FROM MERISTEMS TO FLORAL DIVERSITY: DEVELOPMENTAL OPTIONS AND CONSTRAINTS

EDITED BY: Regine Claßen-Bockhoff, Louis Philippe Ronse De Craene and Annette Becker

PUBLISHED IN: Frontiers in Ecology and Evolution and Frontiers in Cell and Developmental Biology

frontiers Research Topics

frontiers

ISSN 1664-8714
ISBN 978-2-88966-827-4
DOI 10.3389/978-2-88966-827-4

About Frontiers

Frontiers is more than just an open-access publisher of scholarly articles: it is a pioneering approach to the world of academia, radically improving the way scholarly research is managed. The grand vision of Frontiers is a world where all people have an equal opportunity to seek, share and generate knowledge. Frontiers provides immediate and permanent online open access to all its publications, but this alone is not enough to realize our grand goals.

Frontiers Journal Series

The Frontiers Journal Series is a multi-tier and interdisciplinary set of open-access, online journals, promising a paradigm shift from the current review, selection and dissemination processes in academic publishing. All Frontiers journals are driven by researchers for researchers; therefore, they constitute a service to the scholarly community. At the same time, the Frontiers Journal Series operates on a revolutionary invention, the tiered publishing system, initially addressing specific communities of scholars, and gradually climbing up to broader public understanding, thus serving the interests of the lay society, too.

Dedication to Quality

Each Frontiers article is a landmark of the highest quality, thanks to genuinely collaborative interactions between authors and review editors, who include some of the world's best academicians. Research must be certified by peers before entering a stream of knowledge that may eventually reach the public - and shape society; therefore, Frontiers only applies the most rigorous and unbiased reviews.
Frontiers revolutionizes research publishing by freely delivering the most outstanding research, evaluated with no bias from both the academic and social point of view. By applying the most advanced information technologies, Frontiers is catapulting scholarly publishing into a new generation.

What are Frontiers Research Topics?

Frontiers Research Topics are very popular trademarks of the Frontiers Journals Series: they are collections of at least ten articles, all centered on a particular subject. With their unique mix of varied contributions from Original Research to Review Articles, Frontiers Research Topics unify the most influential researchers, the latest key findings and historical advances in a hot research area! Find out more on how to host your own Frontiers Research Topic or contribute to one as an author by contacting the Frontiers Editorial Office: frontiersin.org/about/contact

FROM MERISTEMS TO FLORAL DIVERSITY: DEVELOPMENTAL OPTIONS AND CONSTRAINTS

Topic Editors:
Regine Claßen-Bockhoff, Johannes Gutenberg University Mainz, Germany
Louis Philippe Ronse De Craene, Royal Botanic Garden Edinburgh, United Kingdom
Annette Becker, University of Giessen, Germany

Citation: Claßen-Bockhoff, R., De Craene, L. P. R., Becker, A., eds. (2021). From Meristems to Floral Diversity: Developmental Options and Constraints. Frontiers Media SA. doi: 10.3389/978-2-88966-827-4

Table of Contents

frontiers in Ecology and Evolution

EDITORIAL
published: 31 March 2021
doi: 10.3389/fevo.2021.637954

Editorial: From Meristems to Floral Diversity: Developmental Options and Constraints

Regine Claßen-Bockhoff[1], Louis Philippe Ronse De Craene[2] and Annette Becker[3]*

[1] Institute of Organismic and Molecular Evolution (iomE), Johannes Gutenberg-University, Mainz, Germany, [2] Royal Botanical Garden Edinburgh, Edinburgh, United Kingdom, [3] Department of Biology, Institute of Botany, Justus-Liebig-University, Gießen, Germany

Keywords: flower meristem, floral unit meristem, heterochrony, meristem expansion, spatial constraints, meristem identity

Editorial on the Research Topic

From Meristems to Floral Diversity: Developmental Options and Constraints

Meristems provide growth and shape in flowering plants. They are composed of undifferentiated cells whose fates depend on specific genetic and epigenetic processes. On the molecular level, differential gene expression, and hormone-mediated regulatory feedbacks play key roles, while on the morphogenetic level meristem geometry, mechanical pressure, meristem expansion and the timing of organ initiation and growth processes influence development. Combining the different aspects results in a deeper understanding of the developemental constraints and options underlying growth processes and the genesis of form in plant evolution.

VEGETATIVE AND REPRODUCTIVE MERISTEMS

The shoot apical meristem (SAM) is the primary and dominant meristem maintaining open growth throughout the life of the plant. In the vegetative stage, it continuously segregates leaf primordia and lateral axial meristems. The reproductive stage involves the transition of some (or rarely all) SAMs into reproductive meristems (RMs). Whereas, inflorescence meristems (IMs) grow apically and segregate reproductive units, flower meristems (FMs), and floral unit meristems (FUMs) are determinate lacking apical growth (Claßen-Bockhoff and Bull-Hereñu, 2013).

Molecular studies in the model organism *Arabidopsis thaliana* (Brassicaceae) have shown that the activity of the SAM is regulated by a gene regulatory network mediated by the *WUSCHEL/CLAVATA3* (*WUS/CLA3*) antagonistic system (Laux, 2003), whereas the FM is under the control of the FM identity genes *LEAFY (LFY)* and *APETALA1* (AP1) (Chandler, 2012).

- Interestingly, some genes of the corresponding networks have specific functions whereas others have dual or multiple roles dependent on their respective partners. Chang et al. summarize the present knowledge of the genes with dual functions and show that e.g., *WUS* contributes to the maintenance of SAM activity, when associated with *CLV3*, and to the termination of the FM in association with *AGAMOUS (AG)*. The relative role of genes directly affects floral morphology. Obviously, deducing floral organ homology from single gene expressions may be misleading (Ochoterena et al., 2019).
- Lee et al. investigate the genetic interactions of the transcriptions factors (TF) CRABS CLAW (CRC) and SUPERMAN (SUP) and identify their target genes in *Arabidopsis thaliana*. These TFs not only play a key role in FM determinacy, but also regulate many genes during stamen development, even though *CRC* is only expressed in carpels and nectaries. The authors found that these TFs together influence meristem size, organ number, and stamen elongation, but also stimulate the expression of auxin- and cytokinin-related genes and fine-tune hormonal signaling.

OPEN ACCESS

Edited and reviewed by:
Mark A. Elgar,
The University of Melbourne, Australia

****Correspondence:***
Regine Claßen-Bockhoff
classenb@uni-mainz.de

Specialty section:
This article was submitted to Evolutionary Developmental Biology, a section of the journal Frontiers in Ecology and Evolution

Received: *04 December 2020*
Accepted: *08 March 2021*
Published: *31 March 2021*

Citation:
Claßen-Bockhoff R, Ronse De Craene LP and Becker A (2021) Editorial: From Meristems to Floral Diversity: Developmental Options and Constraints. Front. Ecol. Evol. 9:637954. doi: 10.3389/fevo.2021.637954

The study gives an impressive insight into the interactions between gene expression and epigenetic regulatory mechanisms.

The transition from indeterminate to determinate growth is of central interest for evolutionary developmental questions as it links organ formation with the two elementary features of open growth and reproduction. Meristem morphology, histology, developmental options, and gene regulatory processes completely change when the SAM merges into a FM, challenging the traditional interpretation of the flower as a short shoot with modified leaves (Bateman et al., 2006; Claßen-Bockhoff, 2016).

- In this context, the study of González et al. is of particular interest. The authors use the endoparasitic *Pilostyles boyacensis* (Apodanthaceae) to reconstruct the evolution of FM-related gene expression. This plant has no SAMs and a highly reduced plant body. Nevertheless, it produces flowers by a direct transition from the parenchyma strand to a FM. The authors compare gene expression at three different developmental stages and found that the lack of SAMs and leaves correlates with reductions or even absence in gene expression of specifically genes required for SAM maintenance.

If a SAM is not needed as a precondition for flower formation, why, then, should the FM be homologue to a SAM?

DEVELOPMENTAL OPTIONS AND CONSTRAINTS IN FLOWER MERISTEMS

Determinant meristems (FMs, FUMs) differ from SAMs and IMs by lacking apical growth. They do not segregate new primordia but fractionate until the meristem is completely used. This process can result in spatial constraints, organ suppression, and even organ reduction (Ronse de Craene, 2018). The first organs determine the space available to next organs. Spatial constraints are thus closely linked with the timing of floral organ initiation and development. On the evolutionary scale, heterochrony is one of the major drivers of morphological diversification through abbreviation (paedomorphosis) or extension of development (peramorphosis) (Box and Glover, 2010).

A second characteristic feature of determinate meristems is their ability to expand, thus compensating spatial constraints. Based on the auxin model (Reinhardt et al., 2003), primordia formation is a self-regulating process occupying space completely. Once additional space is generated, new primordia appear (Claßen-Bockhoff and Meyer, 2015) or existing primordia repeat fractionation (Ronse de Craene and Smets, 1991).

Altogether, flower development depends on spatio-temporal correlations in which available space and timing of primordium initiation influence each other and the symmetry, merism, and phyllotaxis of floral structures.

- As to floral symmetry, Naghiloo presents a comprehensive analysis across angiosperms comparing the onset of symmetry during ontogeny. Using published SEM data for early, mid, and late developmental stages, she found that both actinomorphic and zygomorphic patterns originate at different development stages and can be associated with changes and even reversals in symmetry. She concludes that floral symmetry is not necessarily a phylogenetic signal, but rather depends on epigenetic factors, such as mechanical pressure, space limitation, and meristem expansion.
- As to merism and phyllotaxis, Kitazawa and Fujimoto approach the Ranunculaceae as an appropriate model system to study the evolutionary relation between spiral and whorled organ position. They demonstrate that spiral and whorled phyllotaxis mainly depend on organ number and post-meristematic organ displacement. Spiral and whorled phyllotaxis are no alternatives but two sides from the same general law of size dependent growth rate, available space, and timing.
- *Nuphar* belongs to the basal angiosperms and has large bractless flowers occupying leaf positions in the parastichies of the rhizome. Floral organs are not clearly arranged in whorls or spirals. El et al. investigate flower position and floral organ initiation and conclude that the flowers are laterally arranged and the floral organization is primarily whorled. Irregularities are most likely caused by the relative proportions between flower meristem and floral organ primordia, mechanical pressure, and differences in timing.
- Bull-Hereñu and Ronse De Craene illustrate with the example of *Malesherbia* (Passifloraceae) that the diversity of flowers is correlated with the timing of organ initiation and the relative growth rate of the floral organs. While the different flower sizes are correlated with the FM size, the relative proportions between hypanthium and petal length depend on the timing of organ initiation and subsequent spatial constraints.
- Thaowetsuwan et al. investigate the origin of the perianth in the genus *Croton* (Euphorbiaceae) by comparing the development of staminate flowers with well-developed petals and carpellate flowers lacking petals or producing filamentous structures. The authors conclude that the filamentous structures are pedomorphic forms of petals. The reduction of petals is linked to spatial constraints as the alternipetalous whorl is initiated as the outer, but appears at anthesis as the inner whorl.
- Iwamoto et al. investigate the development of a fifth staminode in the labellum of Globbeae (Zingiberaceae). They demonstrate that some species have a well-developed or rudimentary fifth staminode, lacking in the majority of species, and conclude that the repeatedly appearing staminode might be a plesiomorphic character in the group. The loss of the fifth staminode may be linked with mechanical constrictions within the flower bud.

Meristem expansion is particularly obvious in FUMs. Once it exceeds a certain threshold, the meristem fractionates into submeristems.

- Claßen-Bockhoff and Frankenhäuser illustrate that the multistaminate unit in *Ricinus communis* (Euphorbiaceae) might be also interpreted as a floral unit. The structure, traditionally intepreted as a secondary polyandrous flower, develops from a large meristem which fractionates repetitively

with increasing expansion. At the end, anthers associated with leaf-like structures are formed. As this developmental pattern is not known from any other polyandrous flower, the authors interpret the anthers as highly reduced staminate flowers of floral units matching the many monostaminate flowers present in the family.

CONCLUSIONS

The meristem level is often disregarded when morphogenetic processes are explained by developmental genetic studies and modeling approaches. However, gene expression and hormone flow depend on meristem conditions, which on their side are influenced by physical parameters. The Special Issue on Floral Meristems aims to increase the knowledge on meristem conditions and epigenetic processes to bridge the gap between developmental genetics, developmental morphology, and computer modeling. The papers on meristem conditions provide deep insights into the physical and genetic relations between vegetative and reproductive meristems. In particular, the multiple functions of genes and the formation of FMs in parasitic plants raise new questions on homology which need to be discussed in future. The papers on flower development clearly illustrate the effects of growth dynamics, spatial constraints, mechanical pressure, meristem expansion, and novel space generation on the number, size, and shape of floral organs. They underline the need to consider epigenetic processes when dealing with character transformation, heterotopy, and heterochrony on an evolutionary scale.

AUTHOR CONTRIBUTIONS

All authors listed have made a substantial, direct and intellectual contribution to the work, and approved it for publication.

ACKNOWLEDGMENTS

This is the third Special Issue co-edited by members of the FLO-RE-S group (Bull-Hereñu et al., 2014; Iwamoto and Bull-Hereñu, 2018). FLO-RE-S aims to increase interest in organismic aspects of floral development ranging from meristem conditions to biotic interactions (https://flores-network.com). We are grateful for the support of the entire editorial board at Frontiers in Ecology and Evolution. Thanks go also to the external peer reviewers who gave their time and insights to enhance the quality of the manuscripts in this issue.

REFERENCES

Bateman, R. M., Hilton, J., and Rudall, P. J. (2006). Morphological and molecular phylogenetic context of the angiosperms: contrasting the 'top-down' and 'bottom-up' approaches used to infer the likely characteristics of the first flowers. *J. Exp. Bot.* 57, 3471–3503. doi: 10.1093/jxb/erl128

Box, M. S., and Glover, B. J. (2010). A plant developmentalist's guide to paedomorphosis: reintroducing a classic concept to a new generation. *Trends Plant Sci.* 15, 241–246. doi: 10.1016/j.tplants.2010.02.004

Bull-Hereñu, K., Claßen-Bockhoff, R., and Ronse De Craene, L. P. (2014). The FLO-RE-S network for contemporary studies in flower structure and biology. *Flora* 221, 1–3. doi: 10.1016/j.flora.2016.02.005

Chandler, J. W. (2012). Floral meristem initiation and emergence in plants. *Cell. Mol. Life Sci.* 69, 3807–3818. doi: 10.1007/s00018-012-0999-0

Claßen-Bockhoff, R. (2016). The shoot concept of the flower: still up to date? *Flora* 221, 46–53. doi: 10.1016/j.flora.2015.11.012

Claßen-Bockhoff, R., and Bull-Hereñu, K. (2013). Towards an ontogenetic understanding of inflorescence diversity. *Ann. Bot.* 112, 1523–1542. doi: 10.1093/aob/mct009

Claßen-Bockhoff, R., and Meyer, C. (2015). Space matters: meristem expansion triggers corona formation in *Passiflora*. *Ann. Bot*. 117, 277–290. doi: 10.1093/aob/mcv177

Iwamoto, A., and Bull-Hereñu, K. (2018). Floral development: re-evaluation of its importance. *J. Plant Res.* 131, 365–366 doi: 10.1007/s10265-018-1034-9

Laux, T. (2003). The stem cell concept in plants: a matter of debate. *Cell* 113, 281–283. doi: 10.1016/S0092-8674(03)00312-X

Ochoterena, H., Vrijdaghs, A., Smets, E., and Claßen-Bockjoff, R. (2019). The search for common origin: homology revisited. *Syst. Biol*. 68, 767–780. doi: 10.1093/sysbio/syz013

Reinhardt, D., Pesce, E. R., Stieger, P., Mandel, T., Baltensperger, K., Bennett, M., et al. (2003). Regulation of phyllotaxis by polar auxin transport. *Nature* 426, 255–260. doi: 10.1038/nature02081

Ronse de Craene, L. P. (2018). Understanding the role of floral development in the evolution of angiosperm flowers: clarifications from a historical and physicodynamic perspective. *J. Plant Res.* 1313, 367–393. doi: 10.1007/s10265-018-1021-1

Ronse de Craene, L. P., and Smets, E. F. (1991). The impact of receptacular growth on polyandry in the myrtales. *Bot. J. Linn. Soc.* 105, 257–269 doi: 10.1111/j.1095-8339.1991.tb00207.x

Conflict of Interest: The authors declare that the research was conducted in the absence of any commercial or financial relationships that could be construed as a potential conflict of interest.

frontiers in Ecology and Evolution

ORIGINAL RESEARCH
published: 14 November 2019
doi: 10.3389/fevo.2019.00437

CRABS CLAW and SUPERMAN Coordinate Hormone-, Stress-, and Metabolic-Related Gene Expression During *Arabidopsis* Stamen Development

Ze Hong Lee[1], *Yoshitaka Tatsumi*[1], *Yasunori Ichihashi*[2,3], *Takamasa Suzuki*[4], *Arisa Shibata*[5], *Ken Shirasu*[5], *Nobutoshi Yamaguchi*[1,2] *and Toshiro Ito*[1]*

[1] *Division of Biological Science, Graduate School of Science and Technology, Nara Institute of Science and Technology, Ikoma, Japan,* [2] *Precursory Research for Embryonic Science and Technology, Japan Science and Technology Agency, Kawaguchi-shi, Japan,* [3] *RIKEN BioResource Research Center, Tsukuba, Japan,* [4] *Department of Biological Chemistry, College of Bioscience and Biotechnology, Chubu University, Kasugai, Japan,* [5] *RIKEN Center for Sustainable Resource Science, Yokohama, Japan*

OPEN ACCESS

Edited by:
Annette Becker, University of Giessen, Germany

Reviewed by:
Nayelli Marsch-Martinez, Center for Research and Advanced Studies (CINVESTAV), Mexico
Thomas Gross, University of Giessen, Germany

***Correspondence:**
Toshiro Ito
itot@bs.naist.jp

Specialty section:
This article was submitted to Evolutionary Developmental Biology, a section of the journal Frontiers in Ecology and Evolution

Received: *28 August 2019*
Accepted: *25 October 2019*
Published: *14 November 2019*

Citation:
Lee ZH, Tatsumi Y, Ichihashi Y, Suzuki T, Shibata A, Shirasu K, Yamaguchi N and Ito T (2019) CRABS CLAW and SUPERMAN Coordinate Hormone-, Stress-, and Metabolic-Related Gene Expression During Arabidopsis Stamen Development. Front. Ecol. Evol. 7:437. doi: 10.3389/fevo.2019.00437

The appropriate timing of the termination of floral meristem activity (FM determinacy) determines the number of floral organs. In *Arabidopsis*, two transcription factors, CRABS CRAW (CRC) and SUPERMAN (SUP), play key roles in FM determinacy. CRC belongs to the YABBY transcription factor family, whose members contain a zinc finger and a helix-loop-helix domain. The *crc* mutation causes the formation of unfused carpels and leads to an increase in carpel number in sensitized backgrounds. The *SUP* gene encodes a C2H2-type zinc-finger protein, and *sup* mutants produce extra carpels and stamens. However, the genetic interaction between *CRC* and *SUP* is not fully understood. Here, we show that these two transcription factors regulate multiple common downstream genes during stamen development. The *crc sup* double mutant had significantly more stamens and carpels than the parental lines and an enlarged floral meristem. Transcriptome data have implicated several cytokinin- and auxin-related genes as well as stress- and metabolic-related genes to function downstream of CRC and SUP during stamen development. The regulation of common downstream genes of CRC and SUP might contribute to the initiation of an appropriate number of stamens and to subsequent growth and development.

Keywords: *Arabidopsis*, CRABS CLAW, cytokinin, floral meristem, flower, SUPERMAN

INTRODUCTION

Plant development is dependent on the persistent activity of pluripotent meristematic cells that are responsible for organ formation (Laux et al., 1996). In angiosperms, flower development initiates from the floral stem-cell pool that is located in the center of the floral meristem (FM). The FMs produce an appropriate population of cells to initiate a fixed number of floral organs before FM activity terminates (FM determinacy) (Lenhard et al., 2011). In *Arabidopsis*, the FM is maintained by activity of the WUSCHEL (WUS) homeodomain protein and CLAVATA (CLV) ligand–receptor system (Laux et al., 1996; Brand et al., 2000; Schoof et al., 2000).

The WUS–CLV negative feedback loop controls the balance between stem-cell renewal and organ formation and determines the size and number of floral organs, which are sepals, petals, stamens, and carpels (Schoof et al., 2000; Sun et al., 2009). Loss-of-function mutants of any of the *CLV* genes results in enlarged FMs and consequently leads to an increase in floral organ number (Clark et al., 1993, 1995; Kayes and Clark, 1998). Conversely, *wus* mutants have fewer floral organs. Thus, the WUS–CLV negative feedback loop is essential to control FM activity.

The homeotic gene *AGAMOUS* (*AG*) determines when FM activity ceases and limits the size of the FM (Yanofsky et al., 1990; Lohmann et al., 2001; Lenhard et al., 2011). In loss-of-function *ag* mutants, the FM overproliferates, resulting in an increase in floral organ number or in a "flower within flower" phenotype, due to the failure of FM termination (Yanofsky et al., 1990). The AG protein binds to the *WUS* promoter and represses *WUS* expression via the deposition of repressive histone marks (Liu et al., 2011; Guo et al., 2018). During FM termination, AG represses *WUS* expression by directly inducing two key downstream targets, *KNUCKLES* (*KNU*) and *CRABS CLAW* (*CRC*) (Alvarez and Smyth, 1999; Bowman and Smyth, 1999; Payne et al., 2004; Gomez-Mena et al., 2005; Lee et al., 2005; Sun et al., 2014; Bollier et al., 2018). Previous studies have demonstrated that the *crc knu* double mutant shows prolonged *WUS* expression and produces flowers with reiterated floral organs, such as stamens and carpels (Breuil-Broyer et al., 2016; Yamaguchi et al., 2017). The *KNU* gene encodes a C2H2 zinc-finger protein with a conserved transcriptional repressor motif (Payne et al., 2004; Sun et al., 2009, 2014, 2019; Bollier et al., 2018). The KNU transcriptional repressor interacts with Polycomb group proteins and deposits repressive histone marks at the *WUS* locus (Sun et al., 2019). Alternatively, CRC belongs to the YABBY family of transcription factors, members of which contain a zinc finger and a helix-loop-helix domain (Bowman and Smyth, 1999; Baum et al., 2001; Lee et al., 2005). We previously identified two CRC direct and auxin-related targets, which are responsible for FM termination (Yamaguchi et al., 2017, 2018): *TORNADO2* (*TRN2*) encodes a transmembrane protein of the tetraspanin family and controls auxin homeostasis (Cnops et al., 2006; Chiu et al., 2007) and *YUCCA4* (*YUC4*) is one of the 11 *YUCCA* genes that encode flavin monooxygenases involved in tryptophan-dependent auxin biosynthesis (Cheng et al., 2006, 2007). The downregulation of *TRN2* and upregulation of *YUC4* by CRC terminates FM proliferation and triggers floral organ formation (Yamaguchi et al., 2017, 2018).

Other factors have been reported to be involved in FM termination (Uemura et al., 2017): *SUPERMAN* (*SUP*) encodes a C2H2 zinc-finger protein, which has been proposed to act as a boundary gene that specifies the separation between floral whorls 3 and 4 (Bowman et al., 1992; Sakai et al., 1995). The loss-of-function *sup* mutation leads to the formation of supernumerary stamens at the expense of carpel tissues (Sakai et al., 1995, 2000; Prunet et al., 2017). Ectopic *SUP* expression causes altered auxin and cytokinin phenotypes (Nibau et al., 2010). SUP interacts with CURLY LEAF, one of the Polycomb group (PcG) protein components (Xu et al., 2018). Then, the SUP-PcG complex represses two auxin biosynthesis genes, *YUCCA1* (*YUC1*) and *YUC4*, to limit stamen number through deposition of H3K27me3 (Zhao et al., 2001; Cheng et al., 2006, 2007; Sassi and Vernoux, 2013; Xu et al., 2018).

Organ formation is controlled by a complex network of interactions between plant hormones. One simple model of hormone interaction is via antagonism. In antagonistic interactions, the components of one plant hormone signaling pathway interact with those of another hormone. For example, auxin inhibits cytokinin signaling. One cytokinin signaling component, *ARABIDOPISIS HISTIDINE PHOSPHOTRANSFER PROTEIN6* (*AHP6*), is functionally important in auxin–cytokinin crosstalk (Mähönen et al., 2006; Moreira et al., 2013; Besnard et al., 2014a,b). Auxin signaling downstream of *AHP6* inhibits cytokinin signaling to regulate the positioning of floral primordia (Moreira et al., 2013; Besnard et al., 2014a,b). Although it is generally reported that auxin and cytokinin function antagonistically, recent studies have revealed that they also act synergistically during gynoecium formation (Wolters and Jurgens, 2009; El-Showk et al., 2013; Schaller et al., 2015; Müller et al., 2017; Reyes-Olalde et al., 2017a,b). Although these findings have demonstrated that the interplay between auxin and cytokinin via *AHP6* is important for floral primordium positioning and gynoecium formation, the role of *AHP6* in FM determinacy and floral organ initiation remains unclear.

Subsequent floral organ growth and development might also be affected by CRC and/or SUP, potentially via the transcriptional regulation of downstream genes. These might include, for example, the auxin-responsive gene *AUX/IAA19*, which regulates stamen elongation (Tashiro et al., 2009; Ghelli et al., 2018), and *REPRODUCTIVE MERISTEM* (*REM*) genes, which are potentially involved in the early stages of flower development and are often transcriptionally regulated by well-known key floral regulators (Mantegazza et al., 2014). Despite the importance of many genes involved in the regulation of floral organ growth and development, little is known concerning their regulation.

Here, we report the genetic interaction between *SUP* and *CRC*. Molecular genetic analysis revealed that *SUP* and *CRC* cooperatively fine-tune hormone signaling and various stress or metabolic events to regulate stamen formation during flower development.

MATERIALS AND METHODS

Plant Materials and Growth Conditions

The *Arabidopsis thaliana* mutants *crc-1* and *sup-5* used in this study were in the Landsberg *erecta* (L*er*) ecotype background. The *crc-1*, and *sup-5* lines were described previously (Gaiser et al., 1995; Bowman and Smyth, 1999; Jacobsen et al., 2000; Sakai et al., 2000; Yamaguchi et al., 2017, 2018). The double mutants were generated by genetic crossing and genotyped by PCR in subsequent generations. Seeds were sown on soil and stratified at 4°C for 3–7 days. Plants were grown at 22°C under 24 h of continuous light. Plants to be directly compared were grown side-by-side to minimize environmental differences within the growth chamber.

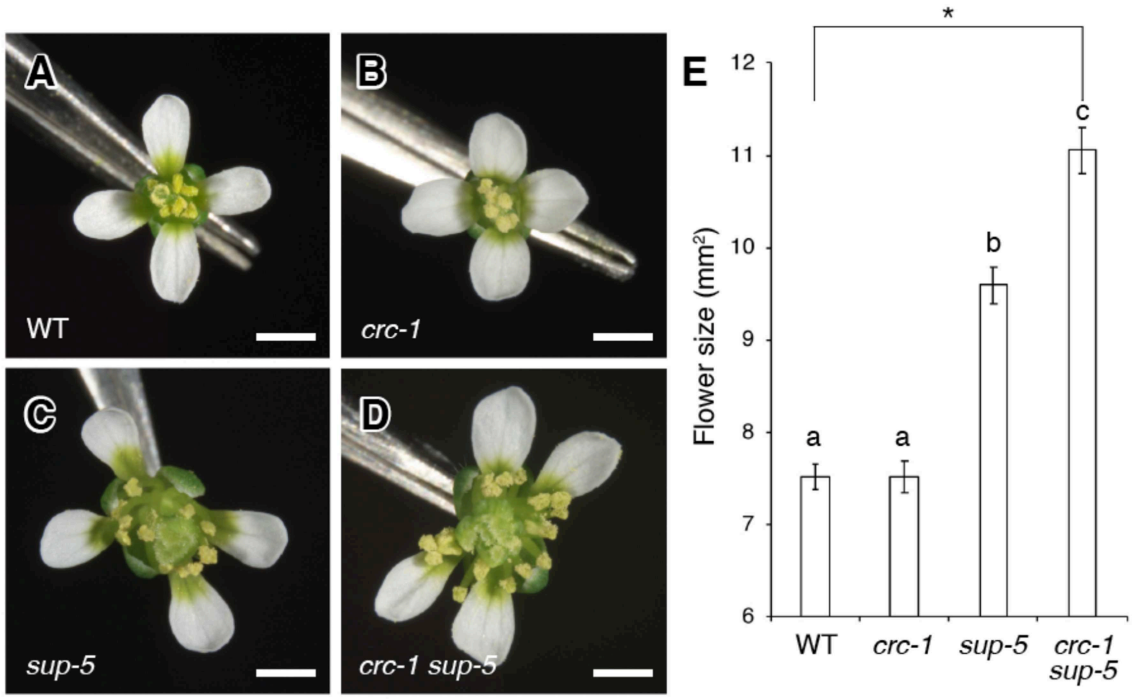

FIGURE 1 | Comparison of flower size among the wild type, *crc-1*, *sup-5*, and *crc-1 sup-5* at floral stage 13. **(A–D)** Top view of flowers. **(A)** The wild type (WT), **(B)** *crc-1*, **(C)** *sup-5*, and **(D)** *crc-1 sup-5*. Scale bars represent 500 μm. **(E)** Quantification of flower size. Mean ± SEM are shown. The asterisk indicates significant difference based on one-way ANOVA. The same letters indicate non-significant differences, whereas different letters indicate significant differences based on the *post-hoc* Tukey HSD test ($p < 0.01$).

Phenotyping Open Flowers

The first 5–10 flowers at developmental stage 13 (according to Smyth et al., 1990) were harvested for phenotyping open flowers (**Figures 1**, **2**). To measure flower size, flowers of L*er*, *crc-1*, *sup-5*, and *crc-1 sup-5* were removed with forceps and fixed onto agar, and photos were taken from above. Flower size was measured using Image J (http://imagej.nih.gov/ij/) software. Thirty flowers (five flowers each from six individual plants) from each genotype were measured. The number of floral organs (sepals, petals, stamen, and carpels) in the wild type (L*er*), *crc-1*, *sup-5*, and *crc-1 sup-5* of stage 13 flowers was counted under a dissecting microscope. Forty flowers (five each from eight individual plants) were counted for each genotype. To test for statistical significance, one-way ANOVA was followed by the *post-hoc* Tukey HSD test.

Measurement of Floral Meristem Size

To measure the size of the FM, inflorescences 1–3 cm tall were harvested immediately after bolting. Inflorescences were fixed with FAA overnight. The resulting inflorescences were dehydrated in an ethanol series (50, 60, 70, 80, 90, 95, and 100%; not <20 min each). The fixed samples were then removed from 100% ethanol and placed in Technovit 7100 resin (Heraeus) before overnight incubation for polymerization. Eight, 10-μm thick sections were prepared using a RM2255 microtome (Leica Microsystems) for each genotype or floral developmental stage. Significance was tested using the Student's *t*-test and one-way ANOVA followed by the *post-hoc* Tukey HSD test.

RNA-Seq

For RNA extraction, floral buds up to floral stage 8 from inflorescences 1–3 cm tall were harvested. Five biological replicates were harvested from wild-type (L*er*), *crc-1*, *sup-5*, and *crc-1 sup-5* backgrounds. Total RNA was extracted using the RNeasy Plant Mini Kit (Qiagen), and genomic DNA was removed using an RNase-Free DNase Set (Qiagen). Library preparation and sequencing were performed as described previously (Uemura et al., 2017; Ichihashi et al., 2018). The created libraries were sequenced by next-generation sequencing (Illumina), and the produced bcl files were then converted into fastq files by bcl2fastq (Illumina). Mapping of sequences to the *Arabidopsis* TAIR10 genome was performed using Bowtie with the following options ("—all—best—strata—trim5 8"). The number of reads for each reference was then counted, and the false discovery rate (FDR), log concentration (Conc) and log fold-change (FC) were obtained using the edge R package (Robinson et al., 2010). To determine DEGs, FDR with adjusted $p < 0.05$ was used. The data were deposited into the DNA Data Bank of Japan (DRA008874).

Transcriptome Analysis

To identify common differentially expressed genes (DEGs), online software (bioinformatics.psb.ugent.be/webtools/Venn/) was used to calculate the overlap between DEGs lists in all mutant backgrounds. Furthermore, Gene Ontology (GO) term analysis was performed using online software agriGO v2.0

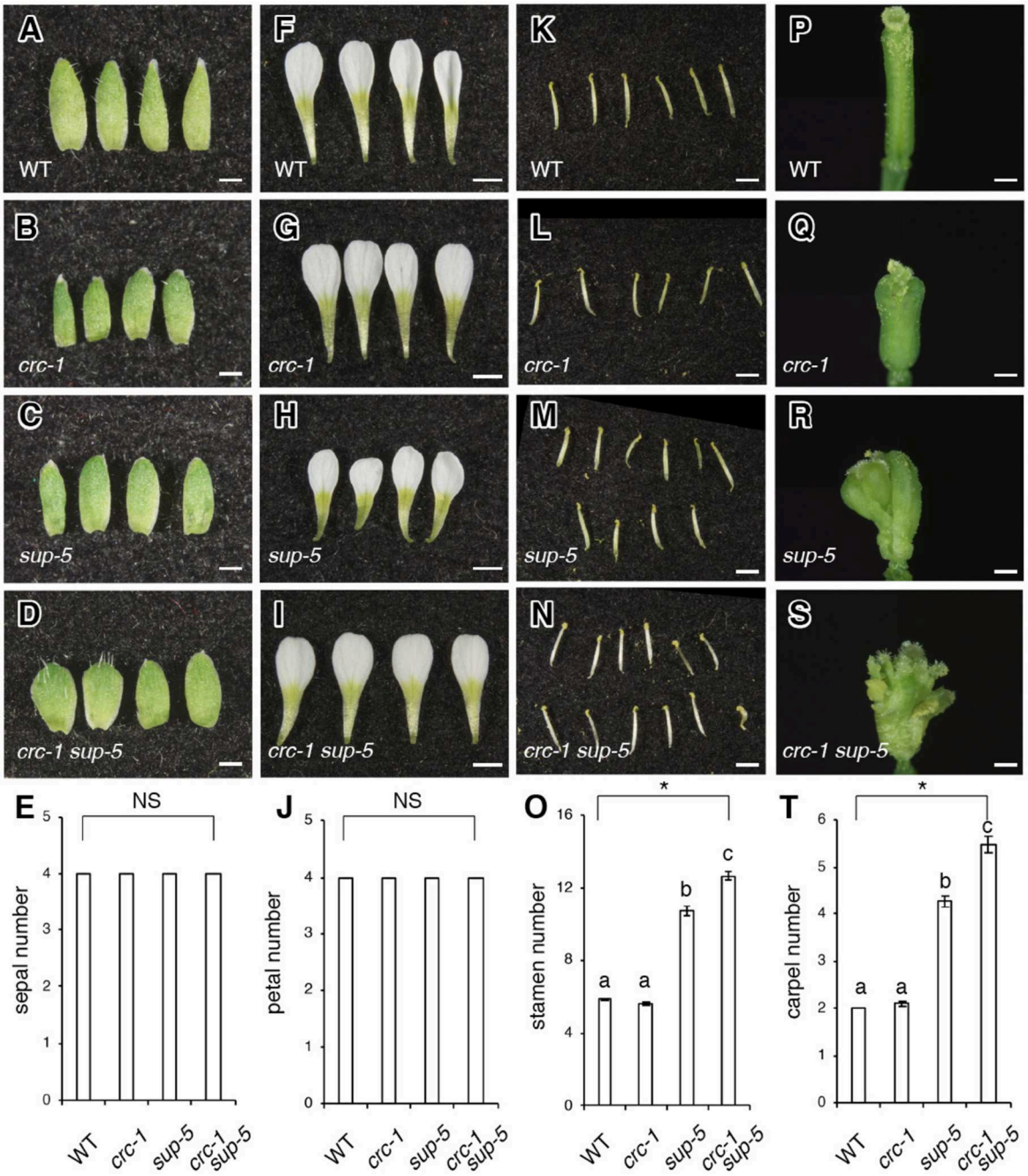

FIGURE 2 | Comparison of floral organ number among the wild type, *crc-1*, *sup-5*, and *sup-5 crc-1* at floral stage 13. **(A–D)** Side view of sepals. **(A)** The wild type (WT), **(B)** *crc-1*, **(C)** *sup-5*, and **(D)** *crc-1 sup-5*. Scale bars represent 500 μm. **(E)** Quantification of sepal number. **(F–I)** Side view of petals. **(F)** The wild type, **(G)** *crc-1*, **(H)** *sup-5*, and **(I)** *crc-1 sup-5*. Scale bars represent 1 mm. **(J)** Quantification of petal number. **(K–N)** Side view of stamens. **(K)** Wild type, **(L)** *crc-1*, **(M)** *sup-5*, and **(N)** *crc-1 sup-5*. Scale bars represent 1 mm. **(O)** Quantification of stamen number. **(P–S)** Side view of carpels. **(P)** The wild type, **(Q)** *crc-1*, **(R)** *sup-5*, and **(S)** *crc-1 sup-5*. Scale bars represent 500 μm. **(T)** Quantification of carpel number. Mean ± SEM are shown. Scale bars represent 500 μm. Asterisks indicate significant differences based on one-way ANOVA. The same letters indicate non-significant differences, whereas different letters indicate significant differences based on the *post-hoc* Tukey HSD test ($p < 0.01$).

(systemsbiology.cau.edu.cn/agriGOvs/) (Tian et al., 2017), followed by REVIGO (Reduced + Visualize Gene Ontology; revigo.irb.hr/) (Supek et al., 2011) to reduce the redundant GO terms.

RT-qPCR

For RNA extraction, floral buds up to floral stage 8 from inflorescences 1- to 3-cm tall were harvested. Plants from mutant backgrounds (*crc-1*, *sup-5*, and *crc-1 sup-5*) and

the controls [wild-type (L*er*)] were grown side-by-side. Approximately 100 mg of floral bud tissue was prepared and frozen immediately after trimming, without fixation. Tissues were kept at −80°C until use (<5 months). RNA extraction was performed using the RNeasy Plant Mini Kit (Qiagen). Genomic DNA was then removed using an RNase-Free DNase Set (Qiagen) to minimize contamination by genomic DNA. The RNA concentration was determined with an IMPLEN NanoPhotometer P-Class spectrophotometer. Synthesis of cDNA was performed with a PrimeScript first-strand cDNA Synthesis Kit (Takara) using <5 μg total RNA, 50 μM oligo dT primer and 200 U PrimeScript RTase with RNase Inhibitor, at 42°C for 30 min. The resulting cDNA was quantified by a LightCycler 480 (Roche) using FastSmart Essential DNA Green Master Mix (Roche) and C_q values were obtained. The expression levels of *AHP6* (*AT1G80100*), *IAA19* (*AT3G15540*), *REM25* (*AT5G09780*), and *TPPI* (*AT5G10100*) were quantified; *EIF4A-1* (*AT3G13920*) was used for the normalization of signals. Five biological replicates were performed and similar results were obtained. The primers used in this study were as follows: AHP6-FW, 5′-CAGCTGGAGCAGCAGAGAAT-3′; AHP6-RV, 5′-TTTCGCTTCGGTAGCTTATAACACA-3′; IAA19-FW, 5′-GATCTAGCCTTTGCTCTTGATAAGC-3′; IAA19-RV, 5′-ATGACTCTAGAAACATCCCCCAAG-3′; REM25-FW, 5′-CTTGGGAGACCACGAGTTTCTTA-3′; REM25-RV, 5′-TTTTGACACGACTAGAAGAAGCGAA-3′; TPPI-FW, 5′-TACAG GTTCGGTCGGTATTAAAGAA-3′; TPPI-RV, 5′-TTGTTAGTGTTCCCAAATCCAAGTG-3′; EIF4-FW, 5′-ACCAGGCGTAAGGTTGATTG-3′; EIF4-RV, 5′-GGTCCATGTCTCCGTGAGTT-3′.

RESULTS

The *sup crc* Double Mutant Has Significantly Larger Flowers and Supernumerary Stamens and Carpels

To analyze the genetic interaction between *SUP* and *CRC*, we generated a *crc-1 sup-5* double mutant and compared the size of flowers between the wild type, *crc-1*, *sup-5*, and *crc-1 sup-5* (**Figures 1A–E**). A wild-type flower consists of four sepals, four petals, six stamens, and two carpels (**Figure 1A**). The mean size of wild-type flowers was 7.5 ± 0.1 mm^2 (**Figure 1E**). Similar to the wild type, the *crc-1* single mutant had a fixed number of four types of floral organs (**Figure 1B**). The size of *crc-1* flowers was 7.5 ± 0.2 mm^2 (**Figure 1E**), which was not significantly different from wild-type and *crc-1* flowers ($p > 0.01$) (**Figure 1E**). As reported previously (Uemura et al., 2017), *sup-5* plants produce significantly larger flowers (9.6 ± 0.2 mm^2) than the wild type ($p < 0.01$) (**Figures 1C,E**). An increase in the size of *sup-5* mutant flowers was accompanied by the presence of extra whorls of stamens, due to sustained floral stem-cell activity (**Figure 1C**) (Xu et al., 2018). In *crc-1 sup-5* double mutants, a large number of stamens and carpels arose from whorls 3 and 4 (**Figure 1C**). The mean size of *crc-1 sup-5* flowers was 11.1 ± 0.2 mm^2 (**Figures 1D,E**) and was thus significantly larger than that of the wild type or either single mutant ($p < 0.01$) (**Figure 1E**).

Combination of *crc* With *sup* Results in a Synergistic Increase in the Number of Stamens and Carpels

To investigate the genetic interaction between *CRC* and *SUP* further, the number of organs was counted in wild-type, *crc-1*, *sup-5*, and *crc-1 sup-5* double mutant flowers (**Figures 2A–T**). Wild-type flowers had four sepals, four petals, six stamens, and two carpels (**Figures 2A,E,F,J,K,O,P,T**). Similarly, the *crc* mutant produced four sepals, four petals, and six stamens (**Figures 2B,E,G,J,L,O,Q,T**). Although *crc-1* mutants produced three or even occasionally four carpels, the mean carpel number for *crc-1* was 2.1 ± 0.0 (**Figure 2T**), which did not differ significantly from the wild type. Indeed, there was no significant difference in the number of all four floral organs between the wild type and *crc-1* mutants ($p > 0.01$) (**Figures 2E,J,O,T**). No significant difference was observed in the number of sepals and petals between wild-type and *sup-5* flowers ($p > 0.01$) (**Figures 2A,C,E,F,H,J**). However, the mean numbers of stamens and carpels in *sup-5* were 10.7 ± 0.3 and 4.3 ± 0.1, respectively (**Figures 2K,M,O,P,R,T**), significantly higher than those of the wild type ($p < 0.01$) (**Figures 2O,T**). Similar to the wild type or the parental lines, *crc-1 sup-5* double mutant flowers also produced four sepals and four petals ($p > 0.01$) (**Figures 2A–J**) but produced significantly more stamens and carpels than the wild type or either single mutant ($p < 0.01$) (**Figures 2K–T**). Thus, the combination of *crc* with *sup* enhanced the *sup* phenotype.

Combining *crc* and *sup* Enhances the FM Width Phenotype of *sup*

Next, we aimed to determine whether the changes in the size of flowers and/or the number of floral organs correlated with changes in FM height and width. Therefore, we quantified the height (from the groove between sepal primordia and the FM to the top of the floral meristem) and the width (between the two grooves along the lateral axis) of the FM by sectioning (**Figures 3A–O**). In wild-type plants, mean FM height and width at stage 3 were 12.0 ± 0.5 and 58.0 ± 1.1 μm, respectively (**Figures 3A,E**), and were 29.2 ± 0.9 and 75.2 ± 2.0 μm, respectively, at stage 5 (**Figures 3A,E**). In *crc-1* mutants, no significant difference in FM height and width at stage 3 or stage 5 was observed compared to wild-type plants ($p > 0.01$) (**Figures 3A,B,E–G,J**). Similarly, no significant difference in FM height and width was observed between wild-type and *sup-5* FMs at stage 3 ($p > 0.01$). Although FM height in the wild type and *sup-5* mutants did not differ significantly ($p > 0.01$) at stage 5, there was a significant difference in FM width ($p < 0.01$) (**Figures 3F,J**). In *crc-1 sup-5*, FM height and width were similar to in *sup-5* by stage 5 (**Figures 3C–E,H–J**). A significant difference in FM width was observed between *sup-5* and *crc-1 sup-5* FMs at stage 6, but no difference in height ($p < 0.01$, Student's *t*-test). Therefore, combining the *crc* mutation with *sup* enhanced the *sup* mutant FM width phenotype.

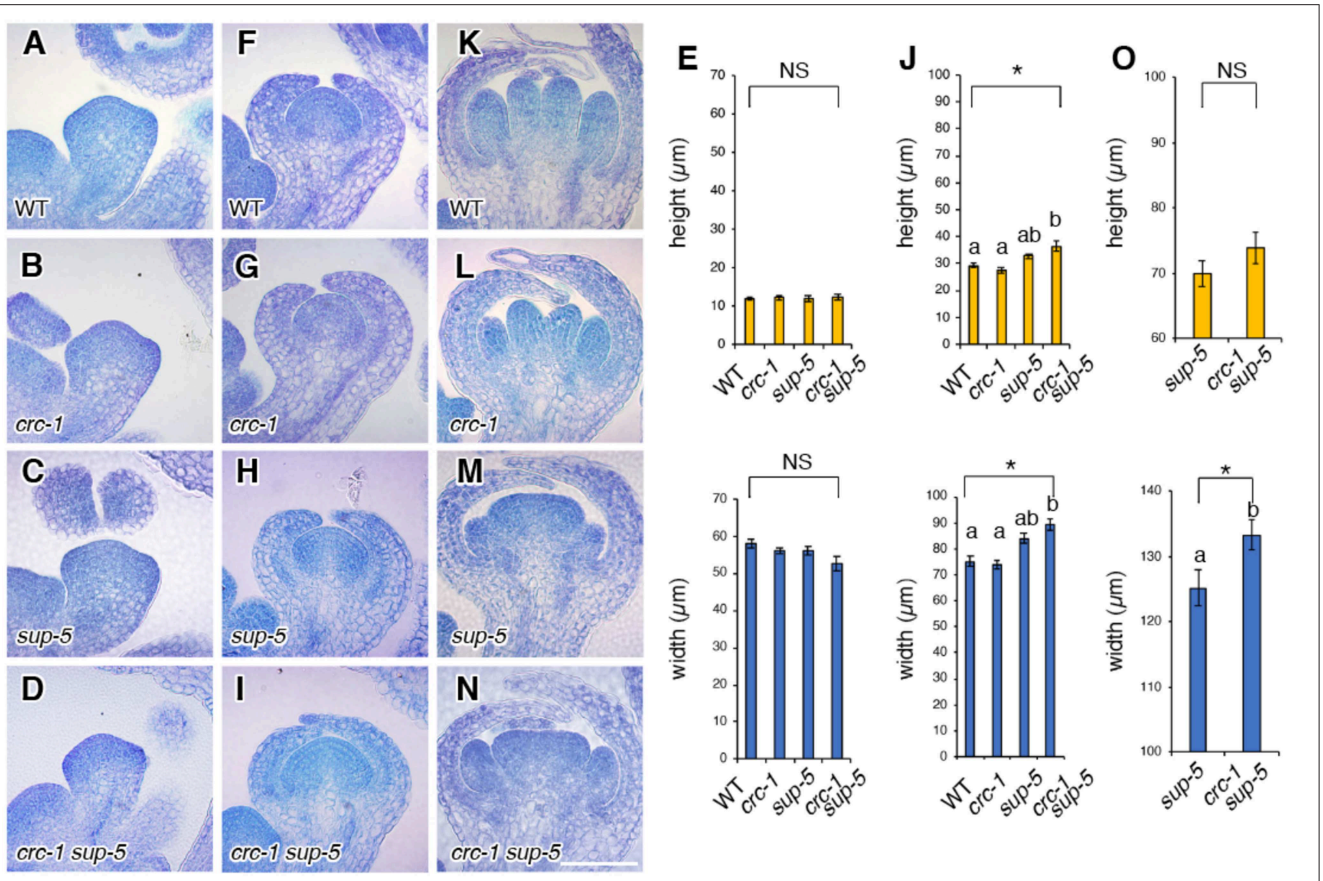

FIGURE 3 | Comparison of floral meristem height and width among the wild type, *crc-1*, *sup-5*, and *sup-5 crc-1* at different floral stages. **(A–D)** Vertical cross sections of stage 3 floral meristems. **(A)** The wild type, **(B)** *crc-1*, **(C)** *sup-5*, and **(D)** *crc-1 sup-5*. **(E)** Quantification of floral meristem height and width at stage 3. **(F–J)** Vertical cross sections of floral meristems at stage 5. **(F)** The wild type, **(G)** *crc-1*, **(H)** *sup-5*, and **(I)** *crc-1 sup-5*. **(J)** Quantification of floral meristem height and width at stage 5. **(K–O)** Vertical cross sections of floral meristems at stage 6. **(K)** The wild type, **(L)** *crc-1*, **(M)** *sup-5*, and **(N)** *crc-1 sup-5*. **(O)** Quantification of floral meristem height and width at stage 6. Mean ± SEM are shown. Scale bars represent 50 μm. For multiple comparisons, asterisks indicate significant differences based on one-way ANOVA. The same letters indicate non-significant differences, whereas different letters indicate significant differences based on the *post-hoc* Tukey HSD test ($p < 0.01$). For single comparisons, the *p*-value was determined using the Student's *t*-test (*$p < 0.01$).

Differentially Expressed Genes in *crc sup*

RNA-seq was performed to examine the genetic interaction at molecular levels in *crc*, *sup*, and *crc sup* (DRA008874). Approximately 10 M reads were sequenced per sample, which were then mapped onto the *Arabidopsis* TAIR 10 genome and differentially expressed genes (DEGs) were identified. In *crc-1* mutants, 263 genes were differentially expressed compared to the wild type (FDR < 0.05) (**Figure 4A**; **Tables S1**, **S2**). Similarly, 65 and 281 genes in total were differentially expressed in *sup* and *crc sup* mutants, respectively (FDR < 0.05) (**Figures 4B,C**; **Tables S1**, **S2**).

To identify genes involved in the enhancement of the *sup* phenotype in the *crc sup* double mutant, we focused on three different categories of DEGs, containing either 20 genes, 11 genes, or 216 genes (**Figures 4B–G**). The "20 genes" category contained the DEGs common to all *crc-1*, *sup-1*, and *crc-1 sup-5* backgrounds (**Figure 4A**). This category contained genes that were differentially expressed in single mutants and whose expression was further altered in the double mutant. To examine the probable functions of these 20 genes, GO term enrichment analysis was performed using agriGO v2.0 online software (Tian et al., 2017). Stimulus-related GO terms such as "response to hormone stimulus," "response to hormone stimulus," and "response to stimulus" were identified (**Figure 4B**; **Table S3**). A further reduction of redundant GO terms by REVIGO categorized ∼70% of the GO terms as "response to endogenous stimulus" (**Figure 4E**; **Table S4**). The "11 genes" category contained the DEGs shared by *sup-5* and *crc-1 sup-5* mutants. This category consisted of the downstream genes of SUP, whose expression was affected by combination with the *crc* mutation. In addition to stimulus-related terms, this category of GO terms also contained development-related GO terms, such as "developmental process" and "anatomical structure development" (**Figures 4C,F**; **Tables S3, S4**). The "216 genes" category contained genes that were differentially expressed only in *crc-1 sup-5*. The GO terms in this category included "response to chemical stimulus," "response to stimulus," and "response to hormone stimulus," which were also present in the "20 genes" and

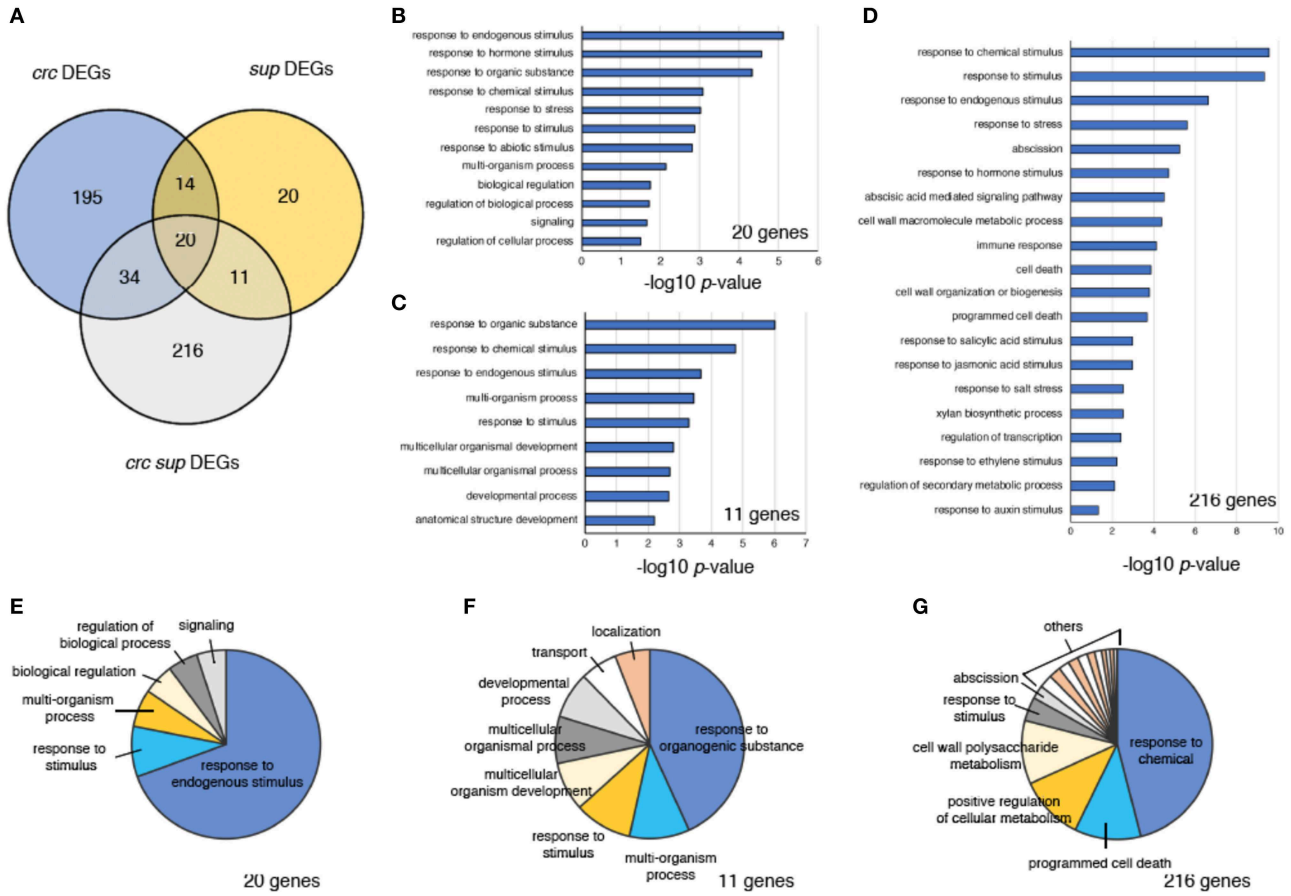

FIGURE 4 | Characterization of DEGs in *crc sup*. **(A)** Venn diagram showing the number of DEGs in *crc*, *sup*, and *crc sup* mutants. **(B–D)** GO term enrichment analysis of categories containing 20 genes **(B)**, 11 genes **(C)**, and 216 genes **(D)**. Selected terms determined by their $-\log_{10}$-adjusted *p*-values are shown. **(E–G)** Pie charts showing summarized GO terms by REVIGO in categories of 20 genes **(E)**, 11 genes **(F)**, and 216 genes **(G)** within the GO term category "biological process".

"11 genes" categories (**Figures 4B–D**; **Tables S3, S4**). In addition, unique GO terms such as "abscission," "programmed cell death," "immune response," and "cell wall organization or biogenesis" were present (**Figure 4D**; **Tables S3, S4**).

Identification of DEGs Related to Stamen Development

To identify the genes involved in supernumerary stamen initiation in *crc-1 sup-5* double mutants, we computationally identified genes involved in stamen development using a published transcriptome dataset (Alves-Ferreira et al., 2007; GSE8864). Previous studies have determined the global expression profile of *Arabidopsis* stamen development using *ap3*, *spl/nzz*, and *ms1* mutants. Among 247 DEGs identified in **Figure 4**, 47 genes were predicted to be expressed at early, intermediate, and late stages of stamen development (**Figure 5A**; **Table S5**). Out of 47 identified genes, 37 were differentially expressed in *ap3* (early stage) (**Figure 5A**). This is consistent with the functions of *CRC* or *SUP*, since both genes are highly expressed from early stages of flower development. Furthermore, an additional 21 and 8 identified genes were differentially expressed in *nzz/spl* (intermediate stage) and *ms1* (late stage), respectively (**Figure 5A**).

To understand the function of the 47 genes involved in stamen development, GO term analysis was performed (**Figure 5B**). The enriched terms included "response to organic substance," "response to chemical stimulus," "cell wall organization or biogenesis," "response to stimulus," "response to hormone," "multicellular organismal development," and "reproductive developmental process" (**Figure 5B**; **Table S6**). The interactive graph view of 47 genes generated by REVIGO identified a cluster of GO terms that contain five different terms: "response to organic substance," "response to hormone," "response to chitin," "response to carbohydrate," and "response to water deprivation" (**Figure 5C**). After removing redundant GO terms, ∼70% of GO terms were involved in "response to chemical" (**Figure 5D**; **Table S7**).

Genes Potentially Involved in Stamen Development

Based on RNA-seq, *SUP* was expressed at normal levels in *crc* and, similarly, *CRC* expression was unaffected in *sup*

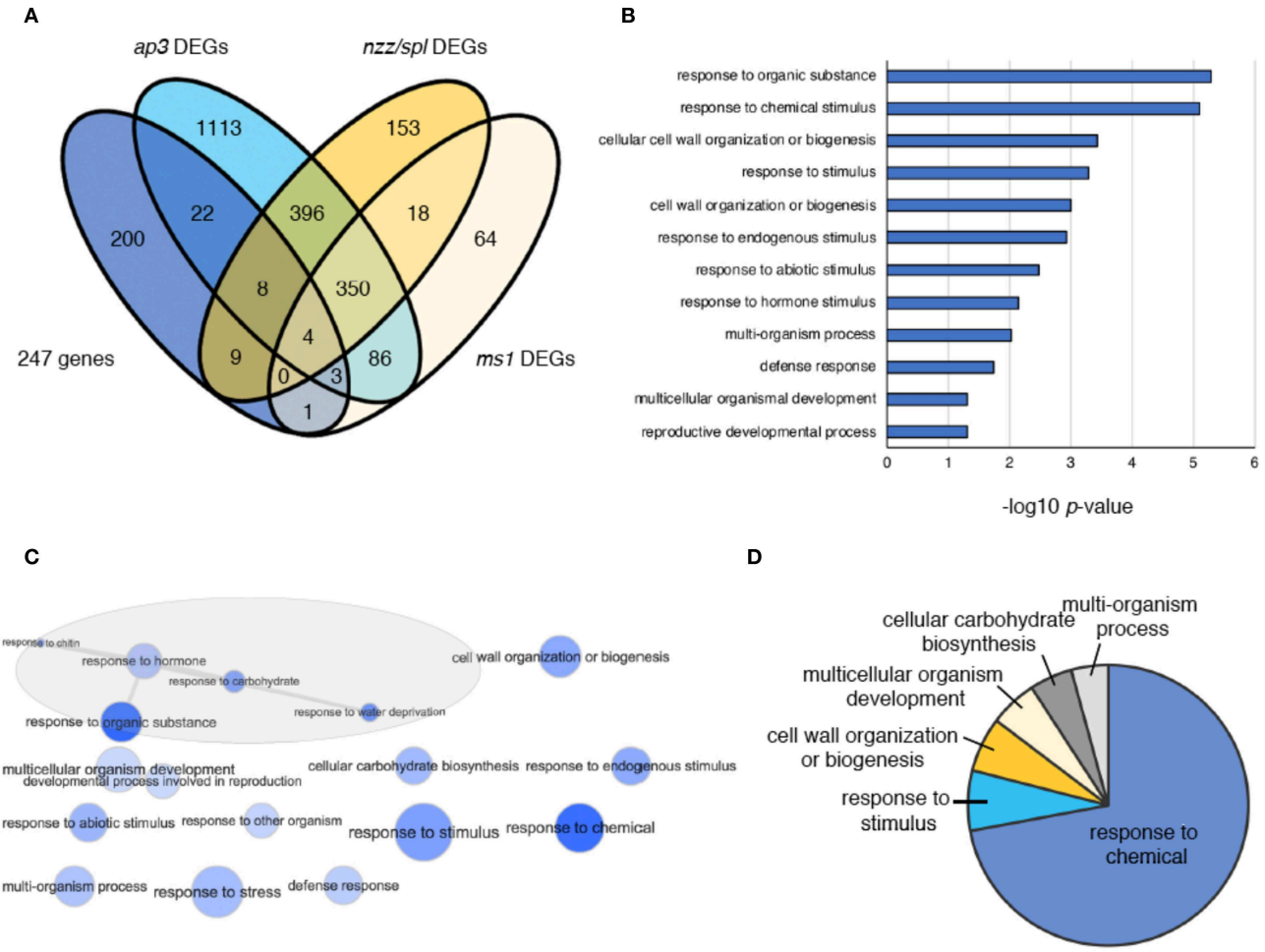

FIGURE 5 | DEGs in *crc sup*, *ap3*, *nzz/spl*, and *ms1* flowers. **(A)** Venn diagram showing 247 DEGs in *ap3*, *nzz/spl*, and *ms1*. **(B)** GO term enrichment analysis of 47 genes coregulated by CRC and SUP and related to stamen development. Selected terms determined by their $-\log_{10}$-adjusted *p*-values are shown. **(C)** The interactive graph view of 47 genes generated by REVIGO. **(D)** Pie charts showing summarized GO terms by REVIGO for 47 genes within the GO-term category "biological process".

(FDR < 0.05). Thus, it is unlikely that either transcription factor transcriptionally regulates the expression of the other (**Figure S1**). All of the 47 DEGs in *crc-1 sup-5* that overlapped with the list of DEGs from the stamen transcriptome dataset were categorized into two different clusters by K-means clustering (**Figure 6A**). Cluster 1 contained 28 genes, which were highly expressed in all mutant backgrounds, whereas cluster 2 contained genes that were downregulated in all mutant backgrounds (**Figures 6A,B**). Compared to the subtle difference in differential gene expression observed in either *crc-1* or *sup-5* single mutants, the expression levels of 47 genes were greatly affected in *crc-1 sup-5* double mutants.

The upregulated genes identified in *crc-1 sup-5* might be direct targets of SUP because SUP is a transcriptional repressor (**Figures 6C–J**). These genes might also be directly regulated by CRC, since CRC can act as a bifunctional transcription factor (Yamaguchi et al., 2017, 2018; Gross et al., 2018). Consistent with the GO term analysis, hormone-related genes such as *AHP6* and *IAA19* were highly expressed in the single mutants (**Figures 6C,D**) (Nakamura et al., 2003; Tatematsu et al., 2004; Mähönen et al., 2006; Besnard et al., 2014a,b). These two genes were also more highly expressed in *crc sup* than in either single mutant. The expression levels of *CELLULOSE SYNTHASE8* (*CESA8*), *REPRODUCTIVE MERISTEM25* (*REM25*), and *AT1G12080* (Turner and Somerville, 1997; Chen et al., 2005; Mantegazza et al., 2014) were also higher in *crc-1 sup-5* (**Figures 6E–G**). Among the potential downstream genes, the roles of *CESA8* and *REM25* have been well studied during cell wall organization and reproductive development, respectively.

By contrast, some of the genes related to hormonal regulation, such as *SMALL AUXIN UPREGULATED36* (*SAUR36*) and *DEHYDRATION-RESPONSIVE ELEMENT BINDING PROTEIN2A* (*DREB2A*) (Sakuma et al., 2006; Kim et al., 2011;

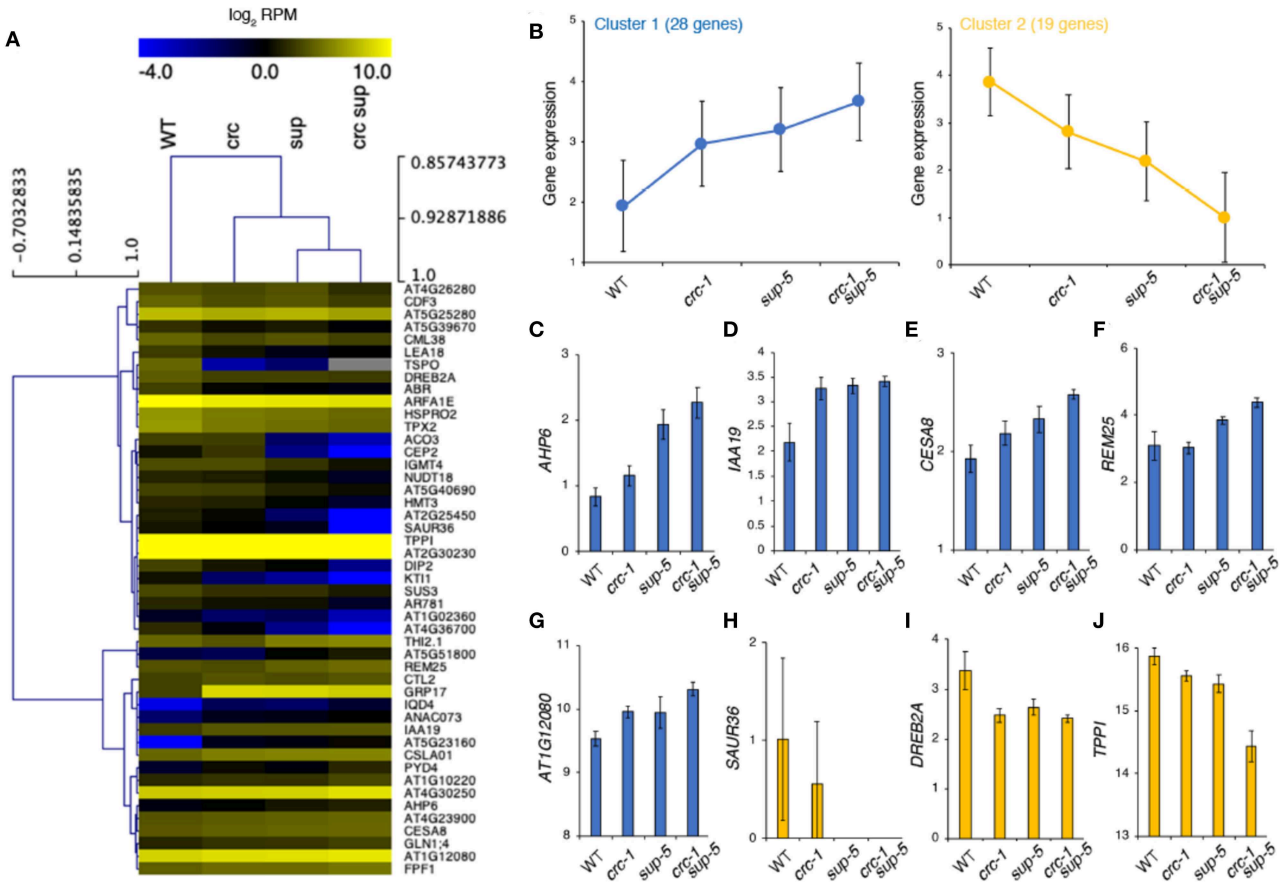

FIGURE 6 | Clustering of high-confidence downstream targets regulated by CRC and SUP. **(A)** Clustering of 47 genes during stamen formation. **(B)** Gene expression from two different clusters: cluster 1 (left) and cluster 2 (right). **(C–J)** Expression level of genes according to RNA-seq. *AHP6* **(C)**, *IAA19* **(D)**, *CESA8* **(E)**, *REM25* **(F)**, *AT1G12080* **(G)**, *SAUR36* **(H)**, *DREB2A* **(I)**, and *TPPI* **(J)**. Mean ± SEM (log_2 of reads per million mapped reads [RPM]) are shown.

Hou et al., 2013; Stamm and Kumar, 2013), were downregulated (**Figures 6H–J**). One sugar metabolism regulator, TREHALOSE-6-PHOSPHATE PHOSPHATASE I (TPPI) (Schluepmann et al., 2004), has also been identified as the downregulated target in the mutant backgrounds. The RNA-seq data were confirmed by RT-qPCR (**Figure S2**).

DISCUSSION

CRC and *SUP* Interact Genetically During Floral Meristem and Stamen Development

Floral meristem determinacy and meristematic cell differentiation are two critical steps in flower development (Sablowski, 2015; Bommert and Whipple, 2017; Xu et al., 2019). Disruption in either or both of these processes caused by the misexpression of FM regulators eventually results in abnormal floral phenotypes (Lohmann et al., 2001; Ma, 2005). Both *SUP* and *CRC* are highly conserved genes in Angiosperms and function as FM activity and identity genes in distinct spatio-temporal manners (Sun and Ito, 2015). Compared to *sup* mutants, *crc* mutants do not have altered floral organ number, despite the occasional presence of more than two carpels (Alvarez and Smyth, 1999; Bowman and Smyth, 1999). However, our data show that combination of the *crc* mutation with *sup-5* resulted in the formation of sterile flowers with significantly more stamens and carpels. The *crc* mutation enhanced FM indeterminacy in *sup-5* mutants, leading to an increase in FM size. Because the increased number of stamens in *sup* mutants is at the expense of carpel tissues due to the expansion of the *APETALA3* gene expression domain into the fourth whorl, an increase in FM size, leading to the formation of more carpels, might increase the rate of floral organ identity conversion, coupled with hormonal changes (Prunet et al., 2017). The sterility of *crc sup* double mutant flowers was probably due to a failure in establishing carpel polarity caused by *crc*. Polarity changes further enhance the carpel defect phenotypes in *sup* single mutants, which produce apically open carpels with abnormal ovule integument development (Gaiser et al., 1995; Baker et al., 1997; Eshed et al., 1999; Breuil-Broyer et al., 2016).

Compared to the *Arabidopsis CRC* gene, its orthologs in other species play broader and prominent roles during plant growth and development (Nagasawa et al., 2003; Yamaguchi et al., 2004;

Li et al., 2011). No clear defects in FM determinacy and no homeotic defects are observed in *crc* single mutants (Alvarez and Smyth, 1999; Bowman and Smyth, 1999; Baum et al., 2001; Nagasawa et al., 2003). By contrast, mutation of *CRC* orthologs in other plant species causes multiple phenotypic defects during the vegetative and reproductive stages. For example, one well-characterized *CRC* ortholog is *DROOPING LEAF* (*DL*) in rice (*Oryza sativa*). Molecular studies have identified the gene functions that specify carpel identity and regulate midrib leaf formation in rice (Yamaguchi et al., 2004). To date, no *crc* alleles that show floral homeotic or leaf defects as strong as those in *dl* mutants have been identified in *Arabidopsis*. When combined with mutants of other key regulators of floral meristem activity or development, these higher-order *crc* multiple mutants show synergistic effects and produce flowers with extra floral whorls or floral organs with abnormal phenotypes (Eshed et al., 2001; Prunet et al., 2008; Zuniga-Mayo et al., 2012). In *sup crc* double mutants, aberrant FM indeterminacy and floral organ identity were observed. Although *CRC* is only expressed in the abaxial region of carpels prior to FM termination, the *crc* mutation enhances not only FM determinacy, but also the initiation of floral organs such as stamens or carpels. Thus, it is conceivable that phytohormones are involved in the genetic interaction between *CRC* and *SUP* because phytohormones exert multiple roles in a non-cell-autonomous manner. Recent studies have identified roles for *CRC* and *SUP* in hormone homeostasis (Yamaguchi et al., 2017, 2018; Xu et al., 2018). Hormonal regulation by CRC might also explain why its orthologs have various functions in different plant species.

CRC and SUP Regulate Common Downstream Targets Involved in Stamen Development

Based on RNA-seq, *SUP* was expressed at normal levels in *crc* and similarly, *CRC* expression was unaffected in *sup* ($FDR < 0.05$). Thus, it is unlikely that either transcription factor transcriptionally regulates the expression of the other (**Figure S1**).

Cytokinins maintain meristem activity by controlling cell division (Riou-Khamlichi et al., 1999; Werner et al., 2001; Yang et al., 2002; Zhang et al., 2013). Consistent with this finding, we identified *AHP6* as a common downstream gene of CRC and SUP. It has been reported that supernumerary stamen primordia in *sup* are formed at stage 7 (Prunet et al., 2017). Considering that *CRC* is expressed from floral stage 6 onwards (Bowman and Smyth, 1999; Lee et al., 2005), the effect of the *crc* mutation in the *sup* background and *AHP6* misexpression was observed after stage 6. Stage-specific gene expression and binding tests using a synchronized system, together with the expression of multiple marker genes, will provide greater insight into how stamen number is defined by CRC and SUP via *AHP6*.

IAA19, which plays a key role in controlling stamen elongation (Tashiro et al., 2009; Ghelli et al., 2018), was also differentially expressed in *crc-1 sup-5* plants. This suggests that SUP might be important not only for early stamen formation, but also for subsequent stamen growth. The *crc* mutation affects the expression of *IAA19*, which is expressed in stamens, even though *CRC* is not expressed in these organs. It is unclear how this regulation occurs, but might involve non-cell-autonomous effects.

The *REM25* and *TPPI* genes were also differentially expressed in *crc-1 sup-5* (Mantegazza et al., 2014). Based on previous *in situ* hybridization data, *REM25* is highly expressed in stamen and carpel primordia at floral stage 6. Since *SUP*, *CRC*, and *REM25* have overlapping expression domains (Sakai et al., 1995; Bowman and Smyth, 1999; Lee et al., 2005), SUP and CRC might be upstream regulators of *REM25*. Genetic redundancy and the physical linkage of *REM* loci hamper functional studies of *REM* family genes (Mantegazza et al., 2014); therefore, the generation of mutants via CRISPR/Cas9 might contribute to understanding the function of genes within this family. *TPPI* is required for the appropriate establishment of organ boundaries (Lor, 2014), which is consistent with the regulation of organ boundary genes, such as *CUC2* (Xu et al., 2018), by SUP. However, the exact function of *TPPI* during flower development is largely unknown and it is relevant to study the molecular function of *TPPI* during stamen/carpel boundary specification.

DATA AVAILABILITY STATEMENT

The datasets generated for this study can be found in the DRA008874.

AUTHOR CONTRIBUTIONS

ZL, YT, NY, and TI conceived and designed the experiments. ZL and YT performed the phenotypic experiments. ZL extracted RNA. YI, AS, and KS generated RNA-seq libraries. TS performed sequencing. NY conducted transcriptome analyses and wrote the paper.

FUNDING

This work was supported by a grant from the Japan Science and Technology Agency Precursory Research for Embryonic Science and Technology (JPMJPR15QA), JSPS KAKENHI Grant-in-Aid for Scientific Research on Innovative Areas (No. 18H04782), JSPS KAKENHI Grant-in-Aid for Scientific Research B (No. 18H02465), Grant-in-Aid for challenging Exploratory Research (No. 19K22431), the NAIST foundation and the LOTTE Foundation to NY, Japan Science and Technology Agency Precursory Research for Embryonic Science and Technology (JPMJPR15Q2) and Cabinet Office, Government of Japan, Cross-ministerial Strategic Innovation Promotion Program (SIP), Technologies for Smart Bio-industry and Agriculture to YI, JSPS KAKENHI Grant-in-Aid for Scientific Research C (No. 15H05955) to TS, JSPS KAKENHI Grant-in-Aid for Scientific Research S (No. 15H05959, 17H06172) to KS, JSPS KAKENHI Grant-in-Aid for Scientific Research on Innovative Areas (No. 17H05843, 18H04839), JSPS KAKENHI Grant-in-Aid for Scientific Research A (No. 15H02405), Grant-in-Aid for challenging Exploratory Research (No. 18K19342) to TI.

ACKNOWLEDGMENTS

We would like to thank Akie Takahashi, Hiroko Egashira, Kyoko Sunuma, Mayumi Nara, Mikiko Higashiura, Taeko Kawakami, and Yuka Kadoya, for technical assistance.

SUPPLEMENTARY MATERIAL

The Supplementary Material for this article can be found online at: https://www.frontiersin.org/articles/10.3389/fevo.2019.00437/full#supplementary-material

REFERENCES

Alvarez, J., and Smyth, D. R. (1999). *CRABS CLAW* and *SPATULA*, two *Arabidopsis* genes that control carpel development in parallel with *AGAMOUS*. *Development* 126, 2377–2386.

Alves-Ferreira, M., Wellmer, F., Banhara, A., Kumar, V., Riechmann, J. L., and Meyerowitz, M. M. (2007). Global expression profiling applied to the analysis of *Arabidopsis* stamen development. *Plant Physiol.* 145, 747–762. doi: 10.1104/pp.107.104422

Baker, S. C., Robinson-Beers, K., Villanueva, J. M., Gaiser, J. C., and Gasser, C. S. (1997). Interactions among genes regulating ovule development in *Arabidopsis thaliana*. *Genetics* 145, 1109–1124.

Baum, S. F., Eshed, Y., and Bowman, J. L. (2001). The *Arabidopsis* nectary is an ABC-independent floral structure. *Development* 128, 4657–4667. Available online at: https://dev.biologists.org/content/128/22/4657.long

Besnard, F., Refahi, Y., Morin, V., Marteaux, B., Brunoud, G., Chambrier, P., et al. (2014a). Cytokinin signaling inhibitory fields provide robustness to phyllotaxis. *Nature* 505, 417–421. doi: 10.1038/nature12791

Besnard, F., Rozier, F., and Vernoux, T. (2014b). The AHP6 cytokinin signaling inhibitor mediates an auxin-cytokinin crosstalk that regulates the timing of organ initiation at the shoot apical meristem. *Plant Signal. Behav.* 9:e28788. doi: 10.4161/psb.28788

Bollier, N., Sicard, A., Leblond, J., Latrasse, D., Gonzalez, N., Gévaudant, F., et al. (2018). At-MINI ZINC FINGER2 and Sl-INHIBITOR OF MERISTEM ACTIVITY, a conserved missing link in the regulation of floral meristem termination in *Arabidopsis* and tomato. *Plant Cell* 30, 83–100. doi: 10.1105/tpc.17.00653

Bommert, P., and Whipple, C. (2017). Grass inflorescence architecture and meristem determinacy. *Semin. Cell Dev. Biol.* 79, 37–47. doi: 10.1016/j.semcdb.2017.10.004

Bowman, J. L., Sakai, H., Jack, T., Weigel, D., Mayer, U., and Meyerowitz, E. M. (1992). *SUPERMAN*, a regulator of floral homeotic genes in *Arabidopsis*. *Development* 114, 599–515.

Bowman, J. L., and Smyth, D. R. (1999). *CRABS CLAW*, a gene that regulates carpel and nectary development in *Arabidopsis*, encodes a novel protein with zinc finger and helix-loop-helix domains. *Development* 126, 2387–2396.

Brand, U., Fletcher, J. C., Hobe, M., Meyerowitz, E. M., and Simon, R. (2000). Dependence of stem cell fate in *Arabidopsis* on a feedback loop regulated by *CLV3* activity. *Science* 289, 617–619. doi: 10.1126/science.289.5479.617

Breuil-Broyer, S., Trehin, C., Morel, P., Boltz, V., Sun, B., Chambrier, P., et al. (2016). Analysis of the *Arabidopsis superman* allelic series and the interactions with other genes demonstrate developmental robustness and joint specification of male–female boundary, flower meristem termination and carpel compartmentalization. *Ann. Bot.* 117, 905–923. doi: 10.1093/aob/mcw023

Chen, Z. Z., Hong, X. H., Zhang, H. R., Wang, Y. Q., Li, X., Zhu, J. K., et al. (2005). Disruption of the cellulose synthase gene, *AtCesA8/IRX1*, enhances drought and osmotic stress tolerance in *Arabidopsis*. *Plant J.* 43, 273–283. doi: 10.1111/j.1365-313X.2005.02452.x

Cheng, Y., Dai, X., and Zhao, Y. (2006). Auxin biosynthesis by the YUCCA flavin monooxygenases controls the formation of floral organs and vascular tissues in *Arabidopsis*. *Genes Dev.* 20, 1790–1799. doi: 10.1101/gad.1415106

Cheng, Y., Dai, X., and Zhao, Y. (2007). Auxin synthesized by the YUCCA flavin monooxygenases is essential for embryogenesis and leaf formation in *Arabidopsis*. *Plant Cell* 19, 2430–2439. doi: 10.1105/tpc.107.053009

Chiu, W. H., Chandler, J., Cnops, G., Van Lijsebettens, M., and Werr, W. (2007). Mutations in the *TORNADO2* gene affect cellular decisions in the peripheral zone of the shoot apical meristem of *Arabidopsis thaliana*. *Plant Mol. Biol.* 63, 731–744. doi: 10.1007/s11103-006-9105-z

Clark, S. E., Running, M. P., and Meyerowitz, E. M. (1993). *CLAVATA1*, a regulator of meristem and flower development in *Arabidopsis*. *Development* 119, 397–418.

Clark, S. E., Running, M. P., and Meyerowitz, E. M. (1995). *CLAVATA3* is a specific regulator of shoot and floral meristem development affecting the same processes as *CLAVATA1*. *Development* 121, 2057–2067.

Cnops, G., Neyt, P., Raes, J., Petrarulo, M., Nelissen, H., Malenica, N., et al. (2006). The *TORNADO1* and *TORNADO2* genes function in several patterning processes during early leaf development in *Arabidopsis thaliana*. *Plant Cell* 18, 852–866. doi: 10.1105/tpc.105.040568

El-Showk, S., Ruonala, R., and Helariutta, Y. (2013). Crossing paths: Cytokinin signalling and crosstalk. *Development* 140, 1373–1383. doi: 10.1242/dev.086371

Eshed, Y., Baum, S. F., and Bowman, J. L. (1999). Distinct mechanisms promote polarity establishment in carpels of *Arabidopsis*. *Cell* 99, 199–209. doi: 10.1016/S0092-8674(00)81651-7

Eshed, Y., Baum, S. F., Perea, J. V., and Bowman, J. L. (2001). Establishment of polarity in lateral organs of plants. *Curr. Biol.* 11, 1251–1260. doi: 10.1016/S0960-9822(01)00392-X

Gaiser, J. C., Robinson-Been, K., and Gasser, C. S. (1995). The *Arabidopsis SUPERMAN* gene mediates asymmetric growth of the outer integument of ovules. *Plant Cell* 7, 333–345. doi: 10.2307/3869855

Ghelli, R., Brunetti, P., Napoli, N., De Paolis, A., Cecchetti, V., Tsuge, T., et al. (2018). A newly identified flower-specific splice variant of *AUXIN RESPONSE FACTOR8* regulates stamen elongation and endothecium lignification in *Arabidopsis*. *Plant Cell* 30, 620–637. doi: 10.1105/tpc.17.00840

Gomez-Mena, C., de Folter, S., Costa, M. M., Angenent, G. C., and Sablowski, R. (2005). Transcriptional program controlled by the floral homeotic gene *AGAMOUS* during early organogenesis. *Development* 132, 429–438. doi: 10.1242/dev.01600

Gross, T., Broholm, S., and Becker, A. (2018). CRABS CLAW acts as a bifunctional transcription factor in flower development. *Front. Plant Sci.* 9:835. doi: 10.3389/fpls.2018.00835

Guo, L., Cao, X., Liu, Y., Li, J., Li, Y., Zhang, K., et al. (2018). A chromatin loop represses *WUSCHEL* expression in *Arabidopsis*. *Plant J.* 94, 1083–1097. doi: 10.1111/tpj.13921

Hou, K., Wu, W., and Gan, S. S. (2013). *SAUR36*, a small auxin up RNA gene, is involved in the promotion of leaf senescence in *Arabidopsis*. *Plant Physiol.* 161, 1002–1009. doi: 10.1104/pp.112.212787

Ichihashi, Y., Fukushima, A., Shibata, A., and Shirasu, K. (2018). "High impact gene discovery: simple strand-specific mRNA library construction and differential regulatory analysis based on gene co-expression network," in *Plant Transcription Factors. Methods in Molecular Biology*, Vol. 1830, ed N. Yamaguchi, 163–189 (New York, NY: Humana Press).

Jacobsen, S. E., Sakai, H., Finnegan, E. J., Cao, X., and Meyerowitz, E. M. (2000). Ectopic hypermethylation of flower-specific genes in *Arabidopsis*. *Curr. Biol.* 10, 179–186. doi: 10.1016/S0960-9822(00)00324-9

Kayes, J. M., and Clark, S. E. (1998). *CLAVATA2*, a regulator of meristem and organ development in *Arabidopsis*. *Development* 125, 3843–3851.

Kim, J. S., Mizoi, J., Yoshida, T., Fujita, Y., Nakajima, J., Ohori, T., et al. (2011). An ABRE promoter sequence is involved in osmotic stress-responsive expression of the *DREB2A* gene, which encodes a transcription factor regulating drought-inducible genes in *Arabidopsis*. *Plant Cell Physiol.* 52, 2136–2146. doi: 10.1093/pcp/pcr143

Laux, T., Mayer, K. F. X., Berger, J., and Jürgens, G. (1996). The *WUSCHEL* gene is required for shoot and floral meristem integrity in *Arabidopsis*. *Development* 122, 87–96.

Lee, J. Y., Baum, S. F., Alvarez, J., Patel, A., Chitwood, D. H., and Bowman, J. L. (2005). Activation of *CRABS CLAW* in the nectaries and carpels of *Arabidopsis*. *Plant Cell* 17, 25–36. doi: 10.1105/tpc.104.026666

Lenhard, M., Bohnert, A., Jürgens, G., and Laux, T. (2011). Termination of stem cell maintenance in *Arabidopsis* floral meristems by interactions between *WUSCHEL* and *AGAMOUS*. *Cell* 105, 805–814. doi: 10.1016/S0092-8674(01)00390-7

Li, H. F., Liang, W. Q., Yin, C. S., Zhu, L., and Zhang, D. B. (2011). Genetic interaction of *OsMADS3*, *DROOPING LEAF*, and *OsMADS13* in specifying rice floral organ identities and meristem determinacy. *Plant Physiol.* 156, 263–274. doi: 10.1104/pp.111.172080

Liu, X., Kim, Y. J., Müller, R., Yumul, R. E., Liu, C., Pan, Y., et al. (2011). *AGAMOUS* terminates floral stem cell maintenance in *Arabidopsis* by directly repressing *WUSCHEL* through recruitment of Polycomb Group proteins. *Plant Cell* 23, 3654–3670. doi: 10.1105/tpc.111.091538

Lohmann, J. U., Hong, R. L., Hobe, M., Busch, M. A., Parcy, F., Simon, R., et al. (2001). A molecular link between stem cell regulation and floral patterning in *Arabidopsis*. *Cell* 105, 793–803. doi: 10.1016/S0092-8674(01)00384-1

Lor, J. L. (2014). *Function of TPPI and TPPJ in Arabidopsis boundary regions* (Unpublished masters dissertation). University of California, Riverside, USA.

Ma, H. (2005). Molecular genetic analyses of microsporogenesis and microgametogenesis in flowering plants. *Annu. Rev. Plant Biol.* 56, 393–434. doi: 10.1146/annurev.arplant.55.031903.141717

Mähönen, A. P., Bishopp, A., Higuchi, M., Nieminen, K. M., Kinoshita, K., Tormakangas, K., et al. (2006). Cytokinin signaling and its inhibitor AHP6 regulate cell fate during vascular development. *Science* 311, 94–98. doi: 10.1126/science.1118875

Mantegazza, O., Gregis, V., Mendes, M. A., Morandini, P., Alves-Ferreira, M., Patreze, C. M., et al. (2014). Analysis of the *Arabidopsis REM* gene family predicts functions during flower development. *Ann. Bot.* 114, 1507–1515. doi: 10.1093/aob/mcu124

Moreira, S., Bishopp, A., Carvalho, H., and Campilho, A. (2013). AHP6 inhibits cytokinin signaling to regulate the orientation of pericycle cell division during lateral root initiation. *PLoS ONE* 8:e56370. doi: 10.1371/journal.pone.0056370

Müller, C. J., Larsson, E., Spichal, L., and Sundberg, E. (2017). Cytokinin-auxin crosstalk in the gynoecial promodium ensures correct domain patterning. *Plant Physiol.* 175, 1144–1157. doi: 10.1104/pp.17.00805

Nagasawa, N., Miyoshi, M., Sano, Y., Satoh, H., Hirano, H. Y., Sakai, H., et al. (2003). *SUPERWOMAN 1* and *DROOPING LEAF* genes control floral organ identity in rice. *Development* 130, 705–718. doi: 10.1242/dev.00294

Nakamura, A., Higuchi, K., Goda, H., Fujiwara, M. T., Sawa, S., Koshiba, T., et al. (2003). Brassinolide induces *IAA5*, *IAA19*, and DR5, a synthetic auxin response element in *Arabidopsis*, implying a cross talk point of brassinosteroid and auxin signaling. *Plant Physiol.* 133, 1–11. doi: 10.1104/pp.103.030031

Nibau, C., Stilio, V. S. D., Wu, H. M., and Cheung, A. Y. (2010). *Arabidopsis* and tobacco *SUPERMAN* regulate hormone signaling and mediate cell proliferation and differentiation. *J. Exp. Bot.* 62, 949–961. doi: 10.1093/jxb/erq325

Payne, T., Johnson, S. D., and Koltunow, A. M. (2004). *KNUCKLES* (*KNU*) encodes a C2H2 zinc-finger protein that regulates development of basal pattern elements of the *Arabidopsis* gynoecium. *Development* 131, 3737–3749. doi: 10.1242/dev.01216

Prunet, N., Morel, P., Thierry, A. M., Eshed, Y., Bowman, J. L., Negrutiu, I., et al. (2008). *REBELOTE*, *SQUINT*, and *ULTRAPETALA1* function redundantly in the temporal regulation of floral meristem termination in *Arabidopsis thaliana*. *Plant Cell* 20, 901–919. doi: 10.1105/tpc.107.053306

Prunet, N., Yang, W., Das, P., Meyerowitz, E. M., and Jack, T. P. (2017). *SUPERMAN* prevents class B gene expression and promotes stem cell termination in the fourth whorl of *Arabidopsis thaliana* flowers. *Proc. Natl. Acad. Sci. U.S.A.* 114, 7166–7171. doi: 10.1073/pnas.1705977114

Reyes-Olalde, J. I., Zuniga-Mayo, V. M., Marsch-Martinez, N., and de Folter, S. (2017a). Synergistic relationship between auxin and cytokinin in the ovary and the participation of the transcription factor SPATULA. *Plant Signal. Behav.* 12:e1376158. doi: 10.1080/15592324.2017.1376158

Reyes-Olalde, J. I., Zúñiga-Mayo, V. M., Serwatowska, J., Chavez Montes, R. A., Lozano-Sotomayor, P., Herrera-Ubaldo, H., et al. (2017b). The bHLH transcription factor SPATULA enables cytokinin signaling, and both activate auxin biosynthesis and transport genes at the medial domain of the gynoecium. *PLoS Genet.* 13:e1006726. doi: 10.1371/journal.pgen.1006726

Riou-Khamlichi, C., Huntley, R., Jacqmard, A., and Murray, J. A. H. (1999). Cytokinin activation of *Arabidopsis* cell division through a D-type cyclin. *Science* 283, 1541–1544. doi: 10.1126/science.283.5407.1541

Robinson, M. D., McCarthy, D. J., and Smyth, G. K. (2010). edgeR: a bioconductor package for differential expression analysis of digital gene expression data. *Bioinformatics* 26, 139–140. doi: 10.1093/bioinformatics/btp616

Sablowski, R. (2015). Control of patterning, growth, and differentiation by floral organ identity genes. *J. Exp. Bot.* 66, 1065–1073. doi: 10.1093/jxb/eru514

Sakai, H., Krizek, B. A., Jacobsen, S. E., and Meyerowitz, E. M. (2000). Regulation of *SUP* expression identifies multiple regulators involved in *Arabidopsis* floral meristem development. *Plant Cell* 12, 1607–1618. doi: 10.1105/tpc.12.9.1607

Sakai, H., Medrano, L. J., and Meyerowitz, E. M. (1995). Role of *SUPERMAN* in maintaining *Arabidopsis* floral whorl boundaries. *Nature* 378, 199–203. doi: 10.1038/378199a0

Sakuma, Y., Maruyama,. K., Qin,. F., Osakabe, Y., Shinozaki, K., and Yamaguchi-Shinozaki, K. (2006). Dual function of an *Arabidopsis* transcription factor DREB2A in water-stress-responsive and heat-stress-responsive gene expression. *Proc. Natl. Acad. Sci. U.S.A.* 103, 18822–18827. doi: 10.1073/pnas.0605639103

Sassi, M., and Vernoux, T. (2013). Auxin and self-organization at the shoot apical meristem. *J. Exp. Bot.* 64, 2579–2592. doi: 10.1093/jxb/ert101

Schaller, G. E., Bishopp, A., and Kieber, J. J. (2015). The Yin-Yang of hormones: cytokinin and auxin interactions in plant development. *Plant Cell* 27, 44–63. doi: 10.1105/tpc.114.133595

Schluepmann, H., van Dijken, A., Aghdasi, M., Wobbes, B., Paul, M., and Smeekens, S. (2004). Trehalose mediated growth inhibition of *Arabidopsis* seedlings is due to trehalose-6-phosphate accumulation. *Plant Physiol.* 135, 879–890. doi: 10.1104/pp.104.039503

Schoof, H., Lenhard, M., Haecker, A., Mayer, K. F. X., Jürgens, G., and Laux, T. (2000). The stem cell population of *Arabidopsis* shoot meristems is maintained by a regulatory loop between the *CLAVATA* and *WUSCHEL* genes. *Cell* 100, 635–644. doi: 10.1016/S0092-8674(00)80700-X

Smyth, D. R., Bowman, J. L., and Meyerowitz, E. M. (1990). Early flower development in *Arabidopsis*. *Plant Cell* 2, 755–767. doi: 10.1105/tpc.2.8.755

Stamm, P., and Kumar, P. P. (2013). Auxin and gibberellin responsive *Arabidopsis SMALL AUXIN UP RNA36* regulates hypocotyl elongation in the light. *Plant Cell Rep.* 32, 759–769. doi: 10.1007/s00299-013-1406-5

Sun, B., and Ito, T. (2015). Regulation of floral stem cell termination in *Arabidopsis*. *Front. Plant Sci.* 6:17. doi: 10.3389/fpls.2015.00017

Sun, B., Looi, L. S., Guo, S., He, Z., Gan, E. S., Huang, J., et al. (2014). Timing mechanism dependent on cell division is invoked by polycomb eviction in plant stem cells. *Science* 343:1248559. doi: 10.1126/science.1248559

Sun, B., Xu, Y., Ng, K. H., and Ito, T. (2009). A timing mechanism for stem cell maintenance and differentiation in the *Arabidopsis* floral meristem. *Genes Dev.* 23, 1791–1804. doi: 10.1101/gad.1800409

Sun, B., Zhou, Y., Cai, J., Shang, E., Yamaguchi, N., Xiao, J., et al. (2019). Integration of transcriptional repression and polycomb-mediated silencing of *WUSCHEL* in floral meristems. *Plant Cell* 31, 1488–1505. doi: 10.1105/tpc.18.00450

Supek, F., Bosnjak, M., Skunca, N., and Smuc, T. (2011). REVIGO summarizes and visualizes long lists of gene ontology terms. *PLoS ONE* 6:e21800. doi: 10.1371/journal.pone.0021800

Tashiro, S., Tian, C. E., Watahiki, M. K., and Yamamoto, K. T. (2009). Changes in growth kinetics of stamen filaments cause inefficient pollination in *massugu2*, an auxin insensitive, dominant mutant of *Arabidopsis thaliana*. *Physiol. Plant* 137, 175–187. doi: 10.1111/j.1399-3054.2009.01271.x

Tatematsu, K., Kumagai, S., Muto, H., Sato, A., Watahiki, M. K., Harper, R. M., et al. (2004). *MASSUGU2* encodes Aux/IAA19, an auxin-regulated protein that functions together with the transcriptional activator NPH4/ARF7 to regulate differential growth responses of hypocotyl and formation of lateral roots in *Arabidopsis thaliana*. *Plant Cell* 16, 379–393. doi: 10.1105/tpc.018630

Tian, T., Liu, Y., Yan, H., You, Q., Yi, X., Du, Z., et al. (2017). agriGO v2.0: a GO analysis toolkit for the agricultural community, 2017 update. *Nucleic Acids Res.* 45, W122–W129. doi: 10.1093/nar/gkx382

Turner, S. R., and Somerville, C. R. (1997). Collapsed xylem phenotype of *Arabidopsis* identifies mutants deficient in cellulose deposition in secondary cell wall. *Plant Cell* 9, 689–701. doi: 10.1105/tpc.9.5.689

Uemura, A., Yamaguchi, N., Xu, Y., Wee, W. Y., Ichihashi, Y., Suzuki, T., et al. (2017). Regulation of floral meristem activity through the interaction of *AGAMOUS*, *SUPERMAN*, and *CLAVATA3* in *Arabidopsis*. *Plant Reprod.* 31, 89–105. doi: 10.1007/s00497-017-0315-0

Werner, T., Motyka, V., Strnad, M., and Schmülling, T. (2001). Regulation of plant growth by cytokinin. *Proc. Natl. Acad. Sci. U.S.A.* 98, 10487–10492. doi: 10.1073/pnas.171304098

Wolters, H., and Jurgens, G. (2009). Survival of the flexible: hormonal growth control and adaptation in plant development. *Nat. Rev. Genet.* 10, 305–317. doi: 10.1038/nrg2558

Xu, Y., Prunet, N., Gan, E. S., Wang, Y., Stewart, D., Wellmer, F., et al. (2018). SUPERMAN regulates floral whorl boundaries through control of auxin biosynthesis. *EMBO J.* 37:e97499. doi: 10.15252/embj.201797499

Xu, Y., Yamaguchi, N., Gan, E. S., and Ito, T. (2019). When to stop: an update on molecular mechanisms of floral meristem termination. *J. Exp. Bot.* 70, 1711–1718. doi: 10.1093/jxb/erz048

Yamaguchi, N., Huang, J., Tatsumi, Y., Abe, M., Sugano, S. S., Kojima, M., et al. (2018). Chromatin-mediated feed-forward regulation of *YUCCA4* expression by AGAMOUS and CRABS CLAW directs gynoecium formation. *Nat. Commun.* 9:5290. doi: 10.1038/s41467-018-07763-0

Yamaguchi, N., Huang, J., Xu, Y., Tanoi, K., and Ito, T. (2017). Fine-tuning of auxin homeostasis governs the transition from floral stem cell maintenance to gynoecium formation. *Nat. Commun.* 8:1125. doi: 10.1038/s41467-017-01252-6

Yamaguchi, T., Nagasawa, N., Kawasaki, S., Matsuoka, M., Nagato, Y., and Hirano, H. Y. (2004). The YABBY gene *DROOPING LEAF* regulates carpel specification and midrib development in *Oryza sativa*. *Plant Cell* 16, 500–509. doi: 10.1105/tpc.018044

Yang, J., Zhang, J., Huang, Z., Wang, Z., Zhu, Q., and Liu, L. (2002). Correlation of cytokinin levels in the endosperms and roots with cell number and cell division activity during endosperm development in rice. *Ann. Bot.* 90, 369–377. doi: 10.1093/aob/mcf198

Yanofsky, M. F., Ma, H., Bowman, J. L., Drews, G. N., Feldmann, K. A., and Meyerowitz, E. M. (1990). The protein encoded by the *Arabidopsis* homeotic gene *AGAMOUS* resembles transcription factors. *Nature* 346, 35–39. doi: 10.1038/346035a0

Zhang, W., Swarup, R., Bennett, M., Schaller, G. E., and Kieber, J. J. (2013). Cytokinin induces cell division in the quiescent center of the *Arabidopsis* root apical meristem. *Curr. Biol.* 23, 1979–1989. doi: 10.1016/j.cub.2013.08.008

Zhao, Y., Christensen, S. K., Fankhauser, C., Cashman, J. R., Cohen, J. D., Weigel, D., et al. (2001). A role for flavin monooxygenase-like enzymes in auxin biosynthesis. *Science* 291, 306–309. doi: 10.1126/science.291.5502.306

Zuniga-Mayo, V. M., Marsch-Martinez, N., and de Folter, S. (2012). JAIBA, a class-II HD-ZIP transcription factor involved in the regulation of meristematic activity, and important for correct gynoecium and fruit development in *Arabidopsis*. *Plant J.* 71, 314–326. doi: 10.1111/j.1365-313X.2012.04990.x

Conflict of Interest: The authors declare that the research was conducted in the absence of any commercial or financial relationships that could be construed as a potential conflict of interest.

frontiers in Ecology and Evolution

ORIGINAL RESEARCH
published: 27 March 2020
doi: 10.3389/fevo.2020.00070

Perianth Phyllotaxis Is Polymorphic in the Basal Eudicot *Anemone* and *Eranthis* Species

Miho S. Kitazawa[1,2] *and Koichi Fujimoto*[2]*

[1] Center for Education in Liberal Arts and Sciences (CELAS), Osaka University, Toyonaka, Japan, [2] Department of Biological Sciences, Graduate School of Science, Osaka University, Toyonaka, Japan

Floral organs are clade-specifically arranged to either spiral or whorled (concentric circles) phyllotaxis. The basic number (merosity) of perianth organs within a whorl is limited to three in most monocots and to four or five in most eudicots. Although the Fibonacci number (3, 5) of merosity is well-known to agree with that of the spirals in phyllotaxis, the evolutionary relationship between whorls and spiral phyllotaxis remains unclear. Focusing on aestivation (the relative positioning of margins of flower organs in the bud) to capture phyllotaxis including merosity of whorled flowers, trimerous-whorled flowers and spiral ones coexist within populations with intraspecific variation in organ numbers. In addition, a recent mathematical model showed that tetramerous and pentamerous whorls developed from spiral organ initiation by incorporating a post-meristematic organ displacement, depending on the interaction among organ primordia. Therefore, integrating the variation of aestivation with the spiral-to-whorl development may elucidate the underlying mechanism of the continuous spiral-whorl relationship with the merosity diversification. Here, we showed that the aestivation of perianth organs (tepals) of mature flowers was intra-specifically variable but constrained in wild populations of several *Anemone* and *Eranthis* species (Ranunculaceae); the spiral arrangements coexisted within a small population, with dimerous, trimerous, tetramerous, and pentamerous double-whorled arrangements, despite considerable possibilities in the geometry. We determined mathematically that most of these constrained aestivations of 5 to 11-tepaled flowers emerge upon the spiral phyllotaxis with a divergence angle between subsequent organs of 90–102 or 135–144° (known as the Lucas and Fibonacci angles, respectively). Incorporating the post-meristematic organ displacement into the model, double-whorled arrangements work as templates to form multiple whorls, the merosity of which is stabilized to trimery, tetramery, or pentamery depending on the divergence angle. These results demonstrate that spiral phyllotaxis promotes the constrained coexistence of whorl and spiral rather than their interspecific dichotomy. This polymorphic phyllotaxis provides an evolutionary scenario in which the floral bauplans of angiosperms could be differentiated into tri-, tetra- and penta-radial symmetries.

Keywords: phyllotaxis, whorl, spiral, Ranunculaceae, floral development, floral evolution, phenotypic polymorphism, Fibonacci number

OPEN ACCESS

Edited by:
Louis Philippe Ronse De Craene, Royal Botanic Garden Edinburgh, United Kingdom

Reviewed by:
Florian Jabbour, Muséum National d'Histoire Naturelle, France
Dmitry D. Sokoloff, Lomonosov Moscow State University, Russia

***Correspondence:**
Koichi Fujimoto
fujimoto@bio.sci.osaka-u.ac.jp

Specialty section:
This article was submitted to Evolutionary Developmental Biology, a section of the journal Frontiers in Ecology and Evolution

Received: *06 December 2019*
Accepted: *04 March 2020*
Published: *27 March 2020*

Citation:
Kitazawa MS and Fujimoto K (2020) Perianth Phyllotaxis Is Polymorphic in the Basal Eudicot Anemone and Eranthis Species. Front. Ecol. Evol. 8:70. doi: 10.3389/fevo.2020.00070

INTRODUCTION

Phyllotaxis is the regular arrangement of plant aerial organs around the plant stem (Adler et al., 1997). There are two major phyllotactic arrangement types, spiral and whorled. In spiral phyllotaxis, organs are arranged spirally around the stem while in whorled phyllotaxis organs are arranged in concentric circles (i.e., whorls) in a radially symmetric manner (**Figure 1A**). The perianth organs (tepals) of a flower are therefore arranged either in whorls or spirals, and this species-specific trait is thought to have emerged during the evolution of flowering plants (Endress, 2001a; Ronse de Craene et al., 2003; Endress and Doyle, 2009). However, it is a matter of debate whether the ancestral state is spiral or whorled (Sauquet et al., 2017; de-Paula et al., 2018; Sokoloff et al., 2018). On the other hand, during the floral development of many families within the angiosperm clade (e.g., Caryophyllaceae, Solanaceae, Rosaceae, Ranunculaceae, and Nymphaeaceae), organ primordia are initiated in a spiral arrangement but converge to whorls at maturity (Lyndon, 1978; Endress, 1987; Hill and Malmberg, 1996; Foster et al., 2003). Thus, the evolutionary relationship between spiral and whorled arrangements should be investigated further.

Merosity (Ronse de Craene and Smets, 1994; Ronse de Craene, 2016), defined as the number of floral organs within a whorl, is typically four or five in most eudicots and three in monocots and magnoliids (**Figure 1C**, upper panel). There is a tendency for all whorls to have the same organ number in the centrifugal development that is common in flowers (Smyth, 2018). It has been emphasized that basic trimerous and pentamerous forms represent Fibonacci numbers (Endress, 1987; Kubitzki, 1987), which define secondary spirals (parastichy) in spiral phyllotaxis. However, the detailed developmental mechanism for the transition from a spiral to a whorled arrangement is still largely unknown. A recent mathematical model of floral phyllotaxis was used to demonstrate that a pseudo-whorled arrangement (multiple organs arranged at nearly equal distance from the shoot apex; Kwiatkowska, 1999) can emerge from spiral initiation (Kitazawa and Fujimoto, 2015). According to this model, tetramerous and pentamerous whorls emerge from spiral initiation by organ displacement depending on post-meristematic interaction; the mechanism leading to trimerous whorls remains unclear.

Trimery and pentamery coexist in several genera and/or species of several clades scattered over angiosperms (Schoute, 1935; Endress, 1987; Kubitzki, 1987; Ronse de Craene et al., 2003; Damerval and Nadot, 2007; Ronse de Craene, 2016); e.g., *Anemone* (Ranunculaceae, eudicot; Schöffel, 1932; Ren et al., 2010; Kitazawa and Fujimoto, 2014), *Eranthis* (Ranunculaceae; Salisbury, 1919; Kitazawa and Fujimoto, 2016a), *Aspidistra* (Asparagaceae, monocot; Vislobokov et al., 2014), *Nuphar* (Nymphaeaceae, Nymphaeales; Endress, 2001b; Schneider et al., 2003; Padgett, 2007; Warner et al., 2008), and *Cabomba* (Cabombaceae, Nymphaeales; Rudall et al., 2009). One way to capture floral organization is aestivation, i.e., the relative positioning of floral organs in the bud (**Figure 1B**, upper panel; Schoute, 1935; Sattler, 1973; Ronse de Craene, 2010), which can explain phyllotaxis including merosity. In five-tepaled *Anemone* species, aestivations appear to be highly constrained: despite four geometrically possible aestivations (Cunnell, 1958), the quincuncial aestivation, which reflects spiral phyllotaxis

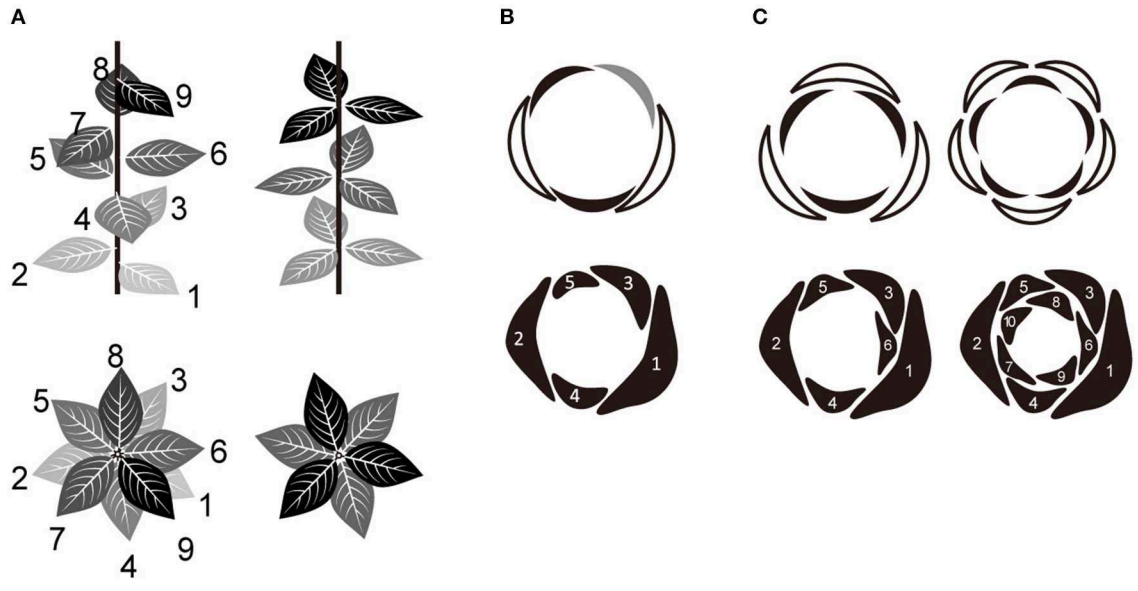

FIGURE 1 | Relationship between spiral and whorl phyllotaxis. **(A)** Two major categories of phyllotaxis; spiral (left) and whorled (right). **(B)** Quincuncial aestivation of five tepals derived from the Fibonacci spiral (with a divergence angle of 137°). The arrangement of each organ in relation to neighboring ones was identified (top) as either external (white), internal (black), or alternating (gray). **(C)** Trimerous and pentamerous double-whorls (top) derived from the Fibonacci spiral (bottom). In some species, primordia initiate individually in a spiral order and then develop into whorled arrangements during floral development via a post-meristematic interaction between them. The numbers in **(A–C)** indicate the initiation order of each organ.

appears to be dominant (**Figure 1B**; Kitazawa and Fujimoto, 2016b, 2018). An aestivation with trimerous double-whorls can emerge from the spiral phyllotaxis upon appearance of an excessive organ (**Figure 1C**, left bottom) and coexist with a quincuncial arrangement within a population (Kitazawa and Fujimoto, 2016b, 2018) with intraspecific variation of organ numbers, as observed in several *Anemone* species (Yule, 1902; Schöffel, 1932). Although the increase of organ numbers also increases the possible geometric arrangements of organs, only few arrangements, including that with double trimerous whorls, appear in natural populations of *Anemone* species (Kitazawa and Fujimoto, 2016b, 2018). Both the quincuncial and the double trimerous whorls are considered to also exist in *Aspidistra* (**Figure 3** in; Vislobokov et al., 2014), *Nuphar* (Endress, 2001b; Schneider et al., 2003), and *Cabomba* (Rudall et al., 2009) species. Theoretically, further increase in organ numbers following the Fibonacci spiral will result in double pentamerous whorls (**Figure 1C**, right); a decrease to four organs will result in double dimerous whorls. The coexistence of whorled and spiral flowers could help clarifying a developmentally constrained pathway of floral organization evolution in angiosperms.

Based on aestivation variation and mathematical modeling approaches, the present report aimed to further investigate the constrained coexistence of whorled and spiral flowers with a wide range of tepal numbers in two Ranunculaceae genera, *Anemone* and *Eranthis*. We theoretically examined the relationship between the merosity and the divergence angle, a major parameter of spiral phyllotaxis, and confirmed that coexisting aestivations work as templates to form multiple whorls while keeping the merosity.

MATERIALS AND METHODS

Positional Arrangement of Perianth Organs

The aestivation of perianth organs (i.e., tepals) was examined in mature flowers with four to 11 tepals only. Following previous studies (Morgan, 1874; Schoute, 1935; Cunnell, 1958; Kitazawa and Fujimoto, 2016b, 2018), we surmised aestivation by referring to the positional arrangements of tepals (**Figures 1B,C**). The aestivation of flowers with the same number of external and internal organs (represented in white and black, respectively; **Figures 1B,C**, upper panel) and no alternating organs (represented in gray; **Figure 1B**) are hereafter referred to as double-whorled. Except for the double-whorls, the aestivations derived from the spiral phyllotaxis that we mathematically confirmed (represented in orange, **Figure 3**), are referred to as spiral flowers. The external, internal, and alternating organs are referred to as E, I, and A, respectively. For simplicity, reflected and rotated arrangements were dismissed, and therefore the position of the flower with respect to the main axis and the direction of the spiral were ignored.

Plant Samples

We measured the positional arrangements of tepals in wild populations of *Eranthis pinnatifida* (Shiga, Hyogo, Okayama, and Hiroshima prefectures), *Anemone nikoensis* (Shiga, Osaka, Hyogo, and Okayama prefectures), *Anemone flaccida* (Hokkaido, Shiga, Osaka, Hyogo, and Okayama prefectures), *Anemone hepatica* (Shiga and Okayama prefectures), and two forms of *Anemone* × *hybrida* (Japanese anemone; designated as *Anemone scabiosa* in Kitazawa and Fujimoto, 2016a,b; Hokkaido, Tokyo, Mie, Shiga, Kyoto, Nara, Osaka, and Hyogo prefectures) in Japan. Perianth organs of these species are not differentiated into sepals and petals. Although there are several forms of *A.* × *hybrida*, we were unable to identify them at many of our observation sites. We used tepal color as the primary feature to distinguish between two of the forms: pale pink (PP) and white (W); the deep pink form was not examined. We did not count the flowers in cases where tepals were so narrow at their basal parts that their positional overlaps were lost as days elapsed after blooming. The absolute frequency of each arrangement was measured as the sum of the multiple populations within the species (**Supplementary Table 1**). The relative frequency was normalized to flower sample sizes and their respective tepal numbers, only when sample size was above 30 (**Supplementary Table 1** and **Figure 2**). The modal tepal number in the sum of the observed populations was 5 for *E. pinnatifida*, *A. flaccida, A. nikoensis*, and *A.* × *hybrida* PP, 6 for *A. hepatica*, and 7 for *A.* × *hybrida* W (**Supplementary Table 2**).

Mathematical Model

To theoretically infer the developmental mechanisms of the observed aestivations, we examined the relationship between divergence angle and merosity using a developmental model for phyllotaxis (Douady and Couder, 1996; Kitazawa and Fujimoto, 2015). In this model, a new primordium i emerges at a constant time interval τ and a constant divergence angle ϕ with the subsequent organ, at the edge of the meristem with radius R_0 in the polar coordinate (R_0, $i\ \phi$ mod 360°), where $i\ \phi$ mod 360° stands for the remainder of the division of $i\ \phi$ by 360°. We considered two types of models, namely the absence (**Figure 3**) and the presence (**Figure 4**) of a post-meristematic organ interaction. In the absence model, analytical calculation rigorously identified aestivation given the primordium number i and angle ϕ. In the presence model, after the initiation, the post-meristematic displacement of organs depending on their interaction was simulated by the Monte Carlo method (Kitazawa and Fujimoto, 2015) to examine which merosity was favored. Monte Carlo steps were repeated for τ multiplied by the number of existing primordia. In each step, a primordium k was selected randomly, and a new position (r'_k, θ'_k) was assigned for it. The new coordinates r'_k and θ'_k followed normal distributions and their means were r_k and θ_k, respectively, with standard deviations σ_r and σ_θ, respectively. The potential energy U_g of each position was formulated as

$$U_g = \sum_j exp\,(-\frac{d_{kj}}{\lambda_g})$$

where d_{kj} denotes the distance between primordia k and j. The new position for k was selected when the energy difference

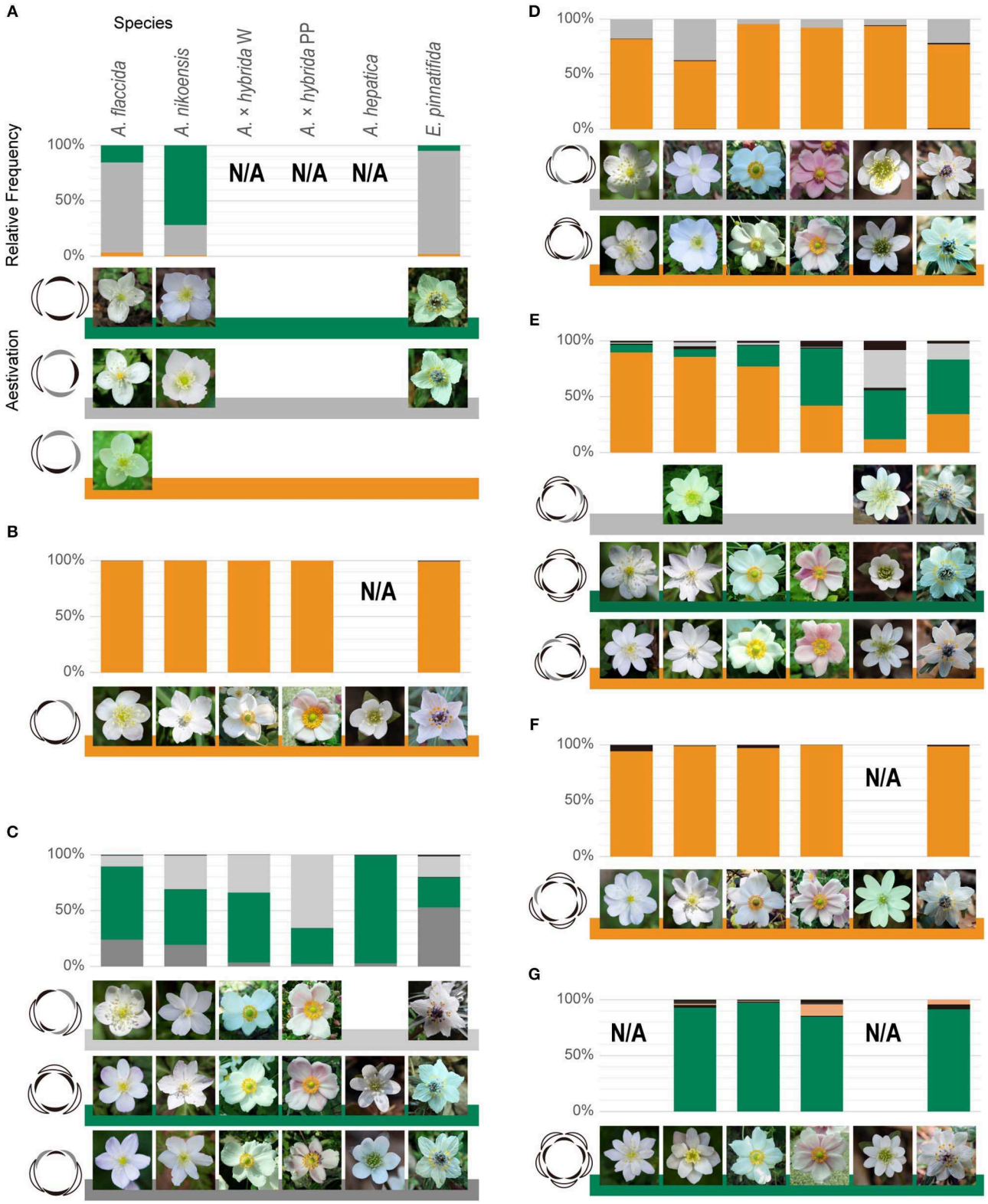

FIGURE 2 | Constrained, intraspecific coexistence of whorled and spiral flowers. Relative frequency of aestivation in flowers with 4 **(A)**, 5 **(B)**, 6 **(C)**, 7 **(D)**, 8 **(E)**, 9 **(F)**, and 10 **(G)** tepals. Green and orange in bar charts denote double-whorled and spiral flowers, respectively, and dark and light gray denote other aestivations,

(Continued)

FIGURE 2 | consistently with coloring in **Supplementary Table 1**. 10-tepaled aestivation in orange denotes EAIEAIEIEI. The other aestivations with relative frequency below 10% are shown in black. Representative images of the major aestivations are shown for each species and form at the right side of the floral diagrams. N/A indicates the sample size was below 30. The rank in each tepal number indicated a negative correlation between tetramerous and trimerous double-whorls; trimerous and tetramerous double-whorls ranked first for 6-tepaled and second for 8-tepaled flowers, respectively, for *A. flaccida, A. nikoensis,* and A. × *hybrida* W; these ranks were the opposite for *A.* × *hybrida* PP and *E. pinnatifida*.

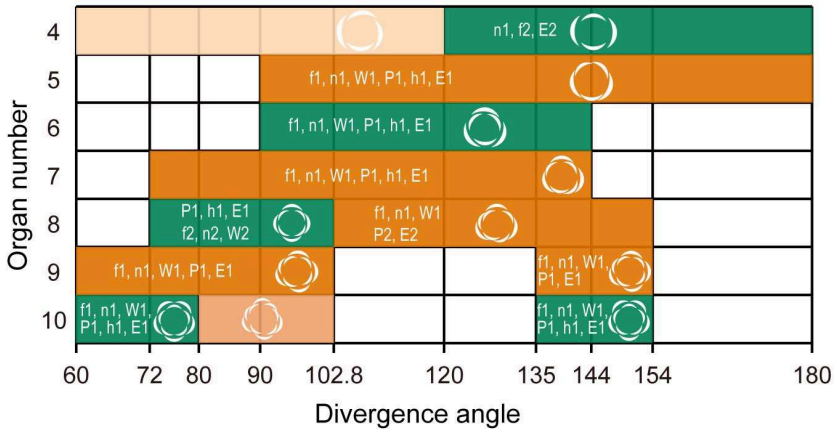

FIGURE 3 | Double-whorls of trimery, tetramery, and pentamery can develop from spiral phyllotaxis at different divergence angles. Aestivation patterns derived from calculations using the spiral phyllotaxis model with a constant divergence angle (degree; horizontal axis) in relation to tepal number (vertical axis). Whorled and spiral flowers observed in *Anemone* and *Eranthis* species are shown in green and orange, respectively; their relative frequency is above 50% in some species or forms, except for the light-colored aestivations (EAAI, 4% maximum; EAIEAIEIEI, 11% maximum). Codes f1, n1, W1, P1, h1, and E1 indicate the most frequent aestivations in *A. flaccida*, *A. nikoensis*, *A.* × *hybrida* W, *A.* × *hybrida* PP, *A. hepatica*, and *E. pinnatifida*, respectively. For the 4-tepaled and 8-tepaled flowers, the second most frequent aestivations are also indicated as f2, n2, W2, P2, and E2, where letters indicate the same species as in the most frequent aestivations. Aestivations in white regions are hardly observed in nature (i.e., <3% of the relative frequency in all the species and forms we examined; see **Supplementary Table 1**).

between the original and the new position ($\Delta_U = U'_g - U_g$) was equal to or smaller than zero. When Δ_U was positive, the new position was selected with probability $\exp(-\beta\Delta_U)$ and the primordium stayed at the original position otherwise. Given $\beta = 1.0\times10^4, \lambda_g = 10.0, \sigma_r = 0.05$ and $\sigma_\theta = 2.0$, the potential-dependent displacement occurs much more largely in the radial direction than in the angular direction.

RESULTS

Constrained Coexistence of Whorled and Spiral Flowers in Populations as a Result of Intraspecific Variation of Tepal Numbers

In line with a previous report (Kitazawa and Fujimoto, 2018), we confirmed that the aestivations of 5- to 7-lobed flowers were constrained to several types including the trimerous double-whorl and the spirals, despite considerable intraspecific variation of tepal numbers in *Anemone* species (**Supplementary Table 2**) (Yule, 1902; Kitazawa and Fujimoto, 2014, 2016a), even when there was a two-fold increase in the sample size (**Figures 2B–D**, **Supplementary Table 1**). Therefore, we explored the constrained coexistence of whorled and spiral flowers in populations with more than 7 and <5 tepals, in four *Anemone* and one *Eranthis* species (sections Positional Arrangement of Perianth Organs and Plant Samples). We found that the aestivations of 8- to 10-lobed flowers were mostly constrained to five types, whereas the relative frequency of the remaining types appeared to be less than 10% in all the species and forms we examined (**Figures 2E–G**). Two of these five dominant types were the tetramerous and pentamerous double-whorled (represented in green, **Figures 2E,G**); two other dominant types were spiral (represented in orange, **Figures 2E,F**). The double pentamerous whorls appeared in more than 85% of the 10-tepaled flowers in each species (**Figure 2G**). One spiral was present in 94% of the 9-tepaled flowers in each species (**Figure 2F**). The tetramerous double-whorled and the other spiral arrangements were dominant in more than 90% of the 8-tepaled flowers, except in *A. hepatica* (57%) and *E. pinnatifida* (83%) where another aestivation (EAIEIEIA) was frequent instead (34% and 14% of flowers, respectively; represented in gray, **Figure 2E**). In addition, the spiral dominantly appeared in 98% of the 11-tepaled flowers in all species ($n = 89$), and the dimerous double-whorl appeared in 29% of the 4-tepaled flowers in all species ($n = 87$; **Supplementary Table 1**; represented in green, **Figure 2A**). These intraspecific coexistences appeared even in a single population of each species where the relative frequency of spirals and whorls showed considerable reproducibility among different years (**Supplementary Table 3**). Taken together, the aestivations of 5- to 11-tepaled flowers were mostly constrained to the double-whorls of trimery, tetramery, and pentamery as well as to spirals.

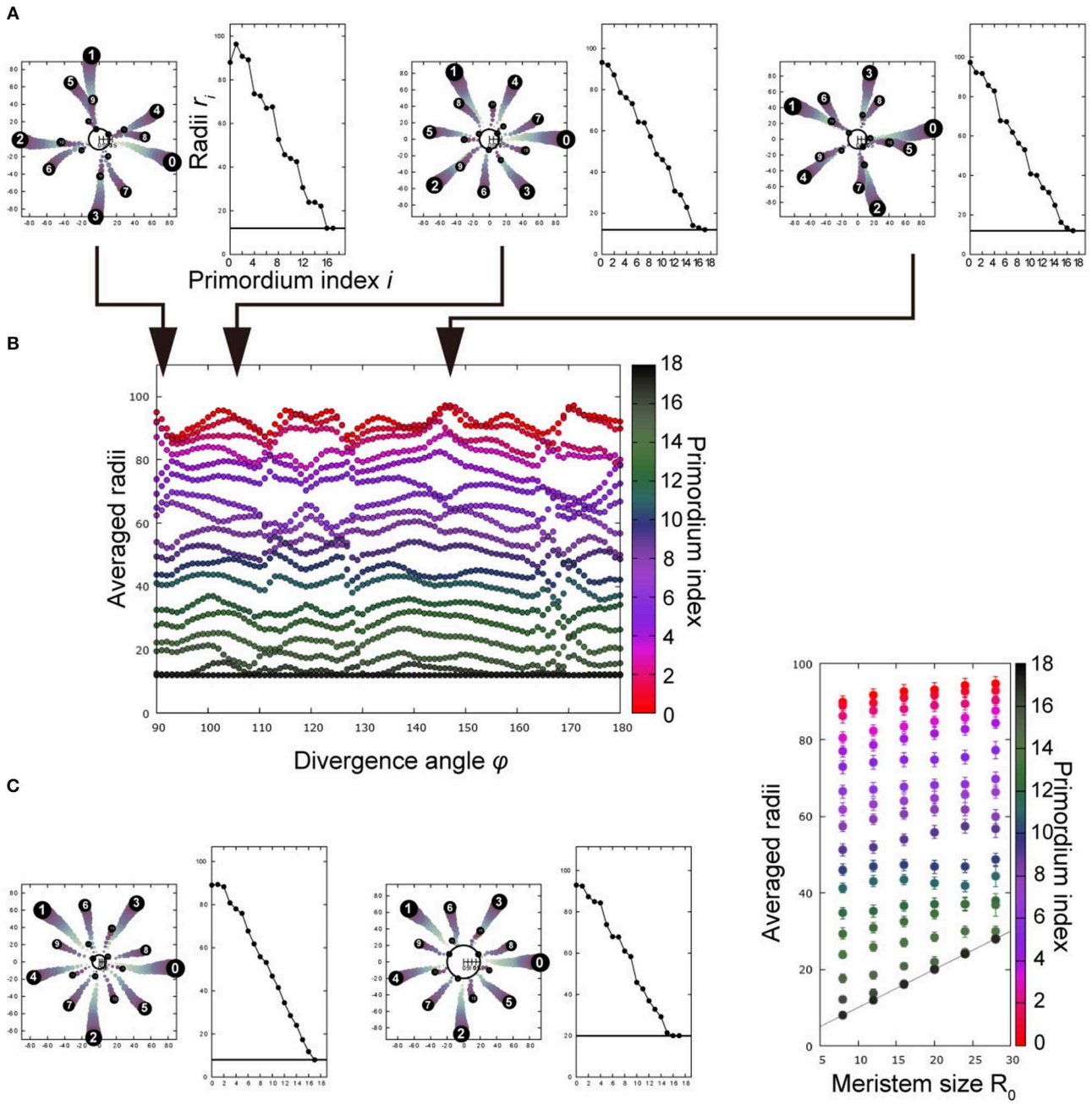

FIGURE 4 | Post-meristematic organ displacement after spiral initiation promotes radial symmetries of trimerous, tetramerous, and pentamerous whorls depending on divergence angles. **(A)** A representative result of Monte Carlo simulation, showing five trimerous whorls. The left panel shows the arrangement in a 2D plane whereas the right panel shows radial positions as a function of primordium indices, evidencing the trimerous whorls separated by radial gaps. $\phi = 91^\circ$ (left), 108° (middle), and 145° (right); $R_0 = 12.0$. **(B)** Radii as a function of ϕ. Radii of primordia were averaged over 200 replicates at the timing of the 18th primordium initiation, and a file was obtained for each ϕ. The color scale indicates the primordium index. The vertical space corresponds to the radial gap between whorls, and the number of primordia separated by the spaces corresponds to the merosity. $R_0 = 12.0$. **(C)** Dependence on the R_0 at $\phi = 136^\circ$. The merosity of the outermost whorl changed from trimery (left, $R_0 = 8.0$) to pentamery (middle, $R_0 = 20.0$), as R_0 increased. The averaged radii are shown in the right panel as in **(B)**, where error bar denotes the standard deviation of 200 simulations.

Species- and Population-Specificity of the Constrained Aestivation

The relative frequencies of the double-whorled and spiral flowers varied across species. The double tetramerous whorls and spiral ranked first and second, respectively, in 8-tepaled flowers for *A.* × *hybrida* PP, *A. hepatica*, and *E. pinnatifida*, whereas these ranks in 8-tepaled flowers were the opposite for *A. flaccida, A. nikoensis*, and A. × *hybrida* W (**Figure 2E**). The relative

frequency distribution of tetramerous double-whorls was more than 40% for *A.* × *hybrida* PP, *A. hepatica,* and *E. pinnatifida*, 19% for *A.* × *hybrida* W, and 7% for *A. flaccida* and *A. nikoensis* (**Supplementary Table 2**). The trimerous double-whorl ranked first in 6-tepaled flowers for *A. flaccida, A. nikoensis, A.* × *hybrida* W, and *A. hepatica*, and second for *A.* × *hybrida* PP and *E. pinnatifida* (EAIEIA and EAIAEI ranked first, respectively, for the last two species; **Figure 2C**), in line with the results of a previous report (Kitazawa and Fujimoto, 2018). In addition, in several populations, the 6-tepaled aestivation exhibited a reproducible difference from the above-mentioned average of total populations. The trimerous double-whorl was first-ranked with more than 73% of the relative frequency in two populations of *E. pinnatifida* (HSB1 and HSB2 in **Supplementary Table 3**) and 27% on average in *E. pinnatifida* (**Supplementary Table 2**). Conversely, it ranked third with <3% of the frequency in a population of *A. nikoensis* (HSY1 in **Supplementary Table 3**), corresponding to an average 50% for this species.

A Spiral Phyllotaxis Model With a Constant Divergence Angle Reproduced the Trimerous, Tetramerous, and Pentamerous Whorls

The spiral phyllotaxis model with a constant divergence angle ϕ (section Mathematical Model) showed that the double trimerous whorls and the spirals observed for the 5-, 7-, 9-, and 11-tepaled flowers simultaneously occur at $90^\circ \leq \phi \leq 102.8^\circ$ and $135^\circ \leq \phi \leq 144^\circ$ angle ranges (**Figure 3**). The aestivations for the 4-, 8-, and 10-tepaled arrangements in nature were reproduced depending on these angular regions in the model; the dimerous double-whorl, spiral (EAIEAIEI), and pentamerous double-whorl appeared at the $135^\circ \leq \phi \leq 144^\circ$ angle range in the model, whereas the spiral (EAAI), tetramerous double-whorl, and spiral (EAIEAIEIEI) appeared at the $90^\circ \leq \phi \leq 102.8^\circ$ angle range (**Figure 3** and **Supplementary Table 1**). The aestivations of 8-tepaled flowers at the $135^\circ \leq \phi \leq 144^\circ$ angle range (i.e., spiral) ranked first in *A. nikoensis, A. flaccida,* and *A.* × *hybrida* W, whereas the double tetramerous whorls at the $90^\circ \leq \phi \leq 102.8^\circ$ angle range appeared most frequently in *A.* × *hybrida* PP, *A. hepatica*, and *E. pinnatifida.* The aestivations of 10-tepaled flowers at the $135^\circ \leq \phi \leq 144^\circ$ and $90^\circ \leq \phi \leq 102.8^\circ$ angle ranges were first- and second-ranked in all the species and forms we observed (**Figure 2G** and **Supplementary Table 1**). Therefore, the spiral phyllotaxis model with constant divergence angles at the $90^\circ \leq \phi \leq 102.8^\circ$ and $135^\circ \leq \phi \leq 144^\circ$ ranges accounted for most aestivations observed in nature (9 of 14 aestivations with relative frequency above 10% in at least one species and form; **Supplementary Table 1**), whereas the aestivations that appeared in the other angular regions of the model are hardly observed in nature (3% at most, highlighted in cyan in **Supplementary Table 1**).

The Spiral Model With Post-meristematic Organ Displacement Promotes Multiple Whorls

We theoretically examined whether spiral initiation with a fixed divergence angle ϕ results in an arrangement with multiple whorls, incorporating the post-meristematic interaction among floral organ primordia (Kitazawa and Fujimoto, 2015; section Mathematical Model). Post-meristematic interaction caused radial displacement of organ primordia, separating outer and inner whorls, where the radial distance of each primordium from the meristem center primordia became almost equal within each whorl. The subsequent primordia were arranged following the whorled phyllotaxis, thereby resulting in more than two whorls (**Figure 4A**). The merosity of whorls was tetramerous near $\phi = 90^\circ$ and pentamerous near $\phi = 144^\circ$ upon initiation (**Figure 4A** left and right; **Figure 4B**), consistent with the above model without post-meristematic interaction. The trimerous whorls stably appeared near $\phi = 120^\circ$ (**Figure 4A**, middle). Merosity can also be affected by another parameter, meristem diameter R_0. For example, when ϕ was 136°, the merosity changed from three to five as R_0 increased (**Figure 4C**, left and middle); when $\phi = 144^\circ$, the merosity of the outermost whorl remained five while R_0 remained in the same range. Therefore, the main parameter of merosity is the divergence angle as in the above model without post-meristematic interaction; around the marginal angles of the arrangements (e.g., $\phi = 136^\circ$ for pentamery, **Figure 4C**), the merosity became unstable and changed depending on R_0.

DISCUSSION

Perianth Phyllotaxis Polymorphism Provides an Evolutionary Scenario for Merosity Differentiation

Our field observations showed that, although *Anemone* and *Eranthis* tepal numbers and arrangements were highly variable, they were not random; rather, they were limited to double-whorled and spiral flowers (**Figure 2**). The spiral model with a constant divergence angle accounted for the observed coexistence of whorled and spiral arrangements, depending mainly on the divergence angle (**Figure 3**). The spiral organ initiation model incorporating the post-meristematic organ displacement further ensured that this double-whorled aestivation works as the template to subsequently form multiple whorls with the same merosity (i.e., trimery, tetramery, or pentamery; **Figure 4**). The debate on the evolution of ancestral flowers has treated whorled and spiral phyllotaxis as opposite hypotheses (Sauquet et al., 2017). The polymorphism of spirals and whorls within populations presented here provides an alternative scenario in which angiosperm floral bauplans evolutionarily diversified to trimerous, tetramerous, and pentamerous whorls. This scenario is further supported by the intraspecific coexistence of spiral and whorled phyllotaxis observed in several clades, including the stamens and carpels of *Anemone* (Schöffel, 1932; Ren et al., 2010) and *Magnolia* (Magnoliaceae; Zagórska-Marek, 1994) species. In addition, some of the tepal arrangement polymorphisms observed in double-whorls of dimery, trimery, and tetramery as well as in spirals (e.g., quincuncial, EAIEIEI; **Figure 2**) are commonly observed in *Aspidistra* (Figure 3 in Vislobokov et al., 2014) and *Cabomba* (Ørgaard, 1991; Rudall et al., 2009) species. To date, the coexistence of spiral and whorled tepal phyllotaxis have only been known among

species in neighboring clades; e.g., spiral in *M. stellata* with a divergence angle of nearly 137° and trimerous-whorled in *M. denudata* and *Liriodendron tulipifera* (Magnoliaceae) within the 120–137° divergence angle range (Kubitzki, 1987). The appearance of trimery at this angle range is consistent with the model with post-meristematic organ displacement (**Figure 4**). Additionally, in Nymphaeales, tepals appear to be tetramerous whorled as well (e.g., *Nymphaea* species; Schneider et al., 2003). Confirming the intraspecific coexistence of spirals and whorls in these clades as well as in *Nuphar* would indicate that such polymorphism is a possible ancestral state of angiosperm flowers.

Possible Developmental Origins of Organ Number and Aestivation Variations

To discuss the frequency of spirals and whorls that differs among species (**Figure 2**), we need to clarify the underlying developmental mechanism of organ number variation. The plausible mechanism of a stochastic increase in tepals is homeosis, where some stamen primordia transform into tepals (Kitazawa and Fujimoto, 2014) due to the fading border of fate determinants (Buzgo et al., 2005; Soltis et al., 2006; Wang et al., 2015). In the mathematical model with post-meristematic modification, the radius of a newer primordium can reach or exceed that of older primordia (**Figure 4**); thus, the newer primordium can assume the outer organ fate, even in an ideal model of concentric fate determination (Coen and Meyerowitz, 1991).

Differences in aestivations among species as well as populations (**Figure 2** and Supporting Table 3) suggest that underlying mechanisms exist genetically and/or geographically. They were mainly observed in the 6- or 8-tepaled flowers. Our present and previous theoretical studies provided two possible scenarios to explain those differences. The present scenario is that floral phyllotaxis is species-specifically biased. Most of the observed aestivations were produced from spiral phyllotaxis with constant divergence angle ranges of 135–144° and 90–102.8° (**Figure 3**). The representative angles of 137° and 99° have been reported in the floral phyllotaxis of a single species, e.g., *A. nemorosa* and *A. hepatica* (Schöffel, 1932) or in the magnollid *Drimys winteri* (Doust, 2001). Theoretically, angles of 137° and 99° are defined as the limits of the Fibonacci sequence ($x_{n+1}= x_n + x_{n-1}$, $x_1= 1$, $x_2= 2$; $\lim_{n\to\infty} 360° \; x_n/x_{n+1} = 137°$) and the Lucas sequence ($x_{n+1}= x_n + x_{n-1}$, $x_1= 1$, $x_2= 3$; $\lim_{n\to\infty} 360° \; x_n/x_{n+1} = 99°$), respectively (Bravais and Bravais, 1837a,b). In addition, these two divergence angles coexisted at a value of the fundamental parameter of spiral phyllotaxis, given by the logarithm of the plastochron ratio ∼0.1 (Douady and Couder, 1996). This value is further consistent with the floral meristem of *Anemone* species (e.g., Figures 7, 10 in Ren et al., 2010). Therefore, even in identical genetic and geographic backgrounds, both Fibonacci and Lucas spiral phyllotaxis can stably coexist showing the polyphenism, while different backgrounds are likely to occur in the *Anemone* spp. and *E. pinnatifida* tepal arrangement. The consistencies between model and nature patterns (sections A Spiral Phyllotaxis Model With a Constant Divergence Angle Reproduced the Trimerous, Tetramerous, and Pentamerous Whorls and The Spiral Model With Post-Meristematic Organ Displacement Promotes Multiple Whorls) suggest that the Fibonacci angle (137°) resulting pentamery is more frequent than the Lucas angle (99°) resulting tetramery in *A. nikoensis, A. flaccida,* and *A.* × *hybrida* W; the opposite is true for *A.* × *hybrida* PP, *A. hepatica*, and *E. pinnatifida.*

On the other hand, this constant divergence angle model cannot account for two aestivations in the 6-tepaled and one of 7-tepaled flowers (represented in light and dark gray, **Figures 2C,D**), which were explained by the other scenario. In the previous model, the divergence angle was variable among organs depending on an inhibitory field potential from preexisting primordia (Kitazawa and Fujimoto, 2016b, 2018); this is probably due to genetic, environmental, or developmental factors that affect phyllotactic parameters such as organ growth rate, as seen in *Arabidopsis thaliana* inflorescence phyllotaxis (Mirabet et al., 2012; Besnard et al., 2014; Refahi et al., 2016). The variable angle model included the constant angle model whereas the latter simply accounted for the coexisting whorls and spiral. Further analyses of the aestivations and angles in the above-mentioned clades would clarify which model is better to summarize the coexistence.

Future Implications of Our Models

The several observed aestivations that have not yet been explained by the constant angle model, were all bilateral (i.e., EAIA, EAIAEI, EAIEIA, and EAIEIEIA; represented in gray, **Figure 2A**). The first arrangement is also widely observed in members of Nymphaeaceae (Schneider et al., 2003; Hu et al., 2009) whereas the others, to our best knowledge, have only been reported in *Anemone* and *Eranthis* species. One possible cause for such bilaterally symmetric arrangements is the presence of certain structures around the flower, such as bracts (Endress, 1999; Ronse de Craene, 2007, 2018; Nakagawa and Fujimoto, 2020). In *Anemone* and *Eranthis* species, three to six bracts are arranged bilaterally. In addition, *A. hepatica* typically has three bracts and trimerous flowers; however, flowers with four bracts tend to have tetramerous double-whorled arrangements. It would also be interesting to study whether such outer structures bias to the 99° and 137° angles resulting in different merosities. Investigating its effect on the polymorphism of spiral and whorls may therefore elucidate the underlying mechanism of merosity diversification in angiosperm flowers.

DATA AVAILABILITY STATEMENT

All datasets generated for this study are included in the article/**Supplementary Material**.

AUTHOR CONTRIBUTIONS

KF contributed conception and design of the study and performed the field work. MK and KF performed the

mathematical modeling, wrote the manuscript, read, and approved the submitted version.

FUNDING

This work was supported by Grants-in-Aid for Scientific Research from Ministry of Education, Culture, Sports, Science, and Technology of Japan to KF (17H06386, and 16H06378).

ACKNOWLEDGMENTS

We thank the Kuwagata family, S. Maeda and K. Horibe for their support in field work.

SUPPLEMENTARY MATERIAL

The Supplementary Material for this article can be found online at: https://www.frontiersin.org/articles/10.3389/fevo.2020.00070/full#supplementary-material

REFERENCES

Adler, I., Barabé, D., and Jean, R. V. (1997). A history of the study of phyllotaxis. *Ann. Bot.* 80, 231–244. doi: 10.1006/anbo.1997.0422

Besnard, F., Refahi, Y., Morin, V., Marteaux, B., Brunoud, G., Chambrier, P., et al. (2014). Cytokinin signalling inhibitory fields provide robustness to phyllotaxis. *Nature* 505, 417–421. doi: 10.1038/nature12791

Bravais, L., and Bravais, A. (1837a). Essai sur la disposition des feuilles curviseriees. *Ann. Sci. Nat. Sec. Ser.* 7, 42–110.

Bravais, L., and Bravais, A. (1837b). Essai sur la disposition symmetrique des inflorescences. *Ann. Sci. Nat. Sec. Ser.* 8, 11–42.

Buzgo, M., Soltis, P., Kim, S., and Soltis, D. E. (2005). The making of the flower. *Biologist* 52, 149–154.

Coen, E. S., and Meyerowitz, E. M. (1991). The war of the whorls: genetic interactions controlling flower development. *Nature* 353, 31–37. doi: 10.1038/353031a0

Cunnell, G. J. (1958). Aestivation in *Ranunculus repens* L. *New Phytol.* 57, 340–352. doi: 10.1111/j.1469-8137.1958.tb05323.x

Damerval, C., and Nadot, S. (2007). Evolution of perianth and stamen characteristics with respect to floral symmetry in *Ranunculales*. *Ann. Bot.* 100, 631–640. doi: 10.1093/aob/mcm041

de-Paula, O. C., Assis, L. C., and de Craene, L. P. R. (2018). Unbuttoning the ancestral flower of angiosperms. *Trend. Plant Sci.* 23, 551–554. doi: 10.1016/j.tplants.2018.05.006

Douady, S., and Couder, Y., (1996). Phyllotaxis as a dynamical self organizing process part I: The spiral modes resulting from time-periodic iterations. *J. Theor. Biol.*178, 255–273. doi: 10.1006/jtbi.1996.0024

Doust, A. N. (2001). The developmental basis of floral variation in *Drimys winteri* (*Winteraceae*). *Int. J. Plant Sci.* 162, 697–717. doi: 10.1086/320790

Endress, P. K. (1999). Symmetry in flowers: diversity and evolution. *Int. J. Plant Sci.* 160, S3–S23. doi: 10.1086/314211

Endress, P. K. (2001b). The flowers in extant basal angiosperms and inferences on ancestral flowers. *Int. J. Plant Sci.* 162 1111–1140. doi: 10.1086/321919

Endress, P. K., (1987). Floral phyllotaxis and floral evolution. Bot. Jahrb. *Syst.* 108, 417–438.

Endress, P. K., (2001a). "Origins of flower morphology," in *The Character Concept in Evolutionary Biology*, ed G. P. Wagner (Academic Press), 493–510. Available online at: https://www.elsevier.com/books/the-character-concept-in-evolutionary-biology/wagner/978-0-12-730055-9

Endress, P. K., and Doyle, J. A. (2009). Reconstructing the ancestral angiosperm flower and its initial specializations. *Am. J. Bot.* 96, 22–66. doi: 10.3732/ajb.0800047

Foster, T., Johnston, R., and Seleznyova, A. (2003). A morphological and quantitative characterization of early floral development in apple (*Malus* × *domestica* Borkh.). *Ann. Bot.* 92, 199–206. doi: 10.1093/aob/mcg120

Hill, J. P., and Malmberg, R. L. (1996). Timing of morphological and histological development in premeiotic anthers of *Nicotiana Tabacum* cv. *Xanthi (Solanaceae). Am. J. Bot.* 83, 285–295. doi: 10.1002/j.1537-2197.1996.tb12709.x

Hu, G.-W., Lei, L.-G., Liu, K.-M., and Long, C.-L. (2009). Floral development in *Nymphaea tetragona* (*Nymphaeaceae*). *Bot. J. Linn. Soc.* 159, 211–221. doi: 10.1111/j.1095-8339.2008.00905.x

Kitazawa, M. S., and Fujimoto, K. (2014). A developmental basis for stochasticity in floral organ numbers. *Front. Plant Sci.* 5:545. doi: 10.3389/fpls.2014.00545

Kitazawa, M. S., and Fujimoto, K. (2015). A dynamical phyllotaxis model to determine floral organ number. *PLoS Comput. Biol.* 11:e1004145. doi: 10.1371/journal.pcbi.1004145

Kitazawa, M. S., and Fujimoto, K. (2016a). Relationship between the species-representative phenotype and intraspecific variation in *Ranunculaceae* floral organ and *Asteraceae* flower numbers. *Ann. Bot.* 117, 925–935. doi: 10.1093/aob/mcw034

Kitazawa, M. S., and Fujimoto, K. (2016b). Stochastic occurrence of trimery from pentamery in floral phyllotaxis of *Anemone* (*Ranunculaceae*). *Acta Soc. Bot. Pol.* 85, 1–10. doi: 10.5586/asbp.3530

Kitazawa, M. S., and Fujimoto, K. (2018). Spiral phyllotaxis underlies constrained variation in *Anemone* (*Ranunculaceae*) tepal arrangement. *J. Plant Res.* 131, 459–468. doi: 10.1007/s10265-018-1025-x

Kubitzki, K. (1987). Origin and significance of trimerous flowers. *Taxon* 36, 21–28. doi: 10.1002/j.1996-8175.1987.tb03919.x

Kwiatkowska, D. (1999). Formation of pseudowhorls in *Peperomia verticillata* (L.) A. *Dietr. shoots exhibiting various phyllotactic patterns. Ann. Bot.* 83, 675–685. doi: 10.1006/anbo.1999.0875

Lyndon, R. F. (1978). Phyllotaxis and the initiation of primordia during flower development in *Silene*. *Ann. Bot.* 42, 1349–1360. doi: 10.1093/oxfordjournals.aob.a085581

Mirabet, V., Besnard, F., Vernoux, T., and Boudaoud, A. (2012). Noise and robustness in phyllotaxis. *PLoS Comput. Biol.* 8:e1002389. doi: 10.1371/journal.pcbi.1002389

Morgan, A. P. (1874). Imbricative aestivation. *Am. Nat.* 8:705–713. doi: 10.1086/271416

Nakagawa, A., Kitazawa, M. S., and Fujimoto, K., (2020). A design principle for floral organ number and arrangement in flowers with bilateral symmetry. *Development* 147:dev182907. doi: 10.1242/dev.182907

Ørgaard, M. (1991). The genus Cabomba (*Cabombaceae*) - a taxonomic study. *Nord. J. Bot.* 11, 179–203. doi: 10.1111/j.1756-1051.1991.tb01819.x

Padgett, D. (2007). A monograph of *Nuphar* (*Nymphaeaceae*). *Rhodora* 109, 1–95. doi: 10.3119/0035-4902(2007)109[1:AMONN]2.0.CO;2

Refahi, Y., Brunoud, G., Farcot, E., Jean-Marie, A., Pulkkinen, M., Vernoux, T., et al. (2016). A stochastic multicellular model identifies biological watermarks from disorders in self-organized patterns of phyllotaxis. *Elife* 5:e14093. doi: 10.7554/eLife.14093

Ren, Y. I., Chang, H.-L., and Endress, P. K. (2010). Floral development in anemoneae (*Ranunculaceae*). *Bot. J. Linn. Soc.* 162, 77–100. doi: 10.1111/j.1095-8339.2009.01017.x

Ronse de Craene, L. P. (2007). Are petals sterile stamens or bracts? The origin and evolution of petals in the core eudicots. *Ann. Bot.* 100, 621–630. doi: 10.1093/aob/mcm076

Ronse de Craene, L. P. (2010). *Floral Diagrams: An Aid to Understanding Flower Morphology and Evolution*. Cambridge: Cambridge University Press.

Ronse de Craene, L. P. (2016). Meristic changes in flowering plants: how flowers play with numbers. *Flora* 221, 22–37. doi: 10.1016/j.flora.2015.08.005

Ronse de Craene, L. P. (2018). Understanding the role of floral development in the evolution of angiosperm flowers: clarifications from a historical and physico-dynamic perspective. *J. Plant Res.* 131, 367–393. doi: 10.1007/s10265-018-1021-1

Ronse de Craene, L. P., Soltis, P. S., and Soltis, D. E. (2003). Evolution of floral structures in basal angiosperms. *Int. J. Plant Sci.* 164, S329–S363. doi: 10.1086/377063

Ronse de Craene, L. P. R., and Smets, E. F. (1994). Merosity in flowers: definitions, origin and taxonomic significance. *Plant Syst. Evol.* 191, 83–104. doi: 10.1007/BF00985344

Rudall, P. J., Remizowa, M. V., Prenner, G., Prychid, C. J., Tuckett, R. E., and Sokoloff, D. D. (2009). Nonflowers near the base of extant angiosperms? *Spatiotemporal arrangement of organs in reproductive units of Hydatellaceae and its bearing on the origin of the flower. Am. J. Bot.* 96, 67–82. doi: 10.3732/ajb.0800027

Salisbury, E. J. (1919). Variation in *Eranthis hyemalis*, *Ficaria verna*, and other members of the *Ranunculaceae*, with special reference to trimery and the origin of the perianth. *Ann. Bot.* 33, 47–79. doi: 10.1093/oxfordjournals.aob.a089702

Sattler, R. (1973). *Organogenesis of Flowers: A Photographic Text Atlas.* Toronto, ON: University of Toronto Press.

Sauquet, H., von Balthazar, M., Magallón, S., Doyle, J. A., Endress, P. K., Bailes, E. J., et al. (2017). The ancestral flower of angiosperms and its early diversification. *Nat. Commun.* 8:16047. doi: 10.1038/ncomms16047

Schneider, E. L., Tucker, S. C., and Williamson, P. S. (2003). Floral development in the *Nymphaeales*. *Int. J. Plant Sci.* 164, S279–S292. doi: 10.1086/376883

Schöffel, K. (1932). Untersuchungen über den Blütenbau der Ranunculaceen. *Planta* 17, 315–371. doi: 10.1007/BF01909279

Schoute, J. C. (1935). On corolla aestivation and phyllotaxis of floral phyllomes. *Verh kon akad Wet Amsterdam Afd Natuurk* 34, 1–77.

Smyth, D. R. (2018). Evolution and genetic control of the floral ground plan. *New Phytol.* 220, 70–86. doi: 10.1111/nph.15282

Sokoloff, D. D., Remizowa, M. V., Bateman, R. M., and Rudall, P. J. (2018). Was the ancestral angiosperm flower whorled throughout? *Am. J. Bot.* 105, 5–15. doi: 10.1002/ajb2.1003

Soltis, P. S., Soltis, D. E., Kim, S., Chanderbali, A., and Buzgo, M. (2006). "Expression of floral regulators in basal angiosperms and the origin and evolution of ABC-function" in *Advances in Botanical Research 44: Developmental Genetics of the Flower*, eds D. E. Soltis, J. H. Leebens-Mack, and P. S. Soltis. (San Diego, CA: Elsevier), 483–506.

Vislobokov, N. A., Sokoloff, D. D., Degtjareva, G. V., Valiejo-Roman, C. M., Kuznetsov, A. N., and Nuraliev, M. S. (2014). Aspidistra paucitepala (Asparagaceae), a new species with occurrence of the lowest tepal number in flowers of Asparagales. *Phytotaxa.* 161, 270–282. doi: 10.11646/phytotaxa.161.4.2

Wang, P., Liao, H., Zhang, W., Yu, X., Zhang, R., Shan, H., et al., (2015). Flexibility in the structure of spiral flowers and its underlying mechanisms. *Nat. Plants* 2:15188. doi: 10.1038/nplants.2015.188

Warner, K. A., Rudall, P. J., and Frohlich, M. W. (2008). Differentiation of perianth organs in *Nymphaeales*. *Taxon* 57, 1096–1109. doi: 10.1002/tax.574006

Yule, G. U., (1902). Variation of the number of sepals in Anemone nemorosa. *Biometrika* 1, 307–308. doi: 10.2307/2331542

Zagórska-Marek, B. (1994). Phyllotaxic diversity in *Magnolia* flowers. *Acta Soc. Bot. Pol.* 63, 117–137. doi: 10.5586/asbp.1994.017

Conflict of Interest: The authors declare that the research was conducted in the absence of any commercial or financial relationships that could be construed as a potential conflict of interest.

frontiers in Ecology and Evolution

REVIEW
published: 03 April 2020
doi: 10.3389/fevo.2020.00089

Same Actor in Different Stages: Genes in Shoot Apical Meristem Maintenance and Floral Meristem Determinacy in Arabidopsis

Wenwen Chang[1,2†], Yinghui Guo[1,2†], Hao Zhang[1,3], Xigang Liu[2,4] and Lin Guo[1*]*

[1] Key Laboratory of Agricultural Water Resources, Hebei Laboratory of Agricultural Water-Saving, Center for Agricultural Resources Research, Institute of Genetics and Developmental Biology, Chinese Academy of Sciences, Shijiazhuang, China, [2] College of Advanced Agricultural Sciences, University of Chinese Academy of Sciences, Beijing, China, [3] College of Life Sciences, Hebei Agricultural University, Baoding, China, [4] State Key Laboratory of Plant Cell and Chromosome Engineering, Center for Agricultural Resources Research, Institute of Genetics and Developmental Biology, The Innovative Academy of Seed Design, Chinese Academy of Sciences, Shijiazhuang, China

OPEN ACCESS

Edited by:
Annette Becker, University of Giessen, Germany

Reviewed by:
Toshiro Ito, Nara Institute of Science and Technology (NAIST), Japan
Benoit Landrein, UMR5667 Reproduction et Developpement des Plantes (RDP), France
Harley M. Smith, Agriculture and Food, Commonwealth Scientific and Industrial Research Organisation (CSIRO), Australia

***Correspondence:**
Xigang Liu
xgliu@sjziam.ac.cn
Lin Guo
guolin@sjziam.ac.cn

[†] These authors have contributed equally to this work

Specialty section:
This article was submitted to Evolutionary Developmental Biology, a section of the journal Frontiers in Ecology and Evolution

Received: *03 December 2019*
Accepted: *18 March 2020*
Published: *03 April 2020*

Citation:
Chang W, Guo Y, Zhang H, Liu X and Guo L (2020) Same Actor in Different Stages: Genes in Shoot Apical Meristem Maintenance and Floral Meristem Determinacy in Arabidopsis. Front. Ecol. Evol. 8:89. doi: 10.3389/fevo.2020.00089

Plant meristems are responsible for producing all post-embryonic organs during organogenesis. While the shoot apical meristem (SAM) maintains its meristematic property throughout the life of a plant, the floral meristem (FM) undergoes precise processes of initiation, maintenance and termination to ensure proper reproductive development and metagenesis. Plant meristem maintenance and termination are controlled by hierarchical genetic networks. While most of the genes in these networks have specific roles in particular processes, some genes have dual roles in SAM maintenance and FM termination through their interactions with different partners. Here, we summarize the molecular mechanisms of these dual-function regulators important for both SAM maintenance and FM termination and discuss the functions of WOX genes mediated gene regulatory networks on meristem maintenance and termination in different species.

Keywords: SAM maintenance, FM determinacy, miRNAs, AGO1/10, ARF3, AP2, FHY3, STM

SHOOT APICAL MERISTEM AND FLORAL MERISTEM

Whereas animals complete the majority of organogenesis and body plan formation during embryogenesis, plants establish the shoot apical meristem (SAM) and root apical meristem (RAM) in the mature embryo (Jürgens, 2001; Lau et al., 2012; Bishopp and Bennett, 2014). During post-embryonic development, the RAM establishes the entire root system, and the SAM gives rise to the above-ground structures, such as leaves, stems and flowers (Miwa et al., 2009; Kaufmann et al., 2010; Satbhai et al., 2015). After the transition from vegetative development to reproductive development, the floral meristems (FMs) are produced in the axils of cryptic bracts at the flanking regions of SAM that is also called Inflorescence Meristem (IM) after floral transition (**Figures 1A–C**; Chandler, 2012). Therefore, the FM, IM and other secondary meristm such as axillary meristems (AMs) are three types of SAM. Subsequently, FMs generate all of the floral organs, such as sepals, petals, stamens and carpels in Arabidopsis (**Figure 1D**). Plant meristems consist of groups of undifferentiated cells that continually initiate new organ primordia, and these undifferentiated cells

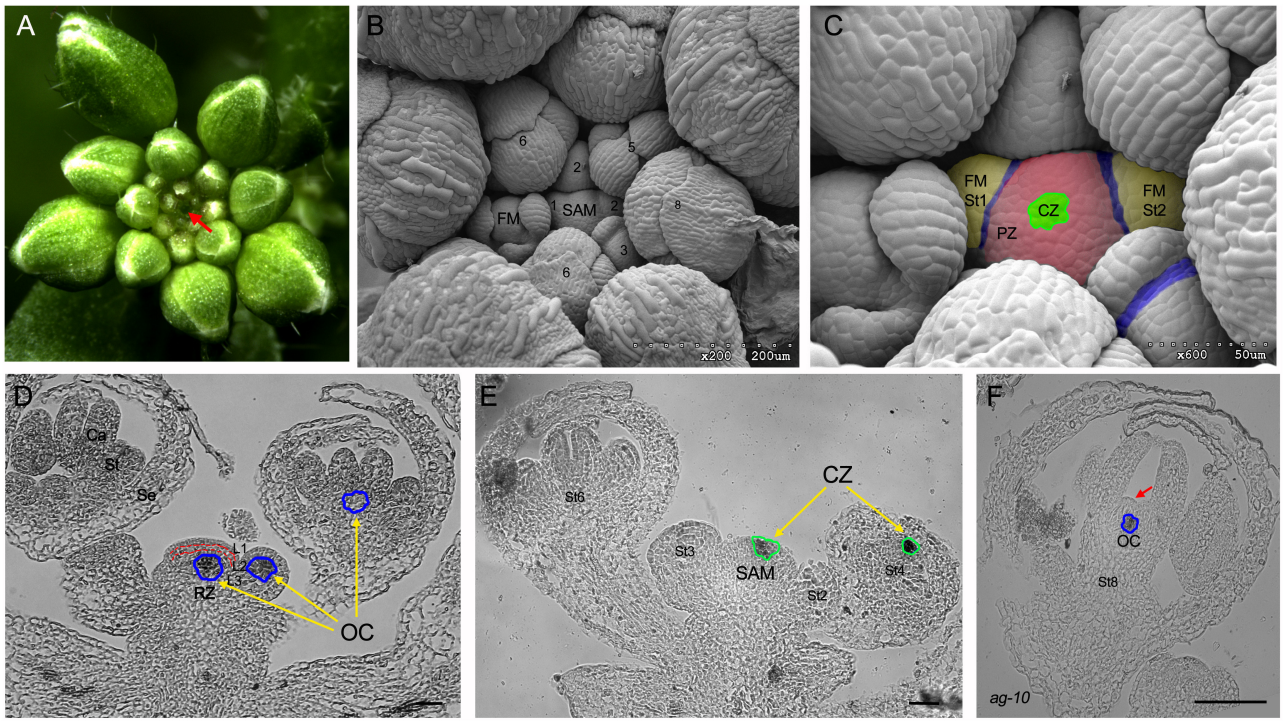

FIGURE 1 | The shoot apical meristem (SAM) and floral meristems (FM) of Arabidopsis. **(A)** Top view of the inflorescence. The SAM is localized at the center and marked by a red arrow. **(B,C)** Overhead view of the SAM and FM. Numbers indicate the developmental stage of flower (Smyth et al., 1990). The central zone (CZ) and peripheral zone (PZ) are labeled by green and magenta color, respectively. The FMs are labeled by pale yellow color. The meristem–organ boundaries are marked in blue. **(D,E)** The longitudinal sections of SAM and FM. The organizing center (OC), in which the *WUS* is expressed, is marked by the blue cycles. The CZ that is marked by the expression of *CLV3* detected by *in situ* hybridization is labeled by green circles. RZ, rib zone; L1, L1 cell layer; L2, L2 cell layer; Se, sepal; St, stamen; Ca, carpel. **(F)** *In situ* assay to show prolonged *WUS* expression (marked by blue circle) in one indeterminate floral bud at stage 8 of *ag-10*, a weak *agamous* allele, and the indeterminate meristem is marked by a red arrow. **(D–F)** Scale bar = 50 μm.

are produced from the limited number of stem cells within the meristem (Groß-Hardt and Laux, 2003; Laux, 2003; Sozzani and Iyer-Pascuzzi, 2014).

The SAM and FM of the model plant Arabidopsis (**Figure 1A**) have similar dome-like structure characterized by the typical tunica/corpus structure found in angiosperms (**Figures 1B–E**). The outer tunica consists of two single cell layers, the epidermal cells (L1) and subepidermal cells (L2), which divide anticlinally to the surface of the meristem; the inner corpus layer is a cluster of cells without clearly oriented divisions (**Figure 1D**; Carles and Fletcher, 2003). From the center outward, the tunica is divided into the central zone (CZ), which harbors a group of stem cells expressing the stem cell marker gene *CLAVATA3* (*CLV3*) (Laux, 2003), and the peripheral zone (PZ), where the descendants of stem cells are displaced and recruited to generate new lateral organ primorida or FMs (**Figure 1E**). Stem cells are a group of pluripotent undifferentiated cells with two distinct capabilities: maintenance through self-renewal and the steady production of precursor cells to form differentiated tissues (Laux, 2003). The CZ is sustained by the underlying organizing center (OC), a part of the rib zone (RZ) underneath the CZ (Mayer et al., 1998; Alvarez-Buylla et al., 2010). The OC cells are characterized by *WUSCHEL* (*WUS*) gene expression (**Figure 1D**).

During development, successful initiation of lateral organ primordia, in which cells are differentiated into specific cell-type of distinct organ like leaf or flower, requires the formation of meristem-to-organ boundary zone to separate the newly formed entity from the rest of plan body (Aida and Tasaka, 2006). The boundary zone is morphologically visible as concave groove with a saddle-shaped surface due to the local growth repression (**Figure 1C**). Cells in the boundary have distinctive property compared to the surrounding cells with reduced rates of cell division, elongated shapes, and unique gene expression program (Breuil-Broyer et al., 2004; Zadnikova and Simon, 2014). Null mutants of boundary-specific genes often display organ fusion, but also impaired organ development and phyllotaxis patterning, indicating that the boundary zone acts as organizing center to control adjacent organ development (Laufs et al., 2004; Zadnikova and Simon, 2014; Wang et al., 2016). Therefore, the dynamic maintenance of meristem depends on the balance between meristem self-renewal and lateral organ formation.

In Arabidopsis, IM, a type of SAM, is indeterminate with its ability to generate new organ throughout the life of a plant, while FM, another type of SAM, undergoes precise processes of initiation, maintenance and termination to ensure proper reproductive development and metagenesis (Sablowski, 2007). During the lifecycle, once a certain number of fruits

are produced, all meristem activity arrests coordinately (termed global proliferative arrest, or GPA) to promote subsequent fruit filling and plant death. Studies showed that both signals from seeds/flowers and the age pathway regulate the GPA of SAM (Hensel et al., 1994; Wuest et al., 2016; Balanzà et al., 2018). After floral transition, the FMs are produced and specified from the flanking of IM under the control of cascaded gene regulatory networks (GRNs) mediated by the FM identity genes, *LEAFY* (*LFY*) and *APETALA1* (*AP1*) (Liu C. et al., 2009; Liu et al., 2013; Chandler, 2012). Subsequently, the FM identity genes, *LFY* and *AP1*, induce the expression of floral organ identity genes that act in a combinatorial manner, termed ABC model, to control floral organ specification at differently developmental stages (Smyth et al., 1990; Coen and Meyerowitz, 1991; Weigel and Meyerowitz, 1994). Briefly, A class genes specify sepals, and A together with B class genes specify petals, while B and C class genes act together leading to stamen development, and C function alone controls carpel formation. In addition, A and C class genes act in an antagonistic manner (Coen and Meyerowitz, 1991). At last, the formation of the innermost carpel primordia is followed by the genetically programmed termination of FMs, termed floral determinacy: it ensures the production of a fixed number of floral organs and subsequent gametogenesis.

Prolonged or enhanced FM activity results in an increased number of floral organs, increased whorls and even extra organs borne on supernumerary whorls due to prolonged stem cell activity (Lenhard et al., 2001; Prunet et al., 2009; Sun et al., 2009; Liu et al., 2011; **Figure 1F**). Genetic analysis showed that the termination of FM is not simple via the differentiation meristem cells into carpel cells since the mutants with 4th whorl carpels are still indeterminate with additional tissue growing inside (Sun et al., 2009; Ji et al., 2011; Liu et al., 2011). Moreover, unlike the GPA of SAM, the temporally precise regulation of the FM ensures that it is terminated at a particular developmental stage (e.g., stage 6 in Arabidopsis) under the control of complex GRNs (Cao et al., 2015; Xu et al., 2019). Therefore, the SAM maintenance and FM determinacy are two distinctly developmental processes.

GENETIC REGULATION OF SAM MAINTENANCE AND FM DETERMINACY

Using forward genetics approaches, researchers have characterized numerous genes that are components of the regulatory networks that maintain SAM activity or terminate FM activity (Cao et al., 2015; Gaillochet and Lohmann, 2015; Soyars et al., 2016; Lee et al., 2019). Since meristems rely on stem cells as their source, FM have similar mechanisms to maintain the stem cell pool as other types of SAM. Similar to animal stem cells, plant stem cells are maintained by stem cell niches (Sablowski, 2004; Zheng and Liu, 2019). *WUS* encodes a homeodomain-containing transcription factor (TF) that is essential for the stem cells maintenance (Mayer et al., 1998; **Figure 1D**). In the *wus* mutant, the SAM fails to properly generate leaf primordia, and the FM is depleted before the production of carpel primordia, due to the rapid consumption of the stem cells contained therein (Laux et al., 1996). In contrast, ectopic *WUS* expression can endow somatic cells with stem cell properties (Zuo et al., 2002; Gallois et al., 2004; Xu et al., 2005). These findings demonstrate that *WUS* is critical for the establishment and maintenance of meristems. Further mechanistic analysis uncovered that WUS moves to the overlying stem cells in the CZ to directly induce *CLV3*, which encodes a secreted peptide (Yadav et al., 2011; Daum et al., 2014; **Figure 1E**). CLV3 subsequently binds to the plasma membrane-localized CLV1 or CLV2/CORYNE(CRN) receptor complex to inhibit *WUS* expression (Soyars et al., 2016). Thus, the *WUS*/*CLV3* negative feedback loop fine-tunes the stem cell pool of the SAM and FM.

Dynamic SAM maintenance is determined by the rates of stem cell proliferation and organ primordia formation. The boundary cells express a set of distinctive TFs that play important roles to locally repress cell proliferation and cell division through crosstalk with the meristem genes and organ primordia specific genes (Heisler and Ohno, 2014; Zadnikova and Simon, 2014). To date, numbers of meristem-to-organ boundary-specific regulators are well studied including NAC family TFs such as CUP-SHAPED COTYLEDON1/2/3 (CUC1/2/3), MYC-domain TFs such as LATERAL ORGAN FUSION1/2 (LOF1/2), and LATERAL ORGAN BOUNDARIES DOMAIN (LBD) family TFs such as JAGGED LATERAL ORGANS (JLO) and LATERAL ORGAN BOUNDARIES (LOB) (Wang et al., 2016). They modulate the boundary establishment as well as organ primordia specification and meristem maintenance through genetic interaction with meristem-specific genes such as *SHOOT MERISTEMLESS* (*STM*) and *WUS*, and organ primordial-specific genes like *ASYMMETRIC LEAVES1/2* (*AS1/2*) and *TEOSINTE BRANCHED1/CYCLOIDEA/PCF1* (*TCP*) genes (Zadnikova and Simon, 2014). However, the molecular mechanisms by which these regulators control cell proliferation and differentiation in the boundaries are still not understood.

At the early stages of flower development, the maintenance and termination of FM activity are highly coordinated with the formation and specification of floral organ to ensure the successful flower development (Smyth et al., 1990; Alvarez-Buylla et al., 2010). Spatially expanded FM activity associated with an increased stem cell population leads to the production of extra floral organs. Temporally enhanced FM activity due to prolonged stem cell maintenance, known as FM indeterminacy, gives rise to supernumerary whorls with extra organs (Prunet et al., 2009; **Figure 1F**). The *WUS/CLV* feedback loop maintain the FM similarly to the way they maintain the SAM, but the regulatory loop alone is incompetent to precisely terminate the FM. AGAMOUS (AG), a C-class MADS domain-containing TF, is a central positive regulator of FM determinacy. The null *ag* mutant displays a flower-in-flower phenotype: the entire fourth whorl of the primary flower is replaced by a new flower bud that in turn produces a new abnormal flower due to the continuous maintenance of stem cells in the FM center (Bowman et al., 1989, 1991; Lenhard et al., 2001). This demonstrated that *AG* has dual-function in the flower development: floral organ (stamen and carpal) identity and FM termination. At stage 3 of floral development (Smyth et al., 1990), *AG* expression is induced by WUS and LFY at the center of the FM, and *WUS* expression is turned off at stage 6, resulting in FM determinacy

(Lohmann et al., 2001). AG indirectly represses *WUS* expression through *KNUCKLES* (Sun et al., 2009, 2019), and AG also directly represses *WUS* through the TERMINAL FLOWER2 (TFL2)-AG complex that triggers chromatin loop formation at the *WUS* locus (Liu et al., 2011; Guo et al., 2018). As a central hub in this network, AG is regulated by numerous factors at the transcriptional, post-transcriptional and protein level through genetic and epigenetic mechanisms (Cao et al., 2015; Xu et al., 2019).

To date, many genes have been characterized in terms of their functions in either SAM maintenance or FM determinacy, while other genes have dual roles in both processes through their genetic interactions with different partners. The following section summarizes recent findings on these dual-function genes with different roles in SAM maintenance and FM determinacy.

INDIVIDUAL FACTORS INVOLVED IN BOTH SAM MAINTENANCE AND FM DETERMINACY

MicroRNA172 (miR172) – APETALA2 (AP2) Module

MicroRNAs (miRNAs) are a class of endogenous 20–24 nt non-coding RNAs. They are encoded by miRNA genes (*MIR*) and processed by DICER-LIKE (DCL) RNase III endonucleases (Margis et al., 2006; Nozawa et al., 2012). Through complementary base pairing, miRNAs guide post-transcriptional regulation of their targets, by either transcript cleavage or translational inhibition, and many of these targets are TFs (D'Ario et al., 2017; Yu et al., 2017b; Liu et al., 2018). Accordingly, miRNAs play dominant roles in plant development and growth. The five *MIR172* genes in Arabidopsis produce three unique mature miR172 species that accumulate in different organs during plant development. When plants are transferred from short-day to long-day to induce flowering, miR172 abundance increases in the SAM (Wollmann et al., 2010), where SQUAMOSA PROMOTER BINDING PROTEIN-LIKE (SPL) proteins, the targets of miR156, promote the expression of miR172 (Wu et al., 2009). In turn, miR172 represses a family of AP2-like TFs, including APETALA2 (AP2), TARGET OF EAT 1 (TOE1), TOE2, TOE3, SCHLAFMÜTZE (SMZ), and SCHNARCHZAPFEN (SNZ), to regulate phase transitions and SAM activity (Aukerman and Sakai, 2003; Chen, 2004; Mathieu et al., 2009). It was well studied that the miR156/*SPL*s module controls the juvenile-to-adult transition by fine-tuning the miR172/*AP2* module (Wang et al., 2009; Wu et al., 2009). At the same time, AP2 directly binds to individual *MIR156* and *MIR172* loci to promote *MIR156* expression and repress *MIR172* expression (Yant et al., 2010; **Figure 2A**). miR172 abundance is high during early floral development then gradually decreases from stage 3 onward. In these later stages, it is mainly detected in the fourth whorl, with the highest levels in the center of the FM, where it represses its target genes *AP2* and *TOE3* to maintain FM activity (Chen, 2004; Wollmann et al., 2010; Jung et al., 2014). Mutations in genes affecting miR172 biosynthesis or accumulation, such as *HUA ENHANCER 1* (*HEN1*) and *CARPEL FACTORY* (*CAF*), result in increased AP2 protein levels and loss of FM termination (Jacobsen et al., 1999; Chen et al., 2002). Additionally, a mutation in *POWERDRESS* (*PWR*) could enhance the weakly indeterminate *ag-10* allele. PWR promotes the expression of *MIR172a*, *b*, and *c*, but not *MIR172d* and *e*, while a mutation in mature miR172d could enhance the determinacy defects of *ag-10* in an AP2-dependent manner, showing that the transcriptional diversification of the *MIR172* family may make the floral determinacy regulatory network more robust (Yumul et al., 2013; **Figure 2B**).

AP2 has numerous roles in floral transition, floral organ patterning, stem cell maintenance and seed development (Bowman et al., 1989; Ohto et al., 2005; Wurschum et al., 2006; Yant et al., 2010). At vegetative stage, *AP2* is highly expressed in incipient leaf primordia, but its transcript levels are low in the SAM and the center of the FM after stage 2 (Wurschum et al., 2006; Wollmann et al., 2010). In early floral development, *AP2* transcripts are concentrated in the sepal and petal primordia and partially overlap with *MIR172* transcript in the third whorl. At later stages, *AP2* is abundant in the developing petals, stamen filaments and the gynoecium, consistent with its multiple roles in floral development (Wollmann et al., 2010).

The semi-dominant *I28* mutant, which harbors a dominant-negative *AP2* allele, exhibits reduced SAM size, premature termination of the SAM and differentiation of the stem cells as in the *wus* mutant. At the early seedling stage, *WUS* and *CLV3* expression are disrupted in the SAM of *I28*. Functional and genetic analysis revealed that *AP2* promotes SAM maintenance either by repressing CLVs signaling or by promoting *WUS* expression independently of the *AG* pathway (Wurschum et al., 2006). Meanwhile, a recent study showed that the MADS-box gene *FRUITFULL* (*FUL*) promotes meristem arrest through direct *AP2* repression. *ful* and *ap2-170,* in which the microRNA binding site of miR172 is mutated, have delayed coordinated arrest of all meristems, or GPA, that correlates with the repression of *WUS* expression. Induction of the miR172-resistant version of *AP2*, $AP2^{170}$, in arrested plants reactivated the SAM and normal flower development, highlighting the important role of *AP2* in SAM maintenance (Balanzà et al., 2018; **Figure 2A**). Since *AP2* is clearly expressed in the emerging leaf primordia but hard to be detected in the SAM, how AP2 regulate *WUS* expression is unclear. A possibility is that AP2 could regulate *WUS* expression non-cell-autonomously.

In the ABC model of flower development (Weigel and Meyerowitz, 1994), *AP2* functions as an A-class gene that acts antagonistically with *AG*, specifies the perianth organs and restricts *AG* expression to the inner two whorls (Drews et al., 1991). Specifically, AP2 directly binds to the second intron of *AG* to repress *AG* expression in the outer two whorls (Wollmann et al., 2010; Yant et al., 2010; Dinh et al., 2012). In the *ag* mutant, *AP2* does not expand to the center of the FM, and miR172 accumulation is unaffected, indicating that *AP2* is mainly regulated by miR172, however, another study showed that *AG* misexpression with the 35S promoter counteracted *AP2* in the outer two whorls (Zhao et al., 2007; Wollmann et al., 2010). Transgenic lines expressing miR172-resistant versions of *AP2* and *TOE3* were found to exhibit floral organ identity defects

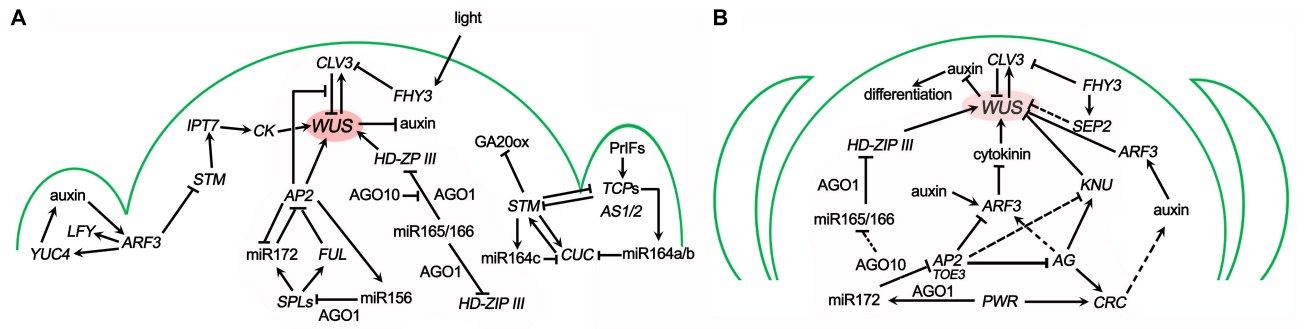

FIGURE 2 | Genetic pathways in the SAM maintenance **(A)** and FM determinacy **(B)**. The arrows represent the activation of gene expression, while the flat arrows represent its repression. The OC is shown in magenta. The genetic interactions are introduced in the text.

and severe FM indeterminacy phenotypes (Zhao et al., 2007; Jung et al., 2014). In addition, AP2 physically interacts with TOE3 *in vivo*, and it inhibits both *KNU* and *AG* expression to promote *WUS* expression and FM activity (Zhao et al., 2007; Yant et al., 2010; Huang et al., 2017). At the same time, AP2 also directly represses the expression of *AUXIN RESPONSE FACTOR3* (*ARF3*) to regulate *WUS* expression (see below) (Liu et al., 2014; **Figure 2B**).

ARGONAUTE1 (AGO1) AND ARGONAUTE10 (AGO10)

Through sequence complementarity with their target transcripts, mature miRNAs that are loaded into the RNA-induced silencing complex (RISC) direct the repression of their targets (Rogers and Chen, 2013). The PAZ and PIWI domain–containing AGO proteins are the central component of the RISC complex. miRNAs are sorted into different AGO proteins according to their 5′-nucleotide (Mi et al., 2008). Of the 10 AGO proteins in Arabidopsis, AGO1 is required for the functions of most miRNAs, and AGO1 deficiency results in pleiotropic developmental phenotypes (Bohmert et al., 1998; Vaucheret et al., 2004; Mallory and Vaucheret, 2010). AGO10, also known as ZWILLE (ZLL)/PINHEAD (PNH), is the closet paralog of AGO1 and is specifically required for SAM maintenance (Moussian et al., 1998; Vaucheret, 2008). While *AGO1* is ubiquitously expressed (Bohmert et al., 1998), *AGO10* expression is restricted to the provasculature underneath the SAM and the adaxial side of lateral organ primordia, where *AGO10* and *AGO1* have overlapping functions (Moussian et al., 1998; Lynn et al., 1999). While *ago1* mutants display pleiotropic defects of general plant architecture including single stem and rare axillary meristems (Bohmert et al., 1998), *ago10* seedlings have an empty apex, a pinhead-like structure or a solitary leaf, and these mutant phenotypes clearly indicate the importance of *AGO10* in SAM establishment and maintenance (Moussian et al., 1998; Tucker et al., 2008).

In the SAM, five class III homeodomain-leucine zipper (HD-ZIP III) TF genes are expressed: *PHABULOSA* (*PHB*), *PHAVOLUTA* (*PHV*), *REVOLUTA* (*REV*), *CORONA* (*CNA*), and *ATHB8*. These genes are targeted by miR165/166 and play important roles in organ polarity, SAM establishment and maintenance as well as FM termination. *rev phb* and *rev phb phv* mutants fail to establish a SAM and often produce single pin-like cotyledons, while gain-of-function *phb-D* and *rev-D* mutants have enlarged meristems (Talbert et al., 1995; Byrne, 2006). The transcripts of HD-ZIP III genes are targets of miR165/166 that is restricted to the abaxial side of organ primordia and excluded from the SAM (Liu Q. et al., 2009). miR165/166 overexpression dramatically reduces the transcript levels of all five *HD-ZIP III* genes, resulting in a range of phenotypes from an enlarged SAM to loss of the SAM (Jung and Park, 2007; Zhou et al., 2007). Thus, fine-tuning of the miR165/166–*HD-ZIP III* module by AGO1 and AGO10 is important for SAM maintenance. While miR165/166 are mainly loaded into AGO1 to repress *HD-ZIP III* gene expression and several genetic analyses showed that *AGO1* and *AGO10* have complementary functions in SAM maintenance (Tucker et al., 2008; Mallory et al., 2009), *AGO10* misexpression leads to increased levels of *HD-ZIP III* mRNAs that are degraded by AGO1 (Liu Q. et al., 2009). Subsequently, the detailed biochemical studies revealed that AGO10 binds miR165/6 with higher affinity than AGO1 and promotes miR165/6 degradation in its restricted expressing tissue (Yu et al., 2017a). Thus, acting as a decoy AGO1 protein, AGO10 competitively binds miR165/166 to protect the *HD-ZIP III* transcripts from post-transcriptional regulation, thereby maintaining SAM activity, in line with the predominant distribution patterns of AGO10 in the SAM (Zhu et al., 2011; Aichinger et al., 2012; Zhang and Zhang, 2012).

Genetic analysis showed that AGO10 activity in the FM contrasts its positive role in SAM maintenance. Mutations in *AGO1* and *AGO10* enhance the FM indeterminacy of *ag-10* indicate that *AGO1* and *AGO10* functional redundantly promote stem cell termination in the FM (Ji et al., 2011), and both AGO1 and AGO10 can bind miR172 and miR165/166 to regulate *AP2* and *HD-ZIP III* gene expression, respectively. While AGO1 mainly mediates the activities of miR165/166, AGO10 sequesters miR165/6 and represses its accumulation to fine-tune *HD-ZIP III* gene expression (Yu et al., 2017a). Correspondingly, reduced *HD-ZIP III* expression and increased *AP2* expression result in prolonged floral stem cell activity in the *ago10* mutant (Ji et al., 2011). The expression of HD-Zip III genes needs to be precisely

controlled to achieve successful FM determinacy since both of HD-ZIP III reduction by over-expression of miR165/166 and mis-expression of HD-Zip III overexpression by rendering them resistant to miR165/166 led to prolonged floral stem cell activity (Ji et al., 2011). Thus, both AGO1 and AGO10 are required for SAM establishment and maintenance as well as FM determinacy, with distinct roles in these processes (**Figure 2**).

SHOOT MERISTEMLESS (STM)

STM, a class-I KNOX gene, encodes a mobile TALE homeodomain TF that is essential for SAM establishment and maintenance (Long et al., 1996). Unlike *WUS*, *STM* is expressed throughout the SAM, where it suppresses cell differentiation, but is down-regulated in incipient organ primordial (Scofield et al., 2018). Loss-of-function *stm* mutants have compromised SAM formation and defective SAM organization, as evidenced by the fused cotyledon phenotype, due to the rapid consumption of the entire SAM (Clark et al., 1996; Endrizzi et al., 1996).

Ectopic expression of *STM* at leaf primordia suppresses cell differentiation and maintains the potential to form additional lateral outgrowths (Lenhard et al., 2002). Genetic analysis has revealed that ectopic expression of *STM* and *WUS* could trigger ectopic organogenesis, while they function in different pathway in meristem regulation (Byrne et al., 2002; Lenhard et al., 2002). Although the *stm* and *wus* mutants display similar developmental defects of SAM organization, the meristem arrest phenotypes of them differ from each other, in which meristematic cells are consumed into developing organs in *stm* mutants but are retained in a non-meristematic state in *wus* (Endrizzi et al., 1996; Laux et al., 1996), indicating that *STM* function is required to prevent meristematic cells from adopting organ-specific cell fates, whereas *WUS* is critical for the stem cell pool maintenance.

In the SAM, *STM* represses the expression of one target gene encoding GA20 oxidase (G20ox) enzyme that is required for phytohormone giberellic acid (GA) biosynthesis, to maintain low level of GA that stimulates growth by promote cell expansion. Exogenous GA treatment and constitutive GA signaling suppress *STM* gain-of-function phenotypes, whilst constitutive GA signaling mutant enhances the defects of weak *stm* mutants (Hay et al., 2002). At the same time, over-expression of cytokinin (CK), another phytohormone, biosynthetic *ISOPENTENYL TRANSFERASE* (*IPT*) genes and the exogenous application of CK can partially rescue the meristem defects of *stm* mutants, indicating that CK mediates the function of *STM* on meristem regulation. Further study showed that STM promotes *IPT7* expression to increase CK activity in SAM, which contributes to the homeostasis of CK and *WUS* expression (see below) (Leibfried et al., 2005; Yanai et al., 2005). Therefore, *STM* may functions on both SAM organization and stem cell maintenance.

At the boundary zone, *CUC1* is required for the boundary specification and restricted to express at boundary (Aida et al., 1999). STM binds and activates *CUC1* expression, and CUC1 can directly activate STM expression to comprise a direct positive-feedback loop, which is attenuated by STM-induced miR164c (Hibara et al., 2003; Spinelli et al., 2011; Scofield et al., 2018). In the regulatory interactions, the movement of STM is important for the meristem function and the correct expression patterns of *CUC1* and *CUC2* at the boundary zone (Lucas et al., 1995; Kim et al., 2003; Balkunde et al., 2017). In the organ primordia, primordium identity factors (PrIFs) specify primordium identity and promote expression of *TCP* family genes, which repress the expression of KNOX genes in primordia by direct interaction with primordium-specific AS1/AS2 complex and *CUC1* expression through miR164a/b, whilst STM represses *T* in the SAM (Byrne et al., 2002; Li et al., 2012; Scofield et al., 2018; **Figure 2A**). Therefore, the genetic interactions among these genes ensure the precise gene expression pattern and the boundary formation.

During flower development, STM is not expressed in FM founder cells or incipient FMs at the flanks of the SAM. However, *STM* is reactivated expression throughout the apical region of the FM proper but not in the basal domain that corresponds to the cryptic bract prior to floral patterning, shortly after the FM becomes distinct from the SAM, and then restricted to whorl 4 at late stages (Long and Barton, 2000). Ectopic expression of *STM* results in the formation of ectopic carpels, carpelloid organs and the conversion of ovules to carpels (Scofield et al., 2007). In the mild *stm-2* mutant, the SAM terminates in flowers that lack a central gynoecium (Clark et al., 1996; Scofield et al., 2007). These findings indicated that *STM* is required for whorl 4 and/or carpel development in FMs. Recent study showed that *STM* is also required for the FM competence. Genetic analysis has revealed that *STM* and *UNUSUAL FLORAL ORGANS* (*UFO*), but in depend of *AP1*, genetically interact to specify FM identity and initiate the floral program by regulation of flower identity genes (Roth et al., 2018). These findings demonstrated the multiple-functions of *STM* on organ identity and meristem activity.

AUXIN RESPONSE FACTOR3 (ARF3)

The phytohormone auxin and CK are critical for many plant growth and developmental processes including establishment, maintenance and termination of meristem (Schaller et al., 2015). Auxin is biosynthesized by *YUCCA* gene family and its signaling is mediated by two protein families: auxin response factors (ARFs) and Aux/IAA proteins, which induce global auxin response by regulate the expression of target genes (Reinhardt et al., 2000; Liscum and Reed, 2002; Cheng et al., 2006; Guilfoyle and Hagen, 2007; Vanneste and Friml, 2009). CK biosynthesis depends on the *IPT* gene family and *LONELY GUY* (*LOG*) gene family, respectively. After perceived by its receptors ARABIDOPSIS HISTIDINE KINASE2/3/4 (AHK2/3/4), CKs trigger the CK transcriptional response through B-type ARABIDOPSIS RESPONSEREGULATORs (ARRs) that are the TFs activated through phosphorylation by CK signaling, while A-types ARRs are negative regulators of CK signaling whose expression is induced by CK (Kieber and Schaller, 2014). In the SAM, auxin maxima are found at locations of primordia formation where it induces cellular differentiation and organ outgrowth, while CK maximum is

found at the OC to promote the proliferation of undifferentiated cells (Schaller et al., 2015). CK is required for the activation of *WUS* expression in an AHK2/AHK4-dependent manner, while WUS represses the expression of several A-type ARR genes, such as *ARR5/7/15*, resulting in increased CK activity in the OC (Leibfried et al., 2005; Gordon et al., 2009; Zhao et al., 2010). *ARF5*/*MONOPTEROS* (*MP*) mediates the crosstalk between auxin and CK signaling required for SAM maintenance. Specifically, auxin induces the expression of *ARF5/MP* to repress *ARR7/15* to fine tune CK activity and *WUS* expression (Zhao et al., 2010). Recent study showed that WUS, in turn, maintains low auxin signaling output in stem cells by reducing target genes expression through regulating the histone acetylation status of target loci (Ma et al., 2019). Thus, *WUS* keeps stem cell pool from auxin induced differentiation, while enhancing CK activity to sustain its expression.

ARF3, also known as ETTIN, is one of the 23 ARF family members in Arabidopsis (Guilfoyle and Hagen, 2007). *ARF3* has numerous roles in plant development, including gynoecium morphogenesis, *de novo* organ regeneration, organ polarity and FM determinacy (Sessions et al., 1997; Nemhauser et al., 2000; Cheng et al., 2013; Liu et al., 2014). During *de novo* organ regeneration, *ARF3* is highly expressed in the emerging SAM at early stage of SAM formation, but is ubiquitously expressed in the SAM at later stage of SAM formation, where *ARF3* mediates the auxin response and directly represses the expression of the CK biosynthesis gene *AtIPT5*. Mutations in *ARF3* lead to ectopic CK biosynthesis as well as disrupted stem cell initiation and meristem formation (Cheng et al., 2013). ARF3 protein is evenly distributed throughout the SAM and early FM, while *ARF3* mRNA is abaxially distributed in the SAM and floral organ primordia (Liu et al., 2014; Simonini et al., 2017). Thus, the dynamic ARF3 distribution is required for its function on SAM formation and maintenance. Genome-wide analysis revealed that ARF3 interacts with its partners in an auxin-dependent manner that determines its repressor or activator roles (Simonini et al., 2017). At the flanking regions of the SAM, ARF3 may directly activate the expression of *LFY* to specified floral primordium fate, and *YUC4* to induce auxin biosynthesis, and then promote cell differentiation (Schultz and Haughn, 1991; Cheng et al., 2006; Simonini et al., 2017). Simultaneously, ARF3 physically interacts with FIL to directly repress *STM* expression, and the resulting histone deacetylation promotes organogenesis (Chung et al., 2019). In addition, given that STM promote CK activity, *ARF3* could fine-tune CK activity in SAM (**Figure 2A**).

Unlike the even distribution pattern of ARF3 observed in the SAM, ARF3 is concentrated in the OC of the FM. It overlaps with *WUS* and the CK receptor gene *AHK4*, indicating different roles of *ARF3* in the FM and SAM (Liu et al., 2014). Genetic analysis showed that *ARF3* promotes FM determinacy by repressing *WUS* expression. In this context, *ARF3* is repressed by AP2 to mediate the functions of *AP2* and *AG* in FM maintenance and termination (Liu et al., 2014). Detailed analysis of the underlying molecular mechanism revealed that during early FM development (stages 3–5), AG transiently represses *ARF3* expression to de-repress the expression of *IPT3/5/7* and cell cycle genes, which helps to maintain FM activity. At later FM stages (stages 5–6), AG and auxin increase *ARF3* expression, while AP2 represses *ARF3* expression. ARF3 directly inhibits *IPT3/5/7* and *AHK4* expression and indirectly inhibits the expression of *LOG* genes. This regulation by ARF3 represses CK activity in the OC and ensures proper temporal termination of *WUS* expression (Zhang et al., 2018). Moreover, ARF3 can bind to the *WUS* promotor in an AG-dependent manner to fine-tune *WUS* expression (Liu et al., 2014; **Figure 2B**). Recent studies showed that fine-tuning of auxin homeostasis is required for the FM determinacy and gynoecium formation. Locally increased auxin production rescued the FM indeterminacy phenotype of *knu crc* (*crabs claw*), which is supposed to be mediated by *ARF3* (Yamaguchi et al., 2017, 2018).

FAR-RED ELONGATED HYPOCOTYL3 (*FHY3*)

Coordination of internal developmental cues, nutrients, hormones, and external environmental signals is important for the meristem maintenance and organogenesis in shoots and roots (Li et al., 2017). Light is one of the most important environmental signals for plant development and growth (Arsovski et al., 2012). In addition, light activates photosynthesis to provide energy by sucrose production. Recent studies found that Glucose energy signaling is essential to activate SAM and RM activity through activating target of rapamycin (TOR) kinase, while light induces auxin synthesis to promote SAM activity (Pfeiffer et al., 2016; Li et al., 2017).

At same time, plants have evolved a family of photoreceptors to perceive the light signal. Phytochrome A (phyA) is a key member with both specific and shared functions (Li et al., 2011). Light exposure triggers the transformation of phyA from the inactive Pr form to the active Pfr form, and it translocates into the nucleus with the help of FAR-RED ELONGATED HYPOCOTYL1 (FHY1) and its homolog FHY1-LIKE (FHL) (Casal et al., 2014). In Arabidopsis, FAR-RED ELONGATED HYPOCOTYLS3 (FHY3) directly actives the expression of *FHY1* and *FHL* to promote phyA signaling (Lin et al., 2007). Additionally, *FHY3* plays diverse roles in different plant developmental and physiological processes, such as circadian signaling, chloroplast biogenesis, chlorophyll biosynthesis and programmed cell death (Wang and Wang, 2015). Genome-wide gene expression profiling showed that under far-red (FR) light conditions, FHY3 mainly acts as a transcriptional activator to promote photomorphogenesis during the vegetative stage (Ouyang et al., 2011), but it acts primarily as transcriptional repressor in flower development (Li et al., 2016).

A genetic analysis uncovered the dual roles of *FHY3* in SAM maintenance and FM determinacy (Li et al., 2016). Specifically, a mutation in *FHY3* led to a smaller SAM size, and *fhy3* enhanced the indeterminacy of *ag-10*, a weak *ag* allele. Additionally, *wus* was found to be epistatic to *fhy3*. Molecular analysis revealed that FHY3 directly represses *CLV3* expression to regulate *WUS* expression in the SAM. When seedlings transition from dark to light conditions, *CLV3* expression decreases in WT plants but not in the *fhy3* and *phyA* mutants, indicating that *FHY3*

mediates the repressive effect of light on *CLV3* expression (Li et al., 2016). The de-repressed expression of *CLV3* in the *fhy3* mutant results in reduced *WUS* expression and a small SAM size. On the other hand, during flower development, FHY3 directly actives *SEPALLATA1* (*SEP1*) and *SEP2* expression, in parallel to the *FHY3-CLV3* pathway, to repress *WUS* expression and to promote FM determinacy (Li et al., 2016; **Figure 2**).

CONCLUSION AND FUTURE PERSPECTIVES

All postembryonic organs in plants develop from the stem cells that reside in the meristems. A key similarity between animal and plant stem cells is that the stem cell niche is critical for the maintenance of their activity (Heidstra and Sabatini, 2014; Zheng and Liu, 2019). The WUS homeobox (HB) TF belongs to the plant-specific WUS homeobox (WOX) protein family, one of a number of plant HB TF families that are characterized by the presence of a homeodomain. More broadly, this DNA-binding domain is important for developmental decisions in eukaryotes (van der Graaff et al., 2009). Phylogenetic and functional analyses have shown that *WOX* genes are conserved in euphyllophytes with distinct functions in a wide range of processes, particularly in the establishment, maintenance and termination of different types of meristems (Dodsworth, 2009; van der Graaff et al., 2009; Zhang et al., 2010; Costanzo et al., 2014; Liu and Xu, 2018). *WUS* homologs with conserved functions among angiosperms act in diverse and intricate regulatory networks (Dodsworth, 2009) in which some key players have dual roles in SAM maintenance and FM termination through their interactions with different partners (this review). However, there are many unanswered questions about how *WOX* members have come to function in diverse developmental processes over the course of evolution.

Poaceae (also called grasses) is one of the largest families of angiosperms containing many agriculturally important crops, such as rice, wheat, barley and maize (Grass Phylogeny Working Group et al., 2001). All grasses have a complex inflorescence composed of one, a few, or many spikelets produced by different type meristems. The IM of Arabidopsis is indeterminate and form two types meristems: indeterminate branch meristem and determinate FM. While the IM of wheat is determinate but the IMs of rice and maize are indeterminate, they produce determinate FMs (Zhang and Yuan, 2014). Therefore, the *WOX* genes mediated GRNs that are composed of homologs of key players in different species have distinct functions on meristem maintenance and FM determinacy through different molecular mechanisms. Phylogenetic analysis indicated, for example, that *FHY3*-like genes, encoding Mutator-like transposase-derived TFs, are widespread in angiosperms but not in other organisms (Lin et al., 2007), indicating that *FHY3* is probably linked to the adaptive evolution of phyA (Mathews et al., 2003). Interestingly, although close orthologs of *FHY3* are widespread in dicots, they are missing in monocot genomes (Lin et al., 2007). Thus, moving forward, comparative analyses of the functions of meristem-related genes in diverse plant species, particularly genes involved in SAM establishment and maintenance as well as FM determinacy, will be critical for an improved understanding of meristem evolution and conductive to agricultural production.

AUTHOR CONTRIBUTIONS

WC and YG contributed equally to the composition of the manuscript. XL and LG contributed equally to the conceptualization of the manuscript. HZ prepared the manuscript figures.

FUNDING

This work was supported by National Key Special Programs for Breeding from the Ministry of Science and Technology (2016YFD0100401); the National Science Foundation of China (NSFC) (31970824); the Guangdong Provincial Key Laboratory for Plant Epigenetics (College of Life Sciences and Oceanography, Shenzhen University); and the State Key Laboratory of Plant Cell and Chromosome Engineering (PCCE-KF-2018-04).

ACKNOWLEDGMENTS

We thank Rae Eden Yumul for valuable advice and language editing. We apologize to those authors whose work could not be cited due to space limitations.

REFERENCES

Aichinger, E., Kornet, N., Friedrich, T., and Laux, T. (2012). Plant stem cell niches. *Annu. Rev. Plant Biol.* 63, 615–636. doi: 10.1146/annurev-arplant-042811-105555

Aida, M., Ishida, T., and Tasaka, M. (1999). Shoot apical meristem and cotyledon formation during arabidopsis embryogenesis: interaction among the cup-shaped cotyledon and shoot meristemless genes. *Development* 126, 1563–1570.

Aida, M., and Tasaka, M. (2006). Morphogenesis and patterning at the organ boundaries in the higher plant shoot apex. *Plant Mol. Biol.* 60, 915–928. doi: 10.1007/s11103-005-2760-7

Alvarez-Buylla, E. R., Benitez, M., Corvera-Poire, A., Chaos Cador, A., de Folter, S., Gamboa de Buen, A., et al. (2010). Flower development. *Arabidopsis Book* 8:e0127.

Arsovski, A. A., Galstyan, A., Guseman, J. M., and Nemhauser, J. L. (2012). Photomorphogenesis. *Arabidopsis Book* 10:e0147.

Aukerman, M. J., and Sakai, H. (2003). Regulation of flowering time and floral organ identity by a microrna and its apetala2-like target genes. *Plant Cell* 15, 2730–2741. doi: 10.1105/tpc.016238

Balanzà, V., Martínez-Fernández, I., Sato, S., Yanofsky, M. F., Kaufmann, K., Angenent, G. C., et al. (2018). Genetic control of meristem arrest and life span in arabidopsis by a fruitfull-apetala2 pathway. *Nat. Commun.* 9:565. doi: 10.1038/s41467-018-03067-5

Balkunde, R., Kitagawa, M., Xu, X. M., Wang, J., and Jackson, D. (2017). Shoot meristemless trafficking controls axillary meristem formation, meristem size and organ boundaries in arabidopsis. *Plant J.* 90, 435–446. doi: 10.1111/tpj.13504

Bishopp, A., and Bennett, M. J. (2014). Hormone crosstalk: directing the flow. *Curr. Biol.* 24, R366–R368. doi: 10.1016/j.cub.2014.03.018

Bohmert, K., Camus, I., Bellini, C., Bouchez, D., Caboche, M., and Benning, C. (1998). Ago1 defines a novel locus of arabidopsis controlling leaf development. *EMBO J.* 17, 170–180. doi: 10.1093/emboj/17.1.170

Bowman, J. L., Smyth, D. R., and Meyerowitz, E. M. (1989). Genes directing flower development in arabidopsis. *Plant Cell* 1, 37–52. doi: 10.1105/tpc.1.1.37

Bowman, J. L., Smyth, D. R., and Meyerowitz, E. M. (1991). Genetic interactions among floral homeotic genes of arabidopsis. *Development* 112, 1–20.

Breuil-Broyer, S., Morel, P., de Almeida-Engler, J., Coustham, V., Negrutiu, I., and Trehin, C. (2004). High-resolution boundary analysis during *Arabidopsis thaliana* flower development. *Plant J.* 38, 182–192.

Byrne, M. E. (2006). Shoot meristem function and leaf polarity: the role of class III hd-zip genes. *PLoS Genet.* 2:e89. doi: 10.1371/journal.pgen.0020089

Byrne, M. E., Simorowski, J., and Martienssen, R. A. (2002). *ASYMMETRIC LEAVES1* reveals *knox* gene redundancy in *Arabidopsis*. *Development* 129, 1957–1965.

Cao, X., He, Z., Guo, L., and Liu, X. (2015). Epigenetic mechanisms are critical for the regulation of wuschel expression in floral meristems. *Plant Physiol.* 168, 1189–1196. doi: 10.1104/pp.15.00230

Carles, C. C., and Fletcher, J. C. (2003). Shoot apical meristem maintenance: the art of a dynamic balance. *Trends Plant Sci.* 8, 394–401. doi: 10.1016/s1360-1385(03)00164-x

Casal, J. J., Candia, A. N., and Sellaro, R. (2014). Light perception and signalling by phytochrome a. *J. Exp. Bot.* 65, 2835–2845. doi: 10.1093/jxb/ert379

Chandler, J. W. (2012). Floral meristem initiation and emergence in plants. *Cell. Mol. Life Sci.* 69, 3807–3818. doi: 10.1007/s00018-012-0999-0

Chen, X., Liu, J., Cheng, Y., and Jia, D. (2002). *HEN1* functions pleiotropically in *Arabidopsis* development and acts in c function in the flower. *Development* 129, 1085–1094.

Chen, X. M. (2004). A microrna as a translational repressor of apetala2 in arabidopsis flower development. *Science* 303, 2022–2025. doi: 10.1126/science.1088060

Cheng, Y., Dai, X., and Zhao, Y. (2006). Auxin biosynthesis by the yucca flavin monooxygenases controls the formation of floral organs and vascular tissues in *Arabidopsis*. *Genes Dev.* 20, 1790–1799. doi: 10.1101/gad.1415106

Cheng, Z. J., Wang, L., Sun, W., Zhang, Y., Zhou, C., Su, Y. H., et al. (2013). Pattern of auxin and cytokinin responses for shoot meristem induction results from the regulation of cytokinin biosynthesis by auxin response factor3. *Plant Physiol.* 161, 240–251. doi: 10.1104/pp.112.203166

Chung, Y., Zhu, Y., Wu, M. F., Simonini, S., Kuhn, A., Armenta-Medina, A., et al. (2019). Auxin response factors promote organogenesis by chromatin-mediated repression of the pluripotency gene shootmeristemless. *Nat. Commun.* 10:886. doi: 10.1038/s41467-019-08861-3

Clark, S. E., Jacobsen, S. E., Levin, J. Z., and Meyerowitz, E. M. (1996). The clavata and shoot meristemless loci competitively regulate meristem activity in Arabidopsis. *Development* 122, 1567–1575.

Coen, E. S., and Meyerowitz, E. M. (1991). The war of the whorls: genetic interactions controlling flower development. *Nature* 353, 31–37. doi: 10.1038/353031a0

Costanzo, E., Trehin, C., and Vandenbussche, M. (2014). The role of wox genes in flower development. *Ann. Bot.* 114, 1545–1553. doi: 10.1093/aob/mcu123

D'Ario, M., Griffiths-Jones, S., and Kim, M. (2017). Small rnas: big impact on plant development. *Trends Plant Sci.* 22, 1056–1068. doi: 10.1016/j.tplants.2017.09.009

Daum, G., Medzihradszky, A., Suzaki, T., and Lohmann, J. U. (2014). A mechanistic framework for noncell autonomous stem cell induction in *Arabidopsis*. *Proc. Natl. Acad. Sci. U.S.A.* 111, 14619–14624. doi: 10.1073/pnas.1406446111

Dinh, T. T., Girke, T., Liu, X., Yant, L., Schmid, M., and Chen, X. (2012). The floral homeotic protein apetala2 recognizes and acts through an at-rich sequence element. *Development* 139, 1978–1986. doi: 10.1242/dev.077073

Dodsworth, S. (2009). A diverse and intricate signalling network regulates stem cell fate in the shoot apical meristem. *Dev. Biol.* 336, 1–9. doi: 10.1016/j.ydbio.2009.09.031

Drews, G. N., Bowman, J. L., and Meyerowitz, E. M. (1991). Negative regulation of the arabidopsis homeotic gene agamous by the apetala2 product. *Cell* 65, 991–1002. doi: 10.1016/0092-8674(91)90551-9

Endrizzi, K., Moussian, B., Haecker, A., Levin, J. Z., and Laux, T. (1996). The *SHOOT MERISTEMLESS* gene is required for maintenance of undifferentiated cells in *Arabidopsis* shoot and floral meristems and acts at a different regulatory level than the meristem genes *WUSCHEL* and *ZWILLE*. *Plant J.* 10, 967–979. doi: 10.1046/j.1365-313x.1996.10060967.x

Gaillochet, C., and Lohmann, J. U. (2015). The never-ending story: from pluripotency to plant developmental plasticity. *Development* 142, 2237–2249. doi: 10.1242/dev.117614

Gallois, J. L., Nora, F. R., Mizukami, Y., and Sablowski, R. (2004). Wuschel induces shoot stem cell activity and developmental plasticity in the root meristem. *Genes Dev.* 18, 375–380. doi: 10.1101/gad.291204

Gordon, S. P., Chickarmane, V. S., Ohno, C., and Meyerowitz, E. M. (2009). Multiple feedback loops through cytokinin signaling control stem cell number within the *Arabidopsis* shoot meristem. *Proc. Natl. Acad. Sci. U.S.A.* 106, 16529–16534. doi: 10.1073/pnas.0908122106

Grass Phylogeny Working Group, Barker, N. P., Clark, L. G., Davis, J. I., Duvall, M. R., Guala, G. F., et al. (2001). Phylogeny and subfamilial classification of the grasses (poaceae). *Ann. Mo. Bot. Gard.* 88, 373–457.

Groß-Hardt, R., and Laux, T. (2003). Stem cell regulation in the shoot meristem. *J. Cell Sci.* 116, 1659–1666. doi: 10.1242/jcs.00406

Guilfoyle, T. J., and Hagen, G. (2007). Auxin response factors. *Curr. Opin. Plant Biol.* 10, 453–460.

Guo, L., Cao, X., Liu, Y., Li, J., Li, Y., Li, D., et al. (2018). A chromatin loop represses *WUSCHEL* expression in Arabidopsis. *Plant J.* 94, 1083–1097. doi: 10.1111/tpj.13921

Hay, A., Kaur, H., Phillips, A., Hedden, P., Hake, S., and Tsiantis, M. (2002). The gibberellin pathway mediates knotted1-type homeobox function in plants with different body plans. *Curr. Biol.* 12, 1557–1565. doi: 10.1016/s0960-9822(02)01125-9

Heidstra, R., and Sabatini, S. (2014). Plant and animal stem cells: similar yet different. *Nat. Rev. Mol. Cell Biol.* 15, 301–312. doi: 10.1038/nrm3790

Heisler, M. G., and Ohno, C. (2014). Live-imaging of the Arabidopsis inflorescence meristem. *Methods Mol. Biol.* 1110, 431–440. doi: 10.1007/978-1-4614-9408-9_25

Hensel, L. L., Nelson, M. A., Richmond, T. A., and Bleecker, A. B. (1994). The fate of inflorescence meristems is controlled by developing fruits in Arabidopsis. *Plant Physiol.* 106, 863–876. doi: 10.1104/pp.106.3.863

Hibara, K., Takada, S., and Tasaka, M. (2003). Cuc1 gene activates the expression of sam-related genes to induce adventitious shoot formation. *Plant J.* 36, 687–696. doi: 10.1046/j.1365-313x.2003.01911.x

Huang, Z. G., Shi, T., Zheng, B. L., Yumul, R. E., Liu, X. G., You, C. J., et al. (2017). Apetala2 antagonizes the transcriptional activity of agamous in regulating floral stem cells in *Arabidopsis thaliana*. *New Phytol.* 215, 1197–1209. doi: 10.1111/nph.14151

Jacobsen, S. E., Running, M. P., and Meyerowitz, E. M. (1999). Disruption of an rna helicase/rnase III gene in Arabidopsis causes unregulated cell division in floral meristems. *Development* 126, 5231–5243.

Ji, L. J., Liu, X. G., Yan, J., Wang, W. M., Yumul, R. E., Kim, Y. J., et al. (2011). *ARGONAUTE10* and *ARGONAUTE1* regulate the termination of floral stem cells through two micrornas in *Arabidopsis*. *PLoS Genet.* 7:e1001358.

Jung, J. H., Lee, S., Yun, J., Lee, M., and Park, C. M. (2014). The mir172 target toe3 represses *AGAMOUS* expression during *Arabidopsis* floral patterning. *Plant Sci.* 215–216, 29–38. doi: 10.1016/j.plantsci.2013.10.010

Jung, J. H., and Park, C. M. (2007). *MIR166/165* genes exhibit dynamic expression patterns in regulating shoot apical meristem and floral development in *Arabidopsis*. *Planta* 225, 1327–1338. doi: 10.1007/s00425-006-0439-1

Jürgens, G. (2001). Apical–basal pattern formation in *Arabidopsis* embryogenesis. *EMBO J.* 20, 3609–3616. doi: 10.1093/emboj/20.14.3609

Kaufmann, K., Pajoro, A., and Angenent, G. C. (2010). Regulation of transcription in plants: mechanisms controlling developmental switches. *Nat. Rev. Genet.* 11, 830–842. doi: 10.1038/nrg2885

Kieber, J. J., and Schaller, G. E. (2014). Cytokinins. *Arabidopsis Book* 12:e0168. doi: 10.1199/tab.0168

Kim, J. Y., Yuan, Z., and Jackson, D. (2003). Developmental regulation and significance of knox protein trafficking in *Arabidopsis*. *Development* 130, 4351–4362. doi: 10.1242/dev.00618

Lau, S., Slane, D., Herud, O., Kong, J., and Jürgens, G. (2012). Early embryogenesis in flowering plants: setting up the basic body pattern. *Annu. Rev. Plant Biol.* 63, 483–506. doi: 10.1146/annurev-arplant-042811-105507

Laufs, P., Peaucelle, A., Morin, H., and Traas, J. (2004). Microrna regulation of the cuc genes is required for boundary size control in *Arabidopsis* meristems. *Development* 131, 4311–4322. doi: 10.1242/dev.01320

Laux, T. (2003). The stem cell concept in plants: a matter of debate. *Cell* 113, 281–283. doi: 10.1016/s0092-8674(03)00312-x

Laux, T., Mayer, K. F. X., Berger, J., and Jurgens, G. (1996). The wuschel gene is required for shoot and floral meristem integrity in Arabidopsis. *Development* 122, 87–96.

Lee, Z. H., Hirakawa, T., Yamaguchi, N., and Ito, T. (2019). The roles of plant hormones and their interactions with regulatory genes in determining meristem activity. *Int. J. Mol. Sci.* 20:4065. doi: 10.3390/ijms20164065

Leibfried, A., To, J. P., Busch, W., Stehling, S., Kehle, A., Demar, M., et al. (2005). Wuschel controls meristem function by direct regulation of cytokinin-inducible response regulators. *Nature* 438, 1172–1175. doi: 10.1038/nature04270

Lenhard, M., Bohnert, A., Jurgens, G., and Laux, T. (2001). Termination of stem cell maintenance in *Arabidopsis* floral meristems by interactions between *WUSCHEL* and *AGAMOUS*. *Cell* 105, 805–814. doi: 10.1016/s0092-8674(01)00390-7

Lenhard, M., Jürgens, G., and Laux, T. (2002). The *WUSCHEL* and *SHOOTMERISTEMLESS* genes fulfil complementary roles in *Arabidopsis* shoot meristem regulation. *Development* 129, 3195–3206.

Li, D., Fu, X., Guo, L., Huang, Z., Li, Y., Liu, Y., et al. (2016). *FAR-RED ELONGATED HYPOCOTYL3* activates *SEPALLATA2* but inhibits *CLAVATA3* to regulate meristem determinacy and maintenance in *Arabidopsis*. *Proc. Natl. Acad. Sci. U.S.A.* 113, 9375–9380. doi: 10.1073/pnas.1602960113

Li, J., Li, G., Wang, H., and Wang Deng, X. (2011). Phytochrome signaling mechanisms. *Arabidopsis Book* 9:e0148. doi: 10.1199/tab.0148

Li, X., Cai, W., Liu, Y., Li, H., Fu, L., Liu, Z., et al. (2017). Differential tor activation and cell proliferation in *Arabidopsis* root and shoot apexes. *Proc. Natl. Acad. Sci. U.S.A.* 114, 2765–2770.

Li, Z., Li, B., Shen, W. H., Huang, H., and Dong, A. (2012). Tcp transcription factors interact with as2 in the repression of class-i knox genes in *Arabidopsis thaliana*. *Plant J.* 71, 99–107. doi: 10.1111/j.1365-313X.2012.04973.x

Lin, R., Ding, L., Casola, C., Ripoll, D. R., Feschotte, C., and Wang, H. (2007). Transposase-derived transcription factors regulate light signaling in *Arabidopsis*. *Science* 318, 1302–1305. doi: 10.1126/science.1146281

Liscum, E., and Reed, J. W. (2002). Genetics of aux/iaa and arf action in plant growth and development. *Plant Mol. Biol.* 49, 387–400. doi: 10.1007/978-94-010-0377-3_10

Liu, C., Teo, Z. W., Bi, Y., Song, S., Xi, W., Yang, X., et al. (2013). A conserved genetic pathway determines inflorescence architecture in arabidopsis and rice. *Dev. Cell* 24, 612–622. doi: 10.1016/j.devcel.2013.02.013

Liu, C., Xi, W., Shen, L., Tan, C., and Yu, H. (2009). Regulation of floral patterning by flowering time genes. *Dev. Cell* 16, 711–722. doi: 10.1016/j.devcel.2009.03.011

Liu, H., Yu, H., Tang, G., and Huang, T. (2018). Small but powerful: function of micrornas in plant development. *Plant Cell Rep.* 37, 515–528. doi: 10.1007/s00299-017-2246-5

Liu, Q., Yao, X., Pi, L., Wang, H., Cui, X., and Huang, H. (2009). The *ARGONAUTE10* gene modulates shoot apical meristem maintenance and establishment of leaf polarity by repressing mir165/166 in Arabidopsis. *Plant J.* 58, 27–40. doi: 10.1111/j.1365-313X.2008.03757.x

Liu, W., and Xu, L. (2018). Recruitment of ic-wox genes in root evolution. *Trends Plant Sci.* 23, 490–496. doi: 10.1016/j.tplants.2018.03.011

Liu, X., Dinh, T. T., Li, D., Shi, B., Li, Y., Cao, X., et al. (2014). Auxin response factor 3 integrates the functions of agamous and apetala2 in floral meristem determinacy. *Plant J.* 80, 629–641. doi: 10.1111/tpj.12658

Liu, X. G., Kim, Y. J., Muller, R., Yumul, R. E., Liu, C. Y., Pan, Y. Y., et al. (2011). Agamous terminates floral stem cell maintenance in arabidopsis by directly repressing wuschel through recruitment of polycomb group proteins. *Plant Cell* 23, 3654–3670. doi: 10.1105/tpc.111.091538

Lohmann, J. U., Hong, R. L., Hobe, M., Busch, M. A., Parcy F, Simon R., et al. (2001). A molecular link between stem cell regulation and floral patterning in *Arabidopsis*. *Cell* 105, 793–803. doi: 10.1016/s0092-8674(01)00384-1

Long, J., and Barton, M. K. (2000). Initiation of axillary and floral meristems in *Arabidopsis*. *Dev. Biol.* 218, 341–353. doi: 10.1006/dbio.1999.9572

Long, J. A., Moan, E. I., Medford, J. I., and Barton, M. K. (1996). A member of the knotted class of homeodomain proteins encoded by the *STM* gene of *Arabidopsis*. *Nature* 379, 66–69. doi: 10.1038/379066a0

Lucas, W. J., Bouche-Pillon, S., Jackson, D. P., Nguyen, L., Baker, L., Ding, B., et al. (1995). Selective trafficking of knotted1 homeodomain protein and its mrna through plasmodesmata. *Science* 270, 1980–1983. doi: 10.1126/science.270.5244.1980

Lynn, K., Fernandez, A., Aida, M., Sedbrook, J., Tasaka, M., Masson, P., et al. (1999). The pinhead/zwille gene acts pleiotropically in Arabidopsis development and has overlapping functions with the argonaute1 gene. *Development* 126, 469–481.

Ma, Y., Miotk, A., Šutiković, Z., Ermakova, O., Wenzl, C., Medzihradszky, A., et al. (2019). Wuschel acts as an auxin response rheostat to maintain apical stem cells in *Arabidopsis*. *Nat. Commun.* 10:5093. doi: 10.1038/s41467-019-13074-9

Mallory, A., and Vaucheret, H. (2010). Form, function, and regulation of argonaute proteins. *Plant Cell* 22, 3879–3889. doi: 10.1105/tpc.110.080671

Mallory, A. C., Hinze, A., Tucker, M. R., Bouche, N., Gasciolli, V., Elmayan, T., et al. (2009). Redundant and specific roles of the argonaute proteins ago1 and zll in development and small rna-directed gene silencing. *PLoS Genet.* 5:e1000646. doi: 10.1371/journal.pgen.1000646

Margis, R., Fusaro, A. F., Smith, N. A., Curtin, S. J., Watson, J. M., Finnegan, E. J., et al. (2006). The evolution and diversification of dicers in plants. *FEBS Lett.* 580, 2442–2450. doi: 10.1016/j.febslet.2006.03.072

Mathews, S., Burleigh, J. G., and Donoghue, M. J. (2003). Adaptive evolution in the photosensory domain of phytochrome a in early angiosperms. *Mol. Biol. Evol.* 20, 1087–1097. doi: 10.1093/molbev/msg123

Mathieu, J., Yant, L. J., Murdter, F., Kuttner, F., and Schmid, M. (2009). Repression of flowering by the mir172 target smz. *PLoS Biol.* 7:e1000148. doi: 10.1371/journal.pbio.1000148

Mayer, K. F. X., Schoof, H., Haecker, A., Lenhard, M., Jurgens, G., and Laux, T. (1998). Role of *WUSCHEL* in regulating stem cell fate in the *Arabidopsis* shoot meristem. *Cell* 95, 805–815. doi: 10.1016/s0092-8674(00)81703-1

Mi, S., Cai, T., Hu, Y., Chen, Y., Hodges, E., Ni, F., et al. (2008). Sorting of small rnas into arabidopsis argonaute complexes is directed by the 5' terminal nucleotide. *Cell* 133, 116–127. doi: 10.1016/j.cell.2008.02.034

Miwa, H., Kinoshita, A., Fukuda, H., and Sawa, S. (2009). Plant meristems: clavata3/esr-related signaling in the shoot apical meristem and the root apical meristem. *J. Plant Res.* 122, 31–39. doi: 10.1007/s10265-008-0207-3

Moussian, B., Schoof, H., Haecker, A., Jurgens, G., and Laux, T. (1998). Role of the zwille gene in the regulation of central shoot meristem cell fate during Arabidopsis embryogenesis. *EMBO J.* 17, 1799–1809. doi: 10.1093/emboj/17.6.1799

Nemhauser, J. L., Feldman, L. J., and Zambryski, P. C. (2000). Auxin and ettin in Arabidopsis gynoecium morphogenesis. *Development* 127, 3877–3888.

Nozawa, M., Miura, S., and Nei, M. (2012). Origins and evolution of microrna genes in plant species. *Genome Biol. Evol.* 4, 230–239. doi: 10.1093/gbe/evs002

Ohto, M. A., Fischer, R. L., Goldberg, R. B., Nakamura, K., and Harada, J. J. (2005). Control of seed mass by apetala2. *Proc. Natl. Acad. Sci. U.S.A.* 102, 3123–3128. doi: 10.1073/pnas.0409858102

Ouyang, X., Li, J., Li, G., Li, B., Chen, B., Shen, H., et al. (2011). Genome-wide binding site analysis of far-red elongated hypocotyl3 reveals its novel function in *Arabidopsis* development. *Plant Cell* 23, 2514–2535. doi: 10.1105/tpc.111.085126

Pfeiffer, A., Janocha, D., Dong, Y., Medzihradszky, A., Schone, S., Daum, G., et al. (2016). Integration of light and metabolic signals for stem cell activation at the shoot apical meristem. *eLife* 5:e17023.

Prunet, N., Morel, P., Negrutiu, I., and Trehin, C. (2009). Time to stop: flower meristem termination. *Plant Physiol.* 150, 1764–1772. doi: 10.1104/pp.109.141812

Reinhardt, D., Mandel, T., and Kuhlemeier, C. (2000). Auxin regulates the initiation and radial position of plant lateral organs. *Plant Cell* 12, 507–518. doi: 10.1105/tpc.12.4.507

Rogers, K., and Chen, X. (2013). Biogenesis, turnover, and mode of action of plant micrornas. *Plant Cell* 25, 2383–2399. doi: 10.1105/tpc.113.113159

Roth, O., Alvarez, J. P., Levy, M., Bowman, J. L., Ori, N., and Shani, E. (2018). The knoxi transcription factor shoot meristemless regulates floral fate in Arabidopsis. *Plant Cell* 30, 1309–1321. doi: 10.1105/tpc.18.00222

Sablowski, R. (2004). Plant and animal stem cells: conceptually similar, molecularly distinct? *Trends Cell Biol.* 14, 605–611. doi: 10.1016/j.tcb.2004.09.011

Sablowski, R. (2007). Flowering and determinacy in *Arabidopsis*. *J. Exp. Bot.* 58, 899–907. doi: 10.1093/jxb/erm002

Satbhai, S. B., Ristova, D., and Busch, W. (2015). Underground tuning: quantitative regulation of root growth. *J. Exp. Bot.* 66, 1099–1112. doi: 10.1093/jxb/eru529

Schaller, G. E., Bishopp, A., and Kieber, J. J. (2015). The yin-yang of hormones: cytokinin and auxin interactions in plant development. *Plant Cell* 27, 44–63.

Schultz, E. A., and Haughn, G. W. (1991). Leafy, a homeotic gene that regulates inflorescence development in Arabidopsis. *Plant Cell* 3, 771–781. doi: 10.1105/tpc.3.8.771

Scofield, S., Dewitte, W., and Murray, J. A. (2007). The *KNOX* gene *SHOOT MERISTEMLESS* is required for the development of reproductive meristematic tissues in Arabidopsis. *Plant J.* 50, 767–781. doi: 10.1111/j.1365-313x.2007.03095.x

Scofield, S., Murison, A., Jones, A., Fozard, J., Aida, M., Band, L. R., et al. (2018). Coordination of meristem and boundary functions by transcription factors in the shoot meristemless regulatory network. *Development* 145:dev157081.

Sessions, A., Nemhauser, J. L., McColl, A., Roe, J. L., Feldmann, K. A., and Zambryski, P. C. (1997). Ettin patterns the Arabidopsis floral meristem and reproductive organs. *Development* 124, 4481–4491.

Simonini, S., Bencivenga, S., Trick, M., and Ostergaard, L. (2017). Auxin-induced modulation of ettin activity orchestrates gene expression in Arabidopsis. *Plant Cell* 29, 1864–1882. doi: 10.1105/tpc.17.00389

Smyth, D. R., Bowman, J. L., and Meyerowitz, E. M. (1990). Early flower development in Arabidopsis. *Plant Cell* 2, 755–767.

Soyars, C. L., James, S. R., and Nimchuk, Z. L. (2016). Ready, aim, shoot: stem cell regulation of the shoot apical meristem. *Curr. Opin. Plant Biol.* 29, 163–168. doi: 10.1016/j.pbi.2015.12.002

Sozzani, R., and Iyer-Pascuzzi, A. (2014). Postembryonic control of root meristem growth and development. *Curr. Opin. Plant Biol.* 17, 7–12. doi: 10.1016/j.pbi.2013.10.005

Spinelli, S. V., Martin, A. P., Viola, I. L., Gonzalez, D. H., and Palatnik, J. F. (2011). A mechanistic link between *STM* and *CUC1* during Arabidopsis development. *Plant Physiol.* 156, 1894–1904. doi: 10.1104/pp.111.177709

Sun, B., Xu, Y. F., Ng, K. H., and Ito, T. (2009). A timing mechanism for stem cell maintenance and differentiation in the *Arabidopsis* floral meristem. *Genes Dev.* 23, 1791–1804. doi: 10.1101/gad.1800409

Sun, B., Zhou, Y., Cai, J., Shang, E., Yamaguchi, N., Xiao, J., et al. (2019). Integration of transcriptional repression and polycomb-mediated silencing of wuschel in floral meristems. *Plant Cell* 31, 1488–1505. doi: 10.1105/tpc.18.00450

Talbert, P. B., Adler, H. T., Parks, D. W., and Comai, L. (1995). The revoluta gene is necessary for apical meristem development and for limiting cell divisions in the leaves and stems of *Arabidopsis thaliana*. *Development* 121, 2723–2735.

Tucker, M. R., Hinze, A., Tucker, E. J., Takada, S., Jurgens, G., and Laux, T. (2008). Vascular signalling mediated by zwille potentiates wuschel function during shoot meristem stem cell development in the *Arabidopsis* embryo. *Development* 135, 2839–2843. doi: 10.1242/dev.023648

van der Graaff, E., Laux, T., and Rensing, S. A. (2009). The wus homeobox-containing (wox) protein family. *Genome Biol.* 10:248. doi: 10.1186/gb-2009-10-12-248

Vanneste, S., and Friml, J. (2009). Auxin: a trigger for change in plant development. *Cell* 136, 1005–1016. doi: 10.1016/j.cell.2009.03.001

Vaucheret, H. (2008). Plant argonautes. *Trends Plant Sci.* 13, 350–358. doi: 10.1016/j.tplants.2008.04.007

Vaucheret, H., Vazquez, F., Crete, P., and Bartel, D. P. (2004). The action of argonaute1 in the mirna pathway and its regulation by the mirna pathway are crucial for plant development. *Genes Dev.* 18, 1187–1197. doi: 10.1101/gad.1201404

Wang, H., and Wang, H. (2015). Multifaceted roles of fhy3 and far1 in light signaling and beyond. *Trends Plant Sci.* 20, 453–461. doi: 10.1016/j.tplants.2015.04.003

Wang, J. W., Czech, B., and Weigel, D. (2009). Mir156-regulated spl transcription factors define an endogenous flowering pathway in *Arabidopsis thaliana*. *Cell* 138, 738–749. doi: 10.1016/j.cell.2009.06.014

Wang, Q., Hasson, A., Rossmann, S., and Theres, K. (2016). Divide et impera: boundaries shape the plant body and initiate new meristems. *New Phytol.* 209, 485–498. doi: 10.1111/nph.13641

Weigel, D., and Meyerowitz, E. M. (1994). The abcs of floral homeotic genes. *Cell* 78, 203–209. doi: 10.1016/0092-8674(94)90291-7

Wollmann, H., Mica, E., Todesco, M., Long, J. A., and Weigel, D. (2010). On reconciling the interactions between apetala2, mir172 and agamous with the abc model of flower development. *Development* 137, 3633–3642. doi: 10.1242/dev.036673

Wu, G., Park, M. Y., Conway, S. R., Wang, J. W., Weigel, D., and Poethig, R. S. (2009). The sequential action of mir156 and mir172 regulates developmental timing in *Arabidopsis*. *Cell* 138, 750–759. doi: 10.1016/j.cell.2009.06.031

Wuest, S. E., Philipp, M. A., Guthorl, D., Schmid, B., and Grossniklaus, U. (2016). Seed production affects maternal growth and senescence in Arabidopsis. *Plant Physiol.* 171, 392–404. doi: 10.1104/pp.15.01995

Wurschum, T., Gross-Hardt, R., and Laux, T. (2006). *APETALA2* regulates the stem cell niche in the *Arabidopsis* shoot meristem. *Plant Cell* 18, 295–307. doi: 10.1105/tpc.105.038398

Xu, Y. F., Yamaguchi, N., Gan, E. S., and Ito, T. (2019). When to stop: an update on molecular mechanisms of floral meristem termination. *J. Exp. Bot.* 70, 1711–1718. doi: 10.1093/jxb/erz048

Xu, Y. Y., Wang, X. M., Li, J., Li, J. H., Wu, J. S., Walker, J. C., et al. (2005). Activation of the wus gene induces ectopic initiation of floral meristems on mature stem surface in *Arabidopsis thaliana*. *Plant Mol. Biol.* 57, 773–784. doi: 10.1007/s11103-005-0952-9

Yadav, R. K., Perales, M., Gruel, J., Girke, T., Jonsson, H., and Reddy, G. V. (2011). Wuschel protein movement mediates stem cell homeostasis in the *Arabidopsis* shoot apex. *Genes Dev.* 25, 2025–2030. doi: 10.1101/gad.17258511

Yamaguchi, N., Huang, J., Tatsumi, Y., Abe, M., Sugano, S. S., Kojima, M., et al. (2018). Chromatin-mediated feed-forward auxin biosynthesis in floral meristem determinacy. *Nat. Commun.* 9:5290. doi: 10.1038/s41467-018-07763-0

Yamaguchi, N., Huang, J., Xu, Y., Tanoi, K., and Ito, T. (2017). Fine-tuning of auxin homeostasis governs the transition from floral stem cell maintenance to gynoecium formation. *Nat. Commun.* 8:1125. doi: 10.1038/s41467-017-01252-6

Yanai, O., Shani, E., Dolezal, K., Tarkowski, P., Sablowski, R., Sandberg, G., et al. (2005). *Arabidopsis* knoxi proteins activate cytokinin biosynthesis. *Curr. Biol.* 15, 1566–1571. doi: 10.1016/j.cub.2005.07.060

Yant, L., Mathieu, J., Dinh, T. T., Ott, F., Lanz, C., Wollmann, H., et al. (2010). Orchestration of the floral transition and floral development in *Arabidopsis* by the bifunctional transcription factor apetala2. *Plant Cell* 22, 2156–2170. doi: 10.1105/tpc.110.075606

Yu, Y., Ji, L., Le, B. H., Zhai, J., Chen, J., Luscher, E., et al. (2017a). Argonaute10 promotes the degradation of mir165/6 through the sdn1 and sdn2 exonucleases in *Arabidopsis*. *PLoS Biol.* 15:e2001272. doi: 10.1371/journal.pbio.2001272

Yu, Y., Jia, T., and Chen, X. (2017b). The 'how' and 'where' of plant micrornas. *New Phytol.* 216, 1002–1017. doi: 10.1111/nph.14834

Yumul, R. E., Kim, Y. J., Liu, X. G., Wang, R. Z., Ding, J. H., Xiao, L. T., et al. (2013). Powerdress and diversified expression of the mir172 gene family bolster the floral stem cell network. *PLoS Genet.* 9:e1003218.

Zadnikova, P., and Simon, R. (2014). How boundaries control plant development. *Curr. Opin. Plant Biol.* 17, 116–125. doi: 10.1016/j.pbi.2013.11.013

Zhang, D., and Yuan, Z. (2014). Molecular control of grass inflorescence development. *Annu. Rev. Plant Biol.* 65, 553–578. doi: 10.1146/annurev-arplant-050213-040104

Zhang, K., Wang, R., Zi, H., Li, Y., Cao, X., Li, D., et al. (2018). Auxin response factor3 regulates floral meristem determinacy by repressing cytokinin biosynthesis and signaling. *Plant Cell* 30, 324–346. doi: 10.1105/tpc.17.00705

Zhang, X., Zong, J., Liu, J., Yin, J., and Zhang, D. (2010). Genome-wide analysis of *WOX* gene family in rice, sorghum, maize, *Arabidopsis* and poplar. *J. Integr. Plant Biol.* 52, 1016–1026. doi: 10.1111/j.1744-7909.2010.00982.x

Zhang, Z., and Zhang, X. (2012). Argonautes compete for mir165/166 to regulate shoot apical meristem development. *Curr. Opin. Plant Biol.* 15, 652–658. doi: 10.1016/j.pbi.2012.05.007

Zhao, L., Kim, Y., Dinh, T. T., and Chen, X. (2007). Mir172 regulates stem cell fate and defines the inner boundary of *APETALA3* and *PISTILLATA* expression domain in Arabidopsis floral meristems. *Plant J.* 51, 840–849. doi: 10.1111/j.1365-313x.2007.03181.x

Zhao, Z., Andersen, S. U., Ljung, K., Dolezal, K., Miotk, A., Schultheiss, S. J., et al. (2010). Hormonal control of the shoot stem-cell niche. *Nature* 465, 1089–1092. doi: 10.1038/nature09126

Zheng, Y., and Liu, X. (2019). Review: chromatin organization in plant and animal stem cell maintenance. *Plant Sci.* 281, 173–179. doi: 10.1016/j.plantsci.2018.12.026

Zhou, G. K., Kubo, M., Zhong, R., Demura, T., and Ye, Z. H. (2007). Overexpression of mir165 affects apical meristem formation, organ polarity establishment and vascular development in *Arabidopsis*. *Plant Cell Physiol.* 48, 391–404. doi: 10.1093/pcp/pcm008

Zhu, H., Hu, F., Wang, R., Zhou, X., Sze, S. H., Liou, L. W., et al. (2011). *Arabidopsis* argonaute10 specifically sequesters mir166/165 to regulate shoot apical meristem development. *Cell* 145, 242–256. doi: 10.1016/j.cell.2011.03.024

Zuo, J., Niu, Q. W., Frugis, G., and Chua, N. H. (2002). The *WUSCHEL* gene promotes vegetative-to-embryonic transition in *Arabidopsis*. *Plant J.* 30, 349–359. doi: 10.1046/j.1365-313x.2002.01289.x

Conflict of Interest: The authors declare that the research was conducted in the absence of any commercial or financial relationships that could be construed as a potential conflict of interest.

frontiers in Ecology and Evolution

ORIGINAL RESEARCH
published: 28 April 2020
doi: 10.3389/fevo.2020.00104

Patterns of Symmetry Expression in Angiosperms: Developmental and Evolutionary Lability

*Somayeh Naghiloo**

Department of Biological Sciences, University of Calgary, Calgary, AB, Canada

Variation in flower symmetry is a remarkable aspect of flowering plant diversity. Multiple evolutionary transitions from an ancestral form of radial symmetry to bilateral symmetry and reversals from bilateral to radial symmetry have occurred during angiosperm evolution. The high incident of symmetry transitions poses the question concerning the homology of underlying developmental processes. I conducted a comprehensive study of developmental expression of symmetry across angiosperms covering 72 families and 39 orders. A wide range of timing for the expression of symmetry was found from organ initiation, to enlargement, to late differentiation of organs. In many studied genera, the symmetry pattern was transient during development. Mapping the floral symmetry patterns on the phylogenetic tree indicated the scattered distribution of patterns across angiosperms. Mid to late onset of actinomorphy/zygomorphy was found in all major clades. The expression of symmetry was also versatile within families. No strong relationship was found between the degree of zygomorphy at mature stage and its time of expression. The developmental constraints exerted by the inflorescence, bracts, neighbor flowers or neighbor organs within a flower could provide a possible explanation for the observed variation of symmetry expression.

Keywords: symmetry expression, angiosperms, developmental constraints, actinomorphy, zygomorphy

OPEN ACCESS

Edited by:
Louis Philippe Ronse De Craene, Royal Botanic Garden Edinburgh, United Kingdom

Reviewed by:
Sophie Nadot, Université Paris-Sud, France
Erik Smets, Naturalis Biodiversity Center, Netherlands

***Correspondence:**
Somayeh Naghiloo
somayeh_naghiloo@yahoo.com

Specialty section:
This article was submitted to Evolutionary Developmental Biology, a section of the journal Frontiers in Ecology and Evolution

Received: *25 September 2019*
Accepted: *30 March 2020*
Published: *28 April 2020*

Citation:
Naghiloo S (2020) Patterns of Symmetry Expression in Angiosperms: Developmental and Evolutionary Lability. Front. Ecol. Evol. 8:104. doi: 10.3389/fevo.2020.00104

INTRODUCTION

One of the fascinating aspects of the floral organization is the balanced and harmonic arrangement of organs within a flower creating specific symmetry patterns. Actinomorphy (i.e., polysymmetry or radial symmetry with several symmetry planes) and zygomorphy (i.e., monosymmetry or bilateral symmetry with one symmetry plane) are the most common types of symmetry among flowering plants (Endress, 1999, 2010). Zygomorphy has diverse expressions in flowers, affecting organ categories in various combination (all organs, or only one organ category) and to various degrees (by differential shape, size, curvature, number) (Citerne et al., 2010; Endress, 2012). A weak degree of monosymmetry which is sometimes expressed due to the positional effect (positional monosymmetry, e.g., bending of stamens and styles due to gravity), may provide a precondition for the evolution of elaborate constitutional monosymmetry in polysymmetric groups (Endress, 1999). Except for Lamiales in which both corolla and androecium are remarkably affected, monosymmetry is commonly concentrated on or restricted to the perianth (Endress, 2012).

The reconstruction of the flower symmetry on the phylogenetic tree of angiosperms indicated actinomorphy as the ancestral state which is in agreement with its prevalence in flowers of basal angiosperms (Endress and Doyle, 2009). While relatively elaborate forms of zygomorphy are found in basal angiosperms (Aristolochiaceae of Piperales) and monocots (Orchidaceae of Asparagales, Commelinaceae of Commelinales), zygomorphy is mainly concentrated among rosids especially in Fabales and Malvales and among asterids especially in Lamiales, Asterales, and Dipsacales (Citerne et al., 2010; Endress, 2012). The analysis of symmetry evolution on the phylogenetic tree of angiosperms indicated frequent transitions from the ancestral actinomorphy to zygomorphy at least two times among the basal angiosperms, 29 times in monocots, and 99 times in the eudicots (Reyes et al., 2016). The high incident of zygomorphy and its homoplastic evolution poses the question concerning the homology of underlying developmental processes.

Floral symmetry is established through the activity of the floral meristem during organ initiation, enlargement, and subsequent differentiation. Several authors studied the manifestation of floral symmetry during ontogeny (Mair, 1977; Endress, 1999; Tucker, 1999). They reported a wide range of timing for the expression of symmetry, from organ initiation, to later enlargement of floral organs, to late differentiation of structures. In many studied genera, the symmetry pattern is transient during development. The symmetry established by the ordered initiation of floral organs at the beginning of development can be reduced, enhanced or changed later through differential growth of floral sectors. The developmental or evolutionary constraints underlying such labile expression of symmetry is poorly understood. It is suggested that the phylogenetic background of taxa and the degree of zygomorphy in mature flowers can influence the time of zygomorphy expression (Endress, 1999; Tucker, 1999). In many families with prevalent elaborate zygomorphy (e.g., Fabaceae), zygomorphy is manifested early at organs initiation and persists throughout development (Tucker, 2003). On the other hand, in zygomorphic taxa embedded in groups with predominantly actinomorphic flowers (e.g., *Aconitum* in Ranunculaceae), the flower is actinomorphic through most of its development and the manifestation of zygomorphy occurs toward the end of the ontogeny (Mair, 1977). However, the reverse condition also occurs. Some lamiaceous flowers with elaborate zygomorphy have shown a preceding actinomorphy in early development (Naghiloo et al., 2013a,b, 2014b). The weakly zygomorphic flowers of *Capparis spinosa* from the actinomorphic family Capparaceae express signs of zygomorphy at organ initiation (Naghiloo et al., 2015).

I conducted a comprehensive study of developmental expression of symmetry across angiosperms covering 72 families and 39 orders. Focusing on corolla symmetry as the most prominent manifestation of symmetry, I traced the evolution of developmental changes on a phylogenetic background. The objectives were (1) to determine patterns of symmetry expression within angiosperms, (2) to map the distribution of patterns on a phylogenetic tree, and (3) to infer evolutionary and developmental constraints underlying diversity of symmetry patterns.

MATERIALS AND METHODS

Data Collection

The pattern of symmetry expression of 227 species belonging to 72 families and 39 orders of angiosperms was extracted from literature (for details of species and list of literature see **Supplementary Appendix S1**). The corolla symmetry in anthetic flowers was identified as zygomorphic (79 species) or actinomorphic (148 species) based on the available descriptions and images of the flower. Focusing on the corolla symmetry, I described tetramerous flowers of Brassicaceae and Oleaceae as actinomorphic while they are otherwise described as dissymmetric considering the whole flower.

I then used SEM micrographs from the literature to indicate the expression of symmetry in three developmental stages: (1) The early/initiation phase in which the first trace of organ primordia was detectable. (2) The mid/enlargement phase in which all primordia enlarged as clear bulges. (3) The late/differentiation phase during which the growth of primordia was accelerated and they started to cover the inner organs. The literatures in which the related stages could not be detected were excluded from the study.

The symmetry pattern in early phase was evaluated based on the order of primordia emergence; the simultaneous appearance was interpreted as actinomrphy, while the sequential appearance with a single dorsoventral axis was described as zygomrphy. The decision about organ initiation was based on clear separation from the floral meristem usually forming a furrow. In mid and late phases, the size difference was used as a criterion to indicate symmetry pattern; the size equality was described as actinomorphy while the size gradient along the dorsoventral axis was interpreted as zygomorphy.

Micrographs

Upon identifying the symmetry patterns, representative micrographs for each developmental pattern were extracted from the author's previous publications and presented. For a description of the microscopic procedure, see the related publications (Dadpour et al., 2011a,b, 2012a; Naghiloo et al., 2012, 2013b, 2014a; Naghiloo and Classen-Bockhoff, 2016; Naghiloo and Claßen-Bockhoff, 2017).

Phylogenetic Framework and Character Optimization

I used the angiosperm phylogeny created by Soltis et al. (2011) to infer the relationships among the 72 families examined in the current study. This well-resolved tree was based on data from 17 DNA regions representing all three plant genomes, i.e., nucleus, plastid, and mitochondrion (Soltis et al., 2011). All branches were set equal with a value of 1.

To infer the evolutionary change in symmetry pattern, character optimization was carried out with the Maximum Parsimony method implemented in Mesquite 3.04 (Maddison and Maddison, 2015). All character changes were treated as an unordered and equally weighted.

The Maximum Likelihood method (ML) was not employed here as this method does not accept polymorphisms which were numerous in my dataset.

RESULTS

Patterns of Symmetry Expression

(A) Actinomorphic Species: The evaluation of symmetry expression in 148 actinomorphic species indicated the occurrence of four developmental patterns (**Figures 1**, **2**):

(1) Early expression: The actinomorphy first appeared during petal initiation (S1) due to the simultaneous emergence of primordia (**Figures 1A,D**). It was maintained during development due to synchronous enlargement (S2) and differentiation (S3) (**Figures 1B,C,E,F**). The flowers were, therefore, actinomorphic throughout development.

(2) Mid expression: The corolla started development with a zygomorphic, non-simultaneous initiation (**Figures 1G,J**). However, the initial zygomorphy soon disappeared due to the synchronous enlargement and growth of corolla members after initiation (**Figures 1H,I,K,L**).

(3) Late expression: The corolla development started with the zygomorphic, non-simultaneous initiation of primordia (**Figures 2A,D**). The zygomorphy was still evident during the enlargement of organ primordia (**Figures 2B,E**). The synchronization of petal growth only happened during organ differentiation (**Figures 2C,F**).

(4) Very late expression: The corolla development started with a zygomorphic, non-simultaneous initiation (**Figures 2G,J**). The zygomorphy maintained during enlargement and differentiation phases due to asynchronous growth (**Figures 2H,I,K,L**). The flowers were, therefore, zygomorphic throughout development and actinomorphy only appeared due to equalization of organ growth in pre-anthetic flowers.

(B) Zygomorphic Species: I could distinguish three developmental patterns among 79 zygomorphic species:

(1) Early expression: The zygomorphy first appeared at organ initiation due to the sequential emergence of petal primordia (**Figures 3A,D**). The first initiated primordium showed the highest growth rate, followed by the second and third initiated primordia (**Figures 3B,E**). The size gradient was evident during enlargement and differentiation phases (**Figures 3C,F**). The flowers were therefore zygomorphic throughout development.

(2) Late expression: The corolla development started with an actinomorphic, simultaneous initiation (**Figures 3G,J**). The petals developed synchronously during enlargement and early differentiation phases (**Figures 3H,I,K,L**). The zygomorphy only appeared at the late differentiation phase prior to anthesis.

(3) The double shift of symmetry: The corolla development started with a zygomorphic, non-simultaneous initiation of primordia (**Figures 4A,D,G**). However, the initial zygomorphy was masked due to the equalization of primordia during enlargement phase (**Figures 4B,E,H**). After this period of actinomorphy, zygomorphy appeared again during the differentiation phase due to asynchronous organ growth (**Figures 4C,F,I**).

Evolution of Symmetry Patterns

Tracing the evolution of symmetry indicated that the ancestral state for angiosperms has been an actinomorphic flower which manifested actinomorphy at mid to late stage of development (**Figure 5** and **Supplementary Appendixes S2–S4**). All major angiosperm clades (rosids, asterids, and monocots) were also characterized by an ancestral actinomorphic flower with a preceding early zygomorphy. The transition to early actinomorphy occurred several times in rosids (Fabaceae, Euphorbiaceae, Malvaceae- Neuradaceae clade, Cleomaceae, Rutaceae, Geraniaceae-Myrtaceae clade, and Vitaceae), asterids (Oleaceae, Rubiaceae, Solanaceae, Apiaceae, and Caprifoliaceae), eudicots (Caryophyllaceae), and basal angiosperms (Annonaceae). On the other hands, the transition to late actinomorphy also happened frequently by a shift to zygomorphy at the enlargement or differentiation phase. Such a transition was found in several families among rosids (Elaeagnaceae, Passifloraceae, and Zygophyllaceae), asterids (Plantaginaceae, Rubiaceae, Apiaceae, Caprifoliaceae, and Hydrangeaceae), eudicots (Portulacaceae, Nyctaginaceae, Phytolaccaceae, Berberidaceae, Loranthaceae, Olacaceae, and Ranunculaceae) monocots (Heliconiaceae, Arecaceae) and basal angiosperms (Lauraceae, Nymphaceae).

The majority of zygomorphic flowers were derived from the ancestral state by the transition to zygomorphy during both enlargement and differentiation phases. Examples of such early zygomorphic flowers were found among rosids (Fabaceae, Bataceae, Cleomaceae, and Sapindaceae), asterids (Orobanchaceae, Paulowniaceae, Gesneriaceae, Solanaceae, Caprifoliaceae, Lecythidaceae, and Balsaminaceae), eudicots (Dilleniaceae, Sabiaceae), monocots (Xyridaceae, Zingiberaceae). However, transition to mid-late zygomorphy also happened several times among rosids (Fabaceae, Brassicaceae, and Cleomaceae), asterids (Orobanchaceae, Phrymaceae, Lamiaceae, Scrophulariaceae, Calceolariaceae, Asteraceae, and Caprifoliaceae), monocots (Commelinaceae, Orchidaceae), and basal angiosperms (Aristolochiaceae).

DISCUSSION

Developmental Flexibility and Variation of Symmetry Patterns

Tracing developmental expression of symmetry indicated that it does not follow a fixed pattern and that the symmetry expression at each stage could be independent of the previous or the following stages. The symmetry in mature flowers is often independent of the early expression of symmetry. Regardless

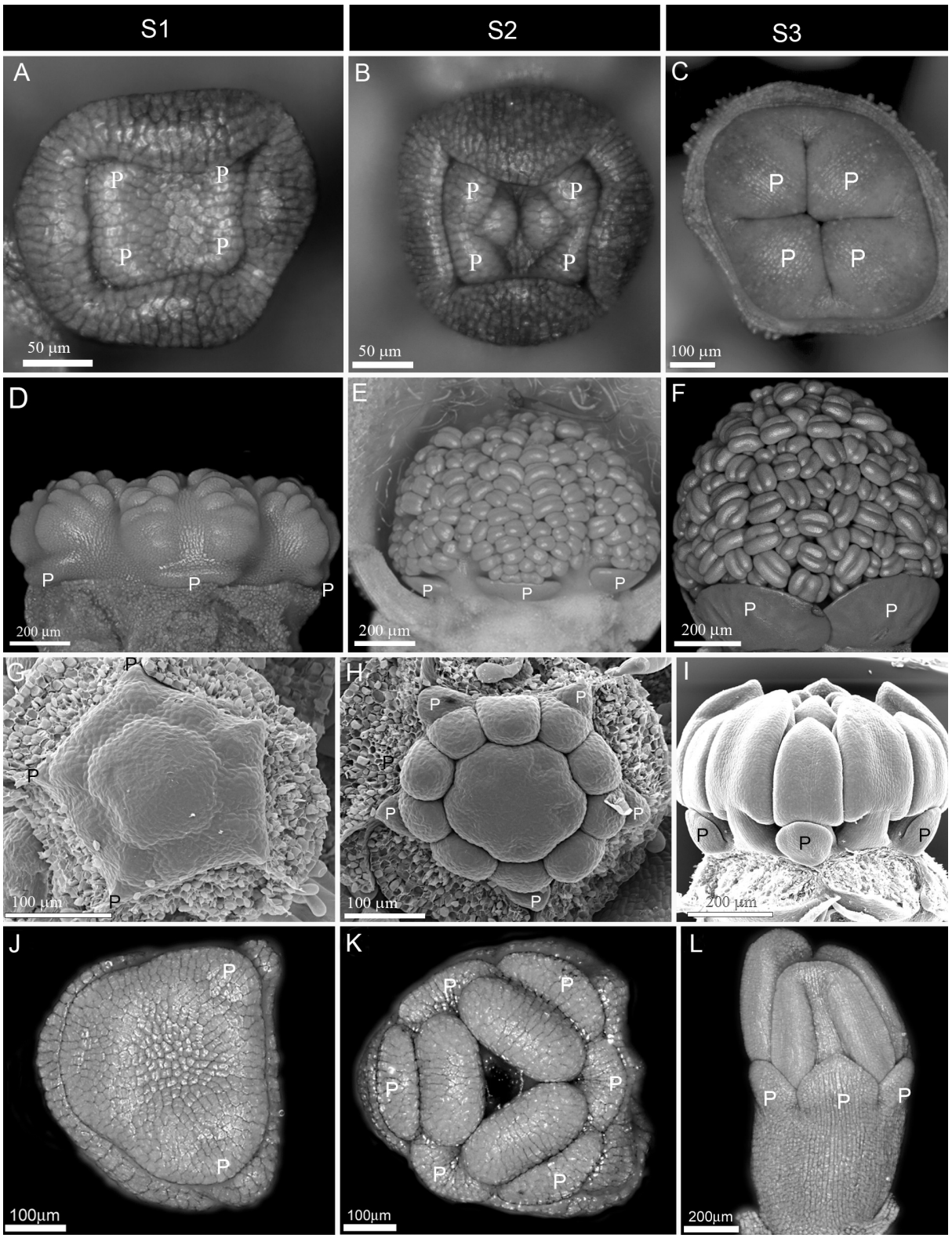

FIGURE 1 | Early to mid-stage establishment of actinomorphy in corolla. **(A–F)** Simultaneous initiation followed by synchronous enlargement and differentiation in *Syringa vulgaris* from Oleaceae **(A–C)** and *Alcea rosea* from Malvaceae **(D–F)**. **(G–I)** Non-simultaneous initiation followed by synchronous enlargement and differentiation in *Zygophyllum fabago* (Zygophyllaceae). **(J–L)** Non-simultaneous initiation of petals within each whorl followed by synchronous enlargement and differentiation in Crocus sativus (Iridaceae). P: petal, S1: Initiation phase, S2: Enlargement phase, S3: Differentiation phase.

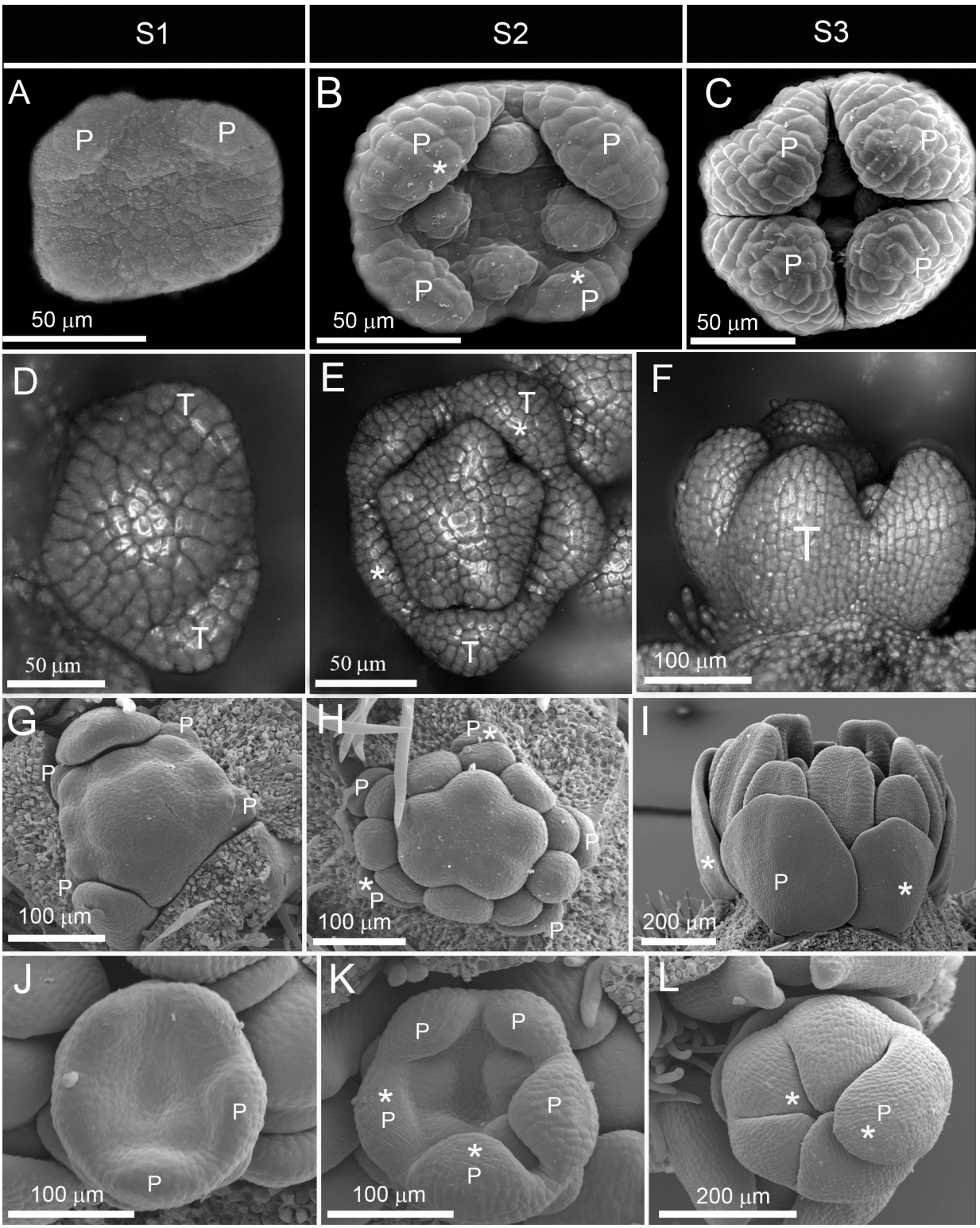

FIGURE 2 | Late establishment of actinomorphy in corolla. **(A–F)** Non-simultaneous initiation followed by asynchronous enlargement and later synchronization of growth during differentiation in *Rubia tinctorium* from Rubiaceae **(A–C)** and *Bougainvillea spectabilis* from Nyctaginaceae **(D–F)**. **(G–L)** Non-simultaneous initiation followed by asynchronous enlargement and differentiation in *Larrea divaricata* from Zygophyllaceae **(G–I)** and *Patrinia gibbosa* from Caprifoliaceae **(J–L)**. P: petal, S1: initiation phase, S2: enlargement phase, S3: differentiation phase. Note the size difference between the largest and the smallest corolla members during asynchronous enlargement and differentiation (shown by stars).

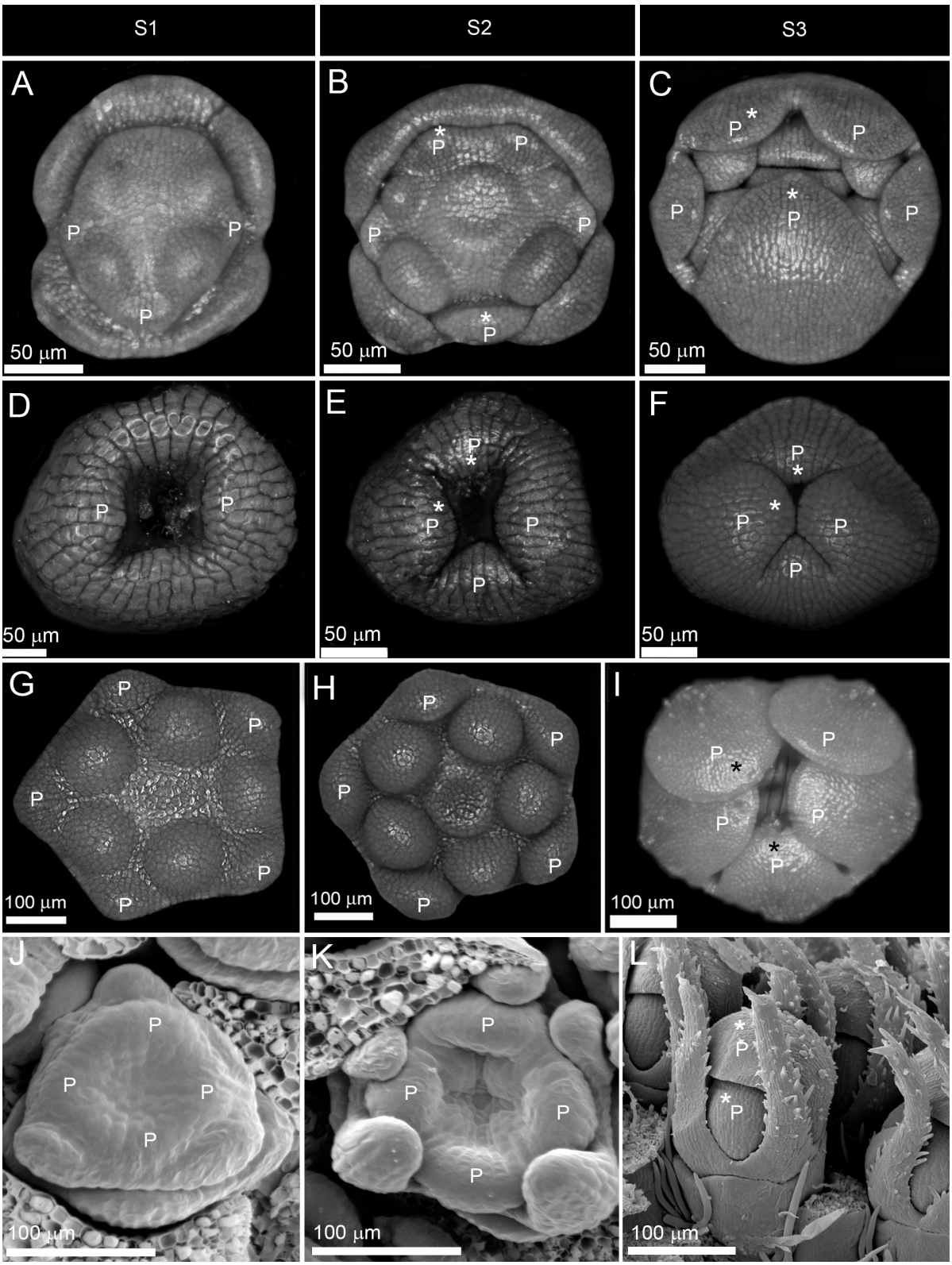

FIGURE 3 | Early and late establishment of zygomorphy in corolla. **(A–F)** Non-simultaneous initiation followed by asynchronous enlargement and differentiation in *Salvia nemorosa* from Lamiaceae **(A–C)** and ray florets of *Osteospermum ecklonis* from Asteraceae **(D–F)**. **(G–L)** Simultaneous initiation followed by synchronous enlargement and asynchronous differentiation in *Verbascum thapsus* from Scrophulariaceae **(G–I)** and *Succisa pratensis* from Caprifoliaceae **(J–L)**. P: petal, S1: initiation phase, S2: enlargement phase, S3: differentiation phase. Note the size difference between the largest and the smallest corolla members during asynchronous enlargement and differentiation (shown by stars).

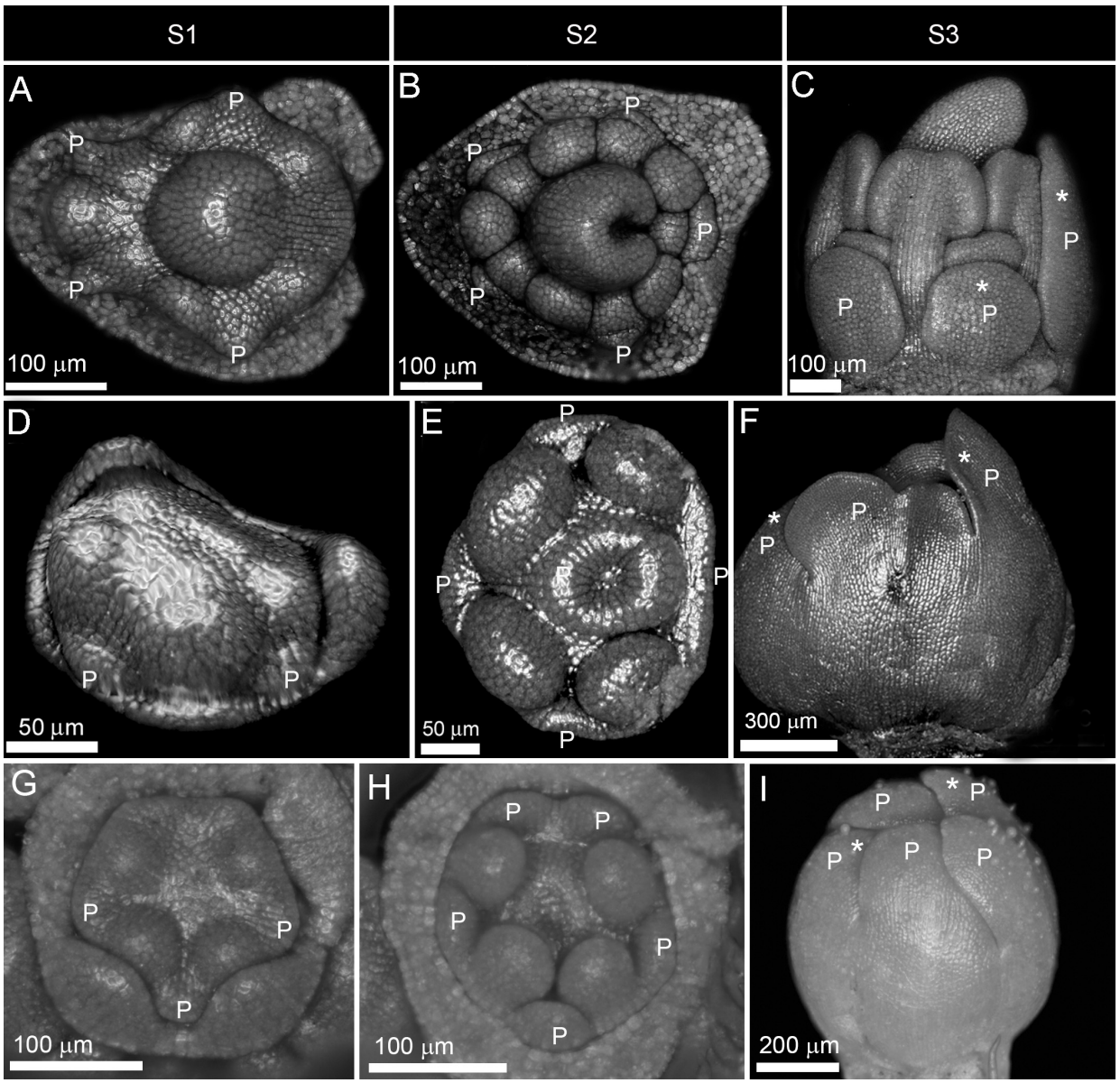

FIGURE 4 | Double change of symmetry in zygomorphic corollas. **(A–I)** Non-simultaneous initiation followed by synchronous enlargement and asynchronous differentiation causing a double shift in symmetry in *Astragalus compactus* from Fabaceae **(A–C)**, *Rhyncocorys elephas* from Orobanchaceae **(D–F)**, and *Ziziphora tenuior* from Lamiaceae **(G–I)**. P: petal, S1: initiation phase, S2: enlargement phase, S3: differentiation phase. Note the size difference between the largest and the smallest corolla members during asynchronous differentiation (shown by stars).

of being actinomorphic or zygomorphic, the majority of flowers were characterized by zygomorphic initiation which was supported as the ancestral state for the angiosperms. The results, therefore, suggest the existence of three independent steps for the establishment of symmetry in the course of ontogeny: organ initiation, enlargement, and differentiation. Hypothetically, if we consider both possible symmetry expressions (zygomorphy or actinomorphy) at each step, the combination of steps will yield eight developmental patterns (**Figure 6**). In agreement with this hypothesis, examples of all predicted symmetry patterns were found among angiosperms. It seems that flexibility in the developmental regulation of floral symmetry provides a broad scope for the evolution of symmetry pattern.

The first insights into the genetic mechanism underlying symmetry expression came from the study of model species *A. majus*. Two recently duplicated TCP family transcription factors, *CYCLOIDEA* (*CYC*) and *DICHOTOMA* (*DICH*), specify the dorsal floral identity (Luo et al., 1996, 1999). The expression of *CYC* and *DICH* is restricted to the dorsal region of the floral meristem, beginning from organ initiation and maintaining throughout enlargement and differentiation (Luo et al., 1996, 1999; Almeida et al., 1997). The function of both genes

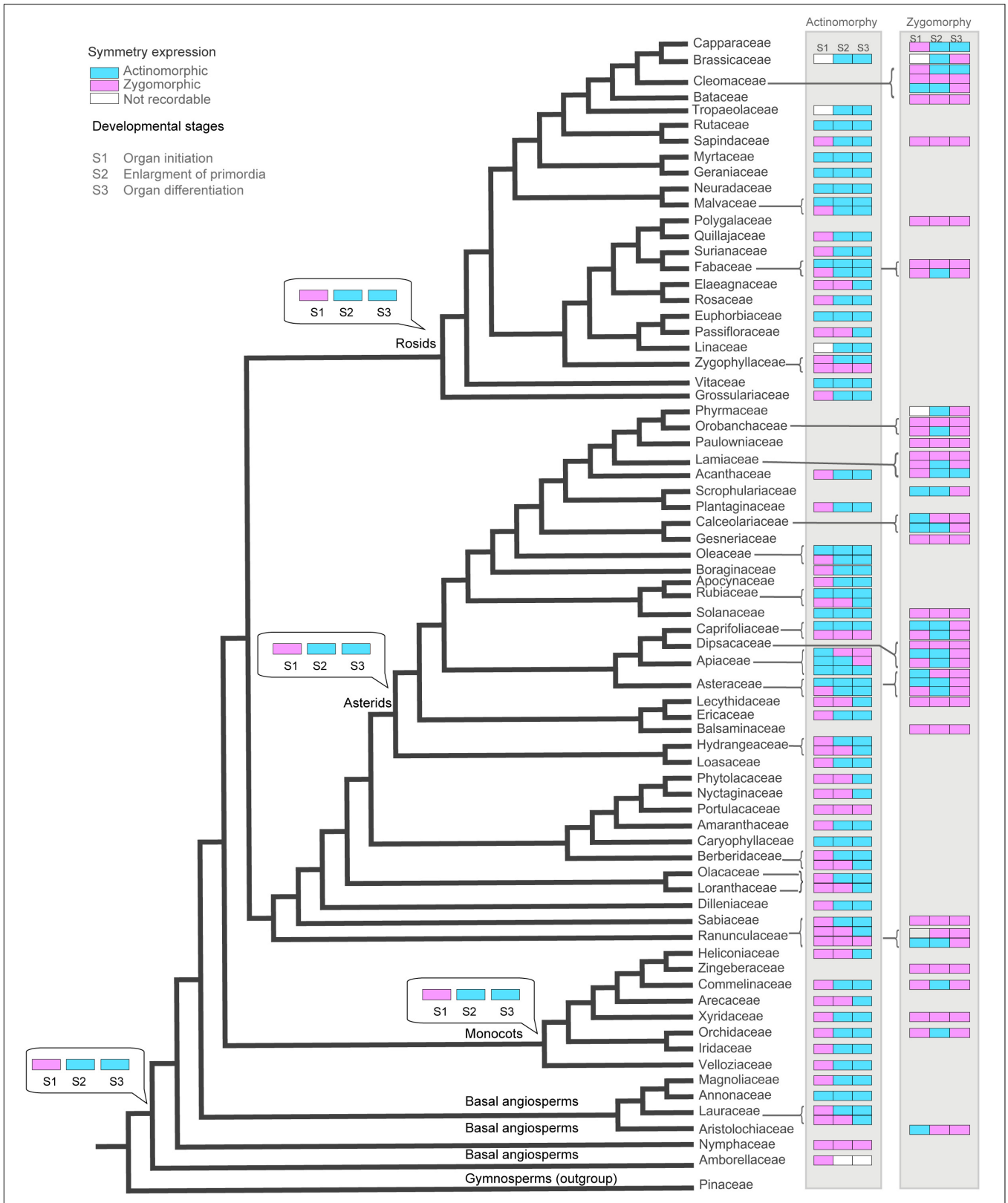

FIGURE 5 | The evolution of corolla symmetry reconstructed on the phylogenetic tree of angiosperms (extracted from Soltis et al., 2011). The ancestral character stats (obtained under Maximum Parsimony method implemented in Mesquite) are shown for the nodes of interest.

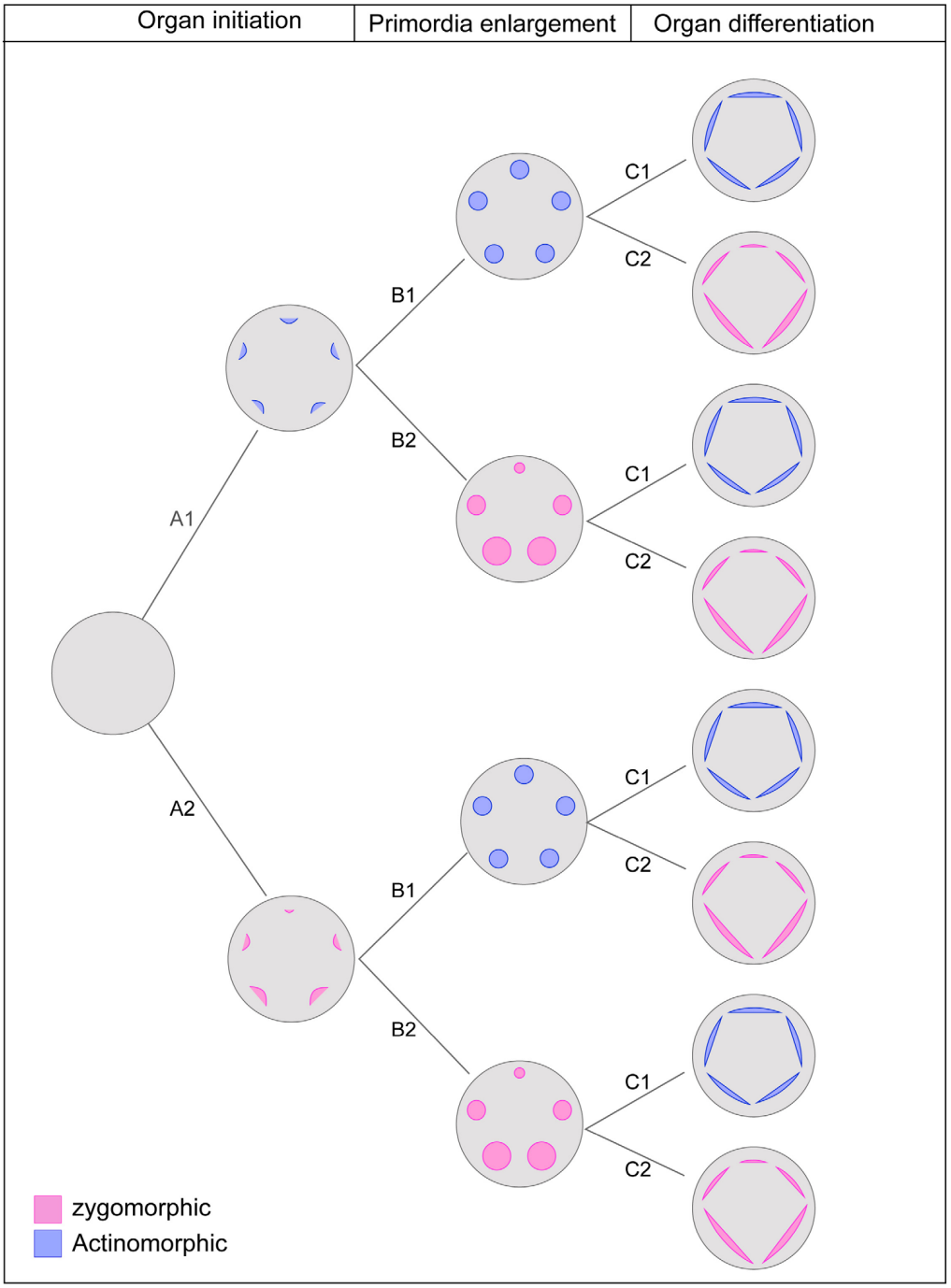

FIGURE 6 | The theoretical pathway of symmetry establishment considering three independent developmental stages with two possible expression of actinomorphy or zygomorphy at each stage. The combination of possible changes results in eight pattern of symmetry expression: Early expression of actinomorphy: A1-B1-C1; Late expression of zygomorphy: A1-B1-C2; Late expression of actinomorphy with a shift at mid stage: A1-B2-C1; Mid-stage expression of zygomorphy: A1-B2-C2; Mid-stage expression of actinomorphy: A2-B1-C1; Late expression of zygomorphy with a shift at mid stage: A2-B2-C1; Late expression of actinomorphy: A2-B2-C1; Early expression of Zygomorphy: A2-B2-C2.

has been shown to be preserved in zygomorphic flowers across different clades of angiosperms (Hileman, 2014). The expression of *CYC* homologes has been studied in relation to the evolutionary transition from zygomorphic to actinomorphic symmetry. In *Plantago*, one *CYC*-like paralog is expressed across the dorsoventral flower axis, while the other paralog has been lost (Reardon et al., 2009; Preston et al., 2011). The combination of expanded *CYC* expression and loss of *CYC* expression, therefore,

mediates the transition to a derived actinomorphy. In *Cadia* and *Tengia*, a similar expansion of one *CYC* paralog across the dorsoventral axis in parallel with the downregulation and loss of expression of the other paralog is suggested to be responsible for the evolution of actinomorphic flowers from zygomorphic ancestors (Citerne et al., 2006; Pang et al., 2010). In contrast, the reversal to radial symmetry in *Psychopterys* and *Sphedamnocarpus* involves the entire loss of both *CYC*-like paralogs (Zhang et al., 2013). An specific pattern of *CYC*-like paralogs is reported in derived actinomorphic flowers of *Bournea* (Zhou et al., 2008). Despite expanded expression of one *CYC*-like paralog, the other paralog is neither lost nor downregulated, but retains dorsal-specific expression at early stage (Zhou et al., 2008). Such transient dorsal-specific expression can explain the initial zygomorphic pattern in *Bournea*. Considering all mentioned examples, I would suggest that changes in the timing, duration, and localization of *CYC*-like gene expression are implicated in the developmental and evolutionary transition of floral symmetry.

Evolution of Symmetry Patterns and Developmental Constraints

Mapping the floral symmetry patterns on the phylogenetic tree indicated the scattered distribution of patterns across angiosperms. Mid-late onset of actinomorphy were found in all major clades including basal angiosperms (Lauraceae), monocots (Arecaceae and Heliconiaceae), eudicots (Ranunculaceae, Olacaceae, Loranthaceae, Berberidaceae, Phytolaccaceae, Nyctaginaceae, and Portulacaceae), asterids (Hydrangeaceae, Lecythidaceae, Caprifoliaceae, Apiaceae, Rubiaceae, and Plantaginaceae), and rosids (Zygophyllaceae, Passifloraceae, and Elaeagnaceae). The same was true for the mid-late onset of zygomorphy with representative examples in eudicots (Ranunculaceae), asterids (Caprifoliaceae, Dipsacaceae, Asteraceae, Calceolariaceae, and Scrophulariaceae), and rosids (Cleomaceae). The expression of symmetry was also versatile within families. The onset of actinomorphy in families such as Ranunculaceae, Oleaceae, Apiaceae, and Zygophyllaceae ranged from early to mid or late development depending on the taxa (see **Supplementary Appendix S1**). A similar variation was found within zygomorphic families. In Lamiaceae, some species like *Marrubium parviflorum*, *Stachys byzantine*, and *Salvia nemorosa* were zygomorphic from petal inception till anthesis, while in *Phlomis armeniana* a double change in symmetry pattern was found (i.e., from early zygomorphy at initiation time to actinomorphy at enlargement and back to zygomorphy at late development) (Naghiloo et al., 2013b, 2014b). Fabaceae represented another zygomorphic family in which both early expression (*Amherstia nobilis*, *Duparquetia orchidacea*) as well as the double change in symmetry pattern (*Astragalus compactus*, *Wisteria sinensis*) were found (Tucker, 2000; Prenner and Klitgaard, 2008; Naghiloo and Dadpour, 2010; Naghiloo et al., 2012). In zygomorphic flowers of Caprifoliaceae, examples of early zygomorphy (*Dipsacus follunum*, *Knautia arvensis*, and *Morina persica*), late zygomorphy (*Succisa pratensis*, *Lonicera periclymenum*) and shift in symmetry pattern (e.g., *Lomelosia palaestina*, *Succisella inflexa*, *Cephalaria transsylvanica*) were found (Naghiloo and Claßen-Bockhoff, 2017). The time of zygomorphy expression in ray flowers of Asteraceae depended on the taxa, ranging from early (e.g., *Osteospermum ecklonis*, *Xeranthemum squarrosum*) to mid or late stages of development (*Senecio glabellus*, *Mutisia coccinea*) (Harris, 1995; Dadpour et al., 2011a, 2012b).

In zygomorphic species of the otherwise radially symmetric family Ranunculaceae, the zygomorphy either expressed at an early stage through precocious initiation of some petal members (e.g., *Delphinium,* Naghiloo Unpublished Data) or at a late stage of development through the formation of a petal spur (*Aconitum*, Mair, 1977; Jabbour et al., 2009). Other examples of zygomorphy in families with predominantly actinomorphic flowers are *Schizanthus* and *Schwenckia* from Solanaceae, and *Iberis amara* from Brassicaceae. In the two first species, zygomorphy is apparent from the onset of organ initiation (Ampornan and Armstrong, 1988, 1989), while in *Iberis amara* zygomorphy establish through heterogeneous growth of petals at the late stage of development (Busch and Zachgo, 2007).

Given the parallel occurrence of symmetry patterns (early, mid or late expression) in different angiosperm clades and their variation among closely related species, the phylogenetic signal (although not tested here) seems unlikely to be the main determinant of the symmetry pattern. I would rather suggest that developmental constraints exerted by the entire inflorescence, bracts, neighbor flowers or neighbor organs within a flower could provide a possible explanation for the observed variation of symmetry expression. As an example, I refer to the correlation found between cymose monochasial inflorescences and late expression of actinomorphy in some taxa (*Centranthus*, Valerianaceae, *Qualea*, and Vochysiaceae) (Eichler, 1878). In *Patrinia*, which expresses actinomorphy at a very late stage of development, the flowers are arranged in dichasia with monochasial peripheral braches. In early floral development, the two petals and stamens on the side toward the weaker subsequent ramification of the dichasium appear earlier than their counterparts (Hofmann and Gottmann, 1990). Beside the ramification pattern of inflorescence, the mechanical forces generated by subtending leaves or bracts can also influence the order of organ initiation (Naghiloo et al., 2012). An association between order of initiation and the presence of bracteoles has been suggested for some members of Papilionoideae (Prenner, 2004).

Another example of developmental constraints which can influence the pattern of symmetry expression is found in species with a double change of floral symmetry (i.e., from zygomorphy to actinomorphy and back to zygomorphy). The size gradient in mature zygomorphic flowers often follows the initiation sequence; organs that are initiated first are usually the largest at maturity and the pattern of early symmetry is maintained throughout development. However, in some taxa (e.g., Papilionoideae, Lamiaceae, Orobanchaceae, Dipsacaceae) the size gradient in mature petals is opposite to the direction of their initiation; the last initiated petal is the largest one at maturity. In such cases, a period of synchronization is required

before the new size gradient establishes through differential growth. The mismatch between the direction of zygomorphy in early and late stages could, therefore, explain double changes of symmetry during development.

DATA AVAILABILITY STATEMENT

The datasets generated for this study is available as **Supplementary Material** online.

AUTHOR CONTRIBUTIONS

SN performed all aspects of this research.

SUPPLEMENTARY MATERIAL

The Supplementary Material for this article can be found online at: https://www.frontiersin.org/articles/10.3389/fevo.2020.00104/full#supplementary-material

REFERENCES

Almeida, J., Rocheta, M., and Galego, L. (1997). Genetic control of flower shape in *Antirrhinum majus*. *Development* 124, 1387–1392.

Ampornan, L., and Armstrong, J. (1988). The floral ontogeny of Schizanthus, a zygomorphic member of the Solanaceae. *Am. J. Bot.* 75:54.

Ampornan, L., and Armstrong, J. (1989). The floral ontogeny of Salpiglossis, a zygomorphic member of the Solanaceae. *Am. J. Bot.* 76:64.

Busch, A., and Zachgo, S. (2007). Control of corolla monosymmetry in the Brassicaceae Iberis amara. *Proc. Natl. Acad. Sci. U.S.A.* 104, 16714–16719. doi: 10.1073/pnas.0705338104

Citerne, H., Jabbour, F., Nadot, S., and Damerval, C. (2010). "The evolution of floral symmetry," in *Advances in Botanical Research*, eds J.-C. Kader and M. Delseny (Cambridge, MA: Academic Press), 85–137. doi: 10.1016/s0065-2296(10)54003-5

Citerne, H., Toby Pennington, R., and Cronk, Q. (2006). An apparent reversal in floral symmetry in the legume Cadia is a homeotic transformation. *Proc. Natl. Acad. Sci. U.S.A.* 103, 12017–12020. doi: 10.1073/pnas.0600986103

Dadpour, M. R, Naghiloo, S., Gohari, G., and Aliakbari, M. (2011a). Inflorescence and floral ontogeny in *Osteospermum ecklonis* L. (Asteraceae). *Botany* 89, 605–614. doi: 10.1139/b11-052

Dadpour, M. R., Naghiloo, S., Peighambardoust, S. H., Panahirad, S., Aliakbari, M., and Movafeghi, A. (2011b). Comparison of floral ontogeny in wild-type and double-flowered phenotypes of *Syringa vulgaris* L. (Oleaceae). *Sci. Horticult.* 127, 535–541. doi: 10.1016/j.scienta.2010.12.004

Dadpour, M. R., Naghiloo, S., and Gohari, G. (2012a). Inflorescence and floral ontogeny in *Crocus sativus* L. (Iridaceae). *Flora* 27, 257–263. doi: 10.1016/j.flora.2012.02.001

Dadpour, M. R., Naghiloo, S., and Neycharan, S. F. (2012b). The development of pistillate and perfect florets in *Xeranthemum squarrosum* (Asteraceae). *Plant Biol.* 14, 234–243. doi: 10.1111/j.1438-8677.2011.00469.x

Eichler, A. W. (1878). *Blüthendiagramme. II*. Leipzig: Engelmann.

Endress, P. (2010). Evolution of floral symmetry. *Curr. Opin. Plant Biol.* 4, 86–91. doi: 10.1016/s1369-5266(00)00140-0

Endress, P. K. (1999). Symmetry in flowers: diversity and evolution. *Int. J. Plant Sci.* 160, S3–S23.

Endress, P. K. (2012). The immense diversity of floral monosymmetry and asymmetry across angiosperms. *Bot. Rev.* 78, 345–397. doi: 10.1007/s12229-012-9106-3

Endress, P. K., and Doyle, J. A. (2009). Reconstructing the ancestral angiosperm flower and its initial specializations. *Am. J. Bot.* 96, 22–66. doi: 10.3732/ajb.0800047

Harris, E. M. (1995). Inflorescence and floral ontogeny in Asteraceae: A synthesis of historical and current concepts. *Bot. Rev.* 61:93. doi: 10.1007/bf02887192

Hileman, L. C. (2014). Trends in flower symmetry evolution revealed through phylogenetic and developmental genetic advances. *Philos. Trans. R. Soc. Lond. B Biol. Sci.* 369:20130348. doi: 10.1098/rstb.2013.0348

Hofmann, U., and Gottmann, J. (1990). Morina L. und Triplostegia Wall. ex DC. im Vergleich mit Valerianaceae und Dipsacaceae. *Bot. Jahrb. Syst.* 111, 499–553.

Jabbour, F., Ronse De Craene, L. P., Nadot, S., and Damerval, C. (2009). Establishment of zygomorphy on an ontogenic spiral and evolution of perianth in the tribe Delphinieae (Ranunculaceae). *Ann. Bot.* 104, 809–822. doi: 10.1093/aob/mcp162

Luo, D., Carpenter, R., Copsey, L., Vincent, C., Clark, J., and Coen, E. (1999). Control of organ asymmetry in flowers of Antirrhinum. *Cell* 99, 367–376. doi: 10.1016/s0092-8674(00)81523-8

Luo, D., Carpenter, R., Vincent, C., Copsey, L., and Coen, E. (1996). Origin of floral asymmetry in Antirrhinum. *Nature* 383, 794–799. doi: 10.1038/383794a0

Maddison, W. P., and Maddison, D. R. (2015). *Mesquite: A Modular System for Evolutionary Analysis*. Available online at: Version 3.04. http://mesquiteproject.org (accessed July, 2019).

Mair, O. (1977). Zur Entwicklungsgeschichte monosymmetrischer Dicotylen-Blüten. *Diss. Bot.* 38, 260–274.

Naghiloo, S., and Classen-Bockhoff, R. (2016). Developmental analysis of merosity and sexual morphs in Rubiaceae: A case study in Rubia and Cruciata. *Flora* 222, 52–59. doi: 10.1016/j.flora.2016.03.010

Naghiloo, S., and Claßen-Bockhoff, R. (2017). Developmental changes in time and space promote evolutionary diversification of flowers: A case study in Dipsacoideae. *Front. Plant Sci.* 8:1665–1665. doi: 10.3389/fpls.2017.01665

Naghiloo, S., and Dadpour, M. (2010). Floral ontogeny in *Wisteria sinensis* (Fabaceae: Faboideae: Millettieae) and its systematic implications. *Aust. Syst. Bot.* 23, 393–400. doi: 10.1071/SB10027

Naghiloo, S., Dadpour, M. R., and Movafeghi, A. (2012). Floral ontogeny in *Astragalus compactus* (Leguminosae: Papilionoideae: Galegeae): variable occurrence of bracteoles and variable patterns of sepal initiation. *Planta* 235, 793–805. doi: 10.1007/s00425-011-1538-1

Naghiloo, S., Esmaillou, Z., and Dadpour, M. R. (2014a). Comparative floral ontogeny of single-flowered and double-flowered phenotypes of *Alcea rosea* (Malvaceae). *Aust. J. Bot.* 62, 217–228. doi: 10.1071/BT14070

Naghiloo, S., Khodaverdi, M., Nikzat Siahkolaee, S., and Dadpour, M. R. (2014b). Comparative floral development in Lamioideae (Lamiaceae): Marrubium, Phlomis, and Stachys. *Plant Syst. Evol.* 300, 1269–1283. doi: 10.1007/s00606-013-0960-1

Naghiloo, S., Esmaillou, Z., Gohari, G., and Dadpour, M. (2013a). Comparative inflorescence and floral ontogeny in the genus Mentha (Mentheae: Nepetoideae: Lamiaceae): Variable sequences of organ appearance and random petal aestivation. *Plant Syst. Evol.* 300, 329–345. doi: 10.1007/s00606-013-0885-8

Naghiloo, S., Khodaverdi, M., Esmaillou, Z., Dadpour, M., and Rudall, P. (2013b). Comparative floral development in the tribe Mentheae (Nepetoideae: Lamiaceae) and its bearing on the evolution of floral patterns in asterids. *J. Syst. Evol.* 52, 195–214. doi: 10.1111/jse.12072

Naghiloo, S., Reza Fathollahi, M., and Claßen-Bockhoff, R. (2015). Flower ontogeny in Capparis spinosa (Capparaceae) with special emphasis on symmetry expression. *Nordic J. Bot.* 33, 754–760. doi: 10.1111/njb.00768

Pang, H., Sun, Q. W., He, S. Z., and Wang, Y.-Z. (2010). Expression pattern of CYC-like genes relating to a dorsalized actinomorphic flower in Tengia (Gesneriaceae). *J. Syst. Evol.* 48, 309–317. doi: 10.1111/j.1759-6831.2010.00091.x

Prenner, G. (2004). New aspects in floral development of Papilionoideae: initiated but suppressed bracteoles and variable initiation of sepals. *Ann. Bot.* 93, 537–545. doi: 10.1093/aob/mch076

Prenner, G., and Klitgaard, B. (2008). Towards unlocking the deep nodes of Leguminosae: Floral development and morphology of the enigmatic *Duparquetia orchidacea* (Leguminosae, Caesalpinioideae). *Am. J. Bot.* 95, 1349–1365. doi: 10.3732/ajb.0800199

Preston, J. C., Martinez, C. C., and Hileman, L. C. (2011). Gradual disintegration of the floral symmetry gene network is implicated in the evolution of a wind-pollination syndrome. *Proc. Natl. Acad. Sci. U.S.A.* 108, 2343–2348. doi: 10.1073/pnas.1011361108

Reardon, W., Fitzpatrick, D. A., Fares, M. A., and Nugent, J. M. (2009). Evolution of flower shape in Plantago lanceolata. *Plant Mol. Biol.* 71, 241–250. doi: 10.1007/s11103-009-9520-z

Reyes, E., Sauquet, H., and Nadot, S. (2016). Perianth symmetry changed at least 199 times in angiosperm evolution. *Taxon* 65, 945–964. doi: 10.12705/655.1

Soltis, D. E., Smith, S. A., Cellinese, N., Wurdack, K. J., Tank, D. C., Brockington, S. F., et al. (2011). Angiosperm phylogeny: 17 genes, 640 taxa. *Am. J. Bot.* 98, 704–730. doi: 10.3732/ajb.1000404

Tucker, S. C. (1999). Evolutionary lability of symmetry in early floral development. *Int. J. Plant Sci.* 160, S25–S39.

Tucker, S. C. (2000). Floral development in Tribe Detarieae (Leguminosae: Caesalpinioideae): Amherstia, Brownea, and Tamarindus. *Am. J. Bot.* 87, 1385–1407. doi: 10.2307/2656867

Tucker, S. C. (2003). Floral development in legumes. *Plant Physiol.* 131, 911–926. doi: 10.1104/pp.102.017459

Zhang, W., Steinmann, V. W., Nikolov, L., Kramer, E. M., and Davis, C. C. (2013). Divergent genetic mechanisms underlie reversals to radial floral symmetry from diverse zygomorphic flowered ancestors. *Front. Plant. Sci.* 4:302. doi: 10.3389/fpls.2013.00302

Zhou, X. R., Wang, Y. Z., Smith, J. F., and Chen, R. (2008). Altered expression patterns of TCP and MYB genes relating to the floral developmental transition from initial zygomorphy to actinomorphy in Bournea (Gesneriaceae). *New Phytol.* 178, 532–543. doi: 10.1111/j.1469-8137.2008.02384.x

Conflict of Interest: The author declares that the research was conducted in the absence of any commercial or financial relationships that could be construed as a potential conflict of interest.

frontiers in Cell and Developmental Biology

ORIGINAL RESEARCH
published: 30 April 2020
doi: 10.3389/fcell.2020.00313

The 'Male Flower' of *Ricinus communis* (Euphorbiaceae) Interpreted as a Multi-Flowered Unit

Regine Claßen-Bockhoff and Hebert Frankenhäuser*

Institute of Organismic and Molecular Evolution, Faculty of Biology, Johannes Gutenberg University of Mainz, Mainz, Germany

One of the most exciting questions in botany refers to the nature of the angiosperm flower. While most flowering structures are easily identified as flowers, there are few examples lying in-between flowers and inflorescences. Such an example is the staminate unit ('male flower') in *Ricinus communis* (Euphorbiaceae) famous for its branched 'staminal trees.' The units were controversially interpreted in the past. Today, they are seen as flowers with multiple branched stamen-fascicles. In the present paper, the recently described floral unit meristem is used to reinterpret the staminate units in *Ricinus*. This meristem shares almost all characteristics with a flower meristem, but differs from it in the number of fractionation steps resulting in multi-flowered units. Reinvestigation of the development confirms previous studies illustrating up to six fractionation steps before the meristem merges into anther-formation. Fractionation starts early at a naked meristem, covers simultaneously its whole surface, shows an all-side instead of unidirectional splitting pattern and continues repeatedly. Based on the present knowledge, it is plausible to interpret the 'male flower' as a floral unit with multiple staminate flowers each reduced to a single anther. This interpretation is in accordance with the many examples of reduced flowers in the Euphorbiaceae.

Keywords: development, floral unit meristem, flower-inflorescence boundary, stamen homology, staminal trees

OPEN ACCESS

Edited by:
Alessandro Minelli, University of Padova, Italy

Reviewed by:
Dmitry D. Sokoloff, Lomonosov Moscow State University, Russia
Clinton Whipple, Brigham Young University, United States

****Correspondence:***
Regine Claßen-Bockhoff
classenb@uni-mainz.de

Specialty section:
This article was submitted to Evolutionary Developmental Biology, a section of the journal Frontiers in Cell and Developmental Biology

Received: *09 January 2020*
Accepted: *08 April 2020*
Published: *30 April 2020*

Citation:
Claßen-Bockhoff R and Frankenhäuser H (2020) The 'Male Flower' of Ricinus communis (Euphorbiaceae) Interpreted as a Multi-Flowered Unit. Front. Cell Dev. Biol. 8:313. doi: 10.3389/fcell.2020.00313

INTRODUCTION

One of the most exciting and fundamental questions in botany refers to the nature of the angiosperm flower. In the past, the flower was interpreted as an euanthium, which is a monaxial shoot with modified leaves (von Goethe, 1790; Arber and Parkin, 1907; Glover, 2007; Ronse De Craene, 2010), or as a highly reduced polyaxial system, a pseudanthium (Delpino, 1889, 1890; von Wettstein, 1901–1908 and followers of alternative flower theories). Today, the euanthium theory is widely accepted though many discrepancies still exist (reviewed by Claßen-Bockhoff, 2016).

Conflicts occur when floral organs change position as in the Triuridaceae *Lacandonia* (Rudall, 2003; Ambrose et al., 2006), when floral organs appear in high numbers as in *Centrolepis* (Centrolepidaceae, Sokoloff et al., 2009) and *Tupidanthus* (Araliaceae, Sokoloff et al., 2007) or when flowers are highly reduced and aggregated as in *Euphorbia* (Prenner and Rudall, 2007). In these cases, the term pseudanthium reappears indicating that the morphological nature of the angiosperm flowers is still up for debate.

An obscure structure is the 'male flower' of the castor oil plant *Ricinus communis* L. (Euphorbiaceae). It is characterized by unique 'staminal trees,' each bearing several anthers on a branched supporter (**Figure 1C**). This peculiar structure was interpreted in various ways (reviewed by Prenner et al., 2008). Delpino (1889, 1890) called it a pseudanthium, a term introduced by him to characterize contracted inflorescences ('infiorescenze contratte') hardly distinguishable from flowers. Zimmermann (1930) used the structure to extend his telome theory to higher plants, a view followed by Wilson (1942). Lam (1948) noticed the appendages below the anthers and argued that these structures could be the subtending bracts of unistaminate flowers, consequently interpreting the 'flower' as an inflorescence. Since van der Pijl (1952) critically discussed the different views, the staminate units were mainly interpreted as flowers with multiple branched stamen fascicles and connective effigurations.

Prenner et al. (2008) reinvestigated the development of the 'male flower' in *Ricinus* to clarify its flower vs. inflorescence nature in a morphogenetic and phylogenetic context. The authors confirmed the repeated meristem fractionation during the process of staminal fascicle formation already documented by Payer (1857) and Michaelis (1924). All authors came to the conclusion that the staminate unit might be rather interpreted as a polyandric flower than an inflorescence.

The difficulty to interpret the unusual structure in *Ricinus* may be intimately connected with the reference system only considering flowers and inflorescences. Consulting the floral unit meristem (FUM), introduced as a third reproductive meristem some years ago (Claßen-Bockhoff and Bull-Hereñu, 2013), may help to disentangle the morphological nature of intermediate structures.

Traditionally, inflorescence and flower meristems are both referred to the shoot apical meristem (SAM). They produce either flower bearing shoot systems (inflorescences) or short shoots with reproductive organs and often preceeding sterile organs (flowers). However, detailed studies on vegetative and reproductive meristems indicate that two different meristems exist producing multi-flowered units, the inflorescence meristem (IM) resembling the SAM and the FUM more similar to a flower meristem (FM) (Claßen-Bockhoff and Bull-Hereñu, 2013; Claßen-Bockhoff, 2016).

- IMs differ from SAMs in having a limited apical growth activity and developing immediately flowers or partial inflorescences from axillary meristems. Only rarely, subtending bracts are lacking. The IMs still produce new primordia in an acropetal sequence and share, thus, the process of segregation with SAMs. Segregation is defined as the lateral separation of meristem parts (primordia) at an ongoing growing meristem (Claßen-Bockhoff and Arndt, 2018).
- FMs differ from SAMs and IMs in being determinate. They lack apical growth activity and are instead able to expand toward different directions. Flower development usually starts with meristem enlargement forming a naked stage which is then used completely by floral organ formation. To distinguish this process from segregation, it is called fractionation (Claßen-Bockhoff, 2016; Claßen-Bockhoff and Arndt, 2018). Fractionation is restricted to determinate meristems, which are much more affected by spatial constraints than segregating meristems.
- FUMs share almost all characteristics with FMs, i.e., they are determinate, able to expand and to use the meristem completely by fractionation. However, they differ from FMs in the number of fractionation steps. In the heads of Asteraceae, for instance, the first fractionation results in the formation of FMs, which, in a second step, gives rise to floral organs. In secondary heads, the first fractionation originates head meristems, the second FMs and the third floral organ primordia (Claßen-Bockhoff, 2016). Subtending bracts are often lacking in floral units.

Beyond Asteraceae, FUMs were already proven in more than 10 angiosperm families (Claßen-Bockhoff and Bull-Hereñu, 2013; Stützel and Trovó, 2013; Naghiloo and Claßen-Bockhoff, 2017; Claßen-Bockhoff and Arndt, 2018). It is, thus, evident that multi-flowered units traditionally summarized as inflorescences fall into two different groups (Bull-Hereñu and Claßen-Bockhoff, 2011).

The present paper reinvestigates the development of the inflorescence, carpellate flowers and staminate units in *R. communis* and tests the hypothesis, that the staminate unit is neither a flower nor an inflorescence, but a floral unit.

MATERIALS AND METHODS

Ricinus is a monotypic genus most likely originating from N-Africa. The only species, *R. communis* L., produces the castor oil which has been used for 1000s of years (van Welzen, 1998). The plant, cultivated and spread throughout the subtropics and tropics, is morphologically highly diverse. The results of the present study refer to plants cultivated in Germany.

Inflorescence architecture, flower morph distribution and flowering sequence were studied on 13 plants cultivated in private and public gardens around Mainz, Germany. Each plant was observed daily for 14 days and branching pattern and flowering sequence were recorded by notes and photos.

For the morphogenetic analysis, plant material was taken from the Botanical Garden of Mainz University. Inflorescence buds and young inflorescences of different developmental stages were collected and fixed in 70% EtOH. In total, 5 buds and 10 young inflorescences were dissected each providing 20–50 floral meristems of different age. The samples were dehydrated in an alcohol-acetone series, critical point-dried (BAL-TEC CPD030) and mounted and sputter coated with gold (BAL-TEC SCD005). Finally, they were observed and analyzed using the scanning electron microscope (ESEM XL-30 Philips). All steps were conducted according to the manufacturer's protocol.

To illustrate meristem expansion during the process of repeated fractionation, the diameter of the meristem (without collar) was measured using SEM pictures. At least 10 samples of each fractionation step were included. As the meristem

FIGURE 1 | *Ricinus communis*. **(A,B)** Inflorescence in different flowering stages. Carpellate flowers in distal and staminate units in proximal positions. **(C)** Staminate unit composed of five reddish bracts/sepals and about 25 much-branched staminal trees, each branch ending in an anther. **(D)** Rare case of inflorescences with a staminate unit in terminal position. **(E)** Rare case of hermaphrodite units consisting of a gynoecium in the center surrounded by few staminal trees.

expands hemispherically, the surface plane was calculated using the formula for measuring the surface of a sphere (3,14 x diameter^2) divided by two. This rough approximation was used to depict meristem expansion rather than to provide reliable quantitative data.

The inflorescence is usually interpreted as being composed of male and female flowers each surrounded by a calyx. As the homology of the staminate unit (male flower) is the topic of the present paper, we use neutral terms.

In the following, we distinguish carpellate flowers with a calyx and staminate units with a collar. We avoid the terms 'female' and 'male' as they belong to the sexual generation of the gamatophyte. We restrict the term 'stamen fascicle' to flowers with secondary polyandry and use the term 'staminal tree' as a descriptive term to characterize the unique structure in *Ricinus*.

RESULTS

Ricinus communis is a fast-growing herb reaching a height of several meters. The main axis and all lateral axes of first and higher branch orders terminate each in a much-branched, monoecious inflorescence (**Figures 1A,B**, **2B**). The terminal inflorescence (**Figure 2A**: T) is the largest one and flowers first. It is followed by first order lateral inflorescences, which decrease in size top down and flower in basipetal sequence

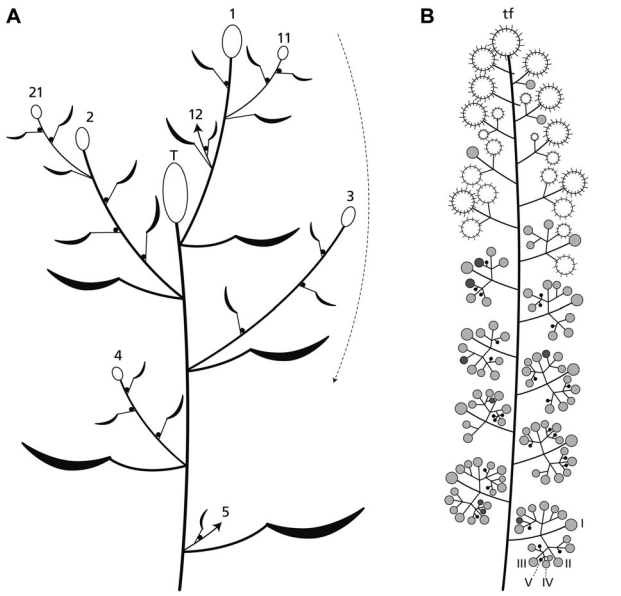

FIGURE 2 | Plant and inflorescence architecture. **(A)** The main axis ends in a terminal inflorescence (T). Lateral axes (1–4) also produce terminal inflorescences which flower in basipetal direction (arrow). Uppermost branches overtop the terminal inflorescence and continue to branch (11, 21) in a sympodial manner. **(B)** The inflorescence is a thyrse with a terminal unit (usually a terminal flower: tf) and up to five branch orders (I–V). Its distal part bears predominantly carpellate flowers (large circles), the proximal one staminate units (small circles). The pictured inflorescence is at the end of anthesis. The carpellate flowers are already fruiting, most of the staminate units are in the postfloral stage (gray) few of them are flowering (dark gray) or still in the bud stage (black).

(**Figure 2A**; arrow). The distal branches overtop the main axis continuing in a sympodial way. All leaves are large and frondose and produce extrafloral nectaries below the peltate part of the lamina. These nectaries and additional ones at the nodes of the plants attract ants.

Inflorescence Architecture and Development

The inflorescence is a thyrse with many laterally arranged, almost sessile cymes. It is usually determined by a carpellate flower (**Figure 2B**: tf) and only rarely by a staminate unit. The proximal cymes are dichasially branched up to the fifth branch order (**Figures 2B**: I–V, **3D**: I–IV), the higher orders sometimes ending monochasially. They bear exclusively staminate units. The tip of the thryrse is usually crowned by a carpellate flower. Only rarely (19%, $n = 39$), a staminate unit occupies the terminal position (**Figures 1D**, **3F**). The distal branches are less branched than the proximal ones and bear carpellate flowers only.

Between the two unisexual zones, an intermediate zone appears bearing carpellate flowers and staminate units in mixed patterns (**Figure 2B**). On average, a single terminal inflorescence produces 15–21 carpellate flowers and 130–140 staminate units ($n = 5$) illustrating that there are about 7.5-times more staminate units than carpellate flowers. However, the general pattern is not strictly fixed as to the size of the inflorescence and the relative number of carpellate flowers vs. staminate units. In one case, an inflorescence was predominantly carpellate producing carpellate flowers even in the proximal part. As further exceptions, hermaphrodite units were found (**Figures 1E**, **4D,E**) occupying the terminal position or the first order position in the intermediate zone.

The inflorescence develops from an inflorescence meristem. It segregates lateral units in an acropetal order each composed of a bract and its axillary meristem (**Figure 3A**: IM). The axillary meristems produce the cymes. While the tip of the young inflorescence still segregates new units, the axillary meristems of the proximal bracts start to initiate meristems of 2nd and 3rd order (**Figure 3A**: I–III). They immediately subdivide into two transversely arranged prophylls and a central primordium giving rise to either a carpellate flower or staminate unit. The central primordium develops a ring-like bulge originating the calyx (carpellate flower) or collar (staminate unit), respectively (**Figures 3A,B**). This structure grows very fast and has to be removed to observe further meristem development.

The terminal unit of the inflorescence, once formed, develops faster than the uppermost lateral flowers (**Figures 3B,C**). The lateral cymes consecutively produce primordia (**Figure 3D**: I–IV) in a sympodial-dichasial manner presenting different developmental stages at the same time (**Figure 3E**).

Development of Carpellate Flowers

The carpellate flower consists of a single trimerous gynoecium surrounded by a synsepalous calyx. In rare cases, single or many staminal trees appear outside the gynoecium altering the carpellate flower into a hermaphrodite unit (**Figures 4D,E**).

The meristem of a young carpellate flower is dome-shaped (**Figure 3B**). The pentamerous calyx early develops and envelops the remaining naked meristem (**Figures 3C**, **4A**: ca). This meristem forms a ring-like bulge which gives rise to the gynoecium wall (**Figure 4A**: gw). Further development involves the continuous growth of this wall and the formation of three septa subdividing the gynoecium into three locules. In each locule, a single ovule appears in axial position (**Figure 4A**: arrow). At an older stage, the three carpel lobes give rise to three bifurcate styles (**Figure 4B**). Their inner side is covered with papillate outgrowths enlarging the surface considerably (**Figure 4C**). During anthesis, the stylar arms are reddish and spread backward (**Figure 1A**); the papillate surface gets sticky and catches pollen grains. In old buds, the gynoecium is covered by long hairs which are greenish during anthesis (**Figure 1A**). In the fruiting stage they become rather long, red and stiff providing the young fruits with their characteristic prickly look (**Figure 1B**).

At the base of young gynoecia bulges appear which do not develop anymore (**Figure 4A**: circles). However, as to their position they may have the potential to originate staminal trees.

Development of Staminate Units and Staminal Trees

Staminate units ('male flowers') consist of 20–26 staminal trees surrounded by five sepal-like structures (**Figure 1C**), which are

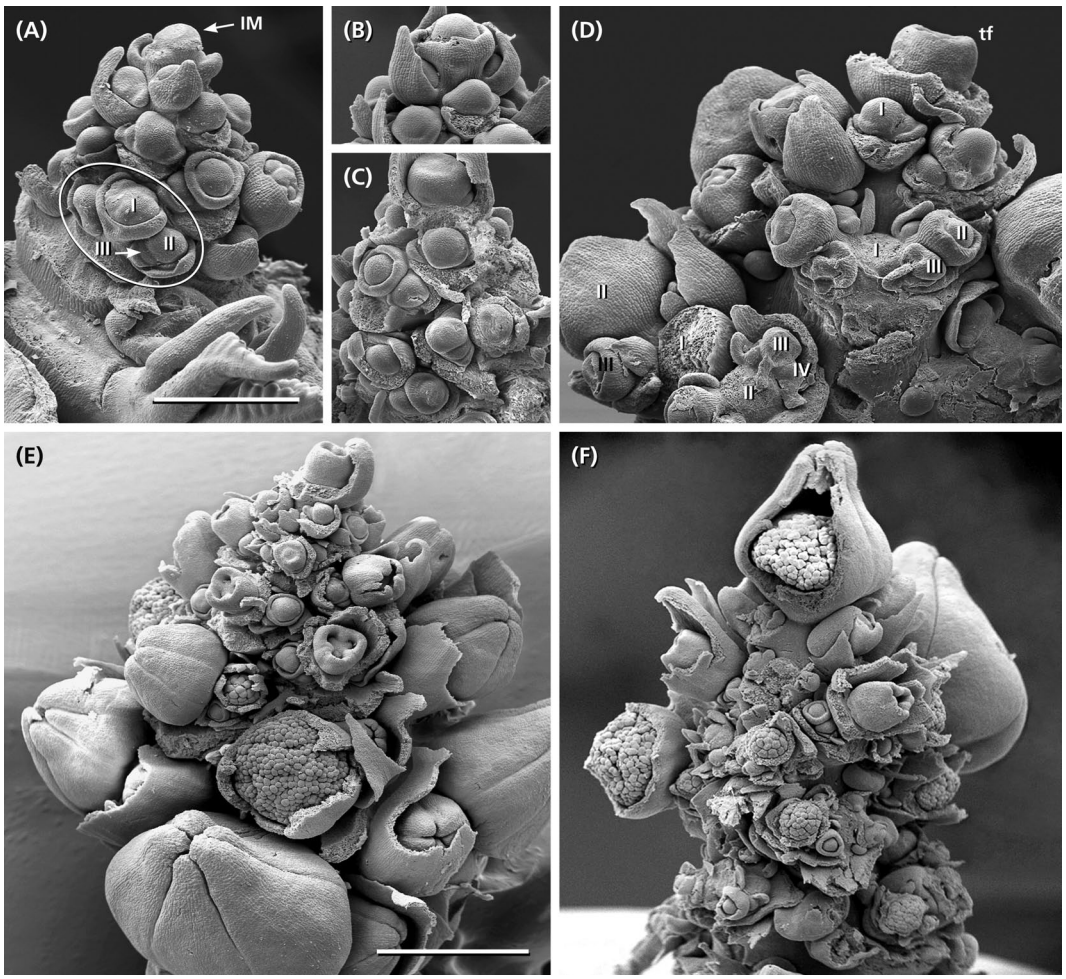

FIGURE 3 | Inflorescence development. **(A)** Young inflorescence with an inflorescence meristem (IM) still segregating bracts and axillary meristems. Developmental sequence is acropetal along the main axis and ordinal within the lateral branches (I, II, III). Cymes start with a regular sympodial-dichasial pattern. **(B,C)** The tip of the IM merges into a carpellate flower surrounded by a synsepalous calyx. **(D)** Detail of a more developed inflorescence already branched up to the forth order (I–IV). Some flowers removed to show the regular dichasial branching pattern. **(E)** Side view of a young inflorescence showing the acropetal development of the lateral branches. In part of the flowers, the outer enveloping elements removed to show the developmental stage of the carpellate flowers and staminate units. **(F)** Developing inflorescence with a terminal staminate unit. Bars: 500 μm **(A)** and 1 mm **(E)**. **(A–D,F)** In the same scale.

basally fused (**Figures 5A–D**). Each staminal tree produces up to 14 bithecate anthers resulting in a total number of 200–350 anthers per staminate unit. Anthers are arranged at the end of bifurcate stalks (**Figures 5L**, **6C,F**) and always associated with a bract-like structure at their abaxial side (**Figure 7D**).

The meristems of the staminate units resemble carpellate flower meristems. They initially produce a ring-shaped, weakly five-lobed bulge (**Figure 5A**). This bulge, which later gives rise to the sepal-like structures, quickly develops and envelops the expanding, still naked center of the meristem (**Figure 5B**).

- In a first step, the center fractionates 8–13 (rarely more) sub-meristems (**Figures 5B,E**: blue) which arch upward (**Figures 6A**). Dependent on their position close to the periphery or in the center of the original meristem, they have an oval or roundish shape (**Figure 5E**).
- In a second step, each sub-meristem of 1st order splits into two (rarely three) equal sub-meristems of 2nd order (**Figure 5F**: green). These sub-meristems are the initials of the 20–26 staminal trees.
- With the expanding meristem (**Table 1**), each of the initials passes up to four further synchronous, occasionally imperfect steps of fractionation generating an average of 14 anthers.

The size of the original meristem and the number of fractions vary considerably (compare **Figures 5B** and **E** and **Table 1**). However, as a general rule, a sub-meristem always splits at right angle to the previous fractionation resulting in a crosswise alternation of splitting directions. Fractionation happens almost simultaneously covering the whole surface of the meristem. In the beginning some meristems show an advanced fractionation activity at the periphery (**Figure 5F**). Interestingly, the fractions

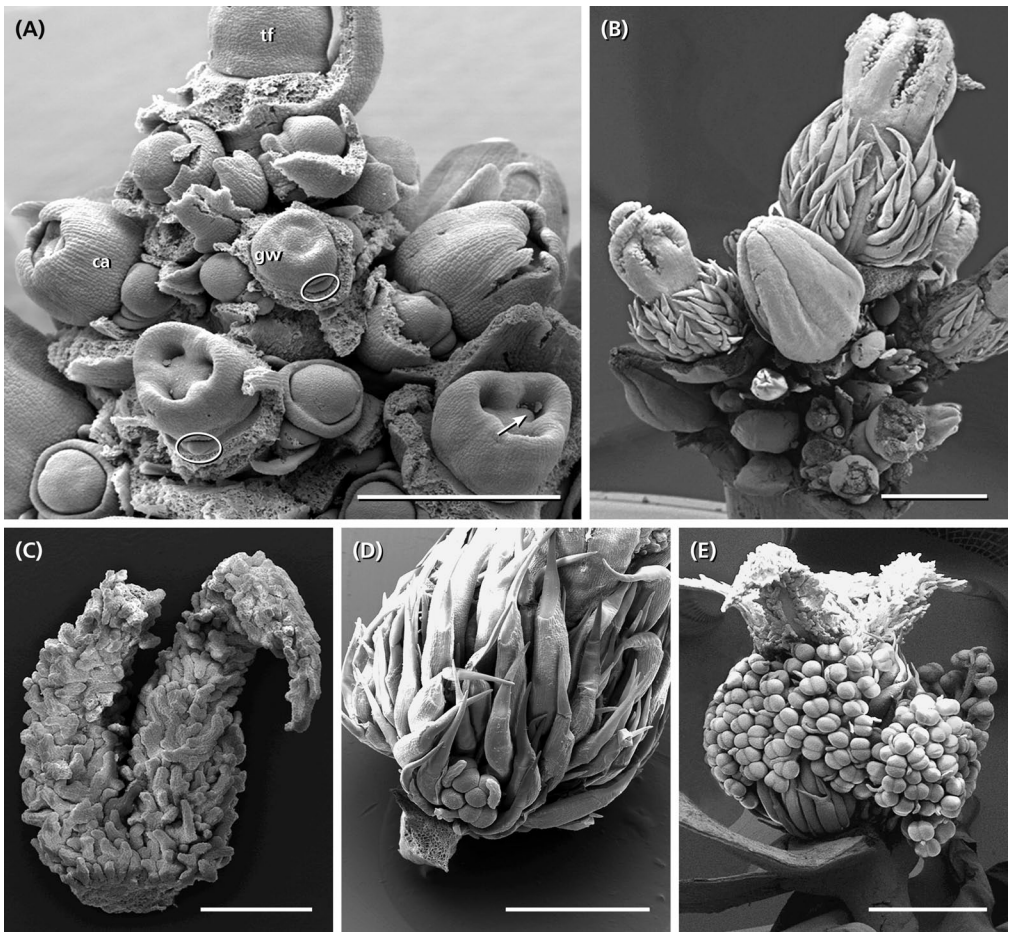

FIGURE 4 | Development of the carpellate flower. **(A)** The developing gynoecium is enclosed by a synsepalous calyx (ca). When the calyx is removed, the formation of a meristematic ring is observable originating the outer gynoecium wall (gw). The ring continues growing, overtops the base of the gynoecium and starts to form the septa of the gynoecium. In each locule, a single ovule appears in axial position (arrow). Quite often, a structure outside the gynoecium appears not further developing (circle). **(B)** The gynoecium of old buds is covered by long hairs and crowned by three bifid styles. **(C)** Bifid style densely covered with papillate outgrowths becoming sticky in the mature stage. **(D,E)** Rare cases of hermaphrodite units with few to many staminal trees surrounding the central gynoecium. Bars: 200 μm **(A)**, 500 μm **(C)**, 1 mm **(B,D)**, 2 mm **(E)**.

are of almost similar size (**Figures 5E–H**) indicating that the meristem surface continuously expands (**Table 1**). Expansion leads to the hemispherical shape of the developing unit and appears to be quite constant. Roughly estimated, the meristem surface expands 1.34-times with each of the first four steps of fractionation reaching a threefold enlargement in total (**Table 1**). After the fourth split, the fractionation processes cannot be followed in detail any longer (**Figures 5I,J**). The fractions remain smaller (**Figure 5I**) and are elevated in groups by the elongating base of the developing staminal tree (**Figures 5K**, **6B**). Thereby, the surface expands significantly generating space for the development of 100s of anthers (**Table 1**). Irregularities in the splitting behavior cause the variable number of anthers per staminal tree.

Formation of Anthers

The last step of fractionation goes along with anther formation (**Figure 5J**). The young anther has a triangular shape and consists of two premature thecae and an abaxially arranged sterile structure (**Figure 7A**). When fractionation is regular, two anthers are arranged in pairs looking like mirror images or single anthers appear (**Figure 5J**). Usually, 12–14 (10–16) anthers are elevated as a group and form a single tree-like bundle (**Figures 5L–N**). The peculiar feature of this staminal tree is its repetitive branching reflecting the successive steps of fractionation by bifurcate segments. Anthers are placed at the ends of the last segments (**Figures 6B,C**). From the very first, thecae are oriented horizontally presenting their longitudinal slit in an upward direction (**Figures 7A,B,E,F**). The unusual position is made available by a broad connective which also clearly separates the thecae from each other. Within the pollen sacs, pollen mother cells develop passing meiosis and producing pollen grains (**Figures 6C,E,F**). In the mature stage of theca development, the epidermis becomes reduced and the endothecium is exhibited as the outermost cell layer (**Figure 6F**).

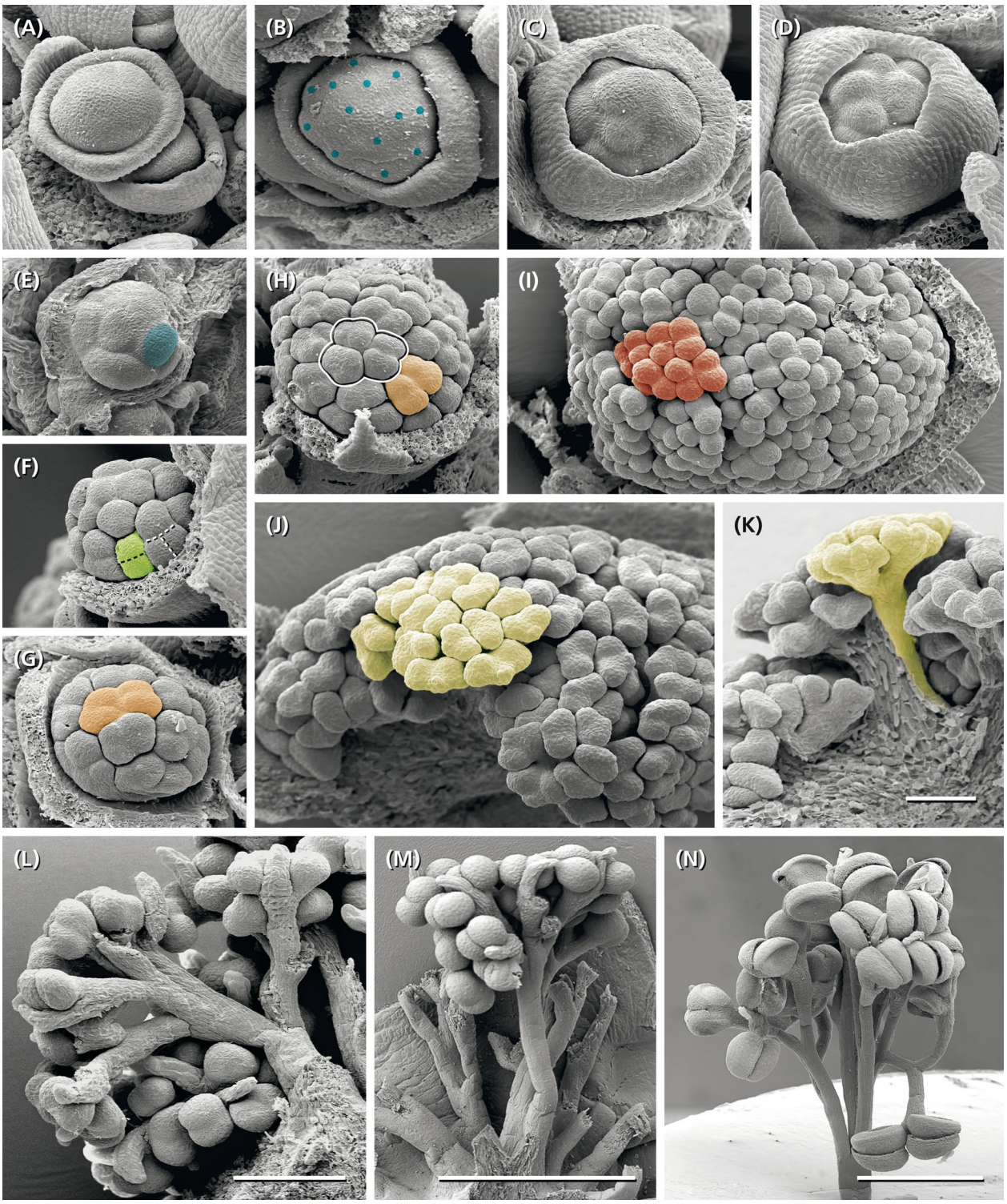

FIGURE 5 | Development of the staminate unit. **(A)** Young dome-shaped primordium with a peripheral, weakly five-lobed meristematic ring. **(B)** Collar clearly separated from central meristem bulge (diameter ~ 215 μm). **(C,D)** Meristem enveloped by the collar starts first fractionation (diameter ~ 250 μm). **(E)** Same stage as in **(C)** but smaller (~165 μm); collar removed, one of the eight submeristems indicated by blue color. **(F)** Second fractionation starting at the peripheral submeristems (green). **(G,H)** Third fractionation at different meristem sizes producing four submeristems (orange) from one original submeristem (blue in **E**). **(I)** Fourth fractionation completed (red, diameter ~600 μm), begin of staminal tree elongation. **(J,K)** Anther formation after the fifth step of fractionation. **(L–N)** Staminal trees on different developmental stages; the bifurcate splits indicating the consecutive steps of fractionation. Colors indicate the fate of a single original submeristem. **(A–K)** All pictures in the same scale. Bar: 100 μm. Bars in **(L)**: 200 μm, in **(M,N)**: 1 mm.

TABLE 1 | Meristem expansion during the process of repeated fractionation (n = 10, except the two latest stages).

Developmental steps	Meristem diameter [μm]	Meristem surface [μm^2]	Degree of surface expansion		
			x-Times		Factor
Original meristem	177.1 ± 13.93	98,484.25			
1st fractionation (blue)	206.4 ± 20.43	133,767.01	1,358	1,358	1.34± 0.13
2nd fractionation (green)	251.5 ± 18.81	198,612.07	2,016	1,485	
3rd fractionation (orange)	292.8 ± 19.84	269,197.98	2,733	1,355	
4th fractionation (. . .)	315.7 ± 25.30	312,952.78	3,177	1,163	
5th fractionation (red)	∼600	1130,400.00	11,478	3,612	
6th fractionation (yellow)	∼930	2715,786.00	27,576	2,403	

x-Times: multiplication of the original meristem surface. Factor: enlargement factor between the single steps of fractionation.

Each staminal tree is provided with a vascular bundle branching at the bifurcation sites and supporting the anthers (**Figures 6C,D**). In contrast, the abaxial structure which reaches a final length of 0.2 mm, has no vascular bundle. It elongates, gets a flat, bract-like shape, overtops the developing thecae (**Figures 7B–D**) and finally desiccates (**Figure 7E**). Epidermis cells of the structure clearly differ from the sculptured thecae walls indicating that the structure originates below the thecae (**Figures 7A,D,F**).

DISCUSSION

For more than 100 years, the staminate unit of *R. communis* has fascinated botanists and provoked controversial interpretations. Prenner et al. (2008) summarized this history and discussed whether the *Ricinus* stamen could represent a reduced flower as in several other Euphorbiaceae that possess an obscure flower-inflorescence boundary, but finally concluded that the staminal trees should be taken as extended stamen fascicles.

While intermediate structures or even 'hybrids' between flowers and inflorescences are widely accepted (e.g., Prenner and Rudall, 2007; Kirchoff et al., 2008), their morphogenetic and phylogenetic significance is not yet fully understood. Gene expression patterns are used to differentiate among flowers and inflorescences. Prenner et al. (2011) found expression of the LFY protein not only in individual flower primordia of *Euphorbia*, but also in the cyathium primordium indicating that pseudanthial meristems may be genetically similarly regulated like flower meristems. Likewise, Zhao et al. (2016) identified a *Gerbera* specific *GhLFY* resembling *LFY* expression in a single flower meristem. Floral identity and floral symmetry genes were furthermore identified in the showy leaves of *Davidia involucrata* (Vekemans et al., 2012) and showy branchlets in *Actinodium cunninghamii* (Claßen-Bockhoff et al., 2013). All these examples illustrate that one should be careful using gene expression patterns for floral organ homology (Ronse De Craene, 2007; Ochoterena et al., 2019).

Considering the clear differences between inflorescence and flower meristems (summarized in Claßen-Bockhoff, 2016), the question rises whether an extended reference system including floral units could be better suited to interpret 'intermediate structures.'

Repeated Fractionation and Spatial Constraints in *Ricinus communis*

The re-investigation of reproductive units in *R. communis* confirms the ontogenetic studies of the 'male flower' by Payer (1857); Michaelis (1924), Kirchoff et al. (2008), and Prenner et al. (2008) showing several steps of meristem fractionation before anthers appear. However, also differences were found questioning the given morphological interpretation.

With respect to Prenner et al. (2008) neither the centrifugal development of the first primordia nor the terminal position of one of the staminal trees and the separate initiation of the stamen fascicles are confirmed. Instead, a pattern of meristem fractionation is documented indicating that the availability of space predominantly guides pattern formation.

The first step of meristem development is an almost simultaneous division into sub-meristems of similar size. Dependent on the variable size of the initial meristem, the number of sub-meristems varies. Thereby, neither a terminal sub-meristem nor a flower-characteristic phyllotaxis is observed. Both findings characterize the process of fractionation as a self-organizing process using the meristem completely (Hernandez and Palmer, 1988; Reinhardt et al., 2003; Prusinkiewicz and Barbier de Reuille, 2010; Claßen-Bockhoff and Meyer, 2015). In the next step, the fractions start to grow. Thereby, some sub-meristems show a more advanced development at the periphery indicating that space and shape of the initial meristem might affect the promotion of individual sub-meristems.

Spatial conditions also influence the ongoing meristem development characterized by repetitive fractionation. The initial meristem continuously expands and thereby generates new space for the developing sub-meristems. During the first four steps of fractionation, the degree of expansion is correlated with the temporal sequence of splitting. The sub-meristems enlarge to a certain size and get subdivided into further sub-meristems which repeat the process. However, when space becomes more and more limited, irregular fractionations increase, cause the suppression of further splits and result in a variable number of anthers per fascicle.

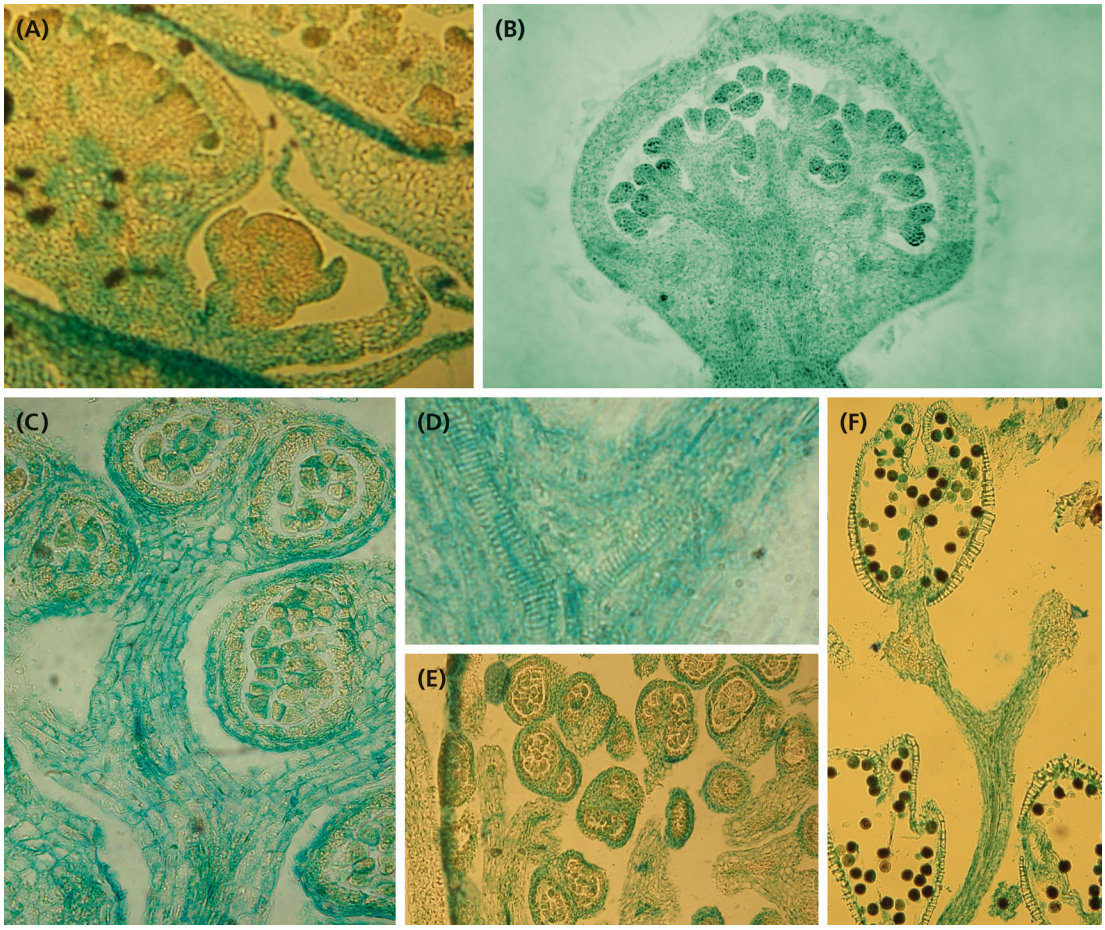

FIGURE 6 | Histology of developing staminate units. **(A)** Longitudinal section of a cyme with two staminate units in different developmental stages. The youngest one corresponds to **Figure 5A**, the second one to **Figure 5H**. **(B)** Longitudinal section of a staminate unit enveloped by the collar. **(C)** Longitudinal section of a stalked, almost mature anther. **(D)** Longitudinal section of the upperpart of a stalk segment showing the splitting vascular bundles. **(E)** Cross section of an old staminate bud showing bithectae anthers and vascularized anther stalks. **(F)** Upper part of a staminal tree showing the split of the fourth and fifth fractionation and one mature theca with naked endothecium and pollen grains.

On average, each staminate unit has 25 staminal trees originating from 8 to 13 sub-meristems. Though the absolute number varies among staminate units, it is evident, that the staminal trees are not initiated separately at the initial meristem, but at least in pairs at the first sub-meristems.

Homology of Stamens and Stamen Fascicles – The Flower Perspective

Stamen fascicles appear in many plant taxa across the angiosperms (Ronse De Craene, 2010). They are defined as groups of stamens originating from a common primordium by a splitting process (Ronse De Craene and Smets, 1987, 1992). Thereby, the number of stamens increases resulting in a polyandrous androecium (**Figure 8B**). More specifically, the androecium is called secondary (or complex) polyandrous as a high number of stamens can also arise from many single primordia (primary polyandry, **Figure 8A**). Usually, the common primordia occupy the position of stamens and are arranged in one or two whorls (Ronse De Craene, 2010). The splitting process proceeds top-down and is centrifugal or centripetal depending on the shape of the flower primordium, local meristem expansion and spatial constraints (Ronse De Craene and Smets, 1991). Secondary polyandry can also arise from a ring primordium and/or proceed in lateral direction, but these forms are not relevant in the present study.

Staminal tree formation in *Ricinus* corresponds with that in secondarily polyandrous flowers in increasing the number of stamens by fractionation. However, neither the position of the fractions nor the direction of splitting conforms to secondary polyandry. Furthermore, the high number of successive steps of subdivision resulting in multiple branched staminal trees is almost unique in *Ricinus*. One may accept these peculiarities as a specific mode of stamen fascicle formation in *R. communis* arguing that the flower meristem is sufficiently plastic to allow this variation. Compared to all other vegetative and reproductive meristems, the FM indeed is the most dynamic one (Ronse De Craene, 2010; Claßen-Bockhoff, 2016). However,

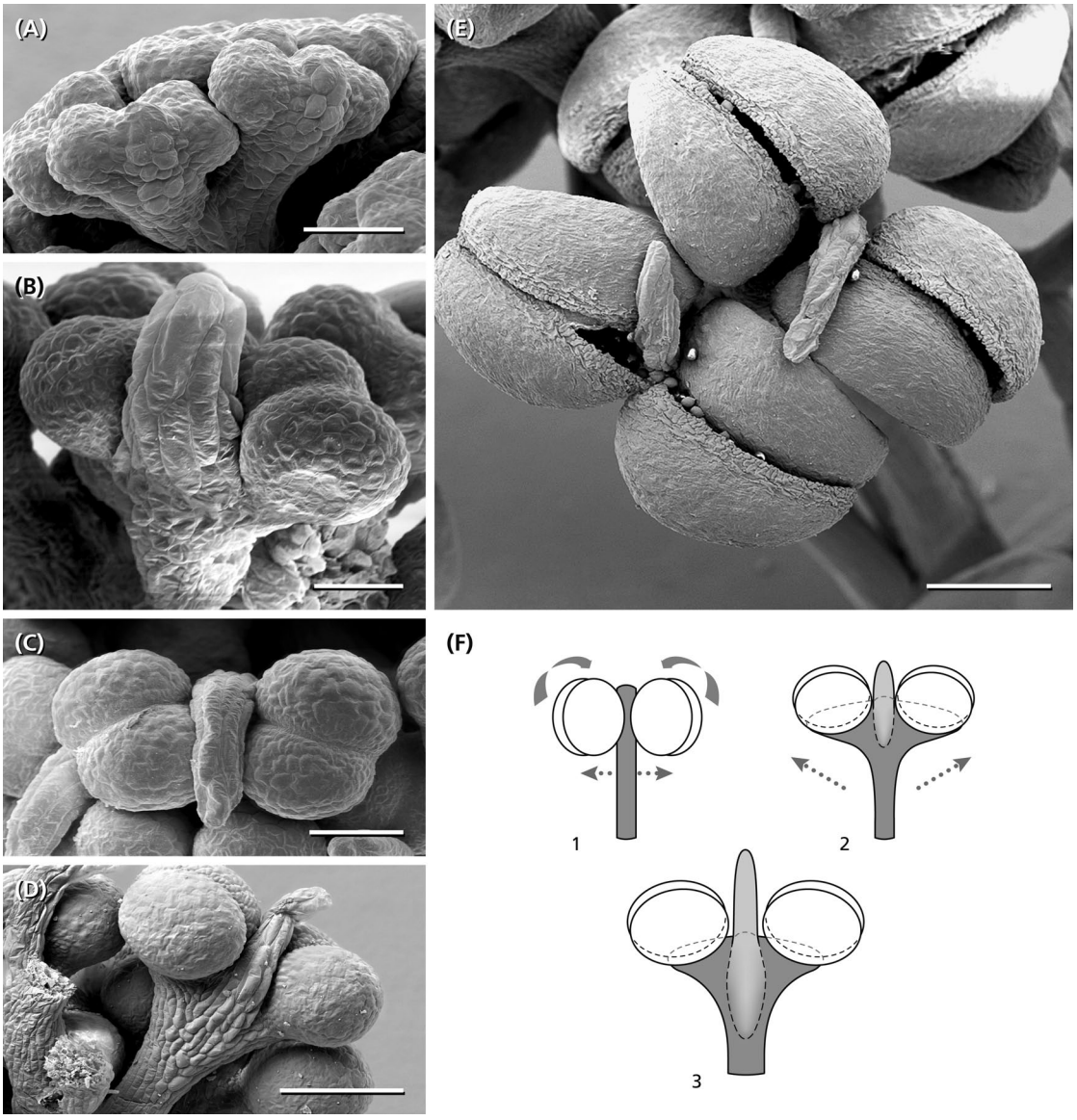

FIGURE 7 | Anther development. **(A)** Young bithectae anthers after the fifth step of fractionation, each with a weak effiguration at the abaxial side. **(B)** Effiguration overtops the two thecae each of them divided into two pollen-sacs. **(C,D)** Anther and abaxial effiguration from above and from the side. **(E)** Two anthers from above presenting their longitudinal dehiscence slits. **(F)** Schematic reconstruction of anther fomation. Compared to a typical bithecate angiosperm anther (*1*), the young anther in *Ricinus* (*2*) shows a widening of the connective turning the thecae around 90° (arrows). At the abaxial side below each theca, an effiguration develops, which in the mature stage (*3*) overtops the pollen-sacs. *1*, angiosperm stamen as reference. *2*, young anther stage corresponding to **(B)**. *(3)* Almost mature stage as shown in **(D)**. Bars: 50 μm **(A,B)**, 100 μm **(C)**, 200 μm **(D,E)**.

interpreting the staminate unit in *Ricinus* as a flower has deep implications on the interpretation of the flower and particularly on the stamen.

While the pollen-sacs correspond to microsporangia arranged in an anther, the question raises what the filament might be? Is it the petiole of a leaf (**Figure 8C**: green; Baum and Leinfellner, 1953; Kunze, 1979) or is it just an anther supporter (antherophor) elevating the pollen-sacs in a position for optimal pollen dispersion (**Figure 8C**: orange; Hagemann, 1984)? In this case, to keep the euanthial theory, one could argue that the common primordium is a leaf homolog, while the filament-anther complex is an emergence without being homologous to any part of the leaf. It develops from the surface of a leaf primordium which itself remains inhibited. The emergence hypothesis is attractive as it could easily explain the high structural diversity of the filaments without the need to refer to leaf development. However, considering the deep differences between SAMs and FMs, one might also question the euanthial theory and prefer interpreting the flower just as the tip of the stem bearing floral organs (Claßen-Bockhoff, 2016). As floral organs originate from a determinate

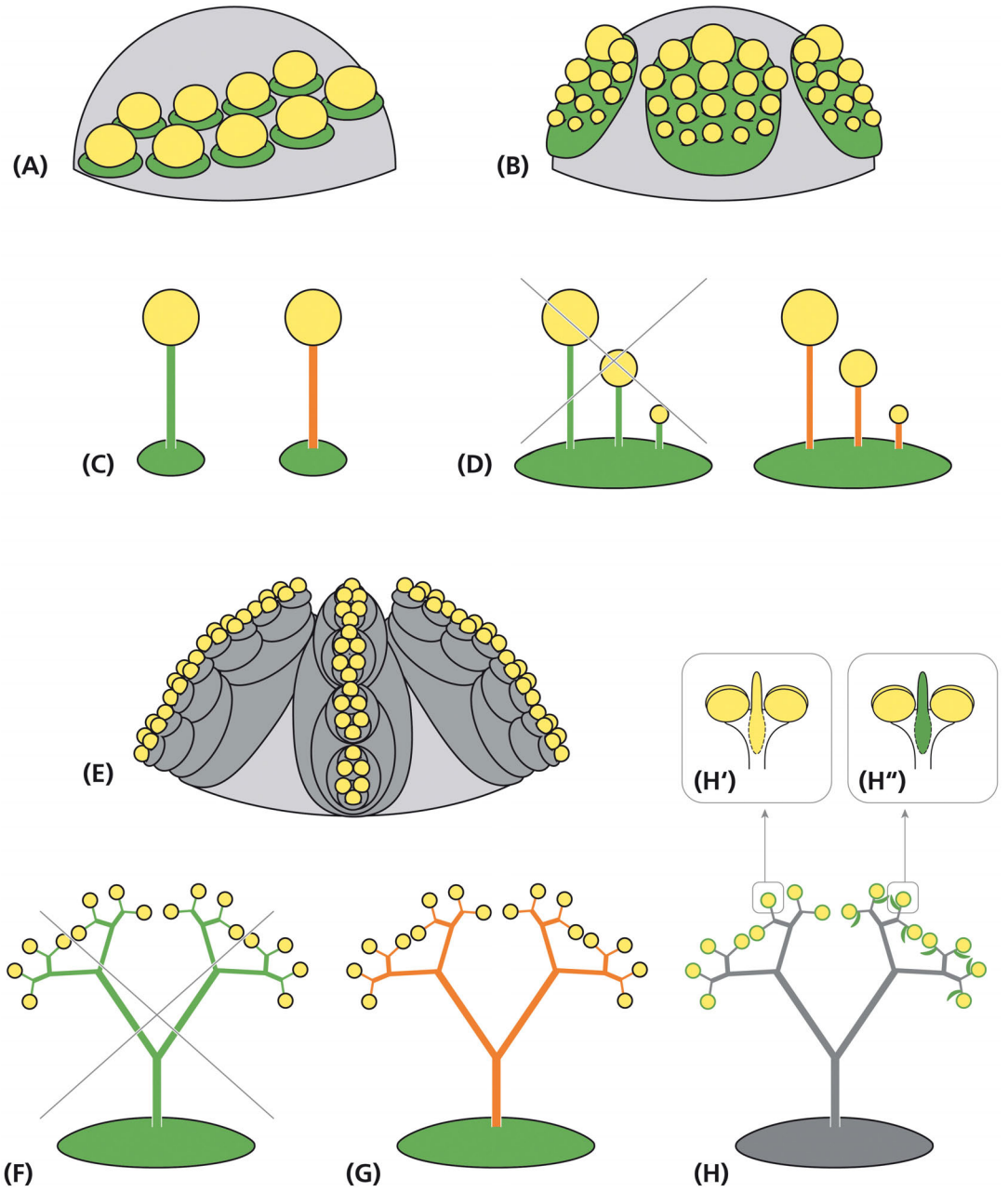

FIGURE 8 | Alternative interpretations of the staminal trees in *Ricinus*. Schematic representation of flower meristems originating single stamens **(A)** and stamen fascicles of the centrifugal type **(B)** from a leaf-homolog primordium (green). **(C)** Morphological interpretation of the filament as part of a sporangiate leaf (left) or an anther supporter (right). **(D)** Sketch of a stamen fascicle interpreted as a compound leaf (left: not confirmed by development) and as a suppressed leaf primordium with stalked anthers (right: uncommon, but acceptable assumption). **(E)** Alternative interpretation: floral unit meristem passing repeated steps of fractionation (gray) before originating reduced, uni-staminate flowers. Interpretations of the staminal tree as **(F)** a stamen fascicle homologous to a compound leaf (not confirmed by development), **(G)** a single stamen with branched anther supporters or **(H)** a floral unit with many uni-staminate flowers arising at the end of bifurcated staminal trees. **(H‴)** Alternative interpretations of the adaxial structure as a connective effiguration (**H′**: yellow) and as a subtending bract (**H″**: green). Green: leaf homolog. Yellow: anther. Orange: effiguration. Gray: meristematic tissue.

FM genetically completely differently regulated than SAMs, there is no need to homologize the flower with a short shoot any longer.

The petiole interpretation of the filament is in conflict with the phenomenon of secondary polyandry where many filaments originate from a single primordium. To solve this problem, Guédès (1979), as Payer (1857) and others before him (summarized in von Wettstein, 1901–1908), compared the branched stamen fascicle with a multi-pinnate leaf (**Figures 8D,F**: green). This comparison, however, cannot be hold as pinnae originate from the fractionating leaf margin

and not from the primordium plain (Hagemann, 1970). Only the emergence interpretation of the filament is in accordance with the phenomenon of secondary polyandry. Accepting this view, the angiosperm filament is an anther supporter. Stamen fascicles only differ quantitatively from solitary stamens as they produce several instead of only one antherophor per underlying primordium (**Figure 8D**: orange). If the staminate unit in *R. communis* is referred to an euanthium, the collar should be homologized with the calyx of the carpellate flower and the stamen fascicle interpreted as a multiple branched emergence bearing anthers (**Figures 8F,G**).

Homology of the Staminal Trees – The Floral Unit Perspective

Multi-flowered units are traditionally called inflorescences. Dependent on the absence or presence of a terminal flower, they are grouped into open and closed inflorescences. In both cases, it is assumed that they develop from IMs sharing many characteristics with SAMs (Prusinkiewicz et al., 2007). However, morphogenetic studies clearly illustrate, that multi-flowered units develop from two different meristems, the IMs generating inflorescences by the process of segregation and FUMs giving rise to floral units (Claßen-Bockhoff and Bull-Hereñu, 2013). FUMs share almost all characteristics with FMs, in particular the determinate nature of the meristem, the initially naked stage and the capacities of expansion and fractionation. For that reason, young FUMs cannot be distinguished from FMs (Claßen-Bockhoff, 2016). The notion of Prenner et al. (2008) that the young stages of the staminate unit meristems in *R. communis* look flower-like is, thus, not necessarily an indication for the flower nature of these units. FUMs differ from FMs in the number of fractionation steps (**Figure 8E**). As the high number of consecutive meristem splits is the most peculiar feature in the development of the staminal trees, FUMs appear to be excellent candidates to explain the staminate unit in *R. communis*.

Interpreting the staminate unit in *R. communis* as a floral unit means at the same time that the staminal trees are not homologous to the stamen fascicles of polyandrous flowers but to clusters of highly reduced flowers (**Figure 8H**). Each anther is homologized with a uni-staminate flower. This flower has neither a pedicel nor a filament, but only a well-developed anther, directly originating from the latest sub-meristem.

The anthers may or may not be associated with laterally arranged sterile structures (van der Pijl, 1952). The structure is traditionally taken as a connective effiguration (**Figure 8H′**), but this interpretation is questionable. First, is it difficult to identify the connective due to the upturned position of the anther. Second, the structure appears to be inserted below the anther directly originating from the sub-meristem. As an alternative, the sterile structure can be taken as the subtending bract of the uni-staminate flower (**Figure 8H″**, Lam, 1948). The position supports this view and the minute length of the bract could explain the lack of a vascular bundle.

The given scenario of the staminate unit development in *Ricinus* corresponds to the present knowledge about FUMs. It only differs from the known examples in the high number of fractionation steps and in the extreme flower reduction to a single anther. All other floral units investigated so far are clearly composed of flowers and have been recognized as inflorescences in the past. An almost simultaneous subdivision of a large hemispherical meristem similar to that in *Riciuns* was observed in the head development of the dove tree *Davidia involucrata* (Nyssaceae; Claßen-Bockhoff and Arndt, 2018). The meristem likewise expands considerably originating new FMs in basipetal direction (Jerominek et al., 2014). After the first step of fractionation, the sub-meristems merge into FMs. Ongoing meristem expansion enlarges the already existing FMs providing them with the space for floral organ formation. In the secondary heads of *Echinops* and *Pycnosurus* (both Asteraceae; Claßen-Bockhoff, 2016), the compound umbels of Apiaceae (Claßen-Bockhoff and Bull-Hereñu, 2013, unpublished data) and the secondary heads of some Eriocaulaceae (Stützel and Trovó, 2013), floral organs are only formed after a second step of fractionation.

It should not be concealed that the inflorescences of some Urticaceae (*Dorstenia*) and Moraceae (*Elatostema sessilis*, *Procris frutescens*) show a high developmental similarity to *Ricinus* (Bernbeck, 1932). In the mentioned Moraceae, development starts with a large, naked meristem which splits crosswise as in *Ricinus*. The splits are associated with bract formation at the margin of the flat meristem, but flowers are only initiated after the fourth fractionation step. The inflorescences are traditionally interpreted as condensed thyrses with dichasial cymes. A re-investigation is needed to elucidate whether the reproductive systems are inflorescences or floral units. In any case, they support the view that the staminate unit in *Ricinus* is rather a multi-flowered unit than a flower.

Evolution of Staminate Units in *R. communis*

There is a general agreement that the staminate units of *R. communis* evolved in adaptation to wind pollination (Delpino, 1889; van der Pijl, 1952). Dusty pollen, exposed anthers, papillate and sticky stigmas and lacking perianth structures are characteristic features of anemophilous blossoms. In *R. communis*, pollen grains are additionally released explosively (Bianchini and Pacini, 1996). The specific release mechanism is associated with the loss of the epidermis of the thecae walls (Staedtler, 1923; Bianchini and Pacini, 1996).

The shift from zoophily to anemophily is often associated with extreme flower reduction resulting in perianth-less unisexual flowers which are aggregated in dense clusters of monoecious and dioecious inflorescences (Friedman and Barrett, 2009 and literature herein). All these characters fit to the interpretation that the staminate unit in *R. communis* is not a flower but a floral unit.

The derived character of the staminate units also fits to the phylogenetic relationship of the species. The monotypic *Ricinus* is placed in subclade A4 of the core acalyphoids (Euphorbiaceae s.str., Wurdack et al., 2005). It is classified, though weakly supported, as sister to *Speranskia*. This genus differs considerably from *Ricinus* notably in the presence of 10–15 free stamens per staminate flower indicating that the formation of staminal

trees is an apomorphy for *Ricinus*. On the other hand, *Ricinus*-like staminal trees appear in the only distantly related genera *Homonoia* and *Spathiostemon* (van Welzen, 1998) placed in the Acalypheae-Lasiococcinae, subclade A3 (Wurdack et al., 2005). Further examples in Euphorbiaceae (Michaelis, 1924) indicate that peculiar stamen structures evolved several times independently within the family. Unfortunately, these species are only little known and it is completely unclear whether their 'male flowers' develop like the staminate units in *Ricinus* or differently. Much better investigated are the cyathia in *Euphorbia* (Prenner and Rudall, 2007) originally interpreted as flowers and then identified as a cluster of unisexual flowers (Čelakovský, 1872; Michaelis, 1924). The terminal position is occupied by a carpellate flower only consisting of a trimerous gynoecium. This flower is surrounded by five groups of staminate flowers each reduced to a single stamen. If the staminate unit in *Ricinus* is interpreted as a floral unit, similarities to *Euphorbia* cannot be denied.

An interesting finding is the appearance of bisexual units in *R. communis* already described by Michaelis (1924) and Prenner et al. (2008). Interestingly, Michaelis (1924) found them also in *Homonoia*, the genus sharing staminal trees with *Ricinus*. As the family is characterized by unisexual flowers, these abnormalities can be either interpreted as rarely appearing perfect flowers or as floral units composed of a single carpellate flower surrounded by several staminate units. Such patterns are known from the floral units in *Davidia involucrata* (Nyssaceae, Claßen-Bockhoff and Arndt, 2018) and from the cyathia in *Euphorbia*.

While cyathia are generally bisexual, both loss of the terminal flower (Narbona et al., 2002; Schardt and Claßen-Bockhoff, 2013) and transition to dioecy result in unisexual cyathia. In *E. balsamifera* and other diecious species, the carpellate cyathium is reduced to a single trimerous gynoecium surrounded by an involucrum bearing the nectaries. Referring to the cyathium, nobody would call this involucrum a calyx. In *R. communis*, the opposite case the obvious. Referring to the assumed flower, the structure surrounding the naked gynoecium is interpreted as a calyx. However, as carpellate and staminate units in *Ricinus* share the same early developmental stages including the naked stage, meristem expansion and calyx/collar formation, it cannot be excluded that the 'carpellate flower' in *Ricinus* is also a reduced floral unit. Similar to diecious cyathia, both carpellate and staminate units in *Ricinus* would then be floral units surrounded by a collar.

CONCLUSION

In the present paper, the staminate unit in *Ricinus* is interpreted as a floral unit composed of highly reduced uni-staminate flowers. The main argument is the high number of fractionation steps, which run almost simultaneously across the whole meristem surface and show a crosswise splitting pattern. These features are not known from secondarily polyandrous flowers. If the staminate unit is nevertheless interpreted as a flower (which is possible), one has to accept a completely new stamen structure and to disregard the meristem similarities between *R. communis* and floral units. Maybe, it is too early for a final morphological interpretation of the staminate units in *Ricinus* as there is too little known about FUMs, their diversity and genetic regulation. In this sense, the present paper and the following attempt to explain the relation between FMs and FUMs are given to stimulate discussion and continuative research projects.

FUMs as Peramorphic FMs

Ongoing fractionation defining the transition from flowers to floral units may be based on a delay in the expression of floral organ identity genes.

- FMs can be defined as determinate reproductive meristems with an early expression of floral organ identity genes (Coen and Meyerowitz, 1991). Their determinancy is regulated by *LEAFY* (*LFY*) suppressing *TERMINAL FLOWER* (*TFL)* and thereby stimulating the expression of *APETALA 1 (AP1*) and other ABC-genes (Turck et al., 2008; Zeevaart, 2008). The meristem fractionates only once and gives rise to sepals, petals, stamens and carpels. If it expands, new space is generated among already existing floral organs as demonstrated by secondary polyandry (Ronse De Craene and Smets, 1991) or corona formation (Claßen-Bockhoff and Meyer, 2015).
- In FUMs, compared to FMs, the expression of floral identity genes starts later allowing the meristem to fractionate before each sub-meristem merges into a flower. Consequently, the result is not a single flower but a multi-flowered unit. As shown in *Euphorbia* (Prenner et al., 2011) and *Gerbera* (Zhao et al., 2016), *LFY*-like genes are expressed most likely defining the determinacy of their meristems in a similar way as in flower meristems. The repeated subdivisions would just be the autonomous response of the meristem to its ongoing expansion (Runions et al., 2014). The resulting fractionation pattern would reflect the geometry of the meristem which explains the repeated cross-wise splits in *Ricinus*. Fractionation only stops after five to six steps of subdivision when the latest sub-meristems are defined as flowers originating anthers.

If the delay of gene expression triggers the process of repeated fractionation, one may interpret the FUM as a peramorphic FM. The process of peramorphosis is defined as an extension of trait development, producing new morphologies in the descendant which are not present in the ancestors (Box and Glover, 2010). In the case of *Ricinus*, it occurs due to a prolongation of the not yet genetically defined stage of meristem development.

Flower-Inflorescence Boundaries

FUMs also offer a new view onto the phenomenon of intermediate structures between flowers and inflorescences. From the evolutionary point of view, one should expect such forms as all types of reproductive meristems originate from the SAM and finally produce flowers.

While in the past, traditionally defined inflorescences (developing from inflorescence meristems) were used as

reference systems demanding a deep re-organization of the inflorescence to generate a flower-like pattern (e.g., Harris, 1999), the use of FUMs easily explains flower-like units from flower-like meristems. Only single steps of fractionation separate a flower from a head and a head from a secondary head (Claßen-Bockhoff, 2016). This easy way to transform a meristem is supported by mutants of *Gerbera* (Asteraceae) illustrating that several flowers develop at a single ray flower position under certain genetic and spatial conditions (Zhao et al., 2016).

While the heads in Asteraceae are composed of clearly identifiable flowers, cyathia in *Euphorbia* show indistinct boundaries between floral organs, flowers and inflorescences. Prenner and Rudall (2007) concluded from their studies that the cyathium should be neither interpreted as a flower nor as an inflorescence, but as a "hybrid." The lacking boundaries are excellent examples for the overlap of two independent processes, the development of the original meristem forming the cyathium and that of its parts. The higher the parts are reduced, the more difficult is the interpretation of the whole as a flower or floral unit as both meristems converge to a flower-like pattern. The extreme case is shown in the staminate unit of *R. communis*, in which the flowers are so extremely reduced that only repeated fractionations indicate the underlying complex nature.

The difficulty to identify flower-inflorescence boundaries may be due to the variability of the FUM in the number of fractionations. The labile balance between meristem expansion (stimulating fractionation) and the time of gene expression (defining flower meristems) may result in transitional forms. However, these are no hybrids but structures indicating a process of evolutionary character transformation.

DATA AVAILABILITY STATEMENT

The datasets generated for this study are available on request to the corresponding author.

AUTHOR CONTRIBUTIONS

RC-B initiated the project conducted by undergraduate students. RC-B and HF supervised the student projects. HF added missing SEM-pictures and histological cuttings. RC-B wrote the manuscript which was discussed with HF and revised by both authors.

FUNDING

Funds for open access publication fees were received from the Johannes Gutenberg University of Mainz.

ACKNOWLEDGMENTS

The first author thanks P. Prusinkiewicz and A. Runions (both Calgary, AB, Canada) for inspiring discussions on meristems and the auxin concept of primordia formation. We are grateful to Martina Flörchinger and Sabine Schmidt for producing part of the SEM pictures and histological cuttings in their student projects. We thank the graphic designers of our institute, Dipl. Designer (FH) Doris Franke and BA Maria Geyer, for preparing the drawings and color plates. We finally thank the editor and reviewers for interesting discussions.

REFERENCES

Ambrose, B. A., Espinosa-Matías, S., Vázquez-Santana, S., Vergara-Silva, F., Martínez, E., Márques-Guzmán, J., et al. (2006). Comparative developmental series of the Mexican Triurids support a euanthial interpretation for the unusual reproductive axes of *Lacandonia schismatica* (Triruidaceae). *Am. J. Bot.* 93, 15–35.

Arber, E. A. N., and Parkin, J. (1907). The origin of angiosperms. *J. Linn. Soc.* 38, 29–80.

Baum, H., and Leinfellner, W. (1953). Die ontogenetischen Abänderungen des diplophyllen Grundbaues der Staubblätter. Österr. *Bot. Z.* 100, 91–135. doi: 10.1007/bf02230791

Bernbeck, F. (1932). Vergleichende Morphologie der Urticaceen- und Moraceen-infloreszenzen. *Bot. Abhandl.* 19, 1–100.

Bianchini, M., and Pacini, E. (1996). Explosive anther dehiscence in *Ricinus communis* L. involves cell wall modifications and relative humidity. *IJPS* 157, 739–745.

Box, M. S., and Glover, B. J. (2010). A plant developmentalist's guide to paedomorphosis: reintroducing a classic concept to a new generation. *Trends Plant Sci.* 15, 241–246. doi: 10.1016/j.tplants.2010.02.004

Bull-Hereñu, K., and Claßen-Bockhoff, R. (2011). Open and closed inflorescences: more than simple opposites. *J. Exp. Bot.* 62, 79–88.

Čelakovský, L. (1872). Noch ein Versuch zur Deutung der *Euphorbia*-Blüthen. *Flora* 55, 153–158.

Claßen-Bockhoff, R. (2016). The shoot concept of the flower: still up to date? *Flora* 221, 46–53.

Claßen-Bockhoff, R., and Arndt, M. (2018). Flower-like heads from flower-like meristems: pseudanthium development in *Davidia involucrata* (Nyssaceae). *J. Plant Res.* 131, 443–458.

Claßen-Bockhoff, R., and Bull-Hereñu, K. (2013). Towards an ontogenetic understanding of inflorescence diversity. *Ann. Bot.* 112, 1523–1542.

Claßen-Bockhoff, R., and Meyer, C. (2015). Space matters: meristem expansion triggers corona formation in *Passiflora*. *Ann. Bot.* 117, 277–290.

Claßen-Bockhoff, R., Ruonala, R., Bull-Hereñu, K., Marchant, N., and Albert, V. A. (2013). The unique pseudanthium of *Actinodium* (Myrtaceae) – morphological reinvestigation and possible regulation by CYCLOIDEA-like genes. *EvoDevo* 4:8.

Coen, E. S., and Meyerowitz, E. M. (1991). The war of the whorls: genetic interactions controlling flower development. *Nature* 353, 31–37.

Delpino, F. (1889). Anemofilia a scatto delle antere presso il *Ricinus communis*. *Malpighia* 3, 337–338.

Delpino, F. (1890). Contribuzione alla teoria della pseudanzia. *Malpighia* 4, 302–312.

Friedman, J., and Barrett, S. C. H. (2009). Wind of change: new insights on the ecology and evolution of pollination and mating in wind-pollinated plants. *Ann. Bot.* 103, 1515–1527.

Glover, B. J. (2007). *Understanding Flowers and Flowering: an Integrated Approach*. Oxford: Oxford University Press.

Guédès, M. (1979). *Morphology of Seed-plants*. Vaduz: Cramer.

Hagemann, W. (1970). Studien zur Entwicklungsgeschichte der Angiospermenblätter. *Bot. Jahrb.* 90,

Hagemann, W. (1984). *Die Baupläne der Pflanzen. Eine Vergleichende Darstellung ihrer Konstruktion*, University of Heidelberg: Germany.

Harris, E. M. (1999). Capitula in the asteridae: a widespread and varied phenomenon. *Bot. Rev.* 65, 348–369.

Hernandez, L. F., and Palmer, J. H. (1988). Regeneration of the sunflower capitulum after cylindrical wounding of the receptacle. *Am. J. Bot.* 75, 1253–1261.

Jerominek, M., Bull-Hereñu, K., Arndt, M., and Claßen-Bockhoff, R. (2014). Live imaging of developmental processes in a living meristem of *Davidia involucrata* (Nyssaceae). *Front. Plant Sci.* 5:613. doi: 10.3389/fpls.2014.00613

Kirchoff, B. K., Pfeifer, E., and Rutishauser, R. (2008). Plant structure ontology: how should we label plant structures with doubtful or mixed identities? *Zootaxa* 1950, 103–122.

Kunze, H. (1979). Typologie und Morphogenese des Angiospermen-Staubblattes. *Beitr. Biol. Pflanzen* 54, 239–304.

Lam, H. J. (1948). Classification and the new morphology. *Acta Biotheor.* 8, 107–154.

Michaelis, P. (1924). Blütenmorphologische Untersuchungen an den Euphorbiaceen unter Besonderer berücksichtigung der Phylogenie der Angiospermenblüte. *Bot. Abhandl.* 3, 1–150.

Naghiloo, S., and Claßen-Bockhoff, R. (2017). Understanding the unique flowering sequence in *Dipsacus fullonum*: evidence from geometrical changes during head development. *PLoS One* 12:e0174091. doi: 10.1371/journal.pone.0174091

Narbona, E., Ortiz, P. L., and Arista, M. (2002). Functional andromonoecy in *Euphorbia* (Euphorbiaceae). *Ann. Bot.* 89, 571–577.

Ochoterena, H., Vrijdaghs, A., Smets, E., and Claßen-Bockhoff, R. (2019). The search for common origin: homology revisited. *Syst. Biol.* 68, 767–780.

Payer, J. B. (1857). *Traité D'organogénie Comparée de la Fleur. Reprint Cramer 1966*. Paris: Masson.

Prenner, G., Box, M. S., Cunniff, J., and Rudall, P. J. (2008). Branching stamens of *Ricinus* and the homologies of the angiosperm stamen fascicle. *Int. J. Plant Sci.* 169, 735–744.

Prenner, G., Cacho, N. I., Baum, D., and Rudall, P. J. (2011). Is *LEAFY* a useful marker gene for the flower-inflorescence boundary in the *Euphorbia* cyathium? *J. Exp. Bot.* 62, 345–350.

Prenner, G., and Rudall, P. J. (2007). Comparative ontogeny of the cyathium in *Euphorbia* (Euphorbiaceae) and its allies: exploring the organ-flower-inflorescence boundary. *Am. J. Bot.* 94, 1612–1629.

Prusinkiewicz, P., Barbier de Reuille, P. (2010). Constraints of space in plant development. *J. Exp. Bot.* 61, 2117–2129.

Prusinkiewicz, P., Erasmus, Y., Lane, B., Harder, L. D., and Coen, E. (2007). Evolution and development of inflorescence architectures. *Science* 316:1452. doi: 10.1126/science.1140429

Reinhardt, D., Pesce, E. R., Stieger, P., Mandel, T., Baltensperger, K., Bennett, M., et al. (2003). Regulation of phyllotaxis by polar auxin transport. *Nature* 426, 255–260.

Ronse De Craene, L. P. (2007). Are petals sterile stamens or bracts? The origin and evolution of petals in the core eudicots. *Ann. Bot.* 100, 621–630.

Ronse De Craene, L. P. (2010). *Floral Diagrams. An Aid to Understanding Flower Morphology and Evolution*. Cambridge: Cambridge University Press.

Ronse De Craene, L. P., and Smets, E. F. (1987). The distribution and the systematic relevance of the androecial characters oligomery and polymery in the Magnoliophytina. *Nord. J. Bot.* 7, 239–253.

Ronse De Craene, L. P., and Smets, E. F. (1991). The impact of the receptacular growth by polyandry in the Myrtales. *Bot. J. Linn. Soc.* 105, 257–269.

Ronse De Craene, L. P., and Smets, E. F. (1992). Complex polyandry in the Magnoliatae: definition, distribution and systematic value. *Nord. J. Bot.* 12, 621–649.

Rudall, P. J. (2003). Monocot pseudanthia revisited: floral structure of the mycoheterotrophic familiy Triuridaceae. *Int. J. Plant Sci.* 164, S307–S320.

Runions, A., Smith, R. S., and Prusinkiewicz, P. (2014). "Computational models of auxin driven development," in *Auxin and its Role in Plant Development*, eds J. Petrášek Zažímalová, and E. Benkova, (Heidelberg: Springer), 315–357.

Schardt, L., and Claßen-Bockhoff, R. (2013). Blütenökologische Untersuchungen an *Euphorbia palustris* und *Euphorbia helioscopia*. *Mainzer Naturwiss. Archiv* 50, 211–232.

Sokoloff, D. D., Oskolski, A. A., Remizowa, M. V., and Nuraliev, M. S. (2007). Flower structure and development in *Tupidanthus calyptratus* (Araliaceae): an extreme case of polymery among asterids. *Pl. Syst. Evol.* 268, 209–234.

Sokoloff, D. D., Remizowa, M. V., Linder, H. P., and Rudall, P. J. (2009). Morphology and development of the gynoecium in Centrolepidaceae: the most remarkable range of variation in Poales. *Am. J. Bot.* 96, 1925–1940.

Staedtler, G. (1923). Über Reduktionserscheinungen im Bau der Antherenwand in Angiospermen-Blüten. *Flora* 116, 85–108.

Stützel, T., and Trovó, M. (2013). Inflorescences in Eriocaulaceae: taxonomic relevance and practical implications. *Ann. Bot.* 112, 1505–1522.

Turck, F., Fornara, F., and Coupland, G. (2008). Regulation and identity of florigen: FLOWERING LOCUS T moves the centre stage. *Ann. Rev. Plant Biol.* 59, 573–594.

van der Pijl, L. (1952). The stamens of *Ricinus*. *Phytomorphology* 2, 130–132.

van Heel, W. A. (1966). Morphology of the androecium in Malvales. *Blumea* 13, 177–394.

van Welzen, P. C. (1998). Revisions and phylogenies of Malesian Euphorbiaceae: subtribe Lasiococcinae (*Homonoia, Lasiococca, Spathiostemon*) and *Clonostylis, Ricinus*, and *Wetria*. *Blumea* 43, 131–164.

Vekemans, D., Viaene, T., Caris, P., and Geuten, K. (2012). Transference of function shapes organ identity in the dove tree inflorescence. *New Phytol.* 193, 216–228.

von Goethe, J. W. (1790). "Versuch die Metamorphose der Pflanzen zu erklären," in *Naturkundliche Schriften II: Schriften zur Morphologie. Johann Wolfgang von Goethe: Schriften zur Morphologie. Sämtliche Werke, Briefe, Tagebücher und Gespräche*, Vol. 24, ed. D. Kuhn, (Frankfurt: Deutscher Klassiker Verlag), 109–152.

von Wettstein, R. (1901–1908). *Handbuch der Systematischen Botanik*. Leipzig: Wien.

Wilson, C. L. (1942). The telome theory and the origin of the stamen. *Am. J. Bot.* 29, 759–764.

Wurdack, K. J., Hoffmann, P., and Chase, M. (2005). Molecular phylogenetic analysis of uniovulate Euphorbiaceae (Euphorbiaceae sensu stricto) using plastid *rbcL* and *trnL-F* DNA sequences. *Am. J. Bot.* 92, 1397–1420.

Zeevaart, J. A. D. (2008). Leaf-produced floral signals. *Curr. Opin. Plant Biol.* 11, 541–554.

Zhao, Y., Zhang, T., Broholm, S. K., Tähtiharju, S., Mouhu, K., Albert, V. A., et al. (2016). Evolutionary co-option of floral meristem identity genes for patterning of the flower-like Asteraceae inflorescence. *Plant Physiol.* 172, 284–296.

Zimmermann, W. (1930). *Die Phylogenie der Pflanzen: ein Überblick über Tatsachen und Probleme*. Fischer: Jena.

Conflict of Interest: The authors declare that the research was conducted in the absence of any commercial or financial relationships that could be construed as a potential conflict of interest.

frontiers in Cell and Developmental Biology

ORIGINAL RESEARCH
published: 19 May 2020
doi: 10.3389/fcell.2020.00303

Developmental Flower and Rhizome Morphology in *Nuphar* (Nymphaeales): An Interplay of Chaos and Stability

Elena S. El[1], *Margarita V. Remizowa*[1,2] *and Dmitry D. Sokoloff*[1]*

[1] *Department of Higher Plants, Faculty of Biology, M.V. Lomonosov Moscow State University, Moscow, Russia,* [2] *Faculty of Biology and Biotechnologies, National Research University Higher School of Economics, Moscow, Russia*

European species of *Nuphar* are among the most accessible members of the basal angiosperm grade, but detailed studies using scanning electron microscopy are lacking. We provide such data and discuss them in the evolutionary context. Dorsiventral monopodial rhizomes of *Nuphar* bear foliage leaves and non-axillary reproductive units (RUs) arranged in a Fibonacci spiral. The direction of the phyllotaxis spiral is established in seedlings apparently environmentally and maintained through all rhizome branching events. The RUs can be located on dorsal, ventral or lateral side of the rhizome. There is no seasonality in timing of their initiation. The RUs usually form pairs in positions N and N + 2 along the ontogenetic spiral. New rhizomes appear on lateral sides of the mother rhizome. A lateral rhizome is subtended by a foliage leaf (N) and is accompanied by a RU in the position N + 2. We hypothesize a two-step process of regulation of RU/branch initiation, with the second step possibly involving environmental factors such as gravitropism. Each RU has a short stalk, 1-2 scale-like phyllomes and a long-pedicellate flower. We support a theory that the flower is lateral to the RU axis. The five sepals initiate successively and form two whorls as 3 + 2. The sepal arrangement is not 'intermediate' between whorled and spiral. Mechanisms of phyllotaxis establishment differ between flowers and lateral rhizomes. Petal, stamen and carpel numbers are not precisely fixed. Petals are smaller than sepals and form a whorl. They appear first in the sectors of the outer whorl sepals. The stamen arrangement is whorled to chaotic. The merism of the androecium tends to be the same as in the corolla. Flowers with odd numbers of stamen orthostichies are found. These are interpreted as having a non-integer merism of the androecium (e.g., 14.5). Carpels form a whorl in *N. lutea* and normally alternate with inner whorl stamens. Sterile second whorl carpel(s) are found in some flowers of *N. pumila.*

Keywords: angiosperms, development, evolution, flower, gravitropism, mechanical forces, phyllotaxis

OPEN ACCESS

Edited by:
Louis Philippe Ronse De Craene, Royal Botanic Garden Edinburgh, United Kingdom

Reviewed by:
Rolf Rutishauser, University of Zurich, Switzerland
Mario Coiro, Université de Fribourg, Switzerland

***Correspondence:**
Dmitry D. Sokoloff
sokoloff-v@yandex.ru

Specialty section:
This article was submitted to Evolutionary Developmental Biology, a section of the journal Frontiers in Cell and Developmental Biology

Received: *14 January 2020*
Accepted: *07 April 2020*
Published: *19 May 2020*

Citation:
El ES, Remizowa MV and Sokoloff DD (2020) Developmental Flower and Rhizome Morphology in Nuphar (Nymphaeales): An Interplay of Chaos and Stability. Front. Cell Dev. Biol. 8:303. doi: 10.3389/fcell.2020.00303

INTRODUCTION

The question of the origin and early evolution of angiosperms and angiosperm flowers remains one of key problems of evolutionary botany (Bateman et al., 2006; Doyle, 2008, 2012; Friis et al., 2011; Herendeen et al., 2017; Wang, 2018; Coiro et al., 2019; Bateman, 2020). Despite the fascinating progress during recent decades, inferring patterns of evolution of floral characters is in some cases problematic or the analyses provide equivocal results (Doyle and Endress, 2000; Endress and Doyle, 2009; Sauquet et al., 2017, 2018; De-Paula et al., 2018; Sokoloff et al., 2018a; Rümpler and Theißen, 2019). Among important limitations of ancestral character reconstructions is the lack of data or insufficient knowledge of morphological and especially developmental characters in many angiosperms species (Sauquet et al., 2017; Sauquet and Magallón, 2018; Sokoloff et al., 2018a).

Throughout the centuries of research in developmental plant morphology, European species *Nuphar* (Nymphaeaceae, Nymphaeales) have been among the most accessible plants currently recognized as members of the basal angiosperm grade. In spite of the great amount of relevant publications and controversial morphological interpretations (Trecul, 1845; Raciborski, 1894a,b; Cutter, 1957a,b, 1958, 1959, 1961; Dormer and Cutter, 1959; Chassat, 1962; Moseley, 1965, 1972; Wolf, 1991; Igersheim and Endress, 1998; Endress, 2001; Schneider et al., 2003; Padgett, 2007; Endress and Doyle, 2009) a comprehensive developmental study of European species of *Nuphar* using scanning electron microscopy is lacking. We are filling this gap and discuss the importance of *Nuphar* for understanding early evolution of angiosperms.

Traditionally, *Nuphar* was regarded as sister to the rest of Nymphaeaceae, a conclusion well-supported by several morphological characters, including superior rather than (semi)inferior ovary (Les et al., 1999; Borsch et al., 2008; Taylor, 2008; see also He et al., 2018). The traditional circumscription of Nymphaeaceae was supported by the occurrence of syncarpy and other characters (e.g., Borsch et al., 2008). Among two other families of the order, Cabombaceae possess free carpels whereas pistils of Hydatellaceae are unicarpellate (Moseley et al., 1984; Igersheim and Endress, 1998; Rudall et al., 2007; Sokoloff et al., 2013). Recent evidence from plastid phylogenetics suggests that placement of *Nuphar* as sister to Cabombaceae cannot be ruled out (Gruenstaeudl et al., 2017; Gruenstaeudl, 2019). As pointed out by Gruenstaeudl (2019), the monophyly of Nymphaeaceae currently remains indeterminate, and specific phylogenetic conclusions are strongly dependent on the precise plastome gene, data partitioning scheme, and codon position evaluated. Other potential problems may include taxon sampling and long-branch effects. The ambiguity in placement of *Nuphar* makes ancestral state reconstruction even more problematic for some characters (especially syncarpy). In this situation, detailed knowledge on morphology of *Nuphar* is important. The genus consists of the primarily Eurasian section *Nuphar* and the American section *Astylus* (Padgett, 2007). To our knowledge, developmental data documented by scanning electron microscopy are only available for two American species, *N. advena* (Endress, 2001) and *N. polysepala* (Schneider et al., 2003). Though extremely useful, published illustrations do not cover all stages of flower development.

The waterlilies possess a lot of interesting and unusual structural and developmental features whose interpretation is problematic. Disentangling these controversies is important for accurate assessment of morphological evolution. For example, lateral branching is normally axillary in seed plants, both in their vegetative parts and inflorescences (e.g., Gatsuk, 1974), but morphological interpretation of shoot branching and especially flower arrangement in all families of Nymphaeales is controversial (Raciborski, 1894a,b; Cutter, 1957a,b, 1958, 1959; Chassat, 1962; Richardson, 1969; Moseley, 1972; Schneider et al., 2003; Grob et al., 2006; Endress and Doyle, 2009; Sokoloff et al., 2009). Interpretation of flower position in *Nuphar* is especially problematic, because the flower of *Nuphar* is associated with a minute phyllome (or two phyllomes) variously interpreted as flower-subtending bract belonging to the rhizome, homolog of the first sepal of *Nymphaea* or phyllome of the lateral axis (Trecul, 1845; Raciborski, 1894a; Cutter, 1959; Chassat, 1962; Moseley, 1972; Endress and Doyle, 2009). Another important question is interpretation of perianth and androecium phyllotaxis of *Nuphar* as whorled or spiral (Hiepko, 1965; Cronquist, 1981; Wolf, 1991; Endress, 2001; Schneider et al., 2003; Padgett, 2007). This is related to the question of whorled vs. spiral arrangement of floral parts in ancestral flowers (Sauquet et al., 2017). The whorled interpretation is dominating in recent literature, but, for example, Padgett (2007) describes spirally arranged appendages enclosing a compound ovary in *Nuphar*. Even within the whorled interpretation, details of organ arrangement such as the number of petal whorls remain questionable. In the present study, we are making at attempt of resolving these problems. Because flower development is strongly related to flower positioning of the rhizome, both flower and rhizome development are covered here.

MATERIALS AND METHODS

Material of *Nuphar lutea* L. (growing tips of rhizomes or entire rhizomes) was collected in river Usmanka, near the Biological Teaching and Scientific Centre 'Venevitinovo' of Voronezh State University (Novousmansky distr., Voronezh prov., Russia) in June 2009 (voucher: *Sokoloff s.n.*, MW1063500) and in Moskva River near village Lutsino (Odintsovsky distr., Moscow prov., Russia) in June-September 2012 (voucher: *Sadovnikova s.n.*, MW1063501). The material of *N. pumila* (Timm) DC. was collected in Vashutinskoe lake (Pereslavl distr., Yaroslavl prov., Russia) in July 2013 (voucher: *Sadovnikova s.n.*, MW1063499).

All material was fixed in 70% ethanol. For scanning electron microscopy (SEM), specimens were dissected under a stereomicroscope and then dehydrated in alcohol-acetone series, critical-point dried in liquid CO_2 using a Hitachi HCP-2 critical point dryer, mounted on aluminum stubs, coated with gold or platinum using an Eiko IB-3 ion-coater and observed using a JSM-6380LA SEM and CamScan 4 DV at the Department of electron microscopy at the Faculty of Biology, Moscow State University. Tips of 25 rhizomes of *N. lutea* (all from

Moskva River) and of 10 rhizomes of *N. pumila* were used for SEM investigations.

Some flowers have been sectioned anatomically after documenting their morphology using SEM. These dry samples were transferred into 70% ethanol through 100% acetone and then processed using standard anatomical methods (Barykina et al., 2004) with paraplast embedding and serial sectioning at a thickness of 15 μm using the HM 355S Automatic Microtome (Thermo Fisher Scientific). A microtome knife sharpener KS-250 (Thermo Fisher Scientific) was used. The sections were stained in picroindigocarmine and carbolic fuchsine using a Varistain GEMINI ES Automated Slide Stainer and mounted in Bio Mount (Bio-Optica, Milano). Sections were examined and images were taken using a Zeiss Axioplan microscope.

Entire rhizomes were analyzed with respect to the arrangement of all lateral organs and scars of all abscised organs in older parts of the rhizomes. Nineteen entire rhizomes of *N. lutea* were used for quantitative study of organ arrangement. The data set is provided in **Supplementary Data 1**. Methods used for visualization of the quantitative data are explained in the caption of **Figure 3**. To study possible seasonality in organ initiation, four plants of *N. lutea* were selected. Rhizome of each plant has been marked in early June of 2012 by a metallic ring applied just below the first leaf appeared in that vegetation season. These rhizomes were collected at the end of the vegetation season in October 2012 and analyzed with respect to organ arrangement.

RESULTS

Rhizome Morphology and Flower Arrangement

The description of rhizomes is based on *N. lutea*. We had less material on *N. pumila*, but the features described below were found in this species, too, except the occurrence of the collateral groups of the rhizome branches. Also, we did not study young rhizomes before the first branching in *N. pumila*.

The one-flowered reproductive units (RUs) with long-pedicellate flower as well as the long-petiolate foliage leaves with floating blades are spirally arranged along a massive thick creeping monopodial rhizome. The RUs are not located in the axils of the foliage leaves (**Figures 1A**, **2A**). There are no cataphylls directly attached to the rhizome. The RUs appear to 'replace' the foliage leaves in some positions of the ontogenetic spiral of phyllotaxis, or, in other words, the RUs are included in the same spiral as the foliage leaves (**Figure 2A**).

The rhizomes are dorsiventrally flattened, except in young plants. Since the rhizome apex is apparently oblique (displaced toward the dorsal side of the rhizome), the leaves are obliquely inserted on the lateral sides of the rhizome (**Figure 1D**) and transversally inserted on the dorsal (**Figure 1C**) and ventral (**Figure 1E**) sides. As a result, the ontogenetic spiral and the parastichies are somewhat 'deformed' relative to their ideal shapes: they are 'shifted forward' on the ventral side and 'shifted backward' on the dorsal side. According to Raciborski (1894a), rhizomes that grow very deep in the ground (e.g., when flooded with earth due to the slippage of a brook bank), are growing straight up and are almost completely built radially.

The arrangement of the leaves and the RUs along the rhizome follows the Fibonacci pattern. Assuming that organs 6 and 90 in **Figure 2A** both occupy positions close to dorsal median, we calculated an empirical divergence angle as 137.2°, which is very close to the theoretical value for the Fibonacci pattern (137.5°). Direction of the ontogenetic spiral is either clockwise or anticlockwise. Sets of 2, 3 and 5 parastichies can be recognized (**Figure 2A**). As predicted by the Fibonacci pattern, the parastichies forming the sets of 2 and 5 spirals have a direction that is opposite to that of the ontogenetic spiral, while those forming the set of 3 spirals follow the direction of the ontogenetic spiral (**Figure 2A**).

The rhizomes remain undamaged during several years after abscission of foliage leaves and flowers. The positions of all abscised organs can be easily inferred from their scars (**Figures 1**, **2A**) that remain clear throughout the life of the rhizome. The pedicel scars are circular or elliptic (**Figures 1A,E,G**, **2A**). The leaf scars are elliptic with acute left and right angles (**Figures 1A,C–E**, **2A**). Adventitious roots arise, usually in groups of 2-4, below leaf bases on the ventral side of the rhizome (**Figures 1D,E**). They are initiated in the same positions but arrested at early stages on the lateral sides of the rhizome (**Figure 1D**). The roots are absent on the dorsal side (**Figure 1C**).

Distribution of the RUs and the lateral shoots (= rhizome branches) along the length of the rhizome follows certain regularities (**Figure 3**). The RUs tend to form pairs (**Figures 1A**, **2A**). The two RUs of a pair are separated by a foliage leaf in the ontogenetic spiral of phyllotaxis, so that the positions N and N + 2 are occupied by the RUs (**Figure 2A**) and the position N + 1 (as well as N-1 and N + 3) has a foliage leaf. The organs are numbered in the sequence of their initiation. For example, in the rhizome in **Figure 2A**, three such pairs of reproductive units can be seen (in positions 4 and 6, 22 and 24, 48 and 50). The two RUs of a pair are spatially close to each other (**Figures 1A**, **2A**). They hold adjacent positions in a parastichy (namely, in one of the parastichies forming a set of two). Much less frequently, the RUs appear singly (not accompanied by another RU in the position N + 2) or in triplets in positions N, N + 2, N + 4. For example, in the rhizome in **Figure 2A**, there is a RU in the position 69, but organs 67 (on the ventral side, not shown) and 71 are leaves. Occurrence of two RUs in adjacent positions of the ontogenetic spiral (N, N + 1) is extremely rare (**Figure 3A**), but one of these rare instances can be seen in **Figure 2A** (in positions 81 and 82). The number of positions of the ontogenetic spiral between the pairs of the RUs (or single RUs or their triplets) is highly variable (**Figure 3B**), and there is no obvious correlation with any other parameter. In particular, the RUs can be located on any side of a rhizome (dorsal, lateral or ventral, **Figures 1A,E**). Indeed, out of the positions of 138 RUs counted in our quantitative study, 69 were associated with roots and 69 had no roots near their bases. Observations on annual dynamics of the rhizome development demonstrated the absence of any clear correlation between year seasons and initiation of the RUs. A rhizome produces 25–35 foliage leaves and typically more than one pair

FIGURE 1 | Rhizomes of *Nuphar lutea*. **(A)** Dorsal view of rhizome with a lateral branch. Scars of five reproductive units (RUs) are visible. Four of them form pairs and the fifth is associated with the lateral branch. **(B)** Detail of rhizome with a lateral branch and a supernumerary bud in axil of the same subtending leaf. Dorsal **(C)**, lateral **(D)**, and ventral **(E)** views of a rhizome. The roots were cut off before taking the images. Inset shows another view of RU scar that is only slightly visible in panel **(E)**. **(F)** Ventral view of entire branching rhizome with the oldest part remaining (roots and fully expanded leaves cut off). **(G)** Close up of the oldest, vertical part of the rhizome illustrated in panel **(F)**. This part was formed when the plant was young. The first branching event was associated with a shift to dorsiventrality in both the branch and the main axis. fl, flower; lb, leaf blade; lf, cut leaf base (this leaf of the current season was still attached to the plant); ma, main axis; ls, leaf scar; op, oldest part of the rhizome; sl, scar of subtending leaf of rhizome branch; rb, rhizome branch; rt, root; ru = scar of RU; sb, supernumerary lateral bud.

of RUs a season (**Table 1**). Our direct observations showed no obvious seasonality in the activity of the rhizome apex (**Table 1**). In the absence of direct observations it is almost impossible to detect the boundaries between successive years in long perennial rhizomes of *Nuphar*. In our quantitative study based on 19 entire rhizomes, 1/2 of all measured distances between RU groups (or branch + unit groups or single units) was in the interval between 11 and 19 with the median value 15 (**Figure 3B**). Based of our field experiments, these figures have nothing to do with potential seasonality of rhizome growth.

Rhizome branching is always axillary. The subtending leaf of lateral rhizome does not differ from other foliage leaves. Formation of lateral rhizomes is in most cases associated with flower formation in the following way (**Figures 4A,B**): instead of

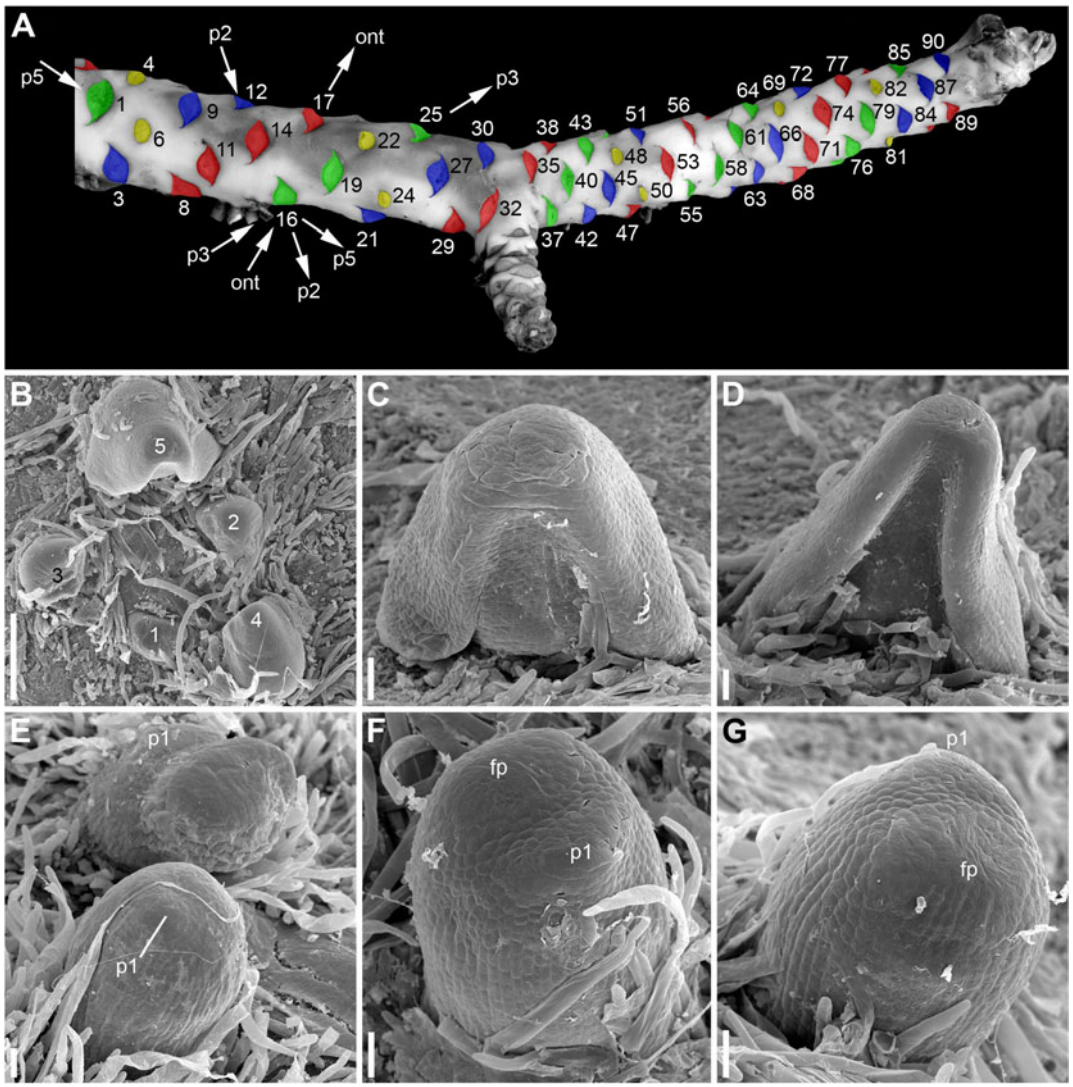

FIGURE 2 | Rhizome morphology and early development of its lateral organs in *Nuphar lutea* (**A**, photo, **B–G**, SEM). **(A)** Dorsal view of rhizome with artificially colored scars of abscised lateral organs. Yellow, scars of RUs, green, blue and red, scars of vegetative leaves. The three colors are used to show that the leaves can be viewed as forming three parastichies, with RUs taking part in formation of these parastichies. The lateral organs of the rhizome are numbered in an acropetal order starting arbitrary from the first visible leaf scar (actually, the rhizome is longer than shown here). The leaf 32 is a subtending leaf of the rhizome branch. There is a RU in the position 34, which is not visible here because it is on the ventral side of the rhizome. Using the leaf 16 as an example, the arrows indicate the four kinds of spirals that can be drawn through each lateral organ of the rhizome. ont = ontogenetic spiral; p2, a spiral that belongs to a set of two parastichies (it comprises all organs with even numbers, the other spiral of this set includes all organs with odd numbers); p3, a spiral that belongs to a set of three parastichies (it includes all leaves colored green plus RUs 4, 22, 34, 82); p5, a spiral that belongs to a set of five parastichies (it includes organs 1, 6, 11, 16, 21, 26, 31, 36, 41, 46, 51, 56, 61, 66, 71, 76, etc.). The spiral p3 has the same direction as the ontogenetic spiral while the spirals p2 and p5 have another direction. B, top view of shoot apex with leaves at different developmental stages (numbered starting from the youngest leaf). **(C,D)** Ventral views of leaf primordia at successive stages (the leaf in **(D)** is the leaf 5 in **B**). **(E)**, RUs at distances of 4 (below) 6 (above) plastochrons from the rhizome apex. **(F,G)** Two views of the same RU at distance of 4 plastochrons from the rhizome apex. **(F)** Oblique abaxial view. **(G)** Adaxial view. fp, flower primordium; p1, the first scale-like phyllome. Scale bars = 300 μm in **(B)**, 50 μm in **(C–G)**.

a pair of RUs in positions N, N + 2, a lateral shoot is formed in the position N and a RU is formed in the position N + 2. Out of 24 instances of rhizome branching found in our quantitative study, 22 had a lateral shoot in the position N and a RU in the position N + 2, as outlined above (**Figures 4A,B**). In two instances, a lateral shoot in the axil of leaf N was accompanied by a RU in the position N-2 (i.e., the lateral shoot was found where the *second* unit of a pair could be expected).

Shoot branching almost always occurs at the lateral sides of the rhizome, though the RUs are present also on the dorsal and ventral sides. Out of many rhizomes examined, only one instance of branching on the dorsal rhizome side was observed. Unfortunately, this particular part of the rhizome was an old one, with the evidence of decay of some organs, so that it was impossible to draw a complete picture of arrangement of all organs. In two instances (in different individual plants),

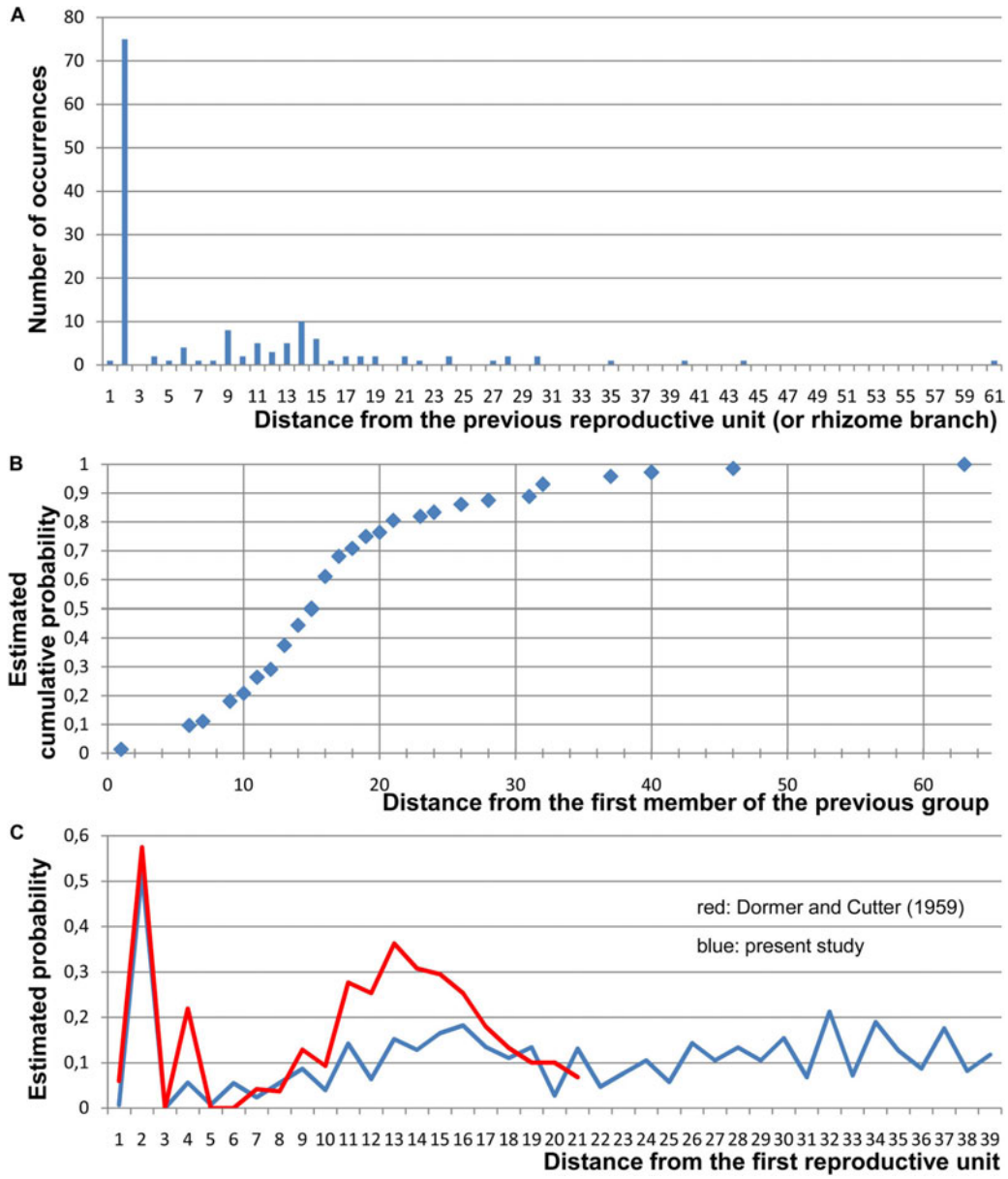

FIGURE 3 | Quantitative data on the arrangement of RUs and rhizome branches in *Nuphar lutea*. For this study, 19 entire rhizomes from the locality in Voronezh province were analyzed and positions of all organs along the ontogenetic spiral were documented. **(A)** Occurrence of different distances (measured in the number of organs along the ontogenetic spiral) between positions of successive lateral RUs and/or positions with rhizome branches (collectively called 'branching sites'). In each rhizome, a distance from each branching site to the next branching site has been measured. Total numbers of occurrences of various distances across all 19 rhizomes are plotted here. In more than 1/2 of the instances, the distance was 2 (i.e., the adjacent branching sites occurred in the positions N and N + 2). **(B)** Occurrence of different distances between the groups, each group containing one, two (N, N + 2), or three (N, N + 2, N + 4) branching sites. Distances from the first site of a group to the first site of the nearest subsequent group have been measured. Estimated cumulative probability rather than absolute numbers of occurrences is shown here. **(C)** Comparison between the present study and the study of Dormer and Cutter (1959). Given that a branching site is present at position 0, each graph shows the frequence of the occurrence of a branching site at each subsequent position of a rhizome. For this analysis, position of the first branching site of a rhizome was treated as 0 and distances to all subsequent branching sites (BS) and non-branching sites (NB) of the rhizome were recorded. Then the second branching site of the rhizome was assigned as position 0 and the same calculation was performed. Following Dormer and Cutter (1959), estimated probability was calculated as BS/(BS + NB) for each distance across all records taken from all rhizomes. Note that Dormer and Cutter (1959) removed positions with lateral rhizomes from their data set (treated these positions as uncertain), but lateral rhizomes were rare in their material.

two rhizome branches were observed in the axil of the same subtending leaf on a lateral side of the rhizome. In both cases, the two branches were located side by side to each other, indicating their development from a collateral group of buds (**Figure 1B**). The larger of the two branches of a pair was in a cathodic position relative to the subtending leaf (the side that is closer

TABLE 1 | Seasonal dynamics of rhizome development in *Nuphar lutea*. Four plants were selected for the experiment.

Rhizome 1. 1 2 3 4 5 6 7 8 (9) 10 11 12 13 14 15 16 17 18 19 20 21 22 23 24
Rhizome 2. 1 2 3 4 5 6 7 8 9 10 11 12 13 (14) 15 (16) 17 18 19 20 21 22 23 24 25 26
Rhizome 3. 1 2 3 (4) 5 (6) 7 8 9 10 11 12 13(rhizome branch in axil of this leaf) 14 (15) 16 17 18 19 20 21 22 23 24 25 26 27
Rhizome 4. 1 2 3 4 (5) 6 (7) 8 9 10 11 12 13 14 15 16 17 18 19 20 21 22 23 24 25 26 27 28 29 (30) 31 (32) 33

Rhizome of each plant has been marked in early June of 2012 by a metallic ring applied just below the first leaf appeared in that vegetation season. These rhizomes were collected at the end of the vegetation season in October 2012 and analyzed with respect to organ arrangement. Diagrams of these rhizomes are provided below. Numbers are organ numbers in the ontogenetic spiral of the rhizome. Numbers without parentheses are vegetative leaves. Number in parentheses are RUs (flowers). Underlined numbers indicate the occurrence of adventitious roots associated with the organ base. Occurrence of a rhizome branch is indicated in parentheses after the number of its subtending leaf. Only organs fully expanded in the current season are considered.

to the beginning of the ontogenetic spiral) while the smaller of the two branches was in an anodic position (closer to the end of the ontogenetic spiral). Like in single branches, in both observed instances, a collateral group in the position N was associated with a RU located in the position N + 2 (in the rhizome in **Figure 1B**, the associated RU is on the ventral side).

The phyllotaxis of the lateral branches starts with foliage leaves (there are no cataphylls). The first leaf is in an anodic position relative to the subtending leaf, the second leaf is in a cathodic position, the third leaf is in an adaxial position being slightly shifted toward the anodic side, then the phyllotaxis continues following the Fibonacci pattern (**Figures 4A,B**). As a result (**Figures 4A,B**), the direction of the ontogenetic spiral of the lateral rhizomes is always the same as in the maternal rhizome (also in both branches of the collateral groups). The shoot chirality (clockwise or anticlockwise) is established at seed germination and conserved throughout the life of the entire plant.

The first rhizome branching in plant ontogeny occurs along with formation of the first flower (**Figures 1F,G**). The oldest part of the rhizome (before the first branching) is upright and not dorsiventrally flattened, with adventitious roots present below all leaf bases (**Figure 1G**). After the first branching, dorsiventrality is conspicuous in the main well as in the lateral rhizome (**Figure 1G**).

Rhizome branching is sylleptic, i.e., the branch growth takes place simultaneously with continuation of growth of the main axis. Dormant buds are absent. The buds are totally absent in the axils of all foliage leaves except those subtending sylleptic rhizome branches as described above. The absence of buds is documented by examination of the external morphology, anatomy and development, including observations of shoot apices using SEM and extensive search of young branches on old rhizomes.

Reproductive Units and Flowers

Each RU consists of a short (about 1 mm long) cylindrical common base, a very long cylindrical pedicel bearing a flower situated at the water surface and one or two scale-like phyllomes (**Figure 5**) at the junction of the cylindrical common base and the pedicel. Almost all examined flowers of *N. lutea* possessed only one phyllome, and its position relative to the rhizome was abaxial (**Figures 4C–F**). The phyllome shape is triangular with acute tip (**Figures 5B,C**) to short and wide with obtuse tip (**Figure 5D**). We found only two flowers with a pair of phyllomes at the base of the pedicel in *N. lutea* (**Figures 5E–K**). In these two flowers, one phyllome was in the abaxial position, while another one was nearly adaxial, but its position slightly differed between the two RUs where it was observed (**Figures 4G,H**). In both units with two phyllomes, the phyllome 2 had a narrower base than phyllome 1 (**Figures 5E,F,H,I**) and in one of the two instances, only the phyllome 2 was vascularized (**Figure 5K**). As the phyllomes are short, they are usually hidden by the long hairs that cover all surrounding organs.

Developmental data are only available for RUs of *N. lutea* with single scale-like phyllome (**Figures 6**, **7**, **8A,B**). The earliest evidence of scale-like phyllome can be seen in RUs at distance of 6 plastochrons from the rhizome apex (**Figures 6A,E–G**). At this stage, the cylindrical common base of RU is already longer than the crescent-shaped phyllome primordium. The phyllome primordium is abaxial relative to the rhizome apex. On the adaxial side of RU, a flower primordium can be seen (**Figures 6F,G**). The flower primordium does not look like a direct continuation of the common base of RU because of its displacement on the adaxial side, its elliptic (elongated transversally) outline and clearly demarcated borders (**Figure 6F**). Similar picture can be seen at slightly older stage (7 plastochrons from the rhizome apex, **Figures 7A,E–G**). The flower primordium is even more transversally elongated (**Figure 7F**) and its borders are clearly demarcated (**Figure 7E**). In these early stages, the width of the scale-like phyllome is compatible to the width of the floral primordium and it is only slightly shorter than the latter (**Figures 6E–G**, **7E–G**). With subsequent flower development, the common stalk of the RU and the scale-like phyllome exhibits only limited growth and become hidden by surrounding structures. Already at the stage with all sepals initiated, special efforts are needed to document the occurrence of the phyllome (**Figures 8A,B**).

Hairs first develop on the abaxial side of the common stalk of RU (**Figures 6E**, **7G**) and then on its adaxial side (**Figure 6C**). Hairs on the pedicel first appear in its distal part (**Figures 8C,I**), probably because the intercalary growth is localized in its proximal part.

The flowers are cup-shaped, with five free rounded sepals, numerous (13–16 in *N. lutea* and 12–13 in *N. pumila*) free narrow nectariferous petals, very numerous (97–150 in *N. lutea* and 55–59 in *N. pumila*) cuneate stamens and a syncarpous superior gynoecium of 14–17 carpels in *N. lutea* and of 8–11 carpels in *N. pumila* (**Figures 9**, **10**). The sepals are convex and much longer and wider than the petals and stamens, forming a protection over the other organs in the bud. Petals and stamens are inserted at the convex receptacle around the club-shaped ovary.

Calyx

The calyx always has a quincuncial aestivation (**Figures 4C–H**, **8A,C,F,H**). Clockwise (**Figures 4C,F,H**, **8C,D**, **11A,B**) and anticlockwise (**Figures 4D,E,G**, **8F,H**) types of the quincuncial

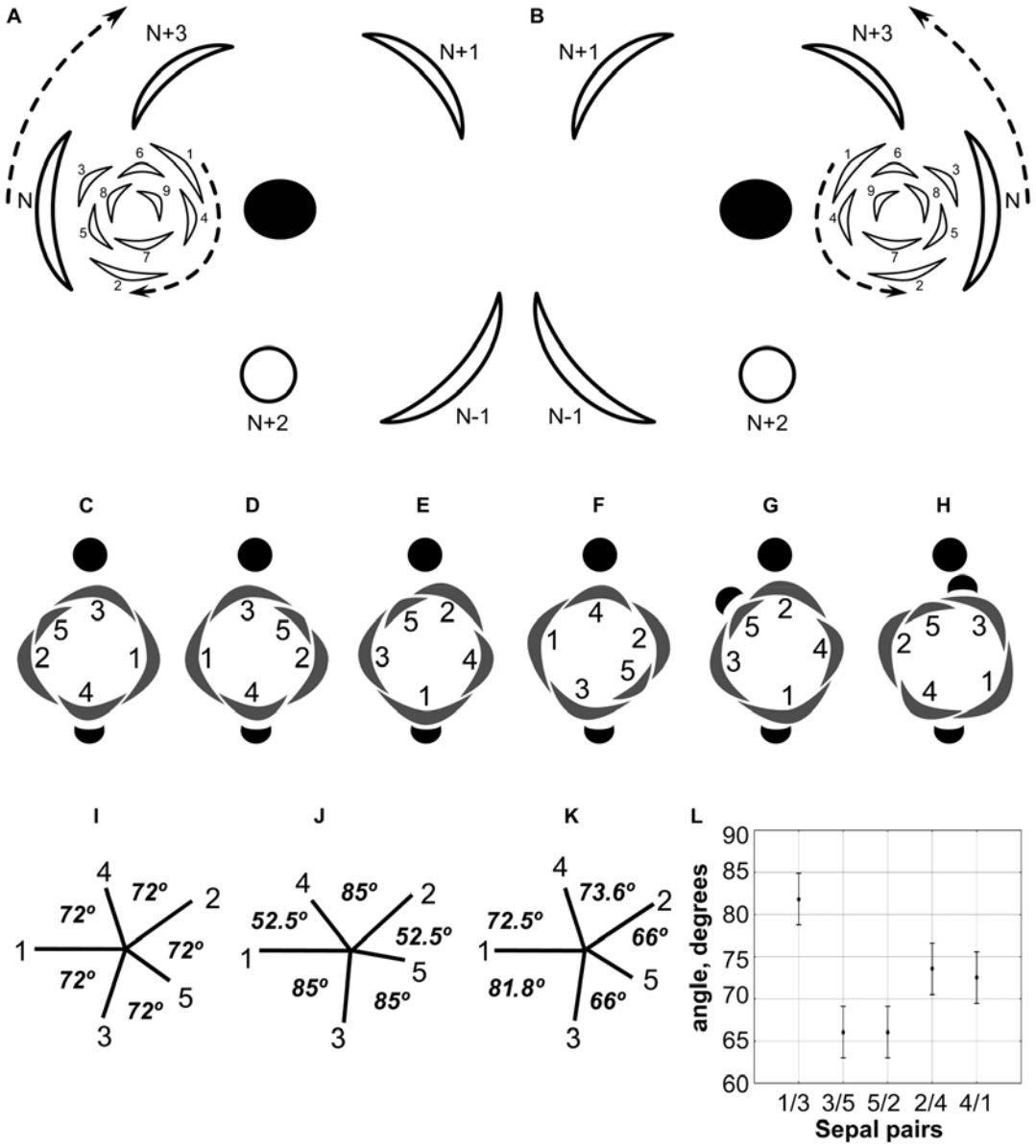

FIGURE 4 | (A,B) Diagrams showing the patterns of rhizome branching and the most common position of the associated RU in *Nuphar lutea*. **(A)** Ontogenetic spirals clockwise. **(B)** Ontogenetic spirals anticlockwise. Black ellipse, rhizome axis that is slightly dorsiventrally flattened; arcs with thick lines, leaves of the main axis; arcs with thin likes, leaves of the branch (1–9); open circle, RU with flower; arrows, direction of ontogenetic spirals; N-1, N, N + 1, N + 2, N + 3, positions in the ontogenetic spiral of the main axis, N is the subtending leaf of the branch and N + 2 is a RU. **(C–H)** Diagrams of all observed patterns of sepal and scale-like phyllome arrangement in *N. lutea*. The most common type in two mirror forms, with clockwise **(C)** and anticlockwise **(D)** sequence of sepal arrangement (and initiation). **(E–H)** Rare types. **(I–K)** Patterns sepal arrangement in calyx with five sequentially initiated sepals. 1,2,3,4,5, sepal numbers. Angles between adjacent sepals are indicated. **(I)** All sepals forming a whorl (theoretical prediction). **(J)** Sepals forming a Fibonacci spiral (theoretical prediction). **(K)** Pattern observed in *Nuphar lutea*, mean values of observed angles are indicated. **(L)** Mean values and confidence intervals for angles between adjacent sepals based on our measurements in 23 flowers of *N. lutea* (see **Supplementary Data 2**, for the data set).

aestivation can be recognized. Both types can be found in different flowers of the same plant, sometimes even in the two RUs in the positions N and N + 2 along a rhizome (**Figure 8A**).

In RUs with single scale-like phyllome, the flowers usually have the two outermost sepals in transversal-abaxial positions, next two larger sepals in almost median positions and an innermost and the smallest sepal in lateral-adaxial position (**Figures 4C,D**, **6B,D**, **7A–D**, **8A,D,E**, **11A**). In this common type of flower orientation, the sepal 3 (the one with one margin external to its adjacent sepal and the other margin internal to another adjacent sepal) is close to an adaxial position (**Figures 4C,D**, **7D**, **8E**). A similar pattern of sepal arrangement was also found in one of the two examined RUs bearing two scale-like phyllomes (**Figure 4G**). The following exceptions from the typical pattern

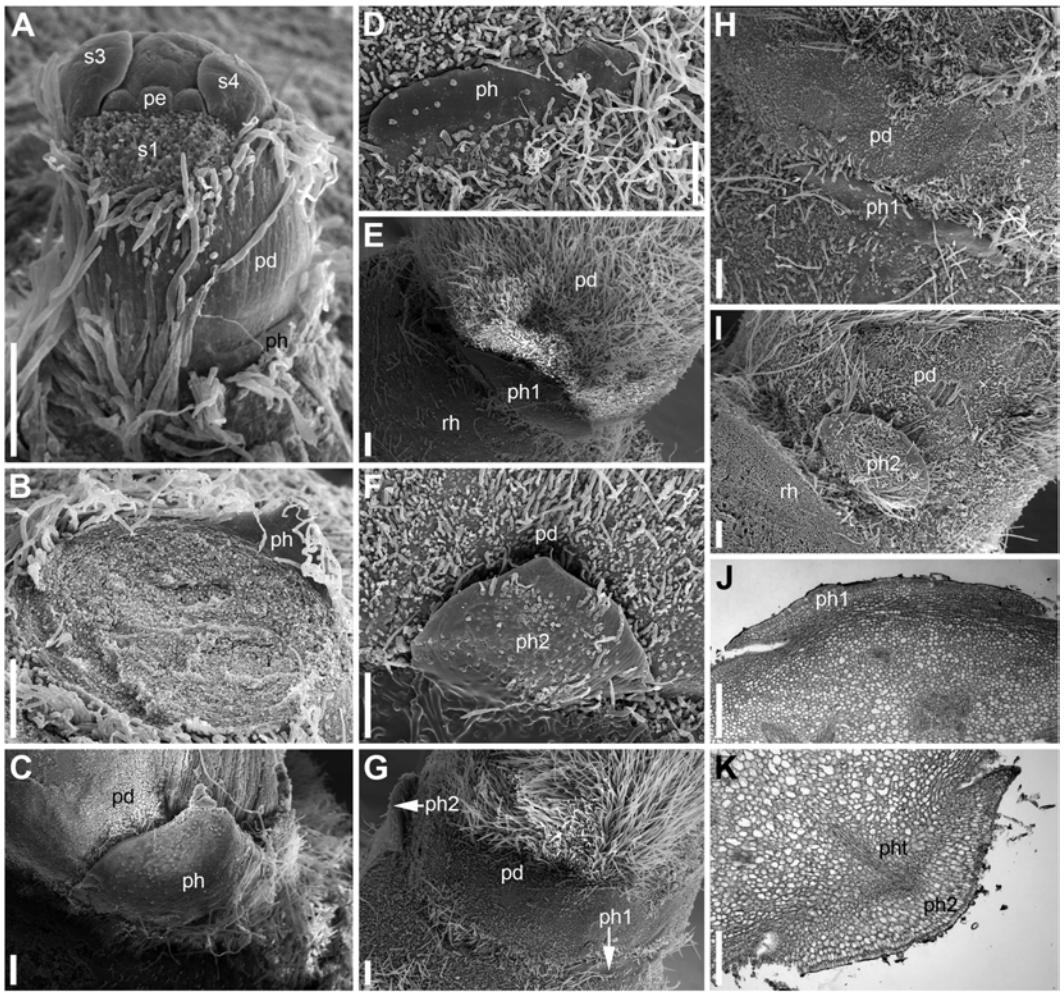

FIGURE 5 | Scale-like phyllomes at the pedicel base of *Nuphar lutea* (**A–I**, SEM; **J,K**, LM). The densely spaced hairs are partially removed in panels **(C–K)**. **(A)** Pre-anthetic RU with single scale-like phyllome. The floral pedicel is yet short. **(B–K)** Anthetic RUs. **(B–D)** RUs with single scale-like phyllome showing variation of its shape. The floral pedicel is removed in **(B)**, so that the phyllome is seen from its adaxial side. **(C,D)** Abaxial view of the phyllome. **(E,F)** RU with two phyllomes (see diagram in **Figure 4H**). **(E)** Phyllome 1. **(F)** phyllome 2. **(G–K)** Another RU with two phyllomes (see diagram in **Figure 4G**). **(G)** Side view showing both phyllomes. **(H,J)** Phyllome 1. **(I,K)** Phyllome 2. pd, pedicel; pe, petal; ph (ph1, ph2), scale-like phyllomes; pht, phyllome trace; rh, rhizome; s1, s3, s4, sepals in sequence of their initiation. Scale bars = 300 μm in **(A–K)**.

of flower orientation have been documented: (1) we found three flowers with the outermost sepal abaxial and the sepal 3 transversal-adaxial (two of them with single scale-like phyllome – **Figures 4E**, **8G–I** – and one with two phyllomes – **Figure 4G**), and (2) a flower with the outermost sepal transversal-adaxial and the sepal 3 transversal-abaxial in a RU with single scale-like phyllome (**Figure 4F**). In the latter case, flower orientation was inverted with respect to the typical condition (**Figures 4C,D**).

Sepal initiation pattern corresponds to the pattern of sepal aestivation, but the process of sepal initiation is very rapid. We only have clear evidence that sepals 1-3 appear before the sepals 4 and 5. In *N. lutea* (for which we had more material), no sepal primordia was observed in flowers until the distance of 7 plastochrons from the rhizome apex unless the transversal elongation of the floral meristem can be interpreted as the earliest manifestation of sepals 1 and 2 (**Figures 7E,F**). At the distance of 8 plastochrons from the rhizome apex, sepals 1 and 2 are well initiated and a smaller primordium of sepal 3 can be seen (**Figures 6A–D**). At the distance of 9 plastochrons from the rhizome apex, all five sepals are initiated in *N. lutea* (**Figures 7A–D**). In *N. pumila,* similar stage of calyx development was found at the distance of only 5 plastochrons from the rhizome apex (**Figure 11A**).

The first three sepal primordia are pronouncedly crescent-shaped whereas the last two are almost rounded in outline and only slightly extended along the apex circumference. After initiation, the sepals grow rapidly to enclose the inner parts of the developing flower. At later stages of flower development, sepals 1 and 2 cover three other petals completely (**Figures 8A,D**).

Angles between sepals were measured in 23 flowers (**Figures 4K,L**). Mean angle between the sepals 1 and 2 was greater than that between the sepals 2 and 3 (about 146° and

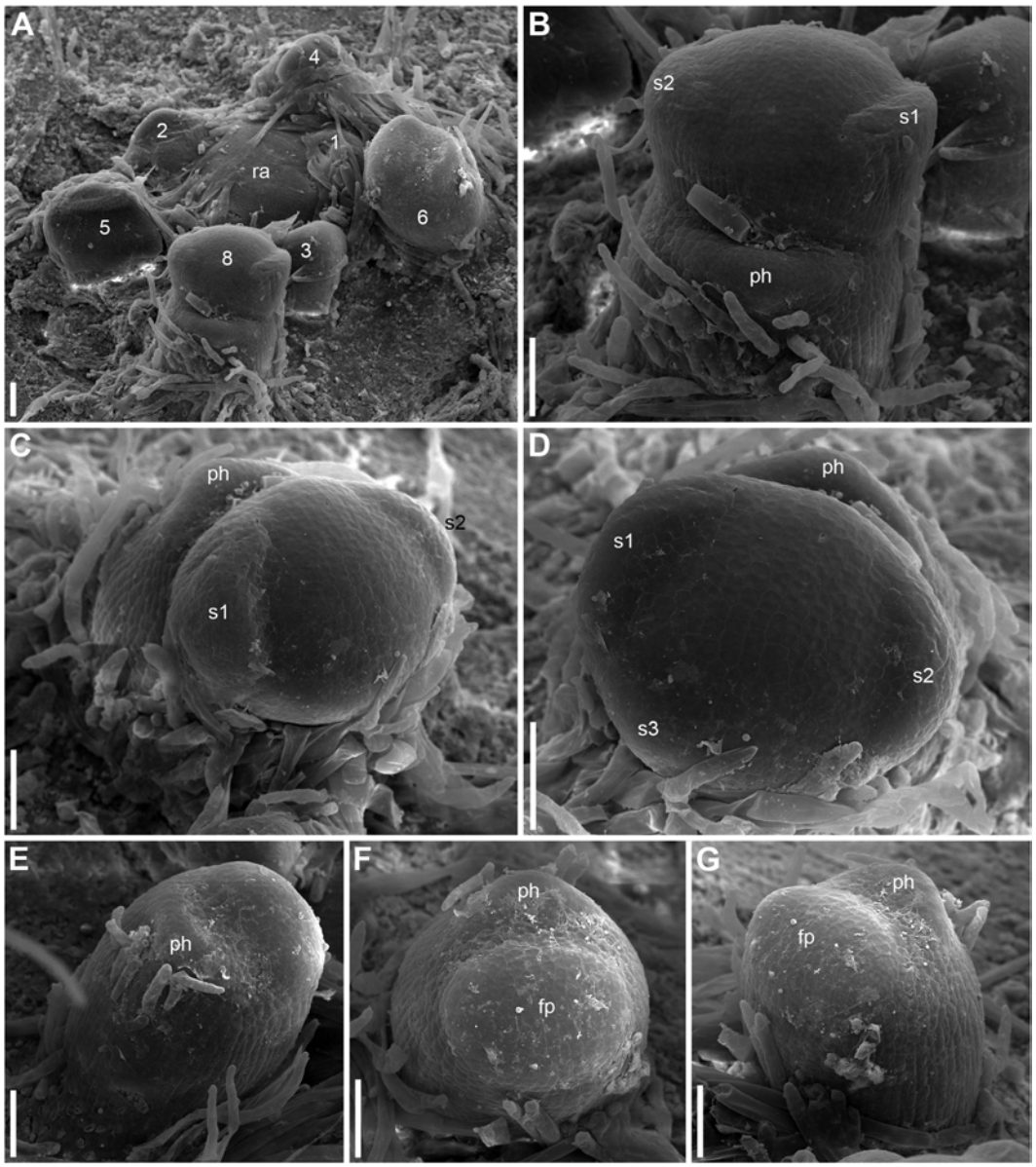

FIGURE 6 | Early development of RUs in *Nuphar lutea* (SEM). **(A)** Rhizome apex surrounded by organs of different age numbered starting from the youngest one. These numbers can be viewed as organ age measured in plastochrons. Organ 7 (leaf) was removed during dissection. 6 and 8 are RUs. **(B–D)** different views of the RU 8 from **(A)**. **(E–G)** Different views of the RU 6 from **(A)**. fp, floral primordium; ph, scale-like phyllome; ra, rhizome apex, s1, s2, s3; sepals in sequence of their initiation. Scale bars = 100 μm in A–G.

132°, respectively). The sepal 4 appeared almost in the middle between the sepals 1 and 4 (mean angles 72.5° and 73.6°, and the difference between these values is not significant, **Figure 4L**). The sepal 5 appeared just in the middle between the sepals 2 and 3 (**Figures 4K,L**).

Corolla

The petals form a series around the flower perimeter. In young flowers, their margins are not overlapping and they are all inserted at almost the same level (**Figures 12**, **13**). At later stages, with increased width of the petals some overlapping of margins can be found (**Figures 14D**, **15B,C**). The petals remain short and do not play important roles in protecting stamens and carpels throughout flower development.

There is a relatively long plastochron between the initiation of the last sepal and the petals. During this time the floral apex becomes more convex. The convexity increases as new organs appear and maintains until all the stamens are produced. Petals differ in shape in early as well as late developmental stages and it may be misleading to use relative size of petal primordia as indication of sequence of their initiation. Petals situated in the sectors of sepals 1, 2 and 3 (these are marked by asterisks in

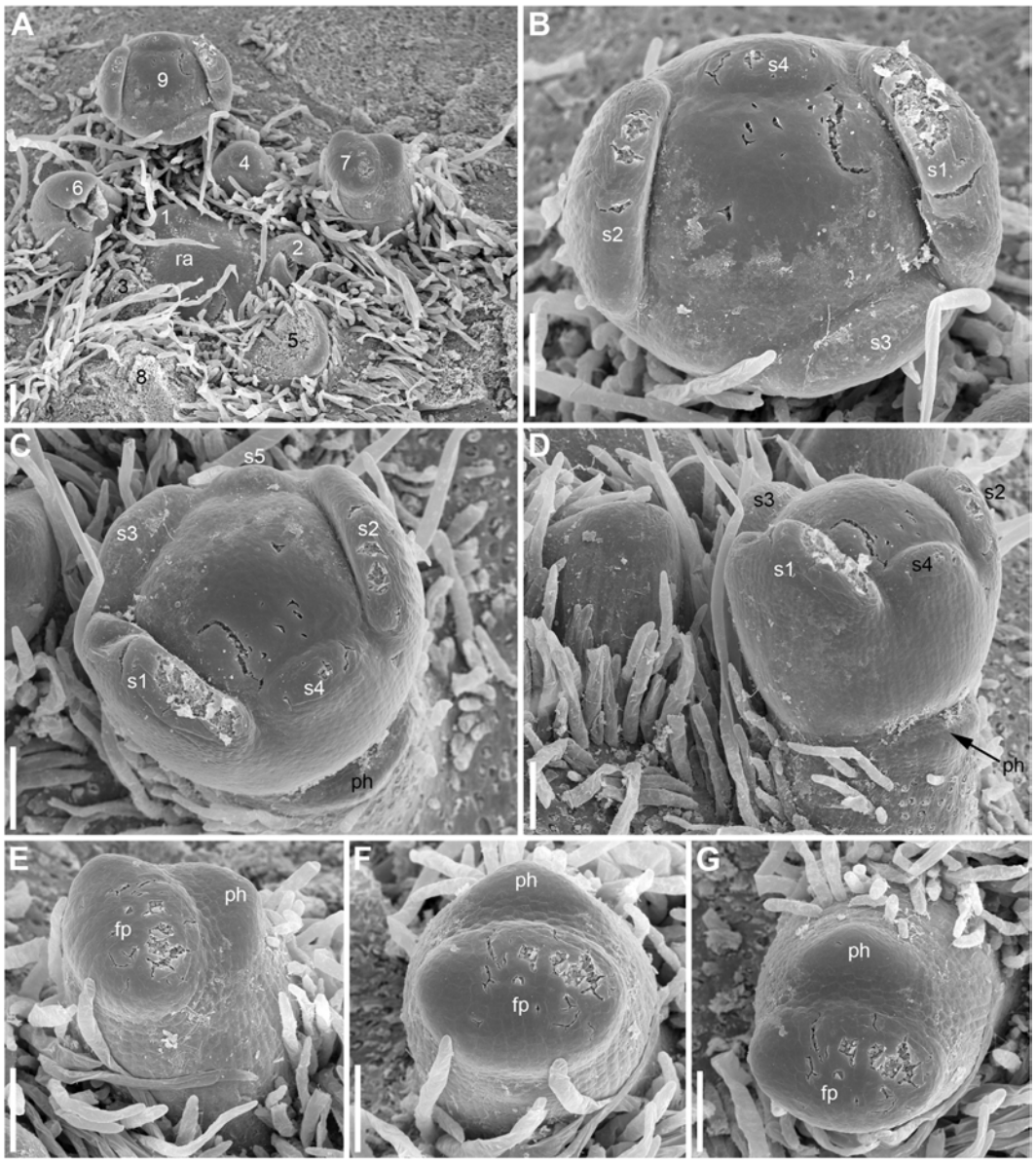

FIGURE 7 | Early development of RUs in *Nuphar lutea* (SEM). **(A)** Rhizome apex surrounded by organs of different age numbered starting from the youngest one. 7 and 9 are RUs. **(B–D)** Different views of the RU 9 from **(A)**. **(E–G)** Different views of the RU 7 from **(A)**. fp, floral primordium; ph, scale-like phyllome; ra, rhizome apex, s1–s5; sepals in sequence of their initiation. Scale bars = 100 μm in **(A–G)**.

Figures 9, **10**) initiate before petals in the sectors of the sepals 4 and 5, at least in *N. lutea* (**Figures 12A–D**). Petals closer to alternisepalous positions are often larger than other petals (note especially the large petal primordia between sepals 1 and 3 in **Figures 13A,B**). On the other hand, there are flowers in which all petals in the sectors of the sepals 1 and 2 are larger than other petals (for example, **Figure 13B**). The corolla is pentagonal in outline reflecting the occurrence of the five lage sepals. The three petals in front of the sepal 1 and the three petals in from of the sepal 2 are the largest ones, the three petals in front of the sepal 3 are slightly smaller and the three and two petals in the sectors of the sepals 4 and 5 are the smallest (**Figure 13B**). Variation of petal numbers in the five sepal sectors is summarized in **Table 2**.

Androecium

The first stamens initiate soon after the petals and normally occupy alternipetalous positions. As petal initiation is delayed in the sectors of the sepals 4 and 5, the very first stamen primordia can be observed in the other sectors when the last petals are yet not recognizable (black arrowheads in **Figures 12B,C**). The stamens form successive alternating whorls whose initiation is centripetal and rapid. These whorls, however, are not always well-recognizable due

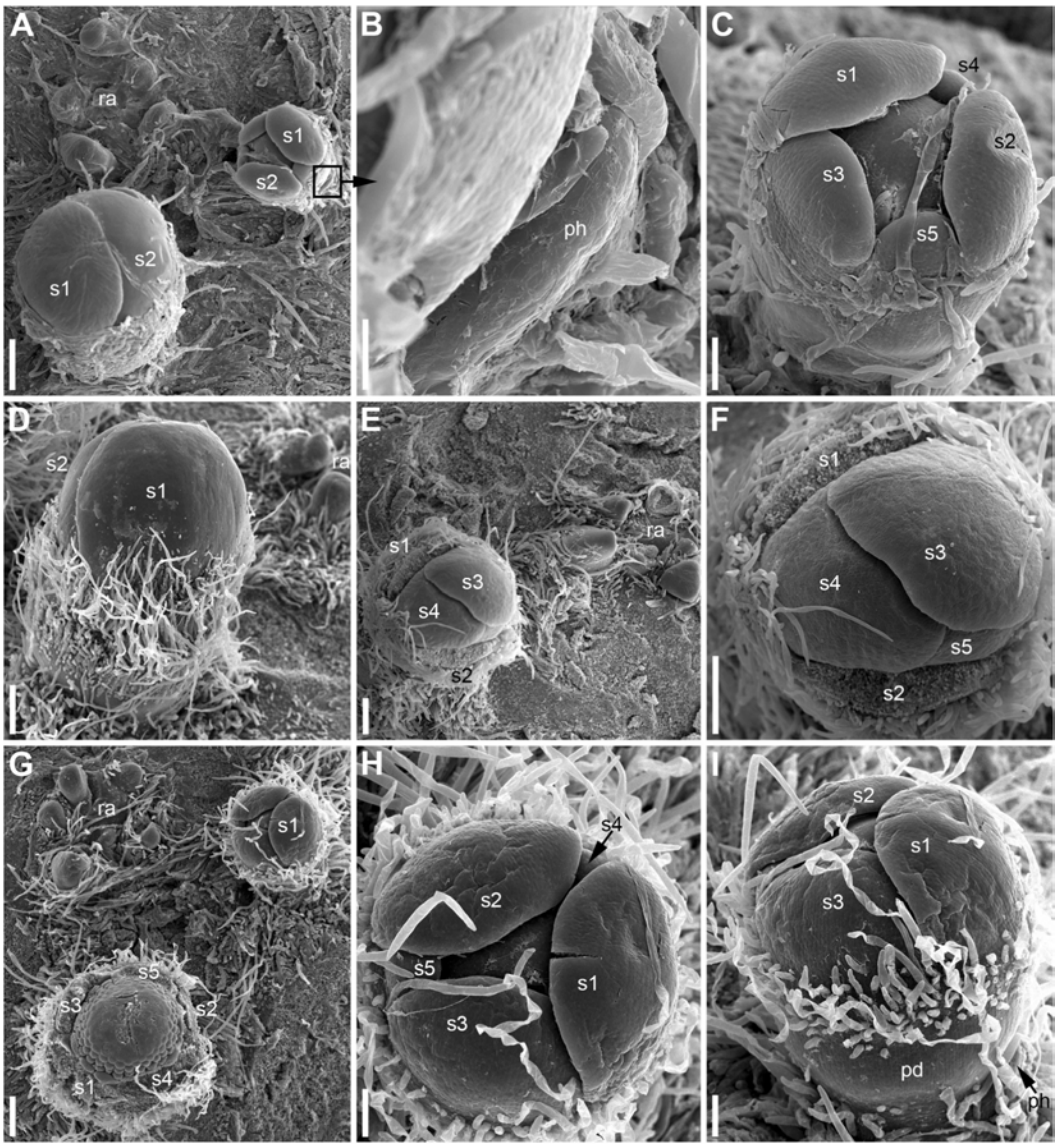

FIGURE 8 | Patterns of flower orientation and calyx aestivation and in *Nuphar lutea* (SEM). **(A–F)** Flowers with the most common type of orientation (see **Figures 4C,D**). **(A)** Two flowers in positions N, N + 2 on the rhizome. The older flower has an anticlockwise sepal arrangement (as in **Figure 4D**), the younger flower has a clockwise sepal arrangement (as in **Figure 4C**). **(B)** Much enlarged detail of **(A)** (marked by a frame in **A**) showing the occurrence of a scale-like phyllome associated with the younger flower. **(C)** The younger flower from **(A)**. **(D)** Flower at about the same stage as the older flower in **(A)**, but with clockwise sepal arrangement. **(E)** Flower with sepals 1 and 2 removed. **(F)** Close up of **(E)**, sepal arrangement anticlockwise (as in **Figure 4D**). **(G)** Two flowers with anticlockwise sepal arrangement and their position relative to rhizome apex. The younger flower with sepal 1 abaxial (as in **Figure 4E**). **(H,I)** Two views of the younger flower from **(G)**. pd, pedicel; ph, scale-like phyllome; ra, rhizome apex; s1–s5 sepals numbered in the sequence of their initiation. Scale bars = 300 μm in **(A,D–G)**, 30 μm in **(B)**, 100 μm in **(C,H,I)**.

to small size of stamen primordia compared with the size of the floral apex and occasional chaotic patterns of stamen arrangement.

At the early stages of development, the petals and stamens are similar in shape and relatively small, though the stamen primordia tend to be more circular in outline. In a few cases we observed individual primordia inserted slightly above typical petals and below typical stamens. We were uncertain in identification of these primordia as future petals or stamens in young flowers (e.g., the organ marked by question mark in **Figure 11C** and the first member of the orthostichy 3 in **Figures 9B**, **13A**). Later, when the thecae of anthers start to differentiate, the transition between petals and stamens is easy to determine. In our experience, the organs initiated in an intermediate position develop as stamens (see the organ labeled st* in **Figure 15D**).

As the outermost stamens usually alternate with petals, an 'ideal' flower would contain N petals, 2N of stamen orthostichies

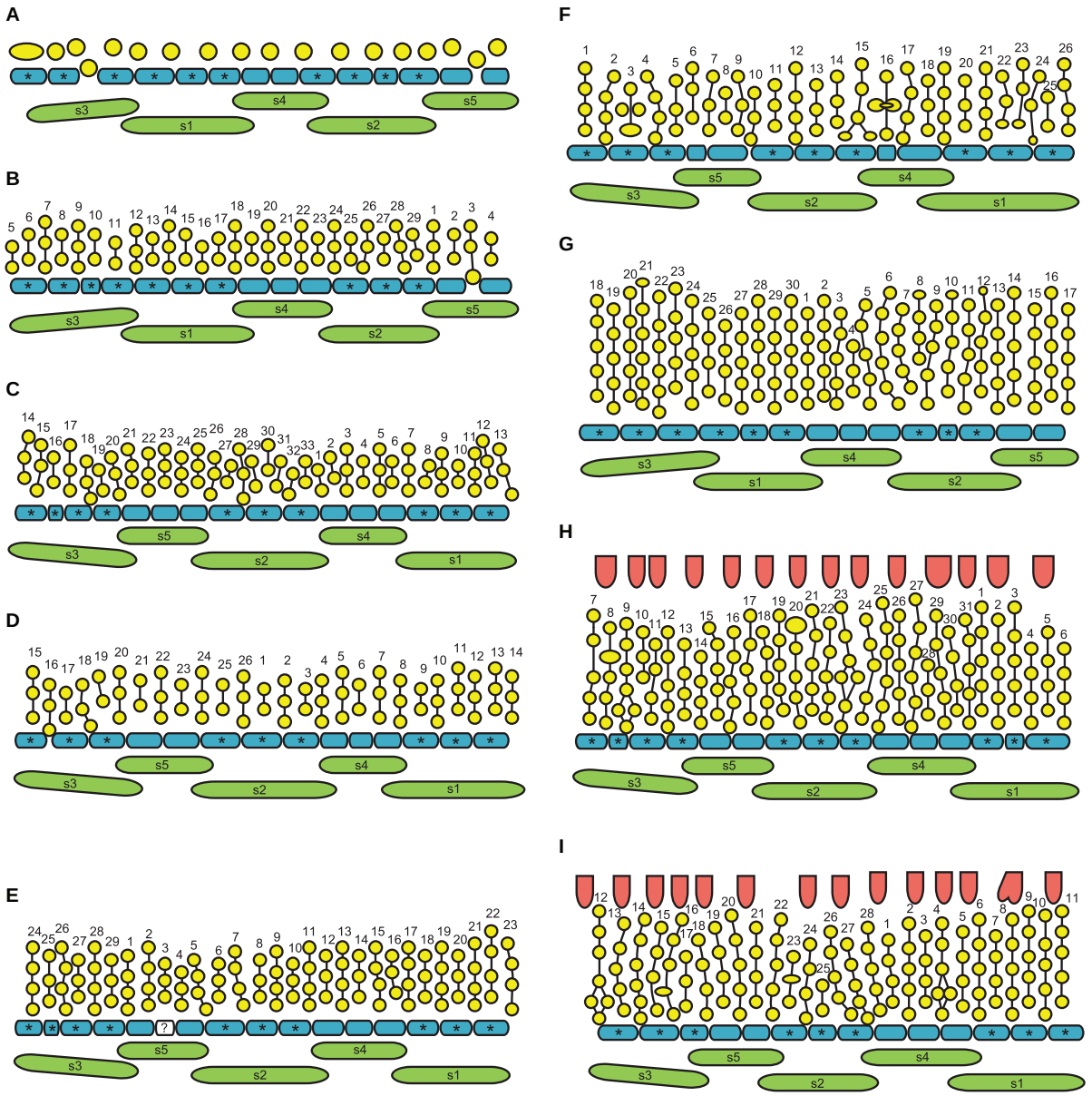

FIGURE 9 | Flower diagrams of *Nuphar lutea*. Here and in **Figure 10**, the diagrams are prepared in a special way. Because the organs are so numerous and the receptacle is so convex, we found it more convenient to present schematical side views (rather than top views) of the flowers. Each flower is 'cut' through a radius near sepal 3 and then 'unrolled' to place all organ positions in the same plane. **(A–F)** Flowers at successive stages of androecium development. **(G)** Flower with androecium initiation completed, but gynoecium not yet formed. **(H,I)** Flowers with all organs initiated. green, sepals (labeled s1–s5 following their aestivation/initiation pattern); blue, petals (asterisks indicate the petals occurring in the sectors of the outer whorl sepals, s1–s3); yellow, stamens; vertical lines, an attempt of recognized stamen orthostichies; red, carpels. The putative orthostichies are numbered starting from an arbitrary point. Question mark indicates an organ that cannot be precisely identified as stamen or petal at this developmental stage.

and two equal sets of N left and N right parastichies. Real androecia deviate from this 'ideal' scheme to a greater or lesser degree (**Figures 9**, **10**). Due to small size of primordia in comparison with the entire floral apex, the regular whorled pattern established by petals is difficult to maintain and the phyllotaxis in most flowers becomes partly chaotic. The degree of irregularity varies from flower to flower. Some (usually 1) orthostichies can be 'missing' or 'added' in particular sites (relative to what can be expected based on the petal number) which leads to presence of unequal subsets of parastichies. Indeed, when the number of orthostichies is 2N-1, then there are sets of N and N-1 parastichies of opposite directions.

Variation in the number of parastichies can be illustrated by some examples (**Figure 13**). In the flower in **Figure 13A** (see also its diagram in **Figure 9B**), the orthostichies 1, 3, 5, 7, 9 are all in alternipetalous positions, but the orthostichy 11 is antepetalous.

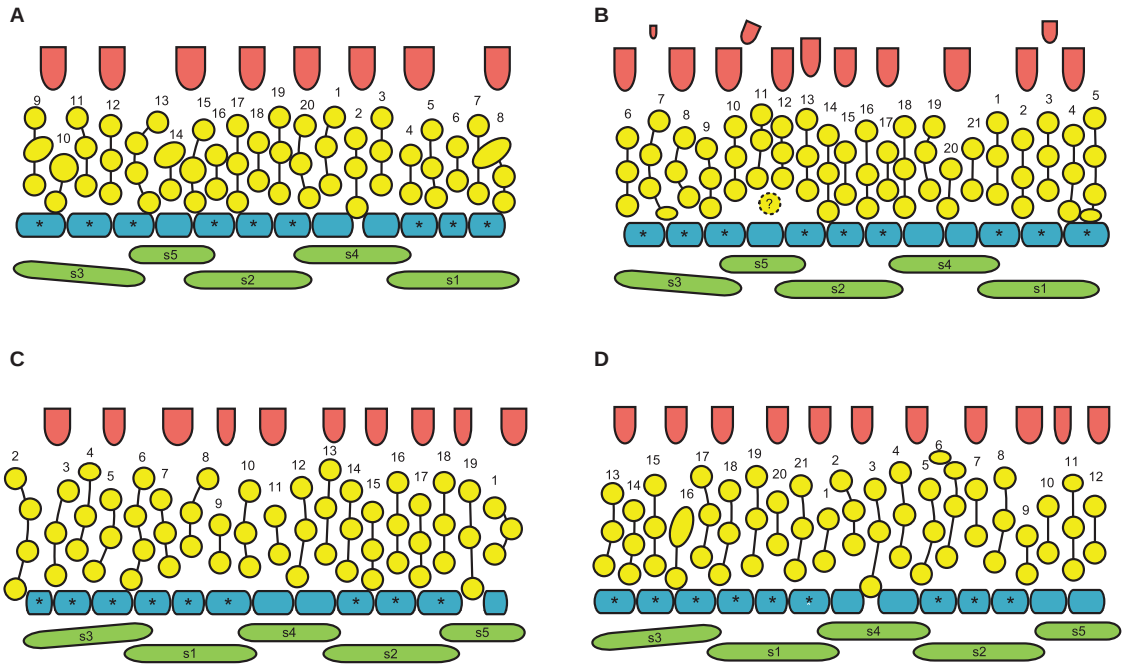

FIGURE 10 | (A–D) Flower diagrams of *Nuphar pumila*. See **Figure 9** for explanations. The second whorl of the gynoecium is only illustrated when more than one carpel was found **(B)**.

This is because one of the three petals in the sector of the sepal 3 is smaller than the other petals and there is no antepetalous orthostichy in the radius of this petal. Because of the absence of this orthostichy, the total of the orthostichies of this flower is 29 despite the presence of 15 petals (**Figure 9B**).

The flower in **Figures 13D–G** has at least 15 (possibly 16, **Figure 9E**) petals and 29 stamen orthostichies (**Figure 13E**). There are sets of 15 (**Figure 13F**) and 14 (**Figure 13G**) parastichies of opposite directions. It is easy to figure out where an expected orthostichy is missing (**Figure 13D**): in the left and central parts of the image, stamen orthostichies colored red are antepetalous, but they are alternipetalous in the right part of the image. The transition is in the sector of the smallest petal where an orthostichy is absent.

The flower in **Figures 13B,C** (diagram in 9D) has 14 petals, but only 26 stamen orthostichies. The petals in the sector of the sepal 4 are smaller than other petals and thus two expected stamen orthostiches are missing here (**Figure 13B**).

The number of stamens is not always equal in all orthostichies (**Figures 9**, **10**). Alternipetalous orthostichies are sometimes one organ longer than the antipetalous ones, and this is what can be expected in a whorled flower. In some cases, just one or a few orthostichies deviate in their organ number. These deviations are mostly localized at the beginning or at the end of the orthostichies. The latter case is illustrated in **Figure 14A**, where there is an orthostichy that is one stamen longer than would be expected (white asterisk) and another orthostichy that is one stamen shorter than would be expected (green arrowhead). There is also a sector where precise recognizing of parastichies is problematic (black dots, **Figure 14A**). There are instances when some orthostichies decline or, alternatively, appear half way to gynoecium. Stamens in double positions can be sometimes observed (**Figure 9F**).

In general, developmental data revealed that the differences in the overall stamen number between *N. lutea* and *N. pumila* are due to the lower number of whorls as well as the lower number of orthostichies in the latter species (**Figures 9**, **10**).

Gynoecium

There is a long plastochron between androecium and gynoecium initiation. The gynoecium starts as a low elevation with lobes usually protruding in free areas between the stamen primordia of the final whorl (**Figure 14A**). The individual carpels appear simultaneously as radial slits (**Figures 11D,E**, **14B**) located on the lobes of the floral apex (or it can be interpreted as a lobed young gynoecium). The number of carpels initiated does not always exactly correspond to the number of the innermost stamens (or to 1/2 of the number of stamen parastichies) because of intervention of chaotic patterns of stamen arrangement (**Figures 9**, **10**). Flowers with branching slits indicating incomplete individuality of carpels are found in *N. lutea* (**Figures 14C,D**, white arrowheads). Similar incompletely subdivided carpels have been illustrated as early as by Trecul (1845).

In *N. lutea*, the central portion of the dome-shaped apex is not involved in carpel formation and remains undifferentiated. The carpel tips do not grow above the initial gynoecial surface. Instead, all the gynoecium enlarges as a whole by intercalary growth and carpel cavities become deeper. This developmental pattern indicates that completely ascidiate carpels form a single whorl and are congenitally united up to their tips. Only in a few

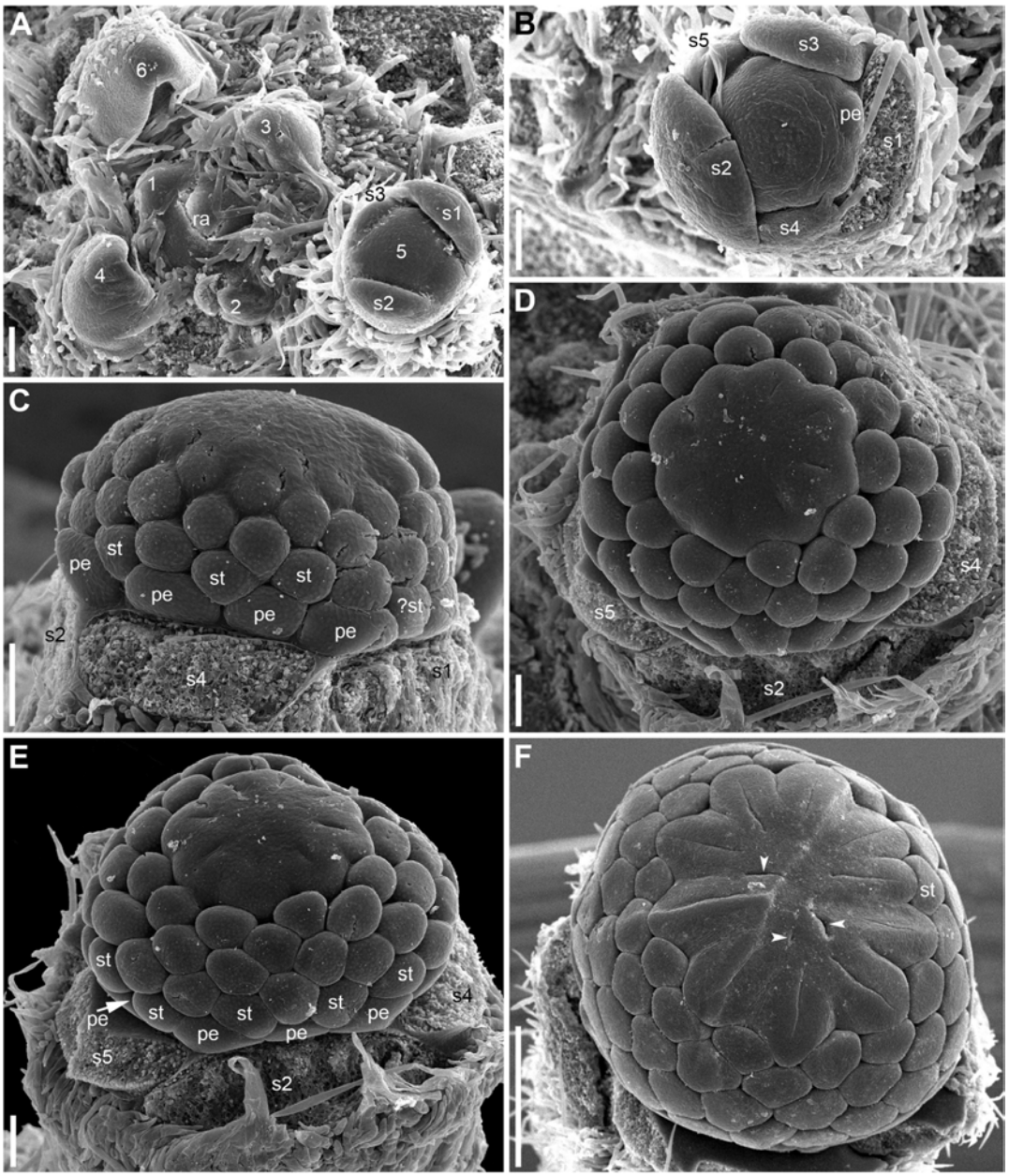

FIGURE 11 | Flower development in *Nuphar pumila* (SEM). **(A)** Flower before petal initiation and its position relative to rhizome axis. Organ age measured in plastochrons is indicated by arabic figures. **(B)** Flower before stamen initiation. **(C)** Flower before carpel initiation. Labels indicate the apparent outer whorl stamens. **(D,E)** Two views of flower with gynoecium just initiated. All carpels are in a single whorl. Diagram of this flower is in **Figure 10A**. Labels in E indicate the apparent outer whorl stamens. **(F)** Flower that is older than in panels **(D,E)**. Its diagram is in **Figure 10B**. Carpels are in two whorls, the second whorl is incomplete and consists of three carpels (arrowheads). The only labeled stamen is one of the innermost stamens and a carpel is located right on its radius. Therefore, this carpel is shifted toward the center of the flower and its position is intermediate between the outer and the inner whorl. It is possible that the asymmetry of the gynoecium caused by this shift triggered the appearance of the inner whorl carpels. It is likely that transference of positional information from androecium to gynoecium was essential in development of this flower, but in our view there is no way of testing a hypothesis that any mechanical pressure (Ronse De Craene, 2018) took place here. pe, petals; ra, rhizome apex; s1–s5, sepals in the sequence of their initiation; st, stamens. Scale = 100 μm in **(A–E)**, 500 μm in **(F)**.

flowers at the latest developmental stages, weak grooves between distal parts of the carpels were found; these never reached the margin of the stigmatic disc (not shown). The length of the carpel slits is less than 1/2 of the radius of the gynoecium, and the slits are located in peripheral parts of the radii (**Figure 14B**). The peripheral part of the gynoecium containing the carpel cavities elongates more extensvely than the central area. As a result, a shallow depression appears in the central area (**Figure 14B**). During subsequent extensive growth of the gynoecium, the upper surface of the gynoecium becomes flat and disc-shaped

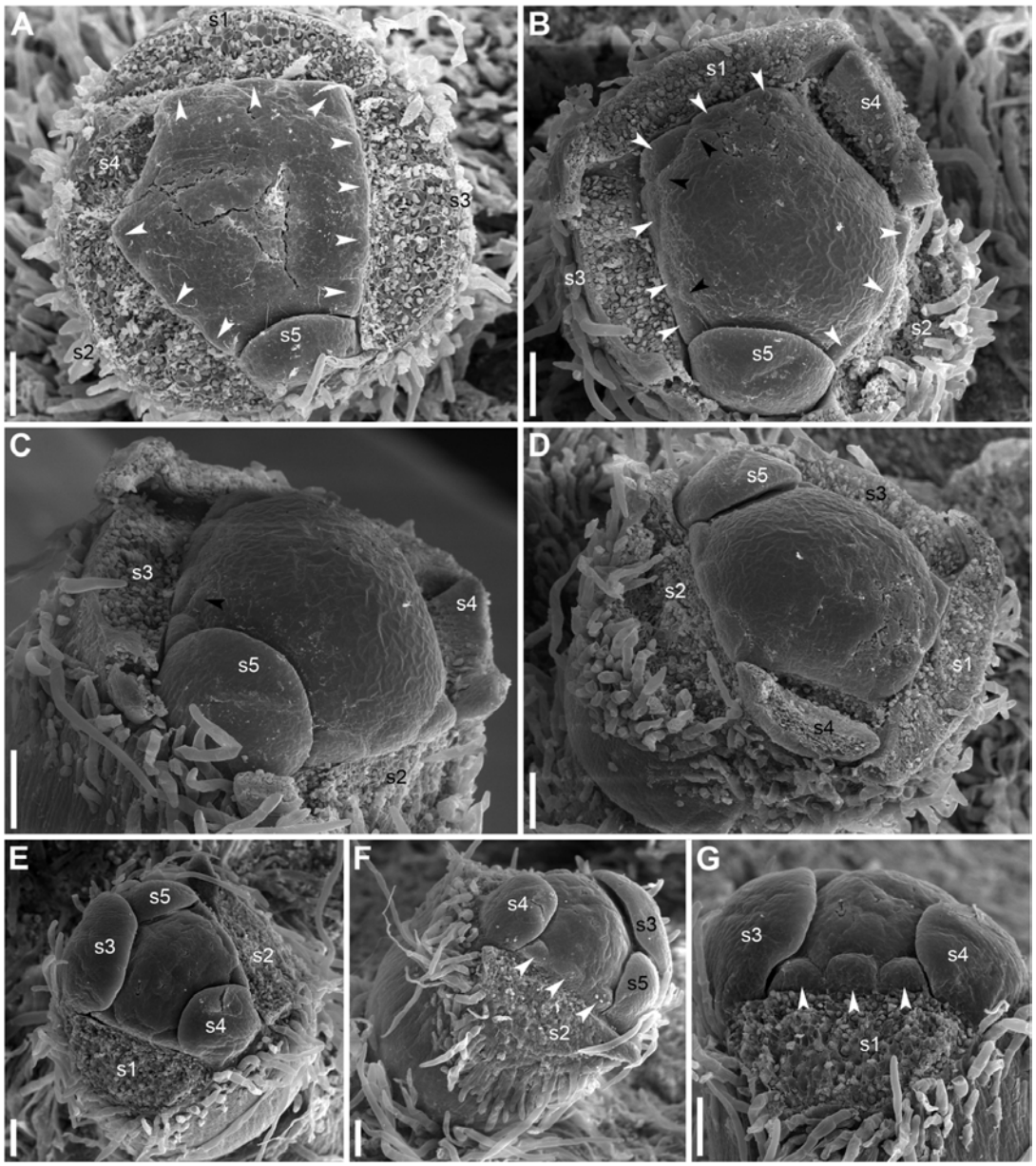

FIGURE 12 | Early corolla development in *Nuphar lutea* (SEM). **(A)** Top view of flower with four of five sepals removed. Note the absence of petals in sectors of the sepals 4 and 5. **(B–D)** Three different views of another flower with four sepals removed. Petals are yet absent in the sectors of the sepals 4 and 5. Note the appearance of the first stamens in the sectors of the sepals 1 and 3. **(E–G)** Three different views of flower with two sepals removed. s1–s5, sepals in sequence of their initiation; white arrowheads, petals; black arrowheads, stamens. Scale bars = 100 μm in **(A–G)**.

(**Figures 14C,D**). Its peripheral area grows radially and the lobes corresponding to individual carpels become much less pronounced. The central depression becomes sealed by irregular growth of more peripheral parts of the gynoecium. As a result, a number of folds can be seen in the center of the gynoecium. Their number and shape are irregular and the folds are in no way related to individual carpels. Sometimes, sealing of the depression takes a more regular form (not shown).

In *N. pumila,* the lobes of the gynoecium are initially almost as weakly pronounced as in *N. lutea* (**Figures 11D,E**), but with subsequent growth of the gynoecium the lobes become conspicuous and the carpel slits extend into the lobes (**Figures 11F**, **15A–C**). There is evidence of mechanical pressure of growing lobes on adjacent stamens. The effect of pressure is only visible on late developmental stages, when anthers adjacent to gynoecium lobes are sometimes partially rotated by displacement (**Figure 15C**). There is no central depression (**Figure 11E**). While at early stages the capels are united with each other throughout their length, late in development their distalmost parts are normally free, though closely spaced. There

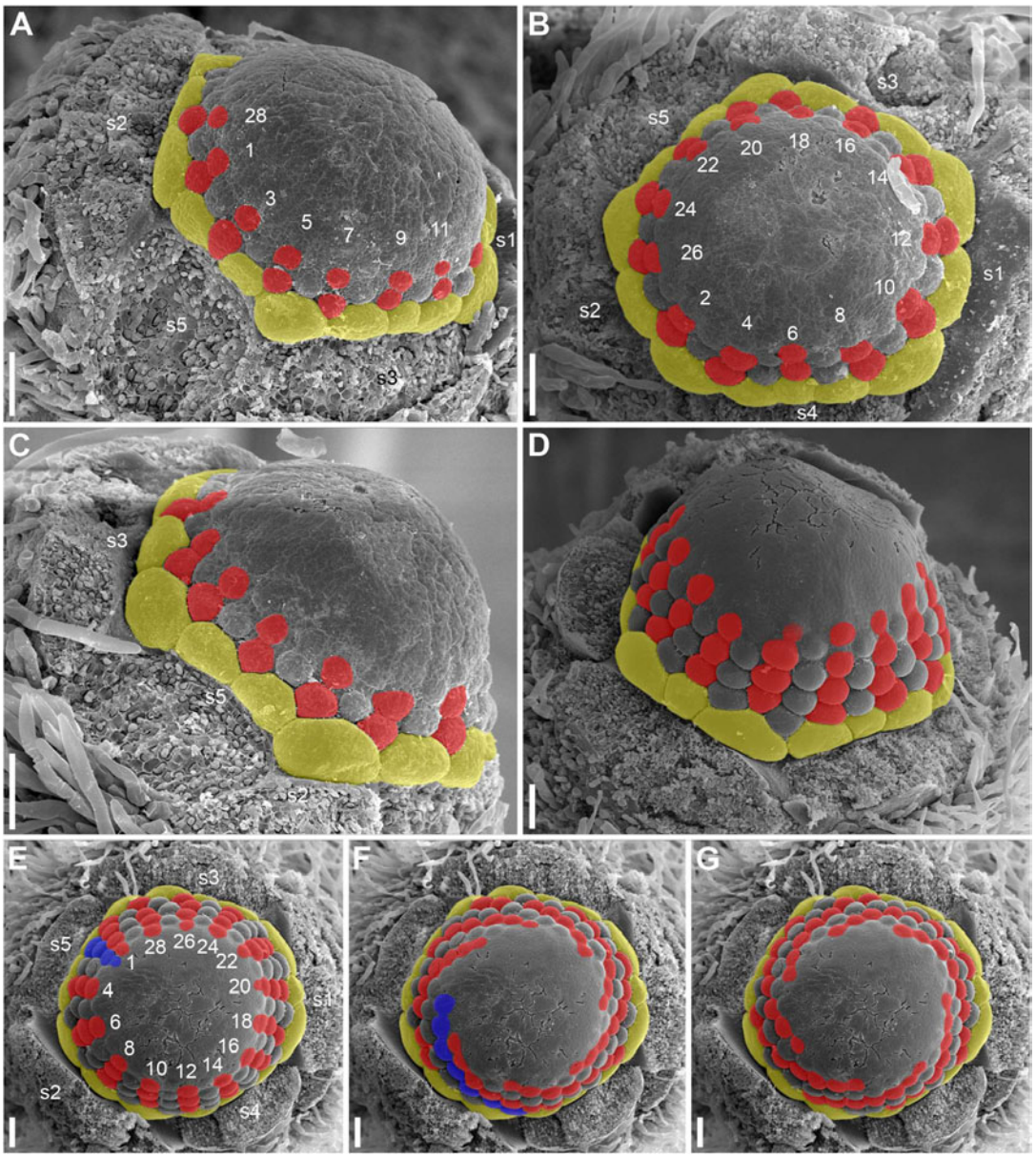

FIGURE 13 | Early androecium development in *Nuphar lutea* (SEM). **(A)** Side view of flower with 15 petals and a 14.5-merous androecium whose diagram is provided in **Figure 9B**. Orthostichies of stamens are highlighted. Note that the first stamen of the orthostichy 3 is shifted toward the level of the petals. **(B,C)** Top and side views of flower with 14 petals and 13-merous androecium whose diagram is provided in **Figure 9D**. Orthostichies of stamens are highlighted. Side **(D)** and top **(E–G)** views of the flower with at least 15 petals and a 14.5-merous androecium whose diagram is provided in **Figure 9E**. Stamen orthostichies are highlighted in panels **(D,E)**. Two sets of stamen parastichies are highlighted in panels **(F,G)**. Yellow, petals; red (and blue), stamen orthostichies in panels **(A–E)** and stamen parastichies in panels **(F,G)**; s1–s5, petals in sequence of their initiation. Stamen orthostichies are numbered in panels **(A,B,E)** in the same way are in **Figures 6B,D,E**. Scale bars = 100 μm in **(A–G)**.

are narrow grooves between the adjacent carpels (**Figures 15A–C,E**). Some of these intercarpellary grooves are incomplete and disappear in their peripheral parts (consider slits between the pairs of labeled carpels in **Figures 15A–C,E**).

Apart from single-whorled (**Figures 11D,E**), two-whorled gynoecia are found in *N. pumila*. The flower in **Figure 11F** is the most instructive in this respect. Here, the outher whorl of the gynoecium is distorted, because one of the innermost stamens (labeled st in **Figure 11F**) lies exactly of a carpel radius. The corresponding carpel is therefore shifted toward the center of the flower: the inner end of the carpel slit is closer to the center than in all other outer whorl carpels. There are three inner whorl carpels, two with short slits and one with a very short slits. The inner ends of the two short slits are at the same distance from the center of the flower as in the unusual outer whorl carpel. The entire gynoecium is rather asymmetrical (**Figure 11F**).

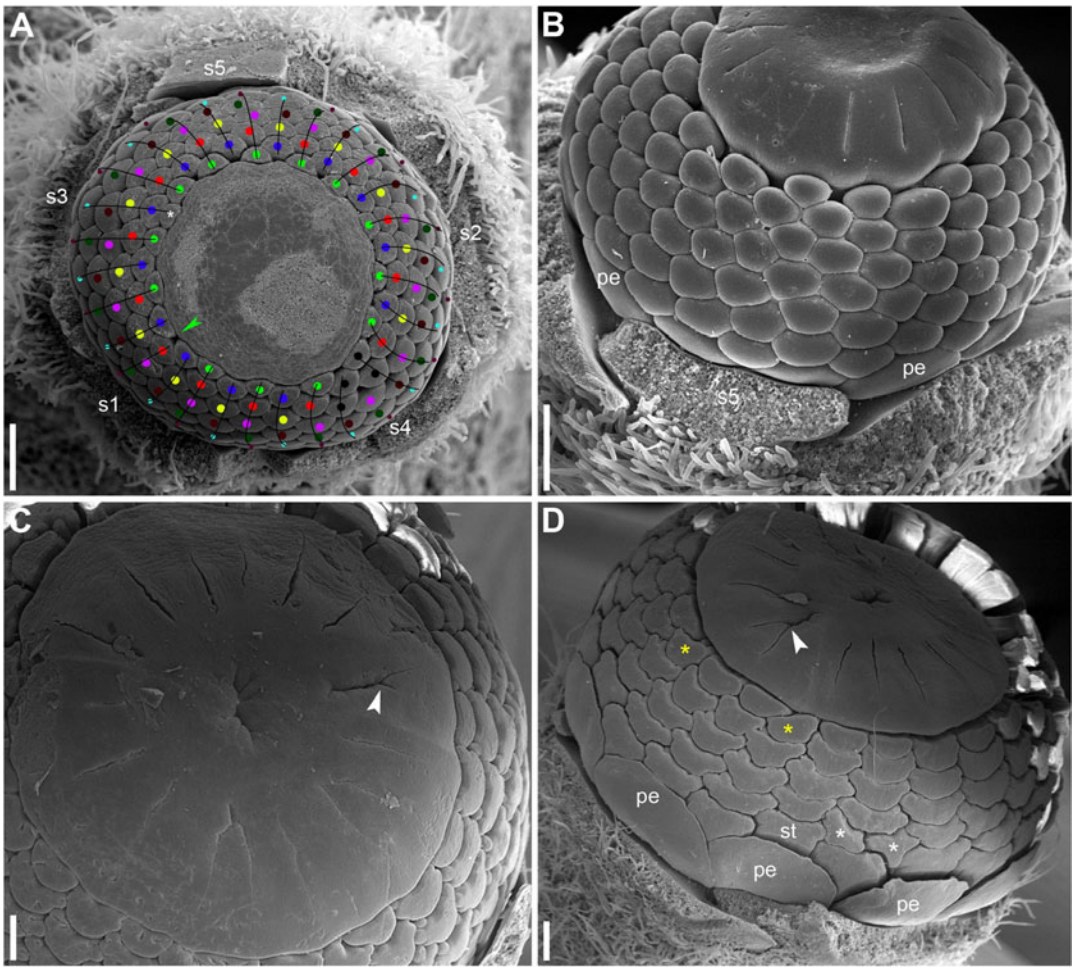

FIGURE 14 | Late stages of flower development in *Nuphar lutea* (SEM). **(A)** Flower whose diagram is provided in **Figure 9G**. Apparent stamen whorls are indicated by dots of different colors. Black dots indicate stamens whose placement in particular whorls is problematic. Apparent orthostichies are indicated by lines. Green arrowhead indicates the position where an inner whorl stamen is missing. There is also an 'extra' stamen inside the innermost whorl (asterisk); note deformation of the receptacle (or very young gynoecium) in the radius of this stamen. **(B)** Flower whose diagram is provided in **Figure 9H**. **(C,D)** Flowers with some carpel clefts bifurcating (white arrowheads). Note the occurrence of some asymmetric stamens in panel **(D)**. Asymmetric are two stamens occupying a double position in a parastichy (white asterisks) and two stamens in the inner part of the androecium (white asterisks). Diagram of **(D)** is provided in **Figure 9I**. pe, petals; s1–s5, sepals; st, stamens. Scale bars = 300 μm in panels **(A–D)**.

Formation of single inner world carpel just in the center of another flower is documented in some flowers (**Figure 15**). The inner whorl carpels are sterile. On cross-sections, they can be recognized in the distal part of the gynoecium only (**Figure 15E**) and not at the level of the ovary (**Figure 15D**).

DISCUSSION

Establishment and Maintainance of Shoot Chirality in Ontogeny

A remarkable feature of rhizomes of both studied species of *Nuphar* is that the direction of the ontogenetic spiral (clockwise or anticlockwise) is repeated in all rhizome branches (i.e., the shoots are homodromous; terminology: Braun, 1835; Dormer, 1965), so that all vegetative progeny of a given plant maintains shoot chirality. Along with genetic markers, this aspect can be used in population-level studies to assess relative roles of vegetative and seed reproduction.

Developmental mechanisms responsible for maintaining shoot chirality in lateral branches may be related to spatial differences between transversal anodic and transversal cathodic positions in the axil of a subtending leaf. The anodic end of a leaf is oriented in the direction up the ontogenetic spiral of phyllotaxis while the cathodic end is oriented toward the beginning of the ontogenetic spiral (Korn, 2006). The first leaf of rhizome branch is always on the anodic side of its subtending leaf in *Nuphar* (**Figures 4A,B**). Patterns differ among various cases of stabilized anodic/cathodic asymmetry in angiosperms (Korn, 2006). For example, in inflorescence (thyrse) of *Dioscorea tokoro*, the bracteole of the first flower of a cincinnus always lies on the cathodic side of the axil of its subtending leaf,

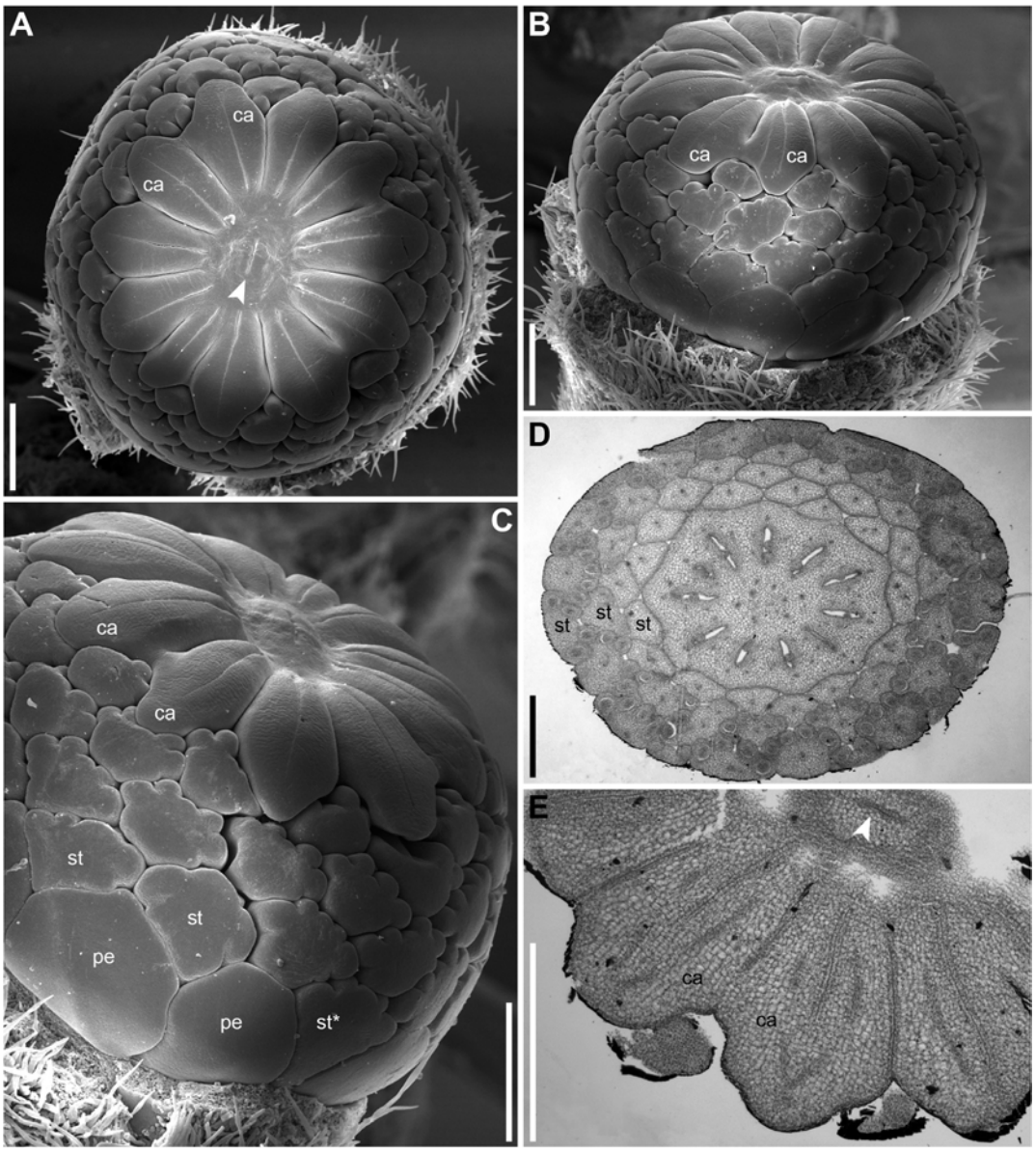

FIGURE 15 | Flower of *Nuphar pumila* whose diagram is provided in **Figure 10D** (**A–C**, SEM; **D,E**, LM). **(A)** Top view. **(B,C)** Side views. **(D)** Cross-section at the level of the ovary. **(E)** Cross-section above the level of the ovules. ca, carpels; pe, petals, st, stamens; st*, stamen attached below the level of the other outermost stamens. Scale bars = 500 μm in panels **(A–E)**.

so the pattern is reverse to what is observed in *Nuphar* (Remizowa et al., 2010a).

As soon as branching takes place on lateral sides of a rhizome in studied species of *Nuphar*, subtending leaves of the branches are always obliquely inserted. As nicely illustrated by Chassat (1962), the branch is thus somewhat displaced from the median position in the axil of its subtending leaf. But the situation is very different on the two sides of the main axis. On one side, the obliquity of leaf bases is in the direction of the ontogenetic spiral whereas on the other side of the main axis the obliquity of leaf bases is nearly perpendicular to the ontogenetic spiral. These impressive differences have no impact on the pattern of initiation of phyllotaxis in lateral branches: the first leaf of the lateral branch is still in an anodic transversal position. We believe that its position is being determined close to the apex of the main axis where the obliquity of the subtending leaf yet not manifested.

The embryo of *Nuphar lutea* has a bilateral symmetry (Meyer, 1960). In mature seed, it contains two cotyledons (organ homologies after Tillich, 1990) and a plumule with two leaves (Guttenberg and Müller-Schröder, 1958). These two leaves lie in a plane between the two cotyledons (Meyer, 1960; Haines and Lye, 1975), and the direction of ontogenetic spiral cannot be yet determined. Shoot chirality becomes pronounced only with appearance of subsequent leaves when certain leaf appears

TABLE 2 | Variation of petal numbers in sectors of sepals 1–5 in the examined material of the two species of *Nuphar*.

	Sector of sepal 1	Sector of sepal 2	Sector of sepal 3	Sector of sepal 4	Sector of sepal 5
N. lutea	3	3–4	3–4	2–3	2–3
N. pumila	2–3	3	3	2	1–2

away from the intercotyledonary plane (either to the left or to the right of it). We believe that the choice between its left or right position is environmentally determined, possibly by gravitropism. Initiation of the third leaf takes place during seed germination (Guttenberg and Müller-Schröder, 1958). If the seed orientation is horizontal, the left and right positions relative to the intercotyledonary plane differ with respect to their proximilty to the Earth. It is likely that gravitropism also plays key roles in determining direction of asymmetric intercalary elongation of cotyledons in Nymphaeaceae (Sokoloff et al., 2014).

Our hypothesis on the roles of gravitropism could be tested experimentally. The experiment should include germination of a sample of seeds of *N. lutea*, with each seed being precisely fixed in a horizontal position. After emergence of epicotyledonary leaves 1, 2 and 3, their position relative to the Earth and shoot apex should be recorded in each seedling. If the leaf 3 always appears on the same side of the shoot apex (e.g., always on the lower side or always on the upper side), then its position and thus the direction of phyllotaxis is determined by gravitropism. If the results turn out to be negative, possible roles of gravitropism in pre-determining future position of the third leaf at the stage of seed development can be further tested. The experiment will require germination of seeds developed within a fruit in various orientations relative to the Earth. Finally, a hypothesis on direct genetic inheritance of shoot chirality can be tested by germination of progeny of self-pollination of plants with clockwise and anticlockwise rhizome spirals. As *N. lutea* is self-compatible (Ervik et al., 1995; Lippok and Renner, 1997), such experiments can be performed.

Flower Arrangement in *Nuphar*

Nuphar and *Nymphaea* share a characteristic pattern of flower arrangement. As demonstrated long time ago (e.g., Raciborski, 1894a) and confirmed in subsequent studies (Cutter, 1957a,b, 1958; Weidlich, 1976a,b; Schneider et al., 2003; Grob et al., 2006), flowers of *Nymphaea* do not possess subtending bracts, but develop in such positions along the rhizome that the flowers can be at least superficially viewed as 'replacing' vegetative leaves in certain positions of ontogenetic spiral. The situation in *Nuphar* is essentially the same, with the difference that there is a tiny phyllome (or two phyllomes) at the base of the pedicel. As revealed earlier (Cutter, 1959; Moseley, 1965, 1972; Schneider et al., 2003) and supported by the present study, none of these tiny phyllomes is situated directly on the rhizome. In both genera, there is a tendency for producing flowers in positions N, N + 2 along the rhizome.

As branching is normally axillary in seed plants, a null-hypothesis that should be tested for a flower that has no obvious subtending bract is that the flower occupies a terminal position. At least for *Nuphar*, this hypothesis can be rejected using arguments summarized in the next paragraph.

If the flowers are morphologically terminal, then the rhizomes are sympodial and the continuation of the rhizome should be a lateral axis developing in the axil of the uppermost foliage leaf. Homodromous sympodial systems superficially resembling a continuous (monopodial) axis with Fibonacci pattern of phyllotaxis are well documented in a few angiosperms, for example in *Pinguicula* (Lentibulariaceae), where a lateral continuation shoot develops in the axil of the uppermost foliage leaf below a reduced 1-3-flowered umbel (Grob et al., 2007; Degtjareva and Sokoloff, 2012). In the case of *Pinguicula*, the first leaf of a continuation shoot is in an anodic position relative to the subtending leaf (like in rhizome branches of *Nuphar*). As a result of this position, only vegetative leaves of the sympodial system mimic a continuous Fibonacci spiral. The flowers (more precisely, umbels, Wydler, 1857; Degtjareva and Sokoloff, 2012) are not members of this spiral. Therefore, the similarity between the sympodial system of *Pinguicula* and the rhizome of *Nuphar* and *Nymphaea* (Raju, 1969) is only superficial (Grob et al., 2007; Degtjareva and Sokoloff, 2012). We can imagine a slightly different situation, where the first leaf of all continuation shoots is in a cathodic position and each elementary shoot is terminated in a flower. Theoretically, such a system will produce a rhizome that fits the features observed in *Nuphar*. However, (1) it is unclear why the position of the first leaf is always cathodic in the hypothetic continuation shoots and always anodic in the actually observed rhizome branches and (2) the proposed sympodial system does not allow occurrence of two flowers as neighboring members of the hypothetical 'composite' Fibonacci spiral in *Nuphar*. A continuation shoot should bear at least one foliage leaf before producing a terminal flower. This foliage leaf is required as a subtending leaf of the next order continuation shoot. In other words, the sympodial model nicely explains the situation of the occurrence of two flowers in positions N and N + 2 (then the leaves N-1 and N + 2 subtend continuations shoots), but the sympodial model fails to explain the occurrence of two flowers in positions N and N + 1. The latter situation is rare, but its occurrence is precisely documented in *Nuphar lutea* (**Figure 2A** of the present study, see also Dormer and Cutter, 1959).

Based on the evidence outlined above, we fully support earlier conclusions (Raciborski, 1894a,b; Cutter, 1957a,b, 1958, 1959; Chassat, 1962; Moseley, 1972; Schneider et al., 2003; Endress and Doyle, 2009) that the rhizome of *Nuphar* is monopodial. Next questions, which are closely related to each other and discussed in the literature cited above are (1) whether the flowers are lateral to the rhizome or to the RU axis (which is then a reduced lateral inflorescence), (2) whether a tiny basal phyllome (or any of the fwo phyllomes) is a (flower-subtending) bract or a sepal homolog and (3) whether the abaxial basal phyllome belongs to the rhizome axis and is just shifted onto its axillary branch (recaulescence) or the abaxial phyllome belongs to the lateral axis, which thus totally lacks a subtending leaf. These problems are

difficult to resolve and we do not think that all the hypotheses are really testable. Moseley (1972) highlighted importance of vascular anatomy (described in Moseley, 1965) and meristem histology in resolving some of these problems. As documented by Moseley (1965), what we describe as a short common stalk of RU remarkably differs from the long flower pedicel in its vasculature. Our preliminary observations (E.S. El, unpubl. data) fully support this conclusion. The common stalk has a ring of vascular bundles, whereas the pedicel above the common stalk has two concentric rings (or stelar and cortical systems) of bundles. In the distal part of the common stalk, the bundles form a vascular complex composed of a continuous circular ring with a cross-bar, and from this there arise the concentric rings of bundles supplying the long floral pedicel (Moseley, 1965, 1972). Using anatomical sections, Moseley (1965) found a circumferential constriction just above the proximal vascular complex demarcating exteriorly the common stalk of RU. These aspects of vasculature (in form of procambial strands) are already recognizable the stage of sepal initiation, long before the intercalary elongation of the pedicel (Moseley, 1972). As pointed out by Moseley (1972), his data as well as the earlier anatomical data of Cutter (1957b, 1959) prove that the scale-like phyllome belongs to the proximal common stalk and its vasculature or procambial strand is derived from the vasculature of the common stalk. Taking into account the fact that rhizome branches and flowers appear in similar positions (forming pairs of N, N + 2), Moseley (1972: 279, see also discussion in Schneider et al., 2003: S287, S289) concluded that the short common stalk at the base of the RU is not part of the peduncle of the flower, but is, rather, 'a short axis which is either a reduced vegetative axis (a possibility considered by Cutter, 1957b) or a vestigial inflorescence axis.' He then favored the idea that *Nuphar* may formerly have had an inflorescence with more than one flower and concluded that the scale-like phyllome(s) do not belong(s) to the flower and should be termed bract(s). As pointed out by Moseley (1972), the meristem of the common stalk has the same histological zonation found in the rhizome apex. He uses this as evidence in favor of his interpretation of the common stalk as a reduced rhizome branch of inflorescence axis, but in our view significance of this observation should not be overestimated. Indeed, the same histological zonation is maintained until the early stage of androecium development (Moseley, 1972).

Our developmental data further support some arguments of Moseley (1972). The plastochron between the initiation of the scale-like phyllome and the first sepal is longer than between the five sepals. The sequence of sepal initiation must be very rapid as it was not possible to find any flower with just one sepal initiated. In RUs with scale-like phyllomes initiated but sepals yet absent, a floral apex can be recognized as a distinct entity. SEM allowed visualizing that the floral apex has well-defined borders throughout its circumference. It does not look like a direct continuation of the common stalk of the RU. With these developmental data, it is tempting to suggest that the scale-like phyllome belongs to the lateral axis and the flower is formed in its axil (i.e., the flower terminates a third order axis). This conclusion agrees with vascular anatomy. We do not insist that this is the only possible conclusion. Initiation of flower-subtending bract and its axillary flower by a common primordium is documented in a range of angiosperms (e.g., Remizowa et al., 2013). The (first) scale-like phyllome always occupies an abaxial position, and it is rather difficult (if not impossible) to prove or disprove the idea that it belongs to the rhizome and junited with the lateral axis (recaulescence). Recaulescence is known in many angiosperms, including some early-divergent lineages such as *Amborella* (Endress and Igersheim, 2000) and some magnoliids (Endress and Lorence, 2020). What can be inferred with more confidence is that the flower and the abaxial phyllome belong to different axes. In particular, this conclusion is supported by relative arrangement of sepals and the abaxial phyllome. Though relative arrangement of sepals is highly conserved in *Nuphar* and they can be easily numbered from sepal 1 to sepal 5 in either clockwise of anticlockwise sequence, the abaxial phyllome in most cases cannot be placed as a member of the same series preceeding the sepal 1 (**Figures 4C–E**). The direction of the angle between this phyllome and the sepal 1 is in most cases opposite to the direction of the angle between sepals 1 and 2 (**Figures 4C,D**).

Unfortunately, like earlier authors (Schneider et al., 2003), we were unable to study development of RUs with two scale-like phyllomes. None of the earlier authors provided information on relative arrangement of sepals and the second phyllome. In both flowers associated with two phyllomes studies here, the *second* phyllome could be viewed as a member of the series series of sepal arrangement preceeding the sepal 1 (**Figures 4G,H**).

In summary, it is most likely that the phyllome 1 is a flower-subtending bract and the phyllome 2 is a bracteole (prophyll). We prefer interpreting the phyllome 1 as belonging to the lateral axis and the flower as terminating a third order axis, but it is difficult to reject a possibility that the phyllome 1 belongs to the rhizome axis and the flower is terminating a second order axis (Raciborski, 1894a; Chassat, 1962; Endress and Doyle, 2009).

Choice of Developmental Programs During Rhizome Development

Our study confirms earlier observations on patterns of distribution of vegetative leaves, RUs and rhizome branches along rhizomes of *Nuphar* (Raciborski, 1894a; Cutter, 1957a,b, 1958, 1959; Dormer and Cutter, 1959; Chassat, 1962). The most remarkable regularity is that RUs or a lateral branch and RU frequently form pairs in positions N, N + 2. Sometimes, this series is continued as N + 4. In *Nymphaea*, much longer series of flowers in even positions can be found. As revealed by Dormer and Cutter (1959; see also Dormer, 1965) and by the present study, given that there is RU in the position N, the probability of the occurrence of another RU in positions N + 1, N + 3 and N + 5 is very low in *Nuphar* (**Figure 3C**). Dormer and Cutter (1959) revealed that apart from this tendency there is a peak of probability of the occurrence of RUs at distances of 11 to 15 positions from an existing RU and interpreted this a periodicity of a longer magnitude. However, they did not analyze probabilities of the occurrence of RUs at distances longer than 21 positions in the ontogenetic spiral. Our data support the conclusion that there is an area of generally low probabilities before the distances of 11 to 15 positions. There is only a weak

depression of our graph after this area (**Figure 3C**). We believe that this depression can be explained by secondary effect from the flowers occurring at distances of 11 to 15 positions. Thus, there are two phenomena (1) a tendency of producing flowers in even positions after an existing flower that disappears after the position N + 4 in *Nuphar* but continues further on in *Nymphaea* (Dormer and Cutter, 1959) and (2) a tendency of inhibition of flowering in certain area after an existing flower. The latter tendency is especially strong in *Nuphar advena* (Dormer and Cutter, 1959 found no RUs at all in positions 3–7). It is very difficult to imagine any environmental factors potentially responsible for these regularities. For example, no periodicity related to seasonality of growth can be seen.

While interpreting these empirical data, one needs to consider that the rhizome apex is nearly flat in waterlilies and therefore physical distances between young organs do not follow the sequence of the ontogenetic spiral. The positions N and N + 2 are closer to each other than the positions N and N + 1. We hypothesize that young primordium of RU or the site of future primordium produces a positional signal (morphogen) that in high concentrations stimulates development of subsequent primordia as RUs but in lower concentrations stimulates their development as vegetative leaves. As can be concluded from surgical experiments (Cutter, 1958), the regulation must take place before the visible appearance of organs on the rhizome apex.

The ideas proposed in the previous paragraph do not explain all features observed in rhizomes of *Nuphar*. Indeed, it is intriguing that the positions with rhizome branches follow the same regularity as those of RUs. If the branch is present in the position N, a RU develops in the position N + 2 (sometimes vice versa). Thus we hypothesize a two-step process of developmental regulation. At the first step, as outlined in the previous paragraph, positions of (pairs of) lateral axes are laid down on the rhizome apex. At the second step, if the first position of a pair is located on a lateral side of the rhizome (relative to the ground level), then a subtending leaf plus a lateral rhizome can arise here instead of RU. This step should involve environmental factors such as gravitropism. See **Supplementary Data 3** for more detailed explanations of the proposed two-step regulation.

There are impressive differences between developmental programs of rhizome branches and RUs. Thus what do they have in common and what may happen at the proposed first step of the regulation (which must take place extremely early in development)? Apparently, at this step branching as such is being allowed. As highlighted by Chassat (1962) and confirmed by the present study, leaves that do not subtend branches do not have any traces of even reduced lateral buds, which is not common in angiosperms.

Five Sepals in Two Unequal Whorls

Interpretation of the perianth organs of Nymphaeaceae and Cabombaceae as sepals and petals or tepals is disputable (Les et al., 1999; Endress, 2001; Ronse De Craene et al., 2003; Schneider et al., 2003; Padgett, 2007; Warner et al., 2009; Ronse De Craene, 2010; Coiro and Barone Lumaga, 2018). Hiepko (1965) concluded that petals of *Nuphar* and *Nymphaea* are not homologous to each other. We use the terms sepals and petals as purely technical, with no claim of petal homologies between waterlilies and eudicots (see Endress, 2006; Yoo et al., 2010; Ronse De Craene and Brockington, 2013).

Members of the section *Nuphar*, including the two species studied here, usually possess five sepals (Padgett, 2007). Sepal aestivation is quincuncial, a condition that is also known in a range of eudicots (Ronse De Craene, 2010). The sequence of sepal initiation agrees with the aestivation pattern and likely determines the latter. Spiral initiation of sepals in core eudicots is an example of spiral organ initiation in whorled flowers (Endress and Doyle, 2007). At first glance, two ideas on sepal arrangement in *Nuphar* can be proposed: (1) the calyx is spiral (spiral flowers are relatively common in basal angiosperms) and (2) the calyx is like in most core eudicots single-whorled, pentamerous. None of these ideas is confirmed. As pointed out by Endress (2001), although in *Nuphar* the outermost five or six (in the section *Astylus*, Padgett, 2007) organs appear sequentially in a spiral pattern, the position is in two whorls. This seems to be effected by a longer plastochron between the third and fourth organ of the flower (Endress, 2001). Our data apparently confirm this idea (**Figures 6D**, **11A**). As such, delayed initiation of some sepals does not indicate that the calyx is necessarily two-whorled. For example, initiation of sepals 4 and 5 is delayed in the pentamerous calyx of some Cistaceae while in other members of the family sepals 3–5 are retarded in initiation (Nandi, 1998). Slightly unequal plastochrons were found in sepal development of some Hydrangeaceae (sometimes with a longer plastochron between sepals 3 and 4, Roels et al., 1997) and Loasaceae (Hufford, 1989).

As suggested by Endress and Doyle (2007), precise interpretation of organ arrangement as spiral or whorled should be based on analyses of divergence angles between the organs. Within a whorl, neighboring organs are equidistant, but the angle is different at the transition from one whorl to another; in spiral systems, divergence angles between successive organs along the ontogenetic spiral are more or less equal (Endress, 1987; Endress and Doyle, 2007). In a whorled pentamerous calyx, the theory predicts angles of 72° between all adjacent sepals (**Figure 4I**). In a trimerous calyx, angles of 120° are expected. In a calyx with five sepals in a Fibonacci spiral, angles between *adjacent* organs are unequal (this follows from equal angles of 137.5° between *successive* organs): two angles are 52.5° and three others are 85° (**Figure 4J**). We tested these ideas using our material of *N. lutea*. At first glance, the results do not fit any theory: mean values are about 73° for two of the five angles between adjacent sepals, 66° for two other angles and about 81° for the fifth angle (**Figures 4K,L**). The differences between these mean values are significant (**Figure 4L**). The inferred angles have nothing in common with what is predicted by the Fibonacci spiral pattern (**Figure 4J**). We interpret our data in the following way. There are three outer whorl sepals. Unlike the common situation, the angles between the outer whorl sepals are unequal: about 146° between sepal 1 and 2, 132° between sepals 2 and 3 and only about 81° between sepals 3 and 1. This is why only two inner whorl sepals are present. There is not enough space for the inner whorl sepal initiation in the sector between the sepals 1 and 3. The sepals 4 and 5 appear in two wider sectors between the outer whorl sepals. Importantly, our quantitative

analysis revealed that the typical position of the sepal 4 is exactly between the outer whorl sepals 1 and 2 (mean angles are inferred as 72.5° and 73.6°, but these differences are not significant, **Figure 4L**). The sepal 5 is inserted exactly between the sepals 2 and 3 (**Figure 4K**). The two-whorled calyx of *Nuphar lutea* maintains the most important feature of the whorled phyllotaxis: the alternation of elements of successive whorls. Each inner whorl sepal is equidistant from the adjacent members of the outer whorl. In contrast to spiral systems, the position of the sepal 4 does not seem to depend on the position of the previously initiated sepal 3, but exclusively on the positions of the adjacent sepals 1 and 2. In the same way, the position of the sepal 5 does not depend on the sepal 4.

Special attention should be paid to use of a consistent way of scoring characters related to floral phyllotaxis in evolutionary analyses (Sauquet et al., 2017). The example of *Nuphar* shows how the ideas based on similar observations can be formulated in different ways. For example, Ronse De Craene et al. (2003) stated that *Nuphar* is occasionally pentamerous by the loss of one sepal of the inner perianth whorl (3 + 2). Endress (2004, 2006) described the perianth of *Nuphar* as spiral, apparently implying the spiral sequence of sepal initiation. Apparently, the calyx of *Nuphar* sect. *Nuphar* should not be scored in morphological data sets as either pentamerous or spiral.

We highlight the importance of the quantitative approach for analyses of organ arrangement in eudicot flowers with five sepals and quincuncial aestivation. They are expected to follow the whorled pattern (Endress and Doyle, 2007), but data on the angles between the sepals are only rarely available. It is possible that further studies will show certain heterogeneity in this group. For example, in the asterid eudicot *Fouquieria columnaris* (Fouquieriaceae, Ericales), the angles between successively initiated sepals are 137°, 137°, 155° and 132° (Schönenberger and Grenhagen, 2005), rather than all equaling 2*72 = 144° (i.e., the value expected in a calyx with five equidistantly spaced sepals).

A highly important member of Nymphaeaceae for which quantitative (and developmental) data are urgently needed is *Barclaya*, which is sister to the rest of Nymphaeaceae except *Nuphar* (Les et al., 1999; Borsch et al., 2008; Taylor, 2008; Gruenstaeudl et al., 2017; He et al., 2018). The flower of *Barclaya* has four or five outermost organs usually interpreted as sepals (Tamura, 1982; Williamson and Schneider, 1994). As pointed out (but not illustrated) by Williamson and Schneider (1994), the mode and sequence of initiation of these organs is the same as described for the sepals of other Nymphaeaceae sensu stricto genera (e.g., *Nymphaea*) with the anterior sepal initiated first, followed by simultaneous initiation of the two lateral sepals, followed lastly by initiation of the posterior sepal. This description is based on flowers with four sepals. According to Tamura (1982), *Barclaya motleyi* consistently possesses five sepals with quincuncial aestivation (just as in *Nuphar* sect. *Nuphar*), though flower orientation relative to main axis is not illustrated. It is unlikely (though not impossible) that development of such calyx follows the unidirectional pattern found in *Nymphaea* and related genera. Published developmental data are not available and urgently needed. There is a useful published image of flower of *Barclaya longifolia* with five sepals. Measurements of angles between all visible organs leaves a question on its interpretation as (1) spiral or (2) whorled with 3 + 2 sepals and 3 + 2 outer petals or (3) whorled with 5 sepals + 5 petals open (**Supplementary Data 4**). Clearly, a quantitative approach is needed here. The first interpretation would contradict the idea of basically whorled nature of flowers in Nymphaeales (Endress, 2001; Schneider et al., 2003), the second interpretation may indicate a plesiomorphic similarity with *Nuphar*, the third interpretation would contradict the idea on the absence of stable pentamery in members of the basal angiosperm grade (Sokoloff et al., 2020).

Calyx Symmetry and Orientation

We found certain autonomy of calyx development from surrounding structures in *Nuphar*. The occurrence of the left or right type of calyx does not depend on the direction of the ontogenetic spiral of the rhizome. This is in a strong contrast with maintainance of shoot chirality in rhizome branches. We hypothesize that the unstable direction of the calyx "spiral" is related to the fact that the sepals appear when the common stalk of the RU is already elongated (Cutter, 1957b, 1959; Moseley, 1972; present study). Also, there is no empirical evidence for sequential initiation of the sepals 1 and 2. The asymmetry only appears with the initiation of the third sepal, and the choice of its left or right position is likely random.

Earlier studies revealed that the flowers of *N. lutea* possess the sepal 3 in a nearly adaxial and sepal 4 in an abaxial position (e.g., Moseley, 1972). We found this as the most common pattern of calyx orientation in *N. lutea* (**Figures 4C,D**). Only this type of flower orientation was found in *N. pumila*, for which we had less material. Other, rare types were revealed in *N. lutea* (**Figures 4E–H**). The differences in calyx orientation did not affect sepal aestivation, which was always quincuncial. This is another evidence of autonomy of calyx development.

According to Moseley (1972), in *N. advena* and *N. variegata*, members of the section *Astylus* with 3 + 3 sepals, two outer whorl sepals are in transversal-adaxial positions and the third one is abaxial (note that the sequence of their initiation is not precisely documented). This differs from the typical condition in *N. lutea* and *N. pumila* (sect. *Nuphar*) where the two first-formed outer whorl sepals are transversal-abaxial and the third one is adaxial. Note that Raciborski (1894a), contrary to Moseley (1972), found two transversal-abaxial and the third adaxial outer whorl sepal in *N. advena*.

Single-Whorled Interpretation of Corolla

Endress (2001) provided the most important and detailed study of early corolla development in *Nuphar*. He studied *N. advena* (with 3 + 3 sepals) and revealed that corolla development begins with initiation of six petals in double positions. Endress (2001) emphasized that flowers of various Nymphaeales share the occurrence of organs in double positions in the third whorl (six stamens in Cabombaceae, six petals in *N. advena*, eight or six petals in *Victoria* and eight petals in *Nymphaea* spp., see also Ronse De Craene and Smets, 1993). Rudall et al. (2009) suggested that the third family of the order, Hydatellaceae, may also fit this pattern, because the involucres of flowerlike reproductive units of

Trithuria occidentalis possess two outer dimerous and the third tetramerous whorl of phyllomes.

We did not reveal petals in double positions in our material of *Nuphar*. We believe that all petals form a whorl in flowers of *N. lutea* and *N. pumila*. Thus, we support the idea that the merism of the third whorl is increased relative to previous whorls, but the increase is more extensive than just appearance of organs in double positions. The petals first appear in the sectors of the outer whorl sepals and later in the sectors of the inner whorl sepals. We suggest that differences in size of young petals not necessarily indicate the sequence of their initiation in *N. lutea*. Larger petals sometimes appear closer to the angles between adjacent sepals, especially in the angle between the sepals 1 and 3, i.e., in the position where one could hypothesize a loss of the third second whorl sepal. The single polymerous whorl of petals of *Nuphar* resembles polymerous single-whorled androecia of some (taxonomically unrelated) angiosperms (Nuraliev et al., 2010; Wanntorp et al., 2011). For example, *Polyscias waialealae* (= *Tetraplasandra waialealae*, Araliaceae) has 6–7 petals and a whorl of 28–46 stamens and some or all alternipetalous stamens are larger or much larger than the others (Nuraliev et al., 2010).

Apparently, the differences in corolla development between *N. lutea* and *N. advena* are not major. The flower of *N. advena* illustrated in Figure 9D of Endress (2001) has nine larger petals forming groups of three in the sectors of the outer sepals. Petals in the sectors of the inner whorl sepals are smaller. The flower in Figure 9C of Endress (2001), which is younger, has three petals in the sector of one of the outer whorl sepals. Petal initiation is retarded in the sectors of the inner sepals (especially in two such sectors). Our interpretation of the corolla in *Nuphar* agrees with a brief description in Wolf (1991) who investigated an unnamed species with five sepals.

It should be noted that the increase of merism in the third whorl is a common, but not universal pattern in flowers of Nymphaeales. Indeed, many members of *Nymphaea* subgen. *Hydrocallis* possess several regularly alternating tetramerous petal whorls (Wiersema, 1987). Thus three conditions can be found in Nymphaeaceae: (1) a single polymerous whorl of petals; (2) the first petal whorl isomerous to calyx, normally tetramerous, the second and subsequent whorls with organs in double positions, sometimes with irregularities; (3) a corolla with many regularly alternating tetramerous whorls. It is an open question whether this series can be read as an evolutionary scenario. Detailed developmental comparisons of various species of *Nymphaea* s.l., including measurements of relative sizes of petal primordia and floral apex are needed.

Androecium Development

We support the idea that the androecium of *Nuphar* and other Nymphaeaceae is fundamentally whorled, with more or less pronounced irregularities (Endress, 2001; Schneider et al., 2003). Wolf (1991) performed detailed investigations of androecia of *Nymphaea alba* and a species of *Nuphar*. He found considerable diversity of androecia in *Nymphaea* (see also Ronse De Craene and Smets, 1993). In a few cases, Wolf (1991) observed androecia with numbers of left and right parastichies are typical for Fibonacci (divergence angle, $\alpha = 137.5°$) or Lucas ($\alpha = 99.5°$) spirals. He considered these cases as exceptions. In most examined flowers, the numbers of parastichies indicated the occurrence of more exotic types of phyllotaxis. For example, androecia with 8 + 11 parastiches of different directions ($\alpha = 132.2°$) and 9 + 10 parastichies ($\alpha = 37.4°$) were found. Flowers with chaotic androecia without clear parastichies were also found (Wolf, 1991). Androecia of *Nuphar* studied by Wolf (1991) were also diverse, including whorled and spiral patterns. In a flower with 15 petals (3 petals in front of each sepal), typical whorled pattern involved 30 orthostichies. This idea perfectly fits our data. An 'ideal' condition for *N. lutea* and *N. pumila* is the presence of equal numbers of antepetalous and alternipetalous orthostichies. Wolf (1991) revealed another situation in *Nuphar* that is close to our observations, namely with 16 + 17 + 33 parastichies ($\alpha = 21.7°$). In his interpretation, which can be easily accepted, what we describe as orthostichies in **Figure 13E** are in fact parastichies (indeed, they are not strictly vertical), so that our flower has 14 + 15 + 29 parastichies.

We prefer describing flowers with N and N + 1 parastichies as whorled, but possessing a non-integer merism of N1/2. For example, the flower in **Figures 13D–G** is 14.5-merous. Such situation appears when a transition between two orthodox, integer values of flower merism is 'frozen halfway,' or a member of one whorl is amalgamated with an adjacent member of another whorl. Situations of this sort have been discussed and variously interpreted for some members of Caryophyllales (e.g., Ronse De Craene et al., 1998; Yurtseva and Choob, 2005; Choob and Yurtseva, 2007).

Application of the concept of non-integer merism, which can be seen as a complementary approach (Rutishauser and Sattler, 1985) to more orthodox view of such flowers as 'simply' spiral, is useful for plant groups with whorled flowers and unstable merism. Vislobokov et al. (2014) explored this while describing flower diversity in the monocot genus *Aspidistra* (Asparagaceae). Flowers of Asparagaceae normally possess 3 + 3 tepals and 3 + 3 stamens. Apart from this trimerous pattern, dimerous, tetramerous and pentamerous flowers are known in *Aspidistra*. In addition, flowers with uneven organ numbers are found, for example with 7 tepals and 7 stamens (or 5 tepals and 5 stamens). Interpreting such flowers as 3.5-merous (2.5-merous) is the simplest way of description (Vislobokov et al., 2014), also for any analyses of character evolution. Alternatives would be interpreting such flowers as tricyclic (considering also gynoecium), but tricyclic flowers are otherwise unknown in Asparagales or as spiral, but spiral flowers are otherwise unknown in monocots (Remizowa et al., 2010b). Similarly, if we accept the occurrence of integer as well as non-integer androecium merism in *Nuphar*, then the character 'androecium phyllotaxis' can be more safely scored as 'whorled' for this taxon for analyses of character evolution. This fits well the idea of the whorled nature of flowers in all Nymphaeales. Alternatively, we will need to score the character as polymorphic (whorled vs. spiral).

An interesting feature of whorled flowers with non-integer merism is that all 'whorls' are united into a continuous, very low spiral (in the case of **Figure 13E** with α = ca. 25°). When we consider a sector of such flower, it seems that it has alternating whorls of stamens, but if we try to trace all

organs of a whorl it happens that one 'whorl' is a direct continuation of another 'whorl.' Apart from androecium of *Nuphar* and examples such as flowers of *Aspidistra*, similar patterns (called biastrepsis) are known as teratological cases in vegetative shoots of some angiosperms, gymnosperms (*Gnetum*) and pteridophytes (*Equisetum*) that normally possess a decussate or whorled phyllotaxis (e.g., De Vries, 1899; Venema, 1937; Snow, 1942; Bierhorst, 1971; Rutishauser, 1999).

Variation of floral phyllotaxis (including chaotic patterns) is well-documented in various angiosperms, especially in those with numerous floral organs (e.g., Endress and Doyle, 2007). The more numerous the floral organs (such as stamens and/or carpels) become, the smaller are their primordia with respect to the floral apex and therefore they become more prone to positional irregularities (Endress and Armstrong, 2011; Rutishauser, 2016). Zagórska-Marek (1994) revealed a great diversity of patterns of carpel arrangement in *Magnolia* flowers, including several 'exotic' types. Interpretation and use of these data depend on focus of discussion. Cladistic approaches require simplification of data. With currently available methods, performing large-scale studies of character evolution without such simplification is nearly impossible. Real taxa often differ in frequencies of certain character states rather than in stable alternative conditions (Meyen, 1973). Variation of floral phyllotaxis in gynoecium and androecium of *Magnolia* (mostly various spiral patterns, see also Xu and Rudall, 2006) and *Nuphar* (mostly more or less typical whorled patterns) nicely illustrates this statement. Many (if not most) other morphological characters in many taxa behave like floral phyllotaxis in *Magnolia* and *Nuphar*, and revealing certain infraspecific variation is probably a matter of sample size.

Gynoecium Diversity in *Nuphar*

The lobed rather than entire edge of the stigmatic disc is traditionally used as a key diagnostic character of *N. pumila* (Padgett, 2007). The present study highlights a need of more detailed developmental studies of gynoecium in *N. pumila* using collections from various localities. We found remarkable features of gynoecium variation in this species. Radial grooves between distal parts of carpels are well-pronounced in *N. pumila*, though some of the grooves are incomplete and do not reach the margin of the stigmatic disc (**Figure 15**). In *N. lutea*, these grooves were only rarely found at the latest developmental stages and never reached the margin of the stigmatic disc. In the New World species *N. advena*, the intercarpellary grooves are absent (Igersheim and Endress, 1998). Thus, there is a variation between complete and incomplete congenital fusion between the ascidiate carpels in *Nuphar*. In *N. pumila*, this variation can be observed within an individual flower. When the fusion in incomplete, it can be classified as early congenital (Sokoloff et al., 2018b), because the intercarpellary grooves are yet absent at the earliest stages of gynoecium development.

We revealed the occasional occurrence of a second whorl of sterile carpels in *N. pumila*. This observation highlights the general phenomenon of developmental plasticity of the floral center in *Nuphar*. In *N. lutea* (our data) and *N. advena* (Igersheim and Endress, 1998; Endress, 2001), the gynoecium is somewhat concave in the center at early developmental stages, and more or less irregular grooves visible at later developmental stages (Figure 32 in Igersheim and Endress, 1998 and **Figures 14C,D** of the present study) merely represent by-products of sealing the central depression. As such, the sealed central depression can be conspicuous in longitudinal sections of young and mature flowers (Moseley, 1965, 1972). What we interpret as single central carpel in some flowers of *N. pumila* (**Figure 15**) cannot be interpreted as by-product of sealing the central depression, because it has a longitudinal slit located on a dome-shaped elevation just in the same way as in the peripheral fertile carpels. Moreover, we did not reveal any central depression in young gynoecia of *N. pumila* (**Figures 11D,F**). The flower interpreted here as having three sterile inner whorl carpels (**Figure 11F**) is even more instructive. It is younger than flowers of *N. lutea* that exhibit sealing of the central depression (**Figures 14C,D**). Based on the stages of carpel and stamen (no distinct microsporangia) development, the flower of *N. pumila* in **Figure 11F** is close to the flower of *N. lutea* in **Figure 14B**. Therefore, the three slits in central part of the gynoecium in **Figure 11F** should be better interpreted as slits of sterile inner whorl carpels. Note that they unlikely represent incipient grooves between fertile carpels, because the developmental stage is too early for appearance of these grooves and one of the three slits that we interpret as belonging to sterile carpels is markedly oblique with respect to the boundary between the closest fertile carpels (**Figure 11F**). Two-whorled gynoecium (or free carpels) is known from a member of Cabombaceae, *Brasenia* (Endress, 2013), and the inner whorl may comprise fewer carpels than the outer whorl (Rudall et al., 2009).

Gynoecia of most Nymphaeoideae possess a conspicuous protrusion of floral apex beyond the level of the carpels (Endress, 2013). The protrusion of the apex is usually not reported from *Nuphar* as well as from *Barclaya* (Williamson and Schneider, 1994; Les et al., 1999; Borsch et al., 2008). Moseley (1972: Figure 38) illustrated a short protusion of the apex inside a deep central depression in *Nuphar japonica*. Interestingly, there are published photographs of *Nuphar pumila* with pronounced central protrusion. In one of them, the protrusion is conspicuous and distally lobed (Bétrisey, 2018). It is tempting to propose that the lobing is due to the occurrence of the second whorl of sterile carpels. An apical protrusion is found in a range of taxa with carpels forming a polymerous whorl (or series: *Illicium*) scattered among angiosperm phylogeny (Endress, 2013). It is not surprising that the character turns to be homoplastic in Nymphaeaceae. Adding fossil record makes it potentially even more homoplastic (von Balthazar et al., 2008; Friis et al., 2009). The sporadic occurrence of the apical protrusion in *Nuphar* illustrates the Krenke's rule (Meyen, 1973): a feature that is characteristic of a given taxon may be found as a rare condition in a related taxon.

Internal and Mechanical Factors in Development

Ronse De Craene (2018) summarized the importance of mechanical pressures in angiosperm floral development. He

highlighted differences between early-developmental and late-developmental pressures. The late-developmental pressures affect already formed organs without influencing their position at initiation (Ronse De Craene, 2018). For example, pressure marks of adjacent organs appear due to organ development in a confined space (Endress, 2008). Androecium development in *Nuphar* apparently provides examples of late developmental pressures. Very young stamens are more or less uniform, hemispherical in both species studied here (**Figures 11C,D**, **13**). At late developmental stages, unusual shape and/or orientation of some anthers can be seen. These can be related to irregularities in stamen arrangement. For example, there is a stamen pair occupying a position where a single stamen could be expected in a whorled system in the flower illustrated in **Figure 14D** (white asterisks). These two stamens are of unusual shapes most likely influenced by mechanical pressures of adjacent stamens. The same flower has two asymmetric stamens in the inner part of the androecium (yellow asterisks). Here, the asymmetry is caused by pressure of an adjacent (left hand in **Figure 14D**) innermost stamen. The innermost stamens, in turn, are compressed by pressure of the late-developing (expanding outwards) stigmatic disc. The asymmetric nature of the pressure on the yellow asterisk stamens appears because the androecium orthostichies are curved in this part of the flower. Where the orthostichies are not curved (right hand part of **Figure 14D**), asymmetry of inner stamens is not manifested. Stigmatic disc is deeply lobed in *N. pumila*. Thus the late-appearing lobes have a stronger impact on the orientation of the innermost stamens. Some anthers thus may be turned to 90° (e.g., the anther between 'ca' and 'ca' in **Figure 15C**). The early-developmental pressures are believed to influence organ position and induce further changes, such as losses or duplications of organs (Ronse De Craene, 2018). In theory, there is no doubt that effects of this sort must take place in floral development. On the other hand, direct testing of this hypothesis is in many cases problematic. For example, in both species studied here, we found instances when a carpel was displaced inwards in the radius of a stamen occupying an unusual position. Clearly, a transference of positional information from androecium to gynoecium took place in these instances. But was this transference at the level of mechanical pressure or pre-patterning (see also Karpunina et al., 2019)?

As highlighted already by Raciborski (1894a), mechanical pressure does not play important roles in rhizome development of *Nuphar*, because young leaves and flowers are not in direct contact with each other at the rhizome apex. Our observations support this conclusion. Especially remarkable is the homodromous nature or rhizome branching that is maintained in spite of strong differences in positions of surrounding organs in branches occurring on the left and right sides of the rhizome. It must be concluded that these differences appear late in development, when branch phyllotaxis is already determined by internal factors. This idea does not necessarily imply that the internal factors are genetic in a simplistic sense. In particular, we do not insist that the occurrence of clockwise or anticlockwise phyllotaxis in rhizomes of *Nuphar* is genetically determined. Instead, we propose a testable hypothesis that it is environmentally determined early in plant ontogeny. Likewise, a possibility of direct genetic inheritance merits experimental testing.

CONCLUSION

Species of *Nuphar* studied here exhibit a mosaic of strong stability and lability in their development. Stable patterns include the maintainance of shoot chirality in all rhizome branches, special positional correlation between rhizome branch and adjacent flower, whorled flowers, overall calyx structure and development with five sepals and quincuncial aestivation. Labile patterns are the distances between flowers along the rhizome length, the number of scale-like phyllomes associated with flower, calyx orientation and its left/right symmetry, petal, stamen and carpel number, relative petal size and the number of stamen orthostichies.

Intriguing tendencies in the arrangement of flowers along the rhizome in *Nuphar* and other waterlilies, especially the N, N + 2 pattern, are known since 19 Century, but we are still far from understanding mechanisms of their regulation. These days various advanced 'omic' (transcriptomic, proteomic, etc.) approaches could be used to compare primordia of various age and position relative to young flower on rhizome apex. With the great progress in understanding regulation of transition to flowering in *Arabidopsis*, some parallels could be found. Another promising direction is mathematical modeling of rhizome growth and organ differentiation in waterlilies.

Interpretation of floral phyllotaxis in *Nuphar* (and many other angiosperms) is problematic for two reasons: (1) infraspecific variation of patterns of arrangement of floral organs in and, importantly, (2) a possibility of use of different criteria to distinguish types of phyllotaxis. In the present paper, we made an emphasis on use of angles between organs while distinguishing whorled and spiral patterns. Another character is the order of organ initiation. A third character (Kitazawa and Fujimoto, 2018; Fujimoto and Kitazawa, 2020) is the pattern of overlapping between margins of adjacent organs (aestivation). Quincuncial aestivation normally correlates with sequential sepal initiation in angiosperms. Is this correlation always empirically demonstrated or sometimes taken as granted? In the case of *Nuphar*, we were unable to collect enough data showing sequential initiation of all five sepals. More importantly, in general, the order of initiation and aestivation are two different characters. There are instances in angiosperms when aestivation clearly does not follow the sequence of initiation, especially in corolla (e.g., Schoute, 1935; Endress, 1999). Use of different criteria may yield in different interpretation of one and the same flower. This is a problem for large scale studies like ancestral character reconstructions. This is why Sauquet et al. (2017) paid special attention to consistent method of character definition across all investigated taxa. Use of literature data for complex characters such as floral phyllotaxis may yield misleading data.

Having in mind all the problems outlined above, we still believe that our study provides further support of the idea that flowers of Nymphaeales are normally whorled (Endress, 2001; Schneider et al., 2003), though their merism and the number of whorls are unstable. Since the flower apex is large and organ primordia are relatively small, interaction of positional information from already formed organs takes place independently in different sectors of the flower. This can be seen (and documented quantitatively) already in the initiation of the two inner whorl sepals. This autonomy of various sectors of developing flowers is likely responsible for the great diversity of androecia and gynoecia in *Nuphar*.

DATA AVAILABILITY STATEMENT

All datasets generated for this study are included in the article/**Supplementary Material**.

AUTHOR CONTRIBUTIONS

EE performed morphological, anatomical, and developmental observations and took all SEM and LM images. DS designed the work and assembled all the figures of the manuscript. EE, MR, and DS interpreted the data and wrote the manuscript.

FUNDING

The work is supported by Russian Foundation for Basic Research (projects 12-04-01070, 12-04-33050, and 18-04-00797). Electron microscopy was performed using the Unique equipment setup "3D-EMC" of Moscow State University (supported by Ministry of Science and Higher Education of Russian Federation, unique identifier RFMEFI61919X0014).

ACKNOWLEDGMENTS

We are grateful to Olesya Pshenichnikova and Piotr Mordvintsev for help in collecting quantitative data on organ arrangement in rhizomes, to Sergey Sadovnikov and Arseny El for help in collecting plant material, to Regine Classen-Bockhoff, Alexander Bobrov, Vladimir Choob, and Paula Rudall for discussion, to Yuri Kopylov-Guskov and Dmitry Sokoloff-IV for help with analyses of quantitative data, to Rolf Rutishauser and Mario Coiro for useful suggestions, to Georgy Davidovich, Anatoly Bogdanov, Svetlana Polevova and their Laboratory of Electron Microscopy at the Biological Faculty, Moscow University for generous technical support.

SUPPLEMENTARY MATERIAL

The Supplementary Material for this article can be found online at: https://www.frontiersin.org/articles/10.3389/fcell.2020.00303/full#supplementary-material

REFERENCES

Barykina, R. P., Veselova, T. D., Deviatov, A. G., Dzhalilova, H. H., Iljina, G. M., and Chubatova, N. V. (2004). *Handbook of the Botanical Microtechniques*. Moscow: Moscow University Press.

Bateman, R. M. (2020). Hunting the snark: the flawed search for mythical Jurassic angiosperms. *J. Exp. Bot.* 71, 22–35. doi: 10.1093/jxb/erz411

Bateman, R. M., Hilton, J., and Rudall, P. J. (2006). Morphological and molecular phylogenetic context of the angiosperms: contrasting the 'top-down' and 'bottom-up' approaches used to infer the likely characteristics of the first flowers. *J. Exp. Bot.* 57, 3471–3503. doi: 10.1093/jxb/erl128

Bétrisey, S. (2018). *Nuphar Pumila va-t-il Disparaître des Alpes?* Available online at: https://www.fr.ch/mhnf/culture-et-tourisme/musees/nuphar-pumila-va-t-il-disparaitre-des-alpes (accessed December 18 2019).

Bierhorst, D. W. (1971). *Morphology of Vascular Plants*. New York, NY: Macmillan.

Borsch, T., Löhne, C., and Wiersema, J. (2008). Phylogeny and evolutionary patterns in Nymphaeales: integrating genes, genomes and morphology. *Taxon* 57, 1052–1081.

Braun, A. (1835). Dr. Carl Schimper's Vorträge über die Möglichkeit eines wissenschaftlichen Verständnisses der Blattstellung, nebst Andeutung der hauptsächlichen Blattstellungsgesetze und insbesondere der neuentdeckten Gesetze der Aneinanderreihung von Cyclen verschiedener Maasse. *Flora* 18, 145–192.

Chassat, J. F. (1962). Recherches sur la ramification chez les Nymphaeacées. *Mém. Soc. Bot. Fr.* 42, 72–95. doi: 10.1080/00378941.1962.10838096

Choob, V. V., and Yurtseva, O. V. (2007). Mathematical modeling of flower structure in the family Polygonaceae. *Bot. Zhurn.* 92, 114–134.

Coiro, M., and Barone Lumaga, M. R. (2018). Disentangling historical signal and pollinator selection on the micromorphology of flowers: an example from the floral epidermis of the Nymphaeaceae. *Plant Biol.* 20, 902–915. doi: 10.1111/plb.12850

Coiro, M., Doyle, J. A., and Hilton, J. (2019). How deep is the conflict between molecular and fossil evidence on the age of angiosperms? *New Phytol.* 223, 83–99. doi: 10.1111/nph.15708

Cronquist, A. (1981). *An Integrated System of Classification of Flowering Plants*. New York, NY: Columbia University Press.

Cutter, E. G. (1957a). Studies of morphogenesis in the Nymphaeaceae. I. Introduction: some aspects of the morphology of *Nuphar lutea* (L.) Sm. and *Nymphaea alba* L. *Phytomorphology* 7, 45–56.

Cutter, E. G. (1957b). Studies of morphogenesis in the Nymphaeaceae. II. Floral development in *Nuphar* and *Nymphaea*: bracts and calyx. *Phytomorphology* 7, 57–73.

Cutter, E. G. (1958). Studies of morphogenesis in the Nymphaeaceae – III. Surgical experiments on leaf and bud formation. *Phytomorphology* 8, 74–95.

Cutter, E. G. (1959). Studies of morphogenesis in the Nymphaeaceae. IV. Early floral development in species of *Nuphar*. *Phytomorphology* 9, 263–275.

Cutter, E. G. (1961). The inception and distribution of flowers in the Nymphaeaceae. *Proc. Linn. Soc. Lond.* 172, 93–100. doi: 10.1111/j.1095-8312.1961.tb00873.x

De Vries, H. (1899). On biastrepsis in its relation to cultivation. *Ann. Bot.* 13, 395–420. doi: 10.1093/oxfordjournals.aob.a088739

Degtjareva, G. V., and Sokoloff, D. D. (2012). Inflorescence morphology and flower development in *Pinguicula alpina* and *P. vulgaris* (Lentibulariaceae: Lamiales): monosymmetric flowers are always lateral and occurrence of early sympetaly. *Org. Divers. Evol.* 12, 99–111. doi: 10.1007/s13127-012-0074-6

De-Paula, O. C., Assis, L. C. S., and Ronse De Craene, L. P. (2018). Unbuttoning the ancestral flower of angiosperms. *Trends Plant Sci.* 23, 551–554. doi: 10.1016/j.tplants.2018.05.006

Dormer, K. J. (1965). "Correlations in plant development: general and basic aspects," in *Handbuch der Pflanzenphysiologie, Band 15, Teil 1*, ed. W. Ruhland (Berlin: Springer), 452–491.

Dormer, K. J., and Cutter, E. G. (1959). On the arrangement of flowers on the rhizomes of some Nymphaeaceae. *New Phytol.* 58, 176–181. doi: 10.1111/j.1469-8137.1959.tb05349.x

Doyle, J. A. (2008). Integrating molecular phylogenetic and paleobotanical evidence on origin of the flower. *Int. J. Plant Sci.* 169, 816–843. doi: 10.1086/589887

Doyle, J. A. (2012). Molecular and fossil evidence on the origin of angiosperms. *Annu. Rev. Earth Planet. Sci.* 40, 301–326. doi: 10.1146/annurev-earth-042711-105313

Doyle, J. A., and Endress, P. K. (2000). Morphological phylogenetic analysis of basal angiosperms: comparison and combination with molecular data. *Int. J. Plant Sci.* 161, S121–S153.

Endress, P. K. (1987). Floral phyllotaxis and floral evolution. *Bot. Jahrb. Syst.* 108, 417–438.

Endress, P. K. (1999). Symmetry in flowers: diversity and evolution. *Int. J. Plant Sci.* 160, S3–S23.

Endress, P. K. (2001). The flowers in basal extant angiosperms and inferences on ancestral flowers. *Int. J. Plant Sci.* 162, 1111–1140. doi: 10.1086/321919

Endress, P. K. (2004). Structure and relationships of basal relictual angiosperms. *Aust. Syst. Bot.* 17, 343–366.

Endress, P. K. (2006). Angiosperm floral evolution: morphological developmental framework. *Adv. Bot. Res.* 44, 1–61. doi: 10.1016/s0065-2296(06)44001-5

Endress, P. K. (2008). The whole and the parts: relationships between floral architecture and floral organ shape, and their repercussions on the interpretation of fragmentary floral fossils. *Ann. Missouri Bot. Gard.* 95, 101–120. doi: 10.3417/2006190

Endress, P. K. (2013). Multicarpellate gynoecia in angiosperms: occurrence, development, organization and architectural constraints. *Bot. J. Linn. Soc.* 174, 1–43. doi: 10.1111/boj.12099

Endress, P. K., and Armstrong, J. E. (2011). Floral development and floral phyllotaxis in *Anaxagorea* (Annonaceae). *Ann. Bot.* 108, 835–845. doi: 10.1093/aob/mcr201

Endress, P. K., and Doyle, J. A. (2007). Floral phyllotaxis in basal angiosperms: development and evolution. *Curr. Opin. Plant Biol.* 10, 52–57. doi: 10.1016/j.pbi.2006.11.007

Endress, P. K., and Doyle, J. A. (2009). Reconstructing the ancestral angiosperm flower and its initial specializations. *Am. J. Bot.* 96, 22–66. doi: 10.3732/ajb.0800047

Endress, P. K., and Igersheim, A. (2000). The reproductive structures of the basal angiosperm *Amborella trichopoda* (Amborellaceae). *Int. J. Plant Sci.* 161, S237–S248.

Endress, P. K., and Lorence, D. H. (2020). Inflorescence structure in Laurales, stable and flexible patterns. *Int. J. Plant Sci.* 181, 267–283. doi: 10.1086/706449

Ervik, F., Renner, S. S., and Johanson, K. A. (1995). Breeding system and pollination of *Nuphar luteum* (L.) Smith (Nymphaeaceae) in Norway. *Flora* 190, 109–113. doi: 10.1016/s0367-2530(17)30639-4

Friis, E. M., Crane, P. R., and Pedersen, K. R. (2011). *Early Flowers and Angiosperm Evolution*. Cambridge: Cambridge University Press.

Friis, E. M., Pedersen, K. R., von Balthazar, M., Grimm, G. W., and Crane, P. R. (2009). *Monetianthus mirus* gen. et sp. nov., a nymphaealean flower from the Early Cretaceous of Portugal. *Int. J. Plant Sci.* 170, 1086–1101. doi: 10.1086/605120

Fujimoto, K., and Kitazawa, M. S. (2020). Perianth phyllotaxis is polymorphic in the basal eudicot *Anemone* and *Eranthis* species. *Front. Ecol. Evol.* 8:70. doi: 10.3389/fevo.2020.00070

Gatsuk, L. E. (1974). Gemmaxillary plants and a system of subordinated units of their shoot body. *Bull. Mosc. Soc. Nat. Biol. Ser.* 79, 100–113.

Grob, V., Moline, P., Pfeifer, E., Novelo, A. R., and Rutishauser, R. (2006). Developmental morphology of branching flowers in *Nymphaea prolifera*. *J. Plant Res.* 119, 561–570. doi: 10.1007/s10265-006-0021-8

Grob, V., Pfeifer, E., and Rutishauser, R. (2007). Sympodial construction of Fibonacci-type leaf rosettes in *Pinguicula moranensis* (Lentibulariaceae). *Ann. Bot.* 100, 857–863. doi: 10.1093/aob/mcm184

Gruenstaeudl, M. (2019). Why the monophyly of Nymphaeaceae currently remains indeterminate: an assessment based on gene-wise plastid phylogenomics. *Plant Syst. Evol.* 305, 827–836. doi: 10.1007/s00606-019-01610-5

Gruenstaeudl, M., Nauheimer, L., and Borsch, T. (2017). Plastid genome structure and phylogenomics of Nymphaeales: conserved gene order and new insights into relationships. *Plant Syst. Evol.* 303, 1251–1270. doi: 10.1007/s00606-017-1436-5

Guttenberg, H. V., and Müller-Schröder, R. (1958). Untersuchungen über die Entwicklung des Embryos und der Keimpflanze von *Nuphar luteum* Smith. *Planta* 51, 481–510. doi: 10.1007/bf01883338

Haines, R. W., and Lye, K. A. (1975). Seedlings of Nymphaeaceae. *Bot. J. Linn. Soc.* 70, 255–265. doi: 10.1111/j.1095-8339.1975.tb01649.x

He, D., Gichira, A. W., Li, Z., Nzei, J. M., Guo, Y., Wang, Q., et al. (2018). Intergeneric relationships within the early-diverging angiosperm family Nymphaeaceae based on chloroplast phylogenomics. *Int. J. Mol. Sci.* 19:3780. doi: 10.3390/ijms19123780

Herendeen, P. S., Friis, E. M., Pedersen, K. R., and Crane, P. R. (2017). Palaeobotanical redux: revisiting the age of the angiosperms. *Nat. Plants* 3:e17015.

Hiepko, P. (1965). Vergleichend-morphologische und entwicklungsgeschichtliche Untersuchungen über das Perianth bei den Polycarpicae. II Teil. *Bot. Jahrb. Syst.* 84, 427–508.

Hufford, L. (1989). Structure of the inflorescence and flower of *Petalonyx linearis* (Loasaceae). *Plant Syst. Evol.* 163, 211–226. doi: 10.1007/bf00936516

Igersheim, A., and Endress, P. K. (1998). Gynoecium diversity and systematics of paleoherbs. *Bot. J. Linn. Soc.* 127, 289–370. doi: 10.1111/j.1095-8339.1998.tb02102.x

Karpunina, P. V., Nuraliev, M. S., Oskolski, A. A., and Sokoloff, D. D. (2019). "Transference of positional information from bracteoles and sepals to petals in species with labile handedness of contort corolla: mechanical forces or prepatterning?" in *Asymmetry in Plants: Biology of Handedness*, eds B. Bahadur, K. V. Krishnamurthy, M. Ghose, and S. J. Adams (Boca Raton. FL: CRC Press), 285–300. doi: 10.1201/9780429492372-18

Kitazawa, M. S., and Fujimoto, K. (2018). Spiral phyllotaxis underlies constrained variation in *Anemone* (Ranunculaceae) tepal arrangement. *J. Plant Res.* 131, 459–468. doi: 10.1007/s10265-018-1025-x

Korn, R. W. (2006). Anodic asymmetry of leaves and flowers and its relationship to phyllotaxis. *Ann. Bot.* 97, 1011–1015. doi: 10.1093/aob/mcl047

Les, D. H., Schneider, E. L., Padgett, D. J., Soltis, P. S., Soltis, D. E., and Zanis, M. (1999). Phylogeny, classification and floral evolution of water lilies (Nymphaeaceae; Nymphaeales): a synthesis of non-molecular, rbcL, matK, and 18S rDNA data. *Syst. Bot.* 24, 28–46.

Lippok, B., and Renner, S. S. (1997). Pollination of *Nuphar* (Nymphaeaceae) in Europe: flies and bees rather than *Donacia* beetles. *Plant Syst. Evol.* 207, 273–283. doi: 10.1007/bf00984392

Meyen, S. V. (1973). Plant morphology in its nomothetical aspects. *Bot. Rev.* 39, 205–261.

Meyer, K. I. (1960). On the embryology of *Nuphar luteum* Sm. *Bull. Mosc. Soc. Nat. Biol. Ser.* 65, 48–60.

Moseley, M. F. (1965). Morphological studies of the Nymphaeaceae. III. The floral anatomy of *Nuphar*. *Phytomorphology* 15, 54–84.

Moseley, M. F. (1972). Morphological studies of Nymphaeaceae. VI. Development of flower of *Nuphar*. *Phytomorphology* 21, 253–283.

Moseley, M. F., Mehta, I. J., Williamson, P. S., and Kosakai, H. (1984). Morphological studies of the Nymphaeaceae (sensu lato). XIII. Contributions to the vegetative and floral structure of *Cabomba*. *Am. J. Bot.* 71, 902–924. doi: 10.1002/j.1537-2197.1984.tb14157.x

Nandi, O. I. (1998). Floral development and systematics of Cistaceae. *Plant Syst. Evol.* 212, 107–134. doi: 10.1007/bf00985224

Nuraliev, M. S., Oskolski, A. A., Sokoloff, D. D., and Remizowa, M. V. (2010). Flowers of Araliaceae: structural diversity, developmental and evolutionary aspects. *Plant Divers. Evol.* 128, 247–268. doi: 10.1127/1869-6155/2010/0128-0012

Padgett, D. (2007). A monograph of *Nuphar* (Nymphaeaceae). *Rhodora* 109, 1–95. doi: 10.3119/0035-4902(2007)109%5B1:amonn%5D2.0.co;2

Raciborski, M. (1894a). Die Morphologie der Cabombeen und Nymphaeaceen. *Flora* 78, 244–279.

Raciborski, M. (1894b). Beiträge zur Kentniss der Cabombeen und Nymphaeaceen. *Flora* 79, 92–108.

Raju, M. V. S. (1969). Development of floral organs in the sites of leaf primordia in *Pinguicula vulgaris*. *Am. J. Bot.* 56, 507–514. doi: 10.1002/j.1537-2197.1969.tb07563.x

Remizowa, M. V., Sokoloff, D. D., and Kondo, K. (2010a). Early flower and inflorescence development in *Dioscorea tokoro* (Dioscoreales): shoot chirality, handedness of cincinni and common tepal-stamen primordia. *Wulfenia* 17, 77–97.

Remizowa, M. V., Sokoloff, D. D., and Rudall, P. J. (2010b). Evolutionary history of the monocot flower. *Ann. Missouri Bot. Gard.* 97, 617–645. doi: 10.3417/2009142

Remizowa, M. V., Sokoloff, D. D., and Rudall, P. J. (2013). "Patterns of bract reduction in racemose inflorescences of early-divergent monocots," in *Early Events in Monocot Evolution*, eds P. Wilkin and S. J. Mayo (Cambridge: Cambridge University Press), 185–207. doi: 10.1017/cbo9781139002950.009

Richardson, F. C. (1969). Morphological studies of the Nymphaeaceae. IV. Structure and development of the flower of *Brasenia schreberi* Gmel. *Univ. Calif. Publ. Bot.* 47, 1–101.

Roels, P., Ronse Decraene, L. P., and Smets, E. F. (1997). A floral ontogenetic investigation of the Hydrangeaceae. *Nord. J. Bot.* 17, 235–254. doi: 10.1111/j.1756-1051.1997.tb00315.x

Ronse De Craene, L. P. (2010). *Floral Diagrams: An Aid to Understanding Flower Morphology and Evolution*. Cambridge: Cambridge University Press.

Ronse De Craene, L. P. (2018). Understanding the role of floral development in the evolution of angiosperm flowers: clarifications from a historical and physico-dynamic perspective. *J. Plant Res.* 131, 367–393. doi: 10.1007/s10265-018-1021-1

Ronse De Craene, L. P., and Brockington, S. F. (2013). Origin and evolution of petals in angiosperms. *Plant Ecol. Evol.* 146, 5–25. doi: 10.5091/plecevo.2013.738

Ronse De Craene, L. P., and Smets, E. F. (1993). The distribution and systematic relevance of the androecial character polymery. *Bot. J. Linn. Soc.* 113, 285–350. doi: 10.1111/j.1095-8339.1993.tb00341.x

Ronse De Craene, L. P., Smets, E. F., and Vanvinckenroye, P. (1998). Pseudodiplostemony, and its implications for the evolution of the androecium in Caryophyllaceae. *J. Plant Res.* 111, 25–43. doi: 10.1007/bf02507147

Ronse De Craene, L. P., Soltis, P. S., and Soltis, D. E. (2003). Evolution of floral structures in basal angiosperms. *Int. J. Plant Sci.* 164, S329–S363.

Rudall, P. J., Remizowa, M. V., Prenner, G., Prychid, C. J., Tuckett, R. E., and Sokoloff, D. D. (2009). Nonflowers near the base of extant angiosperms? Spatiotemporal arrangement of organs in reproductive units of Hydatellaceae and its bearing on the origin of the flower. *Am. J. Bot.* 96, 67–82. doi: 10.3732/ajb.0800027

Rudall, P. J., Sokoloff, D. D., Remizowa, M. V., Conran, J. G., Davis, J. I., Macfarlane, T. D., et al. (2007). Morphology of Hydatellaceae, an anomalous aquatic family recently recognized as an early-divergent angiosperm lineage. *Am. J. Bot.* 94, 1073–1092. doi: 10.3732/ajb.94.7.1073

Rümpler, F., and Theißen, G. (2019). Reconstructing the ancestral flower of extant angiosperms – the war of the whorls is heating up. *J. Exp. Bot.* 70, 2615–2622. doi: 10.1093/jxb/erz106

Rutishauser, R. (1999). Polymerous leaf whorls in vascular plants: developmental morphology and fuzziness of organ identities. *Int. J. Plant Sci.* 160, S81–S103.

Rutishauser, R. (2016). *Acacia* (wattle) and *Cananga* (ylang-ylang): from spiral to whorled and irregular (chaotic) phyllotactic patterns – a pictorial report. *Acta Soc. Bot. Polon.* 85:3531.

Rutishauser, R., and Sattler, R. (1985). Complementarity and heuristic value of contrasting models in structural botany. *Bot. Jahrb. Syst.* 107, 415–455.

Sauquet, H., and Magallón, S. (2018). Key questions and challenges in angiosperm macroevolution. *New Phytol.* 219, 1170–1187. doi: 10.1111/nph.15104

Sauquet, H., von Balthazar, M., Doyle, J. A., Endress, P. K., Magallón, S., Staedler, Y., et al. (2018). Challenges and questions in reconstructing the ancestral flower of angiosperms: a reply to Sokoloff et al. *Am. J. Bot.* 105, 127–135. doi: 10.1002/ajb2.1023

Sauquet, H., von Balthazar, M., Magallón, S., Doyle, J. A., Endress, P. K., Bailes, E. J., et al. (2017). The ancestral flower of angiosperms and its early diversification. *Nat. Commun.* 8:16047.

Schneider, E. L., Tucker, S. C., and Williamson, P. S. (2003). Floral development in the Nymphaeales. *Int. J. Plant Sci.* 164, S279–S292.

Schönenberger, J., and Grenhagen, A. (2005). Early floral development and androecium organization in Fouquieriaceae (Ericales). *Plant Syst. Evol.* 254, 233–249. doi: 10.1007/s00606-005-0331-7

Schoute, J. C. (1935). On corolla aestivation and phyllotaxis of floral phyllomes. *Verh. K. Akad. Wet. Amst. Afd. Natuurkunde* 2, 1–77.

Snow, R. (1942). Further experiments on whorled phyllotaxis. *New Phytol.* 41, 108–124. doi: 10.1111/j.1469-8137.1942.tb07066.x

Sokoloff, D. D., Remizowa, M. V., Bateman, R. M., and Rudall, P. J. (2018a). Was the ancestral angiosperm flower whorled throughout? *Am. J. Bot.* 105, 5–15. doi: 10.1002/ajb2.1003

Sokoloff, D. D., Remizowa, M. V., Timonin, A. C., Oskolski, A. A., and Nuraliev, M. S. (2018b). Types of organ fusion in angiosperm flowers (with examples from Chloranthaceae, Araliaceae and monocots). *Biol. Serb.* 40, 16–46.

Sokoloff, D. D., Remizowa, M. V., Briggs, B. G., and Rudall, P. J. (2009). Shoot architecture and branching pattern in perennial Hydatellaceae (Nymphaeales). *Int. J. Plant Sci.* 170, 869–884. doi: 10.1086/604743

Sokoloff, D. D., Remizowa, M. V., Conran, J. G., Macfarlane, T. D., Ramsay, M. M., and Rudall, P. J. (2014). Embryo and seedling morphology in *Trithuria lanterna* (Hydatellaceae, Nymphaeales): new data for infrafamilial systematics and a novel type of syncotyly. *Bot. J. Linn. Soc.* 174, 551–573. doi: 10.1111/boj.12151

Sokoloff, D. D., Remizowa, M. V., El, E. S., Rudall, P. J., and Bateman, R. M. (2020). Supposed Jurassic angiosperms lack pentamery, an important angiosperm-specific feature. *New Phytol.* [Epub ahead of print].

Sokoloff, D. D., Remizowa, M. V., Macfarlane, T. D., Conran, J. G., Yadav, S. R., and Rudall, P. J. (2013). Comparative fruit structure in Hydatellaceae (Nymphaeales) reveals specialized pericarp dehiscence in some early-divergent angiosperms with ascidiate carpels. *Taxon* 62, 40–61. doi: 10.1002/tax.621005

Tamura, M. (1982). Relationship of *Barclaya* and classification of Nymphaeales. *Acta Phytotax. Geobot.* 33, 336–345.

Taylor, D. W. (2008). Phylogenetic analysis of Cabombaceae and Nymphaeaceae based on vegetative and leaf architectural characters. *Taxon* 57, 1082–1095. doi: 10.1002/tax.574005

Tillich, H.-J. (1990). Die Keimpflanzen der Nymphaeaceae – monocotyl oder dicotyl? *Flora* 184, 169–176. doi: 10.1016/s0367-2530(17)31606-7

Trecul, A. (1845). Recherches sur la structure et le développement du *Nuphar lutea*. *Ann. Sci. Nat. Bot. Ser.* 3, 286–345.

Venema, H. J. (1937). Studies in tropical teratology. 2nd series, no. I. *Blumea Suppl.* 1, 87–96.

Vislobokov, N. A., Sokoloff, D. D., Degtjareva, G. V., Valiejo-Roman, C. M., Kuznetsov, A. N., and Nuraliev, M. S. (2014). *Aspidistra paucitepala* (Asparagaceae), a new species with occurrence of the lowest tepal number in flowers of Asparagales. *Phytotaxa* 161, 270–282.

von Balthazar, M., Pedersen, K. R., Crane, P. R., and Friis, E. M. (2008). *Carpestella lacunata* gen. et sp. nov., a new basal angiosperm flower from the Early Cretaceous (Early to Middle Albian) of eastern North America. *Int. J. Plant Sci.* 169, 890–898. doi: 10.1086/589692

Wang, X. (2018). *The Dawn Angiosperms: Uncovering the Origin of Flowering Plants*. Berlin: Springer.

Wanntorp, L., Puglisi, C., Penneys, D., and Ronse De Craene, L. P. (2011). "Multiplications of floral organs in flowers: a case study in *Conostegia* (Melastomataceae, Myrtales)," in *Flowers on the Tree of Life*, eds L. Wanntorp and L. P. Ronse De Craene (Cambridge: Cambridge University Press), 218–235. doi: 10.1017/cbo9781139013321.009

Warner, K. A., Rudall, P. J., and Frohlich, M. W. (2009). Environmental control of sepalness and petalness in perianth organs of waterlilies: a new Mosaic Theory for the evolutionary origin of a differentiated perianth. *J. Exp. Bot.* 60, 3559–3574. doi: 10.1093/jxb/erp202

Weidlich, W. H. (1976a). The organization of the vascular system in the stems of the Nymphaeaceae. I. *Nymphaea* subgenera *Castalia* and *Hydrocallis*. *Am. J. Bot.* 63, 499–509. doi: 10.1002/j.1537-2197.1976.tb11839.x

Weidlich, W. H. (1976b). The organization of the vascular system in the stems of the Nymphaeaceae. II. *Nymphaea* subgenera *Anechya*, *Lotos* and

Brachyceras. *Am. J. Bot.* 63, 1365–1379. doi: 10.1002/j.1537-2197.1976.tb13222.x

Wiersema, J. H. (1987). A monograph of *Nymphaea* subgenus *Hydrocallis* (Nymphaeaceae). *Syst. Bot. Monogr.* 16, 1–112.

Williamson, P. S., and Schneider, E. L. (1994). Floral aspects of *Barclaya* (Nymphaeaeceae): pollination, ontogeny and structure. *Plant Syst. Evol. Suppl.* 8, 159–173. doi: 10.1007/978-3-7091-6910-0_9

Wolf, M. (1991). *Blütenphyllotaxis von Nymphaeaceae: ist das Androecium von* Nymphaea*, Nuphar etc. spiralig? Symposium Morphologie, Anatomie und Systematik* (Göttingen: University of Göttingen), 85.

Wydler, H. (1857). Morphologische Mittheilungen: *Pinguicula*. *Flora* 39, 609–613.

Xu, F., and Rudall, P. J. (2006). Comparative floral anatomy and ontogeny in Magnoliaceae. *Plant Syst. Evol.* 258, 1–15. doi: 10.1007/s00606-005-0361-1

Yoo, M.-J., Soltis, P. S., and Soltis, D. E. (2010). Expression of floral MADS-box genes in two divergent water lilies: Nymphaeales and *Nelumbo*. *Int. J. Plant Sci.* 171, 121–146. doi: 10.1086/648986

Yurtseva, O. V., and Choob, V. V. (2005). Types of flower structure and pathways of their morphological transformation in Polygonaceae: the preliminary data for the model of floral development. *Bull. Mosc. Soc. Natur., Biol. Ser.* 110, 40–52.

Zagórska-Marek, B. (1994). Phyllotaxis diversity in *Magnolia* flowers. *Acta Soc. Bot. Polon.* 63, 117–137. doi: 10.5586/asbp.1994.017

Conflict of Interest: The authors declare that the research was conducted in the absence of any commercial or financial relationships that could be construed as a potential conflict of interest.

frontiers in Ecology and Evolution

ORIGINAL RESEARCH
published: 04 June 2020
doi: 10.3389/fevo.2020.00133

Floral Development Reveals the Existence of a Fifth Staminode on the Labellum of Basal Globbeae

Akitoshi Iwamoto[1], Shiori Ishigooka[2], Limin Cao[3] and Louis P. Ronse De Craene[4]*

[1] Department of Biological Sciences, Faculty of Science, Kanagawa University, Kanagawa, Japan, [2] Department of Biology, Tokyo Gakugei University, Tokyo, Japan, [3] College of Life Sciences and Environment, Hengyang Normal University, Hengyang, China, [4] Royal Botanic Garden Edinburgh, Edinburgh, United Kingdom

We observed the floral development of *Hemiorchis burmanica* and two species of *Gagnepainia*, which make up the sister group of *Globba* in Globbeae, as well as a selected number of species of *Globba*. Our observations revealed that in *Gagnepainia*, a "fifth staminode," develops as part of the labellum, while it is generally lost in other Zingiberaceae. The fifth staminode, however, was not initiated in the labellum of *Hemiorchis.* A fifth staminode was also observed in *Globba geoffrayi* but was not found in all other species of *Globba* investigated. While the staminode becomes an integral part of the labellum in *Gagnepainia*, it remains small and almost aborts at later stages of development in *G. geoffrayi*. These results indicate that the development of a fifth staminode could be a recurring plesiomorphic trait for Globbeae, only retained in *G. geoffrayi*. The retention of the fifth staminode and its heterochronic shift may be linked with the mechanical constriction within the flower bud. The results may also support the interpretation of an atavistic expression of a once lost staminode.

Keywords: floral development, Globbeae, heterochrony, labellum, staminode, Zingiberaceae

OPEN ACCESS

Edited by:
Alessandro Minelli, University of Padova, Italy

Reviewed by:
Catherine Damerval, UMR8120 Génétique Quantitative et Evolution Le Moulon, France
Chelsea D. Specht, Cornell University, United States

****Correspondence:***
Akitoshi Iwamoto
akitoshi@kanagawa-u.ac.jp

Specialty section:
This article was submitted to Evolutionary Developmental Biology, a section of the journal Frontiers in Ecology and Evolution

Received: *31 December 2019*
Accepted: *22 April 2020*
Published: *04 June 2020*

Citation:
Iwamoto A, Ishigooka S, Cao L and Ronse De Craene LP (2020) Floral Development Reveals the Existence of a Fifth Staminode on the Labellum of Basal Globbeae. Front. Ecol. Evol. 8:133. doi: 10.3389/fevo.2020.00133

INTRODUCTION

The monocots are generally characterized by a common trimerous pentacyclic floral Bauplan (Dahlgren et al., 1985). This trimerous Bauplan (i.e., P3 + 3A3 + 3G3 or K3C3A3 + 3G3) is the most remarkable floral organization of the monocots in the evolutionary context of a derivation from the basal angiosperms (Ronse De Craene, 2010; Iwamoto et al., 2018; **Figure 1A**). In Zingiberaceae, the flower is basically the expression of this floral Bauplan, although its flower developed several distinct features linked with monosymmetry. The flower has a sepal and petal tube consisting of three elements each, a single massive stamen and a slender style inserted between the two pollen sacs of the stamen. These characters are shared with Costaceae (Kress, 1990), considered as the sister group of Zingiberaceae in Zingiberales based on several molecular phylogenetic analyses (Kress et al., 2001; Barrett et al., 2014; Sass et al., 2016). Costaceae, however, differs from Zingiberaceae by its labellum, which is made up of five fused staminodes (Kress, 1990). The large labellum characteristic for the flower of Zingiberaceae is composed of the two lateral staminodes of the inner whorl, while two lateral staminodes of the outer whorl develop as petaloid organs and the abaxial staminode of the outer whorl, the "fifth staminode," is considered to be

lost (Kress, 1990; Kress et al., 2002; **Figure 1B**). Studies of floral development in several species of Zingiberaceae confirmed that the labellum develops from two inner androecial primordia (lateral staminodes), as in *Alpinia* (Song et al., 2007), *Curcuma* (Fukai and Udomdee, 2005), *Globba* (Box and Rudall, 2006), *Hedychium* (Kirchoff, 1997), and *Scaphochlamys* (Kirchoff, 1998).

Hemiorchis and *Gagnepainia* are small genera of the Zingiberaceae, in the subfamily Zingiberoideae tribe Globbeae (Kress et al., 2002). These two genera are closely related to each other, and molecular phylogenetic analyses indicate that they form a monophyletic group (Kress et al., 2002; Williams et al., 2004; Cao et al., 2019). Earlier treatments considered a single genus, *Hemiorchis* Kurz, until Schumann (1904) separated them into two genera sharing a common morphology in leaf shape, inflorescence, fruit, and pollen (Williams et al., 2004). The most important common character in these two genera is the existence of a raised median line along the central region of the labellum terminating as a pointed tip (central carina with apical projection) (Williams et al., 2004; **Figures 2**, **3**). Although this was not explicitly mentioned by the authors, the central carina with apical projection in the labellum might represent the lost "fifth staminode" in Zingiberaceae, corresponding to an outer staminode, which is integrated in the same middle position of the labellum of Costaceae, the sister group to Zingiberaceae (Kress, 1990: **Figure 1C**). In other developmentally investigated species (Kirchoff, 1997, 1998; Fukai and Udomdee, 2005; Box and Rudall, 2006; Song et al., 2007), no traces of the fifth staminode were observed, and the homology of the appendage on the labellum of *Hemiorchis* and *Gagnepainia* remains unclear. Therefore, the observation of the floral development in these two genera is necessary to identify the carina morphologically.

In this study, we observed the detailed floral development in *Hemiorchis* and *Gagnepainia*, in particular focusing on the development of the labellum. We also observed the development of the labellum in a selected number of species of *Globba* and compared the results with those of *Hemiorchis* and *Gagnepainia*. *Hemiorchis* and *Gagnepainia* are sister to *Globba* (including the genus *Mantisia*) forming the tribe Globbeae (Williams et al., 2004). An earlier floral developmental study by Box and Rudall (2006) on two species of *Globba* did not show any evidence of the fifth staminode. *Globba*, however, is the third largest genus of the Zingiberaceae and includes ∼100 species (Kress et al., 2002). Therefore, the morphological variation of flowers within the genus is inferred to be large and may include some variation in the labellum development. Through the observation of the floral development of Globbeae, we examine the potential existence of the fifth staminode in the flower of Zingiberaceae. We also aim to investigate the evolution of labellum morphology in Globbeae,

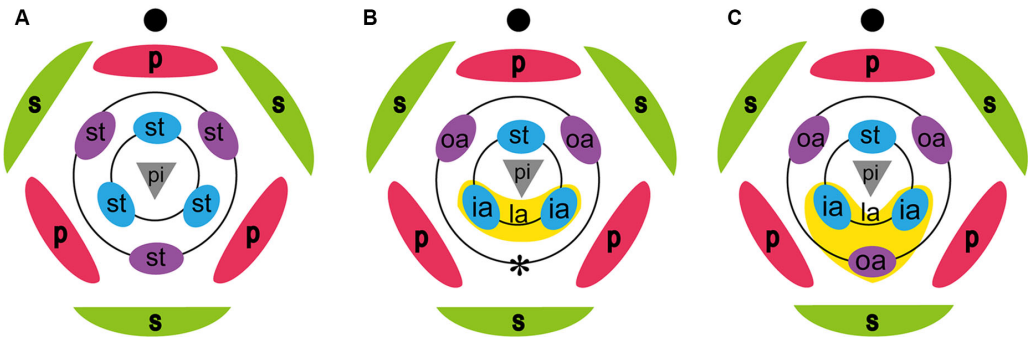

FIGURE 1 | Floral diagrams of a generalized monocot, Zingiberaceae, and possible floral diagram of *Hemiorchis* and *Gagnepainia*. **(A)** Representative monocot. **(B)** Zingiberaceae. The labellum is composed of two inner staminodes (ia), and the abaxial outer stamen is lost (*). **(C)** Possible floral diagram of *Hemiorchis* and *Gagnepainia*. The labellum is composed of three staminodes, two inner staminodes, and the abaxial outer stamen (oa). ia, inner androecial element (staminode); oa, outer androecial element (staminode); pi; pistil; s, sepal; st, stamen. Black circle in each figure indicates the main axis.

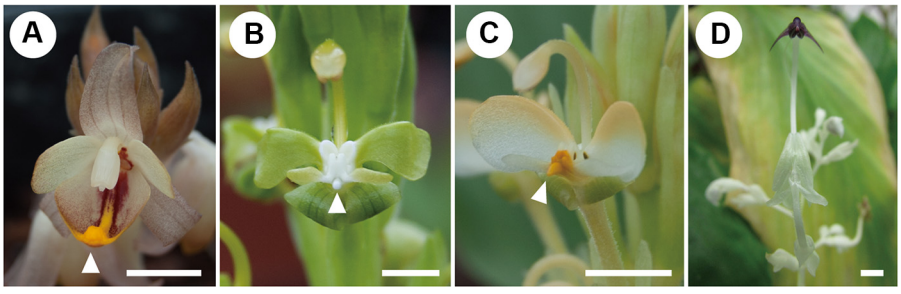

FIGURE 2 | Mature flowers of investigated species. **(A)** *Hemiorchis burmanica*. **(B)** *Gagnepainia harmandii*. **(C)** *Gagnepainia godefroyi*. **(D)** *Globba geofrayii*. White arrows indicate the position of central carina with apical projection. Scale bars = 5 mm.

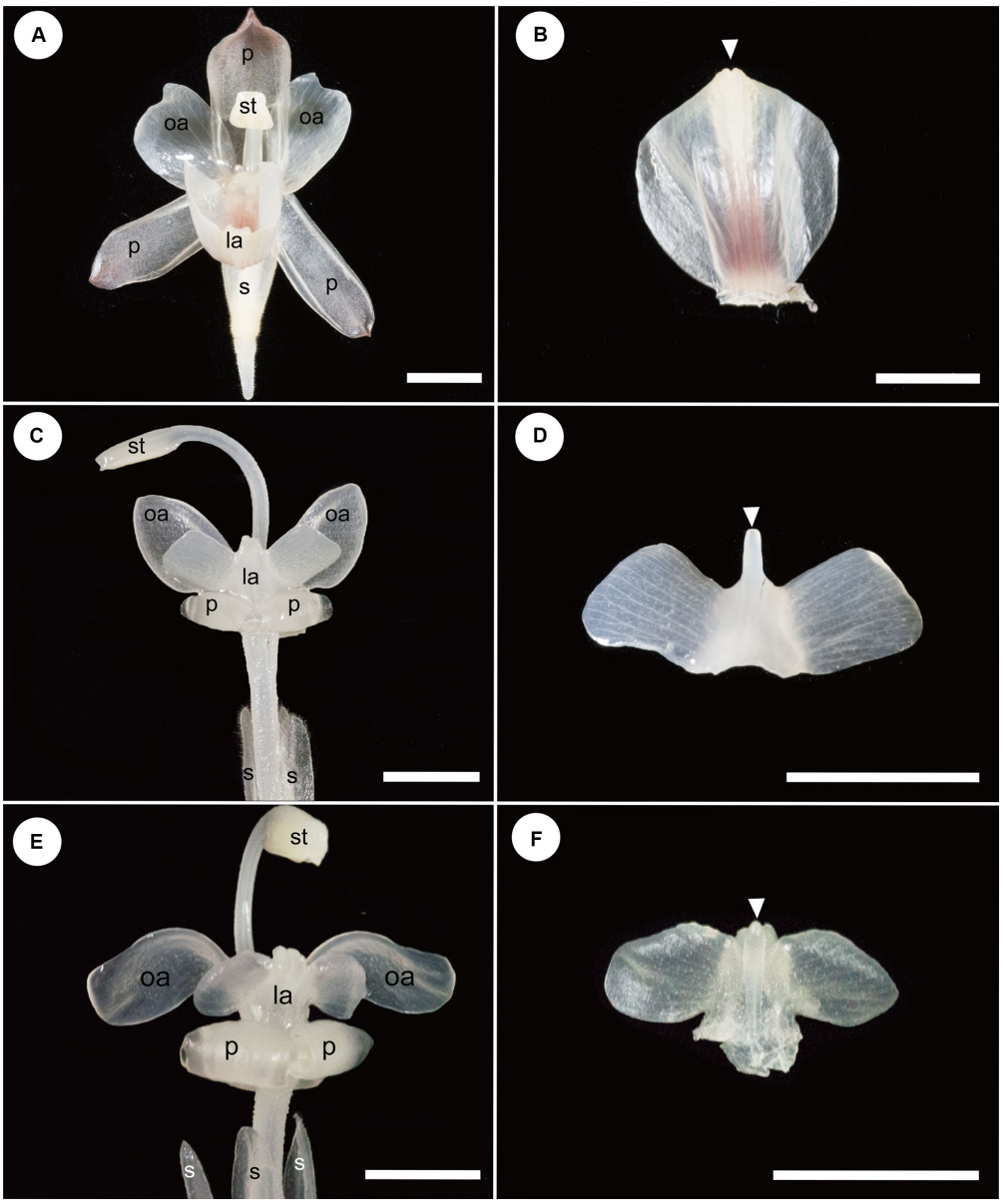

FIGURE 3 | Floral and labellum morphology of *Hemiorchis* and *Gagnepainia.* The adaxial side of the labellum is shown, and the proximal end of the labellum is at the bottom of figures in panels **(B,D,F)**. **(A)** Flower of *Hemiorchis burmanica.* **(B)** Labellum of *H. burmanica*, dissected from **(A)**. White arrowhead points to the bilobed tip of the carina. **(C)** Flower of *Gagnepainia harmandii.* **(D)** Labellum of *G. harmandii.*, dissected from **(C)**. White arrowhead points to the long projection of the carina. **(E)** Flower of *G. godefroyi.* **(F)** Labellum of *G. godefroyi*, dissected from **(E)**. White arrowhead points to the short projection of the carina. Two additional projections are formed on the abaxial side of the labellum. ca; carina of labellum; ia, inner androecial element (staminode); la, labellum; oa, outer androecial element (staminode); p, petal; s, sepal; st, stamen. Scale bars = 5 mm.

which contributes to elucidate the floral evolution of the whole family, Zingiberaceae.

MATERIALS AND METHODS

Plant Material

Living plants of *H. burmanica* Kurz, *Gagnepainia harmandii* (Baill.) K.Schum., and *Gagnepainia godefroyi* (Baill.) K.Schum. were collected at the Royal Botanic Garden Edinburgh (RBGE). All collected materials were fixed for direct or scanning electron microscopy (SEM) observation. Voucher spirit specimens of these three species are preserved in Kanagawa University and RBGE.

Floral materials of eight species of *Globba* were collected at RBGE for SEM observation: *Globba atrosanguinea* Teijsm. & Binn., *Globba fasciata* Ridl., *Globba geoffrayi* Gagnep., *Globba marantina* L., *Globba paniculata* Valeton., *Globba pendula* Roxb.,

TABLE 1 | Source of observed species.

Genus	Subgenus	Species	RBGE living collection accession numbers	Liquid collection number
Gagnepainia		*Gagnepainia harmandii* (Baill.) K.Schum	19991163A	1048 Led
Gagnepainia		*G. godefroyi* (Baill.) K.Schum.	19871253A	1049 Led
Hemiorchis		*Hemiorchis burmanica* Kurz	19991652A	1047 Led
Globba	*Ceratanthera*	*Globba geoffrayi* Gagnep.	20010754	1227 Led
Globba	*Ceratanthera*	*G. pendula* Roxb.	19860743, 20081102	1065 Led
Globba	*Mantisia*	*G. racemosa* Sm.	19920039	1273 Led
Globba	*Globba*	*G. paniculata Valeton*	20010323	1050 Led
Globba	*Globba*	*G. atrosanguinea* Teijsm. & Binn.	19820784	1055 Led
Globba	*Globba*	*G. siamensis* (Hemsl.) Hemsl.	20060813	1051 Led
Globba	*Globba*	*G. marantina* L.	19613981	1068 Led

Globba racemosa Sm., and *Globba siamensis* (Hemsl.) Hemsl. Voucher spirit specimens of the *Globba* species are preserved at RBGE (**Table 1**).

Fixation for Observation

The materials of *H. burmanica*, *G. harmandii*, and *G. godefroyi* were fixed in formalin–acetic acid–alcohol (FAA) containing less ethanol and formalin than usual (absolute ethanol, 30%/water, 62%/glacial acetic acid, 5%/formalin, 3%), and those of *Globba* were fixed in standard FAA (absolute ethanol, 50–70%/glacial acetic acid, 5%/and formalin, 5–7%). The samples were fixed for at least one night at room temperature, and then, FAA was replaced with 70% ethanol for the preservation of samples.

Scanning Electron Microscopy Observations

Preparation for SEM observation involved dissecting the fixed materials at various developmental stages with tweezers and a micromanipulator (MM-333, Narishige, Japan) under a stereoscopic optical microscope.

The dissected tissues were dehydrated in an ethanol series, after which the ethanol was replaced with isoamyl acetate or acetone, critical point dried with a CO_2 critical point dryer (JCPD-5, JOEL, Japan and K850, Leica, Germany), and coated with Pt/Pd using a sputter coater (Ion Sputter E-1030, Hitachi, Japan and K575x, Quorum, United Kingdom).

The coated materials were observed with SEM (S3400, Hitachi, Japan and Supra 55VP, Zeiss, Germany) at 5 kV.

RESULTS

The Floral Morphology of Hemiorchis and Gagnepainia

The results of observations on the mature flowers of *H. burmanica*, *G. harmandii*, and *G. godefroyi* are shown in **Figure 3**.

A mature flower of *H. burmanica* has three sepals fused at the base and three petals (**Figure 3A**). The flower also contains two petaloid staminodes in an outer whorl and a cymbiform labellum and one fertile stamen with a long filament in an inner whorl (**Figure 3A**). Note that the style is slender and contained within the abaxial furrow of the filament, which is not clear in the figure. The unfolded labellum is rhomboid and has two upright wings (**Figure 3B**). The central line of the labellum is raised (=carina), and the tip of the carina is slightly bilobed (**Figure 3B**, white arrowhead).

A mature flower of *G. harmandii* has three sepals fused at the base and three curled petals, although one of them is hidden behind the other two petals (**Figure 3C**). The flower also contains two petaloid staminodes in an outer whorl and a butterfly-shaped labellum and one sterile stamen with a long filament in an inner whorl (**Figure 3C**). The style is slender and contained within the abaxial furrow of filament, which is not shown in the figure. The labellum is butterfly shaped and has two lateral wings (**Figure 3D**). A carina is formed along the central line of the labellum, terminating with a long projection (**Figure 3D**, white arrowhead).

The floral structure of *G. godefroyi* is very similar to that of *G. harmandii* (**Figure 3E**), while the morphology of the labellum is different (**Figure 3F**). The labellum of *G. godefroyi* has also two lateral wings, but their shapes are different from those of the labellum of *G. harmandii.* A carina is also formed along the central line of the labellum, but its distal projection is much shorter than that of *G. harmandii* (**Figure 3F**, white arrowhead). In addition, there are two more projections on the abaxial side of the carina, which are not found in *G. harmandii.*

The Floral Development of *Hemiorchis burmanica*

At a very early developmental stage, a dome-shaped elliptical floral primordium is initiated in the axil of a bract primordium (**Figure 4A**). Next, three sepal primordia are initiated sequentially; the lateral sepal lobes emerge first and precede the adaxial median sepal lobe, which lags behind in growth. Simultaneously, an adaxial and abaxial common primordium are also initiated (**Figure 4B**). At a little later developmental stage, the two common primordia connect laterally and form a ring primordium, while the adaxial and abaxial portions can be still identified (**Figure 4C**). The common primordia divide the flower in two unequal halves. Next, each common primordium rapidly differentiates in the petal and androecium parts; the

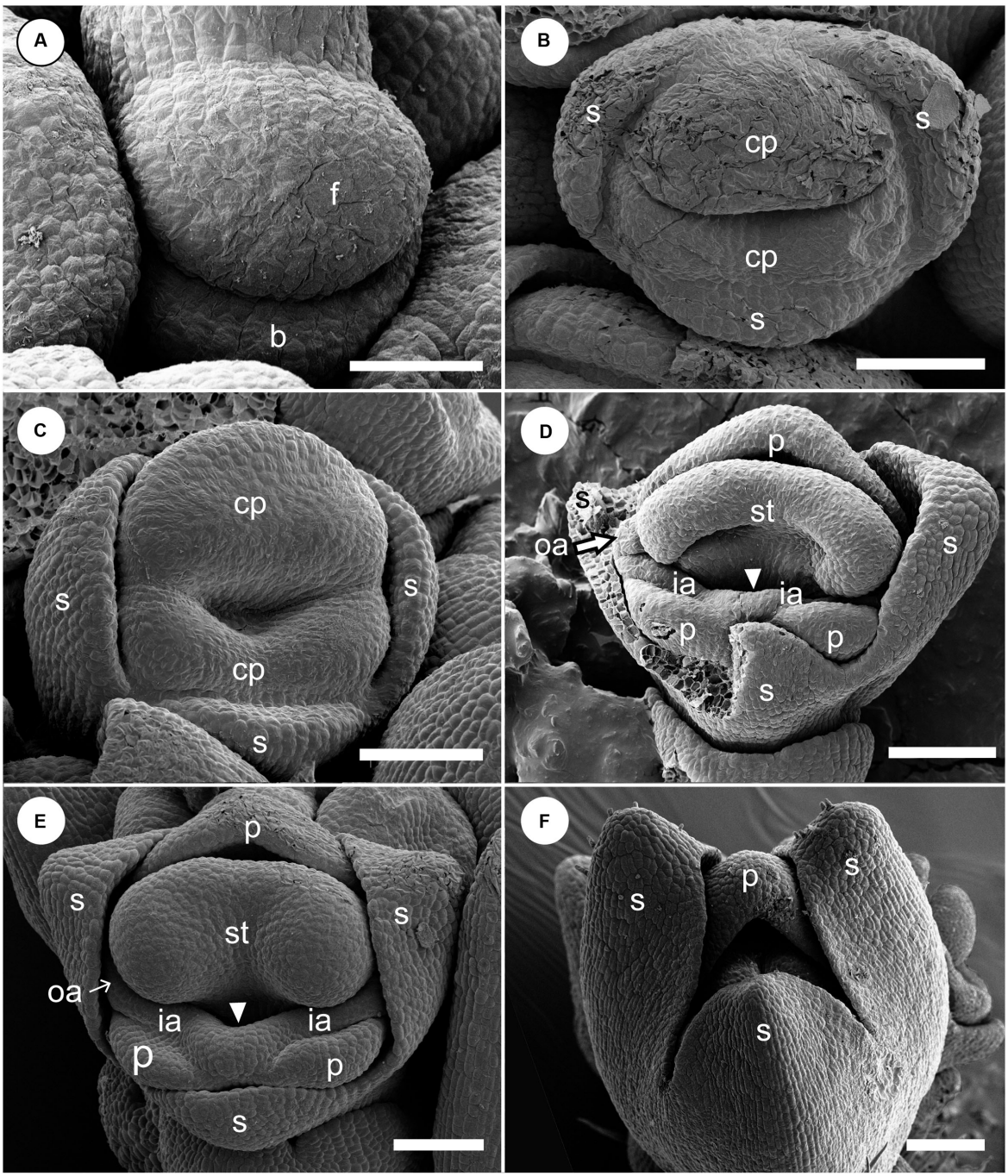

FIGURE 4 | Early floral development of *Hemiorchis burmanica*. **(A)** Flower at the earliest stage. Dome-shaped floral bud (f) and bract (b) are initiated. **(B)** Three sepal primordia (s) and adaxial and abaxial common primordia (cp) are initiated. **(C)** Two common primordia are fused and form a ring primordium. Three sepals develop. **(D,E)** Petal (p), stamen (st), and two outer androecial primordia (oa) develop from the adaxial portion of the ring primordium, while two petals and inner androecial primordia develop from the abaxial portion. Note that there is a bump between the inner androecial primordia (ia), which may not be an abaxial outer androecial primordium (see text for details). **(F)** Three sepal primordia develop and cover the floral apex. b, bract primordium; cp, common primordium; f, floral bud; ia, inner androecial primordium (staminode primordium); oa, outer androecial primordium (staminode primordium); p, petal primordium; s, sepal primordium; st, stamen primordium. Scale bars = **(A)** 50 μm, **(B–F)** 100 μm.

abaxial common primordium gives rise to the lateral inner staminodial primordia and the two abaxial petal primordia, while the adaxial common primordium gives rise to the adaxial petal, two lateral outer staminodial primordia, and the fertile stamen (**Figure 4D**). The stamen primordium differentiates into a massive anther, and the petal and sepal primordia also develop

further (**Figure 4E**). The two outer lateral staminodes are hidden below the large anther. The two anterior lateral staminodes are confluent (**Figure 4E**). At this stage, the only possible evidence of an abaxial outer androecial primordium exists, as a weak bump between the inner androecial primordia (**Figures 4D,E**, white arrowhead). The bump, however, could be regarded as the boundary portion between the inner androecial primordia, which is raised by the distal ends of both primordia (see section "Discussion" for details). The sepal primordia develop further and cover the floral apex at a little later stage (**Figure 4F**).

We removed sepals and petals from young flowers to observe later developmental stages (**Figure 5**). A pistil primordium appears centrally and is adaxially enclosed by the differentiating stamen primordium. A labellum is formed by the common

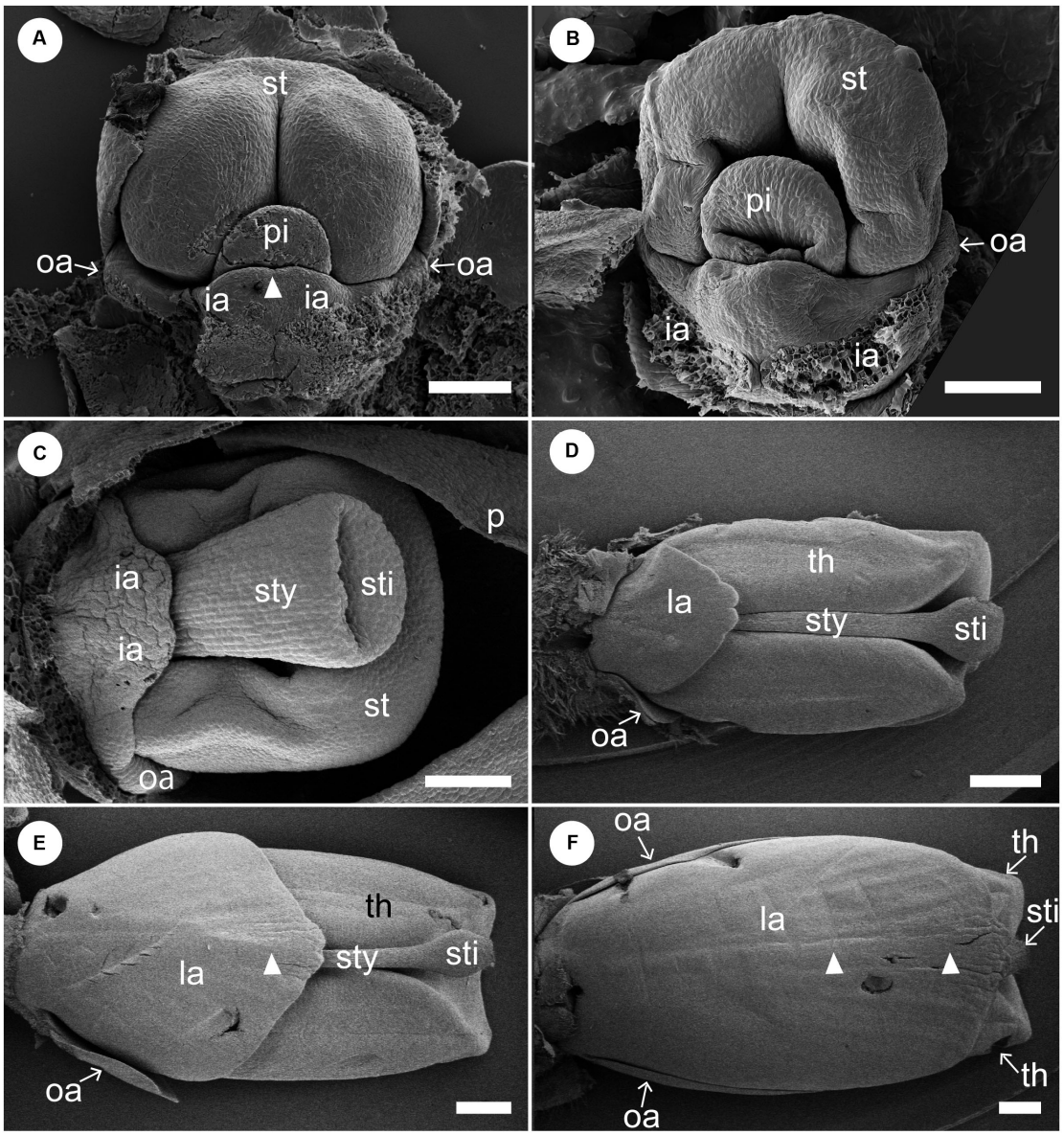

FIGURE 5 | Later floral development of *Hemiorchis burmanica* (continued). Petals and sepals are removed. **(A**,**B)** Flowers at a mid-developmental stage. Two inner androecial primordia (ia) develop and are fused to form a labellum. Note that the tip of the labellum is emarginate (white arrowhead). Outer androecial primordia (oa) do not develop. The stamen primordium (st) develops and encloses the style of the pistil (sty). **(C)** The style elongates and a stigma is differentiated. The inner androecial primordia (labellum primordium) develop further, and outer androecial primordia are still small. The stamen develops thecae. **(D)** Flower at a late stage. The labellum, formed from two inner androecial primordia, and outer androecial primordia expand in size. The style elongates and is tightly enclosed within the thecae. Note that a carina primordium is secondarily initiated along the central line (white arrowhead). **(E,F)** The outer androecial primordia develop into petaloid wing-like staminodes. The labellum grows further and covers the abaxial side of the stamen. Note that there is a slight bump in the central portion of the labellum (white arrowheads). ia, inner androecial primordium or labellum; la, labellum; oa, outer androecial primordium or labellum petaloid staminode; st, stamen primordium; sti, stigma; sty, style; th, thecae. Scale bars = **(A–C)** 100 μm, **(D–F)** 500 μm.

uplift of the two abaxial staminodes (**Figure 5A**). Note that there is a slight depression at the tip of the labellum, which indicates that the labellum is formed by the confluence of the two inner androecial primordia. The outer androecial primordium, if it exists, is not conspicuous (see section "Discussion" for details). The stamen differentiates two thecae, while a concavity develops on the pistil primordium, representing a stigmatic slit (**Figure 5B**). The style elongates and the lateral sides of the labellum expand at later developmental stages (**Figure 5C**). The development of the lateral outer androecial primordia is delayed, as they remain basally connected with the labellum. As the labellum develops further, the outer androecial primordia become independent from the labellum and extend in size; the style elongates and is tightly squeezed between the thecae of the adaxial stamen (**Figure 5D**). Finally, the labellum covers the abaxial side of the flower, and the outer lateral androecial primordia elongate along the sides of the fertile stamen to become adaxial petaloid staminodes (**Figures 5E,F**). Abaxially, the carina also becomes visible as a faint vertical projection (**Figures 5E,F**, white arrowheads).

We also observed the development of the adaxial side of labellum between a middle and late developmental stage corresponding to **Figures 5C–F** (**Figure 6**). At a developmental stage between **Figures 5C,D**, there is still no trace of a bump visible along the central line of the labellum on the adaxial side, while a slight projection is observed at the tip of labellum (**Figure 6A**). At a later developmental stage, a central carina is initiated, and a new lobe is initiated at the tip of carina (**Figure 6B**). As the labellum develops further, the central carina also expands, and its tip is still separated from the labellum as a lobe (**Figure 6C**). At a slight later developmental stage, the central carina expands further, and its tip is fused with the tip of the labellum (**Figure 6D**). A ridge develops along the central line (black arrowhead) and divides higher up in a groove with two parallel ridges. The labellum at these developmental stages (**Figures 6C,D**) corresponds almost to that of **Figure 5D**. The central carina does not develop much at a later developmental stage, which corresponds to **Figure 5E**, although the labellum changes in size and shape (**Figure 6E**). At almost the same developmental stage of **Figure 5F**, the central carina distinctly changes its shape (**Figures 6F,G**). At the upper portion of the labellum, the central groove deepens, and the two ridges expand as narrow crinkly flaps (**Figure 6F**), although at the lower portion of the labellum, the groove is not so obvious (**Figure 6G**).The lower adaxial part of the labellum differentiates as a flap of tissue expanding above the gap leading to the nectaries below and is also touching similar flaps formed by the outer staminodes (**Figures 6C–E,G**).

The Floral Development of *Gagnepainia harmandii* and *G. godefroyi*

The early floral development of *G. harmandii* is almost similar to that of *H. burmanica* (**Figure 7**). The floral development begins with a dome-shaped floral primordium developing in the axil of a broad bract primordium (**Figure 7A**). Two sepal primordia and a two-lobed ring primordium are initiated; it separates into an adaxial and abaxial common primordium (**Figure 7B**). An abaxial sepal primordium eventually separates from the ring primordium but lags behind the lateral sepals (**Figure 7C**). An adaxial petal primordium, stamen primordium, and two lateral outer androecial primordia emerge by the subdivision of the adaxial common primordium, while an abaxial outer androecial primordium, two lateral inner androecial primordia, and two abaxial petal primordia are differentiated from the abaxial common primordium (**Figures 7D,E**). At these stages, the sepals enclose the whole flower (removed), and the petals progressively cover the inner portion of the flower (**Figure 7F**).

We removed the sepals and one abaxial petal and observed the development of the inner portion of the flower (**Figures 8**, **9**). At almost the same developmental stage of the flower in **Figure 7F**, a pistil primordium appears within the groove of the stamen, and each androecial primordium (two lateral outer primordia, one abaxial outer primordium, and two inner primordia) are clearly visible (i.e., the limits between these primordia are conspicuous) (**Figures 8A,B**). At a slightly later stage, the pistil primordium develops a stigma by the unequal development of a central depression. All androecial elements are lifted by common basal growth, but the limits between the elements are still conspicuous (**Figures 8C,D**). Next, the style elongates in a column-like structure with an apical stigmatic slit (**Figure 9**). The labellum is clearly composed of three androecial primordia; in particular, the abaxial outer androecial primordium is conspicuous and independent from the two inner androecial members. The abaxial outer androecial primordium becomes a long, narrow appendage on the labellum, and the elongated style is tightly enclosed by the anther developing a prominent connective (**Figure 9D**).

We observed the floral development of *G. godefroyi* at later developmental stages and confirmed that the labellum clearly includes the abaxial outer androecial primordium similar to *G. harmandii* (**Figure 10**).

The Labellum Development of *Globba*

We found that there are two types of labellum development in the examined eight species of *Globba*. Therefore, the labellum development of two species, *G. paniculata* and *G. geoffrayi*, representing each type, is shown in **Figure 11**.

At a mid-developmental stage of the flower of *G. paniculata*, two inner staminode primordia are initiated (**Figure 11A**). As a pistillate primordium appears and its style elongates, the two inner androecial primordia are lifted by common growth and form a broad primordium (**Figure 11B**, labellum primordium). The boundary between the inner androecial primordia becomes clear at a slight later stage as a notch (**Figure 11C**, white arrowhead). Consequently, a rounded labellum is differentiated retaining the apical depression, indicating its dual nature (**Figure 11D**). An abaxial outer androecial primordium or its vestige was not found throughout the labellum development of *G. paniculata* (**Figures 11A–D**). The other seven *Globba* except for *G. geoffrayi* showed almost the same labellum development.

Two inner androecial primordia and an abaxial outer androecial primordium are initiated at a mid-developmental

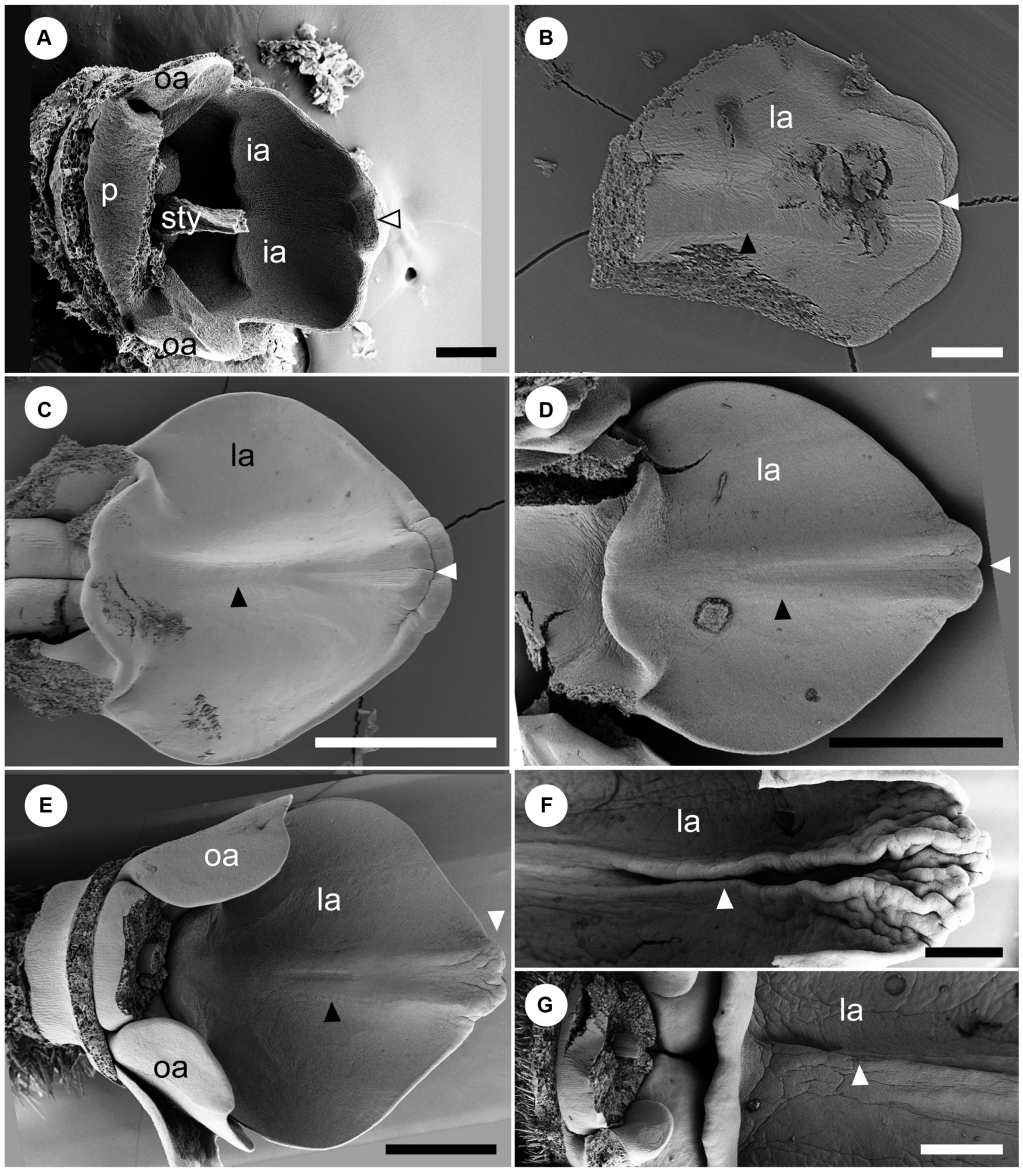

FIGURE 6 | Later floral development of *Hemiorchis burmanica* (continued). The adaxial side of the labellum between middle and late developmental stages. **(A)** The labellum (la) at a developmental stage between **Figures 5C,D**. Stamen, adaxial petal, and upper portion of style are removed. Note that a central carina is not initiated, but there is a projection at the tip of the labellum (white arrowhead). **(B)** The labellum at a slightly later developmental stage than in **(A)**. A carina is initiated (black arrowhead), and the tip of the labellum is horizontally bilobed (white arrowhead). **(C)** The labellum at almost the same developmental stage in **Figure 5D**. The central carina develops as a ridge (black arrowhead), and the tip of the labellum is still horizontally bilobed (white arrowhead). **(D)** The labellum at a slight later developmental stage than **(C)**. The central carina is clear (black arrowhead) separating as two ridges, but the tip of the labellum is covered by the expanded inner lobe (white arrowhead). **(E)** The labellum at almost the same developmental stage in **Figure 5E**. The central carina develops further (black arrowhead) and the tip of the labellum is not horizontally bilobed (white arrowhead). **(F,G)** The labellum at almost the same developmental stage in **Figure 5F**. The **(F)** upper portion and **(G)** lower portion. The central carina (white arrowhead) is a narrow groove enclosed by two flaps and is more obvious in the upper portion. Note the three basal flaps formed by the labellum and outer staminodes, respectively. la, labellum; oa, outer androecial primordium; p, petal primordium; sti, stigma; sty, style. Scale bars = **(A,B)** 100 μm, **(C–G)** 500 μm.

stage of the flower in *G. geoffrayi* when the style appears, and the fertile stamen primordium differentiates anther tissue (**Figure 11E**). Immediately afterward, the style elongates and is enclosed between the thecae, and the limits on both sides of the abaxial outer primordia are clear (**Figure 11F**). As the style elongates, the inner staminodes also develop, although the abaxial outer staminode ceases its development (**Figures 11G,H**). Compared with the inner staminodes, the abaxial outer staminode is very small but still exists even at a late developmental stage. *G. geoffrayi* is the only species showing this type of labellum development among the eight examined *Globba* species.

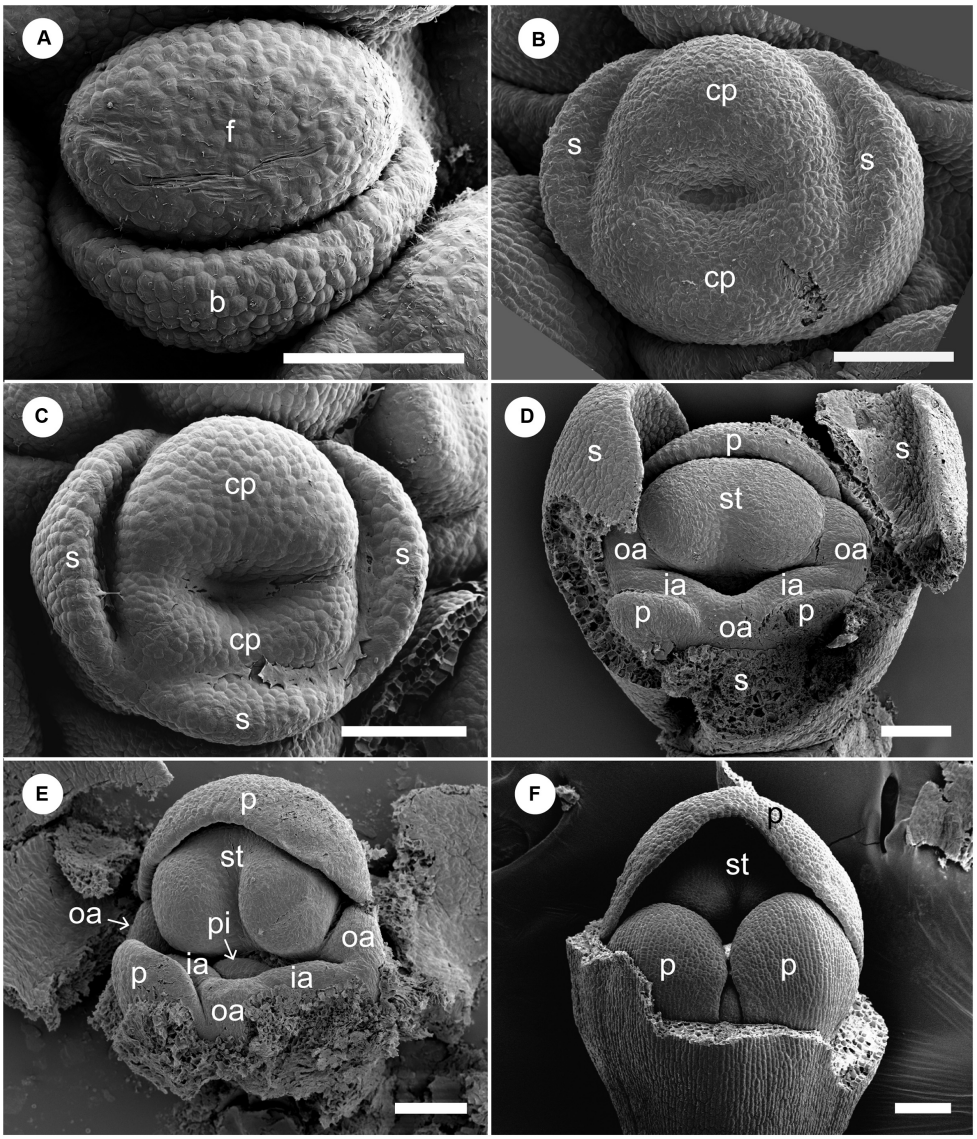

FIGURE 7 | Floral development of *Gagnepainia harmandii*. **(A)** Flower at the earliest stage. Dome-shaped floral bud (f) and bract primordium (b) are initiated. **(B)** Two lateral sepal primordia (s) and ring primordium are initiated. The ring primordium can be separated into three primordia [adaxial and abaxial common primordia (cp), abaxial sepal primordia]. **(C)** An abaxial sepal primordium is separated from the abaxial common primordium. The abaxial common primordium divides into two portions. **(D)** Adaxial petal (p), stamen (st), and two outer androecial primordia (oa) are derived from the adaxial common primordium, while two abaxial petal and inner androecial primordia (ia) are derived from the abaxial common primordium. An abaxial outer androecial primordium is also initiated from the abaxial common primordium, although the boundaries with inner androecial primordia are unclear. **(E)** The style of the pistillate primordium appears. The abaxial outer androecial primordium develops further and the boundaries with inner androecial primordia become clear. Sepal primordia are removed. **(F)** The abaxial petal primordia develop and cover the abaxial side of the stamen. Sepal primordia are removed. b, bract primordium; cp, common primordium; f, floral bud; ia, inner androecial primordium (staminode primordium); oa, outer androecial primordium (staminode primordium); p, petal primordium; s, sepal primordium; st, stamen primordium. Scale bars = 100 μm.

DISCUSSION

The Early Floral Development of *Hemiorchis* and *Gagnepainia* Focusing on Common Primordia

Hemiorchis and *Gagnepainia* are small poorly understood genera in Zingiberaceae (Kress et al., 2002). We revealed the floral development of both genera for the first time in this study. The early floral development of both genera (**Figures 4A–E**, **7A–E**) is generally consistent with that of other genera in Zingiberaceae (Kirchoff, 1997, 1998; Fukai and Udomdee, 2005; Box and Rudall, 2006; Song et al., 2007).

Both flowers of *Hemiorchis* and *Gagnepainia* have a characteristic ring primordium at an early stage that can be separated into an abaxial and adaxial common primordium

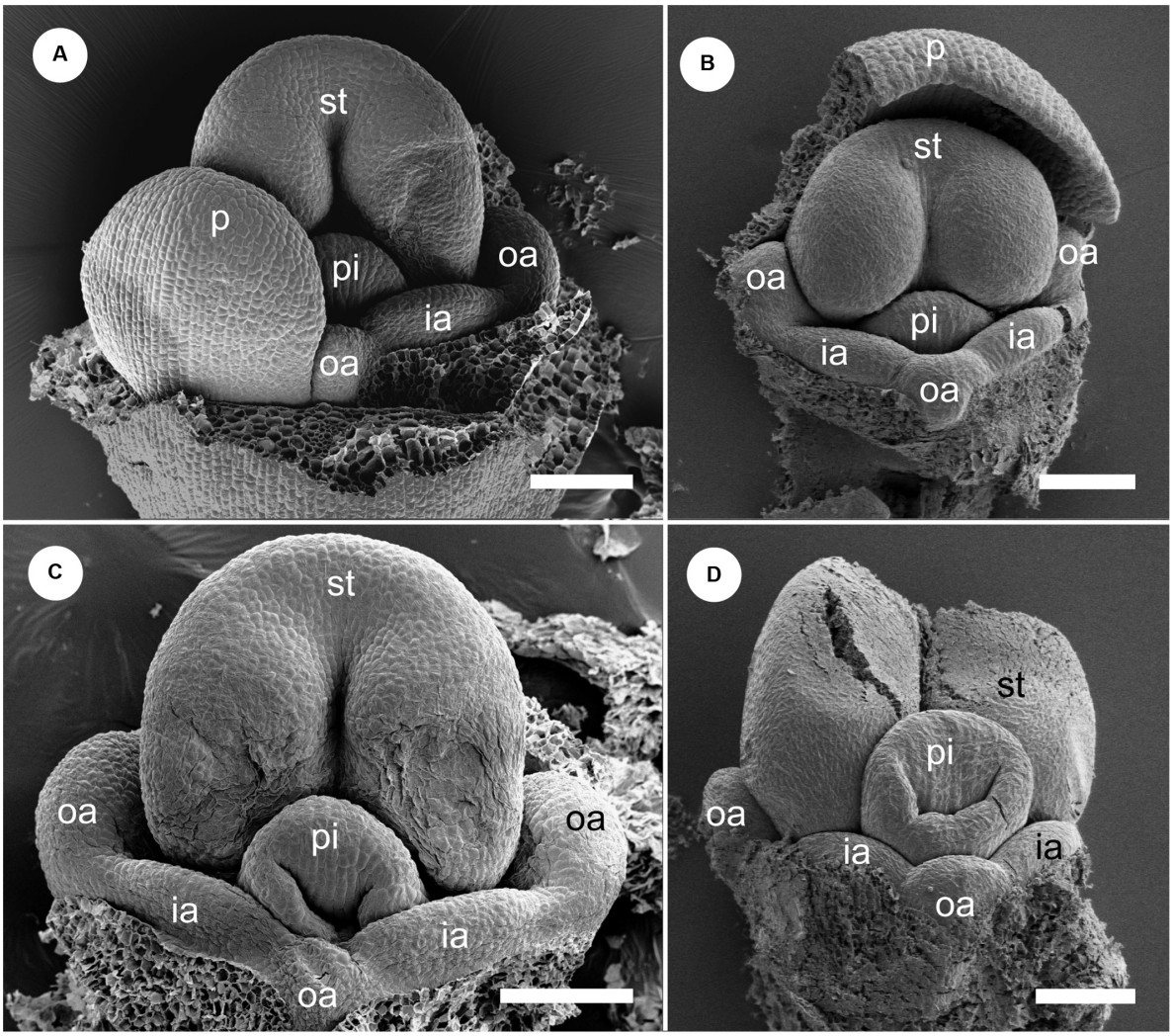

FIGURE 8 | Floral development of *Gagnepainia harmandii* (continued). Petals and sepals are removed. **(A**,**B)** Flowers at almost the same developmental stage as **Figure 6F** (middle stage). One of the abaxial petal primordia (p) is not removed in **(A)**. The androecial primordia are still small, but the boundaries between the abaxial outer androecial primordia (oa) are clear. **(C**,**D)** A slit develop at the top of the style (sty). The androecial primordia develop slightly, and the size of the abaxial outer androecial primordium becomes almost the same as the inner androecial primordia (ia) and outer lateral androecial primordia in **(D)**. ia, inner androecial primordium; la, labellum; oa, outer androecial primordium; p, petal primordium; st, stamen primordium; sty, style. Scale bars = 100 μm.

(**Figures 4C**, **7C**), although all previous studies on the floral development in the family concluded that it can be separated into three common primordia, an adaxial and two lateral abaxial primordia (Kirchoff, 1997, 1998; Fukai and Udomdee, 2005; Box and Rudall, 2006; Song et al., 2007). We interpret that the lateral abaxial common primordia originated from a single primordium because we observed the flowers at critical stages just before the ring primordium is formed (**Figures 4B**, **7B**). A single abaxial common primordium can be identified at this stage, and even an abaxial sepal primordium appears closely connected to the common primordium in *Gagnepainia*. It would be necessary to focus on the early floral development of other members in Zingiberaceae to conclude whether the single abaxial common primordium is a distinct character in the floral development of *Hemiorchis* and *Gagnepainia* or a common character in Zingiberaceae.

The Labellum Development in Globbeae

The existence of an abaxial outer androecial primordium at an early floral developmental stage, the primordium of a "fifth" staminode, has been controversial in Zingiberaceae. Kirchoff (1997, 1998) and Song et al. (2007) recognized the existence of an abaxial outer androecial primordium at early floral developmental stages and concluded that it rapidly ceased to grow and was aborted at later stages in *Alpinia oxyphylla* (Song et al., 2007), *Hedychium gardnerianum* (Kirchoff, 1997), and *Scaphochlamys kunstleri* (Kirchoff, 1998). Fukai and Udomdee (2005) mentioned that there are only two inner androecial primordia on the abaxial side of the

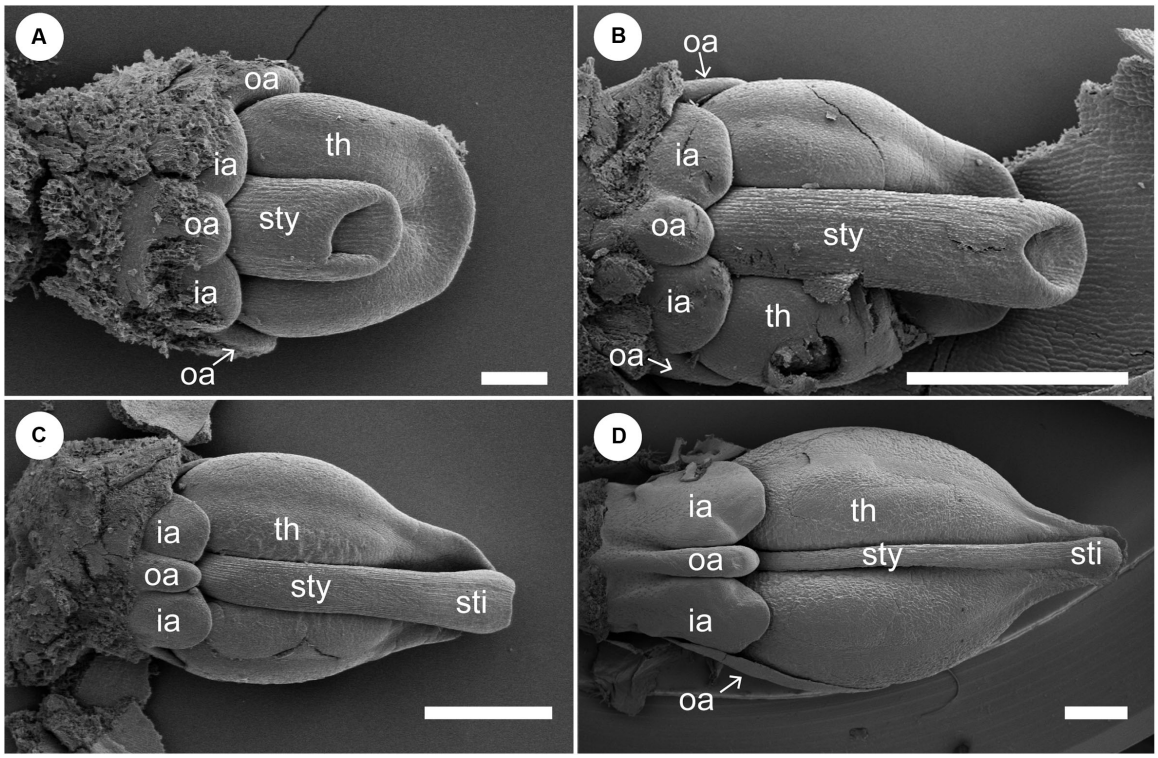

FIGURE 9 | Floral development of *Gagnepainia harmandii* (continued). Petals and sepals are removed. **(A**,**B)** Flowers at a late stage. The style (sty) elongates and is enclosed within the thecae (th). The abaxial outer androecial primordium (oa) and two inner androecial primordia (ia) develop and form a labellum primordium, while the other outer androecial primordia develop along the lateral sides of the stamen. **(C**,**D)** The abaxial outer androecial primordium elongates and becomes a long carina of the labellum. The inner androecial primordia also develop into lateral wings of the labellum. The lateral outer androecial primordia develop into petaloid staminodes along the lateral sides of the stamen. The style elongates and is tightly enclosed within the thecae. ia, inner androecial primordium; oa, outer androecial primordium; th, thecae; sti, stigma; sty, style. Scale bars = 500 μm.

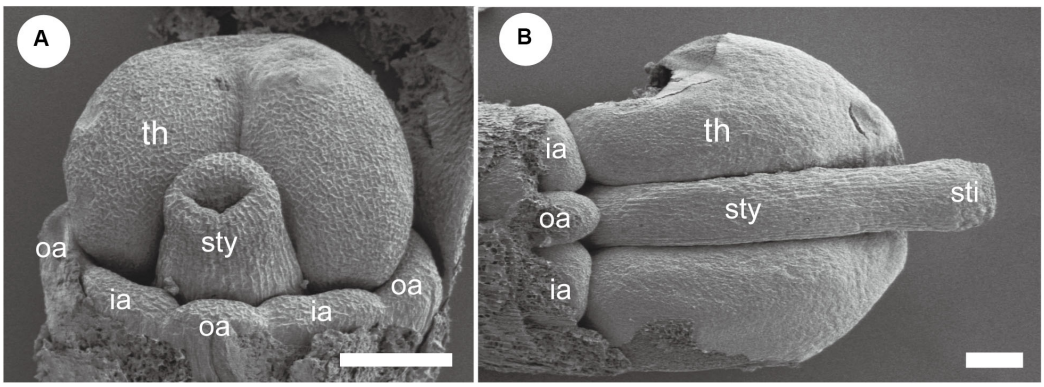

FIGURE 10 | Flower at late mid-developmental stage of *Gagnepainia godefroyi*. Petals and sepals are removed. **(A)** Two inner androecial primordia and three outer androecial primordia (oa), including the abaxial primordium are initiated. **(B)** The style elongates and is enclosed between thecae (th). Two inner androecial primordia (ia) and an outer androecial primordium develop and form the labellum primordium. Abbreviations: ia, inner androecial primordium; oa, outer androecial primordium; pi, pistil primordium; st, stamen primordium. Scale bars = **(A)** 100 μm, **(B)** 500 μm.

flower at an early floral developmental stage in *Curcuma alismatifolia*, and Box and Rudall (2006) found that it was not clear whether the abaxial outer androecial primordium is initiated and subsequently aborted during development or is absent entirely in *Globba spathulata* and *Globba cernua*. Although the morphology of the flower at early developmental stages is almost similar in all studies, their interpretations are different. In this study, we also observed a clear bump in a median position between two inner androecial primordia during early floral development in *Hemiorchis* and *Gagnepainia*,

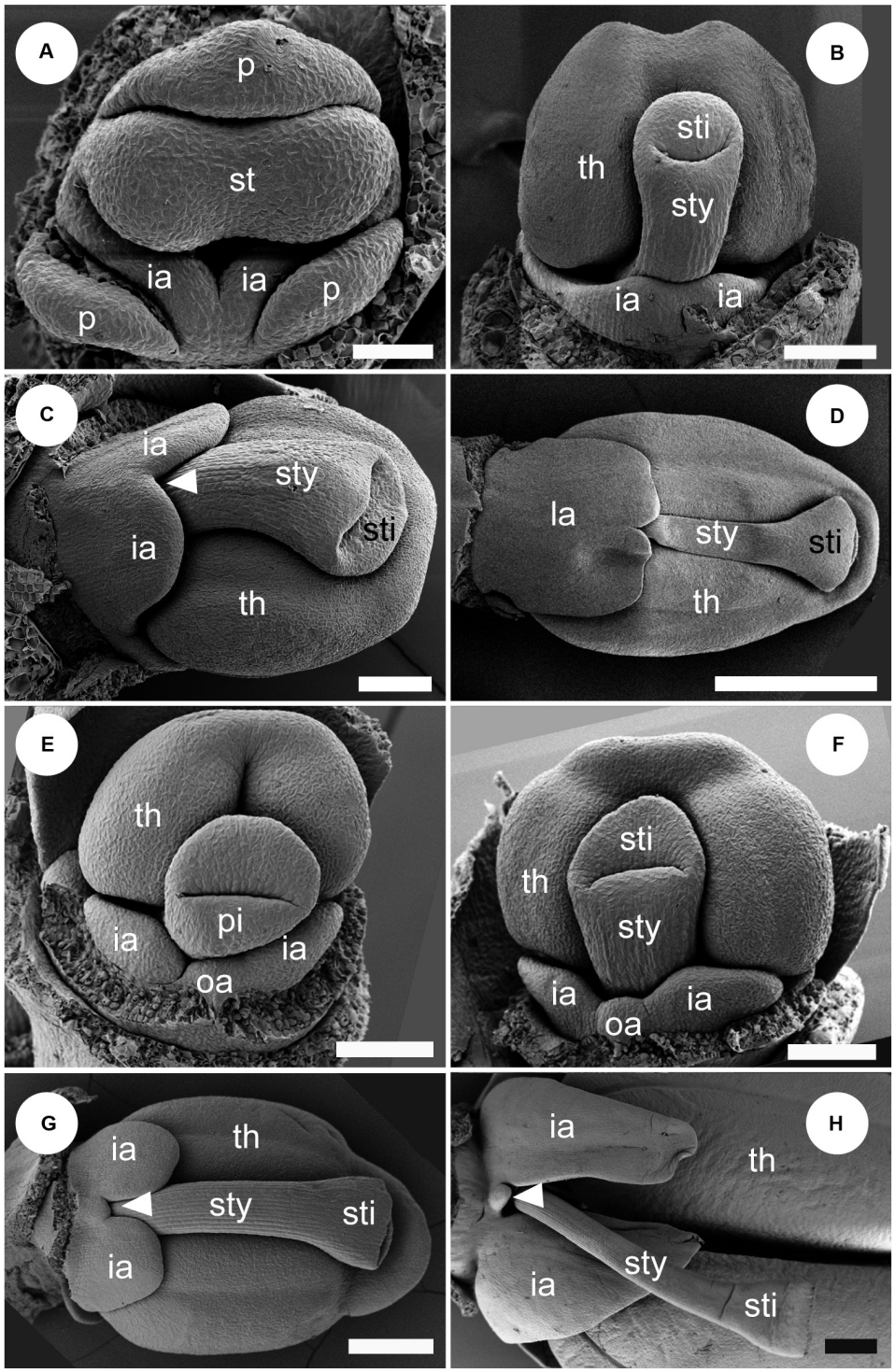

FIGURE 11 | Labellum development of *Globba.* Sepals are removed in panel **(A),** and both sepals and petal are removed in panels **(B–H)**. **(A–D)** Labellum development of *Globba paniculata.* **(A)** Two inner androecial primordia (ia) are initiated, and an outer abaxial androecial primordium (oa) is not observed. **(B)** The two inner abaxial staminodes develop as a broad bilobed primordium. **(C)** The limit between the two staminodes becomes clear as an apical notch (arrowhead). **(D)** The labellum grows upward and progressively covers the abaxial side of the stamen; the tip of the labellum is depressed. **(E–H)** Labellum development of *G. geoffrayi.* **(E,F)** Two inner androecial primordia and an outer abaxial primordium are initiated. **(G,H)** Two inner androecial primordia develop and an outer abaxial primordium is small, although it clearly exists. ia, inner androecial primordium; oa, outer androecial primordium; p, petal primordium; st, stamen primordium; sty, style; th, thecae. Scale bars = **(A)** 50 μm, **(B,C,E,F)** 100 μm, **(D,G,H)** 500 μm.

which could represent the abaxial outer androecial primordium (**Figures 4D,E**, **7D,E**).

However, we consider that the small bump on the young flower of *Hemiorchis* may not be the abaxial outer androecial primordium but just the boundary portion between the inner androecial primordia, which is raised by the distal ends of two inner androecial primordia, while the bump in the early flower of *Gagnepainia* is clearly the abaxial outer androecial primordium. It is indubitable that the bump in *Gagnepainia* is the abaxial outer androecial primordium because it subsequently grows into the central portion of the labellum at later developmental stages (**Figures 7**–**10**).

It would be rather difficult to identify the bump in *Hemiorchis* because there is no vestige of it at later developmental stages but just a depression at a median position of the labellum (**Figure 5**). Kirchoff (1997, 1998) interpreted a similar bump in *Scaphochlamys* and *Hedyosmum* as the abaxial outer androecial primordium, which rapidly ceased to grow and became aborted as a depression at a median position of the labellum. As *Hemiorchis* showed a similar development and if the interpretation about *Scaphochlamys* and *Hedyosmum* is correct, it also initiates the abaxial outer androecial primordium at first and the primordium is rapidly aborted. We observed, however, the labellum development of *G. geoffrayi* and found that the abaxial outer androecial primordium ceases to grow eventually, but it clearly remains visible between two abaxial inner androecial primordia (**Figures 11E–H**). This observation suggests that, if the abaxial outer androecial primordium was once initiated and rapidly ceased to grow at a later developmental stage in *Hemiorchis*, *Scaphochlamys*, and *Hedyosmum*, as Kirchoff (1997, 1998) suggested, the median portion of the labellum would be more depressed as is the case in *G. geoffrayi*, and the labellum would be clearly divided into two lobes without a intermedial bump.

In case that the abaxial outer androecial primordium is not initiated, as in other investigated species of *Globba* (**Figures 11A–D**), and the two inner androecial primordia occupy its position, a labellum with only an apical depression is formed as in most members of Zingiberaceae. We concluded that the labellum development of *Hemiorchis* (**Figures 4E**, **5A–D**), *Scaphochlamys*, and *Hedyosmum* (Kirchoff, 1997, 1998) should be essentially consistent with that of other genera in Zingiberaceae including *Globba* (**Figures 11A–D**; Kirchoff, 1997, 1998; Fukai and Udomdee, 2005; Box and Rudall, 2006; Song et al., 2007). That is, the labellum is clearly composed of two inner staminodes and contains no outer staminode, including a "fifth" staminode. The carina of the mature labellum in *Hemiorchis* (**Figure 3B**) should be considered as a secondary organ because it is initiated and develops only later on the adaxial side of the labellum (**Figure 6**). In particular, an independent lobe is observed at the tip of the labellum on the adaxial side during early labellum developmental stages (**Figures 6B,C**), which strongly suggest that the central carina is not derived from the abaxial outer androecial primordium but is a structure secondarily derived from the adaxial side of the labellum.

The labellum development of *Gagnepainia* is distinct in Zingiberaceae on the other hand. In *G. harmandii*, the abaxial outer primordium is clearly initiated (**Figure 8**) and develops along with two inner androecial primordia to form the labellum (**Figure 9**). The carina of the mature labellum in *G. harmandii* (**Figure 3D**) is certainly derived from the abaxial outer primordium, which corresponds to the abaxial outer staminode. In the other species of *Gagnepainia*, *G. godefroyi*, the abaxial outer primordium is clearly initiated and develops in a similar way (**Figure 10**), which indicates that the carina of this species (**Figure 3F**) is also equivalent to the abaxial outer staminode. We can conclude that the labellum of *Gagnepainia* contains the abaxial outer staminode, the "fifth" staminode, which has been considered to be lost or strongly reduced in the labellum of Zingiberaceae (Kress, 1990; Kress et al., 2002).

In *Globba*, we found two types of labellum development (**Figure 11**). The abaxial outer androecial primordium is not initiated and not included in a labellum of seven of eight observed *Globba* species (**Figures 11A–D**), which is consistent with the previous study on the floral development of *G. cernua* and *G. spathulata* (Box and Rudall, 2006). However, the labellum development of *G. geoffrayi* is distinguished from the dominant type. In *G. geoffrayi*, the abaxial outer androecial primordium is initiated and ceases to grow, but it clearly persists between the two abaxial inner androecial lobes for a considerable part of the development (**Figures 11E–H**). The labellum is an intermediate type between that of *Gagnepainia* and the other species in Zingiberaceae including *Hemiorchis* and *Globba*.

We can conclude that the development of the fifth staminode is a clear case of heterochrony (cf. Ronse De Craene, 2018), showing a gradual transition between a fully developed staminode as in *Gagnepainia*, to a reduced staminode in *G. geoffrayi*, and further to a complete loss of the staminode as in other Zingiberaceae. The loss of the staminode is clearly linked to a progressive termination of initiation of the outer abaxial staminode.

The Evolution of Labellum Morphology in Globbeae

We mapped the labellum development observed in this study and in Box and Rudall (2006) on a simplified phylogenetic tree of the tribe Globbeae based on Cao et al. (2019) (**Figure 12**). We added the other clades, viz., the tribe Zingibereae, subfamily Alpinioideae, and the genera *Tamijia* and *Siphonochilus* based on Kress et al. (2002) and Cole (2018), and mapped the labellum development data from previous studies (Kirchoff, 1997, 1998; Fukai and Udomdee, 2005; Song et al., 2007).

While we do not have observations from all species included in the phylogenetic tree of Globbeae (**Figure 12**, black triangles), that is, not all species from subgenera Mantisia and Globba were observed, observations mapped onto this phylogenetic tree provide a good starting point to discuss the evolution of labellum morphology in Globbeae and do reveal information on evolutionary patterns of labellum development across the tribe.

The labellum comprising only two inner staminodes (type A) is the most common state across the tribe. *Hemiorchis* and *Gagnepainia* form a clade within Globbeae, and the labellum that contains a well-developed fifth staminode (type B) is only

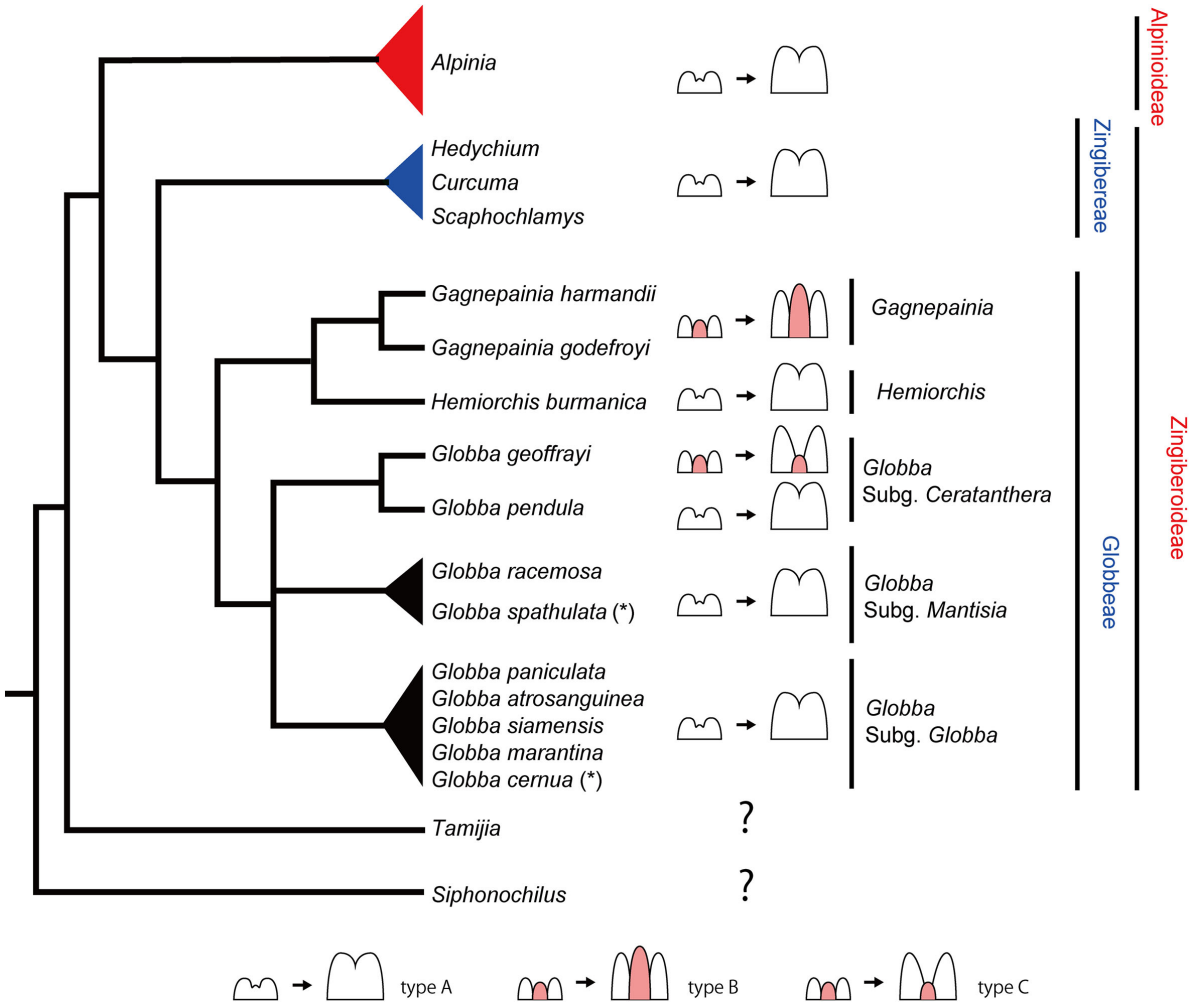

FIGURE 12 | The evolution of labellum development in *Globbeae.* Mapping the labellum development on a simplified phylogenetic tree of the tribe Globbeae based on Cao et al. (2019). The phylogenetic position of Zingibereae, Alpinioideae, *Tamijia*, and *Siphonochilus* are based on Kress et al. (2002) and Cole (2018). Pink highlighted portion in each schematic diagram of labellum development represents the missing fifth staminode. Note that the small bump between bilobed primordia of the left drawing of type A may not be the fifth staminode; therefore, it is not highlighted in pink. For Globbeae, observed species in this study and two species adapted from Box and Rudall (2006) are mapped on the tree, although they do not cover all species included in the original tree of Cao et al. (2019) (some species missing in subgenus *Mantisia* and *Globba*, represented by black triangles). (*) represents a species based on Box and Rudall (2006). The references for the labellum development in Zingibereae and Alpinioideae are as follows: *Alpinia*, Song et al. (2007); *Curcuma*, Fukai and Udomdee (2005); *Hedychium*, Kirchoff (1997); and *Scaphochlamys*, Kirchoff (1998).

found in *Gagnepainia*. The genus *Globba* is sister to the clade containing all *Hemiorchis* and *Gagnepainia* species, with the monophyletic *Globba* subgenus *Ceratanthera* resolved as the earliest diverging lineage within *Globba* (Williams et al., 2004). Within subgenus *Ceratanthera*, while *G. pendula* has the two staminode labellum as most other species in Globbeae, a labellum that includes a remnant of the fifth staminode (type C) has evolved independently in *G. geoffrayi*. *G. geoffrayi* also differs from all other species of *Globba* in distinct floral features, including the unusual development of anther appendages (Cao et al., 2019). All other species investigated, including all species of subgenus *Globba*, develop a type A labellum.

It is not clear whether the strongly developed carina of *Gagnepainia* (type B) is a retained plesiomorphic condition (comparable to the well-developed staminodes of other Zingiberales, for example Costaceae) or a secondary reversal from a staminode in the process of reduction. This evolutionary trend is comparable to staminode evolution in the Primuloid clade, with a different extent of development of the antesepalous staminodial whorls (Ronse De Craene, 2010, 2018). If type B in *Gagnepainia* is the retained plesiomorphic condition, it is only retained in *G. geoffrayi* as the remnant staminode (type C) in the genus *Globba*. Otherwise, the type C labellum evolved independently from *Gagnepainia*, which is a neoteny of type B. The comparative observation of labellum development of *Siphonochilus* and *Tamijia*, which are the most basal lineages in Zingiberaceae (Kress et al., 2002), and further species in Globbeae is necessary to determine whether the existence of a

fifth staminode in Globbeae is plesiomorphic or not. As the fifth staminode exists and is integrated into the labellum of the flower of Costaceae (Kress, 1990), the development of a fifth staminode and integration into the labellum in *Gagnepainia* and *G. geoffrayi* may be its retention in the basal lineages of Globbeae. It is also important to extend the observation of labellum development to the tribe Zingibereae and subfamily Alpinoideae. In these taxa, although only type C has been observed in the previous studies (**Figure 12**), there remains the possibility of the existence of type A and/or type B as observed in Globbeae.

The retention or recovery of the fifth staminode and its heterochronic shift should be linked with the spatial constriction within the flower bud. Iwamoto et al. (2003, 2015) suggested that the initiation and development of floral organs could be suppressed by mechanical pressures on the floral meristem. In fact, the flower buds at early stages in Zingiberaceae including Globbeae observed in this study are tightly packed insides the sepals (e.g., **Figures 4D,E**, **7D,E**), and there could be a strong mechanical pressure between the different elements of the abaxial common primordium, including the labellum and other floral organs, which might cause the suppression of initiation of the abaxial outer androecial primordium and its heterochronic shift (Ronse De Craene, 2018). Detailed anatomical observations, in particular on the longitudinal sections of flower bud at late developmental stages, are necessary to elucidate if there are clear mechanical pressures on the abaxial common primordium.

CONCLUSION

The floral development of *Hemiorchis* and *Gagnepainia* at early stages before the onset of labellum development is generally consistent with that of other members in Zingiberaceae. The fifth staminode develops as part of the labellar carina in *Gagnepainia*, while it is generally lost in Zingiberaceae. The primordium of the fifth staminode is not initiated and lost in the labellum of *Hemiorchis*. As a result, the carina in the labellum of *Hemiorchis* is a secondary organ. The fifth staminode also develops in *G. geoffrayi*, but it is not initiated in all other species of *Globba* investigated. While the staminode becomes the conspicuous carina of the labellum in *Gagnepainia*, it ceases to grow and remains small even at later stages in *G. geoffrayi*.

The fifth staminode could be either a retained plesiomorphy or the recovery of a lost organ in the basal lineage of Globbeae. The initiation of the fifth staminode and its heterochronic shift may be linked to the spatial constriction within the flower bud. It is necessary to investigate the labellum development of other Zingiberaceae, in particular, further species in Globbeae and in the genera *Siphonochilus* and *Tamijia*, which are the most basal lineages in Zingiberaceae to understand to what extent the fifth staminode has persisted among the family.

DATA AVAILABILITY STATEMENT

The datasets generated for this study are available on request to the corresponding author.

AUTHOR CONTRIBUTIONS

AI and LR had substantial contributions to the conception or design of the work, drafted the manuscript. AI and SI observed the floral morphology and development of *Gagnepainia* and *Hemiorchis*. LR and LC observed those of *Globba*.

FUNDING

This work was supported by MEXT KAKENHI Grant-in-Aid for Scientific Research on Innovative Areas "Plant-Structure Optimization Strategy" Grant Number JP19H05358 (to AI), and by JSPS KAKENHI Grant Number JP16K18576 (to AI).

ACKNOWLEDGMENTS

The authors thank the Royal Botanic Garden Edinburgh for support in collecting the materials.

REFERENCES

Barrett, C. F., Specht, C. D., Leebens-Mack, J., Stevenson, D. W., Zomlefer, W. B., and Davis, J. I. (2014). Resolving ancient radiations: can complete plastid gene sets elucidate deep relationships among the tropical gingers (Zingiberales)? *Ann. Bot.* 113, 119–133. doi: 10.1093/aob/mct264

Box, M., and Rudall, P. (2006). Floral structure and ontogeny in Globba (Zingiberaceae). *Plant Syst. Evol.* 258, 107–122. doi: 10.1007/s00606-005-0395-4

Cao, L., Newman, M. F., Kirchoff, B. K., and Ronse de Craene, L. P. (2019). Developmental evidence helps resolve the evolutionary origins of anther appendages in Globba (Zingiberaceae). *Bot. J. Linn. Soc.* 189, 63–82. doi: 10.1093/botlinnean/boy071

Cole, T. C. H. (2018). *Zingiberaceae Phylogeny Poster*. Available online at: www.researchgate.net/publication/314205060_Zingiberaceae_Phylogeny_Poster_ZPP (accessed December, 2019).

Dahlgren, R. M. T., Clifford, H. T., and Yeo, P. F. (1985). *The Families Of The Monocotyledons. Structure, Evolution, and Taxonomy*. Berlin: Springer-Verlag.

Fukai, S., and Udomdee, W. (2005). Inflorescence and flower initiation and development in *Curcuma alismatifolia* Gagnep (Zingiberaceae). *Jpn. J. Trop. Agric.* 49, 14–20. doi: 10.11248/jsta1957.49.14

Iwamoto, A., Izumidate, R., and Ronse De Craene, L. P. (2015). Floral anatomy and vegetative development in *Ceratophyllum demersum*: a morphological picture of an "unsolved" plant. *Am. J. Bot.* 102, 1578–1589. doi: 10.3732/ajb.1500124

Iwamoto, A., Nakamura, A., Kurihara, S., Otani, A., and Ronse De Craene, L. (2018). Floral development of petaloid *Alismatales* as an insight into the origin of the trimerous Bauplan in monocot flowers. *J. Plant Res.* 131, 395–407. doi: 10.1007/s10265-018-1022-0

Iwamoto, A., Shimizu, A., and Ohba, H. (2003). Floral development and phyllotactic variation in *Ceratophyllum demersum* (Ceratophyllaceae). *Am. J. Bot.* 90, 1124–1130. doi: 10.3732/ajb.90.8.1124

Kirchoff, B. K. (1997). Inflorescence and flower development in the *Hedychieae* (Zingiberaceae): *Hedychium*. *Can. J. Bot.* 75, 581–594. doi: 10.1139/b97-065

Kirchoff, B. K. (1998). Inflorescence and flower development in the *Hedychieae* (Zingiberaceae): *Scaphochlamys kunstleri* (Baker) Holttum. *Int. J. Plant Sci.* 159, 261–274. doi: 10.1086/297547

Kress, W. J. (1990). The phylogeny and classification of the Zingiberales. *Ann. Mo. Bot. Gard.* 77, 698–721. doi: 10.2307/2399669

Kress, W. J., Prince, L. M., Hahn, W. J., and Zimmer, E. A. (2001). Unraveling the evolutionary radiation of the families of the zingiberales using morphological and molecular evidence. *Syst. Biol.* 50, 926–944. doi: 10.1080/106351501753462885

Kress, W. J., Prince, L. M., and Williams, K. J. (2002). The phylogeny and a new classification of the gingers (Zingiberaceae): evidence from molecular data. *Am. J. Bot.* 89, 1682–1696. doi: 10.3732/ajb.89.10.1682

Ronse De Craene, L. (2010). *Floral Diagrams: An Aid To Understanding Flower Morphology And Evolution*. Cambridge, MA: Cambridge University Press.

Ronse De Craene, L. (2018). Understanding the role of floral development in the evolution of angiosperm flowers: clarifications from a historical and physico-dynamic perspective. *J. Plant Res.* 131, 367–393. doi: 10.1007/s10265-018-1021-1

Sass, C., Iles, W. J. D., Barrett, C. F., Smith, S. Y., and Specht, C. D. (2016). Revisiting the Zingiberales: using multiplexed exon capture to resolve ancient and recent phylogenetic splits in a charismatic plant lineage. *PeerJ* 4:e1584. doi: 10.7717/peerj.1584

Schumann, K. (1904). Zingberaceae. *Pflanzenreich* 4, 1–4.

Song, J. J., Zou, P., Liao, J. P., Tang, Y. J., and Chen, Z. Y. (2007). Floral ontogeny in *Alpinia oxyphylla* Miq. (Zingiberaceae) and its systematic significance. *Gard. Bull. Singap.* 59, 221–230.

Williams, K. J., Kress, W. J., and Manos, P. S. (2004). The phylogeny, evolution, and classification of the genus Globba and tribe Globbeae (Zingiberaceae): appendages do matter. *Am. J. Bot.* 91, 100–114. doi: 10.3732/ajb.91.1.100

Conflict of Interest: The authors declare that the research was conducted in the absence of any commercial or financial relationships that could be construed as a potential conflict of interest.

frontiers in Ecology and Evolution

ORIGINAL RESEARCH
published: 08 July 2020
doi: 10.3389/fevo.2020.00202

Ontogenetic Base for the Shape Variation of Flowers in *Malesherbia* Ruiz & Pav. (Passifloraceae)

Kester Bull-Hereñu[1,2]* *and Louis P. Ronse De Craene*[3]

[1] *Museo Nacional de Historia Natural, Santiago, Chile,* [2] *Fundación Flores, Santiago, Chile,* [3] *Royal Botanic Garden Edinburgh, Edinburgh, United Kingdom*

The flower of *Malesherbia* Ruiz & Pav. (Passifloraceae) is a suitable model to study how far growth constraints throughout ontogeny are causal for the variation in the proportions of reproductive structures. The *Malesherbia* flower is characterized by a marked hypanthium subtending five alternating sepal and petal lobes plus a coronal rim. In *Malesherbia*, the size relation between hypanthial tube and perianth lobes conditions the general aspect that the flower of a given species may display. For instance, flowers of taxa belonging to the section *Malesherbia* are characterized by a predominant hypanthium much similar to tubular flowers with reduced erect perianth lobes and a protruding paracorollar cylinder, while the opposite is true for the remaining species of the genus resembling a radiate ten-parted open flower with a reduced corona. Further morphological variation in the genus includes the bimodal distribution of absolute size of the mature flower, with some species showing much smaller dimensions (e.g., *M. humilis*) and also the variability in the level of aggregation of the inflorescences ranging from uniflorous (*M. lactea*), through racemose (*M. densiflora, M. lirana*) up to very condensed and globular in shape (*M. fasciculata*). In this work we studied under SEM the flower morphogenesis of 14 *Malesherbia* species collected in the Andean and desertic region of septentrional Chile. Against expectations, our data showed that the growth of petal lobe primordia is relatively faster in tubular flowers than in radiate ones, despite the presence of a much showier perianth at maturity in the latter. Absolute flower size could also be related to absolute meristem size and a relative developmental arrest was detected in the flower buds of very condensed inflorescences. Our results support the idea of a common constraint throughout ontogeny in which earlier inception and faster organ growth leads to relatively smaller dimensions coupled with earlier maturation and arrest of elongation.

Keywords: perianth, petals, sepals, hypanthium, corona, flower development, morphogenesis

OPEN ACCESS

Edited by:
Alistair P. McGregor, Oxford Brookes University, United Kingdom

Reviewed by:
Simone Pádua Teixeira, University of São Paulo, Brazil
Joseph Francis McKenna, Oxford Brookes University, United Kingdom

***Correspondence:**
Kester Bull-Hereñu
kester@laboratorioflores.cl

Specialty section:
This article was submitted to Evolutionary Developmental Biology, a section of the journal Frontiers in Ecology and Evolution

Received: *30 January 2020*
Accepted: *02 June 2020*
Published: *08 July 2020*

Citation:
Bull-Hereñu K and Ronse De Craene LP (2020) Ontogenetic Base for the Shape Variation of Flowers in Malesherbia Ruiz & Pav. (Passifloraceae). Front. Ecol. Evol. 8:202. doi: 10.3389/fevo.2020.00202

INTRODUCTION

Floral phenotypic variation observed in nature is possible due to the existence of unique developmental pathways that lead from floral meristems to mature flowers. How these developmental processes might have diverted through time is doubtless an intriguing question for biologists. One way of dealing with this issue is by trying to understand the drivers that push the development in response to environmental signals and selective forces. A complementary way of

understanding these changes is through the lenses of developmental constraints that may explain why certain changes in the morphogenetic process itself lead to particular phenotypic changes or variation (Ronse de Craene, 2018). Understanding principles behind the shifts of developmental processes, if there are any at all, enables us to understand floral morphology and its diversity from an organism's point of view.

Malesherbia is a South American genus originally considered as the sole representative of the family Malesherbiaceae, but recently placed within the family Passifloraceae (Angiosperm Phylogeny Group, 2016). The genus consists of 27 species that inhabit arid and Andean regions of Perú, Chile and Argentina since the Pliocene colonization of the territory (Gengler-Nowak, 2002; Guerrero et al., 2013). Although the basic bauplan of a *Malesherbia* flower is constant (five alternating sepal and petal lobes subtended by a manifest hypanthium, five stamens attached to a trilocular ovary elevated by an androgynophore and three protruding styles: Harms, 1894; Ricardi, 1967), the floral morphology looks pretty variable in nature (**Figure 1**). Clearly, the size relation between hypanthial tube and perianth lobes conditions the general aspect that a given species may display. For example, flowers of taxa belonging to the section *Malesherbia* (**Figures 1A–D**) are characterized by having a predominant hypanthium with reduced erect perianth lobes and a prominent corona protruding as a paracorollar cylinder. This construction looks pretty much like a tubular flower of the Asterids (**Figures 1A–D**). In the remaining species though, the perianth itself is much showier and remains open evoking rather a typical radiate flower (**Figures 1E–N**). Here, the sepals share a similar coloration as the petals, which creates the aspect of a ten-parted open flower with a corona limited to a discrete toothed rim (**Figures 1E–N**).

Further morphological variation in the genus includes the absolute size of the mature flower, with some species showing much smaller flowers as the ones of the annual species *M. humilis* (below 9 mm in flower width, Ricardi, 1967; **Figure 1M**); and also variability at the level of aggregation of the inflorescences ranging from uniflorous (*M. lactea*), through racemose (*M. densiflora, M. lirana*) up to very condensed and globular in shape as in *M. fasciculata* (Ricardi, 1967; **Figure 1J**).

The reason for this variation is linked to changes in the sizes of the meristem and timing of their development (Ronse de Craene, 2018). For example, meristem size has been shown to be correlated with the absolute size of *Eucryphia* flowers, as the small *Eucryphia milliganii* develops from smaller flower meristems (Bull-Hereñu et al., 2018). Comparable reduction in size of flower organs in relation to their meristematic size have been reported for the reduction in carpel size in *Oxalis* (Bull-Hereñu et al., 2016), the reduced sixth staminode of *Globba* (Iwamoto et al., 2020 this volume), the transformation of stamens into staminodes in *Byttneria* (Malvaceae) or *Sideroxylon* (Sapotaceae, Ronse de Craene and Bull-Hereñu, 2016), and even the abortion of the "fifth" petal of *Koelreuteria* (Sapindaceae, Cao et al., 2018).

On the other hand, the particular globose aspect of *M. fasciculata* could be developmentally explained simply by the inhibition of growth of the inflorescence internodes after flower production, which would account for an open inflorescence type I sensu Bull-Hereñu and Classen-Bockhoff (2011a). However, as the sister species to *M. fasciculata* is the uniflorous *M. lactea* (Gengler-Nowak, 2003), an alternative plausible scenario to explain the globose condensed inflorescence could be the transformation of the ancestor's flower meristem into a flower-like inflorescence meristem = Floral unit meristem (FUM) capable of producing many flowers (Claßen-Bockhoff and Bull-Hereñu, 2013; Claßen-Bockhoff, 2016). FUMs are related to condensed inflorescences of e.g., Asteraceae, Apiaceae, and further pseudanthia in general. They originate from a meristem that initially enlarges to a great extent, giving rise to a considerable spherical or concave meristem, followed by rapid fractionation of flowers covering its surface. Those meristems, also treated as "MC" meristems (Bull-Hereñu and Classen-Bockhoff, 2011b), normally produce floral buds with high phyllotactic numbers (high number of parastichies) resulting in a low arc-angle of the floral buds on it (see "Open II" meristems in Bull-Hereñu and Classen-Bockhoff, 2011a). As the two alternatives show different generative patterns through ontogeny, screening of inflorescence development would help discriminating between them.

In this study we aim to document the morphogenesis of *Malesherbia* flowers with focus on perianth, flower size and inflorescence structure, to ascertain whether developmental patterns are influenced by particular constraints that might explain differences in their later mature appearance.

We hypothesize that tubular flowers with reduced and erect petals and sepals would have perianth primordia arising from relatively smaller or inhibited meristematic tissues. Similarly, we expect that minute flowers of *M. humilis* develop from comparatively smaller floral buds and that the glomerulate inflorescence of *M. fasciculata* responds to either a inhibition of inflorescence internode growth or a unique appearance of a FUM in the genus.

MATERIALS AND METHODS

Material Sampling and Microscopy

This study comprises the observation of fourteen of the sixteen accepted *Malesherbia* species for Chile (Gengler-Nowak, 2003; **Figure 1**). Flower buds were collected from wild populations in the field (**Table 1**) and conserved in ethanol 70% before preparation for microscopy. The two Chilean *Malesherbia* species not considered here are *M. lactea* for which no reproductive material could be obtained, and *M. campanulata* (Ricardi, 1967), whose taxonomic identity is somewhat dubious and probably represents a variety nested within *M. lanceolata*. According to their floral shape, species were designated under one of the four categories: (1) "Tubular," corresponding to the four species of the *Malesherbia* section, characterized by tiny almost erect perianth lobes and a prominent floral tube; (2) "Radiate" corresponding to species with open and showy sepal and petal lobes; (3) "Minute," corresponding to the markedly smaller flowers of the annual *M. humilis*; and (4) "Glomerulate," corresponding to the odd *M. fasciculata* that presents a unique condensed inflorescence

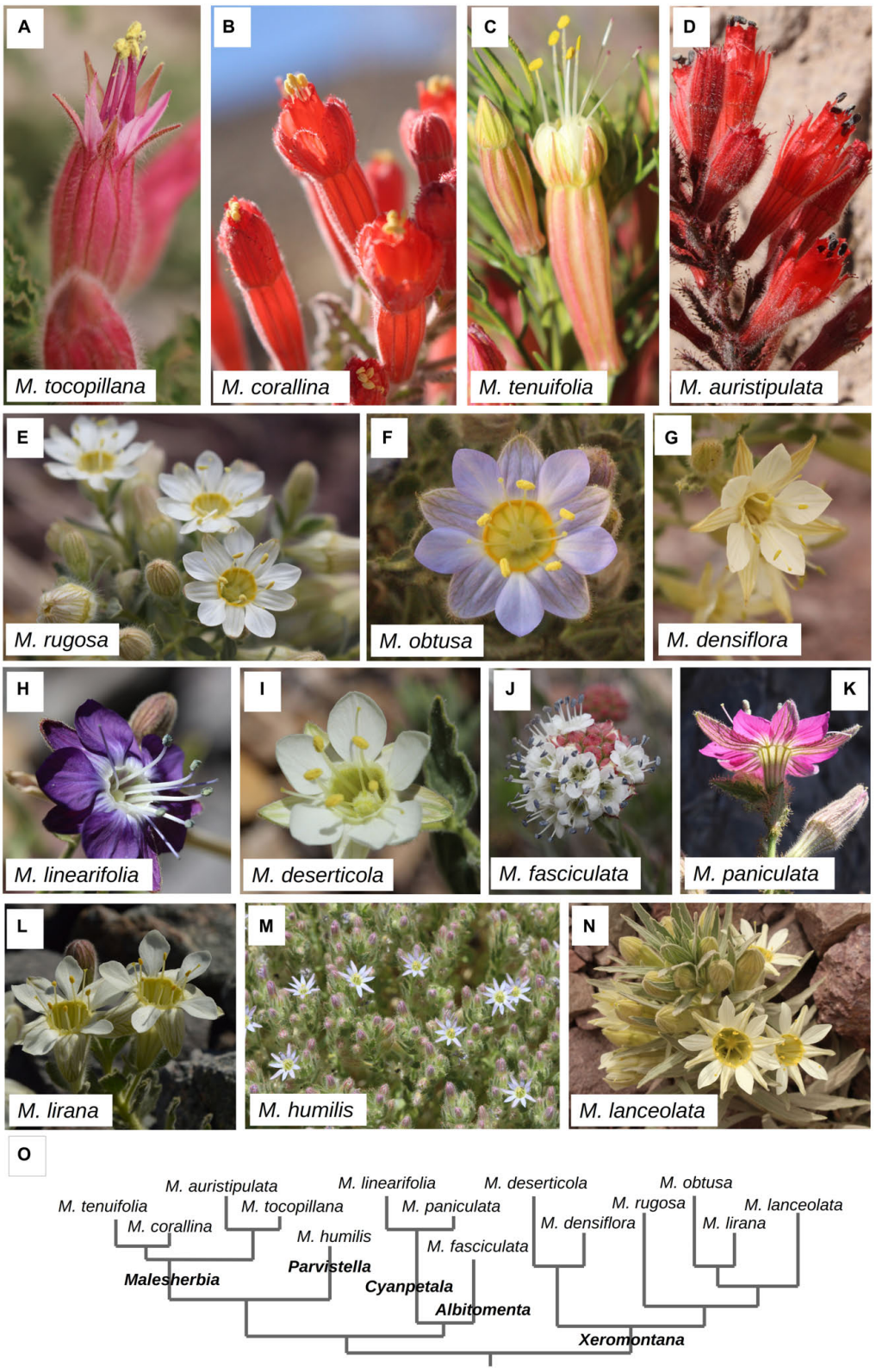

FIGURE 1 | Chilean *Malesherbia* species studied in this work. **(A–D)** Species whose flowers show a prominent reddish tubular shape, all of them belonging to the section *Malesherbia*. **(E–N)** Species with flowers of radiate shape including minute flowers and globular inflorescence and corresponding to the remaining four

(Continued)

FIGURE 1 | Continued
sections of the genus. **(A)** *M. tocopillana* Ricardi, **(B)** *M. corallina* Muñoz-Schick & R.Pinto. Note the prominent corona encircling stamens. **(C)** *M. tenuifolia* D.Don. Note the spatial separation between the five anthers and three pink stigmas. **(D)** *M. auristipulata* Ricardi, **(E)** *M. rugosa* Gay, **(F)** *M. obtusa* Phil., note the pilose ovary at the center. **(G)** *M. densiflora* Phil. **(H)** *M. linearifolia* (Cav.) Pers. **(I)** *M. deserticola* Phil. **(J)** *M. fasciculata* D.Don, note its condensed inflorescence similar to a head or large glomerule, **(K)** *M. paniculata* D.Don seen from the back. Note the hypanthium that sustains the perianth, **(L)** *M. lirana* Gay. Picture courtesy of Ludovica Santilli. **(M)** Annual *M. humilis* Poepp, note the tiny flowers. **(N)** *M. lanceolata* Ricardi. **(O)** Phylogenetic relationship among the studied species after Guerrero et al. (2013). Differences in branch length are for diagrammatic purposes only.

resembling more or less a capitulum of Asteraceae or Apiaceae (**Figure 1**).

Flowers from different stages were dissected under a light microscope (Zeiss Stemi SV6), dehydrated in an alcohol gradient and acetone, dried in a K850 critical-point dryer (Quorum Technologies), further dissected, mounted on aluminum stubs, coated with platinum (Emitech K575X) and observed with a scanning electron microscope (SEM) (Leo Supra 55-VP).

Observations, Measurements and Analysis

From the material visualized from polar views, three stages of flower development were defined (**Figure 2**): (I) Sepal inception, characterized by the existence of a bare floral meristem (fm) surrounded by the sepal lobes; (II) Hypanthial groove, characterized by the appearance of a ridge surrounding the central floral meristem; and (III) Stamen initiation, characterized by the recognition of anther primordia on the flower. The images obtained from stages I–III were used to measure bud width (bw) and monitor the time of inception of petal primordia. In these stages a total of 49 floral buds were screened (**Table 1**).

Buds in stage III and older were also recorded from lateral views (**Figures 2D–F**) to measure the length of organs such as sepal lobes (se), petal (pe) and anthers (an) primordia, and flower bud width (bw) as well (**Table 1**). From lateral views, 231 measurements were taken, which added to the polar views led to a total of 280 measurements taken from SEM micrographs (**Table 1**). Data obtained were then assigned to one of the four groups defined above, according to the species of provenance (**Table 1**).

Bud width was screened in stages I–III in order to inspect for differences in the size of the floral bud among the Tubular, Radiate and Minute groups.

Data regarding organ length were analyzed by plotting petal primordium length (pe) against bud width, and anther and sepal length, in order to understand whether there were differences in the relative rates of elongation of the petals between Tubular and Radiate groups.

TABLE 1 | Material studied in this work including their taxonomic and morphological identity, geographical provenance and N observed.

Section	Species	Plant habit	Latitude (°S)	Altitude (m)	Flower aspect	No of buds measured						
						Polar view			Lateral view			Sum
						I	II	III	se	st	bw	
Malesherbia	*M. auristipulata* Ricardi	subshrub	18°20′	1800	Tubular	2	–	1	11	6	10	30
	M. tenuifolia D. Don	subshrub	20°–20°55′	2500	Tubular	–	–	–	3	1	6	10
	M. tocopillana Ricardi	subshrub	22°5′	300	Tubular	–	1	–	6	3	7	17
	M. corallina M. Muñoz et R. Pinto	subshrub	19°48′	2700	Tubular	2	1	1	3	4	6	17
					Total	4	2	2	23	14	29	74
Cyanpetala	*M. linearifolia* (Cav.) Pers.	subshrub	31°46′–34°17′	1000–2200	Radiate	3	–	2	1	3	4	13
	M. paniculata D. Don	subshrub	28°53′–31°35′	700–1700	Radiate	1	–	2	5	6	6	20
	M. densiflora Phil.	perennial	27°6′–27°12′	3200	Radiate	1	2	1	13	11	11	39
	M. deserticola Phil.	subshrub	24°58′-25°10′	2700	Radiate	1	1	–	–	–	–	2
	M. lanceolata Ricardi	perennial	30°5′–30°10′	2900–3200	Radiate	–	2	4	6	5	8	25
	M. lirana Gay	perennial	29°46′–33°40′	2100–3000	Radiate	2	1	1	3	3	3	13
	M. obtusa Phil.	subshrub	27°29′–27°55′	500–700	Radiate	–	1	3	2	2	2	10
	M. rugosa Gay	perennial	25°53′–27°19′	1000–2500	Radiate	–	–	2	4	3	4	13
					Total	8	7	15	34	33	38	135
Parvistella	*M. humilis* Poepp.	annual	28°27′–33°20′	50–2000	Minute	2	2	7	15	3	14	43
					Total	2	2	7	15	16	14	56
Albitomenta	*M. fasciculata* D. Don	subshrub	29°20′–34°17′	20–1100	Glomerulate	–	–	–	6	4	5	15
					Total	–	–	–	6	4	5	15
					All species	14	11	24	78	67	86	280

*Roman numerals under Polar view indicate developmental stages and abbreviations under lateral view refer to measurements taken. See section "Materials and Methods" and **Figure 2** for more details. se = sepal, st = stamen, bw = bud width.*

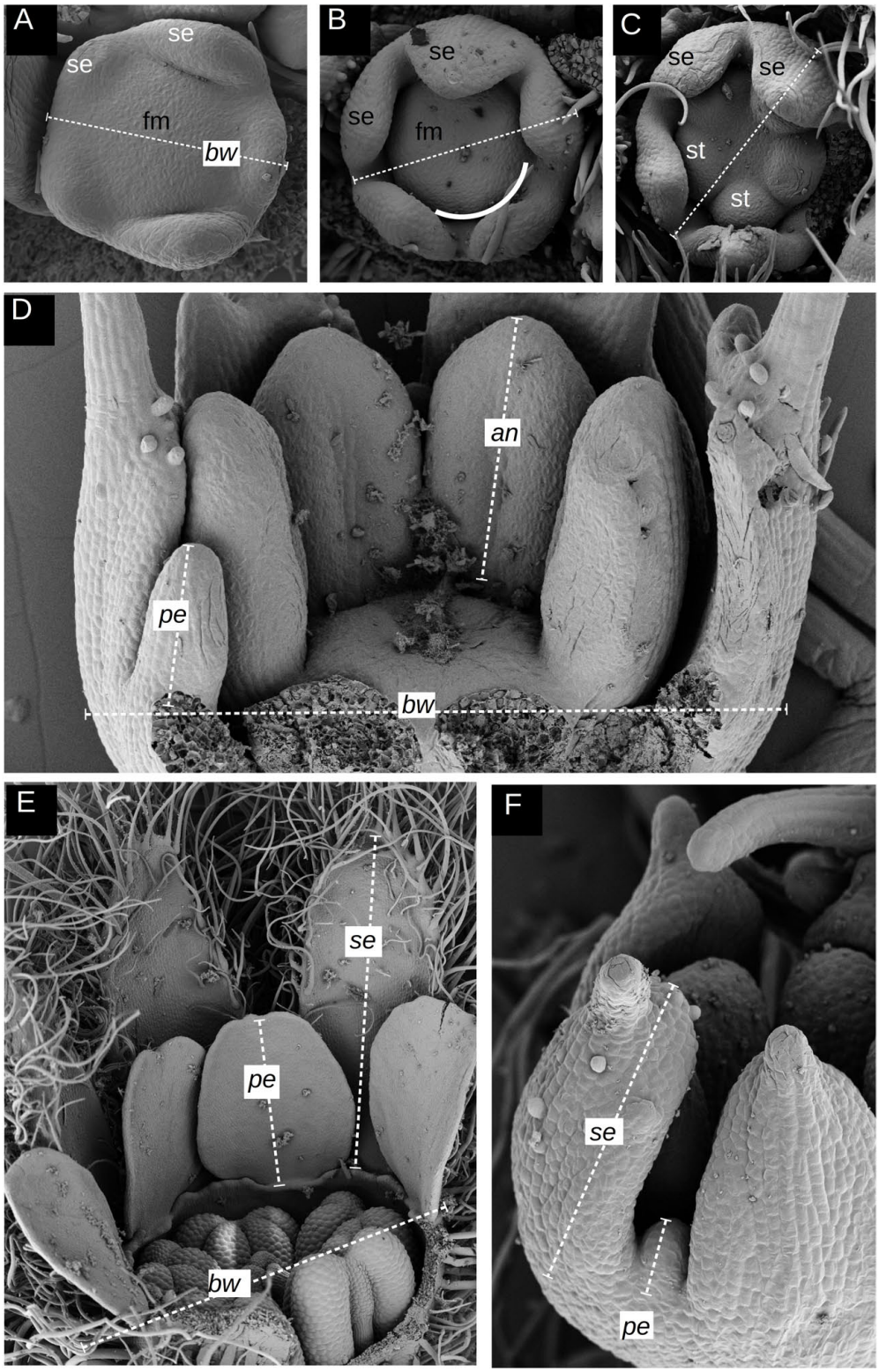

FIGURE 2 | Developmental stages and measurements taken. **(A–C)** definition of stages I–III on polar views; the key organs or attributes whose presence defines the respective stage marked in white. **(D–F)** Examples of measurements obtained from lateral views. **(A)** *M. linearifolia* (Radiate) showing stage I defined by the presence of a bare floral meristem (fm) surrounded by five just initiated sepal primordia (se). The dashed line represents the measurement of the bud width (*bw*) from the tip of

(Continued)

FIGURE 2 | Continued
one of the sepal primordia (on the right) toward the opposite side of the flower bud at the merging point of two other sepal primordia. **(B)** *M. lanceolata* (Radiate) showing stage II defined by the appearance of a groove separating the perianth from the future androecium, marking the position of the future hypanthial tube. A white line illustrates a section of this groove. Dashed line represents the measurement of bud width as explained in panel **(A)**. **(C)** *M. obtusa* (Radiate) showing stage III defined by the recognition of stamen primordia (st). Dashed line same as in panels **(A)** and **(B)**. **(D)** Example of measurements taken from the lateral view of a young flower bud of *M. auristipulata* (Tubular) represented by dashed lines comprising petal (*pe*), anther (*an*) and sepal length (*se*), and bud width (*bw*). **(E)** Example of measurements taken from the lateral view of a relatively older flower bud of *M. humilis* (Minute) showing petal and sepal length plus bud width. **(F)** Similar as in panels **(D)** and **(E)** but at a younger stage of *M. humilis*. fm = floral meristem, st = stamen, se = sepal, *se* = sepal length, *pe* = petal length, *an* = anther length, *bw* = bud width.

Finally, the Glomerulate group was qualitatively inspected in terms of inflorescence development relative to the other groups.

RESULTS

Early Developmental Stages I–III

Floral development in *Malesherbia* starts with the quincuncial inception of sepal lobes around a bare floral apex (Stage I, **Figures 3A,D,G,J**). Radiate species seem to possess a somewhat larger floral meristem (**Figures 3G,J**), but this is not numerically corroborated for all species of both groups (**Figure 5A**). Later on, and after the sepal lobes have grown slightly, a groove surrounding the floral meristem (fm) can be recognized, separating the perianth from the central zone where the stamens will arise (Stage II, **Figures 3B,E,H,K**). This groove represents a circumferential border separating an external side that will expand to form the hypanthium, and an inner side that will rise to build the androgynophore (see **Figure 6N**). At this point Tubular species present the appearance of petal primordia in between the sepal lobes (white arrowheads, **Figures 3B,E**), while these are completely lacking in the Radiate ones (open arrowheads, **Figures 3H,K**). Interestingly, sepal lobes in species of the Radiate group are markedly more advanced (**Figures 3H,K**). Later on, as the floral bud enlarges a bit more in width, stamen primordia appear simultaneously on the central floral meristem (stage III, **Figures 3C,F,I,L**). At this stage, petal primordia are markedly visible in the Tubular group (white arrowheads, **Figures 3C,F**), while these are either absent or very difficult to see in Radiate species (open arrowheads, **Figures 3I,L**). Radiate and Tubular species do not differ in the width of their floral buds at any stage (**Figure 5A**), as the range of the values obtained in both groups fully overlaps. A slight tendency in the increase of the floral width from Stages I through III can be seen in both groups, qualitatively (**Figure 3**) and numerically (**Figure 5A**).

Qualitative Differences in Petal, Sepal and Anther Development

After their inception, floral organs begin to elongate (**Figures 4**, **6**). The difference in growth rate of petal primordia becomes evident when comparing species of both groups with either similar anther or petal sizes. Taking a similar anther size as a reference, it is noticeable that while petal primordia begin to acquire a characteristic shape in Tubular species (**Figures 4A,G**), petals are just visible as small protrusions in Radiate species (**Figures 4C,J**). For a similar petal size in Tubular (**Figures 4B**, **6D**) and Radiate (**Figures 4D**, **6E**) species, differences in stamen size are evident, being larger in the latter. Comparative observations of the perianth also reveal a slight difference in the inception point of petal lobes: Petal primordia are clearly inserted in between the sepal lobes and at a similar distance from the center in tubular species (**Figures 4E**, **6C**), while in Radiate ones, petal primordia are initiated later and more to the inside of the hypanthium (**Figures 4F**, **6A,B**). This difference in position of petal inception is also visible at later stages (**Figures 6D,E**).

While petal lobes have reached and surpassed anthers in Tubular species (**Figure 4H**), they still are lagging far behind the anther tips in Radiate species (**Figure 4K**). A more mature aspect of petal primordia in a Tubular species can be seen in **Figure 4I** showing trichome development on its tip. A similar petal lobe aspect in a Radiate species can be seen in a far more advanced bud stage with larger anthers (**Figure 4L**).

When taking a similar petal size for both Radiate and Tubular species (**Figures 6D,E**), it is evident that the anthers of Radiate species appear to be more developed (**Figure 6D**). This is also true when observing older flower buds as the pair of Tubular and Radiate species shown in **Figures 6F,G**.

Similar observations can be made when taking sepals as reference organs. **Figures 6H,K** present a comparable petal size and shape but with much more reduced sepal lobes in the Tubular species (**Figure 6H**) than in the Radiate ones (**Figure 6K**). A same tendency is encountered when comparing a general view of the perianth in **Figures 6I,J,L**. The first two figures represent Tubular species with sepals approximately double the petal size, while Radiate species at this stage present sepals three to four times larger than the petals. Conversely, Radiate species achieve a relative petal size closer to the 50% of the sepal only when they are much more older and larger, as can be seen in **Figure 6M**.

The petal size pattern observed is reverted when the young flower has grown to a certain extent: petals of Radiate species are capable of overgrowing the floral width as seen in **Figure 6N** (see also **Figure 5B**), while Tubular species attain a relative petal size kept below the flower width as seen in **Figure 6P**. Young flowers of Tubular species show a prominent hypanthium already at this young age and tightly arranged petal lobes at its top (**Figures 6O,P**), while Radiate species seem to have their corolla more loosely arranged within the flower bud (**Figure 6N**).

Quantitative Elongation of Floral Organs

We quantitatively monitored the behavior of petal growth by plotting floral bud width values against petal length (**Figure 5B**). Tubular species present measurable petal primordia at smallest

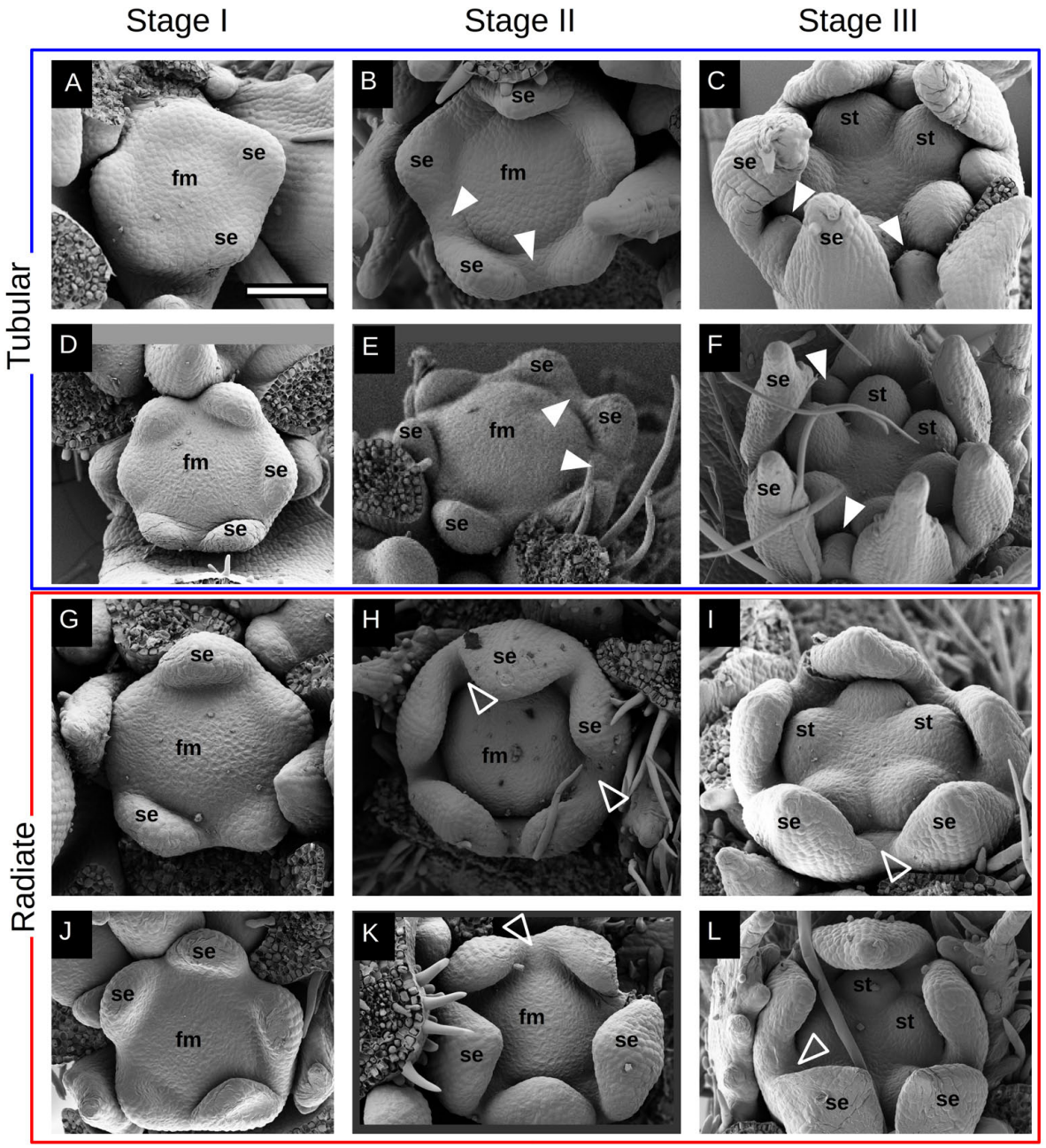

FIGURE 3 | Early development of *Malesherbia* flower. Images in a same row belong to the same species: Tubular group (blue frame): **(A–C)** *M. tocopillana*; and **(D–F)** *M. auristipulata*; Radiate group (red frame): **(G–I)** *M. lanceolata*; **(J–L)** *M. lirana.* Images in the same column correspond to a common developmental stage: **(A,D,G,J)** stage I: sepal inception; **(B,E,H,K)** stage II: hypanthium groove initiation; **(C,F,I,L)** stage III: stamen initiation. **(A)** Sepal primordia (se) arising around a young flower meristem (fm) of Tubular *M. tocopillana.* **(B)** Same species showing a clear hypanthial rim and emergence of petal primordia between sepal lobes (white arrowheads). **(C)** *M. tocopillana* showing five round stamen primordia (st), well defined sepal lobes and in between already developing petal primordia (arrowheads). **(D)** Tubular *M. auristipulata* flower initiating sepal primordia. **(E)** Slightly older flower showing petal initiation (arrowheads) between sepal primordia (se). **(F)** Petal primordia expanding (arrowheads) in between sepal primordia and surrounding the emerging stamen primordia in the center. **(G)** Radiate *M. lanceolata* showing sepal (se) inception and a bare flower meristem (fm) in the center. Note the slightly larger size of the young flower in comparison to the Tubular species shown in panels **(A)** and **(D)**. **(H)** A clear hypanthial rim is established in the young flower while sepal lobes expand toward the center. At this point, no petal primordium can be seen in the space between sepal primordia (open arrowheads) in contrast with the Tubular species shown in panels **(B)** and **(E)**. **(I)** Same species with marked stamen primordia in the center still lacking petal primordia between sepal lobes (open arrowhead). **(J)** Radiate *M. lirana* developing flower with a bare flower meristem in the center (fm) and emerging sepal lobes (se). **(K)** Flower primordium showing hypanthial rim and a sustained growth of sepal lobes. Note the larger sized sepal lobes at this point in Radiate species **(H,K)**, compared to Tubular species **(B,E)**. **(L)** Stamen primordia clearly shown in the flower center while petal primordia are still lacking (open arrowhead). Bar in panel **(A)** for all Figures = 100μm. fm = flower meristem, se = sepal, st = stamen. White arrowhead = petal primordium, open arrowhead = petal primordium still not initiated.

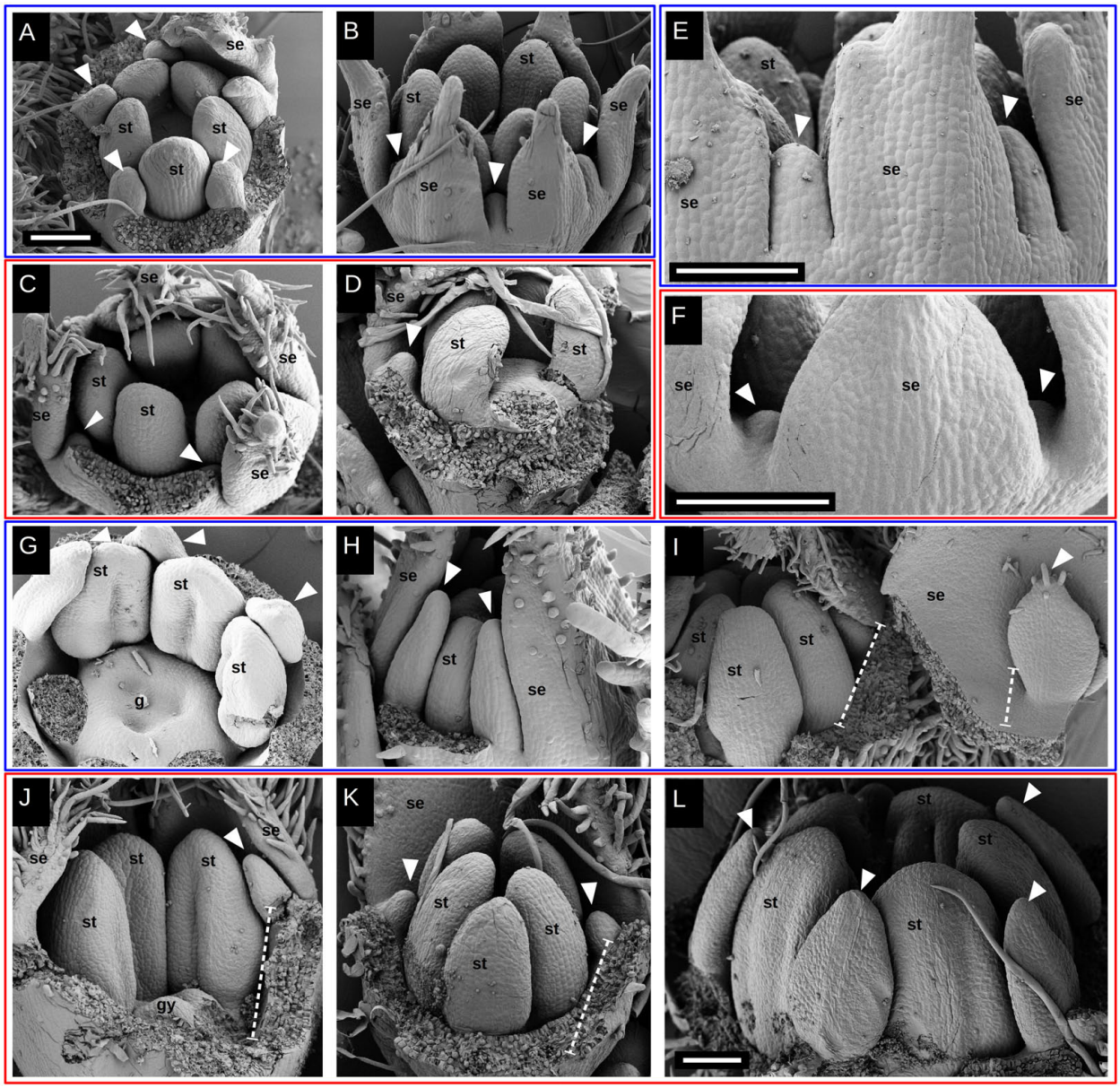

FIGURE 4 | Petal elongation during flower development in *Malesherbia*. Tubular (blue frame) and Radiate (red frame) species at similar stages for comparison: **(A)** and **(B)** v/s **(C)** and **(D)**; **(E)** v/s **(F)**; **(G,H)** and **(I)** v/s **(J,K)** and **(L)**. **(A)** Tubular *M. corallina* showing petals (arrowheads) elongating and alternating with stamens (st). Sepal lobes removed. **(B)** Tubular *M. auristipulata* at a comparable stage showing erect growing young petals. **(C)** *M. lanceolata* showing similar stamen (st) primordium size as in Tubular species **(A)** and **(B)**, but with markedly smaller petal primordia shown by arrowheads. **(D)** *M. densiflora* at similar stage regarding stamen primordium size and also showing a small protruding petal primordium (arrowhead). **(E)** View of perianth of Tubular *M. auristipulata* showing alternating sepal (se) and petal (arrowheads) lobes all inserted on the external perimeter. **(F)** Comparable view of Radiate *M. obtusa* showing much more retarded petal primordia situated more internally than in panel **(E)**. **(G)** *M. auristipulata*; young flower showing stamen (st) with thecal ridge differentiation and well-formed petals outgrowing stamens (arrowheads). A trilocular gynoecium (g) covers the center of the flower. Sepals removed. **(H)** Tubular *M. tocopillana* at a similar stage as G and equivalent large young petals (arrowheads) outgrowing stamens (st). Sepals (se) enclose flower bud, therefore one sepal is removed. **(I)** *M. tenuifolia* showing ventral face of petal (arrowhead) and sepal (se) plus a fraction of the hypanthium (dashed line). This part of the perianth has been torn open from the flower bud that shows young stamens (st). Note the growing trichomes on the petal tip indicating tissue maturation. **(J)** Radiate *M. lanceolata* young flower showing gynoecium and stamen differentiation at a similar stage as **(G–I)**. Note the markedly smaller petal primordium (arrowhead) than in previous species. **(K)** *M. densiflora* at a similar stage as **(J)**, also showing quite retarded and small petal primordia. **(L)** *M. densiflora* showing petals (arrowheads) differentiated to a similar extent as shown for Tubular species in panels **(G–I)**, but with a much larger overall size. Note that even at this size, the petals still do not overgrow the stamens. All bars = 100 μm. fm = flower meristem, se = sepal, st = stamen, gy = gynoecium, white arrowhead = petal primordium, dashed line: hypanthium outline.

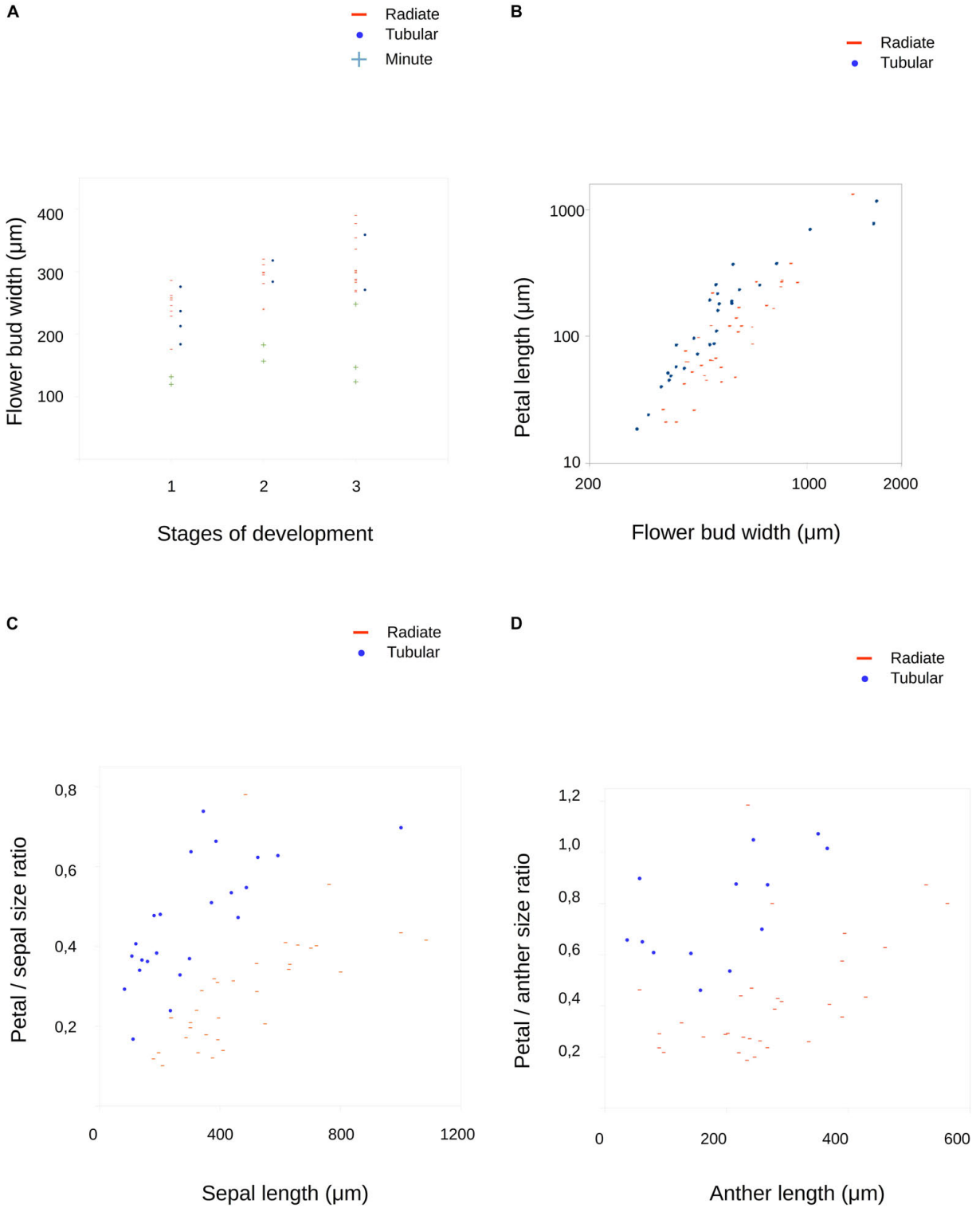

FIGURE 5 | Results of measurements on developing flowers of *Malesherbia*. **(A)** Flower bud width along three developmental stages. Three groups are plotted: Radiate (red stripes), Tubular (blue dots) and Minute (green plus symbol, see **Table 1** and main text for more explanations). Note that data ranges of Radiate and Tubular species fully overlap, while values for Minute are the smallest overall and well outside the ranges of the other two. **(B)** Petal primordium length plotted in relation to bud width. Note that Radiate flowers present smaller values in general. Note the logarithmic scale in both axes. **(C)** Sepal length plotted against relative petal size. **(D)** Anther length plotted against relative petal size. Blue dots = Tubular group, red stripes = Radiate group, green plus symbol = Minute group.

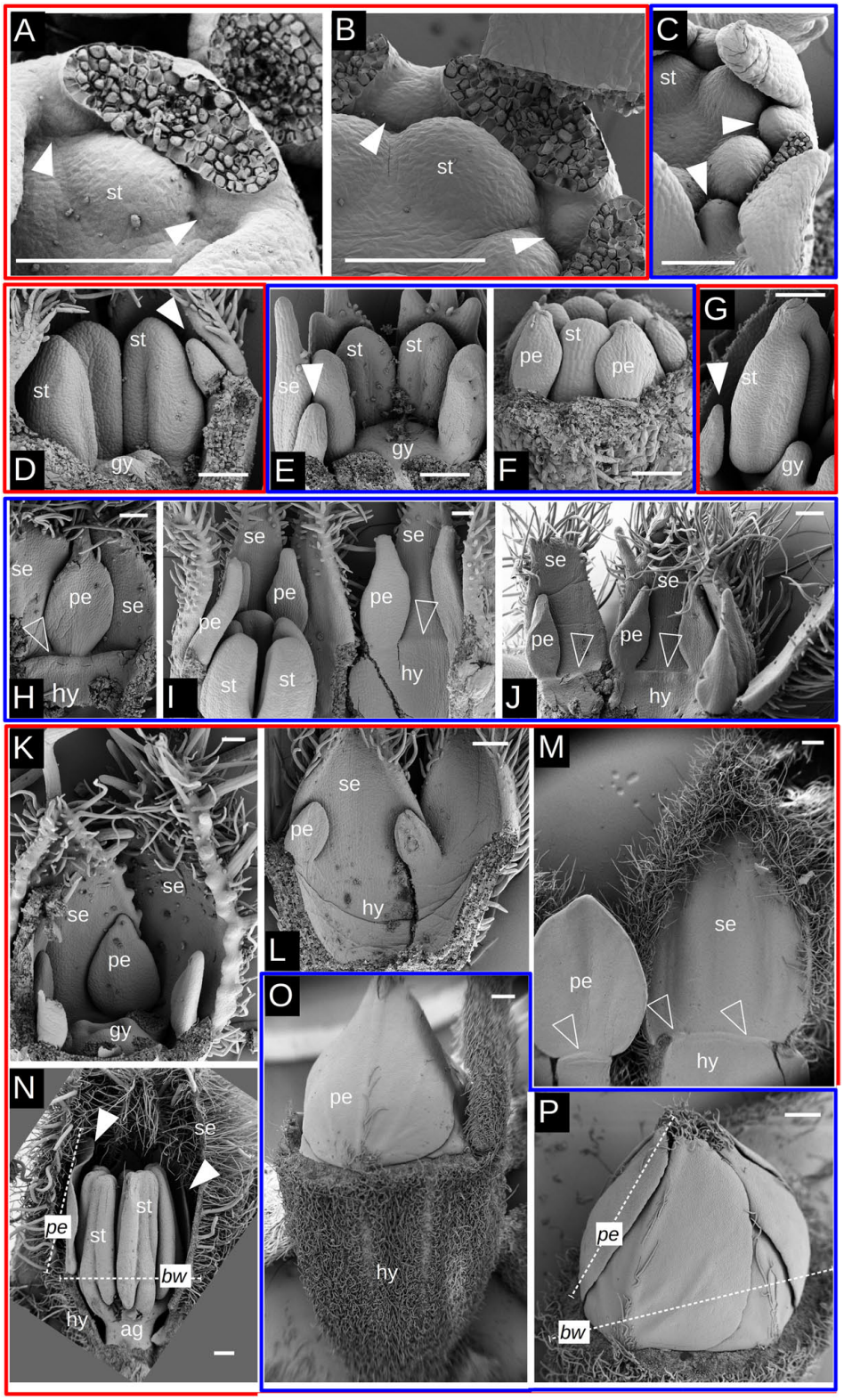

FIGURE 6 | SEM images of petal initiation and elongation in *Malesherbia*. Red frames surround Radiate species and blue frames Tubular species. **(A)** *M. rugosa* (Radiate) showing petal initiation (arrowheads) between stamen primordium (st) and sepals. **(B)** *M. paniculata* (Radiate) at a slightly older stage than in panel **(A)** showing slightly larger petal primordia. Note the position of the petal between stamens (st) and sepals. **(C)** *M. tenuifolia* (Tubular) with petal primordia placed well

(Continued)

FIGURE 6 | Continued
between sepals and being part of the dorsal margin of the flower. **(D)** *M. lanceolata* showing a small young petal (arrowhead) **(E)** *M. auristipulata* with a similar sized young petal (arrowhead) as in panel **(D)**, but with stamens of clearly smaller size. Note the more external position of the petal than in panel **(D)**. Same magnification in panels **(D)** and **(E)**. **(F)** *M. tenuifolia* showing petal primordia (pe) attached at the tip of a developing hypanthium. Also part of stamens (st) visible. Same magnification in panels **(D)** and **(E)** **(G)** *M. linearifolia* showing young petal of comparable size as in panel **(F)**, but with a much larger stamen (st). **(H)** Young petal (pe) and sepal (se) of *M. auristipulata* of a fairly similar size. Open arrowhead signals an incipient corona along the top of the hypanthium (hy) **(I)** *M. tocopillana* flower torn open to show part of the hypanthium, stamens, petals of about half the size of the sepals. **(J)** Perianth and hypanthium of *M. auristipulata* flower showing petals roughly half the size of the sepals. **(K)** *M. rugosa* showing petals of a comparable size as in panel **(H)**, but with much larger sepals (se). Same magnification in panels **(H)** and **(K)**. **(L)** Fraction of perianth of a *M. lanceolata* flower (Radiate). Note the difference in size between petal and sepal primordia in contrast to the situation in Tubular flowers shown in panels **(I)** and **(J)**. Same magnification in panels **(I,J)** and **(L)**. **(M)** *M. lanceolata,* showing petal of around half the size of the sepal. Note that this proportion is achieved in a much later ontogenetic stage in this Radiate flowers than for Tubular ones as shown in panels **(I)** and **(J)**. **(N)** *M. rugosa* young flower with well developed organs. At this advanced stage, the petal length (pe) is close to or already larger than the bud width (wd). See panel **(P)** for the opposite case. **(O)** *M. tenuifolia* young flower showing petals folded in the bud and an important hypanthium formed. **(P)** *M. tenuifolia* (Tubular) showing petals folded with cochlear aestivation. At this advanced stage, the petal length (*pe*) does not surpass the flower bud width (*bw*), contrary to a Radiate flower as shown in N. Bars **(A–L)** = 100 μm, **(M–P)** = 200 μm. Same magnification among **(D–G)**; **(H,K)**; **(I,J)** and **(L)** se = sepal, pe = petal, st = stamen, gy = gynoecium, hy = hypanthium, ag = androgynophore, white arrowhead = petal primordium, open arrowhead = incipient corona, *pe* = petal length, *bw* = bud width, dashed white line = example of measurement.

flower widths (blue dots, **Figure 5B**) and the overall tendency to be larger than the ones of Radiate species (red stripes) at similar bud width (**Figure 5B**).

The growth of petal primordium size relative to sepal or anther primordium size is shown as both increase during bud growth (**Figures 5C,D**). Here, the results found are similar as before: Tubular species present in general relatively larger petal primordia for a given referential organ size. For example, in Tubular species, petals equal anther size when anther primordia reach a length of around 400 μm (blue dots, **Figure 5D**), while in Radiate species petals do not reach anther size at the stages here screened, but attain a size of around 80% of the respective anther (red stripes, **Figure 5D**). A similar observation is made for the size relationship petal /sepal (**Figure 5C**), as the petal relative size in Tubular species is larger than in Radiate species, although not achieving the complete sepal size, but around 75%, while Radiate species achieve around 50% when sepals achieve a size of around 1,000 μm.

Corona Growth

As in other Passifloraceae, *Malesherbia* flowers present a corona rim that surrounds the stamens. This is more prominent in Tubular species (**Figures 1A–D**) where the corona forms a small tube, even reaching the level of the anthers as in *M. auristipulata* (**Figure 1D**). In the remaining species, the corona is limited to a whitish or yellowish toothed rim (**Figures 1H–N**). A corona is already well differentiated in Tubular young flower buds (**Figures 7A–C**). It protrudes ventrally from the hypanthial tissue just below petal and sepal attachment (**Figures 7B,D–H**). The distal margin of the corona is always somewhat toothed but to different degrees, varying from more or less even (**Figures 7A,D,I**), to markedly irregular (**Figures 7C,H,L**). Corona inception occurs when floral organs and hypanthium are already well developed and there seems to be no difference in the petal size of Tubular and Radiate species when it is initiated (**Figures 7E–G**). The first evidence of the corona appears as a swelling of the hypanthial tissue below the petal insertion (**Figures 7E–G**) that later expands and establishes its own growing margin (**Figures 7H–K**). This tissue may proliferate and elongate markedly in Tubular species (**Figures 7D,I**), remain more or less arrested in Radiate ones (**Figures 7J,K**), or also generate irregular crests (**Figure 7L**).

Glomerulate Inflorescence and Minute Flowers

The development of the condensed glomerulate inflorescence of *M. fasciculata* is shown in **Figure 8A**. Many undifferentiated flower primordia subtended by bracts surround an inflorescence meristem (**Figure 8A**). In contrast, inflorescences of Tubular (**Figure 8B**) and Radiate (**Figures 8C,D**) species show floral primordia growing and maturing soon after being produced by the inflorescence apex. Bracteoles and sepals can be seen arising on flower primordia (**Figures 8B–D**). The size of the flower buds is quite different among species, but in particular in the Glomerulate inflorescence (**Figure 8E**) they show the smallest dimensions (compare with **Figures 8D,F**, same magnification).

When observing the stages I–III of flower development of the Minute group (**Figures 8G–I**), they all appear clearly smaller than any other Radiate species (**Figures 8J–L**, same magnification), which is numerically corroborated by the measurements (**Figure 5A**). The size of *M. humilis* (Minute) floral bud width at these stages corresponds to nearly half of the rest.

DISCUSSION

Floral morphogenesis in *Malesherbia* shows that Tubular flowers initiate their petals earlier than Radiate flowers, and also with a faster growth rate. The petal inception in Tubular species occurs in stage II, while Radiate flowers initiate their petals in stage III or even later. The faster growth rate of Tubular petals is recognized both by their higher absolute dimension for a given bud width, and also by their higher relative size in relation to the sepal or anther within the same bud.

This fact may be somehow counterintuitive as Tubular species present the smallest petals at maturity, hence the expectation would be that these would grow slower from the beginning on, but the opposite is true.

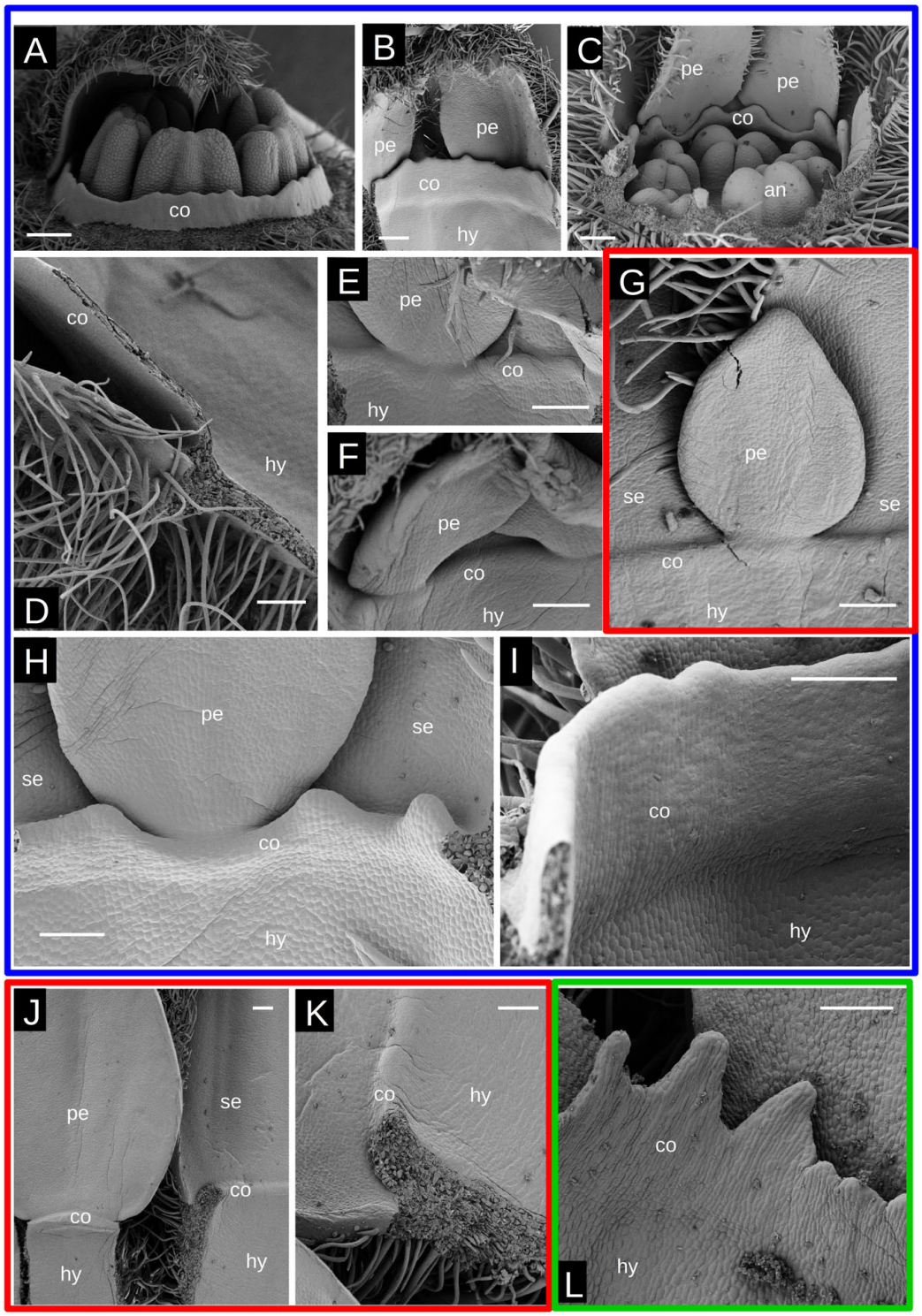

FIGURE 7 | Corona growth in *Malesherbia.* Red frame surrounds a Radiate species, green frame the minute species and blue frames surround Tubular species. **(A)** *M. corallina* showing a corona rim surrounding stamens. **(B)** Same species showing the perianth and corona rim from its ventral side. **(C)** *M. tocopillana* showing its more irregular corona surrounding androecium. **(D)** Detail of longitudinally sectioned well developed corona in *M. auristipulata*. **(E)** Corona being initiated in *M. corallina*. **(F)** Corona initiation in *M. tenuifolia*. **(G)** Corona initiation in *M. densiflora*. Note similar petal size in panels **(E–G)** (same magnification). **(H)** Corona growth in *M. tocopillana*. Note the irregular toothed shape. **(I)** Corona growth in *M. auristipulata* resembling a solid wall. **(J)** Delayed corona growth in *M. lanceolata*. **(K)** Same as in panel **(J)** showing detail of the slow growing corona. **(L)** Corona growth in *M. humilis* showing prominent teeth. co = corona, se = sepal, pe = petal, an = anther, hy = hypanthium. Same magnification panels **(E–G)**. Bars **(A–C)** = 200 μm, **(D–L)** = 100 μm.

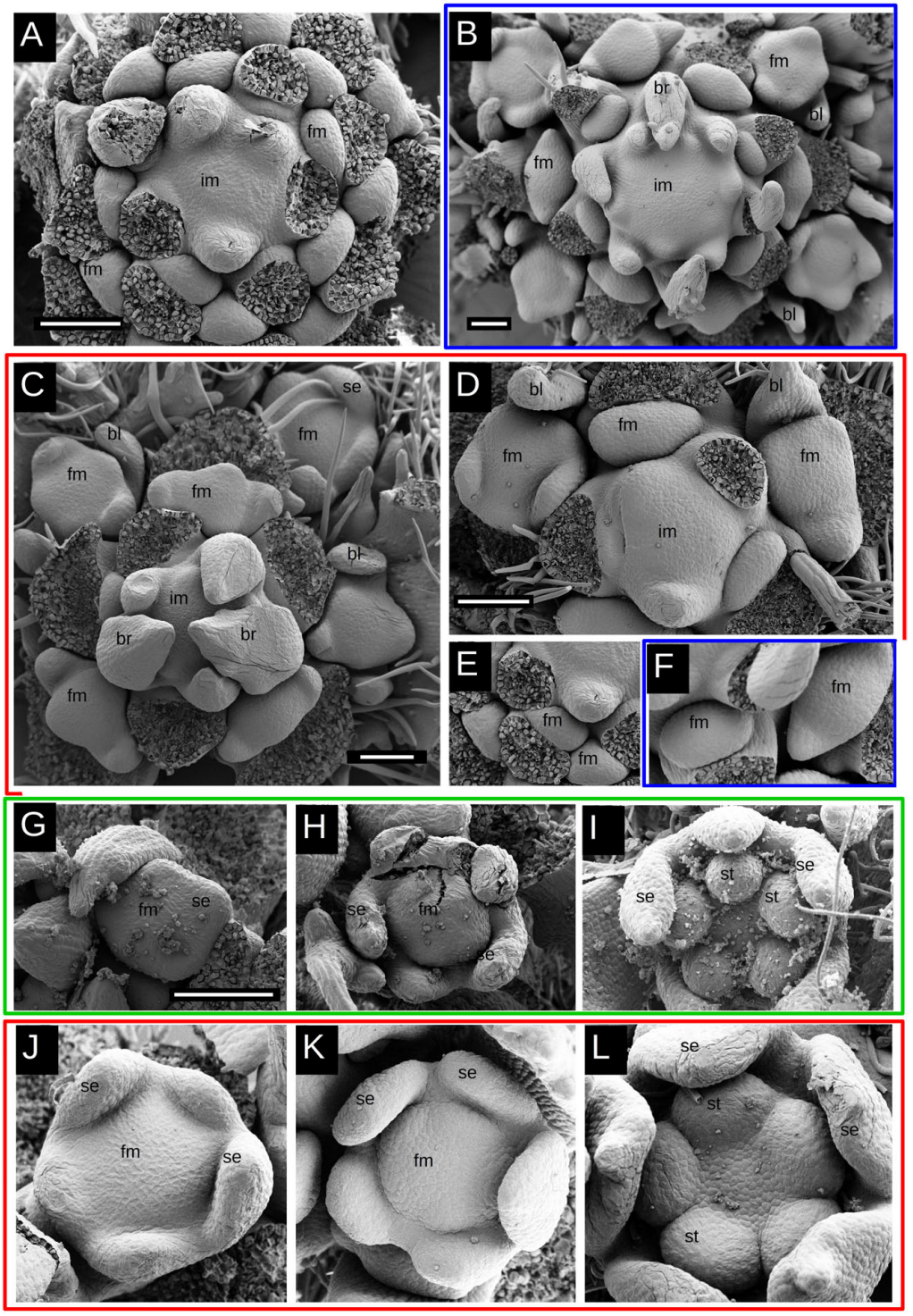

FIGURE 8 | Scanning electron micrographs of flower and inflorescence buds in *Malesherbia.* Red frame surround Radiate species, green frame the minute species and blue frames surround Tubular species. Glomerulate species without a frame. **(A–F)** Inflorescences, **(G–I)** *Malesherbia humilis* (Minute), **(J–K)** Radiate species. **(A)** Developing inflorescence of *M. fasciculata* (Glomerulate). Here, the inflorescence meristem is not particularly more expanded than the other species, nor any particularly higher phyllotaxis is manifest at floral bud initiation, thus there is no evidence for a FUM. **(B)** *M. tocopillana*, **(C)** *M. deserticola*, **(D)** *M. linearifolia*. **(E)** *M. fasciculata;* note the smaller size than **(D)** (same magnification **D,E**). **(F)** *M. tocopillana;* note larger bud size than *M. fasciculata* in panel **(E)** (same magnification **E,F**). **(G)** Stage I of *M. humilis*. **(H)** Same species in stage II. **(I)** Stage III of *M. humilis*. **(J)** Stage I of Radiate *M. rugosa.* **(K)** Stage II in Radiate *M. paniculata*. **(L)** Stage III of *M. rugosa.* Note the overall smaller bud size of *M. humilis* **(G–I)** compared to the equivalent stage of Radiate species **(J–L)**, same magnification **(G–L)**. All bars = 100 μm. im = inflorescence meristem, fm = flower meristem, se = sepal, st = stamen, br = subtending bract, bl = bracteole.

Can this difference in growth rate be explained in terms of meristematic tissues? No evident difference in flower meristem size was found between Radiate and Tubular groups, but the position of the petal primordium was different: in Tubular flowers it is situated well between sepal lobes and at the same level, while in Radiate flowers, the position of the petal primordium is shifted more to the center. This positional shift in Radiate species is probably a consequence of the later initiation of the petal primordium in stage III or later. At this time, sepal lobes are considerably more expanded in Radiate flowers and the space between them is probably no longer available; therefore the site of initiation of the petal is pushed toward the next available space more to the center of the bud. This difference may be linked to the size difference of petals at maturity, as in Tubular flowers the petals remain confined between the erect sepal lobes and corona, and have limited space for expansion, while in Radiate flowers the more inward position of the petals allows for a greater expansion.

Interestingly enough, an initial slower organ growth rate of the petal primordia seems here to be related with a larger mature organ size. This is widely recognized for the petal development in several core eudicots (see Ronse De Craene, 2008). For example, in Caryophyllaceae petals lag very much behind the stamens, even arising from common stamen-petal primordia, but they overtake the stamens in size prior to anthesis (Wei and Ronse De Craene, 2019). Some evidence in the literature has shown this pattern to exist in other flower types affecting other organs. For example, the size of the style in heterostylous *Oxalis* (Oxalidaceae) species has been shown to be inversely related to its initial growth rate, implying that initially faster growing carpels attain a smaller mature size (Bull-Hereñu et al., 2016). In analogy, in a comparative study of the flower development of *Eucryphia* (Cunoniaceae) it has been shown that relatively slow-growing androecia attain larger dimensions at maturity (Bull-Hereñu et al., 2018). At the organismic level, the same phenomenon has been described in the slow-growing regional varieties of the composite *Chaetanthera moenchioides* that attain larger sizes in the adult state (Bull-Hereñu and Arroyo, 2009). Also in controlled experiments, a temperature induced slower plant growth can lead to larger phenotypes as demonstrated for the larger capitula in *Microseris pygmaea* (Battjes and Bachmann, 1994) and *Senecio* (Abbott and Schmitt, 1985) and larger petals in *Capsella* (Neuffer and Paetsch, 2013). This principle allows for hypothesis testing in natural occurring patterns, as e.g., the increase of floral size with elevation: overall lower temperatures in mountain environments that slow growth rates in plants living there, could lead to larger floral aspects at maturity (see Bull-Hereñu et al., 2018).

The corona in *Malesherbia* arises when the organs are fully formed, representing a late morphogenetic phenomenon, similar to the documented observations for the corona of the sister genus *Passiflora* (Prenner, 2014; Claßen-Bockhoff and Meyer, 2016). In *Malesherbia*, the corona seems to initiate when petals have attained a certain size both in Radiate and Tubular flowers, which implies a comparatively earlier initiation in Tubular species, as Radiate petal lobes have been shown to develop slower. The earlier initiation of the corona in Tubular species correlates with its larger dimension and a small perianth at maturity. In radiate species the opposite occurs: a late initiation of the corona is linked to its reduced dimension and a large perianth at maturity. As for petal size, no relation could be found between initial meristematic size and corona size. Such changes in shape of the flower and morphometric adaptations are realized here as a matter of space occupation. Building a long tube is correlated with a longer corona and prevents petals from expanding, while a shorter tube leads to a reduced corona and an expanded perianth.

The Minute flowers of *Malesherbia humilis* proved to be formed by comparatively smaller flower meristems. This phenomenon has been also observed in *Eucryphia milliganii*, a considerably smaller flower within a genus with larger flowers, that also originates from relatively smaller flower meristems (Bull-Hereñu et al., 2018). Similar corroboration has been found for smaller cleistogamous flowers of *Viola* (Violaceae, Mayers and Lord, 1984), *Collomia* (Polemoniaceae, Minter and Lord, 1983) or *Pseudostellaria* (Caryophyllaceae, Luo et al., 2012) that develop from comparatively smaller meristematic sizes.

Smaller flower meristems were also observed in *M. fasciculata*, a species that also presents small flower size at maturity, comparable to that of *M. humilis*. Unfortunately, these flower meristems could only be observed qualitatively at early inception (**Figures 8A,E**), as no measurements of stages I-III could be performed due to a lack of material. The globular inflorescence of *M. fasciculata* does not arise from a FUM as it shows an active inflorescence meristem and no meristematic expansion followed by flower fractionation typical of a FUM (Claßen-Bockhoff and Bull-Hereñu, 2013; Claßen-Bockhoff, 2016). This means that the globose aspect of the inflorescence of *M. fasciculata* is due mainly to inhibition of internode elongation. Here the floral segregation seems to occur very rapidly, as flower primordia appear homogeneous all around the inflorescence meristem. A parallel between inhibited flower meristem size and inhibited inflorescence internodes is here manifest and probably speaks for a common tendency for changing growth rates at various levels of the development. This faster development here is again related to smaller flower and inflorescence sizes, similar to the perianth of Tubular species.

CONCLUSION

We found a general tendency in *Malesherbia* flower ontogeny in showing that timing of development of organs leads to manifest phenotypic variation. As already seen elsewhere for other species, an initial rapid development of organs correlates here with smaller dimensions of petals in Tubular species and in the compact globose inflorescence. Earlier inception of the corona in Tubular species could also account for petal size reduction and a larger corona tube. The absolute size of the meristem was also found to correlate with smaller flower size at maturity. The high diversity in flower morphology among species of *Malesherbia* demonstrates that subtle changes in growth rates are responsible for floral diversification and evolution.

DATA AVAILABILITY STATEMENT

The datasets generated for this study are available on request to the corresponding author.

AUTHOR CONTRIBUTIONS

KB-H collected and prepared the material, made observations with the SEM, performed imaging and measurements, as main writing. LR together with KB-H analyzed and interpreted the data and contextualized it in the present day disciplinary discussion. All authors contributed to the article and approved the submitted version.

FUNDING

This work has been funded by Conicyt-Fondecyt project nr. 11150847.

ACKNOWLEDGMENTS

We appreciate the help of following persons in the field in collecting floral materials: Alan Bull, Diego Penneckamp, Camila Gómez, Stefany Navarrete, Jimena Arriagada, Jaime Martínez, Catalina Rivera, Markus Jerominek, Maria Will, Isidora Sepúlveda, Augusto Cornejo, Ludovica Santilli, and Vanezza Morales. We also appreciate the field access facilities and permissions granted by CONAF, GASCO. We also thank Frieda Christie for technical assistance with the SEM. The Royal Botanic Garden Edinburgh (RBGE) was supported by the Scottish Government's Rural and Environmental Science and Analytical Services Division.

REFERENCES

Abbott, R. J., and Schmitt, J. (1985). Effect of environment on percentage female ray florets per capitulum and outcrossing potential in a self-compatible composite (*Senecio vulgaris* L. var hibernicus Syme). *New Phytol.* 101, 219–229. doi: 10.1111/j.1469-8137.1985.tb02828.x

Angiosperm Phylogeny Group (2016). An update of the Angiosperm Phylogeny Group classification for the orders and families of flowering plants: APG IV. *Bot. J. Linn. Soc.* 181, 1–20. doi: 10.1111/boj.12385

Battjes, J., and Bachmann, K. (1994). Phenotypic plasticity of capitulum morphogenesis in *Microseris pygmaea* (Asteracea: Lactuceae). *Ann. Bot.* 73, 299–305. doi: 10.1006/anbo.1994.1035

Bull-Hereñu, K., and Arroyo, M. T. K. (2009). Phenological and morphological differentiation in annual *Chaetanthera moenchioides* (Asteraceae) over an aridity gradient. *Plant. Syst. Evol.* 278, 159–167. doi: 10.1007/s00606-008-0126-8

Bull-Hereñu, K., and Classen-Bockhoff, R. (2011a). Ontogenetic course ans spatial constraints in the appearance and disappearance of the terminal flower in inflorescences. *Int. J. Plant. Sci.* 172, 471–498. doi: 10.1086/658922

Bull-Hereñu, K., and Classen-Bockhoff, R. (2011b). Open and closed inflorescences: more than simple opposites. *J. Exp. Bot.* 62, 79–88. doi: 10.1093/jxb/erq262

Bull-Hereñu, K., Ronse De Craene, L., and Pérez, F. (2016). Flower meristematic size correlates with heterostylous morphs in two *Chilean Oxalis* (Oxalidaceae) species. *Flora* 221, 14–21. doi: 10.1016/j.flora.2016.02.009

Bull-Hereñu, K., Ronse De Craene, L., and Pérez, F. (2018). Floral meristem size and organ number correlation in *Eucryphia Cav.* (Cunoniaceae). *J. Plant Res.* 131, 429–441. doi: 10.1007/s10265-018-1030-0

Cao, L., Liu, J., Lin, Q., and Ronse de Craene, L. (2018). The floral organogenesis of *Koelreuteria bipinnata* and its variety *K. bipinnata* var integrifolia (Sapindaceae): evidence of floral constraints on the evolution of monosymmetry. *Plant Syst. Evol.* 304, 923–935. doi: 10.1007/s00606-018-1519-y

Claßen-Bockhoff, R. (2016). The shoot concept: still up to date? *Flora* 221, 46–53. doi: 10.1016/j.flora.2015.11.012

Claßen-Bockhoff, R., and Bull-Hereñu, K. (2013). Towards an ontogenetic understanding of inflorescence diversity. *Ann. Bot.* 112, 1523–1542. doi: 10.1093/aob/mct009

Claßen-Bockhoff, R., and Meyer, C. (2016). Space matters: meristem expansion triggers corona formation in *Passiflora*. *Ann. Bot.* 117, 277–290.

Gengler-Nowak, K. (2002). Reconstruction of the biogeographical history of malesherbiaceae. *Bot. Rev.* 68, 171–188. doi: 10.1663/0006-8101(2002)068[0171:rotbho]2.0.co;2

Gengler-Nowak, K. (2003). Molecular phylogeny and taxonomy of Malesherbiaceae. *Syst. Bot.* 28, 333–344.

Guerrero, P. C., Rosas, M., Arroyo, M. T. K., and Wiens, J. J. (2013). Evolutionary lag times and recent origin of the biota of an ancient desert (Atacama–Sechura). *Proc. Natl. Acad. Soc. U.S.A.* 110, 11469–11474. doi: 10.1073/pnas.1308721110

Harms, H. (1894). "Malesherbiaceae," in *Die Natürlichen Pflanzenfamilien. III Teil Abt 6a*, ed. A. Engler (Leipzig: Verlag von Wilhelm Engelmann), 65–68.

Iwamoto, A., Ichigooka, S., Cao, L., and Ronse De Craene, L. P. (2020). Floral development reveals the existence of a fifth staminode on the labellum of basal *Globbeae*. *Front. Ecol. Evol.* 8:133. doi: 10.3389/fevo.2020.00133

Luo, Y., Bian, F., and Luo, Y. (2012). Different patterns of floral ontogeny in dimorphic flowers of *Pseudostellaria heterophylla* (Caryophyllaceae). *Int. J. Plant Sci.* 173, 150–160. doi: 10.1086/663166

Mayers, A., and Lord, E. (1984). Comparative flower development in the cleistogamous species *Viola odorata*. III. A histological study. *Bot. Gaz.* 145, 83–91. doi: 10.1086/337430

Minter, T., and Lord, E. (1983). A comparison of cleistogamous and chasmogamous floral development in *Collomia grandiflora* Dougl. *Ex Lindl.* (Polemoniaceae). *Am. J. Bot.* 70, 1499–1508. doi: 10.1002/j.1537-2197.1983.tb10853.x

Neuffer, B., and Paetsch, M. (2013). Flower morphology and pollen germination in the genus *Capsella* (Brassicaceae). *Flora* 208, 626–640. doi: 10.1016/j.flora.2013.09.007

Prenner, G. (2014). Floral ontogeny in *Passiflora lobata* (Malpighiales, Passifloraceae) reveals a rare pattern in petal formation and provides new evidence for interpretation of the tendril and corona. *Plant. Syst. Evol.* 300, 1285–1297. doi: 10.1007/s00606-013-0961-0

Ricardi, M. (1967). Revisión taxonómica de las malesherbiaceas. *Gayana Bot.* 16, 3–13.

Ronse de Craene, L., and Bull-Hereñu, K. (2016). Obdiplostemony: the occurrence of a transitional stage linking robust flower configurations. *Ann. Bot.* 117, 709–724. doi: 10.1093/aob/mcw017

Ronse De Craene, L. P. (2008). Homology and evolution of petals in the core eudicots. *Syst. Bot.* 33, 301–325. doi: 10.1600/036364408784571680

Ronse de Craene, L. P. (2018). Understanding the role of floral development in the evolution of angiosperm flowers: clarifications from a historical and physicodynamic perspective. *J. Plant Res.* 1313, 367–393. doi: 10.1007/s10265-018-1021-1

Wei, L., and Ronse De Craene, L. P. (2019). What is the nature of petals in Caryophyllaceae? developmental evidence clarifies their evolutionary origin. *Ann. Bot.* 124, 281–295.

Conflict of Interest: The authors declare that the research was conducted in the absence of any commercial or financial relationships that could be construed as a potential conflict of interest.

frontiers in Ecology and Evolution

ORIGINAL RESEARCH
published: 21 July 2020
doi: 10.3389/fevo.2020.00209

Meristem Genes in the Highly Reduced Endoparasitic *Pilostyles boyacensis* (Apodanthaceae)

Angie D. González[1], Natalia Pabón-Mora[2], Juan F. Alzate[3,4] and Favio González[5]*

[1] Departamento de Biología, Facultad de Ciencias, Universidad Nacional de Colombia, Bogotá, Colombia, [2] Instituto de Biología, Universidad de Antioquia, Medellín, Colombia, [3] Centro Nacional de Secuenciación Genómica—CNSG, Sede de Investigación Universitaria—SIU, Universidad de Antioquia, Medellín, Colombia, [4] Grupo de Parasitología, Facultad de Medicina, Universidad de Antioquia, Medellín, Colombia, [5] Instituto de Ciencias Naturales, Facultad de Ciencias, Universidad Nacional de Colombia, Bogotá, Colombia

The family Apodanthaceae comprises two genera (*Apodanthes* and *Pilostyles*) and 11 endoparasitic species, all of them lacking root and shoot apical meristems, stems, and leaves. Their vegetative phase is reduced to a mycelium-like endophyte formed by strands of parenchyma cells that are in close contact to the host vasculature. These plants become apparent only when their tiny gregarious flowers emerge breaking through the host cortex. The lack of vegetative meristems in these plants sharply contrasts to the typical formation of floral meristems. Our target species, *Pilostyles boyacensis*, provides a suitable system to investigate the evolution of meristem-related genes in an endoparasitic flowering plant without a typical vegetative shoot apical meristem. We have generated transcriptomes from two different developmental stages of the parasite (emerged floral buds and fruits), as well as a mixed sample that comprises the endophyte and growing floral buds of the parasite and its host, *Dalea cuatrecasasii* (Fabaceae). We specifically assessed copy number and domain conservation for the *WUSCHEL HOMEOBOX*, *LRR-RLK-IX-a*, and *CLE* families related to the maintenance of the shoot apical meristem (SAM) as well as the *ARF* and *LFY* families responsible for floral meristem identity. Five out of the 11 canonical gene families responsible for SAM maintenance and floral fate determinacy targeted in this study were found in *Pilostyles*. *P. boyacensis* shows at least one transcript with all functional domains conserved for *BAM1*, *WUS*, *WOX9*, *ARF7*, and *LFY*. Other genes implicated in the canonical regulatory network could not be found, including *ARF5*, *ARF19*, *BAM2*, *BAM3*, *CLV1*, and *CLV3*. In conclusion, the endoparasitic lifestyle of Apodanthaceae appears to correlate with a substantial reduction in the transcriptomic machinery linked to SAMs, whereas the genes involved in flower fate have remained intact.

Keywords: ***AUXIN RESPONSE FACTOR 7*, *BARELY ANY MERISTEM*, *holoparasitic plants*, *LEAFY*, *shoot apical meristem*, *WUSCHEL***

Edited by:
Annette Becker, University of Giessen, Germany

Reviewed by:
Lachezar A. Nikolov, University of California, Los Angeles, United States
Luiza Teixeira-Costa, University of São Paulo, Brazil

****Correspondence:***
Natalia Pabón-Mora
lucia.pabon@udea.edu.co

Specialty section:
This article was submitted to Evolutionary Developmental Biology, a section of the journal Frontiers in Ecology and Evolution

Received: *15 January 2020*
Accepted: *08 June 2020*
Published: *21 July 2020*

Citation:
González AD, Pabón-Mora N, Alzate JF and González F (2020) Meristem Genes in the Highly Reduced Endoparasitic Pilostyles boyacensis (Apodanthaceae). Front. Ecol. Evol. 8:209. doi: 10.3389/fevo.2020.00209

INTRODUCTION

The basic body plan in vascular plants results essentially from the activity of two primary meristems that form roots [root apical meristem (RAM)] and shoots [shoot apical meristem (SAM)]. These meristems are established during early embryogenesis and are maintained during plant growth by complex genetic regulatory networks (Ha et al., 2010). In angiosperms, the SAM variously

forms phytomers with photosynthetic phyllomes before its transition to flowering. Several genes are known to control the shoot meristematic activity. In *Arabidopsis thaliana* the *WOX* family gene *WUSCHEL* (*WUS*) maintains the pluripotency and cell division rate (Gaillochet and Lohmann, 2015). In turn, this protein induces the production of the short peptide CLAVATA3 (CLV3, a member of the CLAVATA 3/ESR-related genes, the *CLE* family), which binds to the CLAVATA1 receptor (CLV1, subfamily *LEUCINE-RICH REPEAT RECEPTOR-LIKE KINASE IX-a, LRR-RLK-IX-a*), triggering the negative regulation of *WUS* and leading to cell differentiation at the periphery of the SAM (Gaillochet and Lohmann, 2015). This finely tuned feedback loop keeps a balance between cell division and differentiation and is reinforced by the action of the receptors BARELY ANY MERISTEM 1–3 (BAM1, BAM2, BAM3; members of the *LRR-RLK-IX-a*). BAM receptors are expressed in the periphery of the meristematic field, where they capture other peptides of the CLE family produced on the flanks and avoid complete differentiation of the meristematic cells by the effect of CLE peptides with CLAVATA1 (DeYoung and Clark, 2008). In addition, *WUSCHEL-HOMEOBOX 9* (*WOX9*, another member of the *WOX* family) has been shown to maintain active cell division in the SAM, leaf primordia initiation, and root meristem identity at early stages of seedling growth (Haecker et al., 2004; Wu et al., 2005). Thus, *wox9* mutants develop an abnormal flattened SAM with differentiated cells as well as the arrest of primary root growth (Wu et al., 2005). *WOX9* positively regulates *WUS* expression, and also responds to the negative regulation of CLV3 (Wu et al., 2005).

Hormones also play a key role in the patterning of the SAM. High concentrations of auxin on the SAM flanks are crucial for phyllome patterning, as auxin/indole-3-acetic acid (Aux/IAA) proteins interact with *AUXIN RESPONSE FACTOR 5* (*ARF5*/*MONOPTEROS*, a member of the *ARF* family) (Korasick et al., 2014). *ARF5* is repressed by IAA12/BODENLOS; such repression can be antagonized by high concentrations of auxin, triggering IAA protein degradation (Chandler, 2016). Thus, an increase of auxin in the flanks of the inflorescence meristem (IM) is necessary to release *ARF5,* which can directly induce *LEAFY* (*LFY*) and specify floral meristem (FM) fate (Yamaguchi et al., 2013; Denay et al., 2017). In addition, both *ARF5* and *ARF7* are functionally redundant in embryo axis patterning and auxin-dependent cell expansion (Hardtke et al., 2004). Furthermore, the closely related paralogs *ARF7* and *ARF19* could also induce *LFY* expression indirectly through the positive regulation of *PLETHORA3* (Chandler and Werr, 2015; Taylor-Teeples et al., 2016). *LFY* promotes the transcription of *APETALA1* (*AP1*) (Wagner et al., 1999) in a positive feedback loop responsible for FM identity. *LFY* containing complexes also activate B-, C- and E-class MADS-box genes, which ultimately control floral organ identity (Wils and Kaufmann, 2017).

Parasitic flowering plants have evolved independently at least 12 times (Nickrent, 2020). Hemiparasites are still able to photosynthesize and acquire water and minerals from its host plant. Holoparasites, instead, completely lack photosynthetic organs and relay on the host for all nutritional requirements. Such lifestyle is associated with variations of the typical body plan in response to full nutritional and developmental dependence on the host. The most dramatic reduction occurs in endoparasitic plants, which do not form roots, stems, or leaves (Heide-Jørgensen, 2008). Their vegetative phase is reduced to strands of parenchyma cells inside the host, and their only visible structures are the flowers and the fruits upon their emergence from the host tissues. Flowers frequently retain a variously modified perianth as well as a fully functional androecium and gynoecium (Heide-Jørgensen, 2008; Nikolov et al., 2013). Here, we focus on one of such extraordinary endoparasitic lineages, the Apodanthaceae. The family comprises 11 species in two genera, *Apodanthes* and *Pilostyles* (González and Pabón-Mora, 2014a,b). While the sole species of the former parasitizes members of the Salicaceae and is restricted to the New World, members of the latter grow on various legume lineages in the Americas, Africa, the Near East, and Australia (Bellot and Renner, 2014; González and Pabón-Mora, 2014a,b; Arias-Agudelo et al., 2019). Species of *Pilostyles* have a reduced embryo with 8–10 cells, and it is not known whether RAM or SAM formation occurs during early embryogenesis (Rutherford, 1970; González and Pabón-Mora, 2017; **Figure 1M**). The endophyte consists of mycelium-like cell strands in close contact with the host vasculature (**Figures 1H–J**). The reproductive transition occurs inside of the host passing through a bractless IM that quickly transitions into a FM. Flowers gradually break through the host cortex and emerge in preanthesis (Blarer et al., 2004; Brasil, 2010; Amaral and Ceccantini, 2011; González and Pabón-Mora, 2017; **Figures 1A–G**). Emerging portions are part of the exophyte (**Figures 1A–F**). The lack of recognizable vegetative meristems in these plants sharply contrasts to the typical formation of FMs, which poses a suitable system to study the evolution of meristem-related genes and the interplay between vegetative and FMs across flowering plants (**Figures 1K,L**).

Our study generates for the first time reference transcriptomes from three different developmental time points of the endoparasitic *Pilostyles boyacensis*, namely, endophytic tissue of *P. boyacensis* growing inside the *Dalea cuatrecasasii* host stem, individual floral buds, and fully formed fruits of *P. boyacensis*. We have identified a set of genes involved in shoot apical and FMs. We provide a comprehensive list of meristem-related genes in *Pilostyles* and track their evolution in a broad angiosperm sampling. Altogether, the substantial reduction of the SAM genetic regulatory network affects only the formation of primary meristems, while FM development remains intact. The few SAM meristematic genes found could be functionally recruited in flower, fruit, and early embryogenesis as indicated by their expression in the *P. boyacensis* flowers and fruits.

MATERIALS AND METHODS

Plant Material

Three samples spanning the full life cycle of the endoparasitic *P. boyacensis* were collected: (1) endophytic tissue of *P. boyacensis* growing inside the *D. cuatrecasasii* host stem (hereafter called PbE + D, **Figure 1G**); (2) individual preanthetic flowers of *P. boyacensis* already emerged from the host (hereafter called

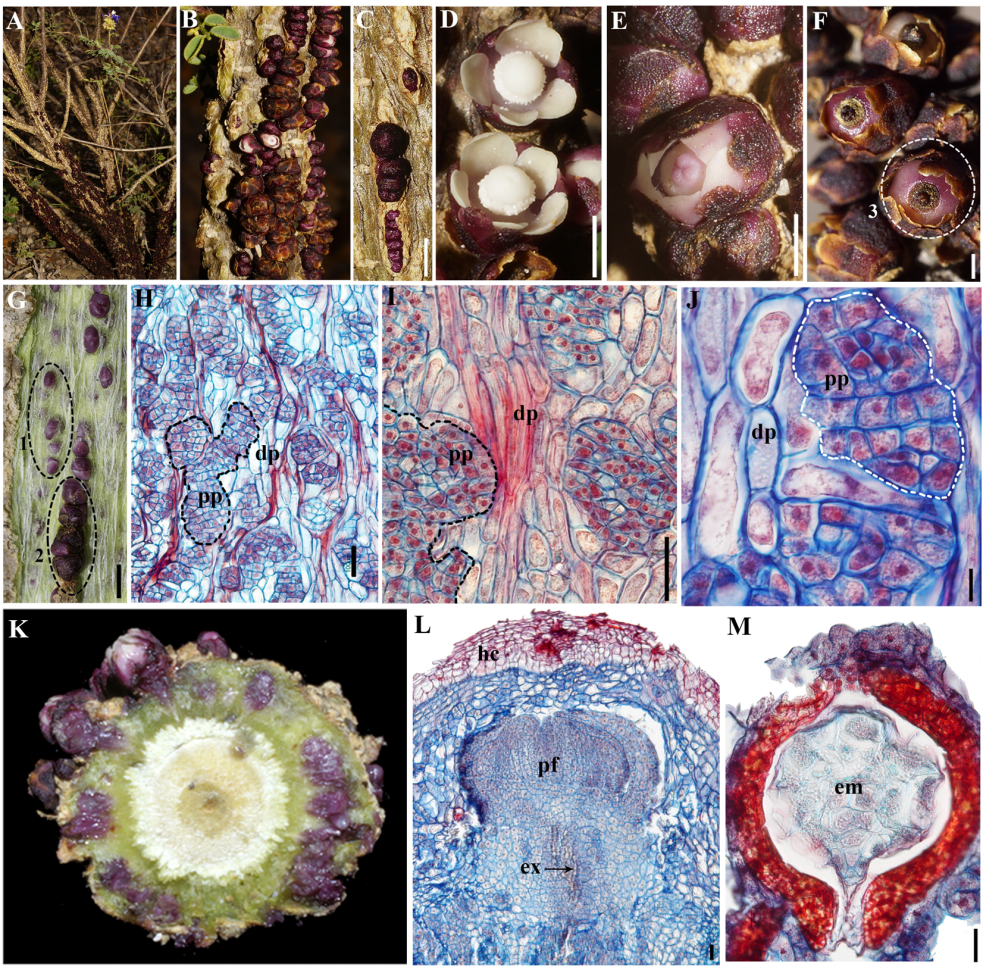

FIGURE 1 | (A–F) *Pilostyles boyacensis* exophyte; **(A–C)** overall view; **(A)** detail of flowers; **(B,C)** flowers emerging from its host *Dalea cuatrecasasii*. **(D)** Staminate flowers; **(E)** carpellate flowers; **(F)** fruits; **(G)** Peeled-off stem portion of *D. cuatrecasasii* showing flowers of *P. boyacensis* at various stages of development and growth; white fibers correspond to the phloem host tissue. **(H–J)** Longitudinal section of infected *D. cuatrecasasii* stem at **(H)** low; **(I)** mid and, **(J)** high magnification showing irregular aggregations of *Pilostyles* parenchymatic cells (pp, dotted) in contact to host phloem (dp). **(K)** Transverse section of infected *D. cuatrecasasii* stem showing flowers of *P. boyacensis* at various stages of development and growth; **(L)** Longitudinal section of *P. boyacensis* floral bud (pf) and its vascular extensor (ex), still inside of the host cortex (hc). **(M)** Longitudinal section of *P. boyacensis* seed with embryo (em). Numbers (1–3) in **(F)** and **(G)** indicate the three tissues sampled for the transcriptomes, as follows: (1) *Dalea*/*Pilostyles* mixed tissue; (2) Preanthetic *Pilostyles* flowers; (3) *Pilostyles* fruits and seeds. Scale bars: **(C–G)** 2 mm; **(H,I,L)** 100 μm; **(J)** 10 μm; **(M)** 20 μm.

PbFl, **Figure 1** G); and (3) young and fully formed fruits and seeds of *P. boyacensis* (hereafter called PbFr, **Figure 1F**). These samples were collected at xerophytic thickets around Villa de Leyva (Boyacá, Colombia) for total RNA extraction (*Pilostyles* voucher *FG 4518*, and *D. cuatrecasasii* voucher *FG 4519*, both deposited at COL). The tissues were flash-frozen in the field and stored in liquid nitrogen until RNA extraction was performed.

RNA Extraction, Sequencing, and Transcriptome Assembly

The TRIzol™ Reagent (Invitrogen) protocol was used for the extraction of total RNA with modifications used by Pabón-Mora et al. (2012). Total RNA was resuspended in 1 ml of EtOH 100% and send out to the Macrogen Sequencing Facility. The RNA-seq experiment was conducted using the Truseq mRNA library construction kit (Illumina) and sequenced on a HiSeq2000 instrument[1]. Read cleaning was performed with a quality threshold of Q30, and a minimum read length of 70 bp, singletons were excluded. Contig assembly was computed using the Trinity V2.5.1 software (Grabherr et al., 2011) with default settings with TRIMMOMATIC adapter removal. Assemblage metrics are summarized in **Table 1**.

Identification of Orthologous Genes Associated With the Regulation of Shoot Apical and Floral Meristems

The canonical genes *ARF5*, *ARF7*, *ARF19*, *BAM1*, *BAM2*, *BAM3*, *CLV1*, *CLV3*, *LFY*, *WOX9*, and *WUS*, involved in the SAM

[1]https://www.illumina.com/

TABLE 1 | Statistics of the PbE + D, PbFl, and PbFr transcriptomes.

	PbE + D	PbFl	PbFr
Number of paired raw reads	72535272	50851360	64546194
Number of contigs	321853	177935	147327
Average contig length	644	592	867
Largest contig	12072	16382	13560
Shortest contig	201	201	201
N50	1009	850	1554
L50	57252	29037	24532
GC%	43.88	42.07	43.5

maintenance and FM fate in *Arabidopsis thaliana*, were retrieved from TAIR (The Arabidopsis Information Resource, Poole, 2007). Then, they were used as queries to search homologs in the transcriptome of *Pilostyles thurberi* (available in the OneKP database; Matasci et al., 2014) as well as in other members of the Cucurbitales, including the genomes of *Cucumis sativus* (available in Phytozome; Goodstein et al., 2012), *Citrullus lanatus* and *Cucurbita maxima* (available in Cucurbit Genomics Database; Zheng et al., 2019). These sequences were compiled and processed to keep exclusively their coding sequences (CDS). A complete matrix for each gene lineage was used as query in the transcriptomes from *P. boyacensis* and *D. cuatrecasasii* described above. BLAST searches were done using an *e*-value of 1×10^{-5} and 1×10^{-30}. *P. boyacensis* genes isolated have been submitted to NCBI under the GenBank numbers MN946521–MN946537.

Sequences resulting from the search in the three *Pilostyles* transcriptomes were then subjected to BLASTN in NCBI. Two searches were performed in order to identify the best hits from the database and to assess their preliminary taxonomic affinity. The first search was done without any taxonomic filters. Here, all *Pilostyles* sequences used as queries resulted in high identity hits with genes from several taxa in the Malpighiales. The second search was done taking into consideration particular taxonomic filters, thus providing the framework to preliminary assign each sequence to either *P. boyacensis* or *D. cuatrecasasii*. This is particularly important for those sequences obtained from the mixed host-parasite transcriptome. Genes were preliminarily assigned to *P. boyacensis* when BLAST searches resulted in high identity and coverage values with sequences from members of Cucurbitales (where Apodanthaceae is currently circumscribed) and Malpighiales (where the first search yielded most hits). On the other hand, genes were assigned to *D. cuatrecasasii* if best hits matched sequences from Fabaceae (as host-related proxies). BLAST searches in Swiss-Prot (sub-base plants) were used to determine whether the sequences extracted corresponded to the target gene.

Characterization of Orthologous Genes Associated With the Regulation of Shoot Apical and Floral Meristems

In order to explore the evolution of the target genes, five independent matrices were compiled for the *ARF5*/*7*/*19*, *CLV1*/*BAMs, LFY*, *WOX9*, and *WUS* genes. These matrices included all sequences isolated from the three reference transcriptomes described above, as well as canonical sequences from *A. thaliana*, and other selected basal angiosperms, monocots, rosids, and asterids. These sequences were extracted from the GenBank, Hardwood Genomics Project[2] Phytozome and OneKP. The CDSs were identified using TransDecoder[3] implemented on the Galaxy platform (Afgan et al., 2018). The complete accession list is in **Supplementary Table S1**.

Sequences were compiled using Bioedit (Hall, 1999) and aligned in two steps: a first, unguided alignment followed by a phylogenetic analysis in order to identify major clades within large gene families such as ARF, BAM, and CLV; and a second, refined alignment guided by sequence similarity found among closely related taxonomic groups for each gene family. Alignments were made using the MAFFT server (Katoh and Standley, 2013) implementing the E-INS-I strategy, a gap opening penalty of -2 and an offset of 0.5 for most genes, except for *WUS* and *WOX9*, where a gap opening value of −3 was used. For the second alignment phase, the merge function of MAFFT was used to compile smaller datasets into a single matrix per gene family[4].

In order to find the evolutionary model that best fits each matrix, ModelTest-NG (Darriba et al., 2019) was used, resulting in the GTR + G model for all gene families. Phylogenetic analyses were carried out by two approaches. First, maximum likelihood using RaxML-HPC2 (Stamatakis et al., 2008) with 500–1000 bootstrap and all other parameters by default. Second, Bayesian inference was applied using MrBayes 3.2.7a (Ronquist et al., 2012) with two independent runs with four chains, convergence between runs assessed by average standard deviation of split frequencies below 0.01, and burn-in of 25% to obtain a majority-rule consensus tree. Some features were adjusted for each gene lineage, as follows: for *WUS* and *WOX9*, three million generations were run with a sample frequency of 500; for *LFY*, six million generations were run with a sample frequency of 500; for *CLV1*/*BAMs*, 30 million generations were run with a sample frequency of 3,000; and for *ARF5*/*7*/*19*, eight million generations were run with a sample frequency of 250. The *Amborella trichopoda* homologs were chosen as outgroup in most phylogenetic analyses with two exceptions; the *A. thaliana PHLOEM INTERCALATED WITH XYLEM* (*PXY*) was used as outgroup in the *LRR-RLK-IX-a* family, given that it predates the *CLV*/*BAM* duplication (Bryan et al., 2012); and the *Physcomitrella patens ARF2* was used as outgroup in the *ARF5/7/19* family, as it precedes the split of *ARF5* and *ARF7/19* (Finet et al., 2013). Software used for the evolutionary model search, maximum likelihood and Bayesian inference were run on the CIPRES Science Gateway (Miller et al., 2010). Resulting trees were visualized and edited using FigTree v. 1.4 (Rambaut, 2006).

Unaligned aminoacidic matrices generated in Bioedit (Hall, 1999) were used to search motifs in the MEME

[2]https://www.hardwoodgenomics.org

[3]https://github.com/TransDecoder/TransDecoder/wiki

[4]https://mafft.cbrc.jp/alignment/server/merge.html

Suite program[5] with the following parameters: Motif Site Distribution: zero or one per sequence; maximum number of motifs: 50; minimum motif width: 7; maximum motif width: 150, and all other default parameters. Selected sequences including those from *Pilostyles boyacensis*, *P. thurberi*, *A. thaliana*, Cucurbitaceae, Salicaceae, Euphorbiaceae, and Fabaceae were subjected to MEME analysis aiming to identify domains and motifs exclusive to Apodanthaceae. *A. thaliana* sequences were included in order to compare the canonical domains reported for those genes. Cucurbitales sequences were included as Apodanthaceae is currently a member of this order. Finally, Salicaceae and Euphorbiaceae (Malpighiales) proteins were included due to high similarity in the BLAST hits with *Pilostyles* sequences. Expanded complete (in the case of WUS, WOX9, and LFY) or partial (for CLV/BAM and ARF5/7/19) datasets of the amino acid matrices were analyzed by MEME to confirm Apodanthaceae exclusive motifs.

RESULTS

Pilostyles boyacensis orthologs of *ARF7, BAM1, LFY,* and *WOX9* were identified from all three transcriptomes. The *WUS* ortholog was found only in the PbFl transcriptome. Orthologs of *ARF5*, *ARF19, BAM2, BAM3, CLV1, CLV3* were not found in any of the three transcriptomes (**Table 2**). *CLE22* and *CLE3*, both of which are *CLE* homologs, were only found in the PbE + D transcriptome. Their CDS size ranges between 288 and 335 nt, and they likely belong to *D. cuatrecasasii*, as both sequences show high identities (70–82%) and coverages (98–100%) with various Fabaceae homologs.

[5]http://meme-suite.org/tools/meme

TABLE 2 | BLAST targeted genes in the three transcriptomes of *P. boyacensis* examined.

Gene family	Gene	PbE + D	PbFl	PbFr
WUSCHEL-related homebox (WOX)	*WUS*	–	*PiboW1* PiboW2*	–
	WOX9	*PiboW9_2*	*PiboW9_1** *PiboW9_2* *PiboW9_3*	*PiboW9_2*
CLAVATA 3/ESR-related (CLE)	*CLV3*	–	–	–
LEUCINE-RICH REPEAT RECEPTOR-LIKE KINASE IX-a, (LRR-RLK-IX-a)	*CLV1*	–	–	–
	BAM1	*PiboBAM1_1*	*PiboBAM2_1*	*PiboBAM1_2** *PiboBAM2_2** *PiboBAM2_3**
	BAM2	–	–	–
	BAM3	–	–	–
AUXIN RESPONSE FACTOR (ARF)	*ARF5*	–	–	–
	ARF7	*PiboARF7_2**	*PiboARF7_1** *PiboARF7_2**	*PiboARF7_2** *PiboARF7_3** *PiboARF7_4**
	ARF19	–	–	–
LEAFY	*LFY*	*PiboLFY3***	*PiboLFY1* *PiboLFY2*	*PiboLFY1* *PiboLFY2*

Single asterisks (*) indicate protein sequences lacking one or more motifs when compared to canonical proteins. Double asterisk (**) indicates incomplete CDS. (–): transcript not found.

The *WUSCHEL* and *WUSCHEL*-Related Homeobox 9 Gene Subfamilies

The phylogenetic reconstruction of the *WUS* genes is mostly consistent with the systematic relationships of the angiosperm groups sampled. The only exception is the odd position of monocot homologs within rosids, likely due to long-branch attraction or convergent sites. Rosid homologs are grouped by family; thus, gene clades from Apodanthaceae, Brassicaceae, Cucurbitaceae, Euphorbiaceae, Fabaceae, Linaceae, Malvaceae, and Salicaceae are recovered (**Figure 2**). *WUS* homologs are mostly single copy genes, except for the duplicates found in *Argemone mexicana* (Papaveraceae), *Cucurbita maxima* (Cucurbitaceae), *Gossypium raimondii* (Malvaceae), *Juglans regia* (Juglandaceae), *Linum usitatissimum* (Linaceae), and *Populus trichocarpa* and *Salix purpurea* (Salicaceae) (**Figure 2** and **Supplementary Figure S1**). Most duplicates appear to be species-specific, except in Salicaceae where the duplication predates the *Populus/Salix* diversification (**Figure 2**).

The two *Pilostyles boyacensis WUSCHEL (WUS)* homologs are closely related to the single sequence recovered from *P. thurberi* (bootstrap/posterior probability BS/PP, 100/1). *WUS* homologs from both *Pilostyles* species are, in turn, clustered with sequences from *Citrullus lanatus*, *Cucumis sativus*, and *Cucurbita maxima* (Cucurbitaceae) (BS/PP, 85/1, **Figure 2**).

The two contigs found in *P. boyacensis* were recovered from the PbFl transcriptome. These two differ in 10 bases and a four-base insertion that extends the reading frame by 38 amino acids toward the 3′ in one of the variants (PiboW2; **Supplementary Figure S2**). The MEME analysis shows that the Homeobox domain (DNA-binding domain), the LELxL WUS motif, and the TLxLFP WOX1 motif are conserved in PiboW2, while PiboW1 lacks the LELxL WUS motif (**Figure 3** and **Table 2**). The single transcript found in the transcriptome of *P. thurberi* shows a premature stop codon and only conserves the Homeobox domain. Our MEME analyses did not identify additional motifs exclusive for Apodanthaceae or Cucurbitaceae.

The phylogeny of the *WUSCHEL-related homeobox 9* genes recovers the monocot and the eudicot homologs with high supports (BS/PP, 86/0.98, and 70/1, respectively). However, the expected relationships within eudicot homologs are not recovered (**Figure 4**). Family-specific duplications were detected in Brassicaceae, resulting in the *WOX8* and *WOX9* clades, as well as in Crassulaceae, Poaceae and Salicaceae (**Figure 4** and **Supplementary Figure S3**). Species-specific duplications were detected in *Cucurbita maxima*, *Gossypium raimondii*, *Juglans regia*, *Linum usitatissimum*, *Musa acuminata*, *Pilostyles boyacensis, P.*

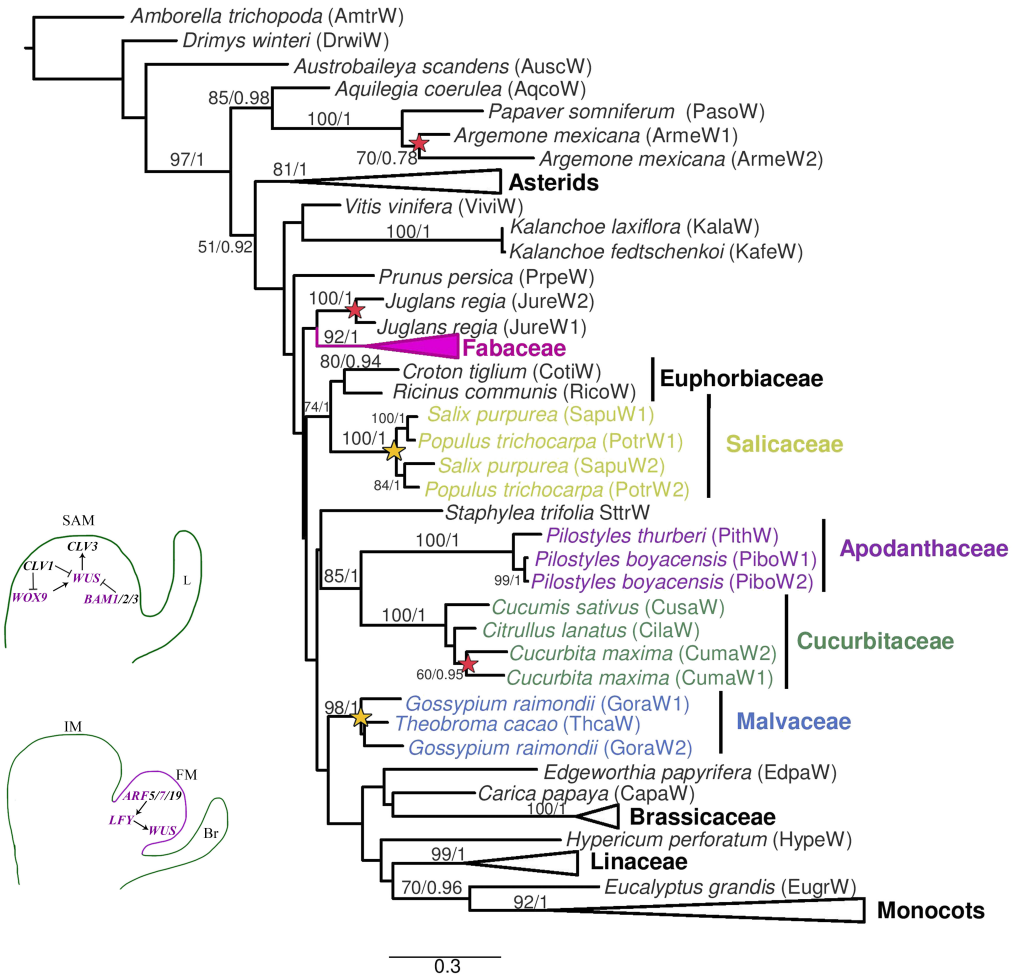

FIGURE 2 | Maximum likelihood reconstruction of the *WUSCHEL* gene lineage. Bootstrap values >50 and posterior probability are shown above the nodes. Yellow stars and red stars indicate family level and species-specific duplication events, respectively. Bottom left, schematic representation of the canonical genes related to the SAM and the transition to IM and FM. Abbreviations: *ARF, AUXIN RECEPTOR FACTOR; BAM, BARELY ANY MERISTEM;* Br, bract; *CLV, CLAVATA;* L, leaf; *LFY, LEAFY; WOX, WUSCHEL HOMEOBOX; WUS, WUSCHEL*.

thurberi, Phaseolus vulgaris, and *Staphylea trifolia* (**Figure 4** and **Supplementary Figure S3**).

All *Pilostyles* homologs cluster with Cucurbitaceae *WOX 9* genes in both phylogenetic reconstructions (BS/PP, 39/0.99, **Supplementary Figure S3**). In the case of *P. boyacensis*, three variants of *PiboWOX9* were detected, all of which were close to one of the two copies found in *P. thurberi* (*PithW9*_1, BS/PP, 100/1, **Figure 4**). The *PiboW9*_2 variant was found in all three transcriptomes, whereas the other two variants where only isolated from the PbFl transcriptome of *P. boyacensis*. The MEME analysis showed an N-terminal motif MASSN, the Homeobox domain, and the C-terminal VFIN/LQxG WOX8 motif, present in all sequences. The only exception was detected in the *PiboW9*_1 variant, which lacks the C-terminal VFIN/LQxG WOX8 motif (**Supplementary Figure S4**; **Table 2**). Two Apodanthaceae-specific motifs and one Cucurbitaceae-specific motif (**Supplementary Figure S4**) were found in a dataset that included 88 representative sequences from *A. thaliana*, Apodanthaceae, Cucurbitaceae, Salicaceae, and Euphorbiaceae (data not shown).

The LEUCINE-RICH REPEAT RECEPTOR-LIKE KINASE IX-a Subfamily

The phylogenetic reconstruction of the LRR-RLK-IX-a subfamily recovered four large clades *CLV1* (BS/PP, 84/0.67), *BAM1*/2 (BS/PP, 16/-), *BAM3* (BS/PP, 88/1), and *BAM3-like* (BS/PP, 65/1) (**Figure 5** and **Supplementary Figure S5**). *Amborella trichopoda* and species of Ranunculales have homologs in each of the four clades, suggesting that duplications occurred prior to the diversification of all angiosperms. However, in 49 out of 74 species, we only detected genes from two or three clades, pointing to heterogeneous expression of the four genes in different taxa. The maximum likelihood (ML) reconstruction of *CLAVATA1* subclade is mostly consistent with the phylogenetic relationships of the angiosperm groups sampled, as the *A. trichopoda CLV1* homolog clusters with the sampled genes from basal eudicots,

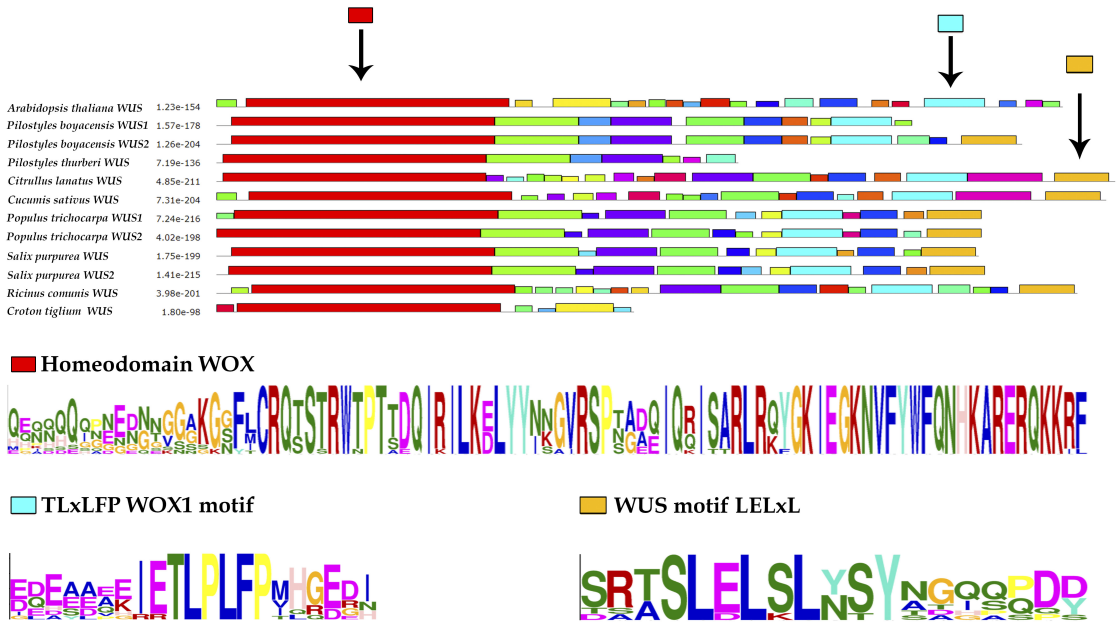

FIGURE 3 | MEME analysis of WUSCHEL proteins of *A. thaliana*, Apodanthaceae, Cucurbitaceae, Salicaceae, and Euphorbiaceae.

and asterid homologs separate from rosid genes (**Supplementary Figure S5**). The *CLV1* representatives from Brassicaceae, Cucurbitaceae, Euphorbiaceae, Fabaceae, Linaceae, Malvaceae, and Salicaceae form well-supported clades (**Supplementary Figure S5**). Local duplications of *CLV1* were detected in the host *Dalea cuatrecasasii*, as well as in *Gossypium raimondii, Kalanchoe laxiflora*, *Linum usitatissimum, Prunus persica*, and Salicaceae.

The clade formed by *BAM3* and *BAM3*-like was retrieved in both analyses (BS/PP, 67/1). The *BAM3*-like subclade includes sequences from *Amborella trichopoda*, representative monocots (*Musa acuminata*) and basal eudicots (Ranunculales; **Supplementary Figure S5**). Asterid and rosid homologs form two separate clades; within the latter, we recovered five variants from the PbE + D transcriptome assigned using BLAST to *Dalea cuatrecasasii* (**Supplementary Figure S5**). The *BAM3* phylogenetic reconstruction mirrors the taxonomic relationships among the angiosperm groups sampled (**Supplementary Figure S5**). The *BAM3* subclade recovers family-level duplications in Fabaceae and Salicaceae, as well as species-specific duplications in *Atropa belladonna, Brassica rapa*, *D. cuatrecasasii*, and *Linum usitatissimum* (**Supplementary Figure S5**).

The ML reconstruction of *BAM1*/2 genes includes sampling from gymnosperms and angiosperms, and like in previous analyses, it is consistent to the phylogenetic relationships of the taxa sampled, with the exception of the position of the monocot genes close to *Eucalyptus grandis* (Myrtaceae) sequences (**Figure 5**). Within eudicots, most asterid genes cluster together (BS/PP, 97/0.94). Family-level duplications are recovered in Apodanthaceae (BAM1/2), Brassicaceae (BAM1/2), Linaceae, Papaveraceae, and Poaceae. Species-specific duplications were detected in *Amaranthus hypochondriacus*, *Begonia* sp., *Chenopodium quinoa, Cladrastis lutea, Cucurbita maxima, Digitalis purpurea, Gossypium raimondii, Linum usitatissimum*, *L. perenne*, *Lonicera japonica, Medicago truncatula, Orobanche fasciculata*, and *Staphylea trifolia* (**Supplementary Figure S5**). Species from Salicaceae and Euphorbiaceae show only one copy of *BAM1/2* (**Supplementary Figure S5**). Apodanthaceae homologs are sisters to gene representatives from Salicaceae, Euphorbiaceae, and Linaceae, but support values are low (BS/PP, 35/0.67, **Supplementary Figure S5**). *BAM1/2* homologs from *P. boyacensis* clustered together with those from *P. thurberi* (BS/PP, 100/1, **Figure 5**).

The MEME analysis for selected sequences within the *BAM1*/2 gene clade detected four leucine-rich regions, two of which were identified using Pfam as LRR4 and LRR8 (both corresponding to the extracellular domain). Additionally, two motifs matched the kinase domains (corresponding to the cytoplasmic domain). The *P. boyacensis PiboBAM1_2*, *PiboBAM2_2*, *PiboBAM2_3* from PbFr, and the *C. sativus CusaBAM1.1* variants lack half of the protein kinase domain (**Supplementary Figure S6**; **Table 2**). Nevertheless, *PiboBAM1_1* isolated from PbE + D, and *PiboBAM2_1*identified in the PbFl transcriptome, as well as *CusaBAM1.2*, exhibit complete domains (**Supplementary Figure S6**; **Table 2**). No motifs exclusive for Apodanthaceae, Cucurbitaceae, or Cucurbitales were found.

The *AUXIN RESPONSE FACTOR 7* Gene Family

The phylogenetic reconstruction of the ARF5/7/19 gene lineages recovers five clades corresponding to *ARF7-A* (BS/PP, 99/1), *ARF7-B* (BS/PP, 61/0.99), *ARF5* (BS/PP, 68/0.88), *ARF7/19-D* (BS/PP, 97/1), and *ARF7-E* (BS/PP, 92/1,

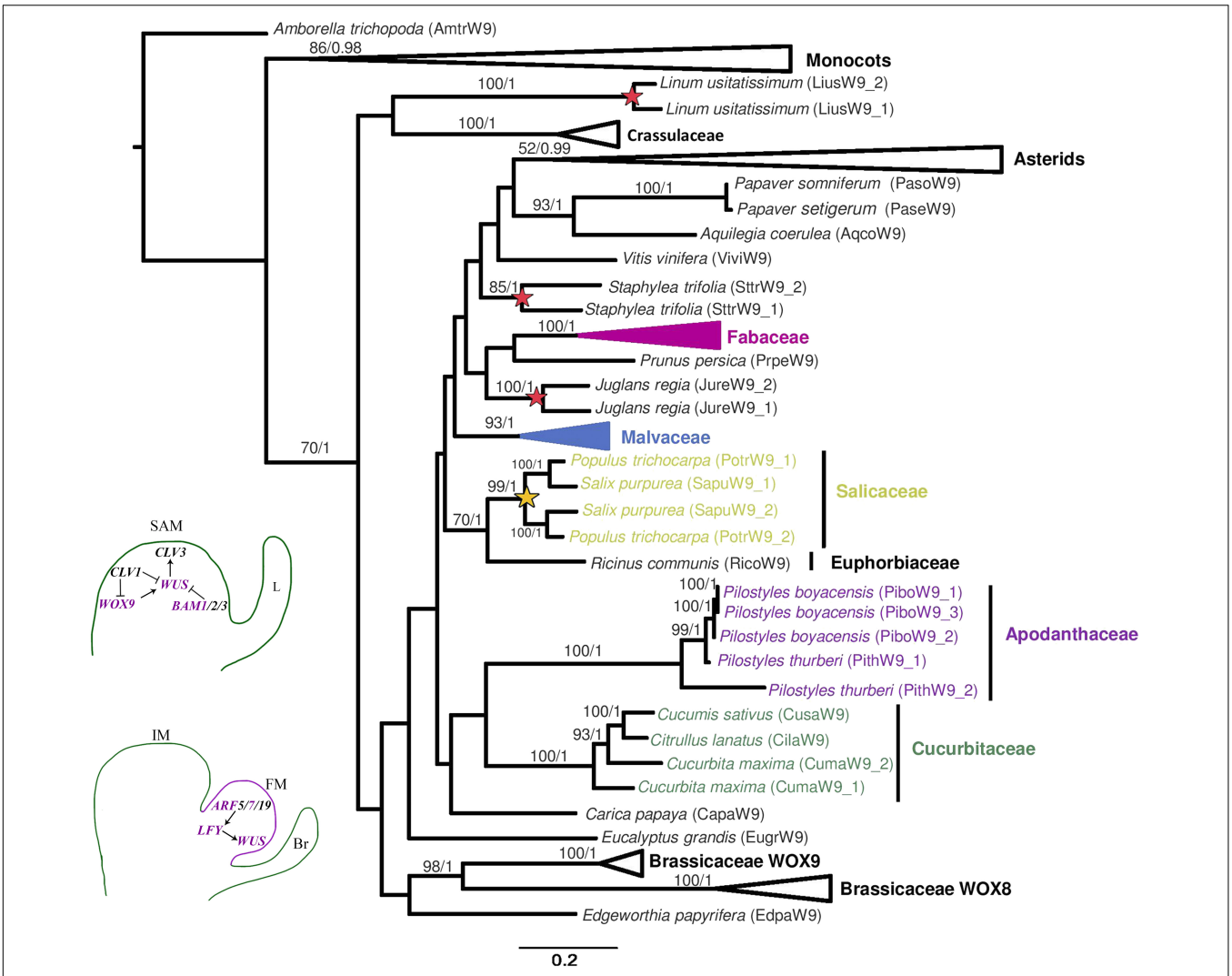

FIGURE 4 | Maximum likelihood reconstruction of the *WUSCHEL-HOMEOBOX 9* gene lineage. Bootstrap values >50 and posterior probability are shown above the nodes. Yellow stars and red stars indicate family-level and species-specific duplication events, respectively. Schemes in the bottom left follow the conventions in **Figure 2**.

Figure 6). The *Amborella trichopoda* and the *Austrobaileya scandens* homologs are found in four and three of the five clades, respectively (**Supplementary Figure S7**). This suggests that duplications occurred before the radiation of all angiosperms. Both *ARF7-A* and *ARF7-B* gene phylogenies are consistent with the phylogenetic relationships of the taxa sampled. Within *ARF7-A* no family-level duplications are detected. Only species-specific duplications are found in *Argemone mexicana, Linum perenne*, *Orobanche fasciculata*, *Papaver somniferum*, and *Papaver setigerum* (**Supplementary Figure S7**).

Within *ARF7-B* a large-scale duplication likely occurred in core eudicots because there are two clades recovered containing asterid and rosid (Salicaceae and Malvaceae) representatives. However, one of the two clades also includes homologs from Brassicaceae, Fabaceae, and Cucurbitaceae. In addition, species-specific duplications are found in *Argemone mexicana, Austrobaileya scandens, Castanea pumila, Gossypium raymondii, Lonicera japonica*, *Musa acuminata, Orobanche fasciculata, Papaver setigerum*, and *Papaver somniferum* (**Supplementary Figure S7**).

The *ARF5* clade has remained largely as a single copy, with no large-scale or family-level duplications (**Supplementary Figure S7**). Thus, well-supported gene clades are recovered for the *ARF5* homologs in Amaranthaceae, Brassicaceae, Euphorbiaceae, Fabaceae, Linaceae, Malvaceae, Orobanchaceae, Papaveraceae, Poaceae, Salicaceae, and Solanaceae (**Supplementary Figure S7**). Species-specific duplications are found only in *Amaranthus hypochondriacus, Conopholis americana, Gossypium raimondii, Mimulus guttatus, Musa acuminata*, and *Orobanche fasciculata* (**Supplementary Figure S7**).

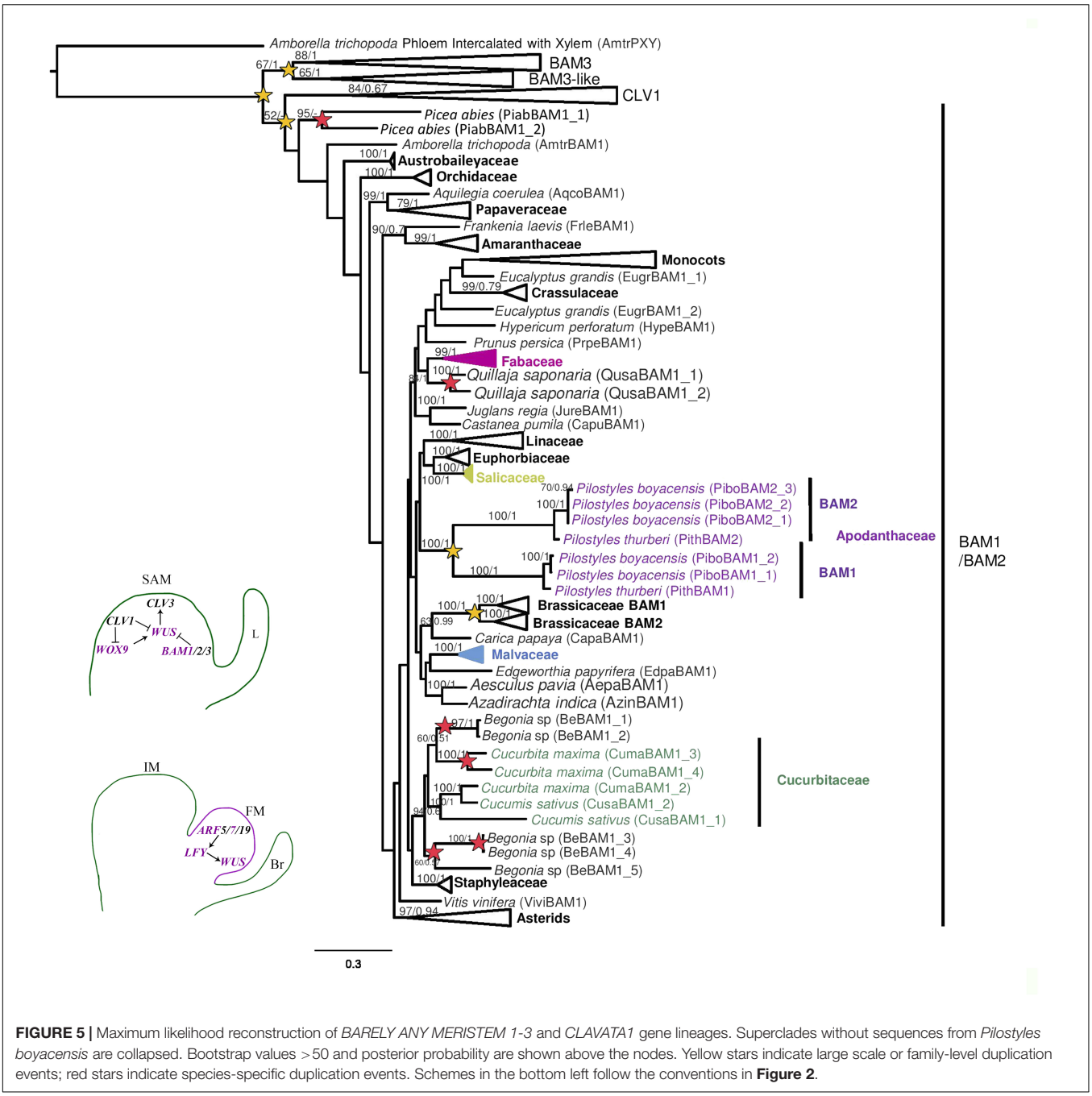

FIGURE 5 | Maximum likelihood reconstruction of *BARELY ANY MERISTEM 1-3* and *CLAVATA1* gene lineages. Superclades without sequences from *Pilostyles boyacensis* are collapsed. Bootstrap values >50 and posterior probability are shown above the nodes. Yellow stars indicate large scale or family-level duplication events; red stars indicate species-specific duplication events. Schemes in the bottom left follow the conventions in **Figure 2**.

In the *ARF7-D* clade, two family-level duplications can be detected, one in the Brassicaceae resulting in the *ARF7* and *ARF19* subclades and a second one within Fabaceae. The remaining *ARF7-D* homologs are retained as single copy except in *Amaranthus hypochondriacus, Argemone mexicana, Atropa belladonna, Castanea pumila, Edgeworthia papyrifera, Gossypium raimondi, Hypericum perforatum, Juglans regia, Linum perenne, Mimulus guttatus,* and *Papaver somniferum* (**Supplementary Figure S7**).

Finally, in the *ARF7-E* clade, family-level duplications were detected in Poaceae and Solanaceae, but most other homologs remain as single copy. Species-specific duplications were found in *Argemone mexicana, Conopholis americana, Hypericum perforatum, Linum perenne, L. usitatissimum, Musa acuminata, Papaver setigerum, P. somniferum, Salix purpurea*, and *Staphylea trifolia* (**Supplementary Figure S7**). In this clade, four variants were isolated from *Pilostyles boyacensis*. *PiboARF7*_2 was found in all three transcriptomes (PbE + D, PbFl, and PbFr), while the variant *PiboARF7*_1 is only found in the PbFl transcriptome, and variants *PiboARF7*_3 and *PiboARF7*_4 were isolated from the PbFr transcriptome. The four *P. boyacensis* and the

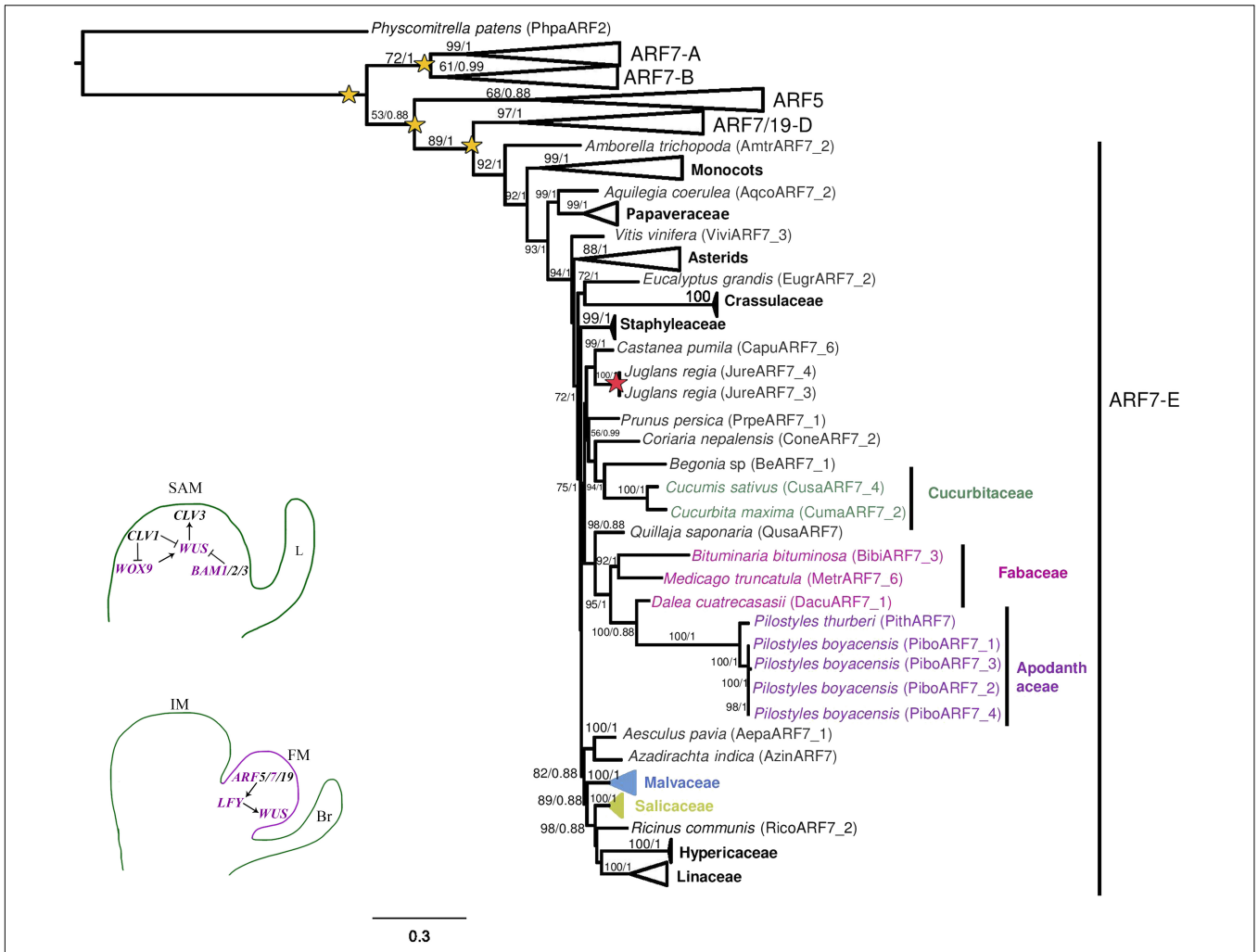

FIGURE 6 | Maximum likelihood reconstruction of the *AUXIN RESPONSE FACTOR 5/7/19* gene lineage. Superclades without sequences from *Pilostyles boyacensis* are collapsed. Bootstrap values >50 and posterior probability are shown above the nodes. Yellow stars indicate large scale or family-level duplication events; red stars indicate species-specific duplication events. Schemes in the bottom left follow the conventions in **Figure 2**.

single *P. thurberi* homologs clustered together (BS/PP, 100/1). The BLASTN comparison showed a similarity percentage of 78% and coverage of 55–74% with homologs from Euphorbiaceae and Salicaceae. Additionally, an *ARF7* homolog isolated from the PbE + D transcriptome, showing an identity of 85% and coverage of 98% with other species of Fabaceae, was assigned here to the host *D. cuatrecasasii* and labeled as *DacuARF7_1* (**Figure 6** and **Supplementary Figure S7**).

The MEME analysis detected the N-terminal B3 DNA binding and the Auxin response factor domains, as well as the C-terminal AUX/IAA domain (with III-IV motifs) and two motifs with QSL-rich regions (**Supplementary Figure S8**). *Pilostyles* proteins present all of these domains, except for one of two QSL-rich regions (**Supplementary Figure S8**, purple domain; **Table 2**). No motifs were found to be exclusive for Apodanthaceae, Cucurbitaceae, or Fabaceae proteins.

The *LEAFY* Gene Family

Finally, the phylogenetic reconstruction of *LEAFY* genes showed that they are retained as single copy in most species, except in *Brassica rapa, Cladrastis lutea, Cucurbita maxima, Kalanchoe laxiflora, Linum perenne, L. usitatissimum*, and *Zea mays* (**Figure 7** and **Supplementary Figure S9**). Three different variants were isolated from *Pilostyles boyacensis*. *PiboLFY1* and *PiboLFY2* were found in the PbFl and PbFr transcriptomes, whereas *PiboLFY3* was detected only in the PbE + D transcriptome. *PiboLFY2* has an additional exon of 135 nt in comparison to *PiboLFY1*. *PiboLFY3* is a partial sequence that differs in two nucleotides located in the 5′UTR (**Supplementary Figure S10**).

The *LFY* variants from *Pilostyles boyacensis* cluster with the single copy found in *P. thurberi* (*PithLFY*, BS/PP, 100/1, **Figure 7**). Interestingly, the ML analysis shows *Pilostyles* homologs as closely related to Euphorbiaceae and Salicaceae genes (BS:38, **Supplementary Figure S9**), whereas in the BI

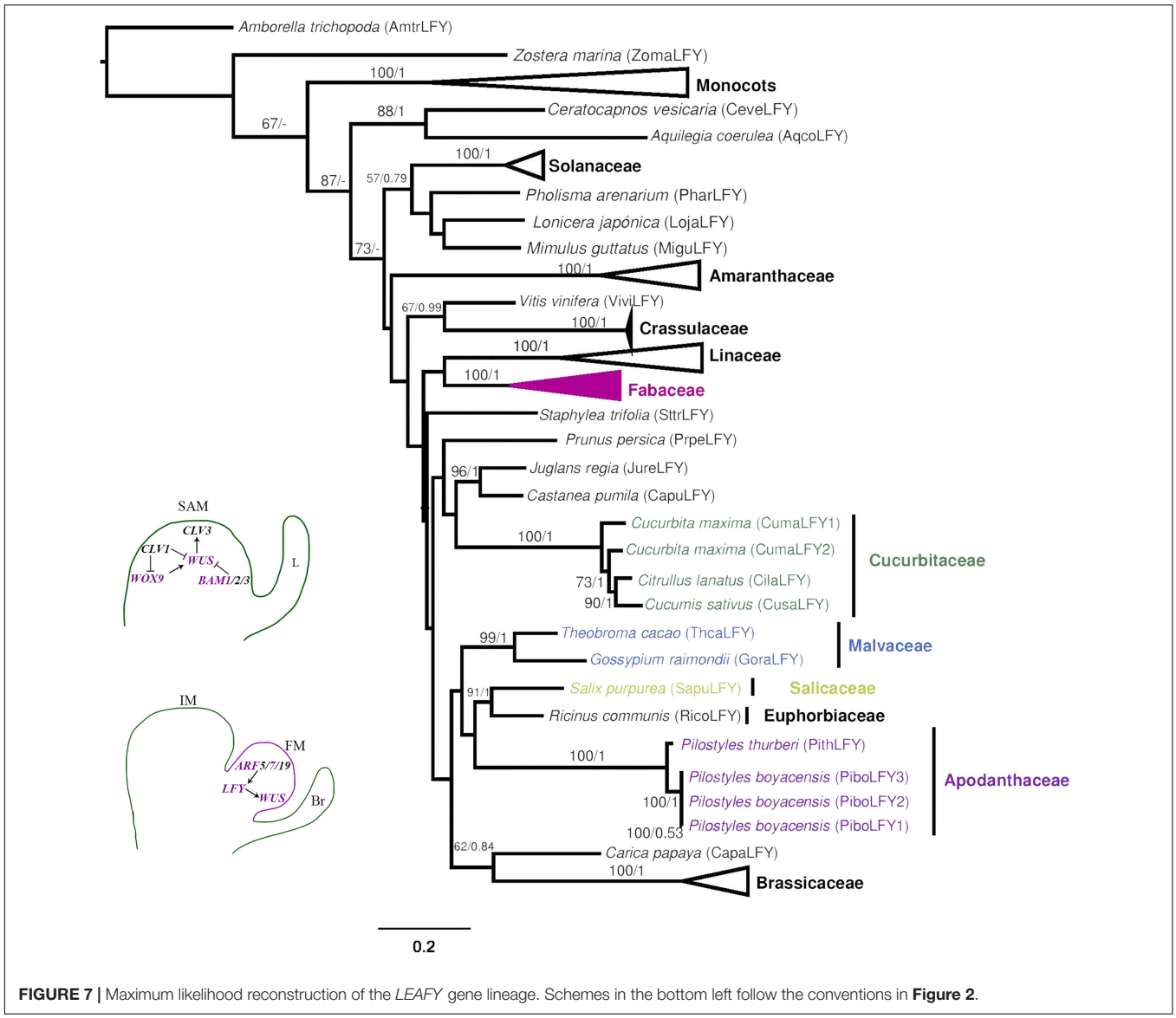

FIGURE 7 | Maximum likelihood reconstruction of the *LEAFY* gene lineage. Schemes in the bottom left follow the conventions in **Figure 2**.

analysis, they cluster with Cucurbitaceae homologs (PP: 0.78, **Supplementary Figure S9**). The MEME analysis detects the highly conserved N-terminal Floricaula/Leafy protein SAM domain and the C-terminal DNA Binding Domain Leafy/F. Additionally, an N-terminal LPPP and a GLSEE motif were detected in the full and the reduced datasets (**Supplementary Figure 10**). Sequences from *Pilostyles* showed all of these domains and motifs, except for the variant *PiboLFY3*, which is an incomplete CDS (**Table 2**). No motifs are exclusive for Apodanthaceae or Cucurbitales sequences.

DISCUSSION

Unlike the typical vegetative SAM to IM to FM developmental sequence that occurs in most angiosperms including Arabidopsis (Ó'Maoiléidigh et al., 2014), the transit to FMs in *Pilostyles* takes place directly from non-specialized endophytic tissue without recognizable vegetative or IMs (Amaral, 2007; González and Pabón-Mora, 2017). Five out of the 11 *A. thaliana* canonical gene families responsible for SAM maintenance and floral fate determinacy targeted in this study were found in *Pilostyles boyacensis*.

The *WUSCHEL* and *WUSCHEL*-Related Homeobox 9 Gene Subfamilies

The *WUSCHEL-related* homologs are represented in *Pilostyles boyacensis* by *PiboWUS*, and *PiboWOX9*. *WOX9* homologs have key roles in early embryo patterning, as well as pluripotency and cell proliferation in the SAM across seed plants (Haecker et al., 2004; Nardmann et al., 2007; Palovaara et al., 2010; Skylar et al., 2010; Zhou et al., 2018). In addition, *WOX9* homologs also play roles in inflorescence architecture and floral identity in petunia and tomato as well as in carpel development in *Arabidopsis*, and possibly in sex determination

in *Cucumis* (Wu et al., 2005; Rebocho et al., 2008; Costanzo et al., 2014; Pawełkowicz et al., 2019). *PiboWOX9* transcripts were found in all three transcriptomes including both early and late developmental stages. Based on the putative roles previously identified in model taxa, we hypothesize that *PiboWOX9* variants have pleiotropic roles in inflorescence architecture, floral identity, carpel development, and perhaps sex determination because they were found in the PbE + D and PbFl transcriptomes. Additionally, *PiboW9_2* could be involved in early embryo patterning because it was found in the PbFr transcriptome. Finally, because their protein sequences have a complete N-terminal motif MASSN and two C-terminal motifs VFIN and LQxG WOX8 (Deveaux et al., 2008; Palovaara et al., 2010), at least the PiboWOX9_2 and PiboWOX9_3 isoforms are fully functional.

PiboWUS variants were isolated exclusively from the PbFl transcriptome. Most *WUS* homologs functionally analyzed control stem cell maintenance in the SAM, the RAM, and the FMs (Laux et al., 1996). Additionally, *WUS* genes are involved in embryo patterning, leaf, perianth, anther, and ovule development (van der Graaff et al., 2009; Tsuda and Hake, 2016; Wu et al., 2019). At least PiboWUS_2 contains the TLxLFP WUS-box and the EAR-like LELxL motif; the latter is crucial in stem cell maintenance because it mediates the repression of target genes (Kieffer et al., 2006; Tsuda and Hake, 2016). Considering that SAMs in *P. boyacensis* are lacking and that *PiboWUS* homologs were not found in the PbE + D or the PbFr transcriptomes, we hypothesize that their functions are restricted to the stem cell maintenance in FMs and perhaps in anther and ovule development.

The LEUCINE-RICH REPEAT RECEPTOR-LIKE KINASE IX—A Subfamily

The LRR-RLK-IX, a subfamily in *Pilostyles*, is represented by *BAM1/2* homologs while *CLAVATA1* homologs are absent. Two copies of *BAM1/2* homologs were detected in each of the two species of *Pilostyles* sampled. The copies are found in different transcriptomes, with *PiboBAM1* active in PbE + D and PbFr, and *PiboBAM2* active in PbFl and PbFr. At least one variant of each copy conserves the extracellular leucine-rich repeat domain, necessary for detection of CLE ligands, as well as the cytoplasmic kinase domains in charge of phosphorylation of target proteins (**Supplementary Figure S6**; Hazak and Hardtke, 2016; Wu et al., 2018).

Four different functions have been assigned to *CLV1*/*BAM* genes in *A. thaliana*. The first is related to the role of *CLV3,* which binds *CLV1/2* to repress *WUSCHEL* related genes in the SAM in order to control cell differentiation and organogenesis (Fletcher, 1999; DeYoung et al., 2006; DeYoung and Clark, 2008; Hazak and Hardtke, 2016; Pan et al., 2016). *CLV1* is reinforced by *BAM* homologs as they sequester CLE ligands secreted in the periphery, resulting in the maintenance of pluripotency in the meristematic field (DeYoung and Clark, 2008). The second, involves *BAM1* in the quiescent center of the RAM restricting cell proliferation (DeYoung et al., 2006). The third role involves *BAM1/2* in the sporogenous cell fate in the anthers and in ovule development (DeYoung et al., 2006; Li et al., 2016). The fourth role is the control of vascular development in roots, shoots, and leaves by *BAM3* (Hazak and Hardtke, 2016).

BAM1/2 transcripts from PbFr lack the kinase domain and have premature stop codons (**Table 2** and **Supplementary Figure S6**). It is likely that such incomplete proteins no longer play a role in early embryogenesis, including putative plumule and radicle differentiation. This is further supported by the fact that *CLV1* homologs were not found in any of the *Pilostyles* transcriptomes, and members of the CLE family (*CLV3*) identified were assigned by similarity to the host *Dalea cuatrecasasii*. The isolation of complete BAM1/2 proteins from the PbE + D and the PbFr transcriptomes strongly suggests that the primary role of *BAM1/2* in *Pilostyles* is restricted to anther and ovule development. Nonetheless, a secondary role related to the vascular development of the floral extensor in *Pilostyles* (Amaral, 2007; González and Pabón-Mora, 2017) cannot be ruled out.

The AUXIN RESPONSE FACTOR 5/7/19 Subclade

The *ARF5/7/19* subclade in *Pilostyles* is represented only by *ARF7E* orthologs. Specifically, *PiboARF7E_2* was found in all three transcriptomes, whereas *PiboARF7E_1* was detected only in the PbFl, and *PiboARF7E_3*, *PiboARF7E_4* were found only in the PbFr transcriptome. Transcripts from *Pilostyles* (except *PiboARFE7_1*) carry intact DNA binding domains as well as AUX/IAA and auxin response factor domains. However, only one out of the two characteristic QSL-rich regions is present in all *Pilostyles* ARF7E proteins. Both, the AUX/IAA domain and the QSL region have been involved in dimerization with other ARFs (Korasick et al., 2014; Chandler, 2016). Thus, sequence analyses indicate that at least three isoforms of *PiboARF7* are fully functional. Nevertheless, the lack of *ARF7E* orthologs in *A. thaliana* hinders a direct functional comparison with *Pilostyles* homologs. Other *ARF5/7/19* are known to play redundant roles in lateral root formation, shoot regeneration, leaf polarity and expansion, FM determination, fertilization, fruit development, senescence, and organ abscission (Chandler, 2016). Altogether, our data suggests that the most likely functions of the *PiboARF7* homologs include FM determination, fertilization, and fruit development. It is possible that *PiboARF7E* genes are taking on the function of *ARF5* in activating *LFY*.

The *LEAFY* Gene Family

LFY homologs in *Pilostyles* species are present as single copy genes, even though in *P. boyacensis* three variants were isolated. *PiboLFY1* and *PiboLFY2* are present in the PbFl and PbFr transcriptomes, while *PiboLFY3* is active in the PbE + D transcriptome. The canonical C-terminal DNA binding and N-terminal FLORICAULA/LEAFY domains reported for *LFY* (Maizel et al., 2005) are conserved in two of the three *PiboLFY* variants, suggesting that they are functional. *LFY* is an indirect

target of *FLOWERING LOCUS T* (*FT*), the florigen, and is a master regulator of FM fate because it represses IM identity and promotes floral organ identity genes (Moyroud et al., 2010). Our results point to conserved roles of *PiboLFY* genes in establishing FM identity and perhaps together with other cofactors activating floral organ identity in *Pilostyles*.

CONCLUSION

The endoparasitic lifestyle of Apodanthaceae is accompanied by a direct transition from a highly reduced endophyte to FMs. We used comparative transcriptomics from three developmental stages of *Pilostyles boyacensis* with and without the host tissues to investigate the genetic regulatory networks involved in SAM and FM identity and maintenance. Eleven canonical gene families responsible for SAM maintenance and floral fate determinacy were targeted in this study. Only five of them were found in *Pilostyles*, namely *ARF7, BAM1, LFY, WOX9*, and *WUS*. No orthologs of *ARF5, ARF19, BAM2, BAM3, CLV1,* or *CLV3* were found. The lack of SAMs and leaves seems to correlate with reductions in the number of genes for the most important gene families controlling the fine-tuning between pluripotency and organogenesis during vegetative growth. Most genes retained are likely to be functioning in establishing reproductive transition and FM fate, as well as early embryogenesis. We provide the first comprehensive comparative platform to assess meristematic activity in the reduced vegetative parts of an endo-holoparasitic plant.

DATA AVAILABILITY STATEMENT

The datasets presented in this study can be found in online repositories. The names of the repository/repositories and accession number(s) can be found below: NCBI GenBank under accession numbers MN946521–MN946537. Alignments used are in **Supplementary Material S11**.

AUTHOR CONTRIBUTIONS

AG, NP-M, and FG conceived and designed the research and performed field and lab procedures, as well as gene evolution analyses. JA performed the assembly and BLAST analyses. All authors wrote, revised, and approved the submitted version.

FUNDING

This project was supported by the Universidad Nacional de Colombia, Vicerrectoría de Investigaciones through the Convocatoria Nacional de Proyectos para el Fortalecimiento de la Investigación, Creación e Innovación de la Universidad Nacional De Colombia 2016–2018, project number 37247, and by Universidad de Antioquia, Estrategia de Sostenibilidad 2018–2019 and Convocatoria Programáticas 2017-16302 grants.

ACKNOWLEDGMENTS

We thank the students Sebastián Guzmán and Paola Piñeros (Universidad Nacional de Colombia) for field work support. We also thank Sebastian González (Massachusetts College of Art and Design) for taking the photographs in **Figure 1**. Preliminary results from this research were presented in the IX Latin American Society for Developmental Biology Meeting (Medellín, Colombia, 2017).

SUPPLEMENTARY MATERIAL

The Supplementary Material for this article can be found online at: https://www.frontiersin.org/articles/10.3389/fevo.2020.00209/full#supplementary-material

REFERENCES

Afgan, E., Baker, D., Batut, B., van den Beek, M., Bouvier, D., Čech, M., et al. (2018). The Galaxy platform for accessible, reproducible and collaborative biomedical analyses: 2018 update. *Nucleic Acids Res.* 46, W537–W544. doi: 10.1093/nar/gky379

Amaral, M. M. (2007). *A estrutura da angiosperma endoparasita Pilostyles ulei (Apodanthaceae): Interface e impacto no lenho de Mimosa spp*. Available online at: http://www.teses.usp.br/teses/disponiveis/41/41132/tde-05112007-095018/ (accessed March 11, 2017).

Amaral, M. M., and Ceccantini, G. (2011). The endoparasite *Pilostyles ulei* (Apodanthaceae – Cucurbitales) influences wood structure in three host species of Mimosa. *IAWA J.* 32, 1–13. doi: 10.1163/22941932-90000038

Arias-Agudelo, L. M., González, F., Isaza, J. P., Alzate, J. F., and Pabón-Mora, N. (2019). Plastome reduction and gene content in New World *Pilostyles* (Apodanthaceae) unveils high similarities to African and Australian congeners. *Mol. Phylogenet. Evol.* 135, 193–202. doi: 10.1016/j.ympev.2019.03.014

Bellot, S., and Renner, S. S. (2014). The systematics of the worldwide endoparasite family Apodanthaceae (Cucurbitales), with a key, a map, and color photos of most species. *PhytoKeys* 36, 41–57. doi: 10.3897/phytokeys.36.7385

Blarer, A., Nickrent, D. L., and Endress, P. K. (2004). Comparative floral structure and systematics in Apodanthaceae (Rafflesiales). *Plant Syst. Evol.* 245, 119–142. doi: 10.1007/s00606-003-0090-2

Brasil, B. D. A. (2010). *Ciclo de Vida, Fenologia e Anatomia Floral de Pilostyles (Apodanthaceae - Rafflesiaceae s.l.): Subsídios Para um Posicionamento Filogenético da Família Apodanthaceae*. Available online at: http://www.teses.usp.br/teses/disponiveis/41/41132/tde-10122010-105707/ (accessed March 11, 2017).

Bryan, A. C., Obaidi, A., Wierzba, M., and Tax, F. E. (2012). XYLEM INTERMIXED WITH PHLOEM1, a leucine-rich repeat receptor-like kinase required for stem growth and vascular development in *Arabidopsis thaliana*. *Planta* 235, 111–122. doi: 10.1007/s00425-011-1489-6

Chandler, J. W. (2016). Auxin response factors. *Plant Cell Environ.* 39, 1014–1028. doi: 10.1111/pce.12662

Chandler, J. W., and Werr, W. (2015). Cytokinin–auxin crosstalk in cell type specification. *Trends Plant Sci.* 20, 291–300. doi: 10.1016/j.tplants.2015.02.003

Costanzo, E., Trehin, C., and Vandenbussche, M. (2014). The role of WOX genes in flower development. *Ann. Bot.* 114, 1545–1553. doi: 10.1093/aob/mcu123

Darriba, D., Posada, D., Kozlov, A. M., Stamatakis, A., Morel, B., and Flouri, T. (2019). ModelTest-NG: a new and scalable tool for the selection of DNA and protein evolutionary models. *Mol. Biol. Evol.* 37, 291–294. doi: 10.1093/molbev/msz189

Denay, G., Chahtane, H., Tichtinsky, G., and Parcy, F. (2017). A flower is born: an update on *Arabidopsis* floral meristem formation. *Curr. Opin. Plant Biol.* 35, 15–22. doi: 10.1016/j.pbi.2016.09.003

Deveaux, Y., Toffano-Nioche, C., Claisse, G., Thareau, V., Morin, H., Laufs, P., et al. (2008). Genes of the most conserved WOX clade in plants affect root and flower development in *Arabidopsis*. *BMC Evol. Biol.* 8:291. doi: 10.1186/1471-2148-8-291

DeYoung, B. J., Bickle, K. L., Schrage, K. J., Muskett, P., Patel, K., and Clark, S. E. (2006). The CLAVATA1-related BAM1, BAM2 and BAM3 receptor kinase-like proteins are required for meristem function in *Arabidopsis*: BAM receptor kinases regulate meristem function. *Plant J.* 45, 1–16. doi: 10.1111/j.1365-313X.2005.02592.x

DeYoung, B. J., and Clark, S. E. (2008). BAM receptors regulate stem cell specification and organ development through complex interactions with CLAVATA signaling. *Genetics* 180, 895–904. doi: 10.1534/genetics.108.091108

Finet, C., Berne-Dedieu, A., Scutt, C. P., and Marlétaz, F. (2013). Evolution of the ARF gene family in land plants: old domains, new tricks. *Mol. Biol. Evol.* 30, 45–56. doi: 10.1093/molbev/mss220

Fletcher, J. C. (1999). Signaling of cell fate decisions by CLAVATA3 in *Arabidopsis* shoot meristems. *Science* 283, 1911–1914. doi: 10.1126/science.283.5409.1911

Gaillochet, C., and Lohmann, J. U. (2015). The never-ending story: from pluripotency to plant developmental plasticity. *Development* 142, 2237–2249. doi: 10.1242/dev.117614

González, F., and Pabón-Mora, N. (2014a). First reports and generic descriptions of the achlorophyllous holoparasites Apodanthaceae (Cucurbitales) of Colombia. *Actualidades Biol.* 36, 123–135.

González, F., and Pabón-Mora, N. (2014b). *Pilostyles boyacensis* a new species of Apodanthaceae (Cucurbitales) from Colombia. *Phytotaxa* 178:138. doi: 10.11646/phytotaxa.178.2.5

González, F., and Pabón-Mora, N. (2017). Floral development and morphoanatomy in the holoparasitic *Pilostyles boyacensis* (Apodanthaceae, Cucurbitales) reveal chimeric half-staminate and half-carpellate flowers. *Int. J. Plant Sci.* 178, 522–536. doi: 10.1086/692505

Goodstein, D. M., Shu, S., Howson, R., Neupane, R., Hayes, R. D., Fazo, J., et al. (2012). Phytozome: a comparative platform for green plant genomics. *Nucleic Acids Res.* 40, D1178–D1186. doi: 10.1093/nar/gkr944

Grabherr, M. G., Haas, B. J., Yassour, M., Levin, J. Z., Thompson, D. A., Amit, I., et al. (2011). Full-length transcriptome assembly from RNA-Seq data without a reference genome. *Nat. Biotechnol.* 29, 644–652. doi: 10.1038/nbt.1883

Ha, C. M., Jun, J. H., and Fletcher, J. C. (2010). "Chapter Four - Shoot Apical Meristem Form and Function," in *Current Topics in Developmental Biology Plant Development*, ed. M. C. P. Timmermans (Cambridge, MA: Academic Press), 103–140. doi: 10.1016/s0070-2153(10)91004-1

Haecker, A., Gross-Hardt, R., Geiges, B., Sarkar, A., Breuninger, H., Herrmann, M., et al. (2004). Expression dynamics of WOX genes mark cell fate decisions during early embryonic patterning in *Arabidopsis thaliana*. *Development* 131, 657–668. doi: 10.1242/dev.00963

Hall, T. A. (1999). BioEdit: a user-friendly biological sequence alignment editor and analysis program for Windows 95/98/NT. *Nucleic Acids Symp. Ser.* 41, 95–98.

Hardtke, C. S., Ckurshumova, W., Vidaurre, D. P., Singh, S. A., Stamatiou, G., Tiwari, S. B., et al. (2004). Overlapping and non-redundant functions of the *Arabidopsis* auxin response factors MONOPTEROS and NONPHOTOTROPIC HYPOCOTYL 4. *Development* 131, 1089–1100. doi: 10.1242/dev.00925

Hazak, O., and Hardtke, C. S. (2016). CLAVATA 1-type receptors in plant development. *EXBOTJ* 67, 4827–4833. doi: 10.1093/jxb/erw247

Heide-Jørgensen, H. (2008). *Parasitic Flowering Plants*. Boston: Brill.

Katoh, K., and Standley, D. M. (2013). MAFFT multiple sequence alignment software version 7: improvements in performance and usability. *Mol. Biol. Evol.* 30, 772–780. doi: 10.1093/molbev/mst010

Kieffer, M., Stern, Y., Cook, H., Clerici, E., Maulbetsch, C., Laux, T., et al. (2006). Analysis of the transcription factor WUSCHEL and its functional homologue in *Antirrhinum* reveals a potential mechanism for their roles in meristem maintenance. *Plant Cell* 18, 560–573. doi: 10.1105/tpc.105.039107

Korasick, D. A., Westfall, C. S., Lee, S. G., Nanao, M. H., Dumas, R., Hagen, G., et al. (2014). Molecular basis for AUXIN RESPONSE FACTOR protein interaction and the control of auxin response repression. *Proc. Natl. Acad. Sci. U.S.A.* 111, 5427–5432. doi: 10.1073/pnas.1400074111

Laux, T., Mayer, K. F., Berger, J., and Jürgens, G. (1996). The WUSCHEL gene is required for shoot and floral meristem integrity in *Arabidopsis*. *Development* 122, 87–96.

Li, H., Shi, Q., Zhang, Z.-B., Zeng, L.-P., Qi, J., and Ma, H. (2016). Evolution of the leucine-rich repeat receptor-like protein kinase gene family: ancestral copy number and functional divergence of BAM1 and BAM2 in Brassicaceae: evolution of the LRR-RLK gene family. *J. Syt. Evol.* 54, 204–218. doi: 10.1111/jse.12206

Maizel, A., Busch, M. A., Tanahashi, T., Perkovic, J., Kato, M., Hasebe, M., et al. (2005). The floral regulator LEAFY evolves by substitutions in the DNA binding domain. *Science* 308, 260–263. doi: 10.1126/science.1108229

Matasci, N., Hung, L.-H., Yan, Z., Carpenter, E. J., Wickett, N. J., Mirarab, S., et al. (2014). Data access for the 1,000 Plants (1KP) project. *Gigascience* 3:17. doi: 10.1186/2047-217X-3-17

Miller, M. A., Pfeiffer, W., and Schwartz, T. (2010). "Creating the CIPRES Science Gateway for inference of large phylogenetic trees," in *Proceedings of the Gateway Computing Environments Workshop (GCE)*, (New Orleans, LA: IEEE), 1–8.

Moyroud, E., Kusters, E., Monniaux, M., Koes, R., and Parcy, F. (2010). LEAFY blossoms. *Trends Plant Sci.* 15, 346–352. doi: 10.1016/j.tplants.2010.03.007

Nardmann, J., Zimmermann, R., Durantini, D., Kranz, E., and Werr, W. (2007). WOX gene phylogeny in Poaceae: a comparative approach addressing leaf and embryo development. *Mol. Biol. Evol.* 24, 2474–2484. doi: 10.1093/molbev/msm182

Nickrent, D. L. (2020). Parasitic angiosperms: How often and how many? *TAXON* 69, 5–27. doi: 10.1002/tax.12195

Nikolov, L. A., Endress, P. K., Sugumaran, M., Sasirat, S., Vessabutr, S., Kramer, E. M., et al. (2013). Developmental origins of the world's largest flowers, Rafflesiaceae. *PNAS* 110, 18578–18583. doi: 10.1073/pnas.1310356110

Ó'Maoiléidigh, D. S., Graciet, E., and Wellmer, F. (2014). Gene networks controlling *Arabidopsis thaliana* flower development. *New Phytol.* 201, 16–30. doi: 10.1111/nph.12444

Pabón-Mora, N., Ambrose, B. A., and Litt, A. (2012). Poppy APETALA1/FRUITFULL orthologs control flowering time, branching, perianth identity, and fruit development. *Plant Physiol.* 158, 1685–1704. doi: 10.1104/pp.111.192104

Palovaara, J., Hallberg, H., Stasolla, C., and Hakman, I. (2010). Comparative expression pattern analysis of WUSCHEL-related homeobox 2 (WOX2) and WOX8/9 in developing seeds and somatic embryos of the gymnosperm *Picea abies*. *New Phytol.* 188, 122–135. doi: 10.1111/j.1469-8137.2010.03336.x

Pan, L., Lv, S., Yang, N., Lv, Y., Liu, Z., Wu, J., et al. (2016). The multifunction of CLAVATA2 in plant development and immunity. *Front. Plant Sci.* 7:1573. doi: 10.3389/fpls.2016.01573

Pawełkowicz, M., Pryszcz, L., Skarzyńska, A., Wóycicki, R. K., Posyniak, K., Rymuszka, J., et al. (2019). Comparative transcriptome analysis reveals new molecular pathways for cucumber genes related to sex determination. *Plant Reprod.* 32, 193–216. doi: 10.1007/s00497-019-00362-z

Poole, R. L. (2007). The TAIR database. *Methods Mol. Biol.* 406, 179–212. doi: 10.1007/978-1-59745-535-0_8

Rambaut, A. (2006). *FigTree Tree Figure Drawing Toll version 1.3.1. Institute of Evolutionary Biology, University of Edinburgh.* Available online at: http://tree.bio.ed.ac.uk/software/figtree/ (accessed January 31, 2013).

Rebocho, A. B., Bliek, M., Kusters, E., Castel, R., Procissi, A., Roobeek, I., et al. (2008). Role of EVERGREEN in the development of the cymose petunia inflorescence. *Dev. Cell* 15, 437–447. doi: 10.1016/j.devcel.2008.08.007

Ronquist, F., Teslenko, M., van der Mark, P., Ayres, D. L., Darling, A., Höhna, S., et al. (2012). MrBayes 3.2: efficient Bayesian phylogenetic inference and model choice across a large model space. *Syst. Biol.* 61, 539–542. doi: 10.1093/sysbio/sys029

Rutherford, R. J. (1970). The anatomy and cytology of *Pilostyles thurberi* Gray (Rafflesiaceae). *Aliso* 7, 263–288. doi: 10.5642/aliso.19700702.13

Skylar, A., Hong, F., Chory, J., Weigel, D., and Wu, X. (2010). STIMPY mediates cytokinin signaling during shoot meristem establishment in *Arabidopsis* seedlings. *Development* 137, 541–549. doi: 10.1242/dev.041426

Stamatakis, A., Hoover, P., and Rougemont, J. (2008). A rapid bootstrap algorithm for the RAxML web servers. *Syst. Biol.* 57, 758–771. doi: 10.1080/10635150802429642

Taylor-Teeples, M., Lanctot, A., and Nemhauser, J. L. (2016). As above, so below: auxin's role in lateral organ development. *Dev. Biol.* 419, 156–164. doi: 10.1016/j.ydbio.2016.03.020

Tsuda, K., and Hake, S. (2016). "Homeobox transcription factors and the regulation of meristem development and maintenance," in *Plant Transcription Factors*, ed. D. H. Gonzalez (Amsterdam: Elsevier), 215–228. doi: 10.1016/b978-0-12-800854-6.00014-2

van der Graaff, E., Laux, T., and Rensing, S. A. (2009). The WUS homeobox-containing (WOX) protein family. *Genome Biol.* 10:248. doi: 10.1186/gb-2009-10-12-248

Wagner, D., Sablowski, R. W., and Meyerowitz, E. M. (1999). Transcriptional activation of APETALA1 by LEAFY. *Science* 285, 582–584. doi: 10.1126/science.285.5427.582

Wils, C. R., and Kaufmann, K. (2017). Gene-regulatory networks controlling inflorescence and flower development in *Arabidopsis thaliana*. *Biochim. Biophys. Acta Gene Regul. Mech.* 1860, 95–105. doi: 10.1016/j.bbagrm.2016.07.014

Wu, C.-C., Li, F.-W., and Kramer, E. M. (2019). Large-scale phylogenomic analysis suggests three ancient superclades of the WUSCHEL-RELATED HOMEOBOX transcription factor family in plants. *PLoS One* 14:e0223521. doi: 10.1371/journal.pone.0223521

Wu, Q., Xu, F., and Jackson, D. (2018). All together now, a magical mystery tour of the maize shoot meristem. *Curr. Opin. Plant Biol.* 45, 26–35. doi: 10.1016/j.pbi.2018.04.010

Wu, X., Dabi, T., and Weigel, D. (2005). Requirement of homeobox gene STIMPY/WOX9 for *Arabidopsis* meristem growth and maintenance. *Curr. Biol.* 15, 436–440. doi: 10.1016/j.cub.2004.12.079

Yamaguchi, N., Wu, M.-F., Winter, C. M., Berns, M. C., Nole-Wilson, S., Yamaguchi, A., et al. (2013). A molecular framework for auxin-mediated initiation of flower primordia. *Dev. Cell* 24, 271–282. doi: 10.1016/j.devcel.2012.12.017

Zheng, Y., Wu, S., Bai, Y., Sun, H., Jiao, C., Guo, S., et al. (2019). Cucurbit Genomics Database (CuGenDB): a central portal for comparative and functional genomics of cucurbit crops. *Nucleic Acids Res.* 47, D1128–D1136. doi: 10.1093/nar/gky944

Zhou, X., Guo, Y., Zhao, P., and Sun, M. (2018). Comparative analysis of WUSCHEL-related homeobox genes revealed their parent-of-origin and cell type-specific expression pattern during early embryogenesis in tobacco. *Front. Plant Sci.* 9:311. doi: 10.3389/fpls.2018.00311

Conflict of Interest: The authors declare that the research was conducted in the absence of any commercial or financial relationships that could be construed as a potential conflict of interest.

frontiers in Ecology and Evolution

ORIGINAL RESEARCH
published: 04 August 2020
doi: 10.3389/fevo.2020.00253

Divergent Developmental Pathways Among Staminate and Pistillate Flowers of Some Unusual *Croton* (Euphorbiaceae)

*Pakkapol Thaowetsuwan[1,2], Stuart Ritchie[1], Ricarda Riina[3] and Louis Ronse De Craene[1]**

[1] Royal Botanic Garden Edinburgh, Edinburgh, United Kingdom, [2] School of Biological Sciences, Institute of Molecular Plant Science, University of Edinburgh, Edinburgh, United Kingdom, [3] Real Jardín Botánico – Consejo Superior de Investigaciones Cientificas (CSIC), Madrid, Spain

Croton is a mega-diverse genus of more than 1,200 species with great morphological diversity and highly dimorphic flowers. Staminate flowers generally possess petals and a variable number of stamens and lack of an ovary. Pistillate flowers generally lack petals or have filamentous structures instead; stamens are lacking, and the ovary is generally tricarpellate with divided styles. However, well-developed petals can be found in pistillate flowers of some African species and two New World sections, i.e., sect. *Alabamenses* and sect. *Eluteria* subsect. *Eluteria*. Our objectives are to compare ontogeny in dimorphic flowers of *Croton* which may elucidate the origin of petals, homology of the filamentous structures, nectaries, and diversity of the androecium. The development of staminate and pistillate flowers of *C. alabamensis* (sect. *Alabamenses*) and *C. schiedeanus* (sect. *Eluteria*) was studied under the scanning electron microscope (SEM) and compared with *C. chilensis* (sect. *Adenophylli*) which has filamentous structures in pistillate flowers. In staminate flowers, petals develop in alternation with sepals and later the outermost stamen whorl develops opposite to the petals. In a much later stage, nectar glands emerge in alternation with the petals. In pistillate flowers, filamentous structures and petals share the same early development in alternation with the sepals. However, growth of the filamentous structures of *C. chilensis* becomes arrested, while petals of *C. alabamensis* and *C. schiedeanus* develop similar to those of the staminate flowers. The main conclusions of the study are: (1) Petals and filamentous structures are homologous based on their location and shape in early development. (2) Nectaries with variable morphology develop in antesepalous position and probably represent receptacular outgrowths and are not staminodial. (3) Staminate flower development displays an unexpected diversity, including a floral cup in *C. alabamensis*. All investigated species have an unusual centrifugal initiation of the second stamen whorl. (4) The possible evolutionary loss and potential regain of petals among different species of *Croton* is discussed in relation to heterochrony. We suggest that the filamentous structures in pistillate flowers represent pedomorphic forms of petals of staminate flowers, and that the well-developed petals in *C. alabamensis* and *C. schiedeanus* are derived via a developmental reversion.

Keywords: bracteopetal, dimorphism, filamentous structure, heterochrony, nectary, petal reduction, spatial constraints, stamen development

OPEN ACCESS

Edited by:
Alessandro Minelli, University of Padua, Italy

Reviewed by:
Paula Rudall, Royal Botanic Gardens, Kew, United Kingdom
Ana Maria Rocha De Almeida, California State University, East Bay, United States
Vidal De Freitas Mansano, Rio de Janeiro Botanical Garden, Brazil

***Correspondence:**
Louis Ronse De Craene
lronsedecraene@rbge.org.uk

Specialty section:
This article was submitted to Evolutionary Developmental Biology, a section of the journal Frontiers in Ecology and Evolution

Received: *06 January 2020*
Accepted: *13 July 2020*
Published: *04 August 2020*

Citation:
Thaowetsuwan P, Ritchie S, Riina R and Ronse De Craene L (2020) Divergent Developmental Pathways Among Staminate and Pistillate Flowers of Some Unusual Croton (Euphorbiaceae). Front. Ecol. Evol. 8:253. doi: 10.3389/fevo.2020.00253

INTRODUCTION

In flowers, "petal" is a term generally applied to the showy pigmented inner perianth whorl, in contrast to the term "sepal" which represents the protective green outermost perianth whorl. The presence of pigments, delicate texture, single vascular bundle and narrow base are common features found in petals (discussions in Endress, 1994; Ronse De Craene, 2007, 2008). However, it is not always easy to classify the perianth as sepals and petals especially in cases where there is only one perianth whorl present, since this may be a result of reduction of either whorl correlated with a functional change (Ronse De Craene, 2010). Petals play a major role in pollinator attraction via visual cues but sometimes they also facilitate scent dispersal, provide nectar, and function as landing platforms for insects (Endress, 1994; Whitney et al., 2011; Ojeda et al., 2016). The presence of both sepals and petals (biseriate perianth) in flowers is the most common pattern in angiosperms, at least in core eudicots (Ronse De Craene and Brockington, 2013). Evolutionary development genetic studies in the model plants *Arabidopsis* and *Antirrhinum* found that interactions between different gene classes give rise to organ determination in each whorl of the flower (ABCDE model) (Soltis et al., 2009; Litt and Kramer, 2010; Rijpkema et al., 2010). Co-expression of A- and B-class genes is found to determine petal identity in core eudicots (Pentapetalae) (Litt and Kramer, 2010; Rijpkema et al., 2010). However, Ronse De Craene (2007) argued that homology of petals should not be deduced based on gene expression pattern alone, but should include historical, phylogenetic and ontological perspectives. There is evidence that "petals" from different groups of angiosperms may have different origins. A continuous transition in the perianth from bracts to petal-like perianth parts is observed in the ANA grade, many magnoliids (Magnoliales, Laurales) and sometimes in core eudicots (e.g., Cactaceae, *Berberidopsis*, *Paeonia,* and Theaceae), while in some magnoliids and monocots, petals may be derived by pigmenting of the inner tepals (Endress, 2008; Ronse De Craene, 2008; Remizowa et al., 2010). Petals derived from transformation of sterile stamens (staminodes) is also reported in Ranunculales (Kosuge, 1994; Erbar et al., 1998). In the core eudicots, the largest group of angiosperms, the presence of a perianth with clear distinction between sepals and petals is prominent (Ronse De Craene, 2008, 2010; Endress, 2010; Soltis et al., 2018). Two possible origins for petals in core eudicots have been proposed, i.e., andropetals (staminodial origin) or bracteopetals (bracteolar origin) (e.g., Takhtajan, 1991). Andropetals generally have a delayed development and small primordia, contrary to bracteopetals which generally have an early development and broad primordia (Ronse De Craene, 2007, 2008). However, Ronse De Craene (2007) suggested that in core-eudicots andropetals are rare, and petals are mostly derived from bracteopetals.

The family Euphorbiaceae belongs to the order Malpighiales, the largest order of the rosid clade in Pentapetalae (The Angiosperm Phylogeny Group, 2016). The family has great diversity in floral morphology and is well-known for the sophisticated inflorescence-flower pseudanthial complex called cyathium, which is found in the genus *Euphorbia* (Wurdack et al., 2005; Prenner and Rudall, 2007; Horn et al., 2012). However, little is known about the morphology of flowers in the whole family. The presence of petals is generally an uncommon character in the Euphorbiaceae with a scattered distribution in distantly related internal groups (Wurdack et al., 2005). The inaperturate crotonoid clade (subfamily Crotonoideae), comprising about 60 genera, is one group in Euphorbiaceae where the presence of petals – at least in staminate flowers – is a key character in defining its affinity (together with inaperturate pollen grains) (**Figure 2A**; Wurdack et al., 2005; Webster, 2014). The putative sister group of this clade is the articulated crotonoid clade, comprising the economically important rubber tree (*Hevea*) and cassava (*Manihot*), which does not have petals but has petaloid tepals instead (**Figure 2A**; Wurdack et al., 2005). So far, no developmental study has been conducted to investigate the origin of petals and their evolution in the inaperturate crotonoid clade, whether they represent the basic condition of bracteopetals or are secondarily derived andropetals.

Croton is a mega-diverse genus of more than 1,200 recognized species with a broad tropical to sub-tropical worldwide distribution in various habitats (Webster, 1993; Govaerts et al., 2000; Berry et al., 2005; van Ee et al., 2011, 2015). Its large size, high morphological variation and wide distribution create great difficulties for taxonomic studies (van Ee et al., 2011). At present, four subgenera of *Croton*, i.e., subg. *Quadrilobi* (Müll. Arg.) Pax in Engl. & Prantl, subg. *Adenophylli* (Griseb.) Riina, subg. *Croton* L. and subg. *Geiseleria* A. Gray., are recognized based on the molecular phylogeny (**Figure 2B**; van Ee et al., 2011, 2015). *Croton* species from African, Asian and Australian lineages belong to the subgenus *Croton*, while other neotropical species belong to the other three subgenera (Berry et al., 2005; van Ee et al., 2011, 2015; Haber et al., 2017). Flowers of *Croton* are unisexual with both genders usually borne on the same indeterminate racemose-thyrsoid inflorescence with pistillate flowers on the proximal part and staminate flowers on the distal one (**Figure 1**; Webster, 1993; Berry et al., 2005; van Ee et al., 2011). Staminate flowers possess a biseriate perianth with well-developed petals and variable numbers of stamens but lack a pistillode (Webster, 1993, 2014; Radcliffe-Smith, 2001; van Ee et al., 2011). In pistillate flowers petals are usually lacking as well as stamens, or filamentous structures are present in the same position as the petals. The ovary is commonly tricarpellate with a single descending ovule per carpel, and topped with three styles with various branching patterns ranging from bifid to multifid (Webster, 1993, 2014; Radcliffe-Smith, 2001; van Ee et al., 2011). Filamentous structures are not just present in *Croton* but also in other genera of the *inaperturate crotonoid clade* (Nair and Abraham, 1962; Venkata-Rao and Ramalakshmi, 1968). The origin of the filamentous structures of pistillate flowers is controversial since they were interpreted as reduced petals (Nair and Abraham, 1962; Webster, 1993; Radcliffe-Smith, 2001; Caruzo and Cordeiro, 2007; De-Paula et al., 2011) or staminodes (Gagliardi et al., 2017). However, well-developed petals instead of filamentous structures were reported in pistillate flowers of two New World sections, i.e., sect. *Alabamenses* (**Figure 1A**) and sect. *Eluteria* subsect. *Eluteria* (**Figure 1B**; van Ee et al., 2011), and some African species (**Figure 1C**; Friis and Gilbert, 2008; Berry et al., 2016). Our study aims to clarify how these petals develop

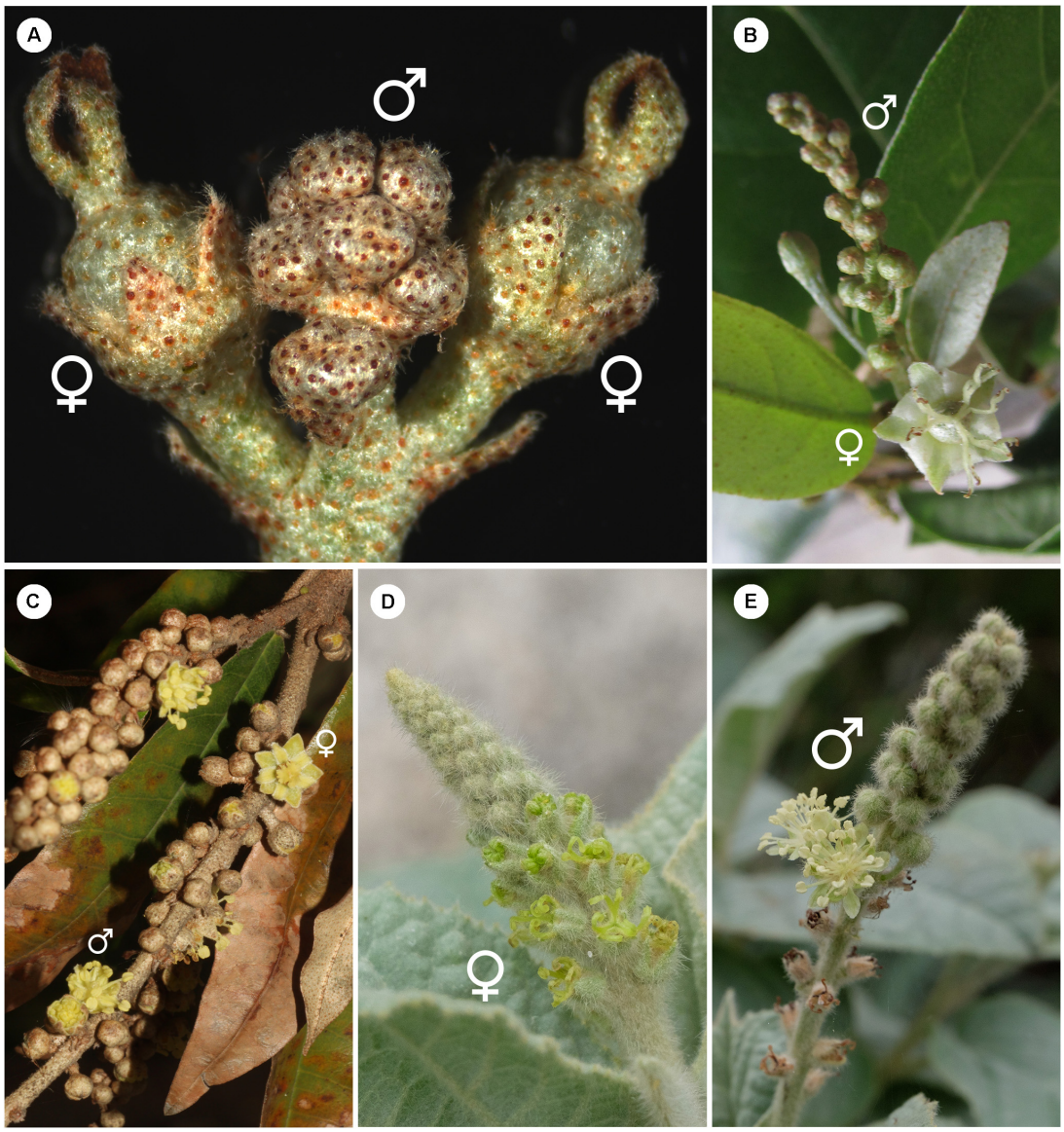

FIGURE 1 | Inflorescence of *Croton* with/without petals in pistillate flower **(A)** Inflorescence of *C. alabamensis* showing blooming pistillate flowers while staminate flowers are still closed. **(B)** Inflorescence of *C. schiedeanus* with long-pedicellate pistillate flower on the proximal part and many staminate flowers on the distal part. **(C)** Inflorescence of *C. gratissimus*, an African species with petals in pistillate flowers. **(D)** Inflorescence of *C. chilensis* showing pistillate stage. **(E)** Inflorescence of *C. chilensis* in the staminate stage (two open staminate flowers).

compared with the filamentous structures from typical pistillate flowers and petals from staminate flowers.

Another important aspect of flower diversity in *Croton* is the presence and homology of nectary tissue. Nectaries are present in both staminate and pistillate flowers of *Croton* in antesepalous position (alternate with petals in staminate flowers or alternate with filamentous structures in pistillate flowers) (Baillon, 1858; Michaelis, 1924; Nair and Abraham, 1962; Venkata-Rao and Ramalakshmi, 1968; De-Paula et al., 2011; Gagliardi et al., 2017). Nectaries could be vascularized or not in *Croton* (Nair and Abraham, 1962; Venkata-Rao and Ramalakshmi, 1968; Freitas et al., 2001; De-Paula et al., 2011) and if vascularized, the source of vascular bundles comes from sepal traces or rarely from the floral stele (De-Paula et al., 2011). A floral nectary (often described as glands or disk) is commonly present in both staminate and pistillate flowers in the subfamily Crotonoideae (Radcliffe-Smith, 2001; Webster, 2014). Nectaries have been reported to arise very late in the development of flowers of *Croton* and other genera in the inaperturate crotonoid clade (Liu et al., 2008, 2015; De-Paula et al., 2011; Gagliardi et al., 2016; Mao et al., 2017). In *Croton* and *Astraea*, nectaries were interpreted as staminodes because of their antesepalous position (De-Paula et al., 2011), but they were interpreted as receptacular outgrowth as well (Caruzo and Cordeiro, 2007). However, little is known of the nectary

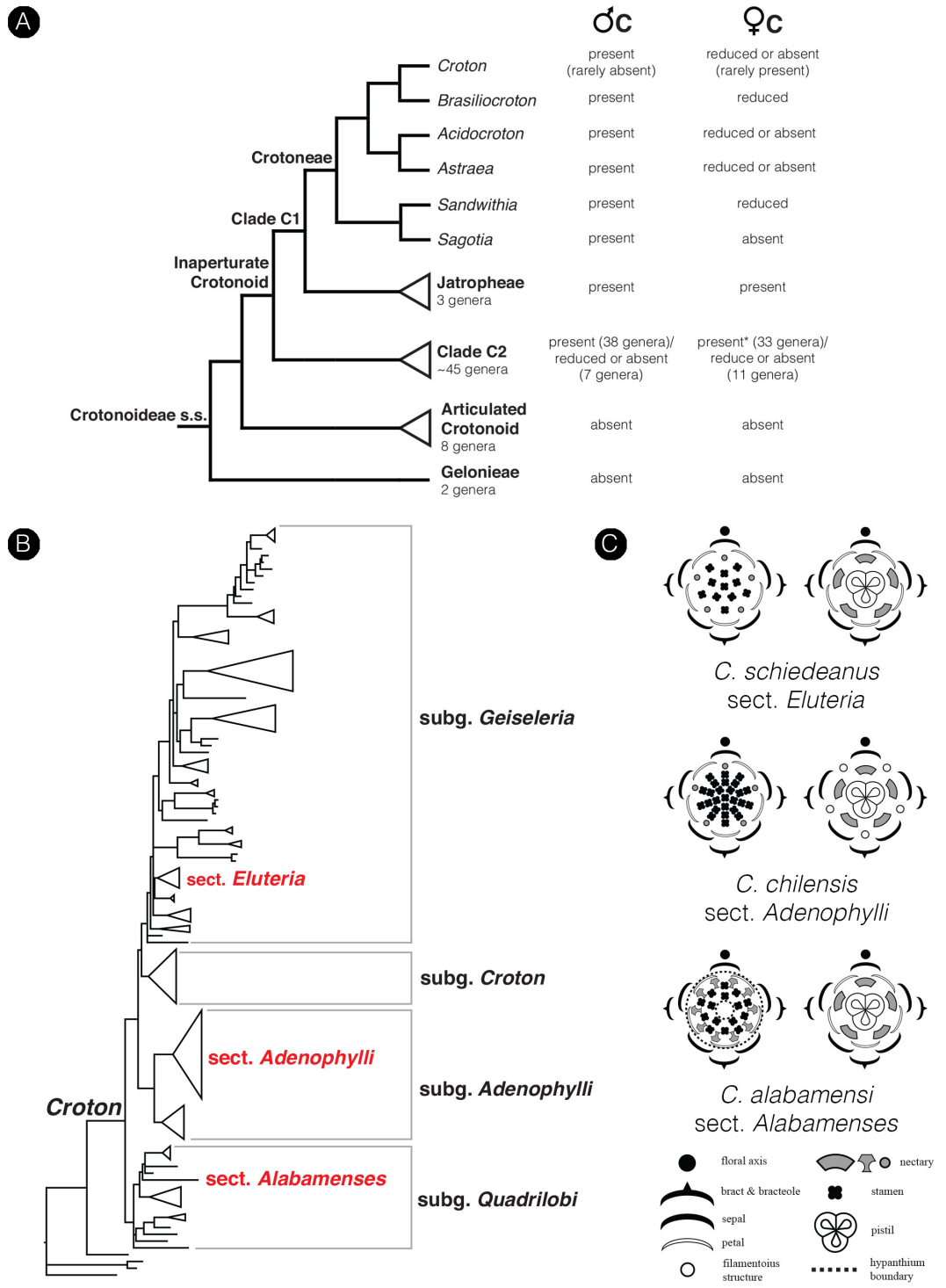

FIGURE 2 | Diagrams show the phylogenetic relationship in the subfamily Crotonoideae and the genus *Croton* mapped with a number of floral characters. **(A)** Simplified phylogenetic cladogram of the subfamily Crotonoideae shows relationships of all subgroups with the relationship of genera in the tribe Crotoneae emphasized (modified from Wurdack et al., 2005; van Welzen et al., 2020). The occurrence of petals in staminate and pistillate flowers were mapped on the tree with data from personal observation and the literature (e.g., Radcliffe-Smith, 2001; Webster, 2014). (Astersisk) There are no data about petals in pistillate flowers of the genus *Tapoïdes*. **(B)** Simplified phylogenetic phylogram of *Croton* indicating four subgenera. Sections which have representative species included in the present study are labeled (modified from van Ee et al., 2011). **(C)** Floral diagrams of both staminate and pistillate flowers from the three species of Croton used in this study. Floral diagrams were drawn following the symbols presented in Ronse De Craene (2010).

development and diversity and our study can throw more light on the origin and homology of the nectaries in *Croton*.

Stamens of *Croton* are well-known for their reflexed filaments in buds (Webster, 1993, 2014; Radcliffe-Smith, 2001; Berry et al., 2005; van Ee et al., 2011). The number of stamen in flower is also found to be highly diverse, ranging from one to more than one hundred (van Ee et al., 2008, 2011; Riina et al., 2009; Webster, 2014). The androecium of many *Croton* also possess the presence of outermost antepetalous stamens which is an unusual character among angiosperms (Baillon, 1858; Marchand, 1860; Michaelis, 1924; Nair and Abraham, 1962; Venkata-Rao and Ramalakshmi, 1968; Gandhi and Thomas, 1983; De-Paula et al., 2011). The origin of this character was thought to be dictated by the presence of an alternipetalous nectary (Venkata-Rao and Ramalakshmi, 1968) or by reduction of a stamen whorl (Gandhi and Thomas, 1983). However, the observation of the late development of the nectary did not support either of these hypotheses (De-Paula et al., 2011; Gagliardi et al., 2017). Investigation of floral development in several species of *Croton* and *Astraea* by De-Paula et al. (2011) found the antesepalous stamen whorl to be the first to develop followed by the antepetalous whorl. However, their studies of transverse sections revealed that the outermost whorl is the antepetalous whorl, while the antesepalous whorl is the next inner whorl, reflected on their floral diagrams (Figure 8 in De-Paula et al., 2011), which is representative for a centrifugal stamen development. More evidence from floral development is required and will be conducted in the present study.

Although our sampling of species is highly limited for such a large genus, results of a comparative floral developmental study of three highly divergent species can address a number of relevant questions linked to the floral evolution of the genus, such as (1) the origin of petals, (2) homology between petals of staminate and pistillate flowers, (3) origin of filamentous structures in the pistillate flowers, (4) androecial diversity in staminate flowers, and (5) diversification among staminate and pistillate flowers with emphasis on the nectaries. A better understanding of petal origins and their evolution in *Croton* will help in understanding similar phenomena in other taxa of subfamily Crotonoideae and also in the family Euphorbiaceae.

MATERIALS AND METHODS

Staminate and pistillate flowers of *Croton alabamensis* (sect. *Alabamenses*) (**Figure 1A**) and *C. schiedeanus* (sect. *Eluteria*, subsect. *Eluteria*) (**Figures 1B**, **2B**), both of which have well-developed petals in pistillate flowers, were studied and compared with flowers of *C. chilensis* (sect. *Adenophylli*) (**Figures 1D,E**, **2B**), which has filamentous structures in pistillate flowers. Samples were collected from cultivated plants grown at the Royal Botanic Garden Edinburgh and in the field (**Table 1**), fixed in FAA solution (90% ethanol at 70%, 5% glacial acetic acid and 5% formalin solution at 40%), then stored in 70% ethanol.

Inflorescence and floral morphology were observed using light microscopy (Zeiss Stemi 2000-C) and photos were captured with an AxioCam MRc 5 (Zeiss).

For the developmental and detailed morphology studies, flowers from different stages were dissected under a light microscope (Zeiss Stemi SV6), dehydrated in an alcohol gradient, dehydrated in acetone, dried at CO_2 critical point in a K850 critical-point dryer (Quorum Technologies), further dissected, mounted on aluminum stubs, coated with platinum (Emitech K575X) and observed with a scanning electron microscope (SEM) (Leo Supra 55-VP). All pictures were later edited in Photoshop (Adobe Inc.). Floral and inflorescence diagrams were drawn with Illustrator (Adobe Inc.).

RESULTS

Croton Chilensis

General Morphology

The inflorescence of *Croton chilensis* is generally a thyrse (an indeterminate inflorescence with lateral cymes) with the presence of solitary pistillate flowers or bisexual cymules (a pistillate flower associated with several staminate flowers) on the lower part and solitary staminate flowers or staminate cymules on the upper part (**Figures 1D,E**). Inflorescences are produced terminally on the stem. The pistillate flowers reach maturity before the staminate flowers (**Figure 1D**). Both staminate and pistillate flowers are subtended by a bract and two bracteoles. Staminate flowers are borne on a slender pedicel while pistillate flowers are nearly sessile (**Figure 1E**). Flowers from both genders are pentamerous (**Figure 2C**).

The perianth of staminate flowers is differentiated into sepals and petals, both with green color (**Figures 2C**, **3A**). Aestivation of the five sepals is quincuncial (**Figure 3B**). Sepals are ovate in shape with a wide base and acute apex (**Figures 3C,D**). The abaxial surface of sepals is covered with stellate trichomes (**Figure 3C**) while the adaxial surface is glabrous (**Figure 3D**). Five petals are arranged in cochlear or quincuncial aestivation (**Figures 3E,F**). Petals are obovate in shape with a narrow base (no claw) and obtuse apex (**Figures 3G,H**). Both surfaces of petals are generally glabrous except for the lower area of the adaxial side which is covered with many simple trichomes (**Figures 3G,H**). The apex of the petals is covered with papillae (**Figures 3G,H**). Inside the corolla whorl, there are five bilobed nectary glands alternating with the petals (**Figures 3I,J**). In the middle of the flowers, there are about 20 (19–24) stamens present, arranged in four whorls on a convex receptacle (could be interpreted as a short androphore by some authors – e.g., De-Paula et al., 2011) (**Figure 3A**). Anthers are inflexed in bud (**Figure 3K**) before expanding at anthesis (**Figures 3A,L**). The outermost stamen whorl is opposite to the petals (**Figure 3A**). There are several simple trichomes at the base of each filament (**Figure 3L**). The receptacle is pilose. There is no evidence of a gynoecial structure in the staminate flowers (**Figure 3A**).

In pistillate flowers, the five sepals are present (**Figures 2C**, **4A**). Aestivation of sepals is quincuncial (**Figure 3B**). Sepal shape is ovate with a wide base, which makes it look triangle-shaped (**Figures 4B,C**). The apex is acute (**Figures 4B,C**). Within the calyx and alternate to the sepals, there are generally filamentous structures (**Figure 4D**), occasionally replaced by

TABLE 1 | Origin of samples of Croton used in this study.

Samples	Plant code	Collection number	Source/Origin
C. alabamensis var. *alabamensis* E.A.Sm. ex Chapm.	–	Pratt & Ferry PFA8	Cultivated plant from Kenneth Wurdack garden/USA
C. alabamensis E.A.Sm. ex Chapm. var. *texensis* Ginzbarg	Grown from seeds at RBGE	(seed code)	Lady Bird Johnson Wild Flower Center/Texas, USA
C. chilensis Müll.Arg.	BGHMR53 (2009.0241A)	1099 Led	RBGE/wild collected in Chile
C. schiedeanus Schltdl.	–	1441/865 La	Wild collected/Belize
C. schiedeanus Schltdl.	–	1331 La	Wild collected/Belize
C. schiedeanus Schltdl.	–	1093 La (Herb. L. Stoddart 02 under name *C. glabellus*)	Wild collected/Belize

petals (**Figure 4A**) or colleters (**Figure 4E**). Opposite to the sepals, there are five nectary glands present, alternate to the filamentous structures (**Figures 4D–F**). Petals, if present, have a narrow ligulate shape with acute apex (**Figures 4A,F**). Stamens are completely absent in the pistillate flowers. At the center of the flower, there is a gynoecium comprising three carpels (**Figure 4G**). The outer surface of the ovary is covered with dense stellate trichomes (**Figures 4G,H**). There are three styles with bifid stigmatic tip (total of six tips) (**Figures 1D**, **4A**).

Ontogeny of Staminate Flowers

Staminate floral primordia arise spirally on the inflorescence axis in the axil of a bract. A pair of bracteoles develops laterally of the floral primordium (**Figures 5A,B**). The first sepal arises abaxially (**Figure 5C**). The remaining sepals develop in a helical order (**Figures 5C,D**). The first sepal is large and almost covers the entire bud during the development (**Figure 5C**). Five petal primordia emerge simultaneously and alternate to the sepals (**Figures 5D–I**). Growth of petals tends to be more rapid on the abaxial side of the flower (**Figure 5H**). Following initiation of all five petals, the first whorl of stamens initiates alternating with the petals (**Figure 5F**). The second whorl of stamens develops next outside of the first whorl opposite the petals. However, in the early stage it is covered by the expanding petals (**Figures 5G–I,K,N**). The third and fourth stamen whorls later develop almost simultaneously and centripetally on the remaining floral meristem (**Figures 5G–J**). Arrangement and number of stamens are observed to be variable among flowers (**Figures 5K,L**). It is difficult to distinguish between the third and fourth whorls. A final set of three to five stamens develops at the apex of the floral meristem and sometimes the last stamen to initiate is shifted toward the center of the flower giving the false impression of a central stamen (**Figures 5J,L–N**). During development, stamens curve and fold inwards, giving *Croton*'s characteristic inflexed anther in bud (**Figure 5O**). Five nectary glands emerge much later in alternation with the petals.

Ontogeny of Pistillate Flowers

Pistillate floral primordia emerge on the proximal to approximately middle part of the inflorescence where there is a transition to the staminate flower zone (**Figures 1D,E**). Each floral primordium is subtended by a bract and sided by two bracteoles. We could not observe the sepal initiation because of the presence of intertwining stellate trichomes obscuring the view. However, we could imply a 2/5 pattern as their arrangement follows a quincuncial aestivation in the mature flowers. Five petal-like primordia develop alternate to the sepals (**Figures 6A–D**). While initiation of primordia is initially similar to staminate flowers, growth of the organs tends to be slower. Different sizes of petal-like organs were observed, which may be the result of a non-simultaneous initiation or unequal development (**Figures 6C,D**). Three congenitally fused carpels arise rapidly, while petals are still in an early developmental stage (**Figures 6A,B**). As the gynoecium develops, petal development terminates (**Figures 6A–H**). Nectary tissue emerges late as a rim at the base of the gynoecium; the pressure of the sepal lobes gives the impression of a pair of nectaries developing between the petals (**Figure 6G**). The nectary expands as a multilobed ring around the ovary (**Figures 6H,I**). A bilobed style develops on top of each carpel (total of three styles/six stigmatic tips) (**Figure 6H**). In closed buds, some petal-like organs are elongated and develop as colleters (**Figures 4D,E**, **6J,K**; P. Thaowetsuwan, unpublished anatomical data). Some petal-like organs develop into miniature petals with various shapes and sizes, resulting in a highly heterogeneous corolla morphology (**Figures 4A,E,F**, **6J–L**).

Croton alabamensis

General Morphology

Flowers of *Croton alabamensis* are borne on racemose inflorescences with up to three pistillate flowers on the lower part and more numerous staminate flowers distally (**Figure 1A**). Inflorescences are produced terminally on shoots. The pistillate flowers mature much earlier than staminate flowers (**Figure 1A**). Both staminate and pistillate flowers are pedicellate, and subtended by a bract and two bracteoles (**Figure 1A**). Both staminate and pistillate flowers are pentamerous (**Figure 2C**).

Perianth of staminate flowers is biseriate (**Figures 2C**, **7A,B**). Sepals have quincuncial aestivation (**Figure 7A**) and an ovate shape with wide base and acute apex (**Figures 7B,C**). The corolla also has quincuncial aestivation (**Figure 7D**). Petals have an ovate shape with narrow base and obtuse apex (**Figures 7E,F**). The abaxial side of sepals is covered with lepidote trichomes (**Figures 7A,B**). On the adaxial side, sepals bear stellate trichomes on their margins (**Figure 7C**) while petals bear simple trichomes on their margins (**Figure 7F**). Petals have stellate-lepidote

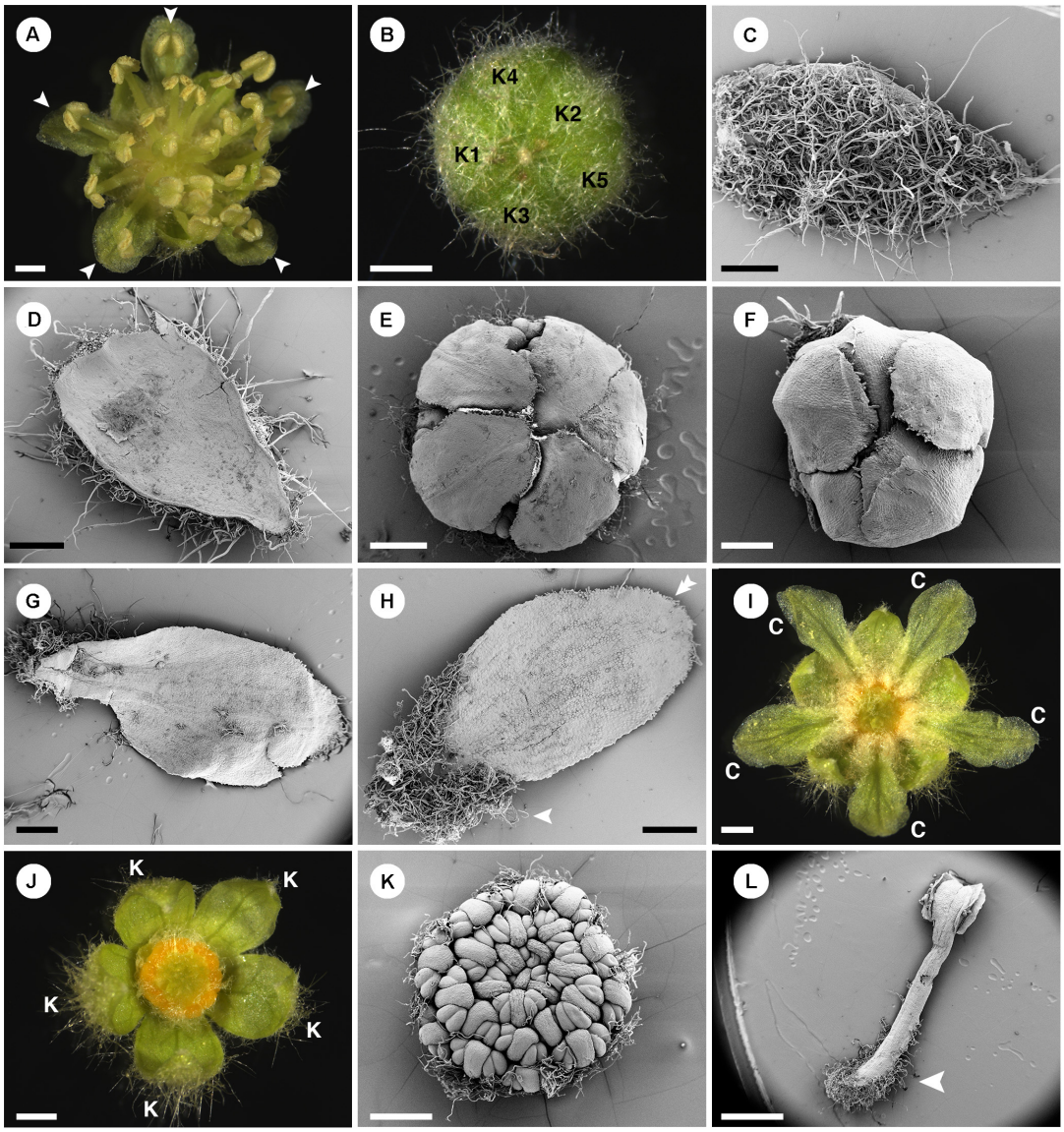

FIGURE 3 | Morphology of staminate flowers of *Croton chilensis*. **(A)** Anthetic flower. Note, the outermost stamens are opposite petals (arrowhead). **(B)** A flower bud near anthesis with quincuncial aestivation. **(C)** Abaxial surface of a sepal covered with long stellate trichomes. **(D)** Adaxial surface of a sepal with glabrous surface. **(E)** Corolla with cochlear aestivation. **(F)** Corolla with quincuncial aestivation. **(G)** Abaxial surface of a petal with few stellate trichomes on the surface. **(H)** Adaxial surface of a petal with long simple trichomes covering the lower part (arrowhead). Note, there are papillae on the margin of the apex (double arrowhead). **(I)** A flower with stamens removed showing trichomes on the lower part of the petals covering nectary glands. **(J)** A flower with petals and stamens removed showing multiple yellow nectary lobes. **(K)** Flower bud with young androecium, perianth removed. Note, anthers are inflexed making them look like facing outward. **(L)** A stamen with lower part of filament covered with many simple trichomes (arrowhead). K, sepal; C, petal. Scale bars: **(A,B,I,J,L)** = 1,000 μm; **(C–E,G,H,K)** = 500 μm; **(F)** = 200 μm.

trichomes covering their abaxial surface (**Figures 7D,E**). Margins and apex of petals are fimbriate comprising simple trichomes (**Figures 7E,F**). Inside the corolla whorl, ten nectary glands alternate with petals and outermost stamens, and are fused pairwise as five horse-shoe shaped nectaries clasping the base of the filaments (**Figure 7G**). There are 15–18 stamens present in the staminate flowers with the outermost whorl alternating with petals (**Figure 7H**). There are some stellate trichomes present on the basal part of the filaments (**Figure 7I**). On the apex of the floral meristem, there is an empty space without trace of carpels (**Figures 2C**, **7H**). Stamens are incurved toward the center of the flower, but the anthers do not inflex (**Figure 7H**). The receptacle is pilose, covered with simple trichomes.

In pistillate flowers, there are two perianth whorls (**Figures 2C**, **8A,B**). Sepal aestivation is quincuncial. Sepals have an ovate shape with a wide base and acute apex (**Figures 8A–D**). In sepals, the abaxial surface is covered by lepidote trichomes (**Figures 8A–C**), while the adaxial surface is glabrous on the lower part but

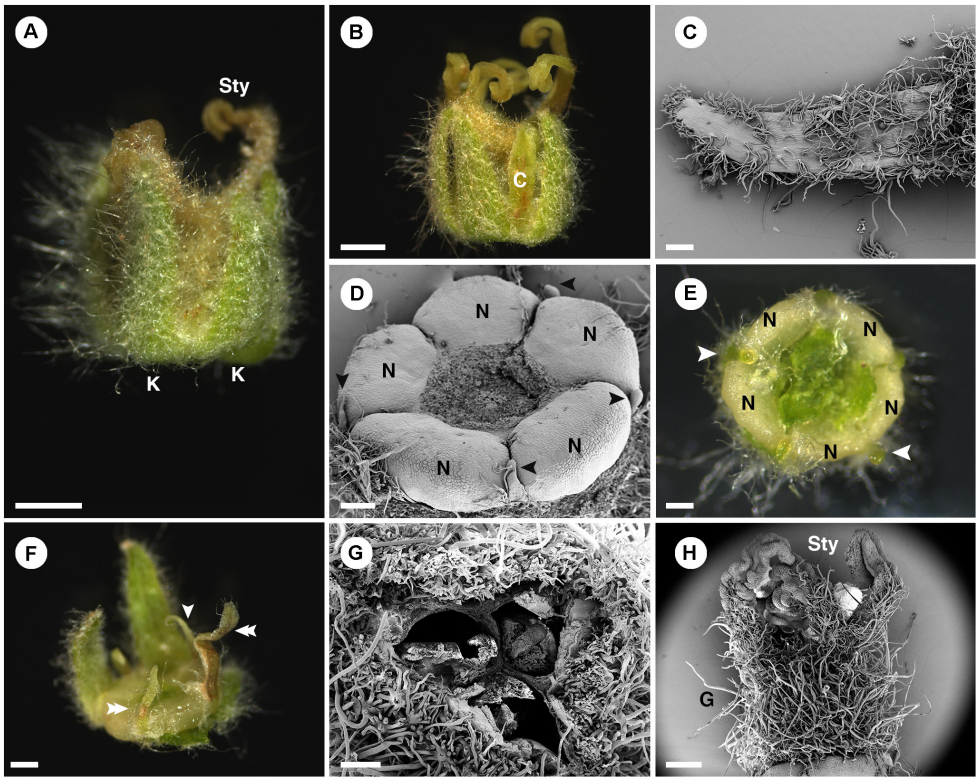

FIGURE 4 | Morphology of pistillate flower of *Croton chilensis*. **(A)** A flower at anthesis. Note, sepals are conspicuous while petals are inconspicuous. Note, the abaxial surface of sepals is covered with long stellate trichomes. **(B)** An anthetic flower with a petal present. **(C)** Adaxial surface of a sepal covered with variably reduced stellate trichomes. **(D)** Five nectary glands with small filamentous structures arranged alternately on the outer part. Note, heteromorphy of filamentous structures in the same flower is present with some becoming colleters (arrowhead). **(E)** Filamentous structures and nectary glands at anthesis. Some filamentous structures become colleters (arrowhead). **(F)** Variable morphologies of organs alternating with nectaries. Some have a filamentous form (arrowhead), while some resemble petals (double arrowhead). **(G)** An ovary consisting of three carpels with axile placentation. **(H)** There are three styles on top of the ovary. The style and stigma have a papillate surface. K, sepal; Sty, style; C, petal; N, nectary; G, ovary. Scale bars: **(A,B)** = 1,000 μm; **(C–E,G)** = 200 μm; **(F,H)** = 500 μm.

covered with some stellate and simple trichomes on the upper part (**Figure 8D**). Petals of pistillate flowers are similar to those of staminate flowers but there is a mix of lepidote and stellate-lepidote trichomes present along the midrib on the abaxial side (**Figure 8E**). Petals have an oblong shape with narrow base and obtuse apex (**Figures 8E,F**). The petals are arranged in alternation with free but confluent nectary glands (**Figure 8G**). Inside the nectary, there is a tricarpellate ovary covered with lepidote trichomes (**Figure 8A**). On top of the ovary, three styles are present with simple style/stigma, but sometimes a slightly divided stigma is present (**Figure 8H**).

Ontogeny of Staminate Flowers

Only staminate flowers from *C. alabamensis* var. *alabamensis* were used in the developmental study. Staminate flowers develop spirally on the upper part of the racemose inflorescence (**Figure 1A**). Each floral primordium is subtended by a bract and two bracteoles (**Figure 9A**). The first sepal emerges on the abaxial side of the flower (**Figures 9A,B**), followed by additional sepals in a 2/5 pattern (**Figure 9B**). Floral primordia are initially convex shaped (**Figures 9A,B**) but later shift vertically to a concave shape due to hypanthium formation during petal initiation (**Figure 9C**). Five petal primordia emerge alternating with sepals (**Figure 9C**). Petals develop unidirectionally toward the abaxial side of the flower (**Figures 9C–E**). Following initiation of petals, two whorls of five stamens emerge almost simultaneously, with the antepetalous stamen primordia developing more rapidly in early stages (**Figure 9D**). A third whorl of five stamens is initiated centripetally (**Figure 9E**), resulting in fifteen stamens arranged in three whorls of five on the slope of the hypanthium (**Figures 9F,G**). Stamen growth tends to be unequal with one side developing faster (**Figure 9E**). No stamen, nor any other floral organ develops at the center of the flower (**Figures 9F–I**). During maturation, stamens curve toward the center but are never inflexed (**Figures 9G–I**). Much later after stamen initiation, five nectary glands develop alternating with petals and opposite the outermost antesepalous stamen whorl. Nectary glands expand to surround the base of the filaments of antesepalous stamens, clearly visible at anthesis (**Figure 7G**).

Ontogeny of Pistillate Flowers

Ontogeny of the pistillate flower was observed in *C. alabamensis* var. *alabamensis*. Pistillate flowers are located on the lower part of the inflorescence (**Figure 1A**). A bract and two

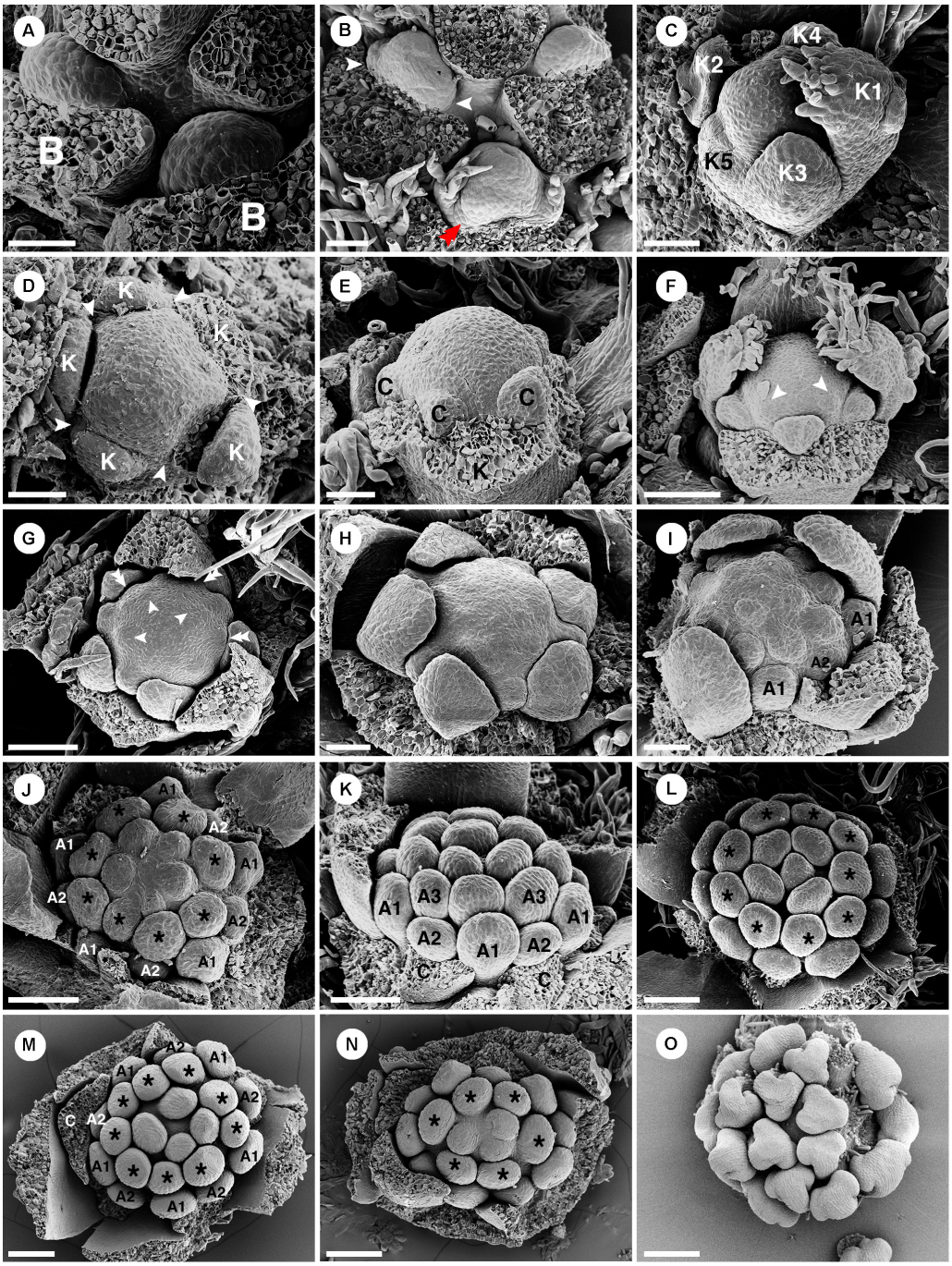

FIGURE 5 | Ontogeny of staminate flowers of *Croton chilensis*. **(A)** Young floral primordia subtended by a bract. Note, the floral apex has a convex shape. **(B)** Sequence of early floral development with formation of bracteoles (arrowhead) and a first sepal (double arrowhead). **(C)** An older bud shows unidirectional unequal growth of sepals with the initiation of petal primordia. **(D)** Apical view of a very young flower bud with initiation of petal primordia (arrowhead). **(E)** In later stages, young petals grow and expand surrounding the central floral apex. **(F)** While petals are growing, the first whorl of stamens develops alternating with petals (arrowhead). **(G)** Next, the second whorl of stamens develops centrifugally opposite petals, while the third whorl develops centripetally alternate with the first stamen whorl. **(H)** Later, the fourth stamen whorl initiates. Only first, third and fourth whorls are visible. The second whorl is covered by the expanding petals which have unequal growth. **(I)** Next, more stamens develop but do not form a complete whorl. **(J)** Anomalous stamen number (eight) in the third and fourth whorls (asterisk). Five stamens are present in the central part forming a complete whorl. **(K)** The antepetalous second stamen whorl is pushed by the petals making the first stamen whorl become the outermost whorl. **(L)** Nine stamens are present in the third and fourth whorls (asterisk). Five central stamens are present but are unequally arranged. **(M)** The outermost stamens during a young developmental stage are stamens from the first whorl. The anomalous stamen number of nine is observed in the third and fourth whorls (asterisk). **(N)** A flower with an anomalous lower stamen number (total 19 stamens). Boundary between third and fourth whorls could not be observed (asterisk). **(O)** Later, young stamens curve toward the floral apex and become inflexed. B, bract; K, sepal; C, petal; A, stamen. Scale bars: **(A–E,H,I)** = 50 μm; **(F,G,K,M,N)** = 100 μm; **(I,J)** = 90 μm; **(L)** = 120 μm; **(O)** = 200 μm.

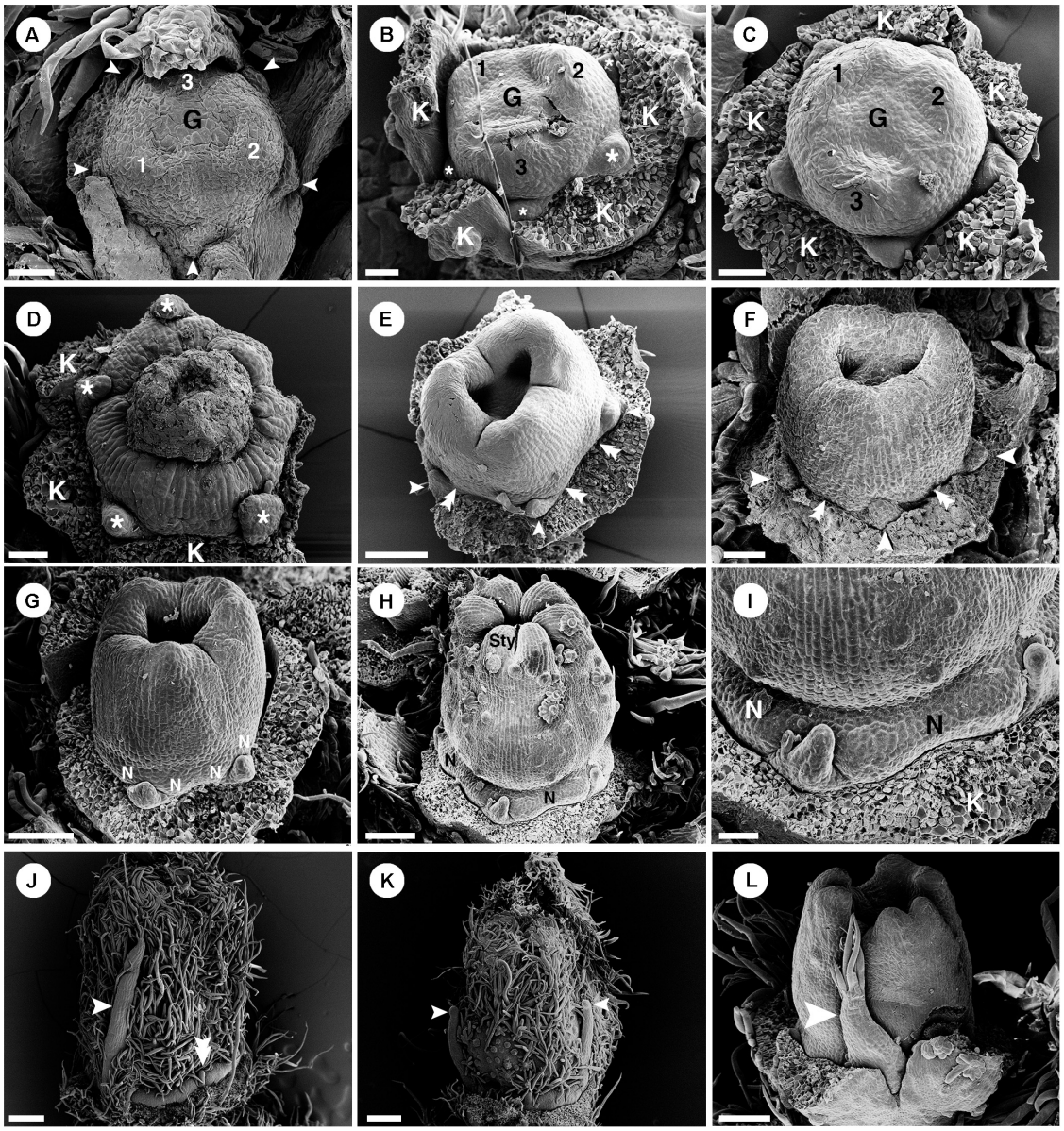

FIGURE 6 | Ontogeny of pistillate flowers of *Croton chilensis*. **(A)** A young flower shows initiation of petal-like primordia (arrowhead) and formation of an ovary by fusion of three carpels. **(B)** Petal-like primordia (asterisk) are arranged alternating with sepals. **(C)** Petal-like organs show slight differences in growth. **(D)** Flower with aborted ovary. Petal-like organs clearly show unequal growth (asterisk). **(E)** Later, three carpels close apically while petal-like organs development is arrested (arrowhead). Nectary primordia start to initiate at the base of the ovary (double arrowhead). **(F)** Petal-like organs stop their development while the ovary grows and expands in size (arrowhead). Nectary tissue starts to form at the base of the ovary opposite to sepals (double arrowhead). **(G)** Later stage; a bilobed style is formed on top of each carpel. Nectary glands appear to be bilobed by pressure of the sepal lobes. **(H)** Next, a bifid style can be seen on top of each carpel. Nectariferous tissue expands to become a ring. **(I)** Magnified view of the previous picture shows the nectary ring expansion while petal-like organs are still minute. **(J)** Later, some petal-like organs grow into filamentous structures (arrowhead) while some are still arrested in their development (double arrowhead). **(K)** Some filamentous structures have a tendency to become a colleter (arrowhead). **(L)** A miniature petal is sometimes present by extension of the petal-like organs (arrowhead). G, ovary; K, sepal; N, nectary; Sty, style. Numbers on the gynoecium in **(A–C)** indicate carpel number. Scale bars: **(A,B,I)** = 40 μm; **(C,D,F)** = 50 μm; **(E,G,L)** = 100 μm; **(H)** = 120 μm; **(J,K)** = 200 μm.

bracteoles subtend the flower. Five sepals are present with quincuncial aestivation implying a helical initiation pattern. Five petals emerge simultaneously alternate to sepals (**Figure 9J**). A congenitally fused tri-carpellate ovary develops rapidly, even when petal primordia are still young (**Figure 9J**). Petal growth is unequal with the abaxial petals developing faster (**Figures 9J–L**). Contrary to *C. chilensis*, all petals in pistillate flowers continue to expand until they resemble petals in staminate flowers at anthesis (**Figures 9J–O**). A bifid style develops on top of each carpel (**Figure 9N**). However, some samples have a simple style at the

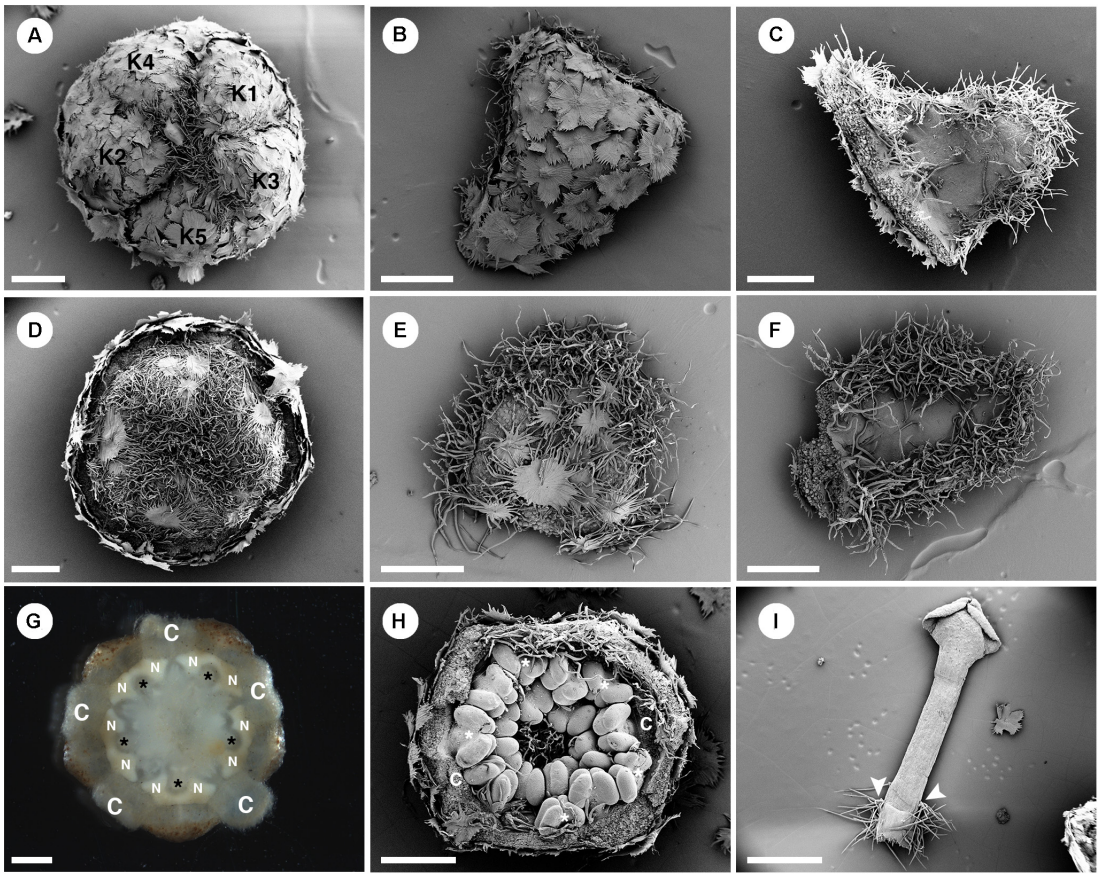

FIGURE 7 | Morphology of staminate flowers from *Croton alabamensis*. **(A)** Calyx in the flower bud with quincuncial aestivation. Note, interlocking of trichomes on the floral apex. **(B)** Abaxial surface of a sepal covered with lepidote trichomes. **(C)** Adaxial surface of a sepal covered with some stellate trichomes on the lower part. There are many stellate trichomes on the margin. **(D)** Corolla in a flower bud with quincuncial aestivation. **(E)** Abaxial surface of a petal covered with stellate-lepidote trichomes. There are many trichomes on the margin. **(F)** Adaxial surface of a petal. The central area is glabrous but there are tufts of simple trichomes on the margin. **(G)** Horse-shoe shaped nectary glands clasping the base of outer antesepalous stamens (asterisk). **(H)** Stamens in the cup-shaped floral bud. The outermost stamens are arranged alternating with petals (asterisk). Note, stamens are not inflexed in bud. **(H)** A stamen with some stellate trichomes on the filament base (arrowhead). K, sepal; C, petal; N, nectary. Scale bars: **(A–F,H)** = 500 μm; **(G,I)** = 1,000 μm.

mature stage, while some flowers retain a bifid style (**Figure 9N**). Much later, nectary glands develop at the base of the ovary in an antesepalous position (**Figure 9O**).

Croton schiedeanus

General Morphology

In *Croton schiedeanus*, flowers are produced spirally on racemose inflorescences (**Figure 1B**). Inflorescences are axillary borne on the main axis. One to two pistillate flowers are present on the proximal part and bloom earlier than staminate flowers on the distal part (**Figure 1B**). Both staminate and pistillate flowers are pedicellate and subtended by a bract and two bracteoles (**Figures 1B**, **2C**). The pedicels of staminate flowers are slender while pedicels of pistillate flowers are bulky and longer (**Figure 1B**). Flowers from both genders are pentamerous.

There are two whorls of perianth parts in staminate flowers (**Figures 10A,D**, **2C**). Sepal shape is ovate with a wide base and acute apex (**Figures 10B,C**). The arrangement of sepals follows a quincuncial pattern (**Figure 10A**). The abaxial side of sepals is covered by lepidote trichomes (**Figure 10B**), while on the adaxial side there are many simple trichomes present near the margin and the apex (**Figure 10C**). Petal shape is ovate with a narrow base and obtuse apex (**Figures 10E,F**) arranged in cochlear aestivation (**Figure 10D**). The abaxial surface of petals is mostly glabrous with one or two lepidote trichomes present (**Figure 10E**). The adaxial surface of petals is also mostly glabrous and sparsely covered with simple trichomes (**Figure 10F**). Margin and apex of petals are fimbriate, lined with simple trichomes (**Figures 10E,F**). Outside the androecium, there are five bilobed nectary glands alternate with the petals (**Figure 10F**). Centrally, about 11 stamens are arranged on a convex receptacle with the outermost whorl opposite to petals (**Figures 2C**, **10H**). Anthers are inflexed in bud (**Figures 10F–H**). Filaments are generally glabrous but sometimes a stellate trichome may be present (**Figure 10H**). There is no indication of an ovary.

Pistillate flowers are borne on longer and thicker pedicels than staminate flowers (**Figure 11A**). In pistillate flowers, both sepals

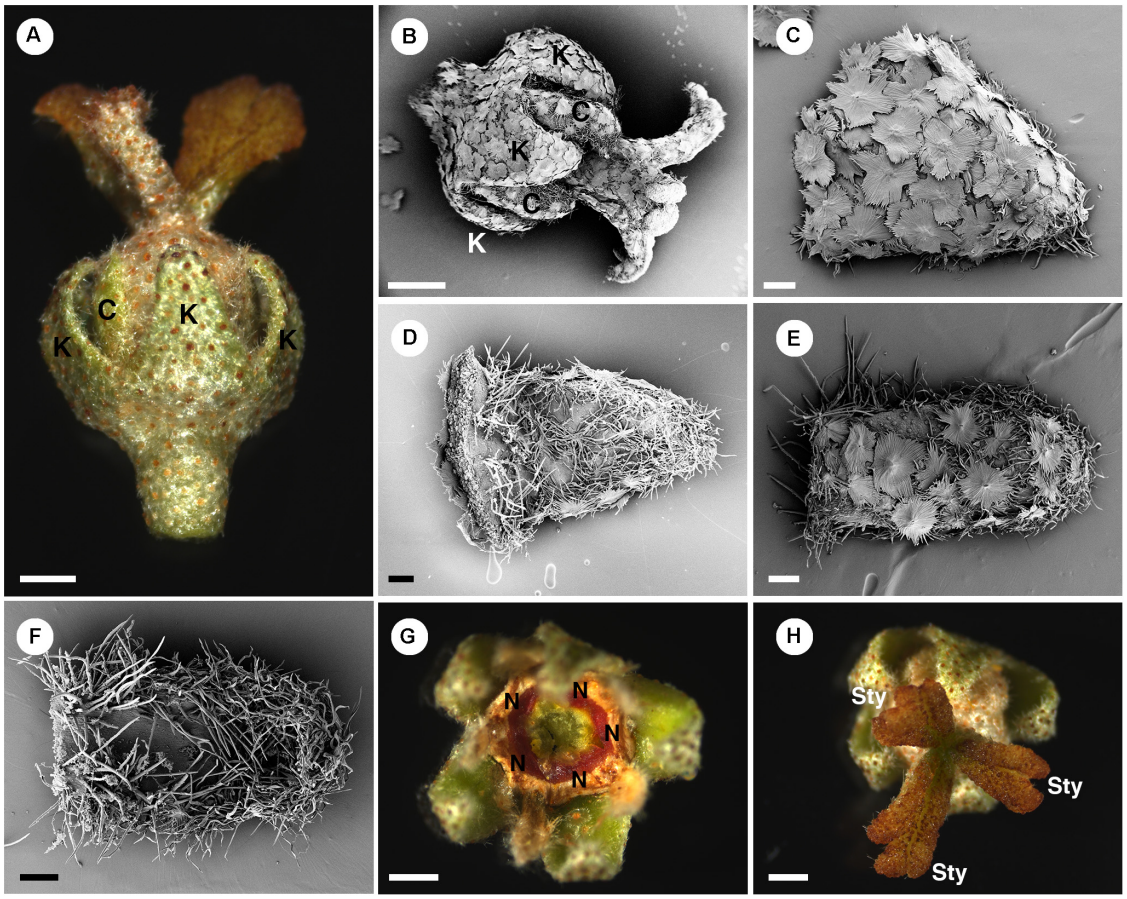

FIGURE 8 | Morphology of pistillate flowers of *Croton alabamensis*. **(A)** A flower near anthesis. Fully developed petals are present. Styles are bilobed but do not fork. **(B)** A flower near anthesis with visible sepals and petals. Styles are slightly bifid in this flower. Note outer surface of all organs is covered with lepidote trichomes. **(C)** Abaxial side of a sepal covered with lepidote trichomes. **(D)** Adaxial side of a sepal. There are many stellate trichomes covering the surface. **(E)** Abaxial side of a petal covered with lepidote and stellate-lepidote trichomes. **(F)** Adaxial side of a petal. The margin is densely covered with simple trichomes. **(G)** A nectary ring inside the corolla initially with yellow color that later changes to red. **(H)** Three styles and stigmatic surfaces. Note, stigmatic lobe number vary from two to four. K, sepal; C, petal; N, nectary; Sty, style. Scale bars: **(A,B,G,H)** = 1,000 μm; **(C–F)** = 200 μm.

and petals are present (**Figures 1B**, **2C**, **11B**). Sepals have an ovate shape with wide base and acute apex (**Figures 11C,D**), arranged in quincuncial aestivation. On the abaxial side of the sepals, there are many lepidote trichomes covering the whole surface (**Figure 11C**). On the adaxial side, there are stellate trichomes on the upper part, but the lower part is glabrous (**Figure 11D**). Petals have an obovate shape with narrow base and obtuse apex and margins of petals overlap in a quincuncial aestivation only in the upper part (**Figures 11C–H**). Petal lobes alternate with nectary glands (**Figures 2C**, **11H,I**). The abaxial surface of petals is mostly glabrous with a few lepidote trichomes on the midrib (**Figures 11E,F**). The adaxial surface is also mostly glabrous with some simple trichomes near the margin (**Figure 11G**). The margin of petals is fimbriate, densely covered with crushed stellate and simple trichomes (**Figures 11E–H**). Five nectary lobes are present opposite the sepals and are basally confluent at the base of the petals (**Figures 11H,I**). Within the nectary, there is a tricarpellate ovary covered with lepidote trichomes (**Figure 11J**). Three styles are present with twice bifid (**Figure 1B**) or multifid stigmatic tips (**Figure 11K**).

Ontogeny of Staminate Flowers

Staminate flowers develop on the distal part of the inflorescence (**Figure 1B**). Flowers are subtended by a bract and two bracteoles. Five sepals are present (**Figure 2C**). The shape of floral primordia is convex, similar to *C. chilensis* (**Figures 12A–I**). Five petals emerge simultaneously alternating to the sepals (**Figures 12B,C**). Later growth is unequal with the abaxial petals developing faster (**Figures 12D–F**). The first whorl of five stamens emerges alternating with the petals (**Figures 12E,F**). Next, the second stamen whorl emerges outside the first whorl (centrifugally) opposite the petals (**Figures 12F,G**). The last stamen to develop is a single stamen occupying the central area of the flower (**Figures 12H,I**). During maturation, stamens curve and fold resulting in an inflexed anther appearance (**Figure 10H**). Nectary glands initiate much later after the stamen development in alternation with petals.

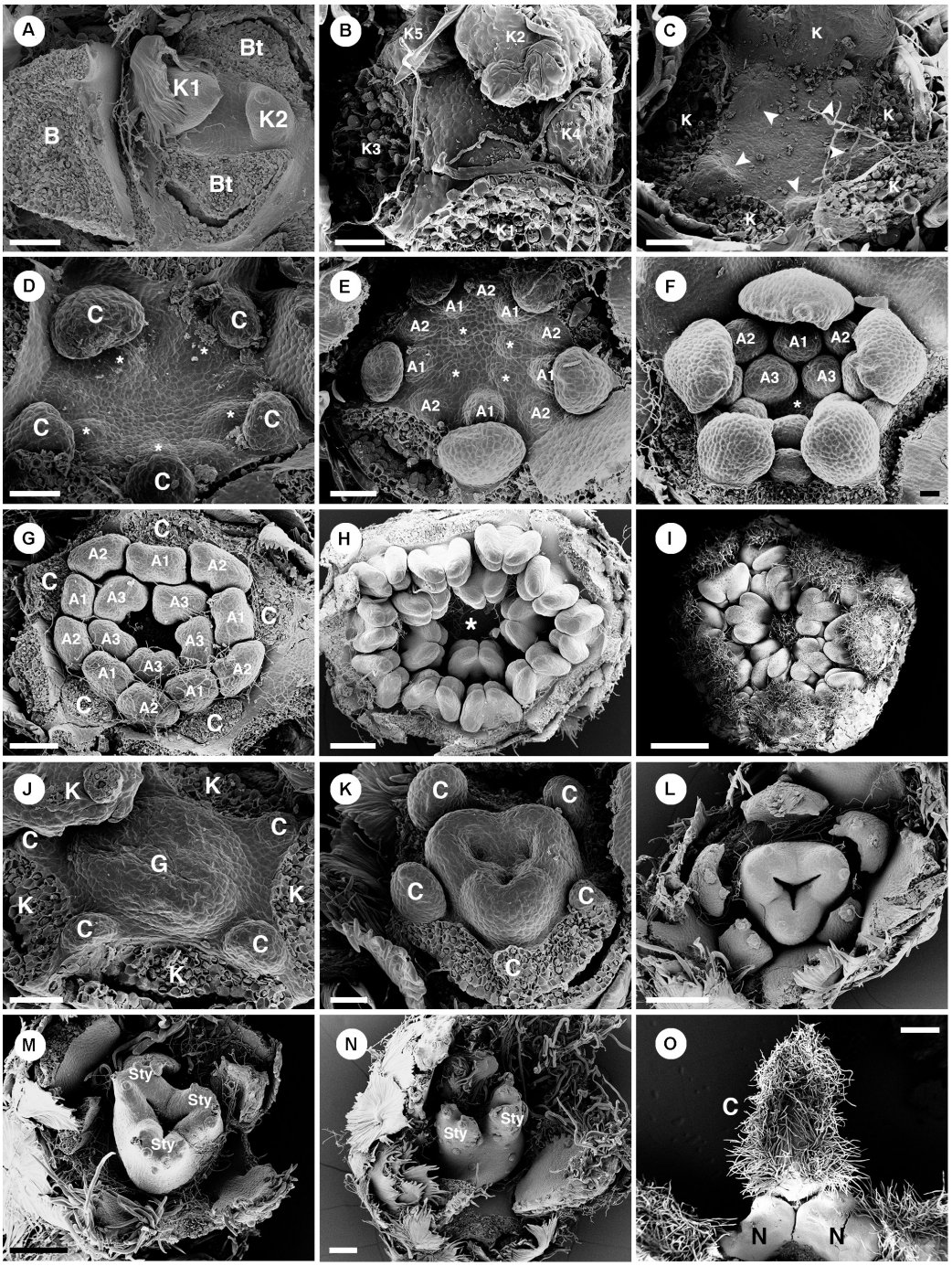

FIGURE 9 | Ontogeny of staminate **(A–I)** and pistillate **(J–O)** flowers of *Croton alabamensis*. **(A)** A young convex floral primordium subtended by a bract and two bracteoles. The first and second sepals are visible. **(B)** Soon, more sepal primordia initiate and grow unequally in a quincuncial (2/5) pattern. Note, the floral primordium is still convex in shape. **(C)** After that, a hypanthium starts to form while five petal primordia initiate alternating with sepals (arrowhead). **(D)** Later, petals continue to grow and clearly show unequal growth. Two whorls of stamens are visible. Stamens from the antepetalous whorl (asterisk) is bigger than stamens from the alternipetalous whorl. Note, a hypanthium is well developed making the flower to become cup-shaped. **(E)** Next, the third whorl of stamens develops centripetally (asterisk). **(F)** The hypanthium starts to grow while petals and three whorls of stamens are visible. There is an empty space in the middle of the flower (asterisk). **(G)** Flower in later stage with all perianth parts removed shows three whorls of stamens. The outermost whorl alternates with petals. **(H)** Apical view of older flower bud shows central empty space (asterisk). **(I)** Later, stamens grow and bend toward the center but never become inflexed. **(J)** Pistillate flower in an early stage shows five petal primordia and a tricarpellate ovary formation. **(K)** In a later stage, petal primordia continue to grow unequally. Three fused carpels are clearly seen. **(L)** Next, petals continue to expand and the ovary start to close. **(M)** A style starts to form on top of each carpel. **(N)** Three bilobed styles are visible on the ovary. **(O)** At a much older stage, five bilobed nectary glands are formed alternating with petals. K, sepal; C, petal; A, stamen; G, ovary; Sty, style; N, nectary. Scale bars: **(A,G,N)** = 100 μm; **(B,F)** = 30 μm; **(C–E,J,K)** = 50 μm; **(H)** = 200 μm; **(I)** = 1,000 μm; **(L,M)** = 150 μm; **(O)** = 400 μm.

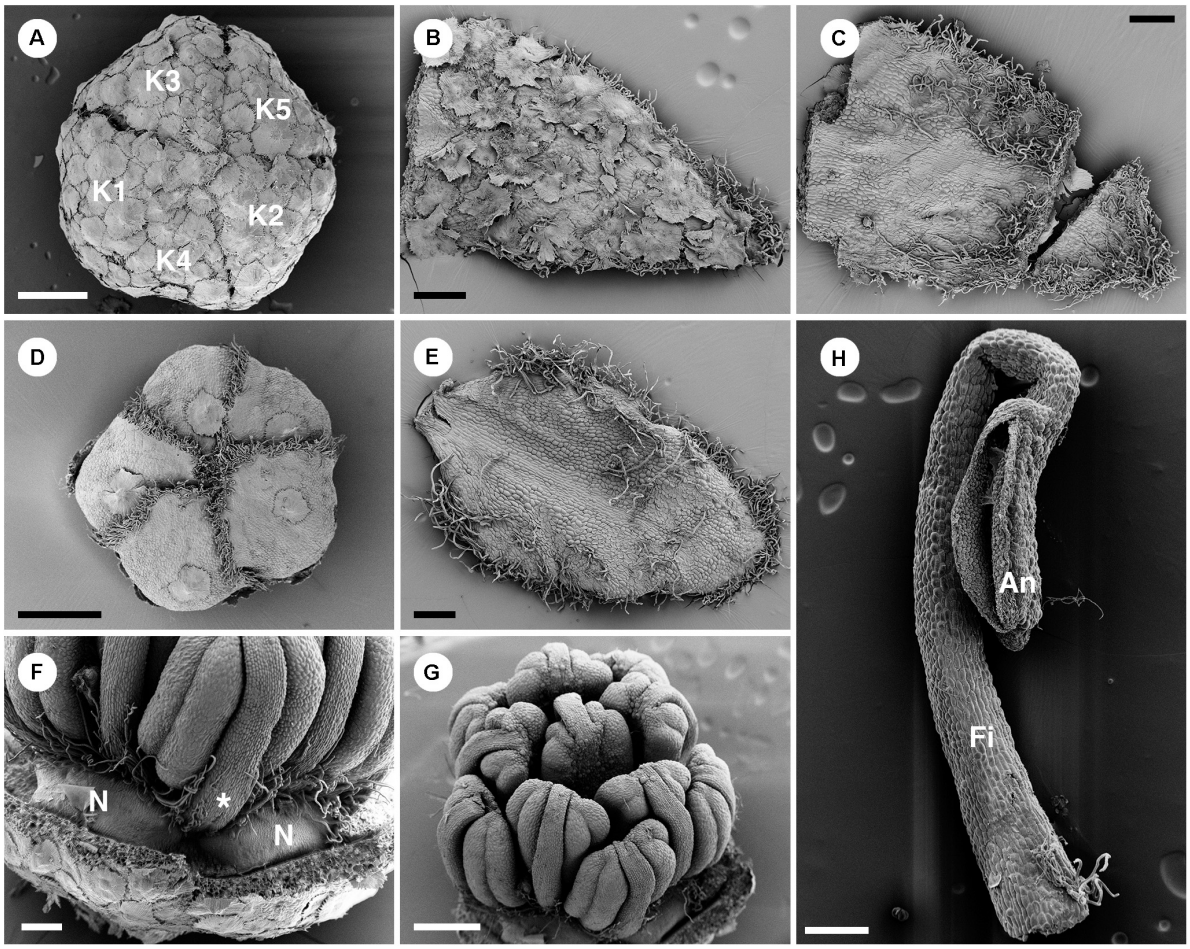

FIGURE 10 | Morphology of staminate flowers of *Croton schiedeanus*. **(A)** Calyx in flower bud with quincuncial aestivation. The surface is covered with lepidote trichomes. **(B)** Abaxial surface of a sepal with lepidote trichomes. **(C)** Adaxial surface of a sepal with many simple trichomes on the margin and apex. **(D)** Corolla in a flower bud with cochlear aestivation. There is a lepidote trichome visible on each petal. Note the frimbriate margin of petals. **(E)** Adaxail side of a sepal with few simple trichomes on the surface. There are many simple trichomes lining the margin and apex. **(F)** Nectaries located in alternation with petals and outermost stamens (asterisk). **(G)** There are 11 stamens arranged in two whorls surrounding a central stamen. The outermost stamens are arranged opposite petals. Note, stamens are inflexed in a flower bud. **(H)** A stamen with a stellate trichome on the base of the filament. K, sepal; N, nectary; Fi, filament; An, anther. Scale bars: **(A,D,G)** = 500 μm; **(B,C,E,F,H)** = 200 μm.

Ontogeny of Pistillate Flowers

There are few pistillate flowers of *C. schiedeanus* located on the proximal part of the inflorescence (**Figures 1B**, **2C**). A pistillate flower is borne in the axil of a bract and sided by two bracteoles. Sepals initiate spirally in a 2/5 pattern (**Figure 13A**). Five petal primordia develop alternate to them (**Figures 13B,C**) and show unequal growth similar to other species (**Figures 13D,E**). Similar to *C. alabamensis*, petals continue to grow and expand throughout the floral development (**Figures 13C–F,I**). Three congenitally fused carpels initiate at the center of flower (**Figures 13E,F**). The ovary continues to develop and enlarge in size (**Figures 13F–I**). Later three styles arise on top of the ovary. Many lobes appear on each style (**Figure 13H**) which later becomes multifid (**Figure 11K**) derived from a bifid pattern (**Figure 13I**). Antesepalous nectaries (**Figure 11I**) develop in the late ontogeny.

DISCUSSION

Petal Evolution in *Croton*

Petals are generally found in staminate flowers of *Croton* (Webster, 1993; Berry et al., 2005; van Ee et al., 2011). Filamentous structures are reported to occur in pistillate flowers in the same position as petals in staminate flowers (De-Paula et al., 2011; Gagliardi et al., 2017). In the past the filamentous structures have been interpreted either as reduced petals or as staminodes (Michaelis, 1924; Nair and Abraham, 1962; Webster, 1993; Radcliffe-Smith, 2001; Caruzo and Cordeiro, 2007; De-Paula et al., 2011; Gagliardi et al., 2017). However, fully developed petals are found in several species from two New World sections, i.e., section *Alabamenses* and section *Eluteria* subsection *Eluteria* (**Figure 2B**; van Ee et al., 2011), and some African species (Friis and Gilbert, 2008; Berry et al., 2016). The section *Alabamenses*

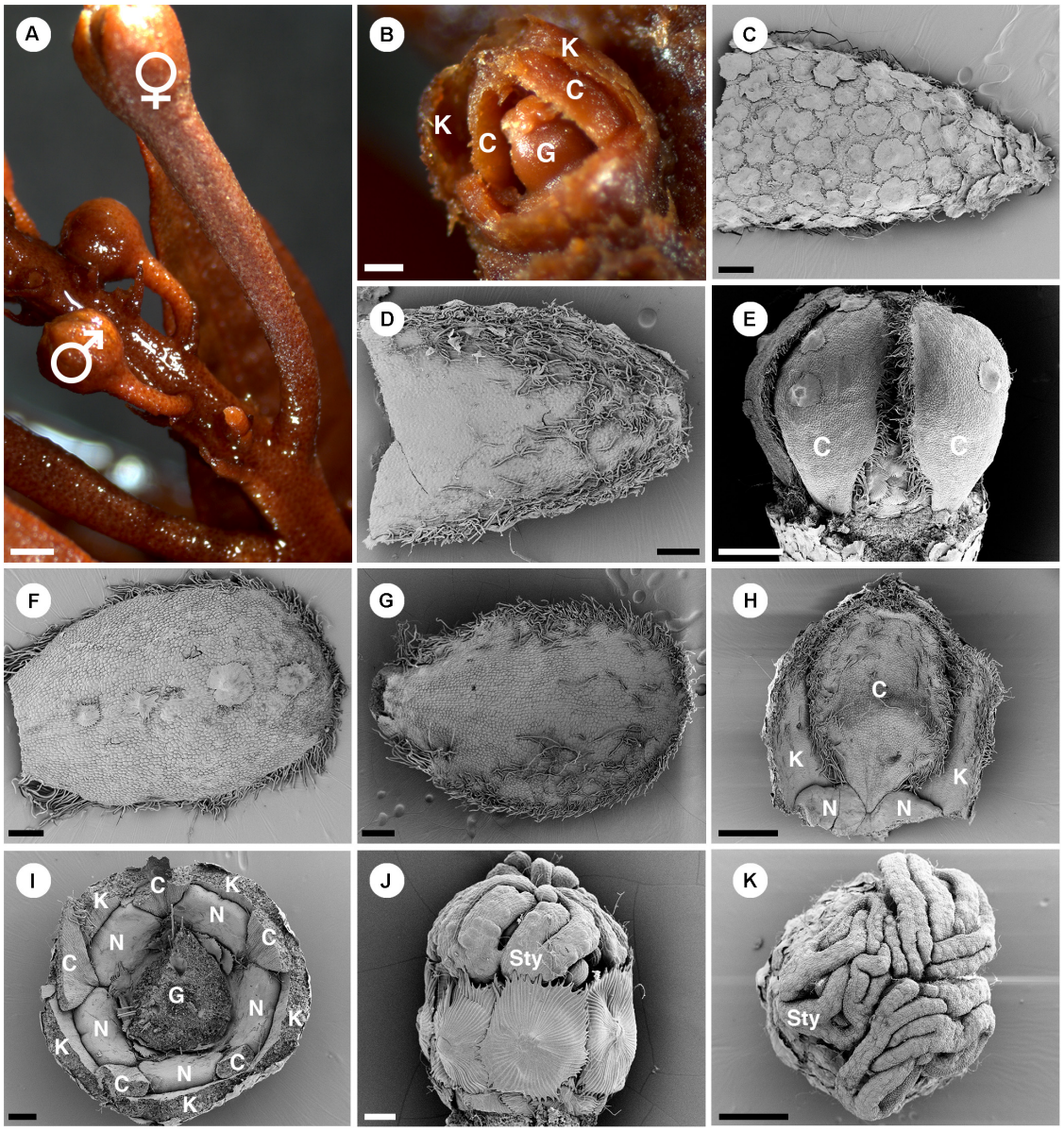

FIGURE 11 | Morphology of pistillate flowers of *Croton schiedeanus*. **(A)** An inflorescence with a pistillate flower on the lower part and many proximal staminate flower buds. The pistillate flower has a longer and thicker pedicel than staminate flower buds. **(B)** A pistillate flower bud with some sepals removed. There are petals visible within. **(C)** Abaxial side of a sepal covered completely with lepidote trichomes. **(D)** Adaxial side of a sepal with simple and stellate trichomes present. **(E)** A pistillate flower bud which calyx and nectary glands removed. Petals show a narrow base. **(F)** Abaxial side of a petal. There are few lepidote trichomes along the midrib. The margin is fimbriate. **(G)** Adaxial side of a petal. The fimbriate margin consists of crushed stellate trichomes and densely packed simple trichomes. **(H)** A petal is arranged alternating with sepals and nectaries. Note, the base looks like a claw due to the influence of the nectary expansion during development. **(I)** A flower bud in which the ovary and part of the perianth were removed. There are five bilobed nectary glands located around the ovary. **(J)** Ovary with surface covered with lepidote trichomes. There are styles on top of it. **(K)** Styles on top of an ovary with multifid stigmatic tips. K, sepal; C, petal; G, ovary; N, nectary; Sty, style. Scale bars: **(A)** = 1,000 μm; **(B–D,F,G,I)** = 200 μm; **(E,H,K)** = 500 μm; **(J)** = 100 μm.

is a monotypic group in subgenus *Quadrilobi* without any close relative with well-developed petals in pistillate flowers (van Ee et al., 2011). The section *Eluteria* (subgenus *Geiseleria*) consists of three subsections comprising 22 species (van Ee et al., 2011). The presence of well-developed petals in pistillate flowers is reported in the 15 species of subsection *Eluteria*, whereas the other two subsections lack well-developed petals in pistillate flowers (van Ee and Berry, 2009; van Ee et al., 2011). In the subgenus *Croton*, pistillate flowers with petals are found in some African species, e.g., *C. gratissimus* and *C. megalocarpus*, which are nested among other species without petals in pistillate flowers (van Ee et al., 2015; Haber et al., 2017). Therefore, it is clear

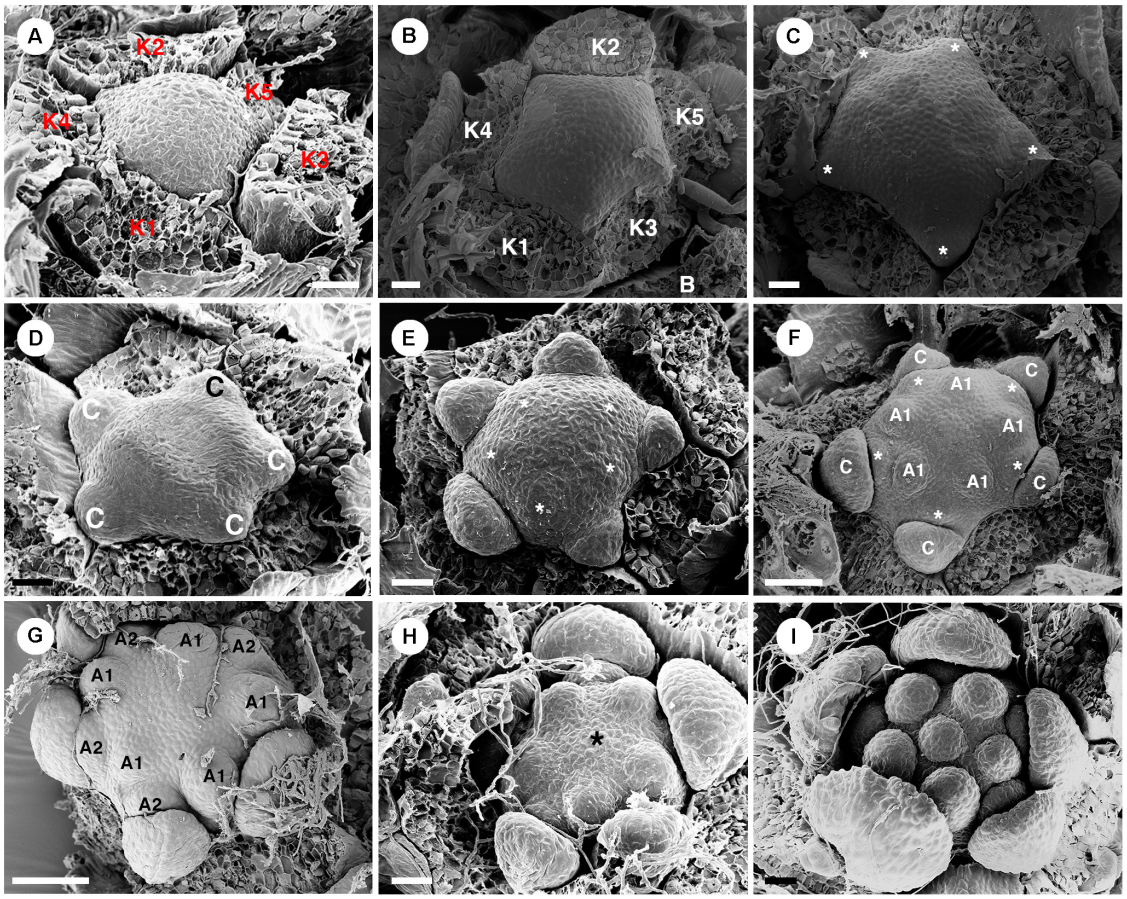

FIGURE 12 | Ontogeny of staminate flowers from *Croton schiedeanus*. **(A)** A very young flower bud with five sepals initiating first. The rest of the floral primordium has a convex shape. **(B)** Apical view of a similar stage; petal primordia start to initiate alternating with sepals. **(C)** Next, petals grow and expand (asterisk). **(D)** Petals show a unidirectional growth pattern. **(E)** Next, the first stamen whorl starts to develop on the convex receptacle alternating with petals (asterisk). **(F)** Soon, the second whorl of stamens develops centrifugally outside of the first whorl opposite petals. **(G)** Apical view of slightly older stage, two stamen whorls are visible with the outermost whorl opposite petals. **(H)** After that, a central stamen starts to initiate on the central empty space (asterisk). **(I)** Apical view of a young flower shows the completion of stamen development. K, sepal; C, petal; A, stamen. Scale bars: **(A–E,I)** = 20 μm; **(F,G)** = 50 μm.

that petals in pistillate flowers have evolved independently among distantly related groups within *Croton* (**Figure 2B**). Our study demonstrates that in the early developmental stages, petals of staminate flowers are similar to petals and filamentous structures of pistillate flowers. Petals develop as broadly based structures in alternation with sepals before the androecium or gynoecium (**Figure 5A** vs. **Figure 6C**: *C. chilensis*; **Figure 9C** vs. **Figure 9J**: *C. alabamensis*; **Figure 12C** vs. **Figure 13C**: *C. schiedeanus*). So, it is interesting to know if petals in *Croton* (and other inaperturate crotonoid taxa) have a tepalar origin (bracteopetals) or staminodial origin (andropetals). Andropetals have a delayed initiation; they develop as part of the androecium (as part of fascicles or an androecial ring primordium), and primordia are characteristically narrow and morphologically comparable to stamens (Ronse De Craene, 2008). However, petals of *Croton* in both staminate and pistillate flowers (including filamentous structures) initiate as broad primordia immediately after sepals (**Figures 5A**, **6C**, **9C,J**, **12C**, **13C**) which are characteristics of bracteopetals (Ronse De Craene, 2008). At maturity, petals of pistillate and staminate flowers are identical. The morphology of petals and sepals also appears to be highly similar, with a broad range of trichomes developing on both organs, implying that perianth parts represent homologous structures.

We consider that the strongly different morphologies of petals and filamentous structures at maturity could be explained by heterochrony. Heterochrony implies a shift in the timing of development of different organs, leading to changes in the shape of size of organs, resulting in evolutionary change. This was recognized as one of the major drivers of morphological evolution (Li and Johnston, 2000; Box and Glover, 2010; Ronse De Craene, 2018; Buendía-Monreal and Gillmor, 2018). After initiation, petals in staminate flowers continue to grow and expand throughout the whole development until maturity (**Figures 5**, **9**, **12**), while growth of pistillate petals is soon arrested or strongly delayed (**Figures 6**, **9**, **13**) suggesting an early developmental blockage of petal development (pedomorphosis). The presence of fully developed petals in pistillate flowers of *C. alabamensis* and *C. schiedeanus* suggests that in those species

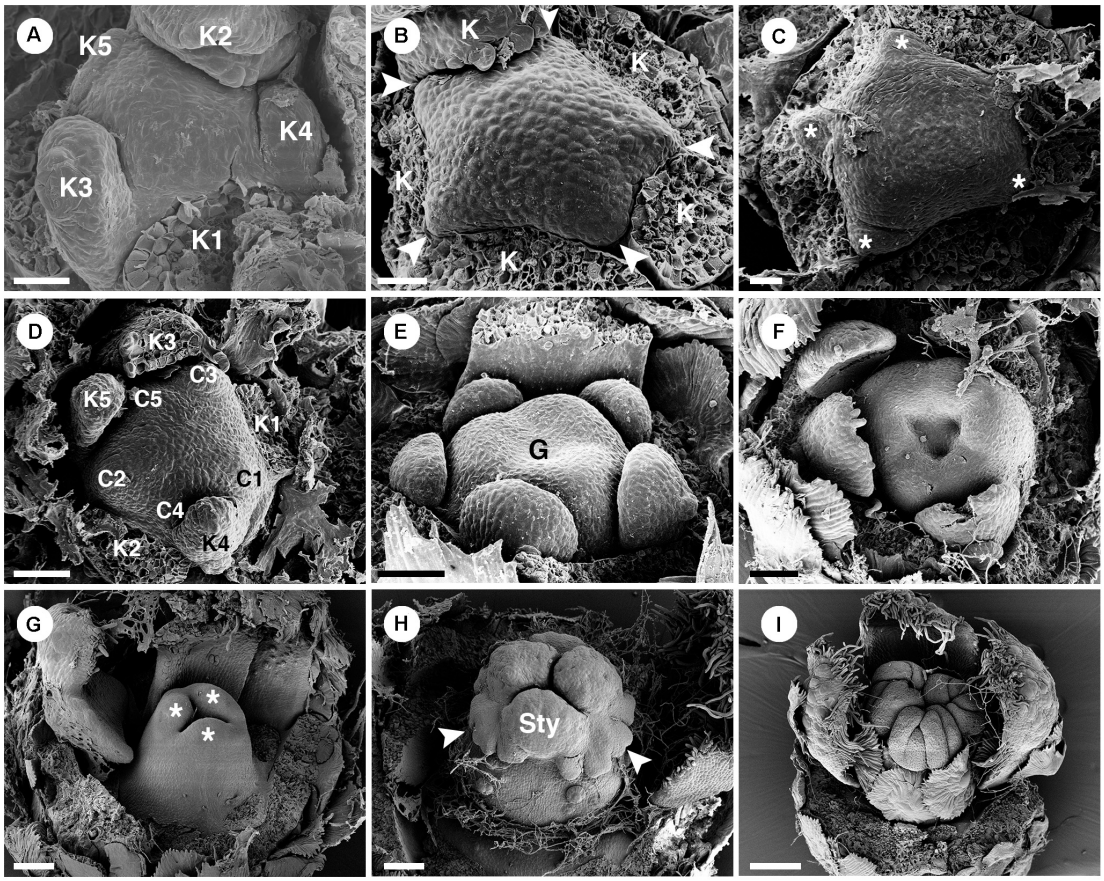

FIGURE 13 | Ontogeny of pistillate flowers of *Croton schiedeanus*. **(A)** An early stage of a flower shows unequal sepal lobes on the convex floral primordium. **(B)** Next, petal primordia start to form alternating with sepals (arrowhead). **(C)** Apical view of older stage; petals start to expand surrounding the convex receptacle (asterisk). **(D)** View of a similar stage shows unequal growth of petals. **(E)** Next, an ovary initiates with three fused carpels. Note, petals continue to grow in a unidirectional pattern. **(F)** An old flower bud shows expansion of petals and ovary. **(G)** Stage of ovary closure. The lobe on top of each carpel starts to form a style (asterisk). **(H)** Three styles are formed on top of the ovary. Note, there are many lobes visible (arrowhead). **(I)** Later, styles dissected into many parts. K, sepal; C, petal; G, ovary; Sty, style. Scale bars: **(A–C)** = 20 μm; **(D–F)** = 5 0μm; **(G)** = 90 μm; **(H)** = 100 μm; **(I)** = 150 μm.

there is a reversal of the process. One could speculate that the presence of fully developed petals in pistillate flowers resembles the ancestral condition. However, *C. alabamensis*, *C. schiedeanus* (sect. *Eluteria*) and the above-mentioned African species are nested in clades containing other *Croton* species having no petals in pistillate flowers (**Figure 2B**; Berry et al., 2005; van Ee et al., 2011, 2015), suggesting that the absence of fully developed petals is plesiomorphic in these clades. Most of the genera in tribe Crotoneae also lack fully developed petals in pistillate flowers (**Figure 2B**; Webster, 2014; Silva et al., 2020). However, among them only pistillate flowers of *Sandwithia* are reported to have miniature petals (Lanjouw, 1932; Secco, 1987; P. Thaowetsuwan, unpublished data). Outside Crotoneae, petals in pistillate flowers are present in several groups. In the tribe Jatropheae, a sister tribe of the Crotoneae, all three genera, i.e., *Jatropha*, *Joannesia,* and *Vaupesia*, have petals in both staminate and pistillate flowers (Velloso, 1798; Ducke, 1922; Schultes, 1955; Dehgan and Webster, 1979; Radcliffe-Smith, 2001; Webster, 2014). Moreover, *Grossera, Cavacoa, Leeuwenbergia,* and *Dodecastigma*, which are in lower grades of another *inaperturate crotonoid clade*, are reported to have petals in pistillate flowers as well (Radcliffe-Smith, 2001; Webster, 2014; van Welzen et al., 2020). Therefore, the presence of fully developed petals may be an ancestral character of the inaperturate crotonoids (clade C1 and C2 of the subfamily Crotonoideae following Wurdack et al., 2005). However, the articulated crotonoid clade and Gelonieae clade, at the basal nodes of the subfamily Crotonoideae, do not have petals (**Figure 2B**; Radcliffe-Smith, 2001; Wurdack et al., 2005; Webster, 2014).

Since fully developed petals occur in groups distantly related with *Croton* (**Figure 2B**), one could consider the occurrence of fully developed petals in pistillate flowers of some *Croton* species as a case of "homoplasy." However, combining both phylogenetic and ontogenetic perspectives, we conclude that this phenomenon is preferably explained as an "apomorphic tendency" (or cryptic apomorphy). This represents a morphological character (fully developed petals in pistillate flowers) that appears in some members but not in all species (*Croton*) and can be genetically

switched on or off because of deeply shared genetic attributes. As a result this character is not recognized as a synapomorphy on the phylogenetic tree (**Figure 2B**; Endress, 2003; Endress and Matthews, 2006; Ronse De Craene, 2010, 2018). Our idea is supported by the mixture of petal-like and filamentous structures in some pistillate flowers from various species of *Croton* (**Figure 4F**; P. Thaowetsuwan, unpublished data). The reduction of petals in pistillate flowers may also be explained by a shift in B gene expression. In *Arabidopsis*, the mutation of *AP3* and *PI genes* (B-class genes) results in the transformation of petals into sepals and stamens into carpels (Bowman et al., 1991; Jack et al., 1992; Goto and Meyerowitz, 1994; Litt and Kramer, 2010; Rijpkema et al., 2010). In strongly heteromorphic species, pistillate flowers often have reduced petals or lack petals altogether, as in *Croton* (e.g., *Gunnera* in Gunneraceae: Ronse De Craene and Wanntorp, 2006; *Grevea* in Montiniaceae: Ronse De Craene, 2016; *Myriophyllum* in Haloragaceae: Kubitzki, 2007). This suggests that petal reduction is linked to a shifting balance of B-genes responsible for petal identity in these plants. A reduced B-gene expression may be responsible for the reduction of petals to small appendages, and in the case of *Croton schiedeanus* and *C. alabamensis* a reversed shift might be the cause of a strong petal morphology.

Mechanical pressure is another important factor that shapes the morphology of floral organs (Ronse De Craene, 2018). We found that the growth and mature morphology of petals in *Croton* is affected by the pressure exercised on the flower bud during development. As filamentous structures develop more slowly than well-developed petals, they are more prone to be squeezed between the enclosing calyx and the massive ovary. As a result, the filamentous structures become long and narrowly shaped (**Figures 4F**, **6J,K**) differing greatly from fully developed petals. The morphology of fully developed petals in pistillate flowers is also shaped by the alternating nectary glands in both staminate and pistillate flowers (**Figures 4A,F**, **6L**). However, nectary glands in pistillate flowers are much larger and sometimes confluent in a ring. Pressure from adjacent nectary glands induce the petals in pistillate flowers to have a very narrow base resembling clawed petals or staminodial structures (**Figures 11H,I**). However, with ontogenetic data, we could confirm that the petals of pistillate flowers represent bracteopetals and the claw-like morphology is a result of spatial pressure from nectary glands in the later stages.

We could not find any concrete evidence of ecological factors that lead to the development of fully developed petals in pistillate flowers. Evolutionary pressure from flower-insect interaction may be an important factor. However, very little attention has been paid to pollination studies in *Croton*. Three pollination syndromes were reported in *Croton*, e.g., wind pollination (Domínguez et al., 1989), insect pollination (Freitas et al., 2001; Pires et al., 2004; Narbona and Dirzo, 2010), or mixed pollination (Novo et al., 2010). However, those studies were conducted in few species of *Croton*. *C. alabamensis* was initially reported to have wind pollination but later observation suggested insect pollination, supported by the presence of nectaries in both genders (van Ee et al., 2006). It is known that all pistillate flowers of *Croton* have nectar producing glands surrounding the ovary to attract insects. The presence of petals in pistillate flowers may help increase flower visibility. However, petals in *Croton* are generally green or white in color similar to sepals and may not contribute to insect attraction (**Figures 1C**, **3A,I**). We also observed in the present study that in two *Croton* species with fully developed petals, there are fewer pistillate flowers in the inflorescence, suggesting that the presence of petals may increase the chance of pollination; however, many other *Croton* species possess a smaller number of pistillate flowers in inflorescences without having fully developed petals (P. Thaowetsuwan, unpublished data). All neotropical *Croton* and African species with petals in pistillate flowers also have lepidote trichomes. However, we think that this association is just a coincidence because other *Croton* with lepidote trichomes do not have fully developed petals in pistillate flowers (P. Thaowetsuwan, unpublished data; van Ee et al., 2011). Further interdisciplinary studies, including genetics, pollination ecology, and morphology, are needed to clarify the presence of fully developed petals in pistillate flowers of some *Croton*.

The Interpretation of Nectaries in *Croton*

Nectaries are either found as five bilobed antesepalous nectaries or as an interrupted nectary ring in both staminate and pistillate flowers of all three species (**Figures 3J**, **4D**, **7G**, **8G**, **10F**, **11I**). Nectary lobes appear bilobed in pistillate flowers, apparently developing as two primordia adjacent to each petal (total of ten) which later expand and fuse together (see De-Paula et al., 2011). However, closer detail reveals that the nectary develops from a rim of tissue below the ovary and becomes increasingly dissected by the intervening filamentous structures (**Figures 6E–I**). We could not observe the initiation stage of the nectary primordia in staminate flowers. However, results from a previous study suggest the emergence of a single primordium (De-Paula et al., 2011). In staminate flowers of *C. alabamensis*, however, there are ten nectary lobes alternating with petals and stamens, arranged into five horse-shoe shaped nectaries clasping the base of the outermost stamens (**Figure 7G**). We hypothesized that during development, nectary glands initiate alternating with the petals similar to other species of *Croton* (**Figure 2C**). However, this space is already occupied by stamens in *C. alabamensis*. Therefore, the nectary glands develop preferentially on the available space (adjacent to stamens/petals) rather than opposite the sepals (**Figure 7G**).

Throughout the genus, nectaries of pistillate flowers are variously fused, often in a ring at the base of the gynoecium (Freitas et al., 2001; Caruzo and Cordeiro, 2007; De-Paula et al., 2011) while nectaries of staminate flowers are generally free (P. Thaowetsuwan, unpublished data; De-Paula et al., 2011). Different authors interpreted the origin of nectaries either as receptacular outgrowths (Caruzo and Cordeiro, 2007) or as transformed staminodes (De-Paula et al., 2011; Gagliardi et al., 2017). De-Paula et al. (2011) interpreted nectaries as secretory staminodes based on their antesepalous position in the flower, despite their late initiation. Ronse De Craene and Smets (2001) suggested that staminodes can be transformed into nectaries with a retention of the original stamen vasculature diverging from the stele (e.g., *Harungana*, Hypericaceae; *Averrhoa*, Oxalidaceae). However, in *Croton*, the nectaries are generally not supplied by

a clear whorl of bundles as would be the case with stamen-derived nectaries (as in *Harungana* of Hypericaceae: Ronse de Craene and Smets, 1991a). Instead, nectaries from most species are supplied by traces derived from sepal bundles (De-Paula et al., 2011). Moreover, nectaries in some species of *Jatropha* were found to be supplied by vascular bundles from both sepals and petals, or from petals alone (Venkata-Rao and Ramalakshmi, 1968). Venkata-Rao and Ramalakshmi (1968) interpreted the nectary of *Jatropha* as of receptacular origin because they are not supplied by bundles from the floral stele. In the Crotoneae genus *Acidocroton*, non-vascularized multi-lobed nectary glands are present forming a ring around the androecium in staminate flowers or the gynoecium in pistillate flowers (P. Thaowetsuwan, unpublished data; Fawcett and Rendle, 1920). Further expansion of the nectary into the androecial zone forming a honeycomb-like nectary is observed in some *Acidocroton* species, emphasizing the variability of the nectary development in the tribe (P. Thaowetsuwan, unpublished data). Vascular connections in *Croton* appear to be opportunistic, since non-vascularized nectaries have also been reported in *C. bonplandianus* (Venkata-Rao and Ramalakshmi, 1968), *C. sarcopetalus* (Freitas et al., 2001), and in the related genus *Astraea* (De-Paula et al., 2011). Non-vascularized floral nectaries were also found in the genus *Brasiliocroton*, the sister genus of *Croton* (P. Thaowetsuwan, unpublished data). The late initiation, variation in number and shape, as well as the variability in its vasculature have been used as criteria to justify the interpretation of the floral nectary in the family Brassicaceae as of receptacular origin (Arber, 1931; Bowman and Smyth, 1998). A similar variability in shape, number, development and opportunistic vascular connections was found in the genus *Croton*, supporting a receptacular origin of the nectaries in the genus, while the only argument supporting the staminodial origin is their antesepalous (alternipetalous) position. Considering the nectary as of receptacular origin, links the floral morphology of Euphorbiaceae with other families in the order Malpighiales. A systematic survey by Bernardello (2007) suggests that most nectaries of Malpighiales are of receptacular (and hypanthial) origin, with the occasional presence of staminodial nectaries, e.g., Bonnetiaceae, some Clusiaceae and Linaceae. Interpreting the nectaries as staminodial in *Croton* because of their position in alternation with the other stamens is a static approach that does not consider the spatial constraints during development, where space is mostly available between the petals. The outer stamen whorl in most *Croton* is antepetalous and the greatest space for the late development of nectaries is in antesepalous position. The presence of horse-shoe shaped nectaries clasping the stamen bases in staminate flowers of *C. alabamensis* (**Figure 7G**) also show plasticity of nectary position supporting the interpretation of a receptacular origin.

Floral Diversity in Staminate Flowers

Our observations suggest that diversity of structures and their development in staminate flowers of *Croton* is unexpectedly high. At maturity, the receptacle of staminate flowers of *C. chilensis* and *C. schiedeanus* is convex, as reported in many species from previous studies (Michaelis, 1924; De-Paula et al., 2011; Gagliardi et al., 2017) while *C. alabamensis* has a concave receptacle in the form of a hypanthium (**Figures 2C**, **7G,H**, **9**). Cup-shaped flowers of *C. alabamensis* were reported before (Ginzbarg, 1992) but it has never been considered to be unique among the genus *Croton* before. A similar condition has been found in staminate flowers from other Crotoneae genera, viz., *Sagotia racemosa* (slightly concave) and *Brasiliocroton muricatus* (flat receptacle), but in those species, stamens fully occupy the floral apex area, contrary to *C. alabamensis* with a central empty space (P. Thaowetsuwan, unpublished data).

Moreover, our observation found that the second whorl of stamens from all three species develops centrifugally opposite to petals (**Figures 5**, **9**, **12**). In *C. schiedeanus*, this whorl appears to be the outermost whorl throughout the whole ontogeny (**Figures 2C**, **10G**, **12**) as was previously reported for other *Croton* species (De-Paula et al., 2011). In early stages of development of *C. chilensis*, the alternipetalous whorl is the outermost whorl (**Figures 5G–N**) while at anthesis, it is the antepetalous whorl (**Figures 2C**, **3A**). This shift in stamen position in *C. chilensis* could be explained by the fact that in the early stages, growth of the outermost antepetalous stamens is restricted by the expanding petals. Therefore, the alternipetalous whorl appears to be outermost and the first to arise. In later stages, nectary glands which develop on the empty space opposite the sepals emphasize the more central position of the alternipetalous stamen whorl. Finally, at anthesis petals start to spread out, allowing the antepetalous stamens to appear as the outermost whorl. *Croton alabamensis* also has a centrifugal stamen development but with the alternipetalous stamens as the initially smaller outermost whorl, while antepetalous stamens are initially larger and arranged as an inner whorl (**Figures 7H**, **9D–I**). One possible explanation is that the vertical expansion of the hypanthium makes petals appear in a higher position than the stamen developing zone (**Figure 9D**), eliminating pressure from petals on the stamen primordia; therefore, antepetalous stamens have the possibility to emerge first or at least grow faster.

The centrifugal stamen development is unusual among angiosperms. This phenomenon is normally linked with a high stamen number (polyandry) (Corner, 1946; Ronse De Craene and Smets, 1992; Rudall, 2010, 2011). However, staminate flowers of *Croton* generally have about 11–16 stamens (P. Thaowetsuwan, unpublished data) which fall in the range of oligandry (flowers with the number of stamen two times the number of petals) to lower scale polyandry (flowers with the number of stamens much higher than petals). The development of the androecium in *Croton* is also different from other patterns of centrifugal stamen development, which is caused by a subdivision of primordia and represent a secondary stamen increase (cf. Ronse De Craene and Smets, 1992). Some cases of centrifugal stamen development in oligandric and lower-polyandric flower were reported before (**Table 2**). The centrifugal stamen development has often been linked with a reduction from ancestral flowers with polyandric centrifugal stamen development (Corner, 1946; Leins and Erbar, 1994). Alternatively, a centrifugal stamen development in oligandric flowers is interpreted as the result of a shift linked with obdiplostemony (Ronse De Craene and Bull-Hereñu, 2016). However, as discussed in Ronse De Craene and

TABLE 2 | Examples of centrifugal stamen development in oligandric and lower-polyandric flowers.

Species/Family	Stamen arrangement*	References
Arabidopsis thaliana (L.) Heynh./Brassicaceae	A $\overleftarrow{2}$ + **4**	Smyth et al., 1990
Asarum caudatum Lindl./Aristolociaceae	A $\overleftarrow{3}$ + $\overleftarrow{3}$ + **6**	Leins and Erbar, 1985
Bruguiera parviflora (Roxb.) W. A. ex Griff./Rhizophoraceae	A $\overleftarrow{7}$-$\overleftarrow{8}$ + **7–8**	Juncosa and Tomlinson, 1987
Callisia Loefl. & *Tradescantia* L./Commelinaceae	A $\overleftarrow{3}$ + **3**	Payer, 1857; Hardy and Stevenson, 2000
Combretum indicum (L.) DeFillps/Combretaceae	A $\overleftarrow{5}$ + **5**	Payer, 1857
Hibbertia (= Adrastaea) salicifolia (DC.) F.Muell./Dilleniaceae	A $\overleftarrow{5}$ + **5**	Tucker and Bernhardt, 2000
Monococcus echinophorus F.Muell./Petiveriaceae	A $\overleftarrow{2}$ **4**** (total 12 stamens)	Vanvinckenroye et al., 1997
Nitraria L. & *Peganum* L./Nitrariaceae	A $\overleftarrow{2}$ **5**** (total 15 stamens)	Ronse de Craene and Smets, 1991b; Ronse De Craene et al., 1996; Bachelier et al., 2011
Suriana maritima L./Surianaceae	A $\overleftarrow{3^{\circ}}$ + **5**	Bello et al., 2008
Visnea mocanera L.f./Pentaphyllaceae	A $\overleftarrow{10}$ + **5**	Payer, 1857
Astraea and *Croton*/Euphorbiaceae	A $\overleftarrow{5}$ + **5** + n***; A $\overleftarrow{5}$ + **5** + 5 + n***; A $\overleftarrow{5}$ + **5** + 5 + 5 + n***	De-Paula et al., 2011 and the present study

*Family names follow APG IV systems. *Left-to-right arrangement represents outermost to innermost stamen whorls. Numbers in bold indicates the first whorl to develop. Centrifugal whorls were indicated with an uppercase arrow. **Indicate centrifugal secondary increase of stamens from a common fascicle. ***Variable number ranging from 1 to 5.*

Bull-Hereñu (2016), a shift in position is linked with differential growth processes associated with pressures in the flower. The different shifts in position of outer alternipetalous stamens in the investigated *Croton* are caused by differential pressures during the development of the flower. For *Croton*, it is possible that polyandry is a derived character since it is mostly found in subgenus *Adenophylli* (van Ee et al., 2011). Moreover, previously described cases of oligandric centrifugal stamen development occur in bisexual flowers, while centrifugal stamen development in unisexual (staminate) flowers is rare. There are few reports of this phenomenon in staminate flowers of Phytelephantoid palms (Uhl and Moore, 1977), *Populus* in Salicaceae (Kaul, 1995), *Medusagyne oppositifolia* in Ochnaceae (Ronse De Craene, 2017) and *Monococcus echinophorus* in Petiveriaceae (Vanvinckenroye et al., 1997), but those developmental patterns are different from the one found in *Croton* (**Table 2**). Therefore, centrifugal stamen development in unisexual oligandric to lower-polyandric flowers such as *Croton* and *Astraea,* may be a unique feature. So far there is no floral ontogenetic study in other genera in the tribe Crotoneae apart of *Astraea* and *Croton*. Since the presence of centrifugal stamen development appears in all previous studied *Croton*, and also *Astraea* (De-Paula et al., 2011), we hypothesize that this developmental pattern may be present in the ancestor of *Croton* and perhaps in the common ancestor of *Croton* and *Astraea* too. Further studies in other genera in the tribe Crotoneae are needed to confirm our hypothesis.

The presence of the outermost stamen whorl opposite to the petals is found in all previously investigated *Croton* (and also *Astraea*) (Baillon, 1858; Marchand, 1860; Michaelis, 1924; Nair and Abraham, 1962; Venkata-Rao and Ramalakshmi, 1968; Gandhi and Thomas, 1983; De-Paula et al., 2011; Gagliardi et al., 2017) and is likely an ancestral character. In the present study, the arrangement of stamens with the alternipetalous stamens as an outermost whorl is almost unique for *C. alabamensis* and has never been reported in *Croton* before. The only other case of the alternipetalous stamen whorl as an outermost whorl is found in some species of *Croton* section *Moacroton* [Figure 1F in van Ee et al., 2008 (*C. ekmanii*); P. Thaowetsuwan, unpublished data] which is a specialized group adapted to serpentine soils found in the Caribbean islands (Borhidi, 1991). Despite *C. alabamensis* and *Croton* section *Moacroton* belonging to the same subgenus *Quadrilobi*, they are not closely related (van Ee et al., 2008, 2011). Therefore, the presence of the alternipetalous outermost whorl should be considered as the result of parallel evolution (cf. Vasconcelos et al., 2017). *Croton alabamensis* and *Croton* section *Moacroton* (except *C. poecilanthus* and *C. maestrensis*) also share the presence of non-inflexed stamens which is unique among all *Croton* species (Berry et al., 2005; van Ee et al., 2008, 2011). Nevertheless, stamen morphology from these two groups is different.

Inner stamen whorls of *Croton chilensis* show great variation in number and arrangement among different flowers. The variation may be influenced by spatial constraints between adjacent organs, which result in a different floral architecture in each flower. Developmental irregularity could occasionally happen as shown in a staminate flower of *C. fuscescens* (section *Julocroton*) from De-Paula et al. (2011). However, our

observations found that irregular stamen development occurs more often in *Croton* subgenus *Adenophylli* in which many species have high stamen numbers (more than 20 stamens) leading to more than 100 stamens in some species from the medusae group in section *Cyclostigma* (P. Thaowetsuwan, unpublished data). Further studies on *Croton* with very high stamen numbers (section *Adenophylli*, section *Cyclostigma*), and very low numbers (section *Moacroton*, section *Crotonopsis*, section *Eremocarpus*, *C. monanthogynus*, etc.) may reveal novel stamen development patterns.

CONCLUSION

Our study reveals that floral development in both staminate and pistillate flowers of three species of *Croton* is highly diverse. Staminate flowers show a high variation of stamen number and development of the androecium that can be linked to spatial constraints during development. Sepals and petals in *Croton* are recognized as homologous structures, with petals equivalent to bracteopetals. In pistillate flowers, a heterochronic shift is responsible for the development of filamentous structures as under-developed petals. The presence of fully developed petals in *C. alabamensis* and *C. schiedeanus* suggests the independent reversal of this process and represents apomorphic tendencies rather than homoplasies. Nectaries are demonstrated to have a receptacular origin rather than staminodial, as supported by developmental and anatomical evidence.

Being a mega-diverse genus of the family Euphorbiaceae, *Croton* represents a great model system for the study of floral evolution. However, there have been few detailed floral morphological investigations until now, possibly hampered by the small size of flowers. We hope that this study will trigger further investigations on the floral ontogeny of *Croton* and other Euphorbiaceous genera to explore the evolutionary dynamics of their floral morphology.

DATA AVAILABILITY STATEMENT

The raw data supporting the conclusions of this article will be made available by the authors, without undue reservation, to any qualified researcher.

AUTHOR CONTRIBUTIONS

PT: manuscript preparation, experiment design, and conducting the experiment. SR: manuscript preparation, and conducting the experiment. RR: manuscript preparation and sample provision. LR: manuscript preparation and experiment design. All authors contributed to the article and approved the submitted version.

FUNDING

PT was funded by the Development and Promotion of Science and Technology talents project (DPST) Scholarship, Royal Thai Government. SR was supported by the Scottish International Education Trust. The Royal Botanic Garden Edinburgh was supported by the Scottish Government's Rural and Environment Science and Analytical Services Division.

ACKNOWLEDGMENTS

We thank Lady Bird Johnson Wild Flower Center/Texas, USA for seeds of *C. alabamensis* var. *taxensis*. We also thank Gunnar Ovstebo and the horticultural team at RBGE for growing and maintaining living collections of *Croton*. Technical assistance of Frieda Christie with light microscopy and scanning electron microscopy is acknowledged. This paper is part of the Ph.D. thesis of the PT funded by the Development and Promotion of Science and Technology talents project (DPST) Scholarship, Royal Thai Government and the MSc dissertation of the second author supported by The Scottish International Education Trust.

REFERENCES

Arber, A. (1931). Studies in floral morphology. I. On some structural features of the cruciferous flower 1. *New Phytol.* 30, 11–41. doi: 10.1111/j.1469-8137.1931.tb07402.x

Bachelier, J. B., Endress, P. K., and Ronse De Craene, L. P. (2011). "Comparative floral structure and development of Nitrariaceae (Sapindales) and systematic implications," in *Flowers on the Tree of Life*, eds L. Wanntorp and L. Ronse De Craene (Cambridge: Cambridge University Press), 181–217. doi: 10.1017/CBO9781139013321.008

Baillon, H. (1858). *Etude Générale Du Groupe Des Euphorbiacées*. Paris: V. Masson.

Bello, M. A., Hawkins, J. A., Rudall, P. J., Bello, M. A., Hawkins, J. A., and Rudall, P. J. (2008). Floral morphology and development in Quillajaceae and Surianaceae (Fabales), the species-poor relatives of Leguminosae and Polygalaceae. *Ann. Bot.* 101, 1433–1434. doi: 10.1093/aob/mcn073

Bernardello, G. (2007). "A systematic survey of floral nectaries," in *Nectaries and Nectar*, eds S. W. Nicolson, M. Nepi, and E. Pacini (Dordrecht: Springer), 19–128. doi: 10.1007/978-1-4020-5937-7_2

Berry, P. E., Hipp, A. L., Wurdack, K. J., Van Ee, B., and Riina, R. (2005). Molecular phylogenetics of the giant genus *Croton* and tribe *Crotoneae* (*Euphorbiaceae sensu* stricto) using ITS and *TrnL-TrnF* DNA sequence data. *Am. J. Bot.* 92, 1520–1534. doi: 10.3732/ajb.92.9.1520

Berry, P. E., Van Ee, B. W., Kainulainen, K., and Achtemeier, L. (2016). *Croton cupreolepis* (Euphorbiaceae), a new coppery-lepidote tree species from eastern Madagascar. *Syst. Bot.* 41, 977–982. doi: 10.1600/036364416X694099

Borhidi, A. (1991). *Phytogeography and Vegetation Ecology Of Cuba*. Budapest: Akadémiai Kiadó.

Bowman, J. L., and Smyth, D. R. (1998). Patterns of petal and stamen reduction in Australian species of *Lepidium* L. (Brassicaceae). *Intern. J. Plant Sci.* 159, 65–74. doi: 10.1086/297522

Bowman, J. L., Smyth, D. R., and Meyerowitz, E. M. (1991). Genetic interactions among floral homeotic genes of *Arabidopsis*. *Development* 112, 1–20.

Box, M. S., and Glover, B. J. (2010). A plant developmentalist's guide to paedomorphosis: reintroducing a classic concept to a new generation. *Trends Plant Sci.* 15, 241–246. doi: 10.1016/j.tplants.2010.02.004

Buendía-Monreal, M., and Gillmor, C. S. (2018). The times they are A-changin': heterochrony in plant development and evolution. *Front. Plant Sci.* 9:1349. doi: 10.3389/fpls.2018.01349

Caruzo, M. B. R., and Cordeiro, I. (2007). Sinopse da tribo Crotoneae dumort (Euphorbiaceae s.s.) no Estado de São Paulo, Brasil. *Hoehnea* 34, 571–585. doi: 10.1590/S2236-89062007004000011

Corner, E. J. H. (1946). Centrifugal stamens. *J. Arnold Arbor.* 27, 423–437.

Dehgan, B., and Webster, G. L. (1979). Morphology and infrageneric relationships of the genus *Jatropha* Euphorbiaceae. *Univer. Calif. Public. Bot.* 74, 1–73.

De-Paula, O. C., das Graças Sajo, M., Prenner, G., Cordeiro, I., and Rudall, P. J. (2011). Morphology, development and homologies of the perianth and floral nectaries in *Croton* and *Astraea* (Euphorbiaceae-Malpighiales). *Plant Syst. Evol.* 292, 1–14. doi: 10.1007/s00606-010-0388-389

Domínguez, C. A., Dirzo, R., Bullock, S. H., and Dominguez, C. A. (1989). On the function of floral nectar in *Croton suberosus* (Euphorbiaceae). *Oikos* 56:109. doi: 10.2307/3566093

Ducke, A. (1922). Plantes ouvelles ou peu connues de la région amazonienne. *Archiv. Jardim Botânico do Rio de Janeiro* 3, 269.

Endress, P., and Matthews, M. (2006). Elaborate petals and staminodes in eudicots: diversity, function, and evolution. *Org. Div. Evol.* 6, 257–293. doi: 10.1016/j.ode.2005.09.005

Endress, P. K. (1994). *Diversity and Evolutionary Biology Of Tropical Flowers*. Cambridge: Cambridge University Press.

Endress, P. K. (2003). "What should a 'complete' morphological phylogenetic anaylsis entail?," in *Deep Morphology: Towards A Renaissance Of Morphology In Plant Systematics*, eds T. F. Stuessy, V. Mayer, and E. Hörandl (Liechtenstein: Ganter Verlag), 131–164.

Endress, P. K. (2008). Perianth biology in the basal grade of extant angiosperms. *Intern. J. Plant Sci.* 169, 844–862. doi: 10.1086/589691

Endress, P. K. (2010). Flower structure and trends of evolution in eudicots and their major subclades. *Ann. Missouri Bot. Garden* 97, 541–583. doi: 10.3417/2009139

Erbar, C., Kusma, S., and Leins, P. (1998). Developmental and interpretation of nectary organs in Ranunculaceae. *Flora* 194, 317–332. doi: 10.1016/s0367-2530(17)30920-9

Fawcett, W., and Rendle, A. B. (1920). *Flora of Jamaica, Containing Descriptions Of The Flowering Plants Known From The Island Vol. 4 Dicotyledons Family Leguminosae to Callitrichae*. London: The trustees of the british museum.

Freitas, L., Bernardello, G., Galetto, L., and Paoli, A. A. S. (2001). Nectaries and reproductive biology of *Croton sarcopetalus* (Euphorbiaceae). *Bot. J. Linnean Soc.* 136, 267–277. doi: 10.1111/j.1095-8339.2001.tb00572.x

Friis, I., and Gilbert, M. G. (2008). *Croton megalocarpoides* sp. nov. an arborescent Euphorbiaceae from semi-evergreen vegetation in S Somalia and E Kenya. *Nordic J. Bot.* 4, 327–331. doi: 10.1111/j.1756-1051.1984.tb01503.x

Gagliardi, K. B., Cordeiro, I., and Demarco, D. (2016). Protection and attraction: bracts and secretory structures in reduced inflorescences of Malpighiales. *Flora* 220, 52–62. doi: 10.1016/j.flora.2016.02.003

Gagliardi, K. B., Cordeiro, I., and Demarco, D. (2017). Flower development in species of *Croton* (Euphorbiaceae) and its implications for floral morphological diversity in the genus. *Austr. J. Bot.* 65:538. doi: 10.1071/BT17045

Gandhi, K. N., and Thomas, R. D. (1983). A note on the androecium of the genus *Croton* and flowers in general of the family Euphobiaceae. *Phytologia* 54, 6–8.

Ginzbarg, S. (1992). A new disjunct variety of *Croton alabamensis* (Euphorbiaceae) from Texas. *SIDA Contribut. Bot.* 15, 41–52.

Goto, K., and Meyerowitz, E. M. (1994). Function and regulation of the *Arabidopsis* floral homeotic gene *PISTILLATA*. *Genes Dev.* 8, 1548–1560. doi: 10.1101/gad.8.13.1548

Govaerts, R., Frodin, D. G., and Radcliffe-Smith, A. (2000). *World Checklist And Bibliography Of Euphorbiaceae (And Pandaceae) 2*. Kew: Royal Botanic Garden Kew.

Haber, E. A., Kainulainen, K., Van Ee, B. W., Oyserman, B. O., and Berry, P. E. (2017). Phylogenetic relationships of a major diversification of *Croton* (Euphorbiaceae) in the western Indian Ocean region. *Bot. J. Linn. Soc.* 183, 532–544. doi: 10.1093/botlinnean/box004

Hardy, C. R., and Stevenson, D. W. (2000). Floral Organogenesis in some species of *Tradescantia* and *Callisia* (Commelinaceae). *Int. J. Plant Sci.* 161, 551–562. doi: 10.1086/314279

Horn, J. W., van Ee, B. W., Morawetz, J. J., Riina, R., Steinmann, V. W., Berry, P. E., et al. (2012). Phylogenetics and the evolution of major structural characters in the giant genus *Euphorbia* L.(Euphorbiaceae). *Mol. Phyl. Evol.* 63, 305–326. doi: 10.1016/j.ympev.2011.12.022

Jack, T., Brockman, L. L., and Meyerowitz, E. M. (1992). The homeotic gene APETALA3 of *Arabidopsis thaliana* encodes a MADS box and is expressed in petals and stamens. *Cell* 68, 683–697. doi: 10.1016/0092-8674(92)90144-2

Juncosa, A. M., and Tomlinson, P. B. (1987). Floral development in mangrove *Rhizophoraceae*. *Am. J. Bot.* 74, 1263–1279. doi: 10.1002/j.1537-2197.1987.tb08740.x

Kaul, R. B. (1995). Reproductive structure and organogenesis in a cottonwood, *Populus deltoides* (Salicaceae). *Int. J. Plant Sci.* 156, 172–180. doi: 10.1086/297238

Kosuge, K. (1994). Petal evolution in Ranunculaceae. *Plant Syst. Evol. Suppl.* 8, 185–191. doi: 10.1007/978-3-7091-6910-0_11

Kubitzki, K. (2007). "Haloragaceae," in *The Families And Genera Of Vascular Plants Volume IX Flowering Plants. Eudicots Berberidopsidales, Buxales, Crossosomatales, Fabales p.p., Geraniales, Gunnerales, Myrtales p.p., Proteales, Saxifragales, Vitales, Zygophyllales, Clusiaceae Alliance, Passifloraceae Alliance, Dilleniaceae, Huaceae, Picramniaceae, Sabiaceae*, ed. K. Kubitzki (London: Springer), 184–190.

Lanjouw, J. (1932). Contributions to the flora of tropical America: XI. *Bull. Miscellan. Inform.* 1932:183. doi: 10.2307/4118526

Leins, P., and Erbar, C. (1985). Ein beitrag zur blütenentwicklung der aristolochiaceen, einer vermittlergruppe zu den monokotylen. *Bot. Jahrb. Syst.* 107, 343–368.

Leins, P., and Erbar, C. (1994). Flowers in Magnoliidae and the origin of flowers in other subclasses of the angiosperms II. The relationships between flowers of Magnoliidae, Dilleniidae, and Caryophyllidae. *Plant Syst. Evol. Suppl.* 8, 209–218. doi: 10.1007/978-3-7091-6910-0_13

Li, P., and Johnston, M. O. (2000). Heterochrony in plant evolutionary studies through the twentieth century. *Bot. Rev.* 66, 57–88. doi: 10.1007/BF02857782

Litt, A., and Kramer, E. M. (2010). The ABC model and the diversification of floral organ identity. *Semin. Cell Dev. Biol.* 21, 129–137. doi: 10.1016/j.semcdb.2009.11.019

Liu, H., Lin, S., and Liao, J. (2015). Floral ontogeny of two *Jatropha* species (Euphorbiaceae s.s.) and its systematic implications. *Pakist. J. Bot.* 47, 959–965.

Liu, H.-F., Deng, Y.-F., and Liao, J.-P. (2008). Floral organogenesis of three species of *Jatropha* (Euphorbiaceae). *J. Syst. Evol.* 46, 53–61.

Mao, Y., Liu, W., Chen, X., Xu, Y., Lu, W., Hou, J., et al. (2017). Flower development and sex determination between male and female flowers in *Vernicia fordii*. *Front. Plant Sci.* 8:1291. doi: 10.3389/fpls.2017.01291

Marchand, L. (1860). Recherches botaniques sur le *Croton tiglium*. *Adansonia* 1, 232–245.

Michaelis, P. (1924). Blütenmorphologische Untersuchungen an den euphorbiaceen, unter besonderer berücksichtigung der phylogenie der angiospermenblüte. *Bot. Abhandlungen* 3:150.

Nair, N. C., and Abraham, V. (1962). Floral morphology of a few species of Euphorbiaceae. *Proc. Indian Acad. Sci. Sect. B* 56, 1–12.

Narbona, E., and Dirzo, R. (2010). A reassessment of the function of floral nectar in *Croton suberosus* (Euphorbiaceae): a reward for plant defenders and pollinators. *Am. J. Bot.* 97, 672–679. doi: 10.3732/ajb.0900259

Novo, R. R., Souza, J. T., and Cardoso de Castro, C. (2010). First report of predation on floral visitors by crab spiders on *Croton selowii* Baill (Euphorbiaceae). *Acta Bot. Brasil.* 24, 592–594. doi: 10.1590/S0102-33062010000200029

Ojeda, D. I., Valido, A., Fernández de Castro, A. G., Ortega-Olivencia, A., Fuertes-Aguilar, J., Carvalho, J. A., et al. (2016). Pollinator shifts drive petal epidermal evolution on the Macaronesian Islands bird-flowered species. *Biol. Lett.* 12:20160022. doi: 10.1098/rsbl.2016.0022

Payer, J. B. (1857). *Traité D'organogénie Comparée De La Fleur*. Paris: Victor Masson.

Pires, M. M. Y., de Souza, L. A., and Terada, Y. (2004). Biologia floral de *Croton urucurana* Baill (Euphorbiaceae) ocorrente em vegetação ripária da ilha Porto Rico, Porto Rico, Estado do Paraná, Brasil. *Acta Scientiar. Biol. Sci.* 26, 209–215. doi: 10.4025/actascibiolsci.v26i2.1638

Prenner, G., and Rudall, P. J. (2007). Comparative ontogeny of the cyathium in *Euphorbia* (Euphorbiaceae) and its allies: exploring the organ, flower, inflorescence boundary. *Am. J. Bot.* 94, 1612–1629. doi: 10.3732/ajb.94.10.1612

Radcliffe-Smith, A. (2001). *Genera Euphorbiacearum*. Kew: Royal Botanic Garden Kew.

Remizowa, M. V., Sokoloff, D. D., and Rudall, P. J. (2010). Evolutionary history of the monocot flower. *Ann. Missouri Bot. Garden* 97, 617–645. doi: 10.3417/2009142

Riina, R., Berry, P. E., and van Ee, B. W. (2009). Molecular phylogenetics of the dragon's blood *Croton* section *Cyclostigma* (Euphorbiaceae): a

polyphyletic assemblage unraveled. *Syst. Bot.* 34, 360–374. doi: 10.1600/036364409788606415

Rijpkema, A. S., Vandenbussche, M., Koes, R., Heijmans, K., and Gerats, T. (2010). Variations on a theme: changes in the floral ABCs in angiosperms. *Semin. Cell Dev. Biol.* 21, 100–107. doi: 10.1016/j.semcdb.2009.11.002

Ronse De Craene, L. (2018). Understanding the role of floral development in the evolution of angiosperm flowers: clarifications from a historical and physicodynamic perspective. *J. Plant Res.* 131, 367–393. doi: 10.1007/s10265-018-1021-1

Ronse De Craene, L., and Bull-Hereñu, K. (2016). Obdiplostemony: the occurrence of a transitional stage linking robust flower configurations. *Ann. Bot.* 117, 709–724. doi: 10.1093/aob/mcw017

Ronse De Craene, L. P. (2007). Are petals sterile stamens or bracts? The origin and evolution of petals in the core eudicots. *Ann. Bot.* 100, 621–630. doi: 10.1093/aob/mcm076

Ronse De Craene, L. P. (2008). Homology and evolution of petals in the core eudicots. *Syst. Bot.* 33, 301–325. doi: 10.1600/036364408784571680

Ronse De Craene, L. P. (2010). *Floral Diagrams: An Aid To Understanding Flower Morphology And Evolution*. Cambridge: Cambridge University Press.

Ronse De Craene, L. P. (2016). "Montiniaceae," in *The Families and Genera of Vascular Plants, Volume 14 Flowering Plants: Eudicots - Aquifoliales, Boraginales, Bruniales, Dipsacales, Escalloniales, Garryales, Paracryphiales, Solanales (except Convolvulaceae), Icacinaceae, Metteniusaceae, Vahliaceae*, eds J. W. Kadereit, V. Bittrich, and K. Kubitzki (London: Springer), 269–274. doi: 10.1007/978-3-319-28534-4_24

Ronse De Craene, L. P. (2017). Floral development of the endangered genus *Medusagyne* (Medusagynaceae-Malpighiales): Spatial constraints of stamen and carpel increase. *Int. J. Plant Sci.* 178, 639–649. doi: 10.1086/692989

Ronse De Craene, L. P., and Brockington, S. F. (2013). Origin and evolution of petals in angiosperms. *Pl. Ecol. Evol.* 146, 5–25. doi: 10.5091/plecevo.2013.738

Ronse De Craene, L. P., Laet, J. D., and Smets, E. E. (1996). Morphological Studies in Zygophyllaceae. II. The floral development and vascular anatomy of *Peganum harmala*. *Am. J. Bot.* 83, 201–215. doi: 10.1002/j.1537-2197.1996.tb12698.x

Ronse de Craene, L. P., and Smets, E. (1991a). Androecium and floral nectaries of *Harungana madagascariensis* (Clusiaceae). *Plant Syst. Evol.* 178, 179–194.

Ronse de Craene, L. P., and Smets, E. (1991b). Morphological studies in *Zygophyllaceae* I. The floral development and vascular anatomy of *Nitraria retusa*. *Am. J. Bot.* 78, 1438–1448. doi: 10.1002/j.1537-2197.1991.tb12610.x

Ronse De Craene, L. P., and Smets, E. (1992). Complex polyandry in the Magnoliatae: definition, distribution and systematic value. *Nordic J. Bot.* 12, 621–649. doi: 10.1111/j.1756-1051.1992.tb01839.x

Ronse De Craene, L. P., and Smets, E. F. (2001). Staminodes: their morphological and evolutionary significance. *Bot. Rev.* 67, 351–402. doi: 10.1007/BF02858099

Ronse De Craene, L. P., and Wanntorp, L. (2006). Evolution of floral characters in *Gunnera* (Gunneraceae). *Syst. Bot.* 31, 671–688. doi: 10.1600/036364406779695951

Rudall, P. J. (2010). All in a spin: centrifugal organ formation and floral patterning. *Curr. Opin. Plant Biol.* 13, 108–114. doi: 10.1016/j.pbi.2009.09.019

Rudall, P. J. (2011). "Centrifugal stamens in a modern phylogenetic context: was Corner right?," in *Flowers on The Tree of Life*, eds L. Wanntorp and L. P. Ronse De Craene (Cambridge: Cambridge University Press), 142–155. doi: 10.1017/CBO9781139013321.006

Schultes, R. E. (1955). A new generic concept in the Euphorbiaceae. *Bot. Museum Leaf. Harv. Univer.* 17, 27–36.

Secco, R. D. S. (1987). Aspectos sistemáticos e evolutivos do gênero *Sandwithia* Lanj (Euphorbiaceae) em relação às suas afinidades. *Boletim do Museu Paraense Emilio Goeldi Ser. Bot.* 3, 157–181.

Silva, O. L. M., Riina, R., and Cordeiro, I. (2020). Phylogeny and biogeography of Astraea with new insights into the evolutionary history of *Crotoneae* (Euphorbiaceae). *Mol. Phylogenet. Evol.* 145:106738. doi: 10.1016/j.ympev.2020.106738

Smyth, D. R., Bowman, J. L., and Meyerowitz, E. M. (1990). Early flower development in *Arabidopsis*. *Plant Cell* 2:755. doi: 10.2307/3869174

Soltis, D. E., Soltis, P. S., Endress, P. K., Chase, M. W., Manchester, S. R., Judd, W. S., et al. (2018). *Phylogeny and Evolution Of The Angiosperms. Revised And Updated Edition*. London: The university of chicago press.

Soltis, P. S., Brockington, S. F., Yoo, M.-J., Piedrahita, A., Latvis, M., Moore, M. J., et al. (2009). Floral variation and floral genetics in basal angiosperms. *Am. J. Bot.* 96, 110–128. doi: 10.3732/ajb.0800182

Takhtajan, A. (1991). *Evolutionary Trends In Flowering Plants*. New York, NY: Columbia University Press.

The Angiosperm Phylogeny Group (2016). An update of the angiosperm phylogeny group classification for the orders and families of flowering plants: APG IV. *Bot. J. Linnean Soc.* 181, 1–20. doi: 10.1111/boj.12385

Tucker, S. C., and Bernhardt, P. (2000). Floral ontogeny, pattern formation, and evolution in *Hibbertia* and *Adrastaea* (Dilleniaceae). *Am. J. Bot.* 87, 1915–1936. doi: 10.2307/2656843

Uhl, N. W., and Moore, H. E. (1977). Centrifugal stamen initiation in *Phytelephantoid* palms. *Am. J. Bot.* 64, 1152–1161. doi: 10.1002/j.1537-2197.1977.tb10805.x

van Ee, B. W., and Berry, P. E. (2009). A phylogenetic and taxonomic review of *Croton* (Euphorbiaceae S.S.) on Jamaica including the description of *Croton jamaicensis*, a new species of section *Eluteria*. *Syst. Bot.* 34, 129–140. doi: 10.1600/036364409787602203

van Ee, B. W., Berry, P. E., Riina, R., and Amaro, J. E. G. (2008). Molecular phylogenetics and biogeography of the caribbean-centered *Croton* subgenus *Moacroton* (Euphorbiaceae s.s.). *Bot. Rev.* 74, 132–165. doi: 10.1007/s12229-008-9003-y

van Ee, B. W., Forster, P. I., and Berry, P. E. (2015). Phylogenetic relationships and a new sectional classification of *Croton* (Euphorbiaceae) in Australia. *Austr. Syst. Bot.* 28:219. doi: 10.1071/SB15016

van Ee, B. W., Jelinski, N., Berry, P. E., and Hipp, A. L. (2006). Phylogeny and biogeography of *Croton alabamensis* (Euphorbiaceae), a rare shrub from Texas and Alabama, using DNA sequence and AFLP data. *Mol. Ecol.* 15, 2735–2751. doi: 10.1111/j.1365-294X.2006.02970.x

van Ee, B. W., Riina, R., and Berry, P. E. (2011). A revised infrageneric classification and molecular phylogeny of New World *Croton* (Euphorbiaceae). *Taxon* 60, 791–823. doi: 10.1002/tax.603013

van Welzen, P. C., Guerrero, S. A., Arifiani, D., Bangun, T. J. F., Bouman, R. W., Eurlings, M. C. M., et al. (2020). *Weda*, a new genus with two new species of Euphorbiaceae-Crotonoideae from Halmahera (North Maluku, Indonesia) and phylogenetic relationships of the Australasian tribe *Ricinocarpeae*. *J. Syst. Evol.* (in press). doi: 10.1111/jse.12581

Vanvinckenroye, P. F., Ronse De Craene, L. P., and Smets, E. F. (1997). The floral development of *Monococcus echinophorus* (Phytolaccaceae). *Can. J. Bot.* 75, 1941–1950. doi: 10.1139/b97-906

Vasconcelos, T. N. C., Prenner, G., Santos, M. F., Wingler, A., and Lucas, E. J. (2017). Links between parallel evolution and systematic complexity in angiosperms—A case study of floral development in *Myrcia* s.l. (Myrtaceae). *Perspect. Plant Ecol. Evol. Syst.* 24, 11–24. doi: 10.1016/j.ppees.2016.11.001

Velloso, J. M. D. C. (1798). "Joannesia," in *Alographia Dos Alkalis Fixos*, ed. S. T. Ferreira (Lisbon: Na offc. de simão thaddeo ferreira), 199–201.

Venkata-Rao, C., and Ramalakshmi, T. (1968). Floral anatomy of the Euphorbiaceae-I. Some non-*Cyathium* taxa. *J. Indian Bot. Soc.* 47, 278–300.

Webster, G. L. (1993). A provisional synopsis of the sections of the genus *Croton* (Euphorbiaceae). *Taxon* 42, 793–823. doi: 10.2307/1223265

Webster, G. L. (2014). "Euphorbiaceae," in *The Families and Genera Of Vascular Plants Volume XI. Flowering plants. Eudicots: Malpighiales*, ed. K. Kubitzki (London: Springer), 51–216.

Whitney, H. M., Bennett, K. M. V., Dorling, M., Sandbach, L., Prince, D., Chittka, L., et al. (2011). Why do so many petals have conical epidermal cells? *Ann. Bot.* 108, 609–616. doi: 10.1093/aob/mcr065

Wurdack, K. J., Hoffmann, P., and Chase, M. W. (2005). Molecular phylogenetic analysis of uniovulate Euphorbiaceae (Euphorbiaceae sensu stricto) using plastid rbcL and *trnL-F* DNA sequences. *Am. J. Bot.* 92, 1397–1420. doi: 10.3732/ajb.92.8.1397

Conflict of Interest: The authors declare that the research was conducted in the absence of any commercial or financial relationships that could be construed as a potential conflict of interest.

Advantages of publishing in Frontiers

OPEN ACCESS
Articles are free to read for greatest visibility and readership

FAST PUBLICATION
Around 90 days from submission to decision

HIGH QUALITY PEER-REVIEW
Rigorous, collaborative, and constructive peer-review

TRANSPARENT PEER-REVIEW
Editors and reviewers acknowledged by name on published articles

Frontiers
Avenue du Tribunal-Fédéral 34
1005 Lausanne | Switzerland

Visit us: www.frontiersin.org
Contact us: frontiersin.org/about/contact

REPRODUCIBILITY OF RESEARCH
Support open data and methods to enhance research reproducibility

DIGITAL PUBLISHING
Articles designed for optimal readership across devices

FOLLOW US
@frontiersin

IMPACT METRICS
Advanced article metrics track visibility across digital media

EXTENSIVE PROMOTION
Marketing and promotion of impactful research

LOOP RESEARCH NETWORK
Our network increases your article's readership